Agenzia nazionale per le nuove tecnologie, l'energia
e lo sviluppo economico sostenibile

Ministero dello Sviluppo Economico

RICERCA DI SISTEMA ELETTRICO

SPES3 facility: RELAP5 simulations, from 65% power, of the DBE DVI line split break, BDBE EBT top line DEG break, Fukushima type SBO, for design support

Roberta Ferri

Report RdS/2012/017

SPES3 FACILITY: RELAP5 SIMULATIONS, FROM 65% POWER, OF THE DBE DVI LINE SPLIT BREAK, BDBE EBT TOP LINE DEG BREAK, FUKUSHIMA TYPE SBO, FOR DESIGN SUPPORT

Roberta Ferri, SIET

Settembre 2012

Report Ricerca di Sistema Elettrico
Accordo di Programma Ministero dello Sviluppo Economico - ENEA
Area: Governo, gestione e sviluppo del sistema elettrico nazionale
Progetto: Nuovo nucleare da fissione: collaborazioni internazionali e sviluppo competenze in materia nucleare

Responsabile del Progetto: Paride Meloni, ENEA

Titolo

SPES3 facility: RELAP5 simulations, from 65% power, of the DBE DVI line split break, BDBE EBT top line DEG break, Fukushima type SBO, for design support

Ente emittente SIET

PAGINA DI GUARDIA

Descrittori

Tipologia del documento: Rapporto Tecnico

Collocazione contrattuale: Accordo di programma ENEA-MSE: tema di ricerca "Nuovo nucleare da fissione"

Argomenti trattati: Reattori e sistemi innovativi
Sicurezza Nucleare
Analisi incidentale

Sommario

This report has been issued in the frame of the ENEA and MSE research program on "Nuovo Nucleare da fissione". It is the deliverable D1 of the task LP2 of the work program PAR-2011 "Verifiche analitiche a supporto dell'impianto SPES3, simulatore integrale di SMR".
The document deals with the results of the RELAP5 simulations performed in support of the SPES3 facility design. In particular, three transients have been simulated: 1-inch equivalent DVI line split break, in design basis conditions, 4-inch equivalent EBT top line DEG break, in beyond design conditions, and SBO, Fukushima type, with further confirmation the plant configuration and safety systems are suitable to cope with such accidental conditions. Moreover, after the final mechanical design review of the EHRS, the results of 2-inch equivalent DVI line DEG break and SBO simulations have been compared to analogous transients with the original EHRS configuration, showing the new design is suitable to transfer the required power.

Note

Copia n. **In carico a:**

REV.	DESCRIZIONE	DATA		CONVALIDA	VISTO	APPROVAZIONE
2			NOME			
			FIRMA			
1			NOME			
			FIRMA			
0	EMISSIONE	27/08/2012	NOME	P. Meloni		P. Meloni
			FIRMA			

Società Informazioni Esperienze Termoidrauliche
Via Nino Bixio, 27c - 29121 Piacenza (I)

EMITTENTE
issued by
Unità di Produzione
Production Unit

CLIENTE: ENEA client:	**COMMESSA:** 1PN00ING10608 job:	**DISCO:** disk:	**PAGINA:** 1 **DI:** 204 page: of:

IDENTIFICATIVO: SIET 01 811 RT 11 Rev.0 document:	**Classe Ris.:** confidential	**ALLEGATI:** 1 CD-ROM enclosures:

TITOLO: **SPES3 facility: RELAP5 simulations, from 65% power, of the DBE DVI line split break, BDBE EBT top line DEG break, Fukushima type SBO, for design support**
title:

REDATTORI: **R. Ferri**
prepared by:

LISTA DI DISTRIBUZIONE
distribution list

ENEA	Paride	Meloni
SIET	Andrea	Achilli
SIET	Gustavo	Cattadori
SIET	Cinzia	Congiu
SIET	Roberta	Ferri
SIET	Stefano	Gandolfi
SIET	Alfredo	Luce

REV. rev.	DATA date	DESCRIZIONE description	REDAZIONE prepared by	APPROVAZIONE approved by
0	2012-03-23	ISSUE	Roberta Ferri R. Ferri	Gustavo Cattadori G. Cattadori

Informazioni strettamente riservate di proprietà SIET SpA - Da non utilizzare per scopi diversi da quelli per cui sono state fornite.
Confidential information property of SIET SpA - Not to be used for any purpose other than those for which it is supplied.

CONTENTS

I. LIST OF TABLES *3*
II. LIST OF FIGURES *4*
III. NOMENCLATURE *11*
1. SCOPE *13*
2. INTRODUCTION *14*
3. SPES3 NODALIZATION AND ANALYZED TRANSIENTS *15*
3.1 SPES3 schemes and RELAP5 nodalization 15
3.2 Analysed transients and related nodalizations 15
4. BDBE EBT TOP LINE DEG BREAK: SPES3-180 ..... *24*
4.1 SPES3-180 24
4.1.1 Transient phases and description 24
4.1.2 Case conclusions 28
5. DBE DVI LINE 1-INCH EQUIVALENT SPLIT BREAK: SPES3-179 ..... *71*
5.1 SPES3-179 71
5.1.1 SPES3-179 transient phases and description 71
5.1.2 Case conclusions 76
6. DBE STATION BLACK-OUT FUKUSHIMA TYPE: SPES3-177 ..... *114*
6.1 SPES3-177 114
6.1.1 SPES3-177 transient phases and description 114
6.1.2 Case conclusions 116
7. DBE DVI LINE DEG BREAK FROM 65% POWER – NEW EHRS: SPES3-181 ..... *142*
7.1 SPES3-181 and SPES3-175 transient phases and description 142
7.1.1 SPES3-181 and SPES3-175 transient phases and description 142
7.1.2 Case conclusions 146
8. DBE STATION BLACK-OUT, FUKUSHIMA TYPE, FROM 65% POWER – NEW EHRS: SPES3-178 ..... *174*
8.1 SPES3-178 and SPES3-177 174
8.1.1 SPES3-178 and SPES3-177 transient phases and description 174
8.1.2 Case conclusions 176
9. CONCLUSIONS *201*
10. REFERENCES *202*
11. ATTACHMENTS *203*

I. LIST OF TABLES

Tab.3. 1 – SPES3 and IRIS RWST-EHRS stand alone models 17

Tab.4. 1 – SPES3-180 steady state conditions 30
Tab.4. 2 – SPES3-180 list of the main events 31

Tab.5. 1– SPES3-179 list of the main events 77

Tab.6. 1 – SPES3-177 list of the main events 118

Tab.7. 1 – SPES3-181 and SPES3-175 list of the main events 147

Tab.8. 1 – SPES3-178 and SPES3-177 list of the main events 177

II. LIST OF FIGURES

Fig.3. 1 – SPES3 general view 18
Fig.3. 2 – SPES3 primary, secondary loop B, and containment system layout 19
Fig.3. 3 – SPES3 secondary system A and C layout 20
Fig.3. 4 – SPES3 Primary System RELAP5 nodalization 21
Fig.3. 5 – SPES3 Secondary Systems and EHRSs RELAP5 nodalization 22
Fig.3. 6 – SPES3 Containment System RELAP5 nodalization 23

Fig.4.1 – SPES3-180 EBT top line break flow (window) 32
Fig.4.2 – SPES3-180 EBT top line break flow (window) 32
Fig.4.3 – SPES3-180 EBT top line break flow (window) 33
Fig.4.4 – SPES3-180 EBT break line liquid fraction (window) 33
Fig.4.5 – SPES3-180 PRZ pressure (window) 34
Fig.4.6 – SPES3-180 PRZ pressure 34
Fig.4.7 – SPES3-180 DW pressure (window) 35
Fig.4.8 – SPES3-180 DW pressure 35
Fig.4.9 – SPES3-180 PRZ and DW pressures (window) 36
Fig.4.10 – SPES3-180 PSS to DW flow (window) 36
Fig.4.11 – SPES3-180 PSS to DW flow 37
Fig.4.12 – SPES3-180 DW non-condensable gas quality (window) 37
Fig.4.13 – SPES3-180 DW non-condensable gas quality 38
Fig.4.14 – SPES3-180 PSS pressure (window) 38
Fig.4.15 – SPES3-180 PSS pressure 39
Fig.4.16 – SPES3-180 LGMS pressure (window) 39
Fig.4.17 – SPES3-180 LGMS pressure 40
Fig.4.18 – SPES3-180 PSS temperature (window) 40
Fig.4.19 – SPES3-180 PSS temperature 41
Fig.4.20 – SPES3-180 core power (window) 41
Fig.4.21 – SPES3-180 core power 42
Fig.4.22 – SPES3-180 SG power (window) 42
Fig.4.23 – SPES3-180 SGss mass flow (window) 43
Fig.4.24 – SPES3-180 SGss outlet pressure (window) 43
Fig.4.25 – SPES3-180 SG ss outlet pressure 44
Fig.4.26 – SPES3-180 SG-A ss level (window) 44
Fig.4.27 – SPES3-180 SG-A ss level 45
Fig.4.28 – SPES3-180 PRZ level (window) 45
Fig.4.29 – SPES3-180 pump inlet liquid fraction (window) 46
Fig.4.30 – SPES3-180 core inlet flow (window) 46
Fig.4.31 – SPES3-180 core inlet flow 47
Fig.4.32 – SPES3-180 RI-DC check valve mass flow (window) 47

Fig.4.33 – SPES3-180 RI-DC check valve mass flow 48
Fig.4.34 – SPES3-180 ADS Stage-I mass flow (window) 48
Fig.4.35 – SPES3-180 ADS Stage-I mass flow (window) 49
Fig.4.36 – SPES3-180 ADS Stage-I mass flow and PRZ liquid fraction (window) 49
Fig.4.37 – SPES3-180 ADS Stage-II mass flow (window) 50
Fig.4.38 – SPES3-180 ADS Stage-II mass flow (window) 50
Fig.4.39 – SPES3-180 ADS Stage-II mass flow and PRZ liquid fraction (window) 51
Fig.4.40 – SPES3-180 EBT injection mass flow (window) 51
Fig.4.41 – SPES3-180 EBT mass (window) 52
Fig.4.42 – SPES3-180 EBT level (window) 52
Fig.4.43 – SPES3-180 EBT balance line mass flow (window) 53
Fig.4.44 – SPES3-180 EBT balance line mass flow (window) 53
Fig.4.45 – SPES3-180 Core liquid fraction (window) 54
Fig.4.46 – SPES3-180 Core liquid fraction 54
Fig.4.47 – SPES3-180 Core inlet and outlet temperatures (window) 55
Fig.4.48 – SPES3-180 Core inlet and outlet temperatures 55
Fig.4.49 – SPES3-180 Core heater rod clad surface temperatures (normal rods) 56
Fig.4.50 – SPES3-180 Core heater rod clad surface temperatures (hot rods) 56
Fig.4.51 – SPES3-180 RPV mass 57
Fig.4.52 – SPES3-180 PCC mass flow 57
Fig.4.53 – SPES3-180 PCC tank level 58
Fig.4.54 – SPES3-160 PCC inlet and outlet temperature 58
Fig.4.55 – SPES3-180 PCC liquid fraction (window) 59
Fig.4.56 – SPES3-180 PCC liquid fraction 59
Fig.4.57 – SPES3-180 PCC power (window) 60
Fig.4.58 – SPES3-180 PCC power 60
Fig.4.59 – SPES3-180 LGMS injection mass flow (window) 61
Fig.4.60 – SPES3-180 LGMS injection mass flow 61
Fig.4.61 – SPES3-180 LGMS mass 62
Fig.4.62 – SPES3-180 LGMS level 62
Fig.4.63 – SPES3-180 PSS and DW pressure (window) 63
Fig.4.64 – SPES3-180 PSS and DW pressure 63
Fig.4.65 – SPES3-180 PSS vent pipe level (window) 64
Fig.4.66 – SPES3-180 PSS vent pipe level 64
Fig.4.67 – SPES3-180 PSS level (window) 65
Fig.4.68 – SPES3-180 PSS level 65
Fig.4.69 – SPES3-180 PSS mass 66
Fig.4.70 – SPES3-180 RC level (window) 66
Fig.4.71 – SPES3-180 RC level 67
Fig.4.72 – SPES3-180 RC to DVI line mass flow 67
Fig.4.73 – SPES3-180 DVI line mass flow 68

Fig.4.74 – SPES3-180 DW level 68
Fig.4.75 – SPES3-180 DW mass 69
Fig.4.76 – SPES3-180 DW to RC mass flow (window) 69
Fig.4.77 – SPES3-180 QT level 70
Fig.4.78 – SPES3-180 QT mass 70

Fig.5. 1 - SPES3-179 DVI break mass flow (window) 78
Fig.5. 2 - SPES3-179 DVI break mass flow (window) 78
Fig.5. 3 - SPES3-179 DVI break mass flow 79
Fig.5. 4 - SPES3-179 EBT injection mass flow (window) 79
Fig.5. 5 - SPES3-179 PRZ pressure (window) 80
Fig.5. 6 - SPES3-179 PRZ pressure 80
Fig.5. 7 - SPES3-179 LGMS mass flow (window) 81
Fig.5. 8 - SPES3-179 PRZ and DW pressures (detail) 81
Fig.5. 9 - SPES3-179 PRZ and DW pressures (window) 82
Fig.5. 10 - SPES3-179 RPV down domer level 82
Fig.5. 11 - SPES3-179 RC level 83
Fig.5. 12 - SPES3-179 RC mass 83
Fig.5. 13 - SPES3-179 DW pressure (window) 84
Fig.5. 14 - SPES3-179 DW pressure 84
Fig.5. 15 - SPES3-179 ADS Stage-I mass flow (window) 85
Fig.5. 16 - SPES3-179 ADS Stage-I mass flow (window) 85
Fig.5. 17 - SPES3-179 DW to PSS mass flow (window) 86
Fig.5. 18 - SPES3-179 DW to PSS integral flow (window) 86
Fig.5. 19 - SPES3-179 DW non-condensable gas quality (window) 87
Fig.5. 20 - SPES3-179 DW non-condensable gas quality 87
Fig.5. 21 - SPES3-179 PSS pressure (window) 88
Fig.5. 22 - SPES3-179 PSS pressure 88
Fig.5. 23 - SPES3-179 LGMS pressure (window) 89
Fig.5. 24 - SPES3-179 LGMS pressure 89
Fig.5. 25 - SPES3-179 DW and PSS pressure (window) 90
Fig.5. 26 - SPES3-179 DW and PSS pressure 90
Fig.5. 27 - SPES3-179 PSS vent pipe level (window) 91
Fig.5. 28 - SPES3-179 PSS temperatures 91
Fig.5. 29 - SPES3-179 Core and SG power(window) 92
Fig.5. 30 - SPES3-179 Core and SG power 92
Fig.5. 31 - SPES3-179 SG secondary side mass flow (window) 93
Fig.5. 32 - SPES3-179 SG secondary side mass flow 93
Fig.5. 33 - SPES3-179 EHRS cold leg mass flow (window) 94
Fig.5. 34 - SPES3-179 EHRS cold leg mass flow 94
Fig.5. 35 - SPES3-179 EHRS power (window) 95

Fig.5. 36 - SPES3-179 EHRS power 95
Fig.5. 37 - SPES3-179 SG secondary side outlet pressure (window) 96
Fig.5. 38 - SPES3-179 SG secondary side outlet pressure 96
Fig.5. 39 - SPES3-179 SG secondary side collapsed level (window) 97
Fig.5. 40 - SPES3-179 SG secondary side collapsed level 97
Fig.5. 41 - SPES3-179 PRZ level (window) 98
Fig.5. 42 - SPES3-179 Pump inlet liquid fraction (window) 98
Fig.5. 43 - SPES3-179 Pump velocity (window) 99
Fig.5. 44 - SPES3-179 Pump by-pass mass flow (window) 99
Fig.5. 45 - SPES3-179 Core inlet mass flow (window) 100
Fig.5. 46 - SPES3-179 Core inlet mass flow 100
Fig.5. 47 - SPES3-179 RI-DC check valve mass flow (window) 101
Fig.5. 48 - SPES3-179 RI-DC check valve mass flow 101
Fig.5. 49 - SPES3-179 RPV mass (window) 102
Fig.5. 50 - SPES3-179 RPV mass 102
Fig.5. 51 - SPES3-179 Core liquid fraction (window) 103
Fig.5. 52 - SPES3-179 Core liquid fraction 103
Fig.5. 53 - SPES3-179 ADS Stage-I integral flow 104
Fig.5. 54 - SPES3-179 RC to DVI mass flow (window) 104
Fig.5. 55 - SPES3-179 EBT level (window) 105
Fig.5. 56 - SPES3-179 EBT to RPV balance line mass flow (window) 105
Fig.5. 57 - SPES3-179 Core inlet and outlet fluid temperature (window) 106
Fig.5. 58 - SPES3-179 Core inlet and outlet fluid temperature 106
Fig.5. 59 - SPES3-179 Core heater rod surface temperature –normal rod (window) 107
Fig.5. 60 - SPES3-179 Core heater rod surface temperature –normal rod 107
Fig.5. 61 - SPES3-179 Core heater rod surface temperature –hot rod (window) 108
Fig.5. 62 - SPES3-179 Core heater rod surface temperature –hot rod 108
Fig.5. 63 - SPES3-179 DVI mass flow (window) 109
Fig.5. 64 - SPES3-179 DVI mass flow 109
Fig.5. 65 - SPES3-179 QT level 110
Fig.5. 66 - SPES3-179 LGMS level (window) 110
Fig.5. 67 - SPES3-179 LGMS mass (window) 111
Fig.5. 68 - SPES3-179 ADS Stage-II mass flow (window) 111
Fig.5. 69 - SPES3-179 ADS Stage-II mass flow 112
Fig.5. 70 - SPES3-179 RWST temperature 112
Fig.5. 71 - SPES3-179 RWST mass 113
Fig.5. 72 - SPES3-179 RWST pressure 113

Fig.7. 1 - SPES3-181 and SPES3-175 DVI break mass flow (window) 148
Fig.7. 2 - SPES3-181 and SPES3-175 DVI break mass flow (window) 148
Fig.7. 3 - SPES3-181 and SPES3-175 DVI break mass flow 149

Fig.7. 4 - SPES3-172 and SPES3-175 PRZ pressure (window) 149
Fig.7. 5 - SPES3-181 and SPES3-175 PRZ pressure (window) 150
Fig.7. 6 - SPES3-181 and SPES3-175 PRZ pressure 150
Fig.7. 7 - SPES3-181 and SPES3-175 DW pressure (window) 151
Fig.7. 8 - SPES3-181 and SPES3-175 DW pressure 151
Fig.7. 9 - SPES3-181 and SPES3-175 PRZ and DW pressures (window) 152
Fig.7. 10 - SPES3-181 and SPES3-175 PRZ and DW pressures 152
Fig.7. 11 - SPES3-181 and SPES3-175 DW to PSS mass flow (window) 153
Fig.7. 12 - SPES3-181 and SPES3-175 DW and PSS pressure (window) 153
Fig.7. 13 - SPES3-181 and SPES3-175 DW and PSS pressure 154
Fig.7. 14 - SPES3-181 and SPES3-175 LGMS pressure 154
Fig.7. 15 - SPES3-181 and SPES3-175 Core and SG power (window) 155
Fig.7. 16 - SPES3-172 and SPES3-175 Core and SG power 155
Fig.7. 17 - SPES3-181 and SPES3-175 SG ss mass flow (window) 156
Fig.7. 18 - SPES3-181 and SPES3-175 SG ss mass flow 156
Fig.7. 19 - SPES3-181 and SPES3-175 EHRS cold leg mass flow (window) 157
Fig.7. 20 - SPES3-181 and SPES3-175 EHRS cold leg mass flow 157
Fig.7. 21 - SPES3-181 and SPES3-175 EHRS power (window) 158
Fig.7. 22 - SPES3-181 and SPES3-175 EHRS power 158
Fig.7. 23 - SPES3-181 and SPES3-175 SG ss outlet pressure (window) 159
Fig.7. 24 - SPES3-181 and SPES3-175 SG ss outlet pressure 159
Fig.7. 25 - SPES3-181 and SPES3-175 SG-Ass collapsed level (window) 160
Fig.7. 26 - SPES3-181 and SPES3-175 SG-Ass collapsed level 160
Fig.7. 27 - SPES3-181 and SPES3-175 PRZ level (window) 161
Fig.7. 28 - SPES3-181 and SPES3-175 Core inlet mass flow (window) 161
Fig.7. 29 - SPES3-181 and SPES3-175 Core inlet mass flow 162
Fig.7. 30 - SPES3-181 and SPES3-175 RI-DC check valve mass flow (window) 162
Fig.7. 31 - SPES3-181 and SPES3-175 RI-DC check valve mass flow 163
Fig.7. 32 - SPES3-181 and SPES3-175 RPV mass (window) 163
Fig.7. 33 - SPES3-181 and SPES3-175 RPV mass 164
Fig.7. 34 - SPES3-181 and SPES3-175 Core liquid fraction (window) 164
Fig.7. 35 - SPES3-181 and SPES3-175 ADS Stage-I mass flow (window) 165
Fig.7. 36 - SPES3-181 and SPES3-175 RC to DVI mass flow IL (window) 165
Fig.7. 37 - SPES3-181 and SPES3-175 RC to DVI mass flow IL 166
Fig.7. 38 - SPES3-181 and SPES3-175 EBT injection mass flow (window) 166
Fig.7. 39 - SPES3-181 and SPES3-175 EBT level (window) 167
Fig.7. 40 - SPES3-181 and SPES3-175 Core inlet and outlet fluid temperature (window) 167
Fig.7. 41 - SPES3-181 and SPES3-175 Core inlet and outlet fluid temperature 168
Fig.7. 42 - SPES3-181 and SPES3-175 Core heater rod surface temperature –normal rod (window) 168
Fig.7. 43 - SPES3-181 and SPES3-175 Core heater rod surface temperature –normal rod 169
Fig.7. 44 - SPES3-181 and SPES3-175 Core heater rod surface temperature –hot rod (window) 169

Fig.7. 45 - SPES3-181 and SPES3-175 Core heater rod surface temperature –hot rod 170
Fig.7. 46 - SPES3-181 and SPES3-175 LGMS injection mass flow (window) 170
Fig.7. 47 - SPES3-181 and SPES3-175 RC level (window) 171
Fig.7. 48 - SPES3-181 and SPES3-175 LGMS level 171
Fig.7. 49 - SPES3-181 and SPES3-175 LGMS mass 172
Fig.7. 50 - SPES3-181 and SPES3-175 ADS Stage-II mass flow 172
Fig.7. 51 - SPES3-181 and SPES3-175 RWST temperature (window) 173
Fig.7. 52 - SPES3-181 and SPES3-175 RWST temperature 173

Fig.8. 1 – SPES3-178 and SPES3-177 RCP velocity (window) 178
Fig.8. 2 – SPES3-178 and SPES3-177 RCP head (window) 178
Fig.8. 3 – SPES3-178 and SPES3-177 RI-DC check valve mass flow (window) 179
Fig.8. 4 – SPES3-178 and SPES3-177 RI-DC check valve mass flow (window) 179
Fig.8. 5 – SPES3-178 and SPES3-177 RI-DC check valve mass flow 180
Fig.8. 6 – SPES3-178 and SPES3-177 Pump by-pass mass flow (window) 180
Fig.8. 7 – SPES3-178 and SPES3-177 Pump by-pass mass flow (window) 181
Fig.8. 8 – SPES3-178 and SPES3-177 SG power (window) 181
Fig.8. 9 – SPES3-178 and SPES3-177 Pump inlet liquid fraction (window) 182
Fig.8. 10 – SPES3-178 and SPES3-177 SG secondary side mass flow (window) 182
Fig.8. 11 – SPES3-178 and SPES3-177 SG secondary side mass flow (window) 183
Fig.8. 12 – SPES3-178 and SPES3-177 SG secondary side mass flow 183
Fig.8. 13 – SPES3-178 and SPES3-177 Core and SG total power (window) 184
Fig.8. 14 – SPES3-178 and SPES3-177 Core and SG power (window) 184
Fig.8. 15 – SPES3-178 and SPES3-177 Core and SG power 185
Fig.8. 16 – SPES3-178 and SPES3-177 SG secondary side collapsed level (window) 185
Fig.8. 17 – SPES3-178 and SPES3-177 SG secondary side collapsed level (window) 186
Fig.8. 18 – SPES3-178 and SPES3-177 SG secondary side collapsed level 186
Fig.8. 19 – SPES3-178 and SPES3-177 EHRS cold leg mass flow (window) 187
Fig.8. 20 – SPES3-178 and SPES3-177 EHRS cold leg mass flow 187
Fig.8. 21 – SPES3-178 and SPES3-177 EHRS power (window) 188
Fig.8. 22 – SPES3-178 and SPES3-177 EHRS power 188
Fig.8. 23 – SPES3-178 and SPES3-177 RWST temperature 189
Fig.8. 24 – SPES3-178 and SPES3-177 RWST mass 189
Fig.8. 25 – SPES3-178 and SPES3-177 Core mass flow (window) 190
Fig.8. 26 – SPES3-178 and SPES3-177 Core mass flow (window) 190
Fig.8. 27 – SPES3-178 and SPES3-177 Core mass flow 191
Fig.8. 28 – SPES3-178 and SPES3-177 SG secondary side outlet pressure (window) 191
Fig.8. 29 – SPES3-178 and SPES3-177 SG secondary side outlet pressure 192
Fig.8. 30 – SPES3-178 and SPES3-177 PRZ pressure (window) 192
Fig.8. 31 – SPES3-178 and SPES3-177 PRZ pressure 193
Fig.8. 32 – SPES3-178 and SPES3-177 Core inlet and outlet temperature (window) 193

Fig.8. 33 – SPES3-178 and SPES3-177 Core inlet, outlet and saturation temperature 194
Fig.8. 34 – SPES3-178 and SPES3-177 Core liquid fraction 194
Fig.8. 35 – SPES3-178 and SPES3-177 PRZ level (window) 195
Fig.8. 36 – SPES3-178 and SPES3-177 RPV down comer level 195
Fig.8. 37 – SPES3-178 and SPES3-177 EBT injection mass flow (window) 196
Fig.8. 38 – SPES3-178 and SPES3-177 EBT to RPV balance line mass flow (window) 196
Fig.8. 39 – SPES3-178 and SPES3-177 DVI mass flow 197
Fig.8. 40 – SPES3-178 and SPES3-177 EBT level 197
Fig.8. 41 – SPES3-178 and SPES3-177 RPV mass 198
Fig.8. 42 – SPES3-178 and SPES3-177 Core heater rod surface temperature –normal rod (window) 198
Fig.8. 43 – SPES3-178 and SPES3-177 Core heater rod surface temperature –normal rod 199
Fig.8. 44 – SPES3-178 and SPES3-177 Core heater rod surface temperature –hot rod (window) 199
Fig.8. 45 – SPES3-178 and SPES3-177 Core heater rod surface temperature –hot rod 200

III. NOMENCLATURE

ADS	Automatic Depressurization System
ADS-DT	ADS-Double Train
ADS-ST	ADS-Single Train
BAF	Bottom of Active Fuel
BDBE	Beyond Design Basis Event
Bot, bot	Bottom
BC	Base Case
D	Diameter
Di	inner Diameter
Do	outer Diameter
DBE	Design Basis Event
DC	Downcomer
DEG	Double Ended Guillotine
DP	Differential pressure
DT	Difference of temperature
DVI	Direct Vessel Injection
DW	Dry Well
EBT	Emergency Boration Tank
EHRS	Emergency Heat Removal System
FER	University of Zagreb
FL	Feed Line
FW	Feed Water
GOTHIC	Generation Of Thermal-Hydraulic Information for Containments
HX	Heat Exchanger
IRIS	International Reactor Innovative and Secure
LGMS	Long Term Gravity Make-up System
LM	LOCA Mitigation signal
LOCA	Loss of Coolant Accident
mid	middle
MFIV	Main Feed Isolation Valve
MSIV	Main Steam Isolation Valve
NPP	Nuclear Power Plant
P	Pressure
PAR	Piano Annuale di Realizzazione
PCC	Passive Containment Cooling
PRZ	Pressurizer
PSS	Pressure Suppression System

PWR	Pressurized Water Reactor
QT	Quench Tank
RC	Reactor Cavity
RELAP	Reactor Excursion and Leak Analysis Program
RI	Riser
RPV	Reactor Pressure Vessel
RWST	Refuelling Water Storage Tank
S	Safeguard signal
SBLOCA	Small Break Loss of Coolant Accident
SBO	Station Black-Out
SG	Steam Generator
SIET	Società Informazioni Esperienze Termoidrauliche
SL	Steam Line
SMR	Small Modular Reactor
SPES	Simulatore Pressurizzato per Esperienze di Sicurezza
T	Temperature
TAF	Top of Active Fuel

1. SCOPE

The primary goal of this document is to describe the results of the SPES3 facility numerical simulations for two tests, included in the test matrix (DBE DVI line split break and BDBE EBT top line DEG break), and a test of SBO, based on the Fukushima accident sequence.

All the transients starts from steady conditions at 65% power, actual operating limit of SPES3 facility, and provide information on the plant behaviour, useful to identify eventual critical points that may need special test procedures.

The DBE, 1-inch equivalent DVI line split break simulation allowed to investigate the plant response under a SBLOCA at low elevation, and to identify phases and events of the transient.

The BDBE, 4-inch equivalent, EBT top line DEG break simulation allowed to investigate phases and events of the transient and to verify the plant can cope with such kind of accident relaying on the PCC performance, when all the EHRS are unavailable.

The simulation of the Fukushima type SBO was performed, assuming the loss of off-site power at time zero, corresponding to the earthquake. It allowed to investigate the plant response to this event.

2. INTRODUCTION

The SPES3 facility was designed for testing on integral layout SMR and it is being built at SIET laboratories. The facility is based on the IRIS reactor design and it is suitable to simulate postulated Design and Beyond Design Basis Events, providing experimental data for code validation and plant safety analyses, [1].

The IRIS reactor is an advanced medium size, integral layout, pressurized water reactor developed by an international consortium of utilities, industries, research centres and universities. It is based on the proven technology of PWR with innovative configuration and safety features suitable to cope with Loss of Coolant Accidents through a dynamic coupling of the primary and containment systems, [2] [3].

The SPES3 facility reproduces the primary, secondary and containment systems of the reactor with 1:100 volume scale, full elevation, prototypical fluid and thermal-hydraulic conditions, [4] [5] [6] [7] [8] [9] [10] [11] [12] [13].

The RELAP5 Mod.3.3 thermal-hydraulic code was chosen to simulate the whole SPES3 facility: primary and secondary circuits, safety systems and containment. During the SPES3 design, a complex calculation-design feedback process led to optimize model and design up to the present configuration suitable to simulate the IRIS reactor and reproduce the IRIS results obtained by FER at Zagreb University with the RELAP5 and GOTHIC coupled codes [14] [15] [16] [17] [18] [19] [20].

The process included the simulation of all design basis events specified in the test matrix with a great attention to the DVI line DEG break, considered the most challenging LOCA in IRIS, potentially maximizing RPV mass depletion. The simulation of the beyond design basis event DVI line DEG break, specified in the test matrix, allowed to verify the PCC performance and optimize the PCC and ADS Stage-II actuation time to cope with accidents where all the EHRS are unavailable. The need of testing SPES3, starting from 65% nominal power, due to the limit of SIET power supply, led to define proper steady conditions at reduced power and mass flows, suitable to provide the same transient trend as if starting from full power.

Work, described in this document, is part of SPES3 facility design support and transient analyses. It is mainly aimed at deepening the knowledge of plant behaviour and transient phases under postulated accidents and at identifying specific critical aspects that can arise during the tests and require special test procedures.

3. SPES3 NODALIZATION AND ANALYZED TRANSIENTS

This section reports the schemes of the SPES3 facility and the RELAP5 nodalization utilized for the cases described in the following chapters.

3.1 SPES3 schemes and RELAP5 nodalization

The general view of SPES3 is reported in Fig.3. 1. The SPES3 flow diagram for primary loop, secondary loop B and containment system is reported in Fig.3. 2. The flow diagrams for secondary loops A and C are reported in Fig.3. 3.

The details of SPES3 base nodalization are reported in [15]. The calculation-design feedback process, carried out to optimize the SPES3 design to better simulate the IRIS plant, led to update the model as described in [18]. Further design optimization are described in [20], mainly aimed at simulating beyond design basis events with optimization of PCC heat exchanger geometry and actuation procedures. In particular, the PCC horizontal bundle consists of 20 U-tubes, 1-inch size (Do = 33.4 mm, Di = 27.86 mm, average length 4.27 m), actuated at the LM-signal together with the ADS-Stage-II in case of BDBE LOCA with EHRS total failure. Also the resistance of the RC to DVI line was optimized by reducing the pressure drops (orifice diameter increased from 1 mm to 7 mm).

The SPES3 nodalizations, starting point for the present analyses, are SPES3-175 for the DBE and SPES3-176 for the BDBE, both from 65% power [20]. Fig.3. 4, Fig.3. 5, Fig.3. 6 report the SPES3 RELAP5 nodalization.

3.2 Analysed transients and related nodalizations

Three transients have been run and analyzed based on the above nodalizations:

SPES3-177: DBE Station black-out, Fukushima type;

SPES3-180: BDBE EBT top line DEG break, 4-inch equivalent;

SPES3-179: DBE DVI split break, 1-inch equivalent.

The executive final design of the EHRS, according to PED requirements, imposed to change the heat exchanger tube geometry due to the use of AISI 304 instead of INCONEL-600 (IRIS material).

The SPES3 design conditions for the secondary side (17.25 MPa pressure and 353.5 °C temperature, specified in [1]) would require a great increase in tube thickness, to satisfy the PED requirements, substituting Inconel with AISI. So, as the SPES3 transient analyses [16] [18] [20] showed the secondary side pressure never reached 12 MPa, it was decided to limit the design conditions to 12 MPa pressure and 324.65 °C temperature. The final tube geometry (AISI 304) is 60.3 mm outer diameter and 5.54 mm thickness with no variation of length and header geometry.

The tube thickness increase limits the global heat transfer coefficient, so it was decided to reduce the Teflon thermal insulation, foreseen on the tubes to correctly scale the heat transfer surface. The Teflon thickness reduction compensates for extra thickness of metal.

Stand-alone cases were run on the EHRS/RWST to define the correct Teflon thickness suitable to let the SPES3 EHRS transfer the same power as IRIS. Based on the stand-alone models for IRIS and SPES3, described in [18], the EHRS-A and B and EHRS-C were simulated separately. The summary of cases is reported in Tab.3. 1.

The final EHRS-A and B configuration is with one tube, for each HX, covered with 0.096 mm Teflon and headers covered with 10 mm Teflon.

The final EHRS-C configuration is with no thermal insulation on the tubes and headers covered with 0.2 mm Teflon.

After the EHRS design optimization, the SPES3 nodalization was updated and two cases were run for comparison with the previous configuration, to demonstrate the EHRS re-design does not affect transferred power. In particular, the cases are listed below:

SPES3-178: DBE Station back-out, Fukushima type;

SPES3-181: DBE DVI line DEG break, 2-inch equivalent.

Tab.3. 1 – SPES3 and IRIS RWST-EHRS stand alone models

ehrs-iris5.i (IRIS Perseo) [18]	Reference case. IRIS tube geometry and INCONEL-600. Inlet P 70 bar steam; Outlet P 70. bar liquid. RES: 2 EHRS total power 65.6 MW/100 = 0.656 MW.
rwstsi70_TT_2inch5_54.i (SPES3-AB)	Three tubes for each HX, size 60.3 x 5.54 mm. AISI 304. No Teflon on the tubes. Headers insulated with 30 mm Teflon. Inlet P 70 bar steam; Outlet P 70.0 bar liquid. RES: Total 2 EHRS power at 3000 s 0.718 MW. 9.4% power higher than ehrs-iris5. Need to cover one tube with Teflon.
rwstsi70_UU_2inch5_54.i (SPES3-C)	Five tubes, size 60.3 x 5.54 mm. AISI 304. Inlet P 70 bar steam; Outlet P 70.0 bar liquid. No Teflon on the tubes. Headers insulated with 30 mm Teflon. RES: Total 2 EHRS power at 3000 s 0.590 MW. 10% power lower than ehrs-iris5. Need to reduce the header insulation.
rwstsi70_TT2inch5_54teflonreduction.i (SPES3-AB)	Three tubes for each HX, size 60.3 x 5.54 mm. AISI 304. No Teflon on the tubes. Headers insulated with 10 mm Teflon. Inlet P 70 bar steam; Outlet P 70.0 bar liquid. RES: Total 2 EHRS power at 3000 s 0.653 MW. 0.44% power lower than ehrs-iris5.
rwstsi70_UU2inch5_54teflonreduction.i (SPES3-C)	Five tubes, size 60.3 x 5.54 mm. AISI 304. Inlet P 70 bar steam; Outlet P 70.0 bar liquid. No Teflon on the tubes. Headers insulated with 0.2 mm Teflon. RES: EHRS-C power at 3000 s 0.654 MW. 0.38 % power lower than ehrs-iris5.

Fig.3. 1 – SPES3 general view

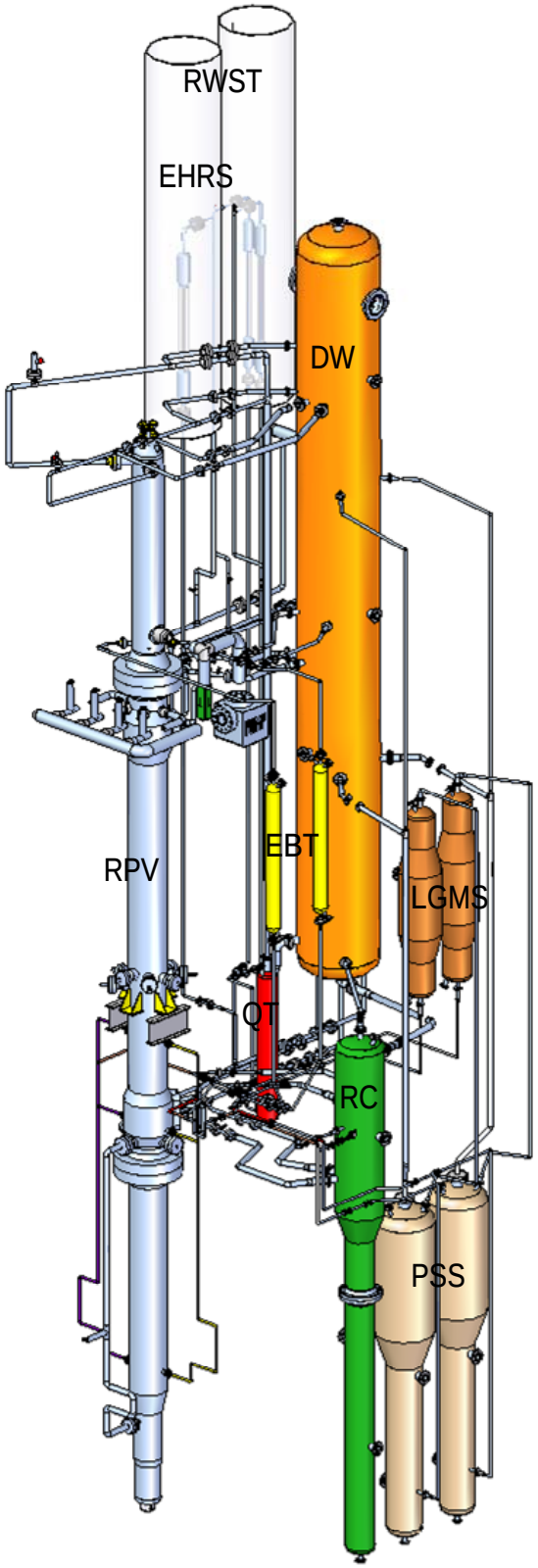

Fig.3. 2 – SPES3 primary, secondary loop B, and containment system layout

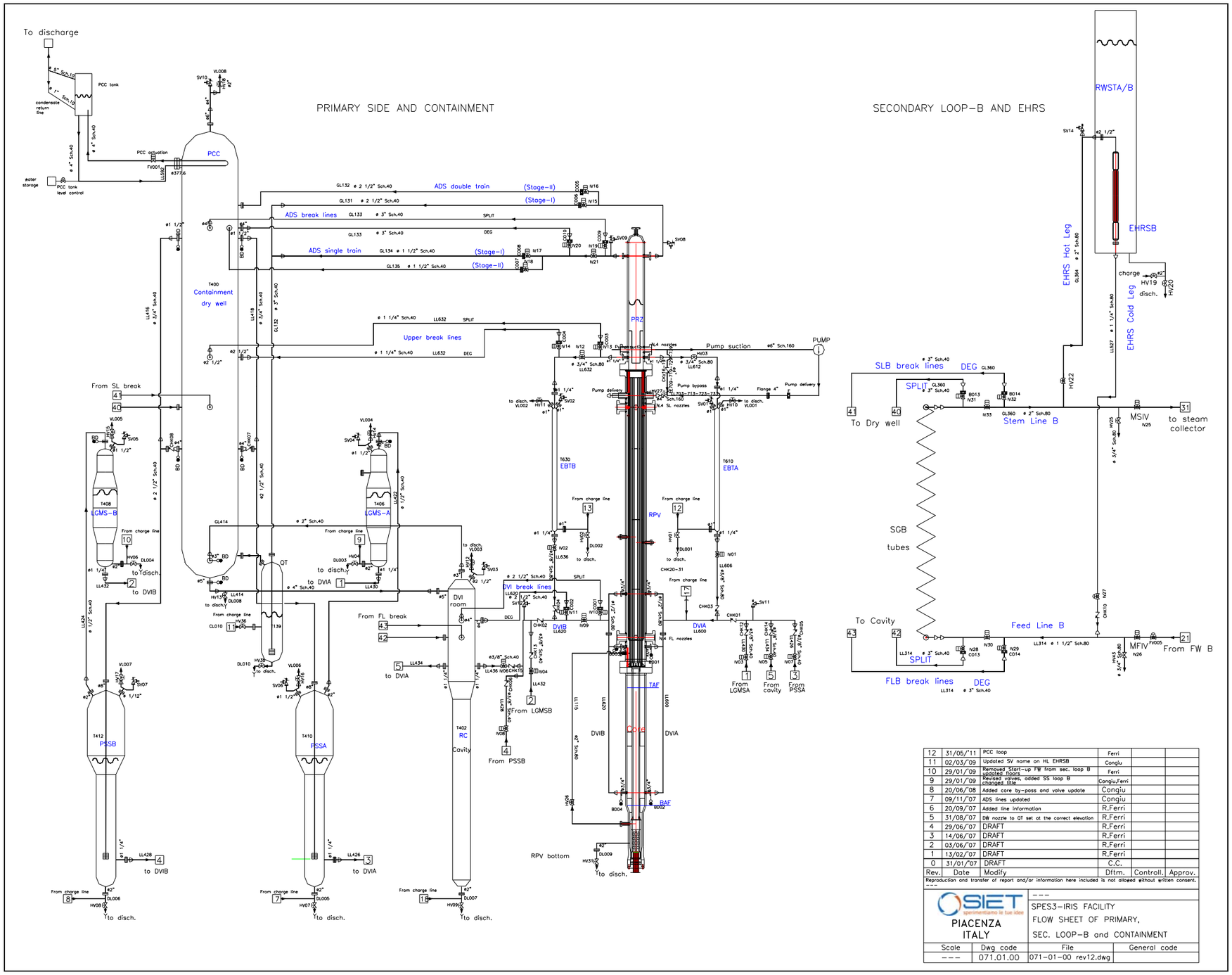

Rev.	Date	Modify	Dftm.	Controll.	Approv.
12	31/05/'11	PCC loop	Ferri		
11	02/03/'09	Updated SV name on HL EHRSB	Congiu		
10	29/01/'09	Removed Start–up FW from sec. loop B updated floors	Ferri		
9	29/01/'09	Revised valves, added SS loop B changed title	Congiu,Ferri		
8	20/06/'08	Added core by–pass and valve update	Congiu		
7	09/11/'07	ADS lines updated	Congiu		
6	20/09/'07	Added line information	R.Ferri		
5	31/08/'07	DW nozzle to QT set at the correct elevation	R.Ferri		
4	29/06/'07	DRAFT	R.Ferri		
3	14/06/'07	DRAFT	R.Ferri		
2	03/06/'07	DRAFT	R.Ferri		
1	13/02/'07	DRAFT	R.Ferri		
0	31/01/'07	DRAFT	C.C.		

Reproduction and transfer of report and/or information here included is not allowed without written consent.

SIET sperimentiamo le tue idee
PIACENZA
ITALY

SPES3–IRIS FACILITY
FLOW SHEET OF PRIMARY,
SEC. LOOP–B and CONTAINMENT

Scale	Dwg code	File	General code
---	071.01.00	071–01–00 rev12.dwg	

Fig.3. 3 – SPES3 secondary system A and C layout

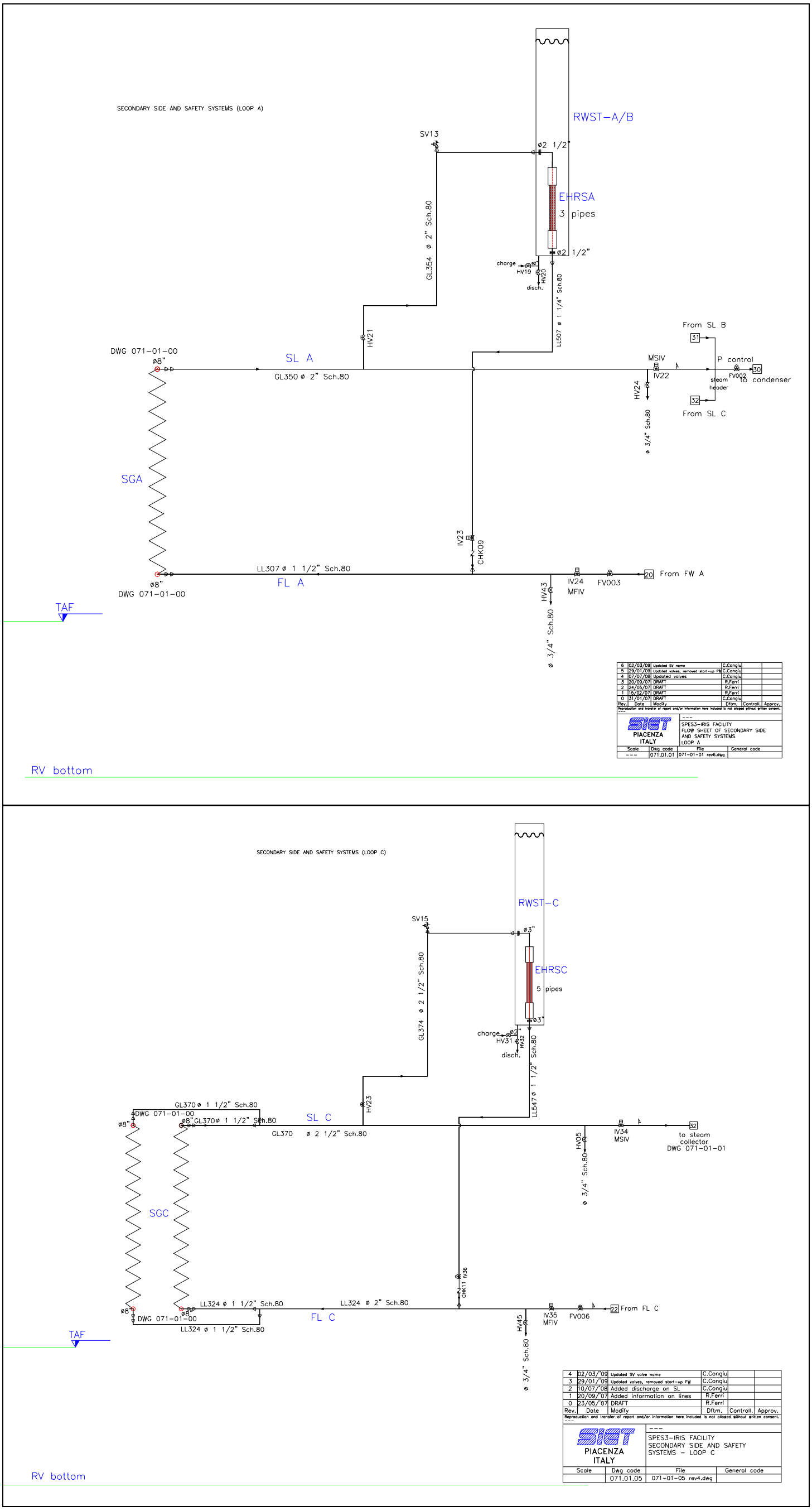

Fig.3. 4 – SPES3 Primary System RELAP5 nodalization

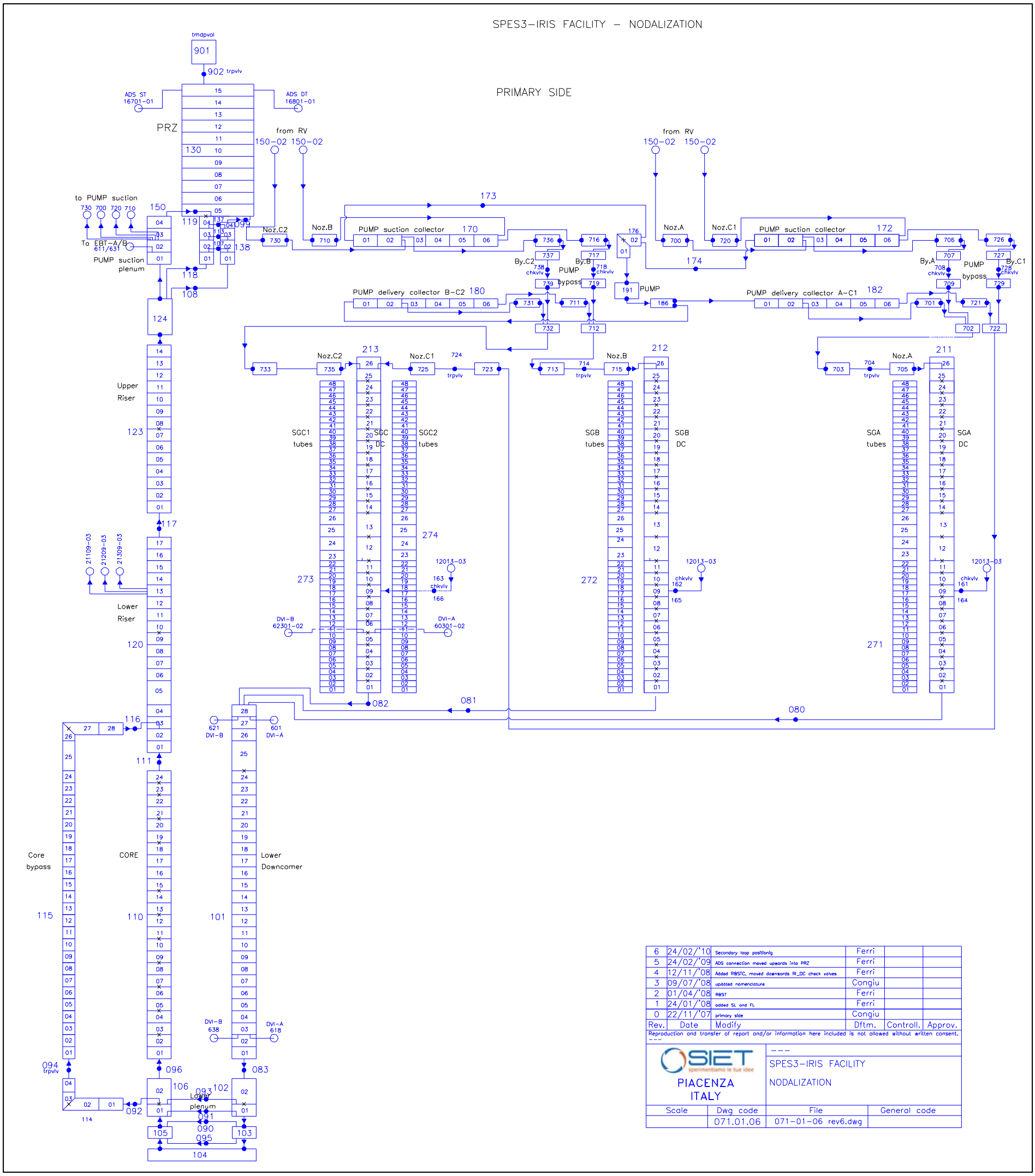

Fig.3. 5 – SPES3 Secondary Systems and EHRSs RELAP5 nodalization

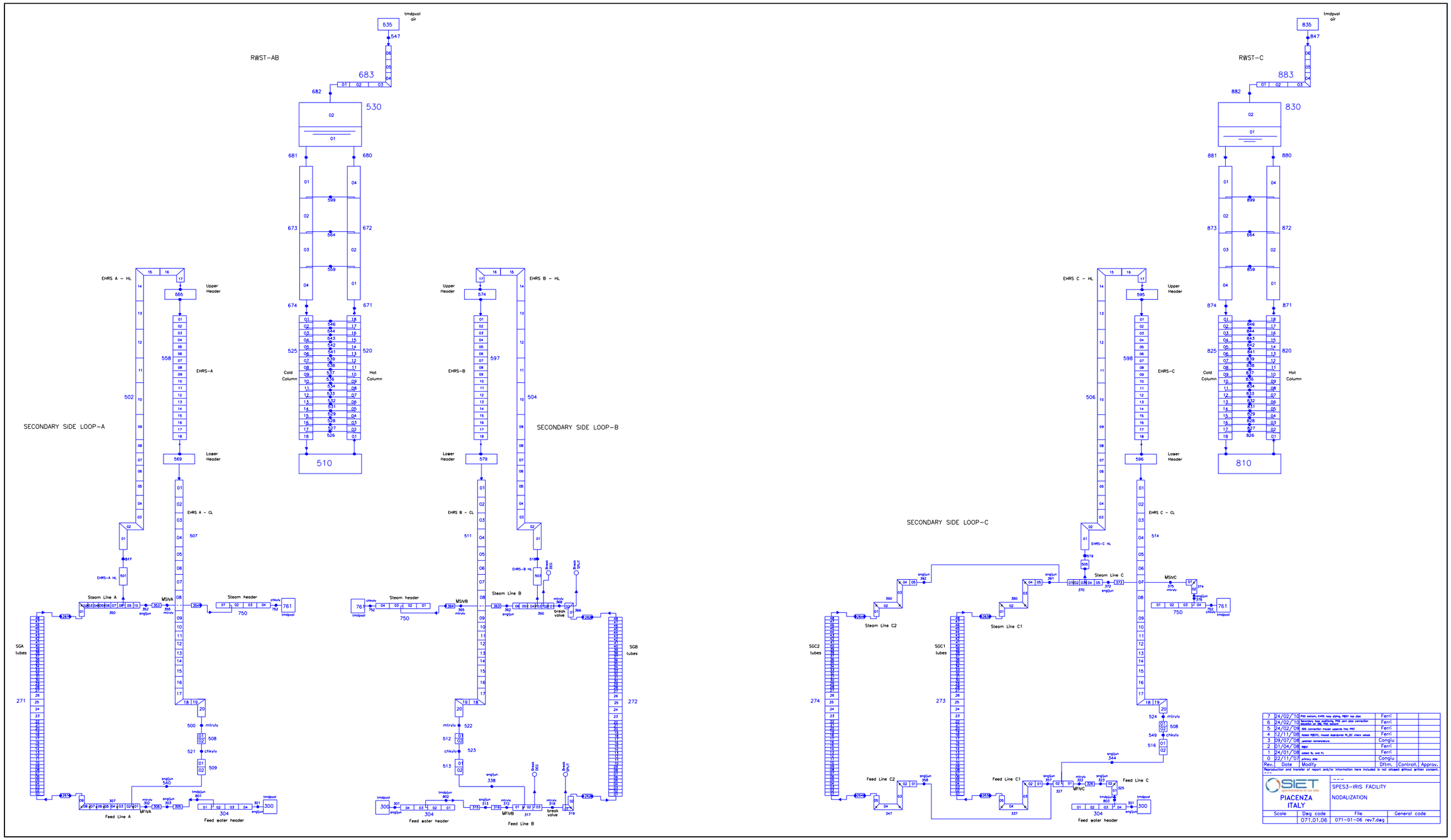

Fig.3. 6 – SPES3 Containment System RELAP5 nodalization

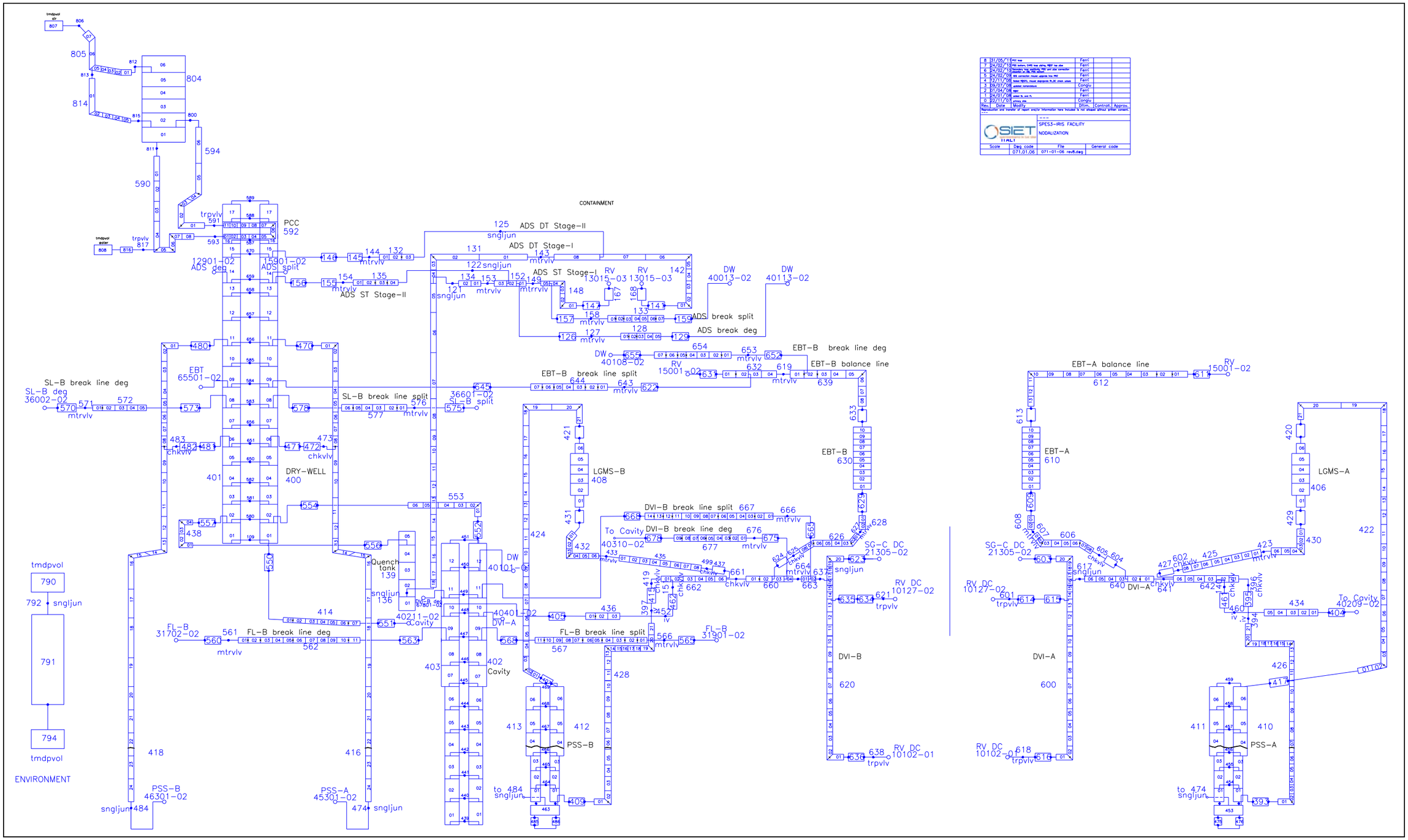

4. BDBE EBT TOP LINE DEG BREAK: SPES3-180

The EBT top line double ended guillotine break, in beyond design conditions, is foreseen in the test matrix for SPES3 experimental program [1]. It is a 4-inch equivalent break with all EHRS unavailable and PCC as the only device to remove decay power and maintain the plant in safe conditions.

SPES3-180 case is based on SPES3-176 nodalization, with 13 tubes SGs and 20 tubes PCC heat exchanger. Due to the EHRS total failure, the PCC is triggered on a signal combination of high containment pressure (0.9 MPa) AND 1800 s delay on LM-signal. The ADS Stage-II intervenes together with the Stage-I at LM-signal [20]. PCC maintains the containment pressure between 0.8 and 0.9 MPa.

SPES3-180 starts from steady conditions at 65% power, in order to investigate the actual SPES3 test conditions.

The RELAP5 nodalization used for SPES3-180 case is shown in Fig.3. 4, Fig.3. 5, Fig.3. 6.

The only changes in the model, with respect to SPES3-176 case, concern the break valves: the DVI-B line valve configuration is set to let the pipe intact while the EBT-B top line valves are set to simulate the DEG break. The RC to DVI line orifice is set to 7 mm diameter for the mtrvlv 452 to correct a mistake in SPES3-176 (where it didn't affect the results).

The following paragraphs describe the BDBE EBT top line DEG break transient results.

4.1 SPES3-180

Steady conditions at 65% power, starting point for the transient, are summarized in Tab.4. 1.

The list of the main events occurring during the transient, with timing and quantities, is reported in Tab.4. 2.

4.1.1 Transient phases and description

The first 10 s of SPES3 data (-10 s to 0 s) are steady state conditions.

All times of the events are given with respect to the break time assumed as time 0 s.

The main phases of the transient are shortly summarized here, while a more detailed description is provided in the followings.

- The break opening causes the RPV blowdown and depressurization, containment pressurization and steam dumping into PSS with air build-up at PSS top;
- the S-signal triggers the reactor scram and secondary loop isolation. EHRS-A and B actuation fails;
- the low PRZ water level signal triggers the pump coast-down and natural circulation in the core is guaranteed until the RPV water level is above the check valves connecting riser and downcomer at one third of the SG height;
- the LM-signal triggers the ADS Stage-I and ADS Stage-II for the fast RPV depressurization and triggers the EBT intervention to inject cold borated water into the primary circuit. EHRS-C actuation fails;
- the PCC water flow is actuated when the 0.9 MPa containment pressure threshold is reached and after 1800 s from the LM-signal;
- the PCC depressurizes the containment and, when the PSS pressure is sufficiently high to win the gravity head of PSS vent pipes, cold water flows from PSS to DW increasing the containment depressurization and flooding the RC;

- the low differential pressure signal between RPV and DW triggers the LGMS injection into the DVI line and opens the valves connecting RC and DVI line to increase water back-flow from containment to primary system;
- the PCC maintains the DW pressure between specified set points;
- in the long term, the PCC maintains the system pressure between specified set points by condensing steam exiting the RPV with water back-flow from RC to RPV.

Break

The break line mass flow, RPV side (SPLIT) and containment side (DEG), is shown in Fig.4.1, Fig.4.2, Fig.4.3. The peak of 4.74 kg/s is observed at 2 s, RPV side. At 75 s the loss of mass from the break decreases due to the ADS intervention that, depressurizing the RPV, causes water flashing and reduces the liquid fraction at the break. The liquid fraction in the break lines is shown in Fig.4.4.

Mass flow, containment side, is negligible soon after the break until 660 s, when a little reverse flow occurs from the DW towards the EBT-B that starts to empty.

Mass flow oscillations, observed through the SPLIT line in the long term, are related to the PCC operation.

Blowdown, RPV depressurization, containment pressurization

The blowdown phase depressurises the RPV with mass and energy transfer to the containment.

The PRZ pressures is shown in Fig.4.5, Fig.4.6.

While the PRZ depressurises, the containment pressure increases as shown in Fig.4.7, Fig.4.8, Fig.4.9. The ADS Stage-I and Stage-II intervention, at the LM-signal, causes the RPV depressurization increase at 69 s and the contemporary DW pressure increase up to reach the peak of 1.62 MPa at 1880 s.

The PCC intervention at 1867.92 s dumps the DW pressure and, removing energy from the containment, brings the pressure to oscillate between set the points of 0.8 and 0.9 MPa, Fig.4.7, Fig.4.8.

At 1980 s, the water injection from PSS to DW contributes to the system depressurization for steam condensation.

Steam dumping into PSS

Containment space (DW and RC) pressurization causes the transfer of steam-gas mixture from DW to PSS through the PSS vent lines, starting at 4 s and lasting until the PCC intervention and subsequent DW depressurization, Fig.4.10, Fig.4.11.

Within 200 s, almost all DW non-condensable gas is transferred to the PSS, Fig.4.12, Fig.4.13. Steam is dumped underwater through the PSS sparger and air pressurizes the PSS and LGMS gas space, Fig.4.14, Fig.4.15, Fig.4.16, Fig.4.17.

The PSS water temperature increases thanks to mass transfer from the DW, Fig.4.18, Fig.4.19. Both liquid and gas temperatures are reported and they are very similar. The PSS water temperature always remains below saturation.

S-Signal: Reactor scram, secondary loop isolation. EHRS-A and B actuation failure

The high containment pressure set-point (1.7e5 Pa) is reached at 6.77 s and it triggers the S-signal.

The S-signal (Safeguard) starts the reactor SCRAM and isolates the three secondary loops. EHRS-A and B actuation is assumed to fail.

Power released to fluid in the core is shown in Fig.4.20, Fig.4.21. After the reactor isolation, no power is removed through the SGs toward the EHRSs, as failed, Fig.4.22.

The MFIV and MSIV of the secondary loops are contemporarily closed in 5 s and secondary loop mass flows set to zero, Fig.4.23.

The secondary side pressures are shown in Fig.4.24, Fig.4.25. After isolation, pressure increases up to about 11.3 MPa, due to heat transfer from the primary side and tube water evaporation. Water evaporation causes tube level decrease, as shown in Fig.4.26, Fig.4.27, as power is transferred from SGs to primary side. Between 4300 s and 7000 s, little power is removed again from the SGs, as the natural circulation in the RPV starts through the RI-DC check valves, causing steam condensation in the tubes and level increase, Fig.4.22, Fig.4.26. In the long term, SG tube levels slightly decreases as power is removed from the primary side by the PCC.

Pump coastdown and primary circulation through RI-DC check valves

The PRZ level is shown in Fig.4.28. The early phase of level decrease, until the ADS Stage-I and Stage-II intervention (67.92 s), is due to the loss of mass from the break. Level increase after ADS actuation is due to water swelling and suction toward the QT (Stage-I) and the DW (Stage-II). Due to the loss of mass from the break and ADS, the pump uncovers soon, Fig.4.29.

The pump coastdown is triggered by the Low PRZ level signal delayed of 15 s (36.26 s + 15 s). Soon after the pump suction is uncovered, RPV natural circulation through the pump interrupts.

The core inlet flow is shown in Fig.4.30, Fig.4.31. Natural circulation lasts until the RI to DC check valves are covered (398 s), Fig.4.32. In the long term, when the RPV level is restored, natural circulation occurs again driven by the heat transfer to the PCC, Fig.4.33.

LM-Signal: ADS Stage-I, ADS Stage-II and EBT actuation. EHRS-C actuation failure. PCC actuation counter start.

The LM-signal (LOCA mitigation) occurs at 67.92 s, when the low PRZ pressure set-point (11.72e6 Pa) is reached, Fig.4.5.

The EHRS-C actuation on LM-signal is assumed to fail. The failure of EHRS-C starts the counter for PCC start with 1800 s delay on LM-signal. Such delay is assumed as time required to fill the containment refuelling cavity, heat sink for PCC.

The failure of all the EHRSs causes a beyond design accident and the emergency procedures foresee that the LM-signal triggers contemporarily the ADS Stage-I and ADS Stage-II. LM-signal triggers also the EBT actuation valves.

All the ADS Stage-I and Stage-II trains are actuated contemporarily and the valves are fully open in 10 s. The ADS Stage-I mass flows are shown in Fig.4.34, Fig.4.35 and the ADS Stage-II mass flow in Fig.4.37, Fig.4.38 (ADS Stage-II negative value is due to the junction direction definition in the model). The peaks of mass flow are related to the liquid fraction at the ADS nozzles, when the PRZ level increases at the ADS opening, Fig.4.36, Fig.4.39, Fig.4.28.

The LM-signal triggers the EBT valves that are fully open in 15 s. EBT injection mass flows are shown in Fig.4.40. EBT-B (broken loop) injection into the DVI line is delayed until the RPV pressure is sufficiently low, close to the containment one. The EBT masses and levels are shown in Fig.4.41 and Fig.4.42, respectively. The EBT-A is empty at 3690 s while the EBT-B is empty at 2680 s.

Soon after EBT actuation, liquid circulation from RPV toward the EBT-A (intact loop) starts at the EBT-A balance line to RPV, then, after such connection is uncovered (128 s), steam replaces water contained in the EBT-A top lines and tank, Fig.4.43, Fig.4.44. Circulation through the EBT-B (broken loop) balance line occurs just after the break, with flow toward the containment through the SPLIT line. When EBT-B starts to inject into the DVI line, steam coming from the DW replaces water in the tank, Fig.4.43, Fig.4.44.

RPV saturation

The fast RPV depressurization and loss of mass from the break, rapidly cause water flashing in the primary circuit and void begins at core outlet at 84 s, Fig.4.45, Fig.4.46. Liquid fraction between 0.7 (core bottom) and 0.4 (core top) occurs in the core, until the PCC is actuated that, depressurizing the DW, allows the water back-flow from PSS to DW and from RC to RPV through the DVI lines (2730 s). High liquid fraction is definitively restored in the RPV after 8000 s, when the PCC operation is at regime conditions.

The inlet and outlet core temperatures are shown in Fig.4.47, Fig.4.48.

Core heater rod surface temperatures are shown in Fig.4.49 and Fig.4.50 for the normal and hot rods, respectively. No temperature excursion is observed even in the periods of low liquid fraction in the core and low RPV mass inventory, Fig.4.51.

PCC actuation

The containment pressure peak of 1.63 MPa occurs at 1870 s, Fig.4.7.

Pressure is rapidly dumped thanks to the PCC intervention at 1867.91 s (i.e. 1800 s delayed on LM-signal AND DW pressure > 0.9 MPa (103.47 s)). After that, pressure is dumped and successively the primary and containment coupled pressure is maintained between 0.8 MPa and 0.9 MPa, accordingly to PCC operation logic, Fig.4.7, Fig.4.8, Fig.4.9.

The PCC tube mass flow is shown in Fig.4.52. The tubes discharge into and are fed by the PCC tank that operates as steam condenser and water supply. PCC tank level is controlled by a PI (proportional-integral) control system, 0.7 m level set-point, that injects cold water into the feed line from an auxiliary circuit, Fig.4.53. The PCC inlet and outlet temperatures are shown in Fig.4.54. Water enters slightly subcooled and exits saturated with a liquid fraction at the outlet of about 0.2, Fig.4.55, Fig.4.56. Power removed by The PCC is shown in Fig.4.57, Fig.4.58.

Low DP RPV-Containment signal, PSS water flow to DW, RC flooding; LGMS and RC to DVI valve actuation, reverse flow from containment to RPV

The “Low DP RPV-Containment” signal set point of 50 kPa is reached at 658.16 s.

Combination of LM-signal AND Low DP RV-Containment signal actuates the LGMSs and opens the valves on the lines connecting RC to DVI lines.

The LGMS isolation valves are fully open in 2 s as well as the RC to DVI line isolation valves.

LGMS injection into the DVI lines is mostly due to non-condensable gas pressurization, occurred from the DW in the blowdown phase, and to gravity. Injection starts at 1320 s, when LGMS pressure overcomes the primary system pressure. LGMS injection mass flow is shown in Fig.4.59, Fig.4.60. The reduction of the injection mass flow, around 2700 s, is due to the PSS sparger uncovering and pressure equalization with the DW. After that, injection is driven by gravity. The LGMS mass and level are reported in Fig.4.61 and Fig.4.62, respectively. LGMS injection into the RPV, through the DVI lines occurs when the DVI pressure is lower than LGMS pressure, accordingly to the PCC operation, and this explains the oscillatory trend of injection, Fig.4.60, Fig.4.58. The LGMS-B is empty at 36790 s and LGMS-A at 40240 s.

PSS water flow to DW, RC flooding, reverse flow from containment to RPV

The containment depressurization due to PCC intervention, takes the DW pressure below the PSS pressure, Fig.4.63, Fig.4.64. When the differential pressure is sufficient to win the PSS vent pipe gravity head, water is pushed upwards into the DW, until the PSSs are empty. The PSS to DW injection starts at 1980 s, Fig.4.10, Fig.4.11, with the fill-up of the PSS vent pipes, Fig.4.65, Fig.4.66. Injection lasts until the PSS sparger remains covered and PSS and DW volumes are separated from the pressure point of view. After 2740 s, the PSS and DW pressures are coupled and follow the oscillations determined by PCC, Fig.4.64. The PSS levels are shown in Fig.4.67, Fig.4.68 and the PSS masses in Fig.4.69.

Due to the PCC operation, mass is extracted and re-injected into the RPV. In the phase where the DW pressure is higher than RPV pressure, steam is pushed from DW to PSS with slow water level increase, Fig.4.67, Fig.4.68. The non-symmetric behaviour of PSS level, observed since about 51000 s, is probably a result of nodalization choices, in fact the PSS vent line-B connection to the DW are on the same slice where the break lines are connected to, more interested by steam coming from the RPV. The slow, but continuous cyclic mass transfer from DW to PSS, slowly stores water in the tanks, making it no more available to be injected into the RPV. It may be a critical point if the amount of water above the core is little.

The RC level, initially increased for the break and ADS Stage-I and Stage-II mass flow collection, rapidly increases in correspondence of the PSS to DW injection up to the complete fill-up at 2690 s (11 m level from bottom), Fig.4.70, Fig.4.71.

At 2470 s, the RC level reaches the DVI line elevation and water back-flow from RC to RPV occurs through the RC to DVI line valves opened at 658.16 s. Injection is allowed when the RPV pressure is lower than the containment one, Fig.4.72, Fig.4.73.

After the RC is full of water, the DW level and mass increase with steps corresponding to the PCC operation, Fig.4.74, Fig.4.75. Between 50000 s and 63000 s, an apparent level decrease occurs in the DW, not corresponding to a mass decrease. The phenomenon occurs in correspondence of the start-up of natural circulation between DW and RC, through the two connecting pipes (liquid and gas, pipes Fig.3. 6) and it is probably due to the vertical-slice nodalization of the DW, Fig.4.76.

The QT, initially empty, is partially filled-up by the ADS Stage-I discharge, Fig.4.77, Fig.4.34. Around 39000 s, water transfer occurs from DW to QT, increasing the QT level and mass, filling the tank since about 75000s, Fig.4.77, Fig.4.78.

Long term conditions

In the long term of the transient, system pressure is maintained between 0.8 and 0.9 MPa by the PCC.

Core power, average value between 100000 and 150000 s, is 46.76 kW.

PCC removed power, average value between 100000 and 150000 s, is 67.92 kW, greater than the core power, and this contributes to slowly cool-down the system.

4.1.2 Case conclusions

The detailed analysis of the BDBE 4-inch equivalent EBT top line DEG break transient, on the SPES3 facility, allowed to understand and investigate the phenomena related to the plant behavior in case of total EHRS failure.

It showed that the accident management procedures, optimized for the BDBE DVI line DEG break [20], in particular the ADS-Stage-II intervention at LM-signal and the PCC actuation with 1800 s delay on LM-signal, allow the system to cope with this kind of transient.

After the blowdown phase and the loss of mass from the ADS, the RPV mass water inventory is restored by the safety system injection and the heater rod clad temperature are kept at low values.

The ADS Stage-I and Stage-II intervention at LM-signal causes a peak of pressure (1.63 MPa) in the containment higher than the design pressure of SPES3 containment tanks (1.5 MPa). Special test procedures will be needed to perform this test on SPES3 facility.

Tab.4. 1 – SPES3-180 steady state conditions

SPES3-169[1]	Primary/Core	SG-A	SG-B	SG-C	EBTA/B	QT	DW	PSSA/B	RC	LGMSA/B	RWSTAB	RWSTC
Pressure (MPa)	15.51 (PRZ) 0.041 (pump head)	6.01 (out)	6.01 (out)	6.03 (out)	Primary	Cont.	0.1013	Cont.	Cont.	Cont.	0.1013	0.1013
Tin (°C)	290.6	223.8	223.8	223.8	48.9	48.9	48.9	48.9	48.9	48.9	20	20
Tout (°C)	328.5	324.8	324.4	324.3								
DT (°C)	37.9	101.0	100.6	100.5								
Superheating (°C)		49.1 (Tsat 275.7)	48.7 (Tsat 275.7)	48.4 (Tsat 275.3)								
Mass flow (kg/s)	29.566 (1.342 in by-pass)	0.8125	0.8125	1.619								
Power (MW)	6.5	1.625	1.624	3.246								
Level (m) -collapsed-	2.145 (PRZ)	1.466	1.625	1.640	3.14 full	empty	empty	3.77	empty	2.454	6.961	6.954
Mass (kg)	3322 (RV)				127			1480		985	11869	11876

[1] SPES3-180, SPES3-179, SPES3-177, SPES3-181, SPES3-178 cases are restart of SPES3-169 steady state [20].

Tab.4. 2 – SPES3-180 list of the main events

	BDBE EBT-B top line DEG break (4-inch equivalent)	**SPES3-180**		
N.	**Phases and events**	**Time (s)**	**Quantity**	**Notes**
Break				
1	Break initiation	0		break valves stroke 2 s
2	Break flow peak (Containment side)	2	1.74 kg/s	Break flow = 0 kg/s at 3 s
3	Break flow peak (RPV side)	2	4.74 kg/s	
Blowdown, RPV depressurization, containment pressurization, steam dumping into PSS				
4	Steam-air mixture begins to flow from DW to PSS	4		
S-Signal: Reactor scram, secondary loop isolation. EHRS-A and B actuation failure				
5	**High Containment pressure signal**	6.77	1.7e5 Pa	**S-signal. Set-point for safety analyses**
6	SCRAM begins	6.77		
7	MFIV-A,B,C closure start	6.77		MFIV-A,B,C stroke 5 s
8	MSIV-A-B-C closure start	6.77		MSIV-A,B,C stroke 5 s.
9	EHRS-A and B actuation failure (EHRS 1 and 3 in IRIS)	6.77		EHRS-A,B IV stroke 2 s.
10	**High SG pressure signal**	24.41	9e6 Pa	
11	SG-A high pressure reached	24.41		
12	SG-B high pressure reached	26.50		
13	SG-C high pressure reached	25.91		
Pump coastdown and primary circulation through RI-DC check valves				
14	**Low PRZ water level signal**	36.26	1.189 m	
15	RCP coastdown starts	51.26		Low PRZ level signal + 15 s delay
16	Secondary loop pressure peak	60 60 74	11.0 MPa 11.2 MPa 11.3 MPa	SG-A SG-B SG-C
LM-Signal: ADS Stage-I and EBT actuation, EHRS-C actuation failure. PCC actuation counter start. RPV saturation				
17	**Low PRZ pressure signal**	67.92	11.72e6 Pa	**LM-Signal** (High P cont + Low P PRZ)
18	EHRS-C actuation failure (EHRS 2 and 4 in IRIS)	67.92		
19	ADS Stage-I opening start (3 trains)	67.92		ADS valve stroke 10 s
20	ADS Stage-II start opening	67.92		ADS Stage-II valve stroke 10 s.
21	EBT-A and B valve opening start	67.92		EBT valve stroke 15 s
22	Natural circulation interrupted at SGs top	72		Pump inlet uncovered (voidf 176-01 ~0)
23	Natural circulation begins through shroud valves	85		
24	Core in saturation conditions	79		
25	Flashing begins at core outlet	84		voidf 110 (core) < 1
26	ADS Stage-I first peak flow (3 trains)	95	3.77 kg/s	ST 1.250 kg/s; DT 2.520 kg/s. Due to liquid fraction
27	ADS Stage-II first peak flow (3 trains)	93	13.43 kg/s	ST 4.55 kg/s; DT 8.88 kg/s. Due to liquid fraction
28	ADS Stage-I second peak flow (3 trains)	180	1.474 kg/s	ST 0.394 kg/s; DT 1.080 kg/s. Due to liquid fraction.
29	ADS Stage-II second peak flow (3 trains)	179 DT 203 ST	5.16 kg/s	ST 1.28 kg/s; DT 3.88 kg/s. Due to liquid fraction.
30	**High containment pressure set-point for PCC**	103.47	0.9 MPa	
31	EBT-RV connections uncovered	128		
32	**Low DP RV-Containment**	658.16	50e3 Pa	
33	LGMSA/B valve opening start	658.16		LM + low DP RV-cont. LGMS valve stroke 2 s.
34	RC to DVI line valve opening	658.16		RC to DVI valve stroke 2 s.
35	LGMS-A/B starts to inject into RC through DVI broken loop	1320		
36	PCC actuation	1867.92		LM-signal + 1800 s + P cont > 0.9 MPa
Low DP RPV-Containment signal, PSS water flow to DW, RC flooding, LGMS and RC to DVI valve actuation; reverse flow from containment to RPV				
37	Containment pressure peak	1870	1.63 MPa	P > P design (1.5 MPa)
38	Containment and RV pressure equalization	1870		
39	DW pressure lower than PSS pressure	1890		
40	Water starts to flow from PSS to DW	1980		
41	RC level at DVI elevation	2470		
42	EBT-A empty (intact loop)	2680		
43	RC full of water	2690		
44	Water starts to flow from RC to DVI-A	2730		
45	EBT-B empty (broken loop)	3690		
46	LGMS-B empty (broken loop)	36790		
47	QT fill-up starts from DW connection	39240		
48	LGMS-A empty (intact loop)	40240		
Long Term conditions				
49	Containment and RPV pressure	100000 s to 150000 s	0.8–0.9 MPa	Controlled by PCC
50	Core power		46.76 kW	Average between 100000 s and 150000 s
51	PCC removed power		67.92 kW	Average between 100000 s and 150000 s

Fig.4.1 – SPES3-180 EBT top line break flow (window)

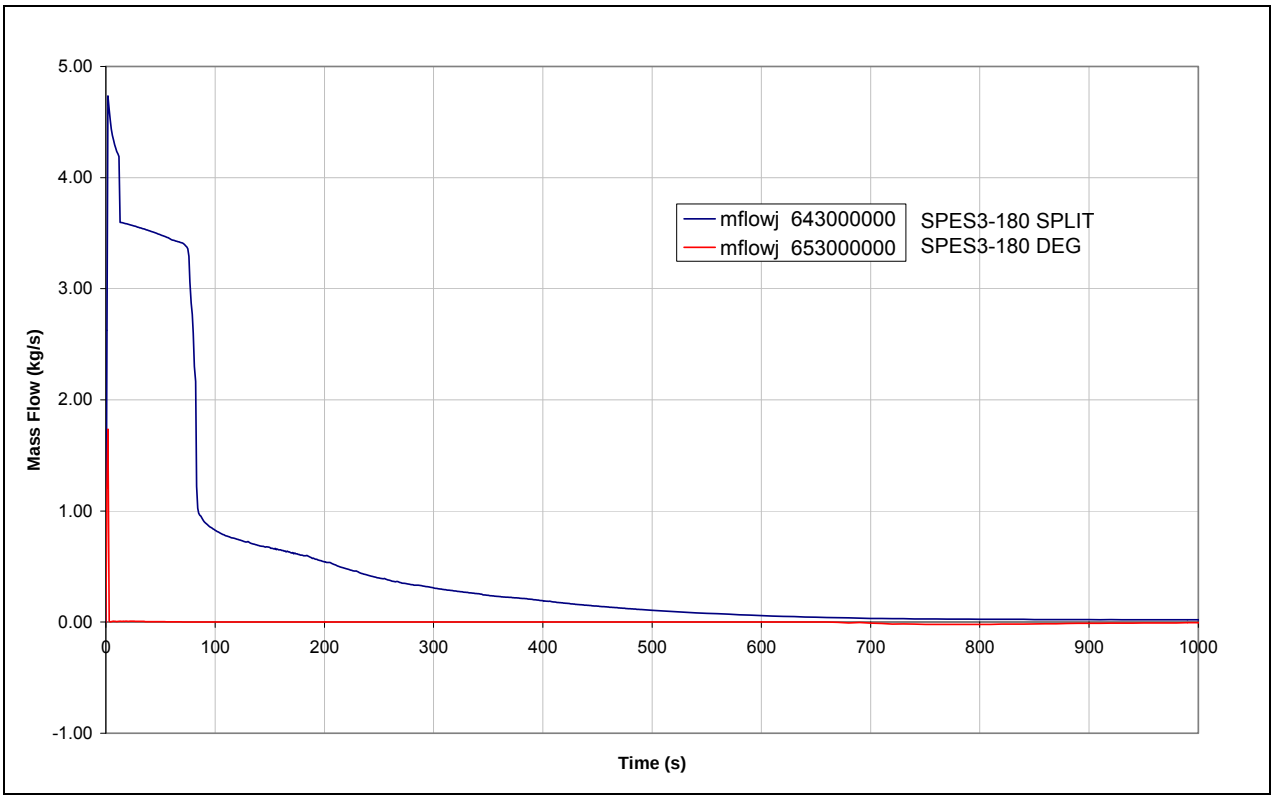

Fig.4.2 – SPES3-180 EBT top line break flow (window)

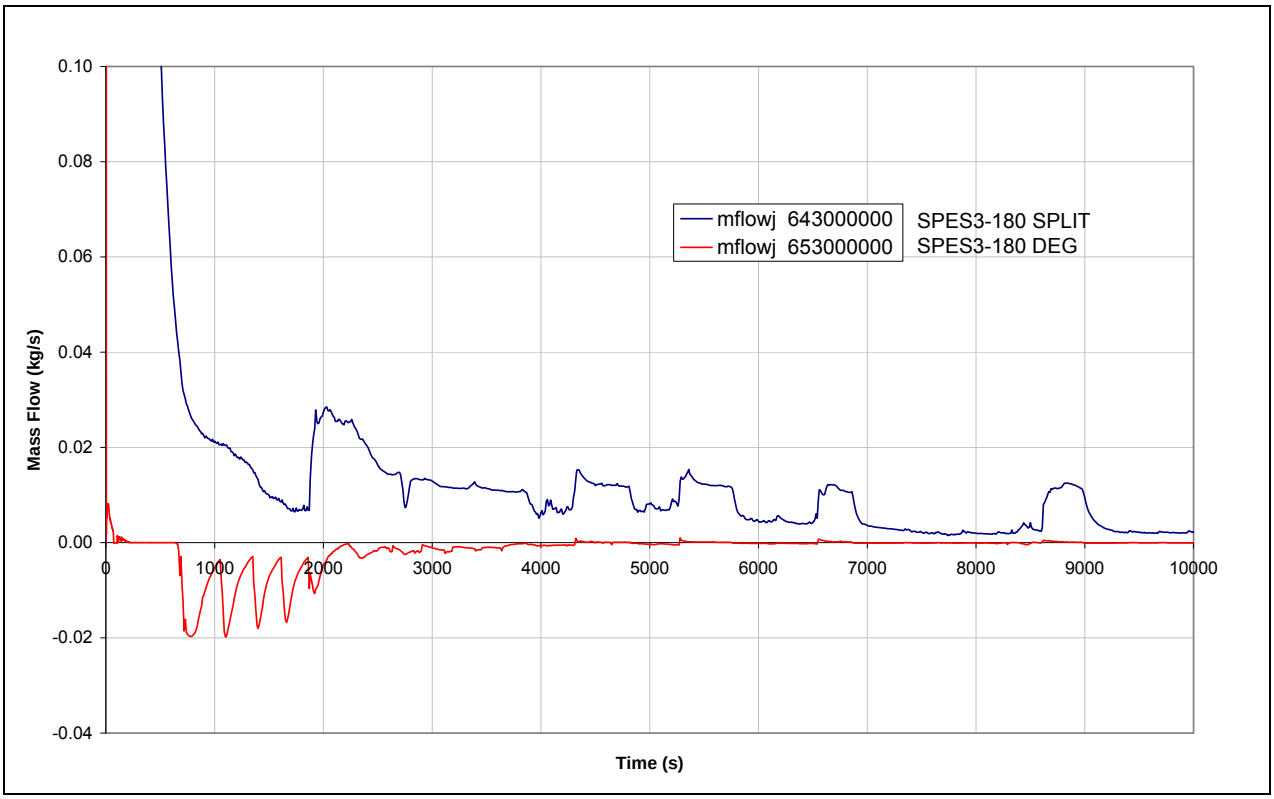

Fig.4.3 – SPES3-180 EBT top line break flow (window)

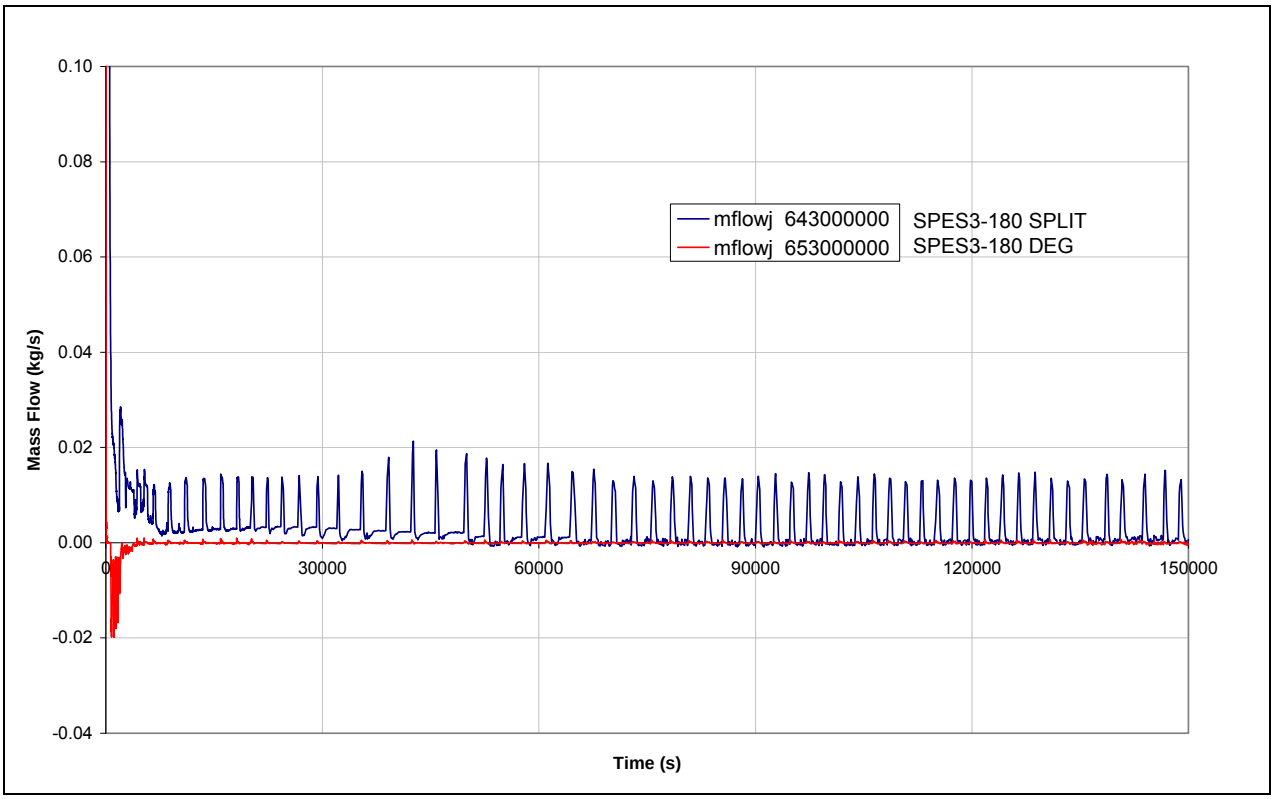

Fig.4.4 – SPES3-180 EBT break line liquid fraction (window)

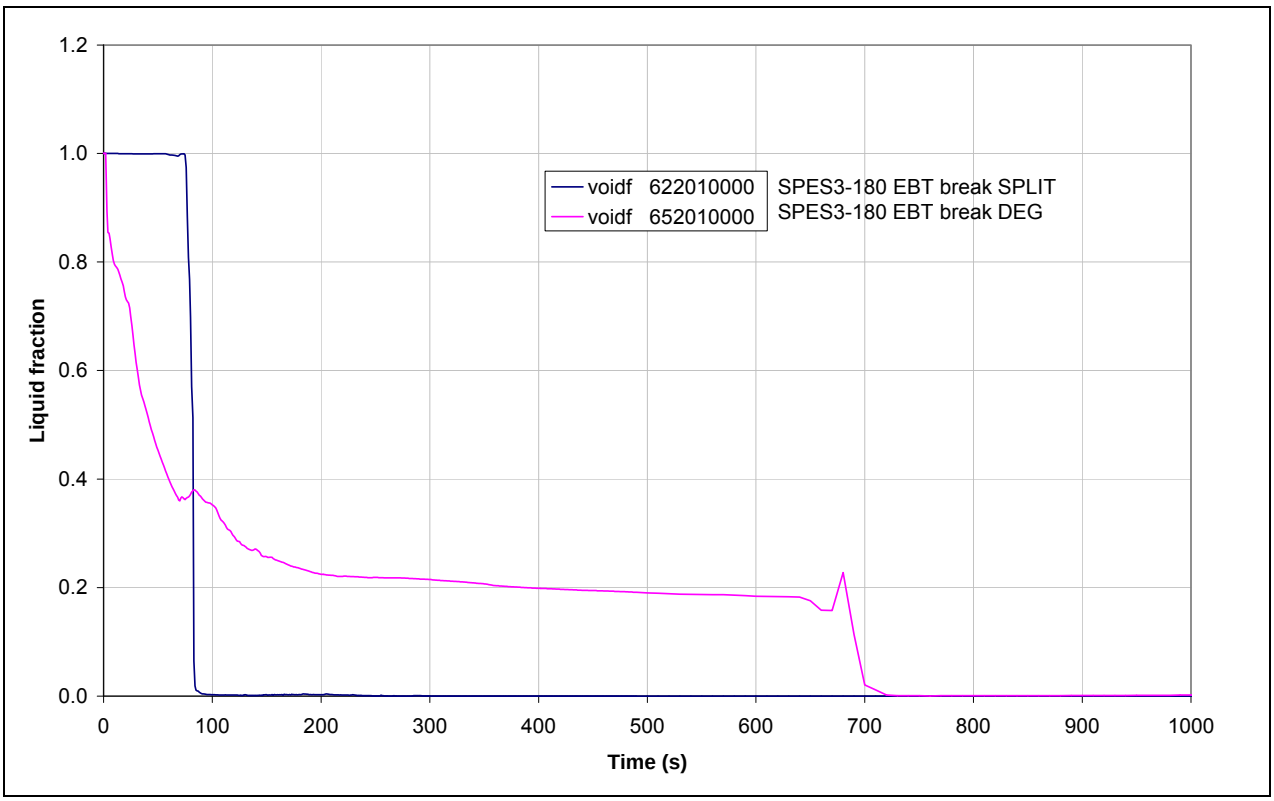

Fig.4.5 – SPES3-180 PRZ pressure (window)

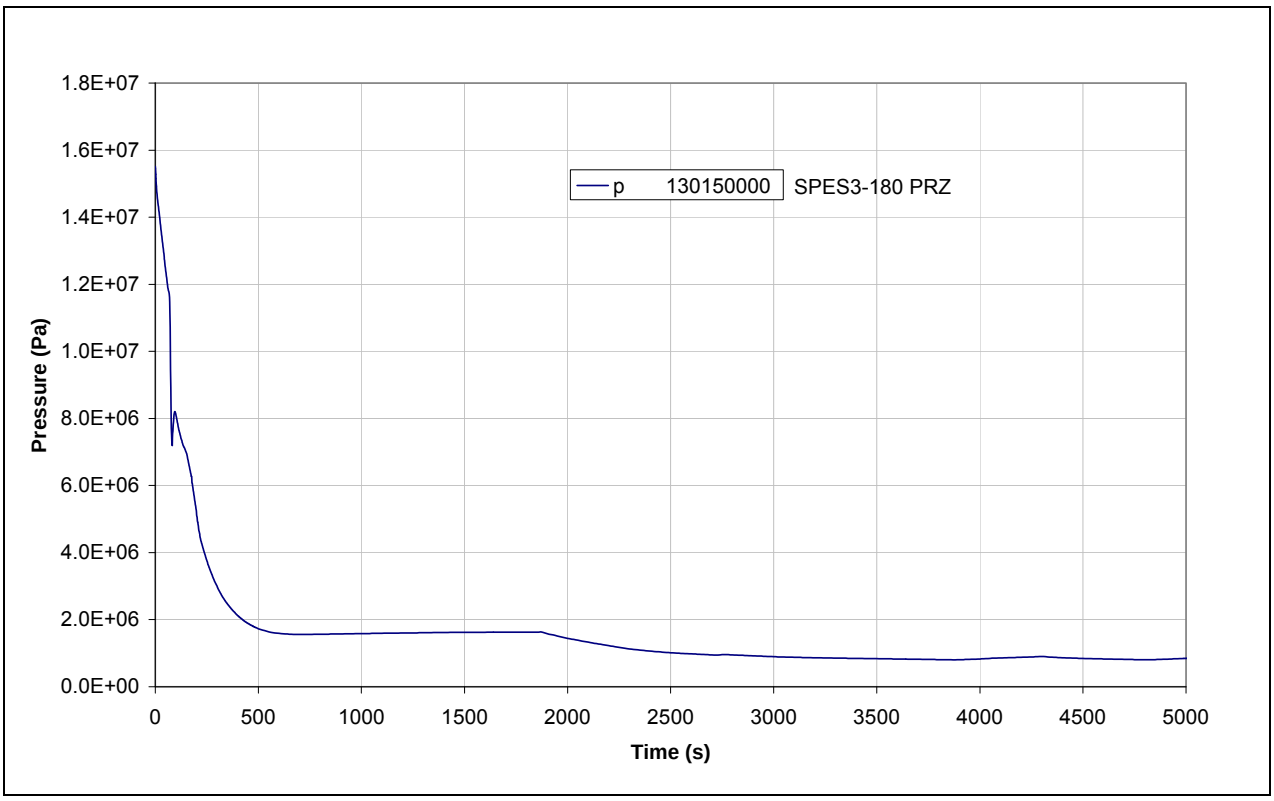

Fig.4.6 – SPES3-180 PRZ pressure

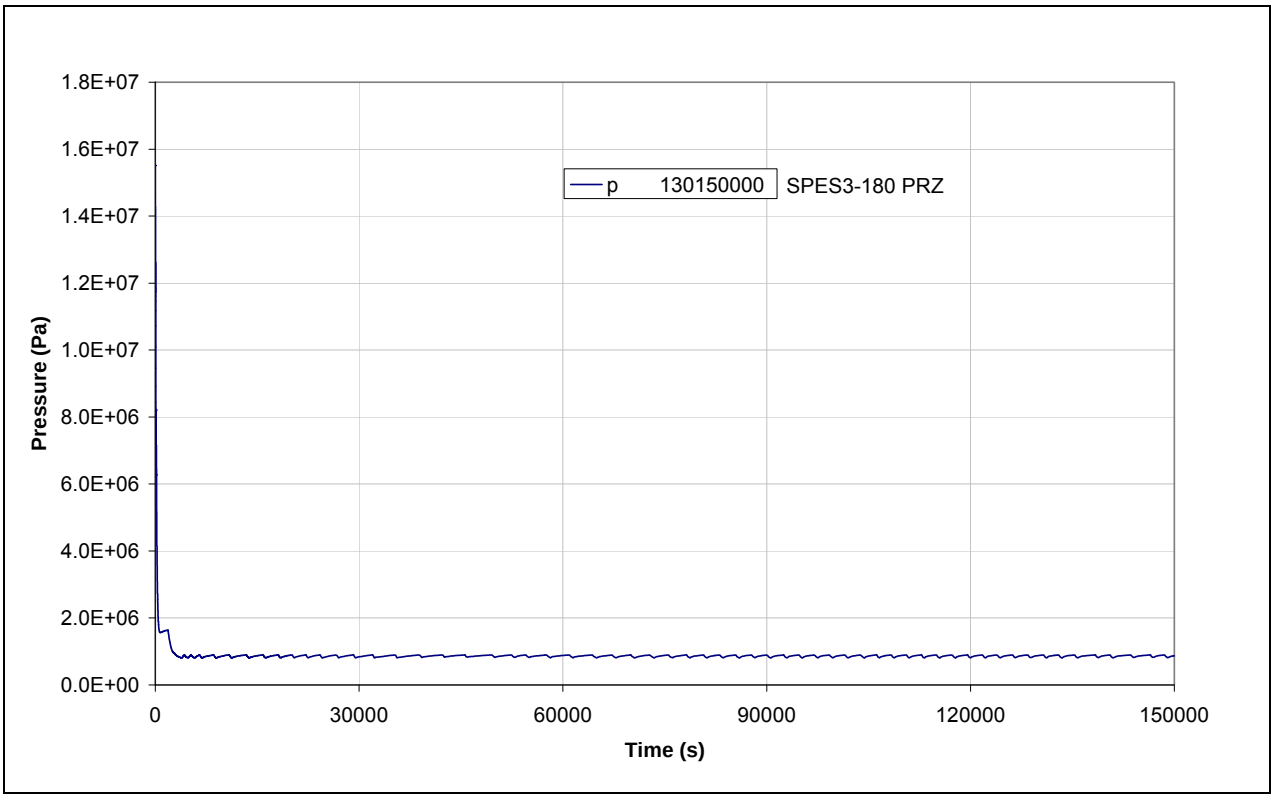

Fig.4.7 – SPES3-180 DW pressure (window)

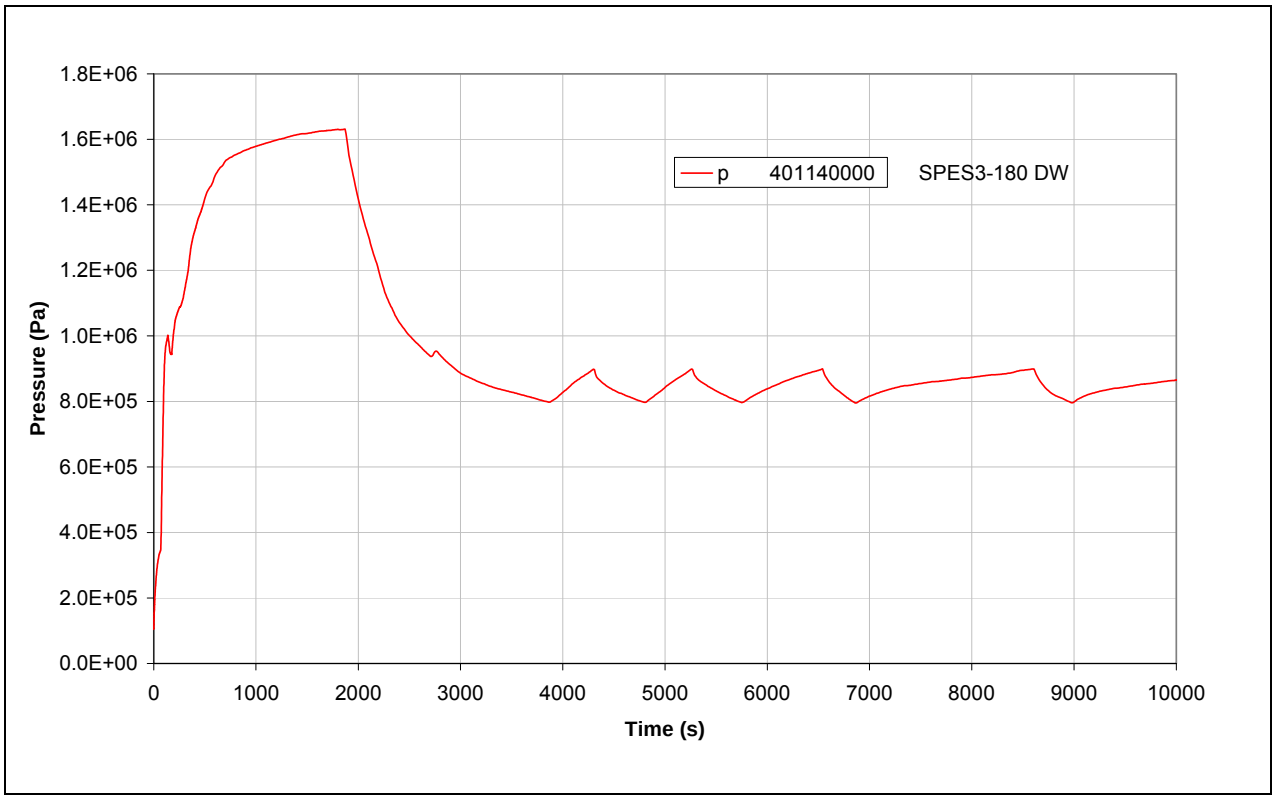

Fig.4.8 – SPES3-180 DW pressure

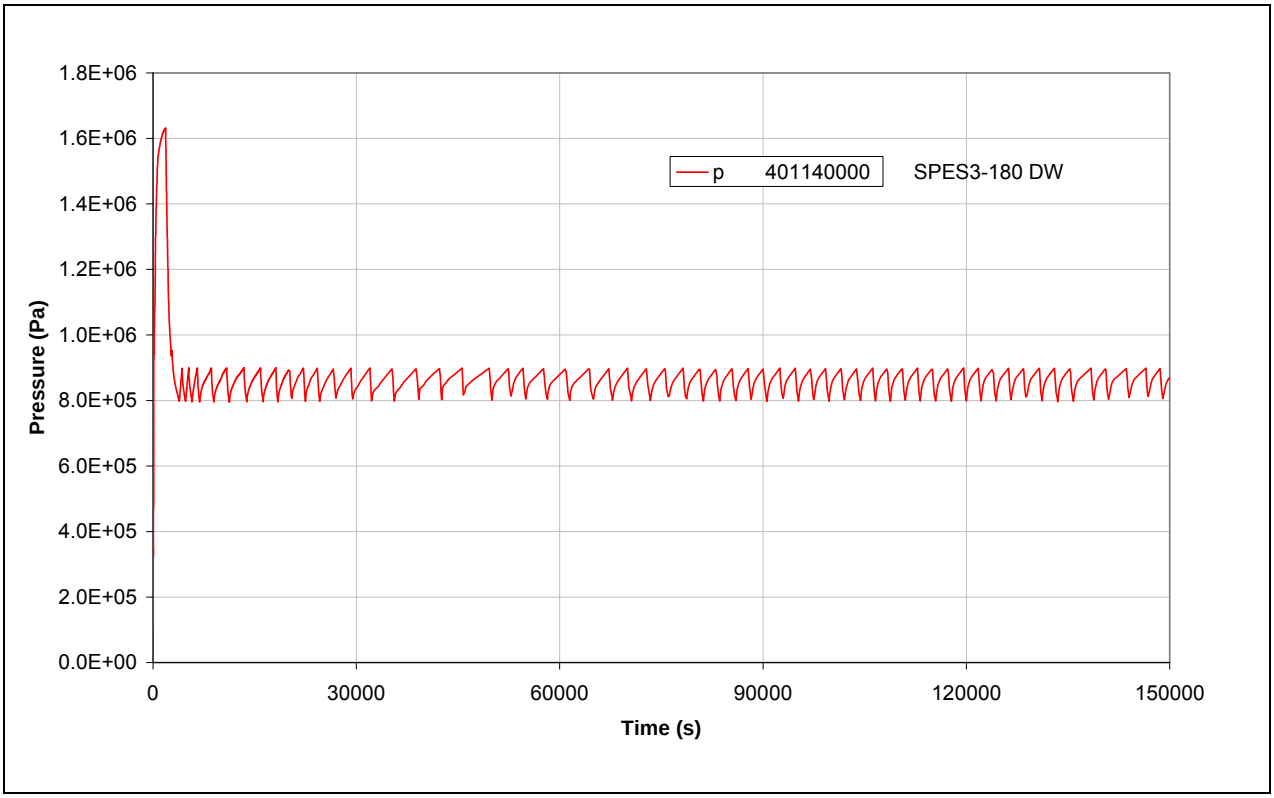

Fig.4.9 – SPES3-180 PRZ and DW pressures (window)

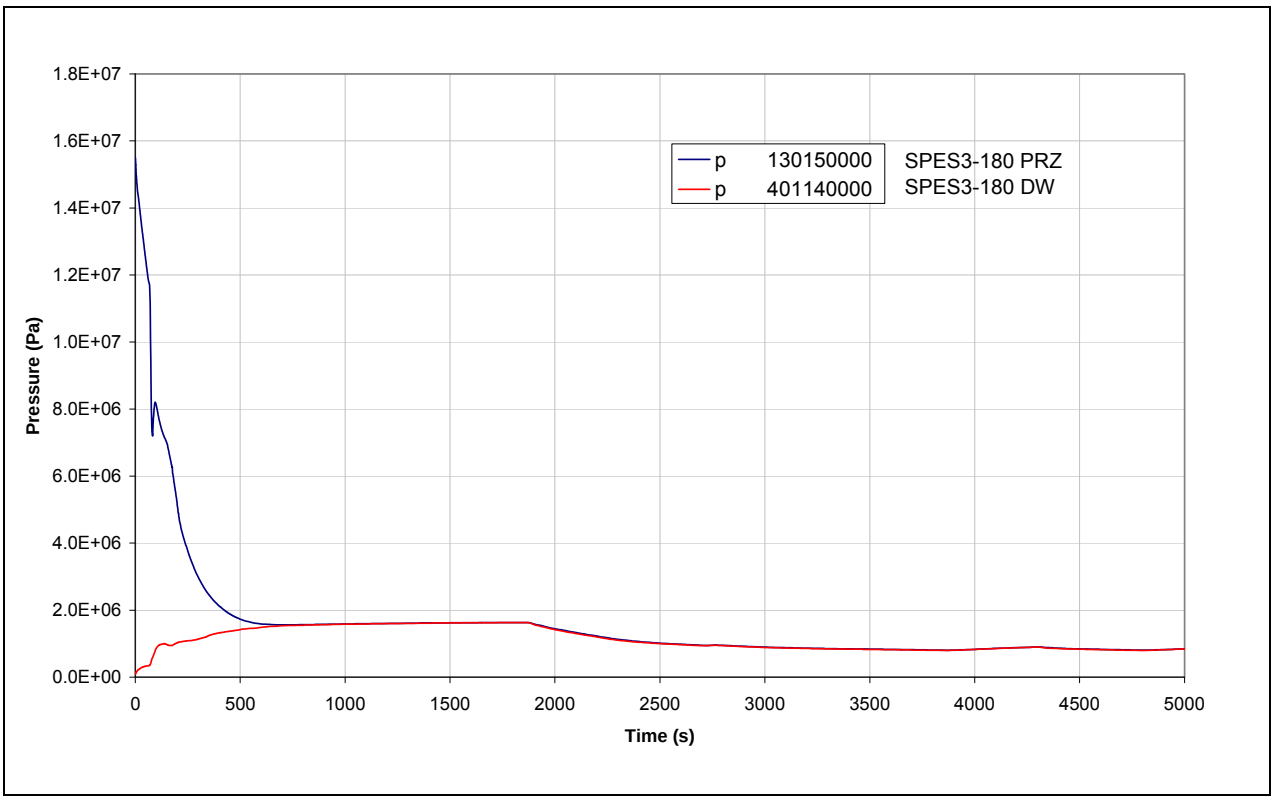

Fig.4.10 – SPES3-180 PSS to DW flow (window)

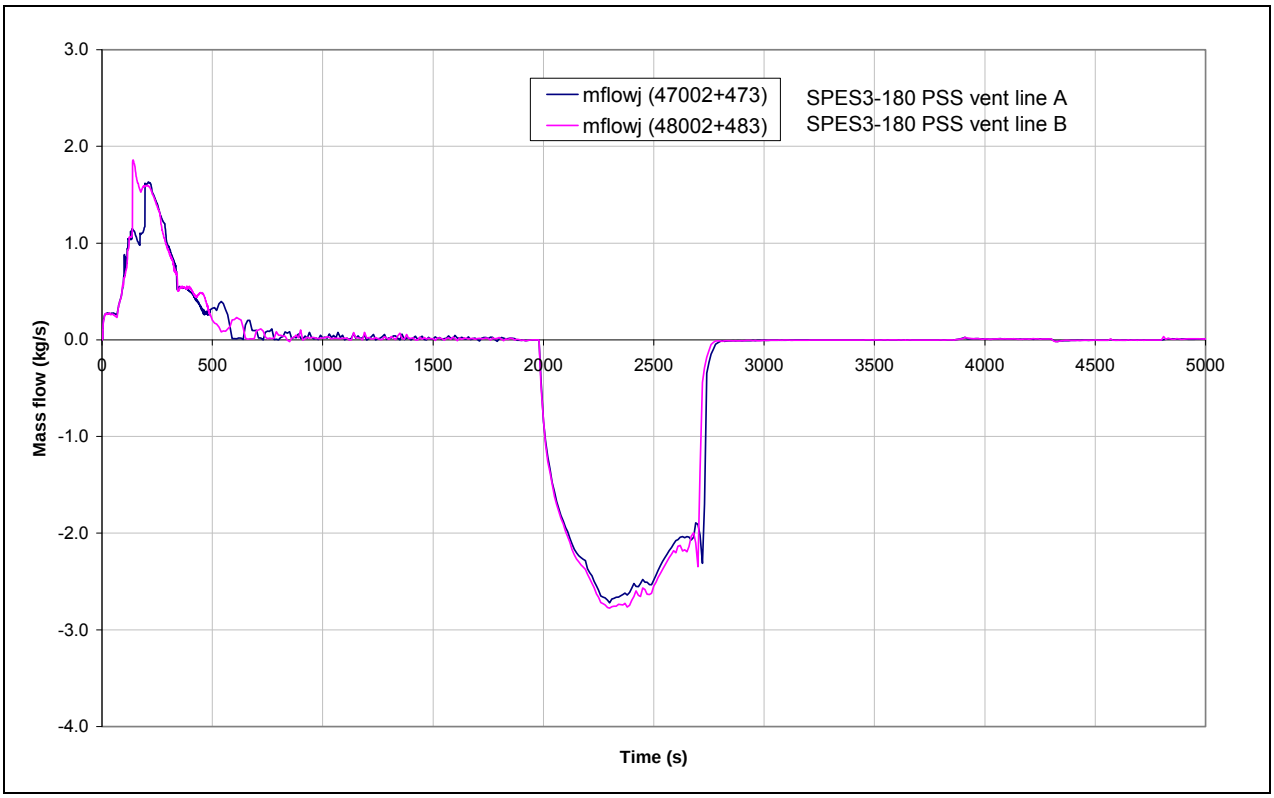

Fig.4.11 – SPES3-180 PSS to DW flow

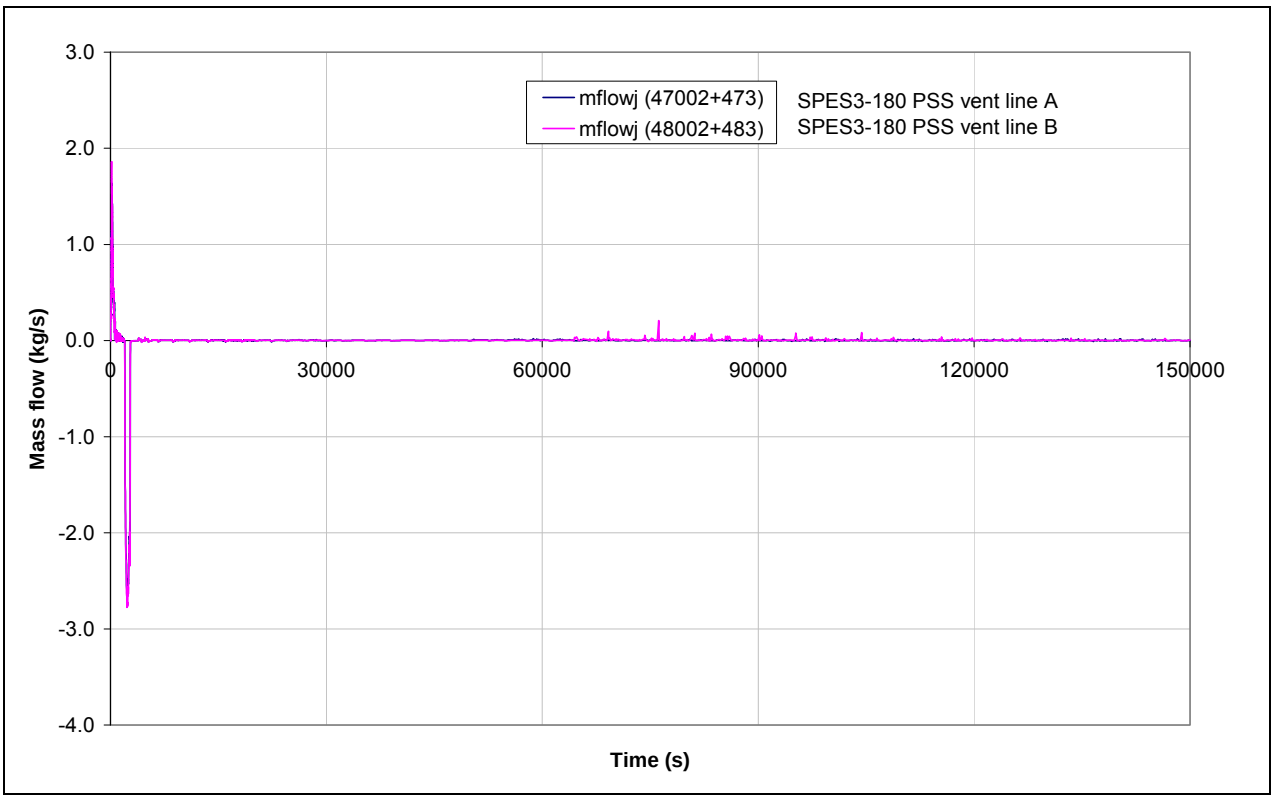

Fig.4.12 – SPES3-180 DW non-condensable gas quality (window)

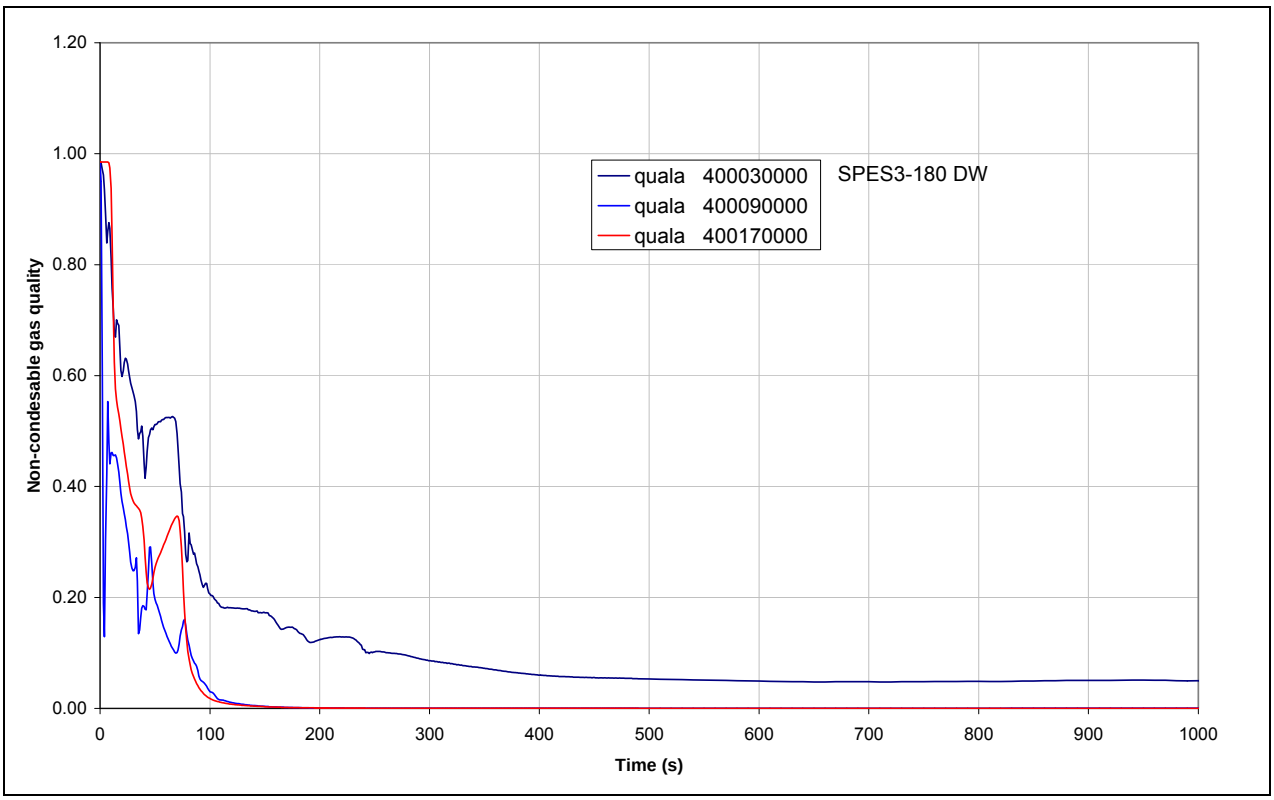

Fig.4.13 – SPES3-180 DW non-condensable gas quality

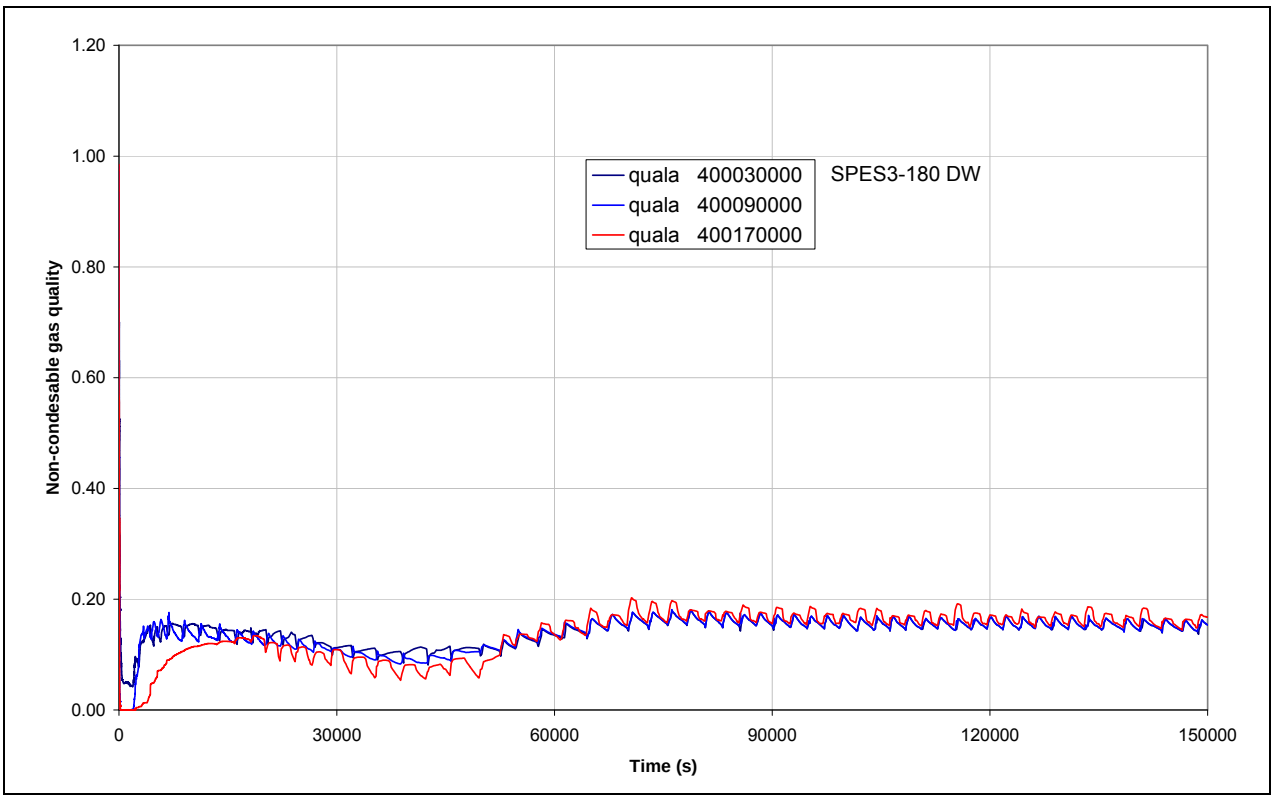

Fig.4.14 – SPES3-180 PSS pressure (window)

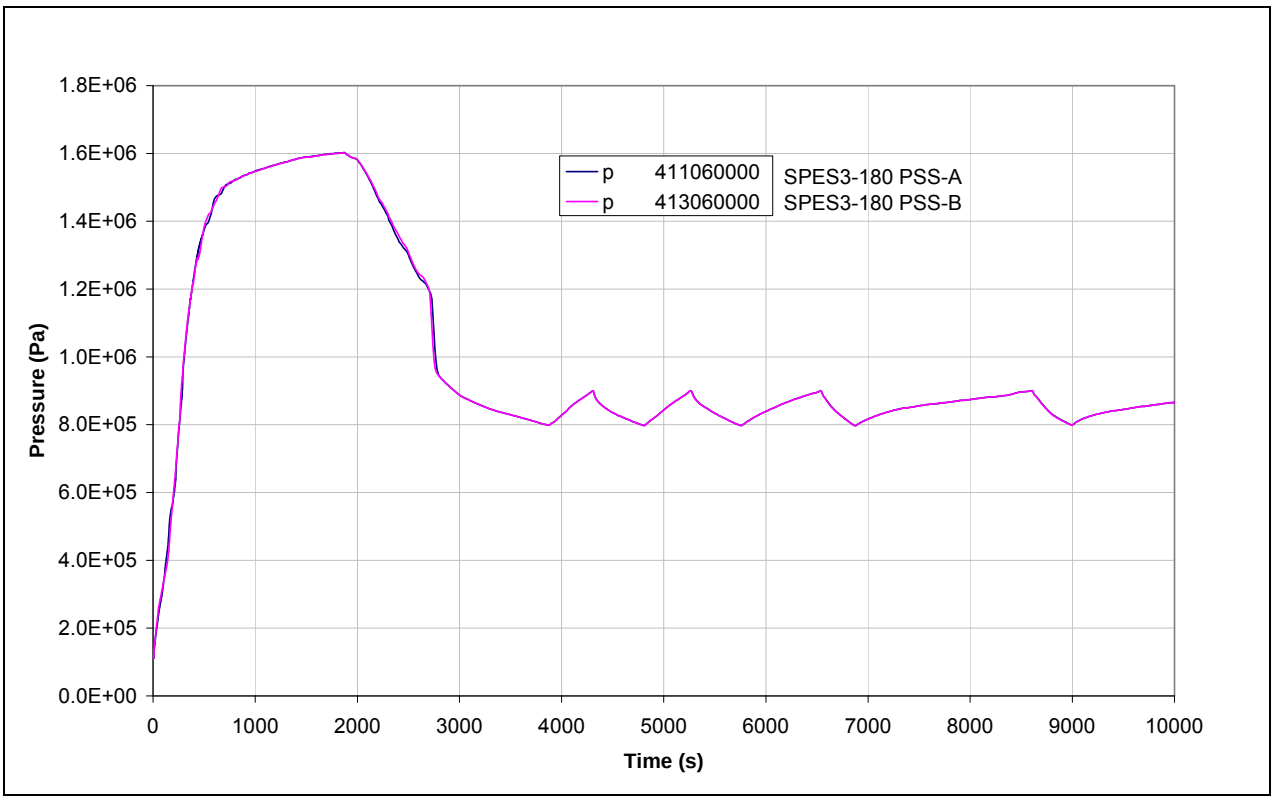

Fig.4.15 – SPES3-180 PSS pressure

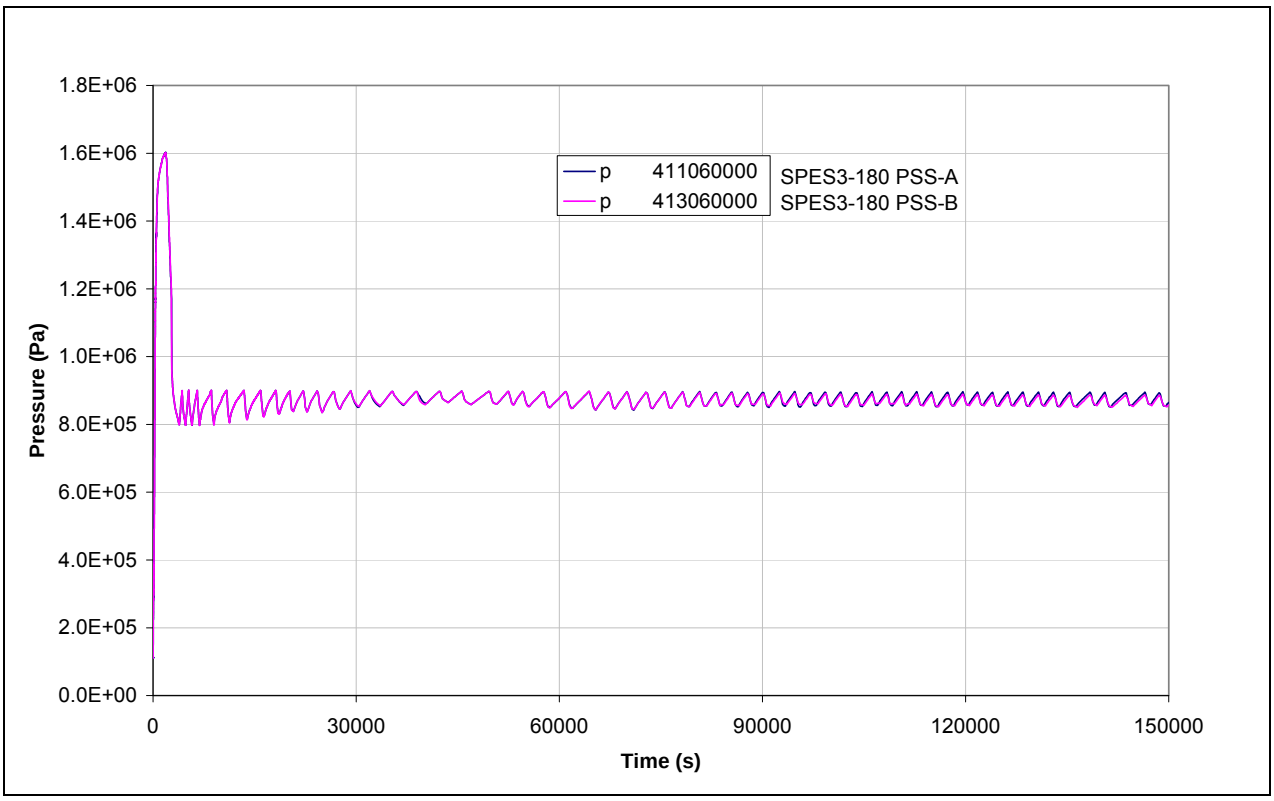

Fig.4.16 – SPES3-180 LGMS pressure (window)

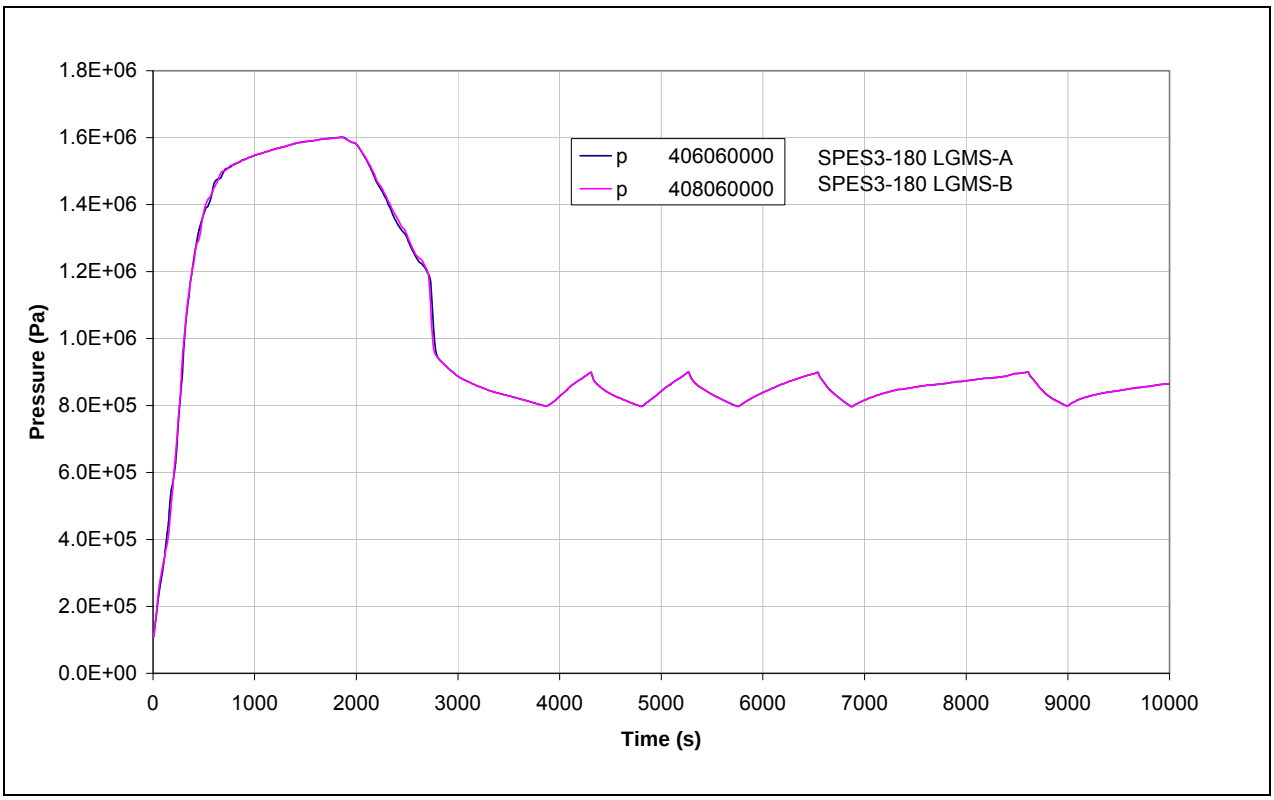

Fig.4.17 – SPES3-180 LGMS pressure

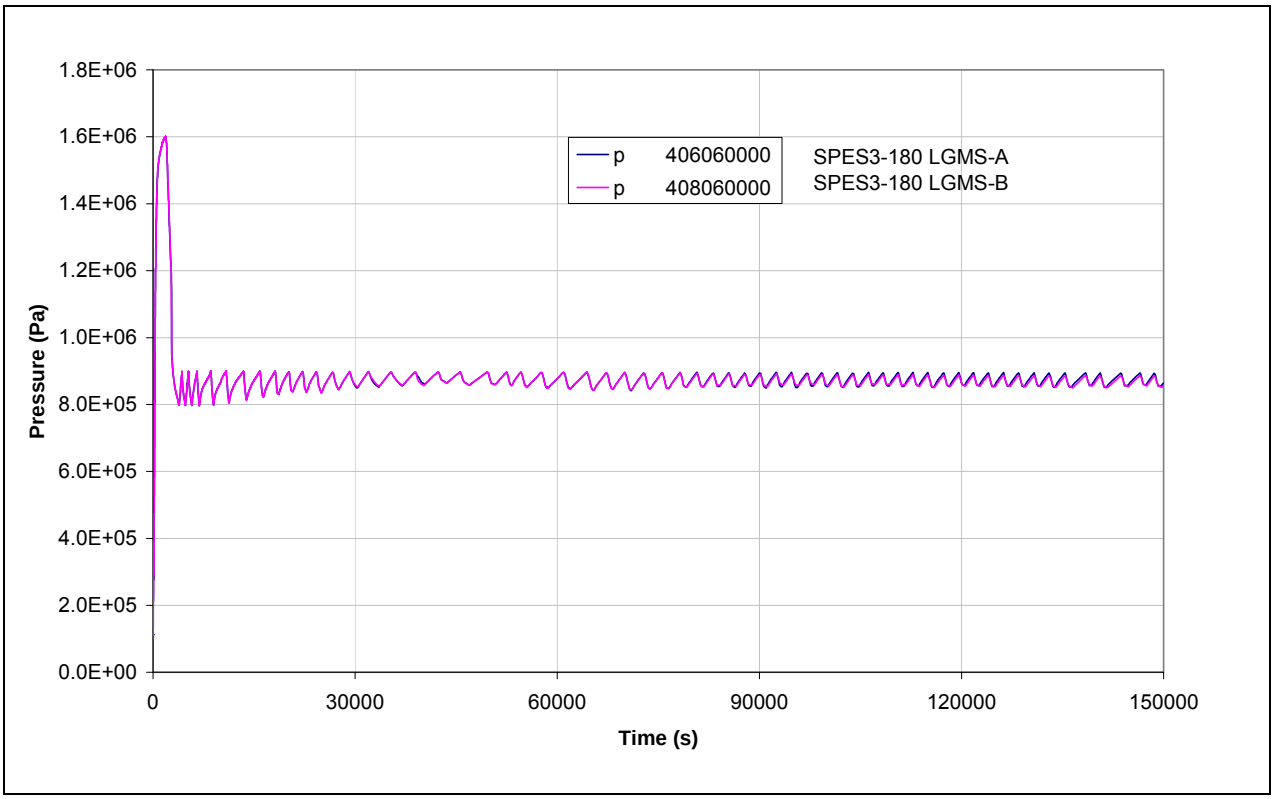

Fig.4.18 – SPES3-180 PSS temperature (window)

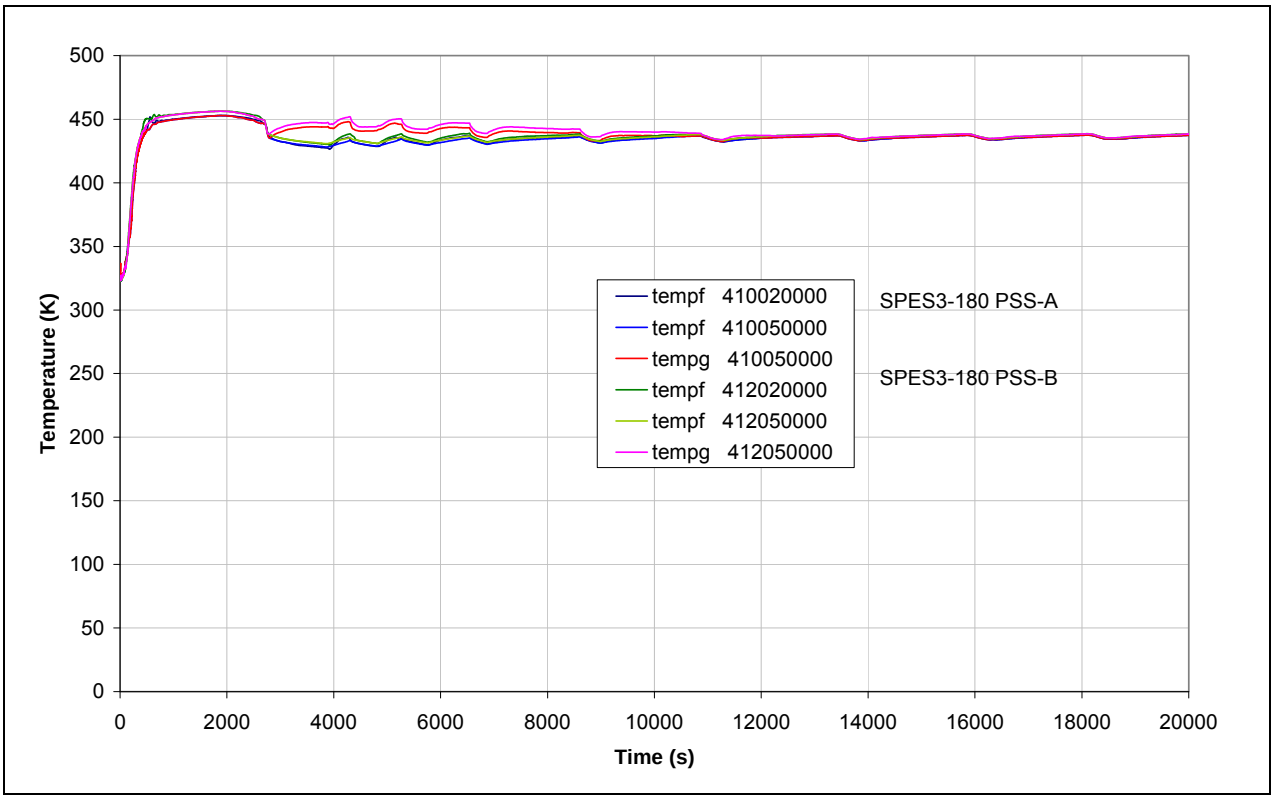

Fig.4.19 – SPES3-180 PSS temperature

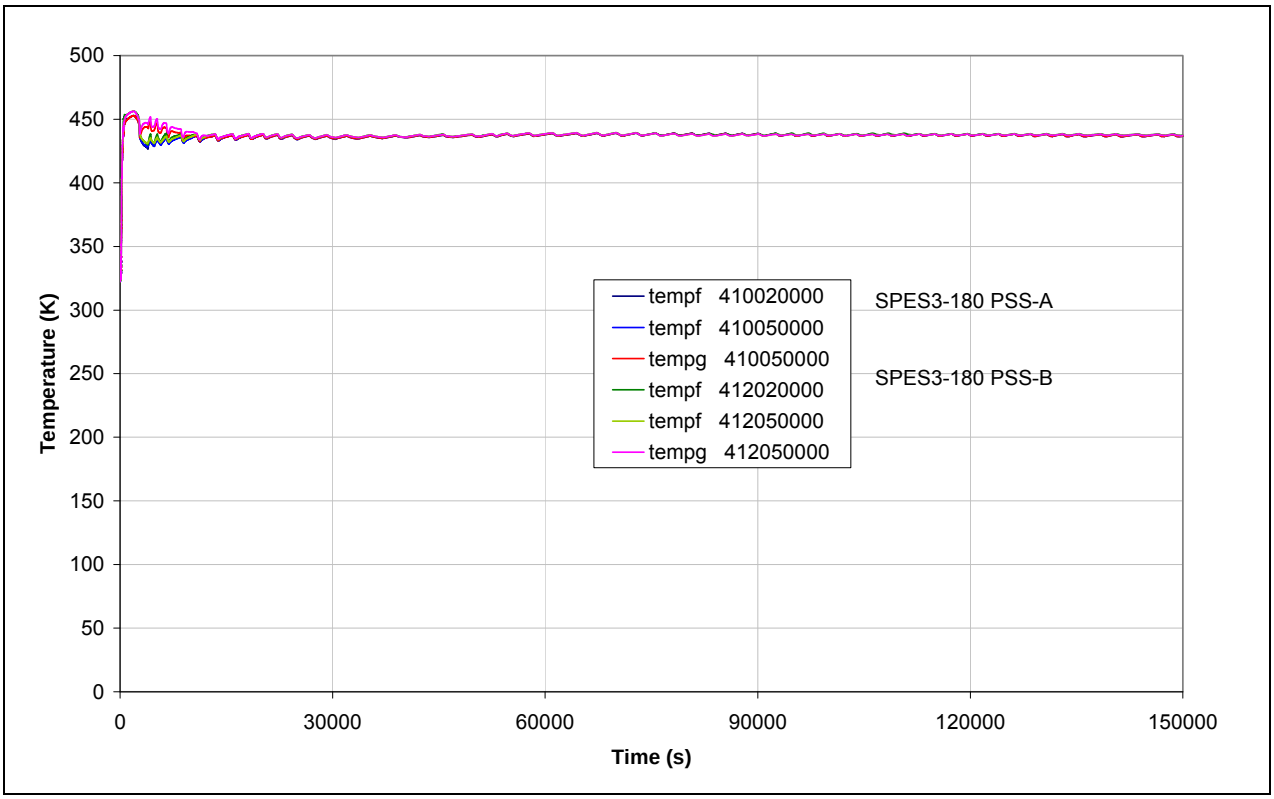

Fig.4.20 – SPES3-180 core power (window)

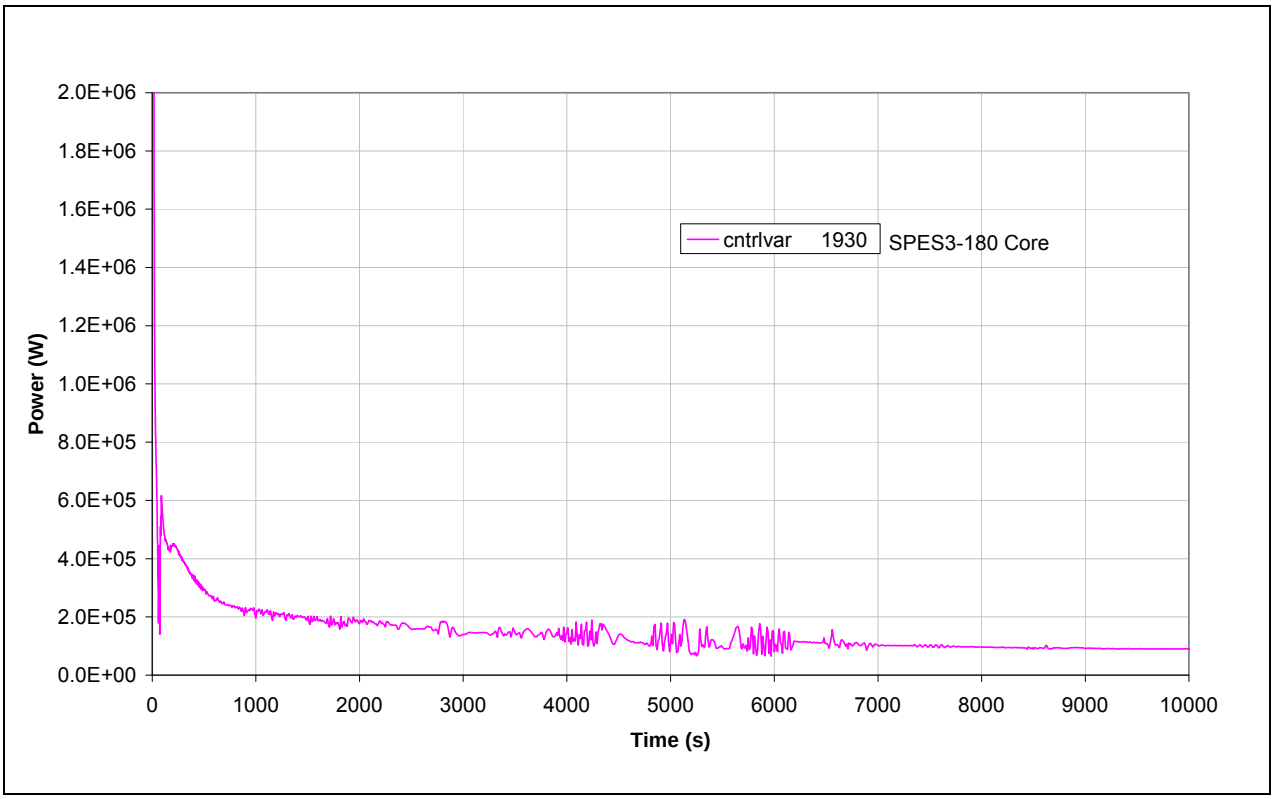

Fig.4.21 – SPES3-180 core power

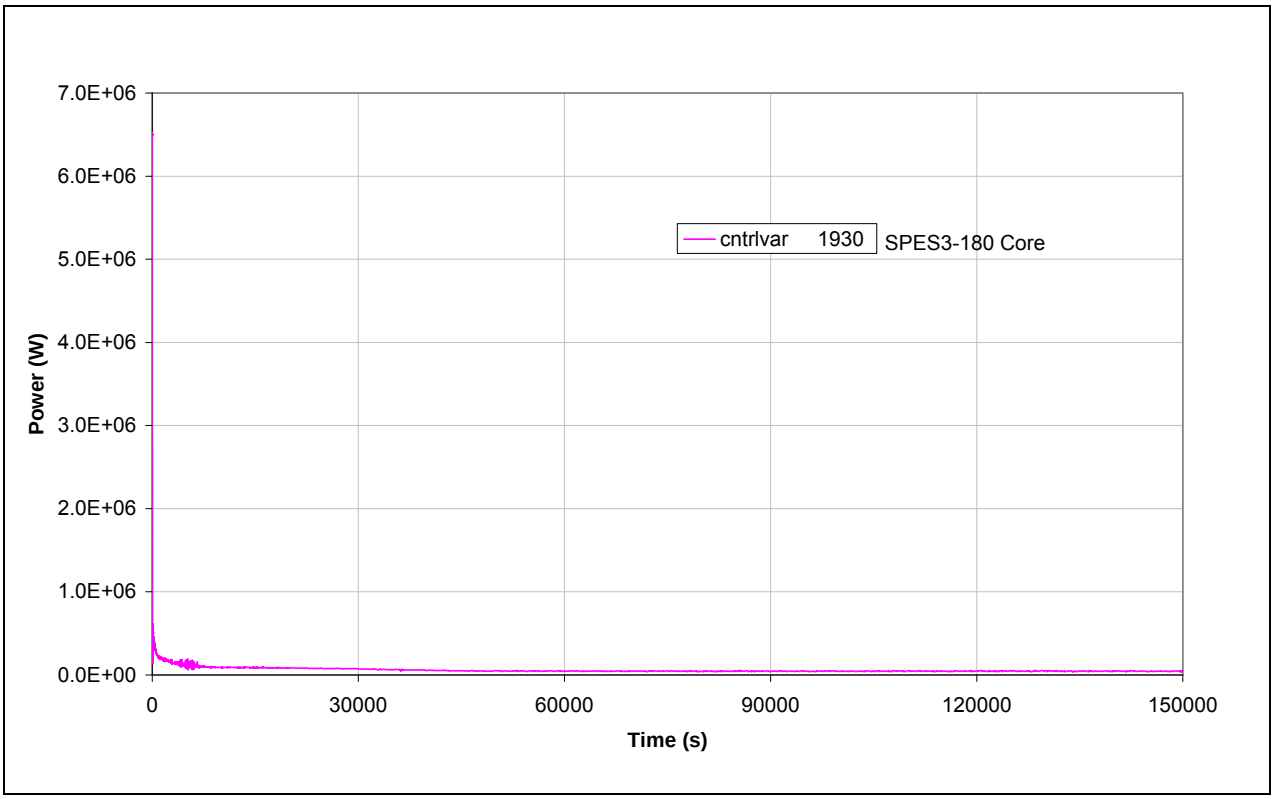

Fig.4.22 – SPES3-180 SG power (window)

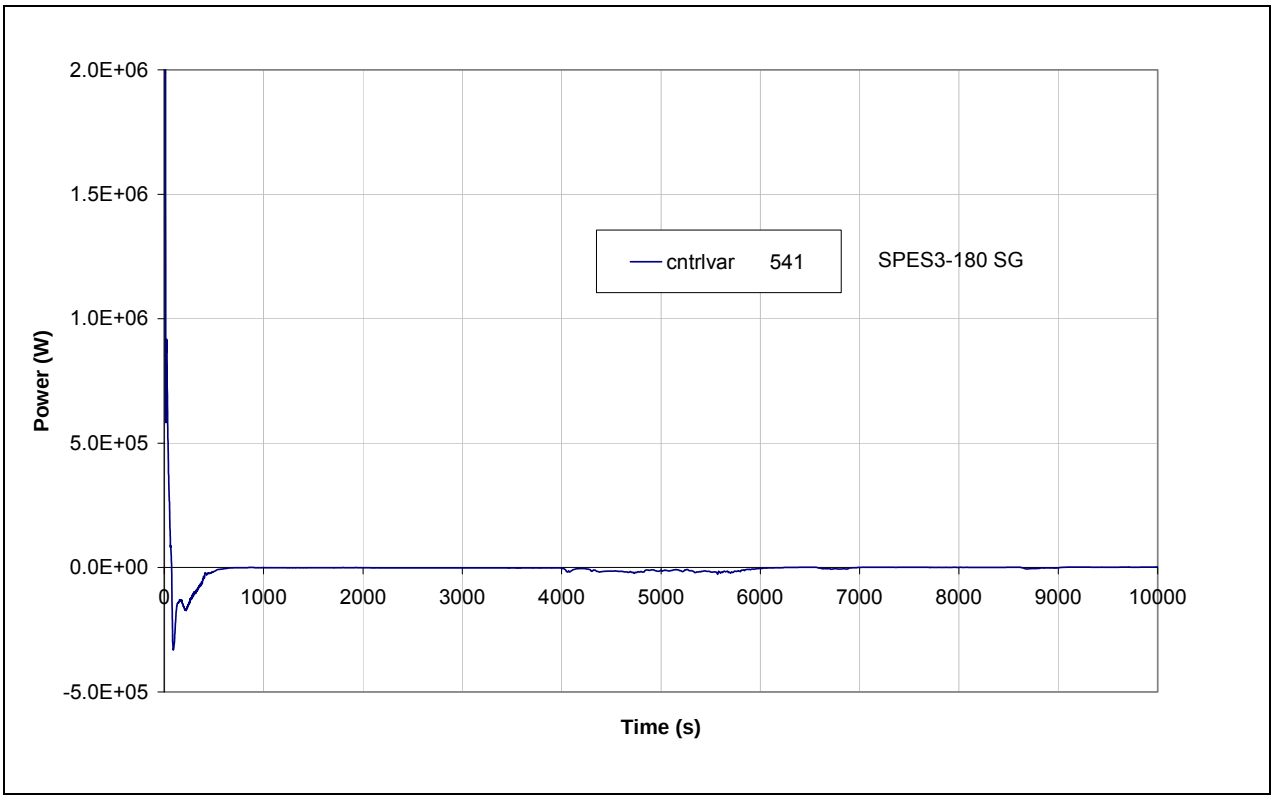

Fig.4.23 – SPES3-180 SGss mass flow (window)

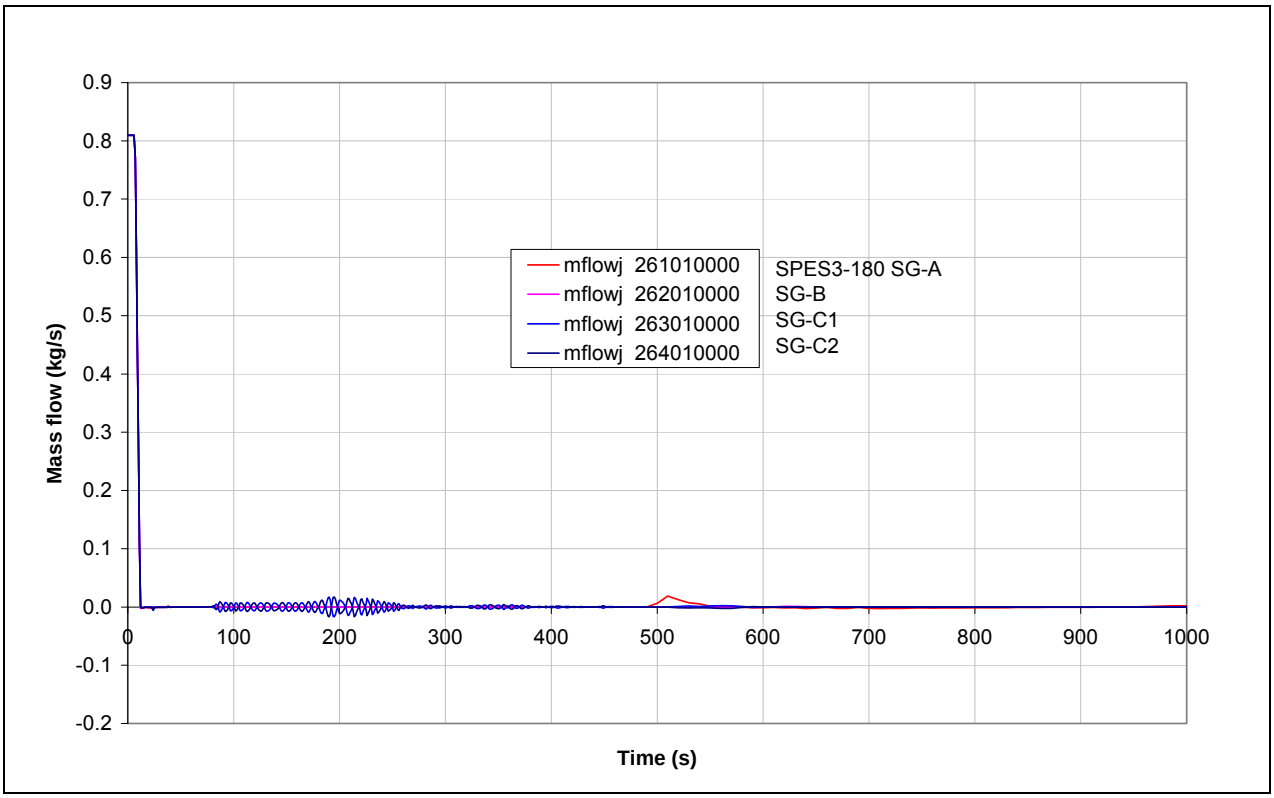

Fig.4.24 – SPES3-180 SGss outlet pressure (window)

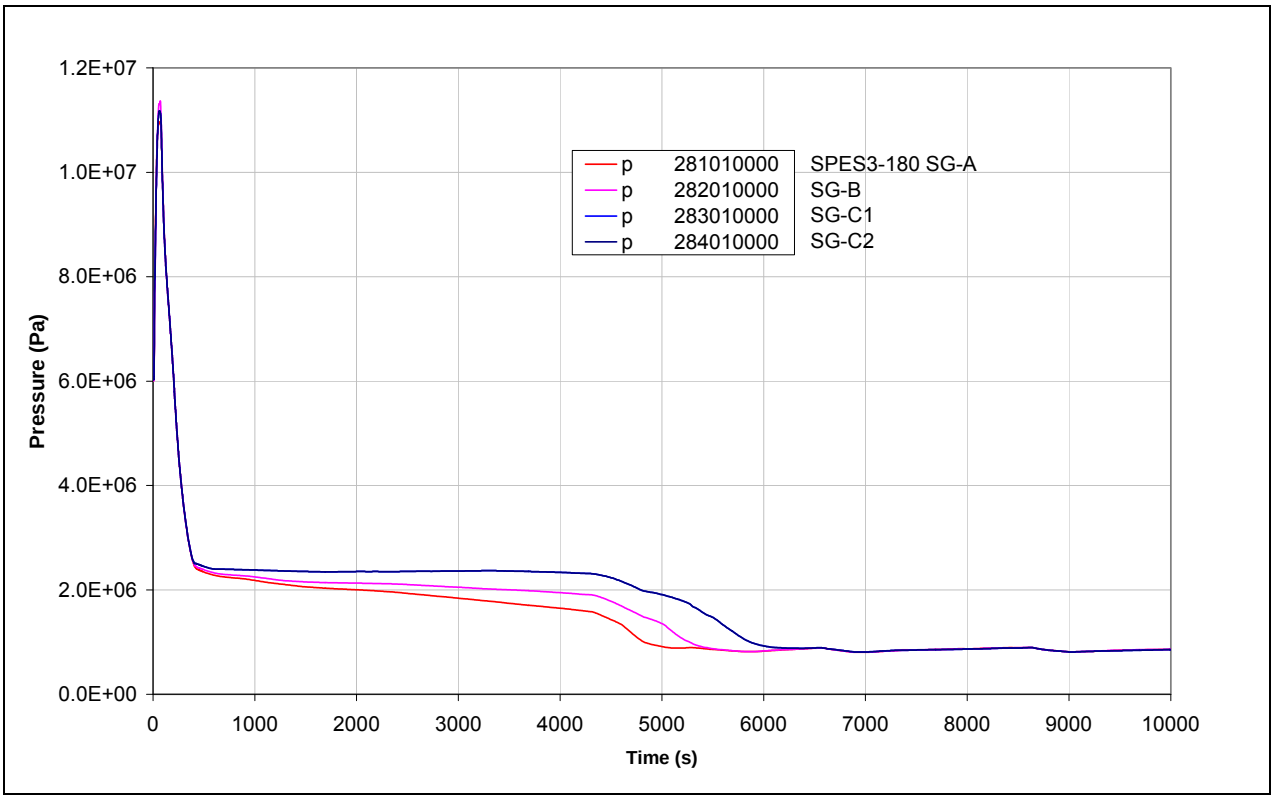

Fig.4.25 – SPES3-180 SG ss outlet pressure

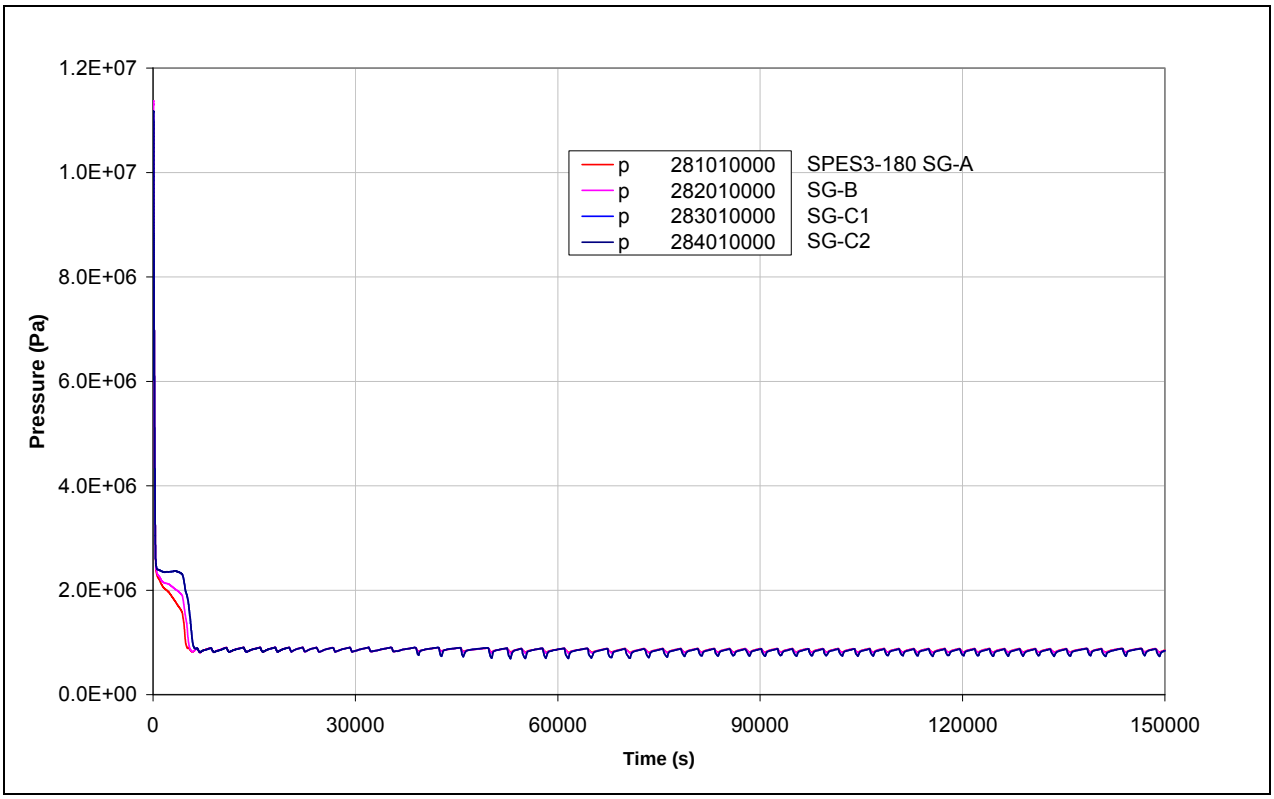

Fig.4.26 – SPES3-180 SG-A ss level (window)

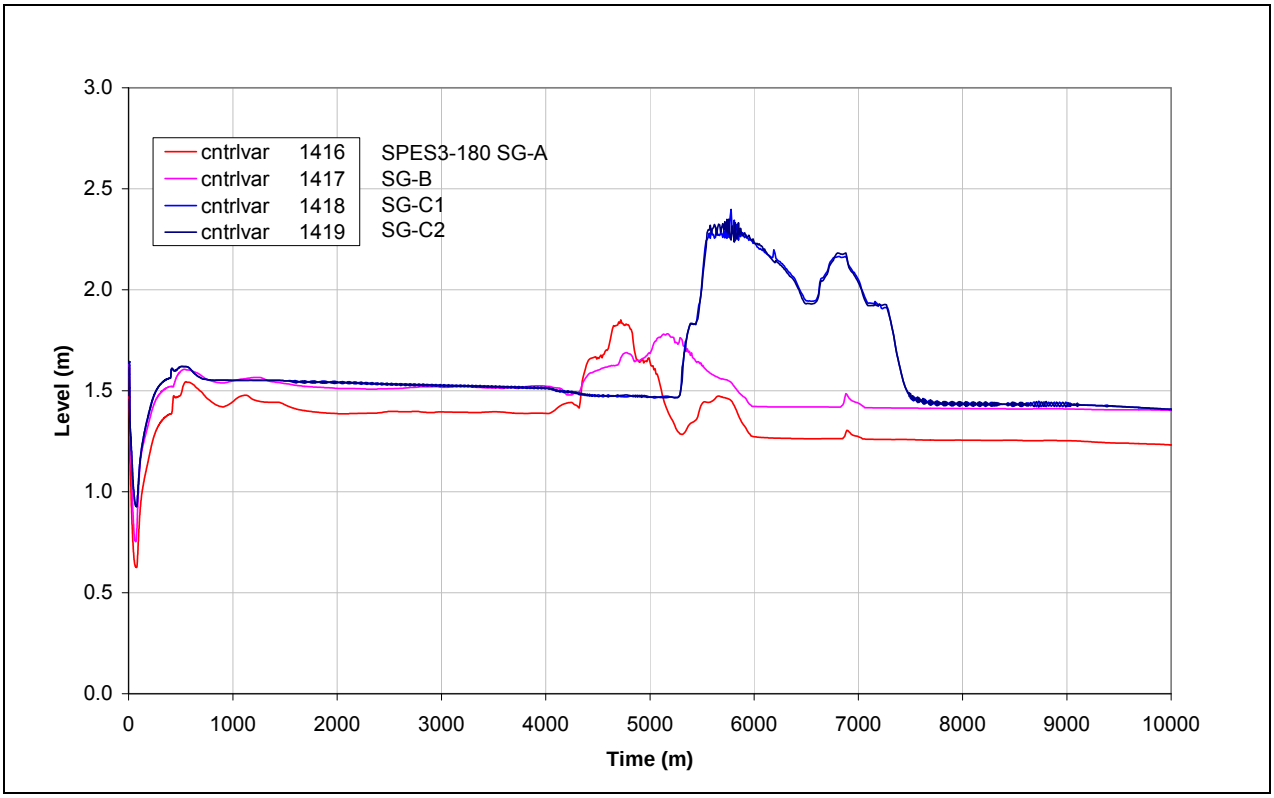

Fig.4.27 – SPES3-180 SG-A ss level

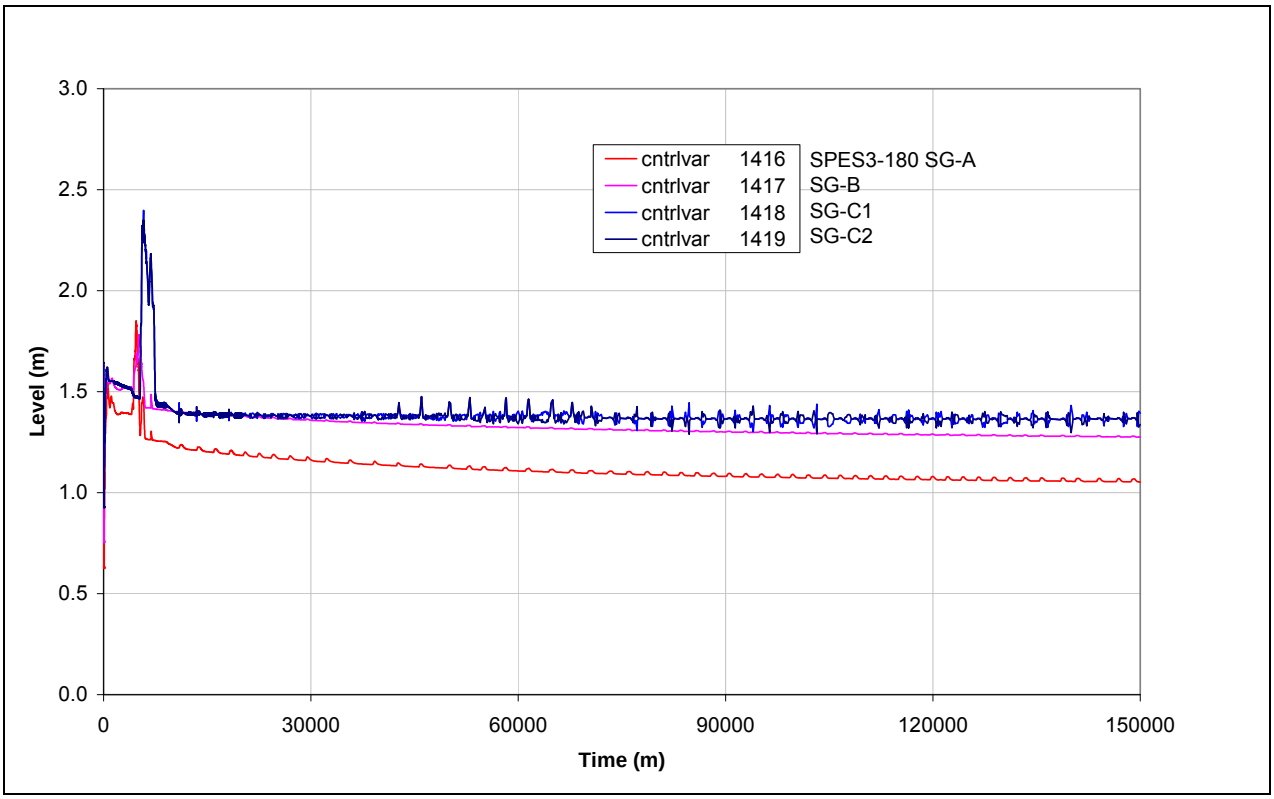

Fig.4.28 – SPES3-180 PRZ level (window)

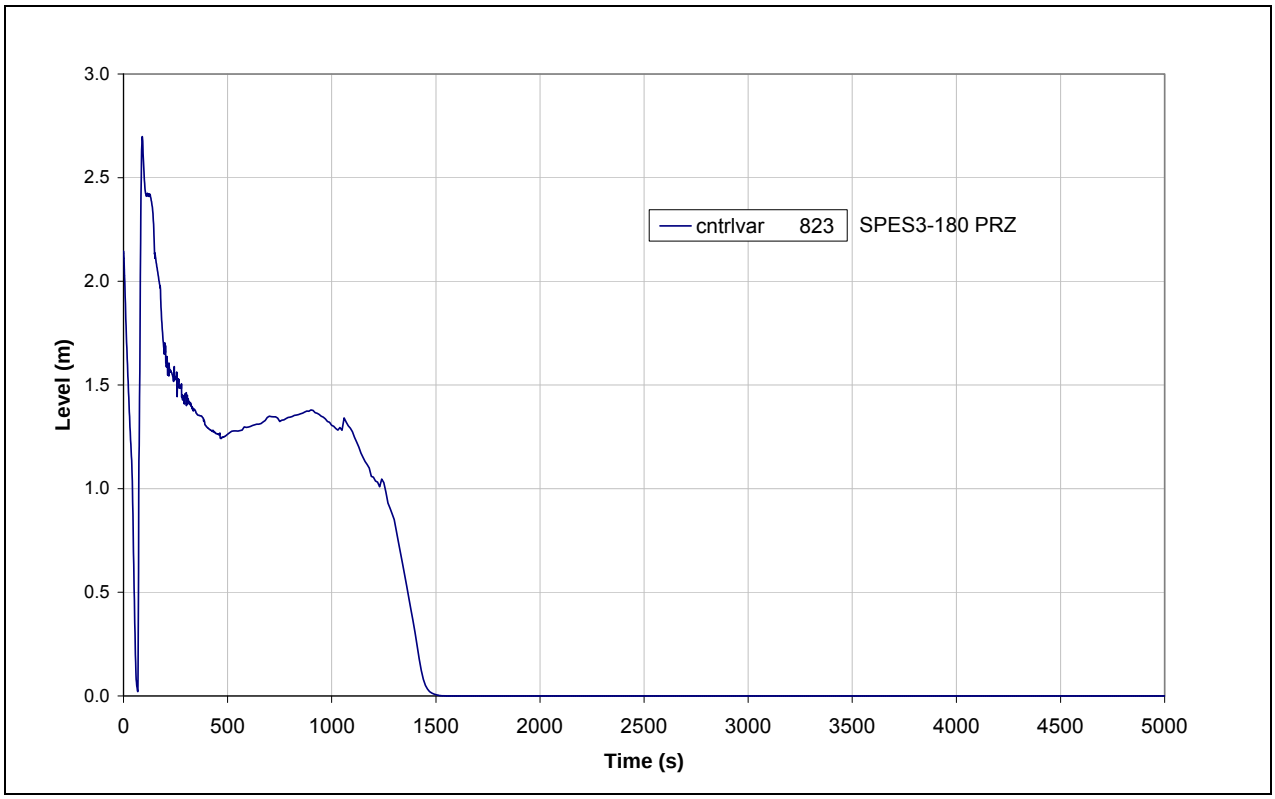

Fig.4.29 – SPES3-180 pump inlet liquid fraction (window)

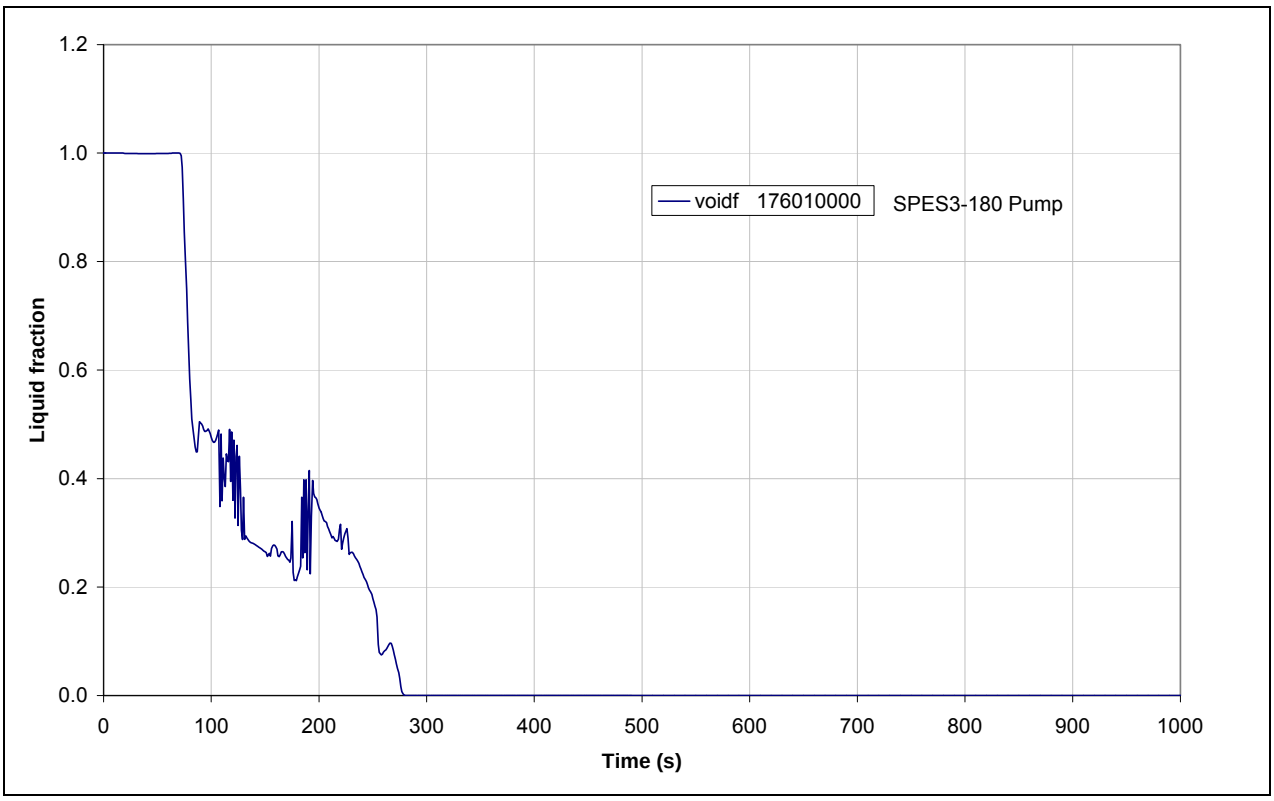

Fig.4.30 – SPES3-180 core inlet flow (window)

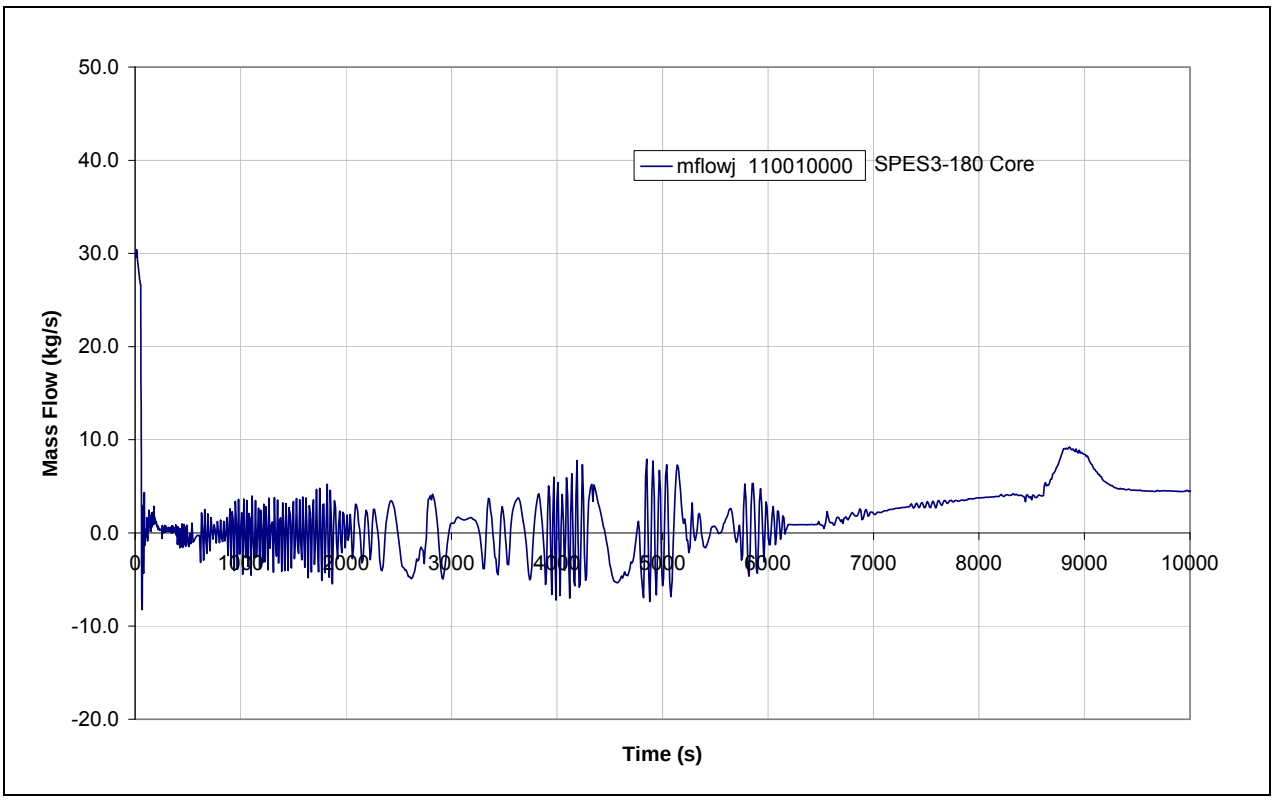

Fig.4.31 – SPES3-180 core inlet flow

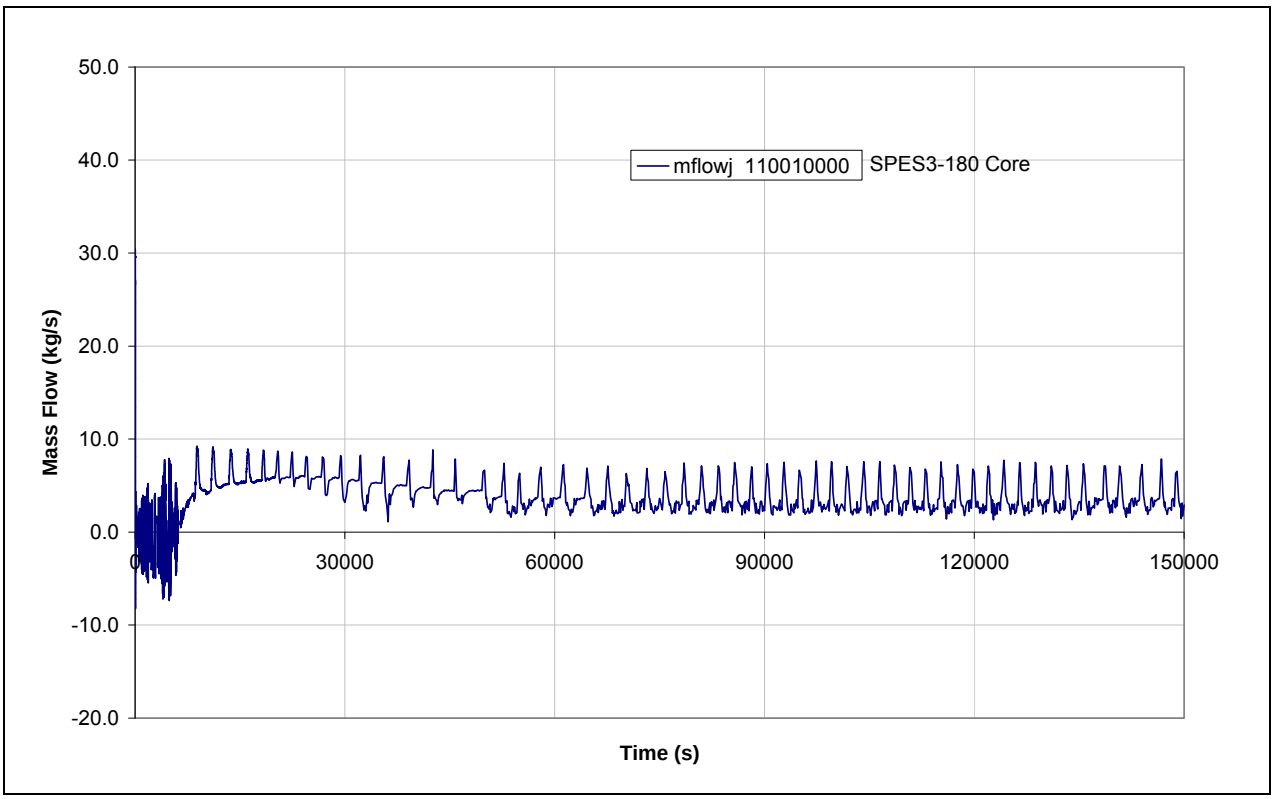

Fig.4.32 – SPES3-180 RI-DC check valve mass flow (window)

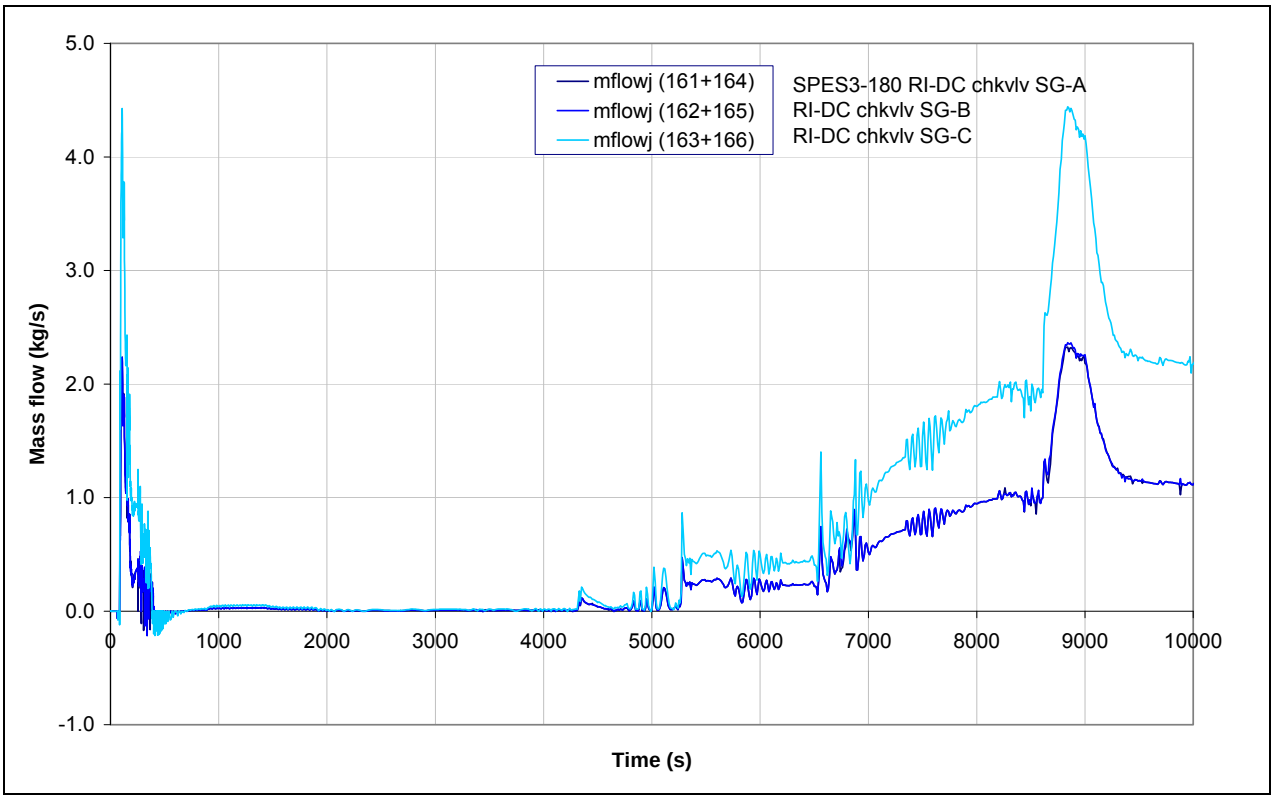

Fig.4.33 – SPES3-180 RI-DC check valve mass flow

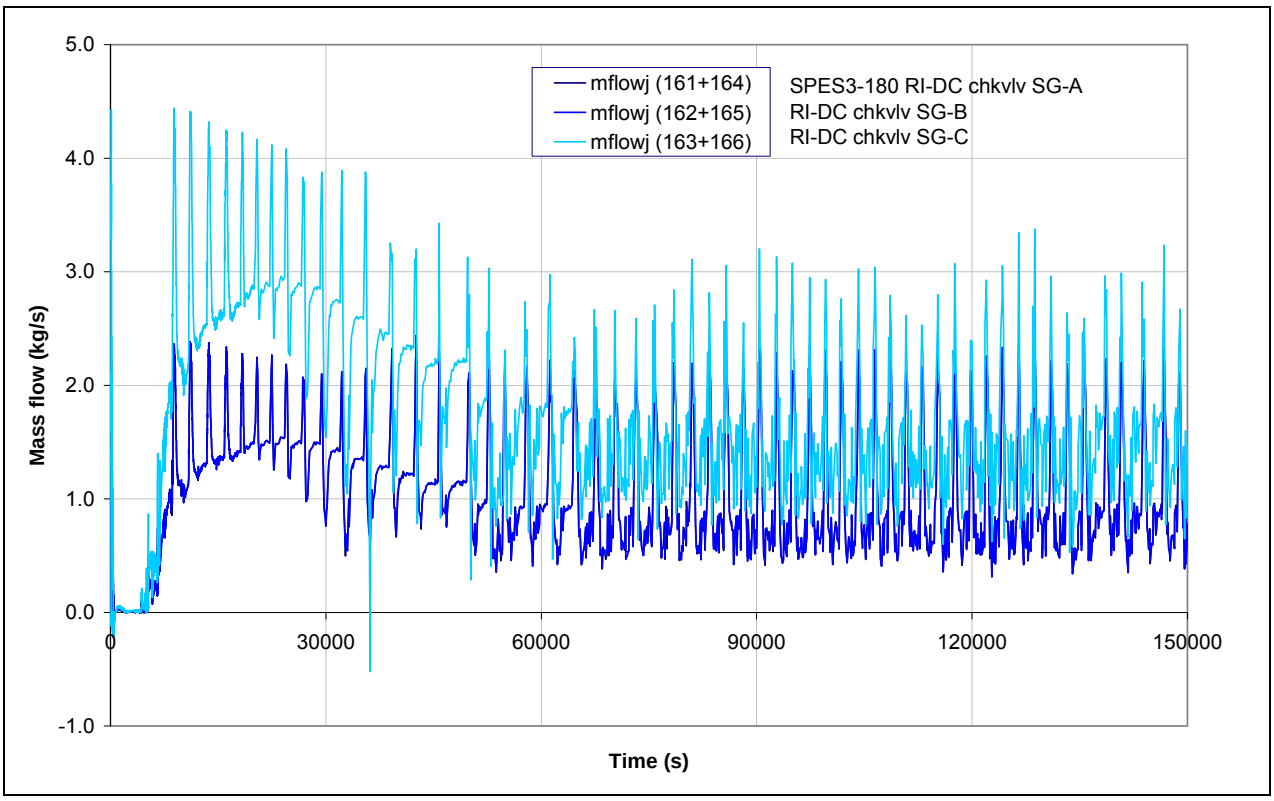

Fig.4.34 – SPES3-180 ADS Stage-I mass flow (window)

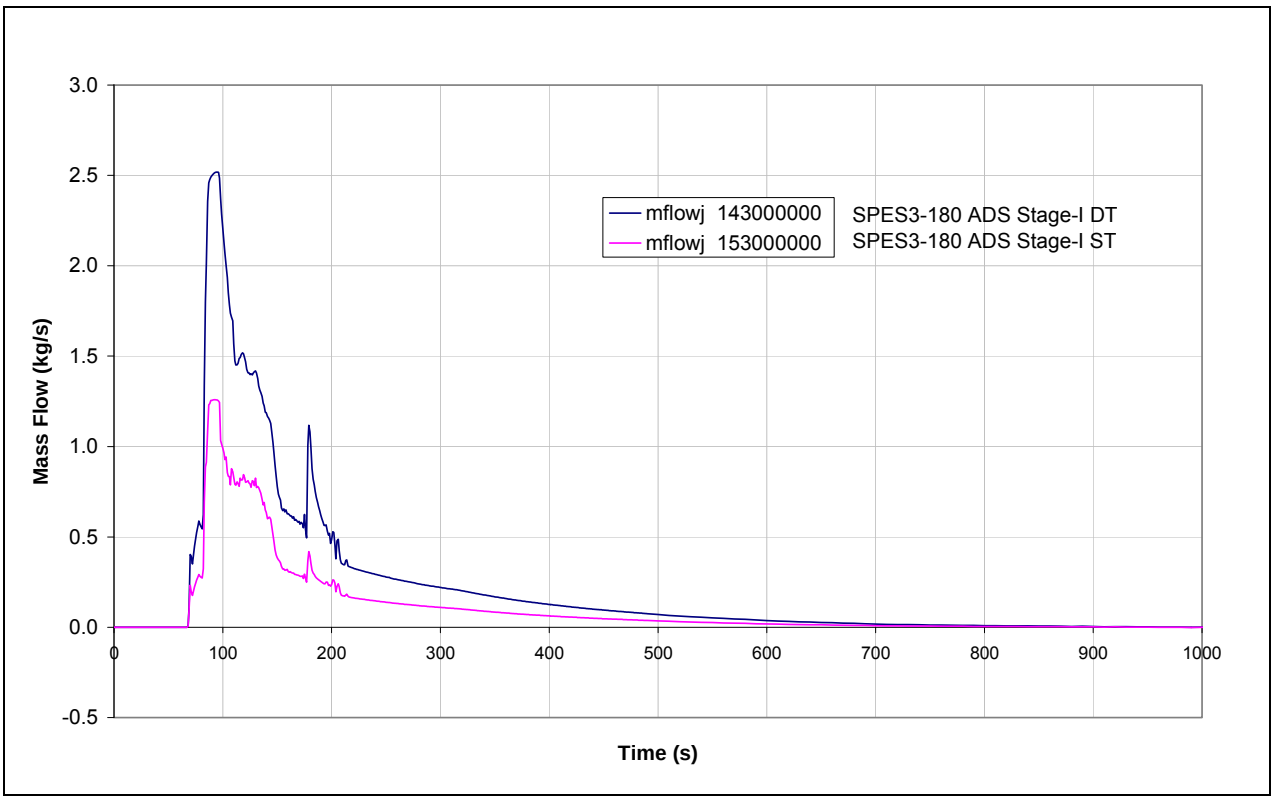

Fig.4.35 – SPES3-180 ADS Stage-I mass flow (window)

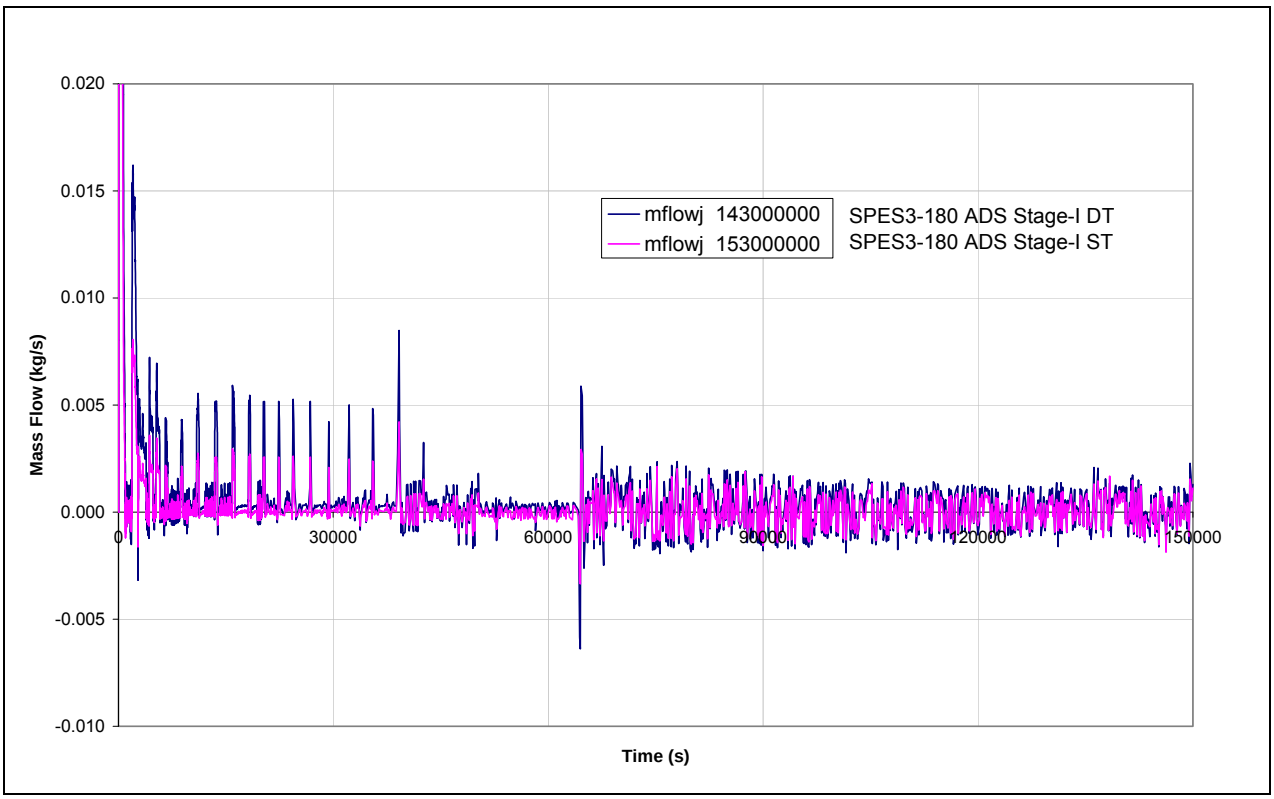

Fig.4.36 – SPES3-180 ADS Stage-I mass flow and PRZ liquid fraction (window)

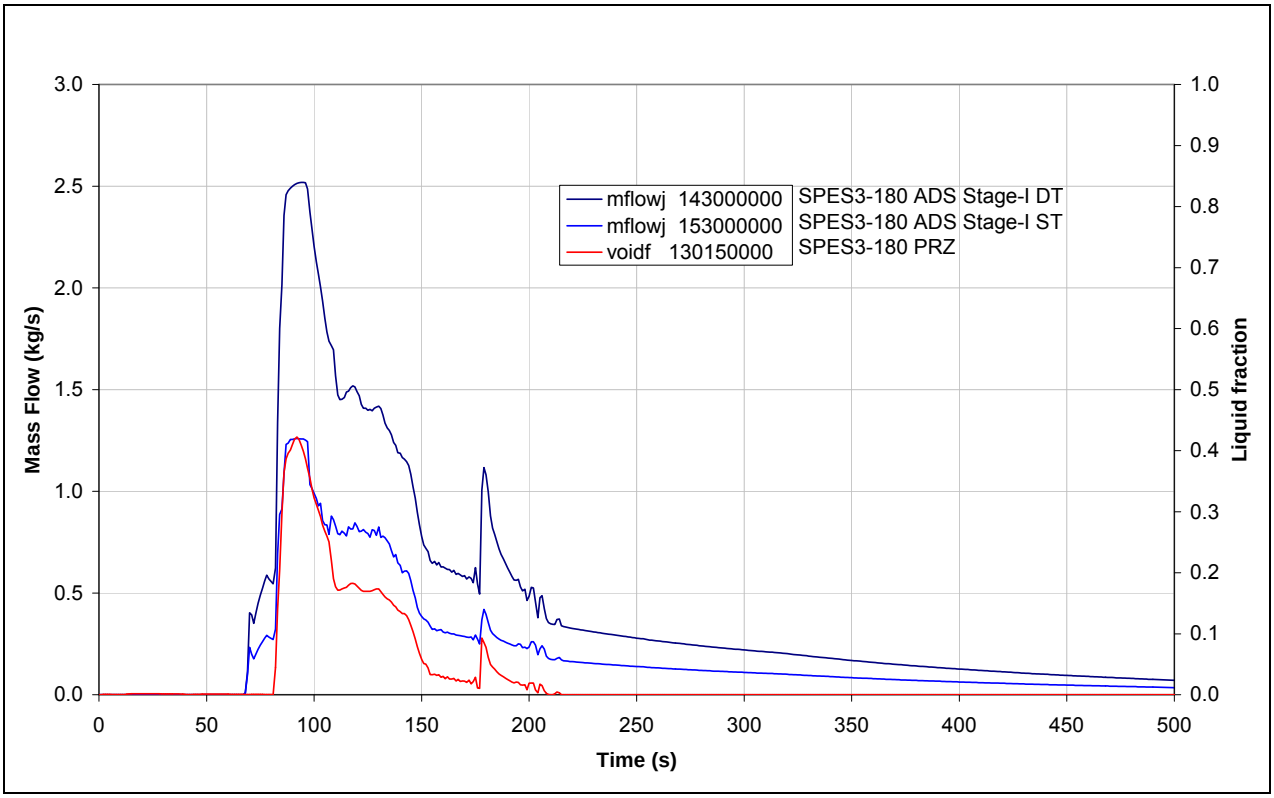

Fig.4.37 – SPES3-180 ADS Stage-II mass flow (window)

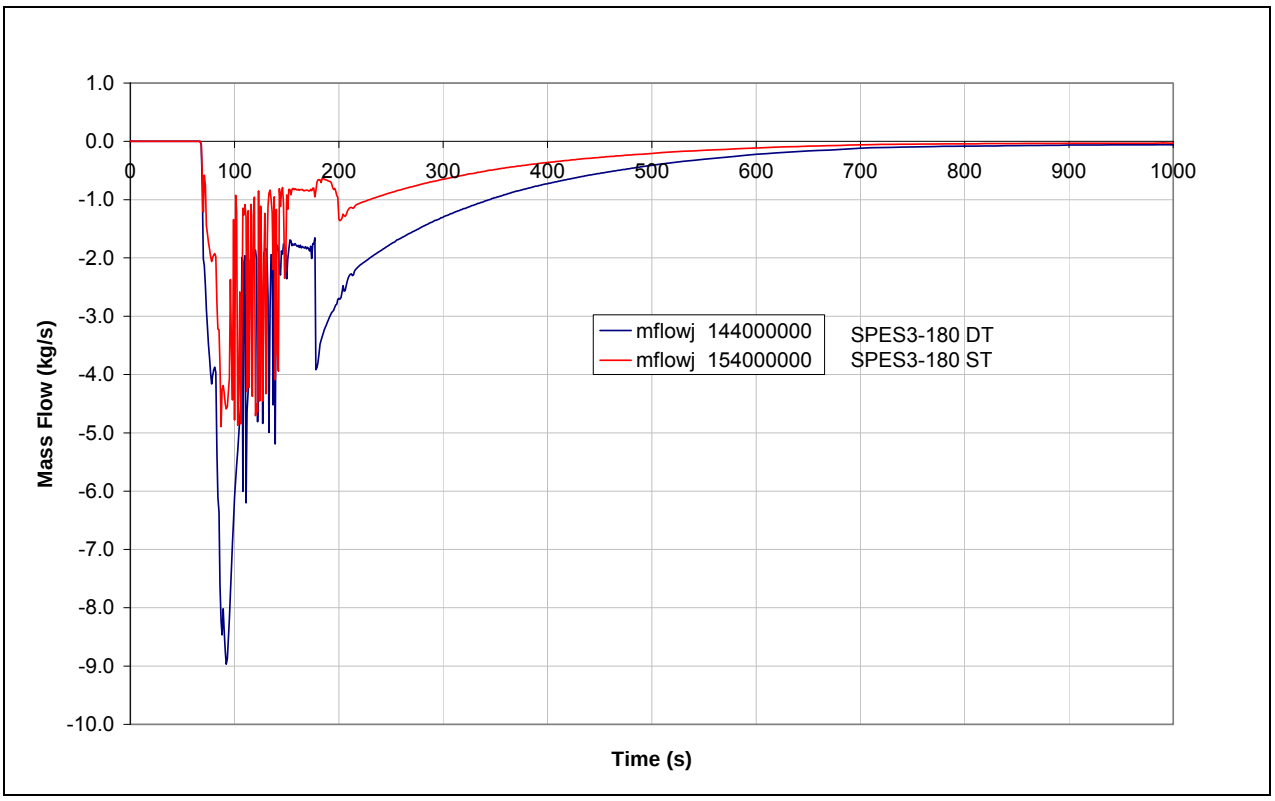

Fig.4.38 – SPES3-180 ADS Stage-II mass flow (window)

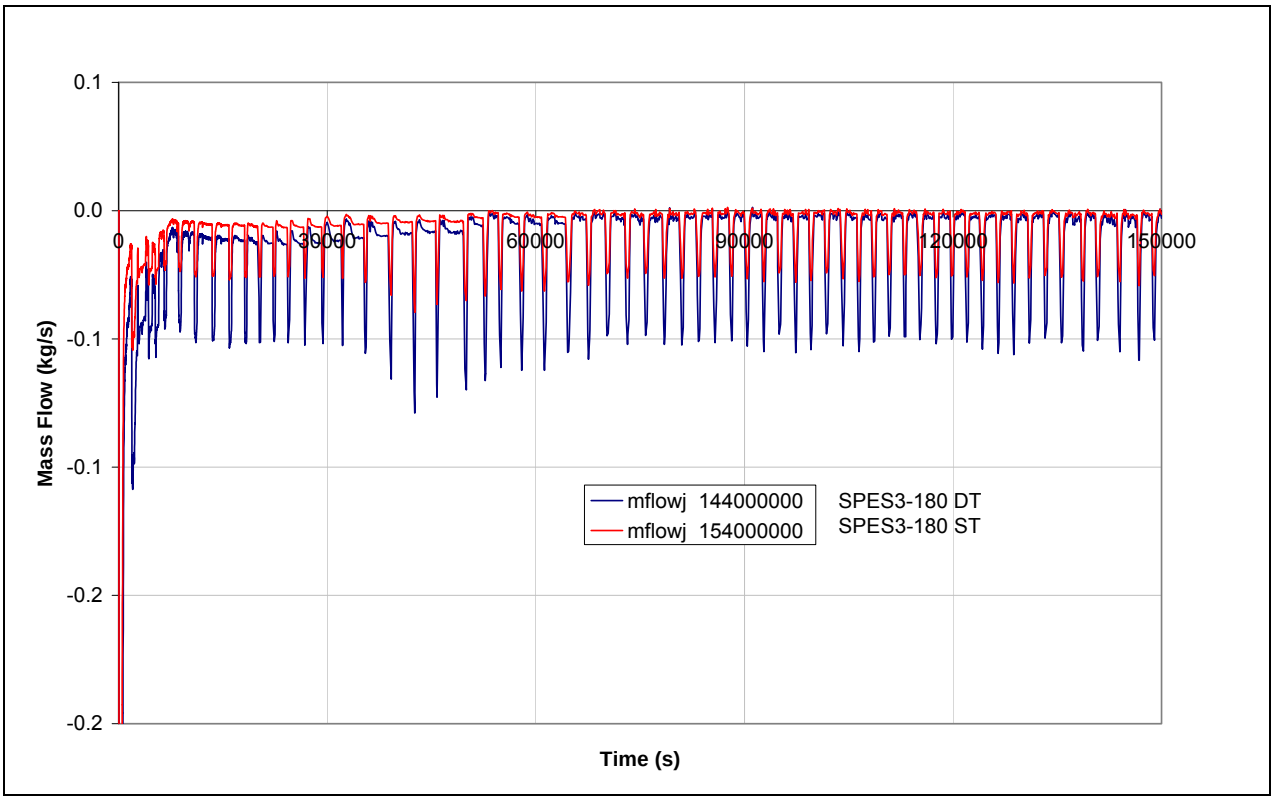

Fig.4.39 – SPES3-180 ADS Stage-II mass flow and PRZ liquid fraction (window)

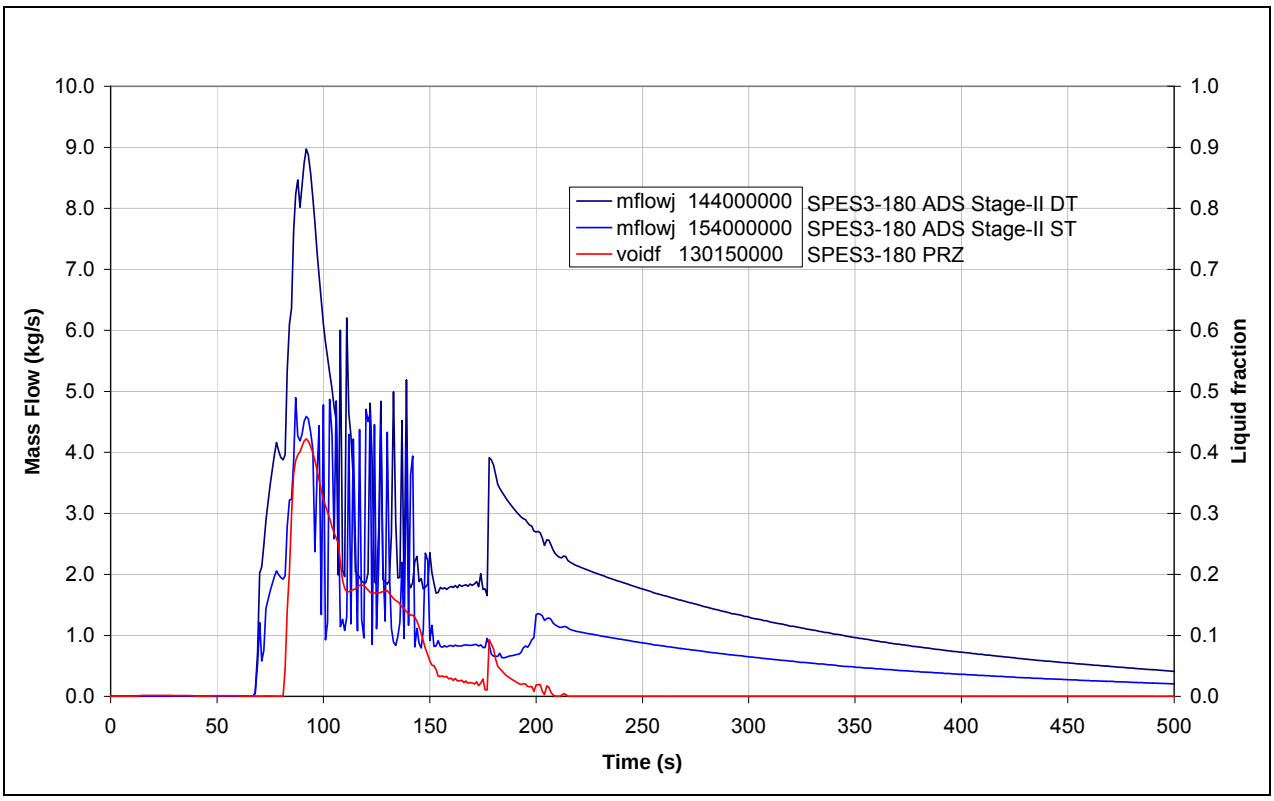

Fig.4.40 – SPES3-180 EBT injection mass flow (window)

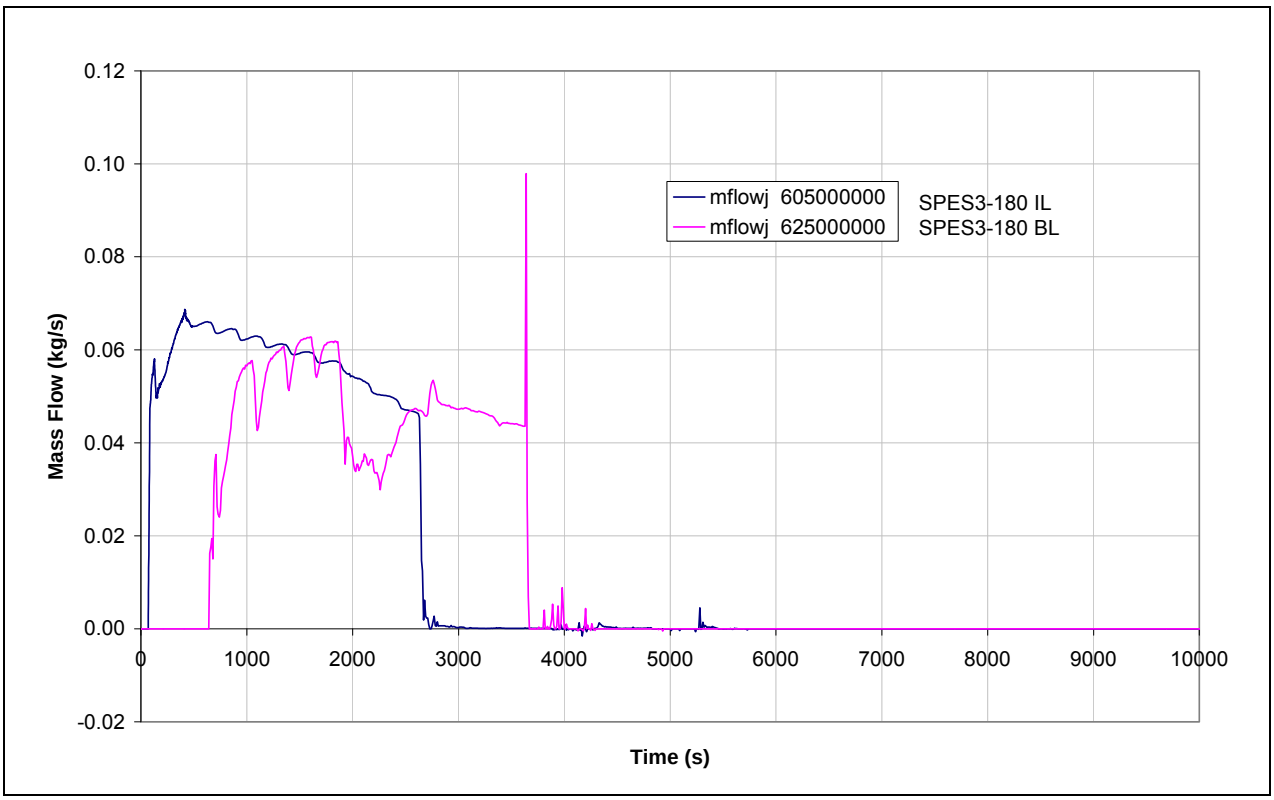

Fig.4.41 – SPES3-180 EBT mass (window)

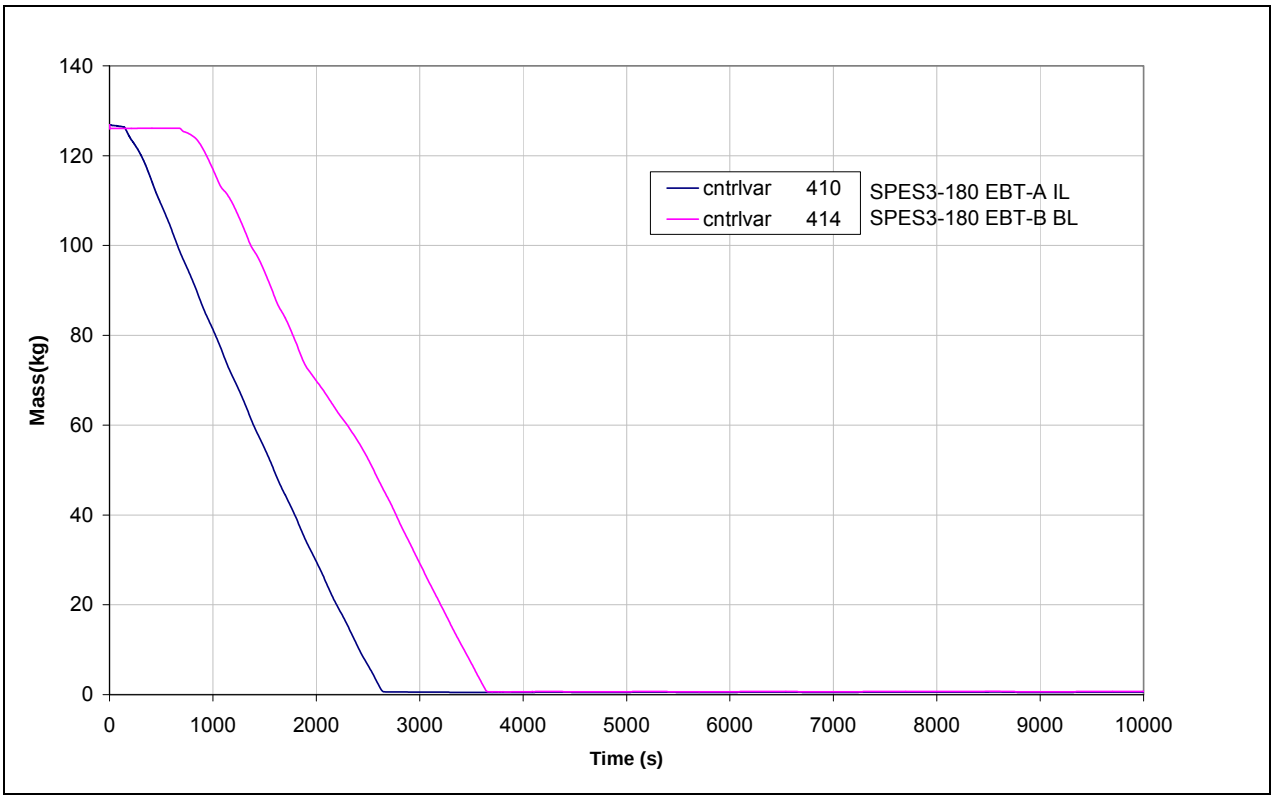

Fig.4.42 – SPES3-180 EBT level (window)

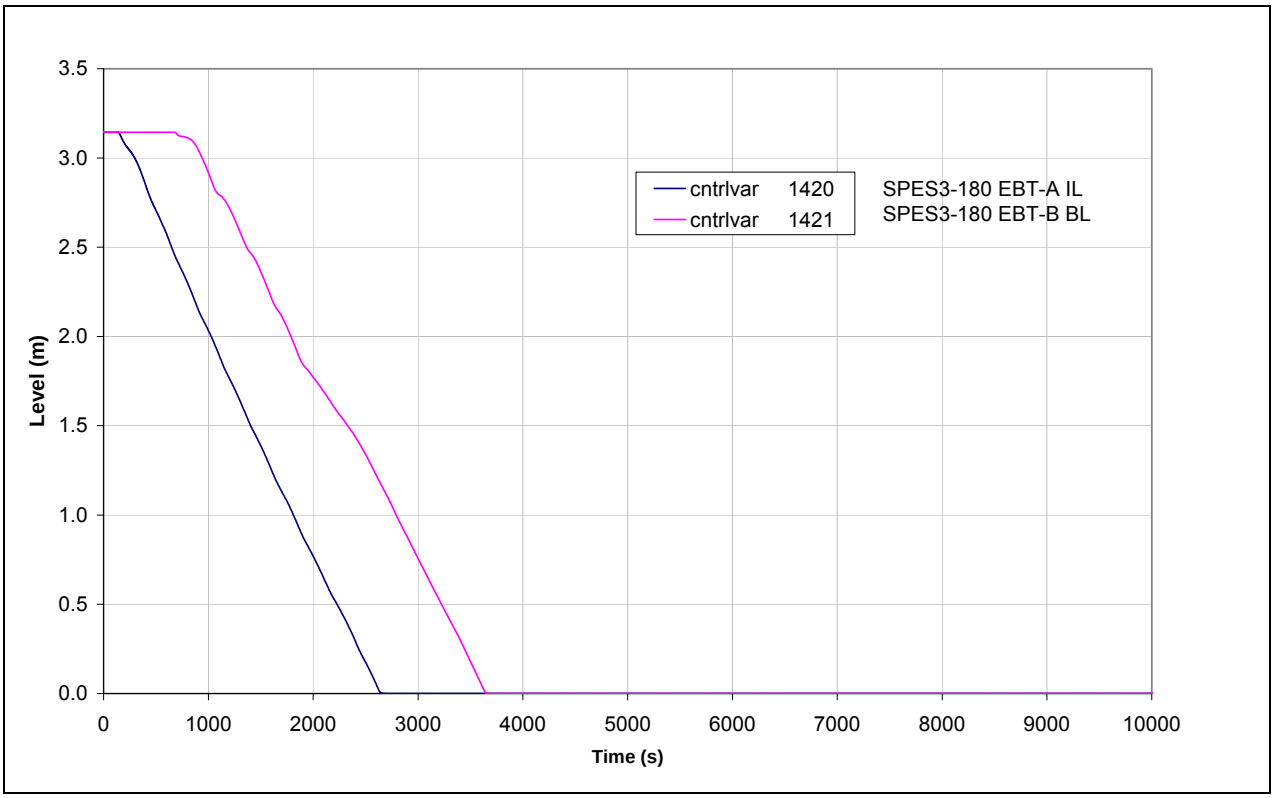

Fig.4.43 – SPES3-180 EBT balance line mass flow (window)

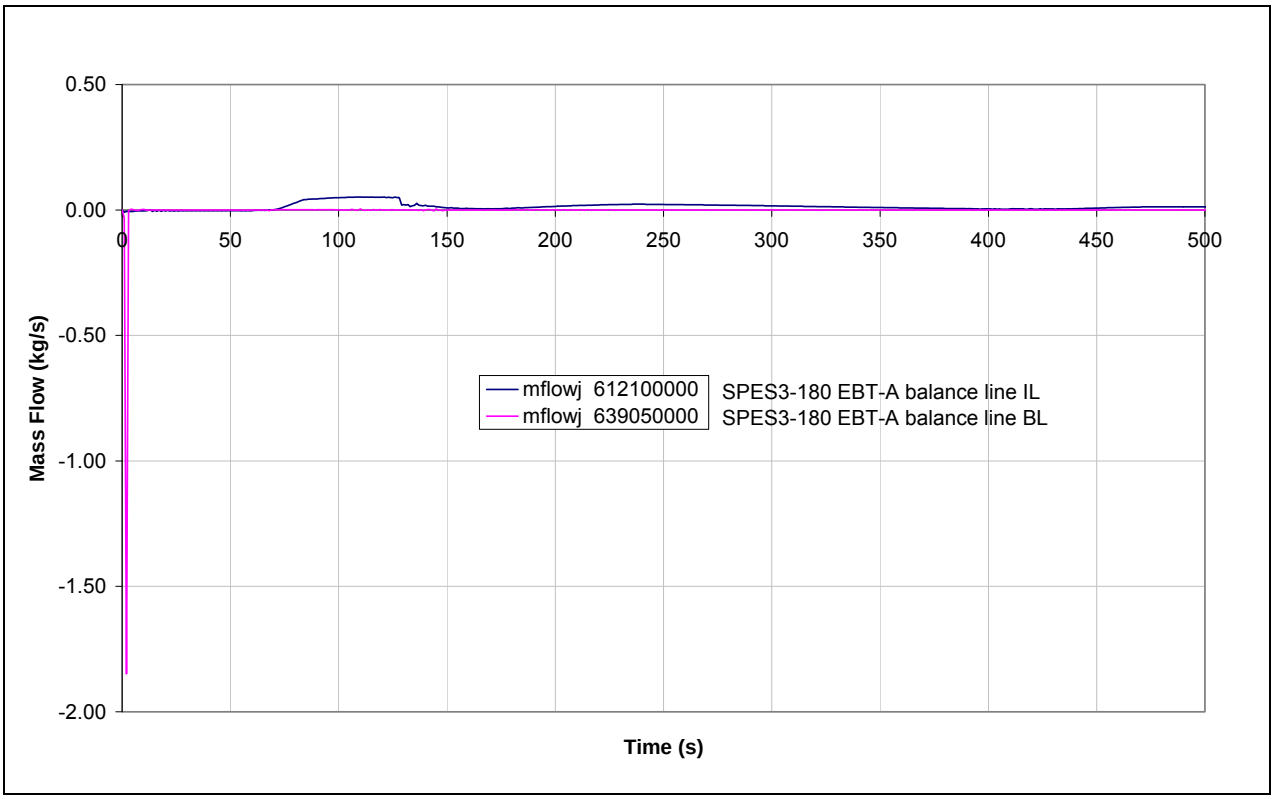

Fig.4.44 – SPES3-180 EBT balance line mass flow (window)

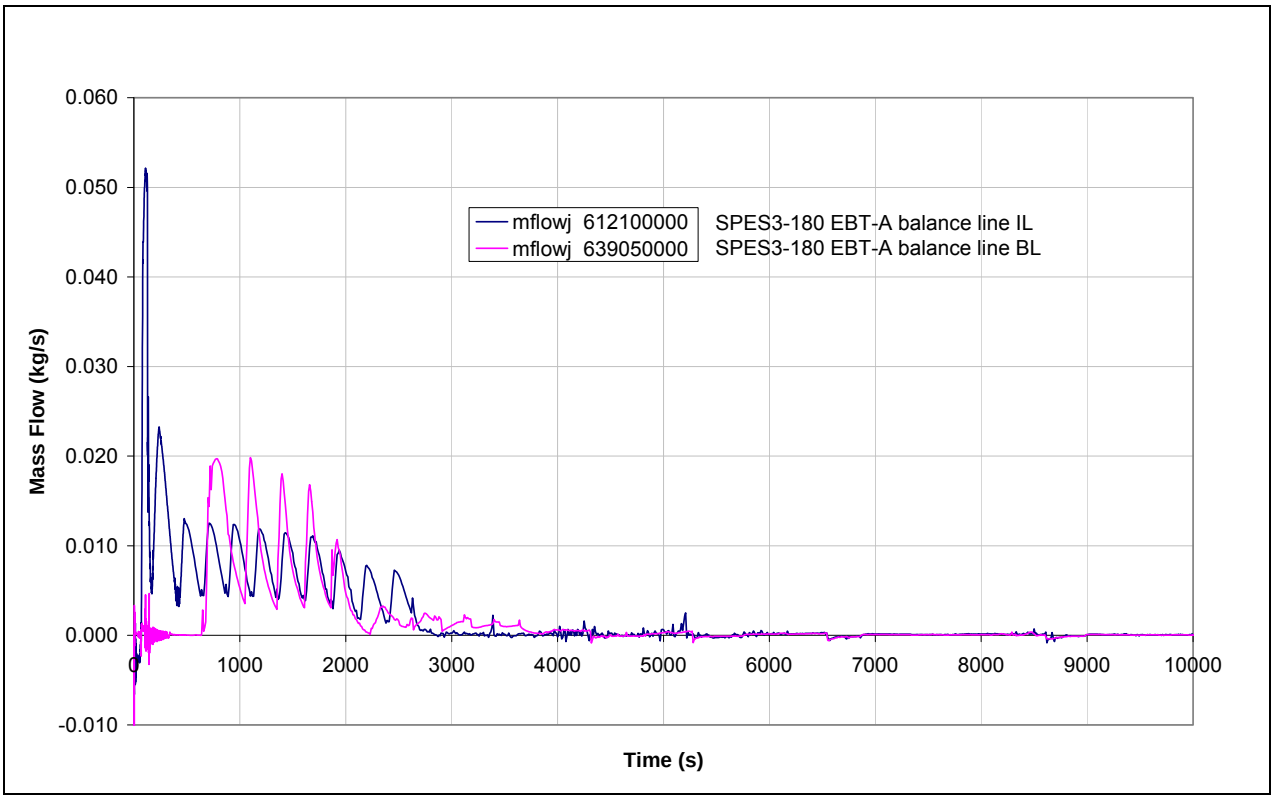

Fig.4.45 – SPES3-180 Core liquid fraction (window)

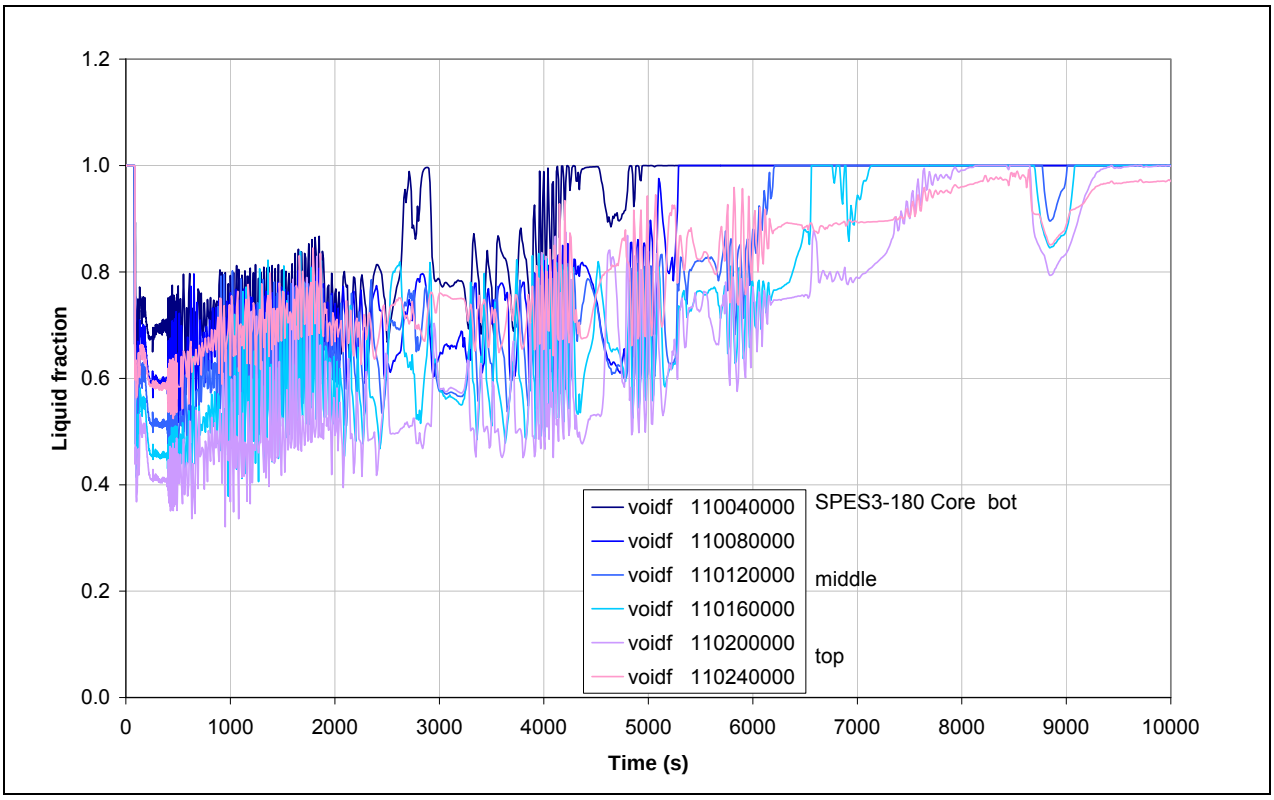

Fig.4.46 – SPES3-180 Core liquid fraction

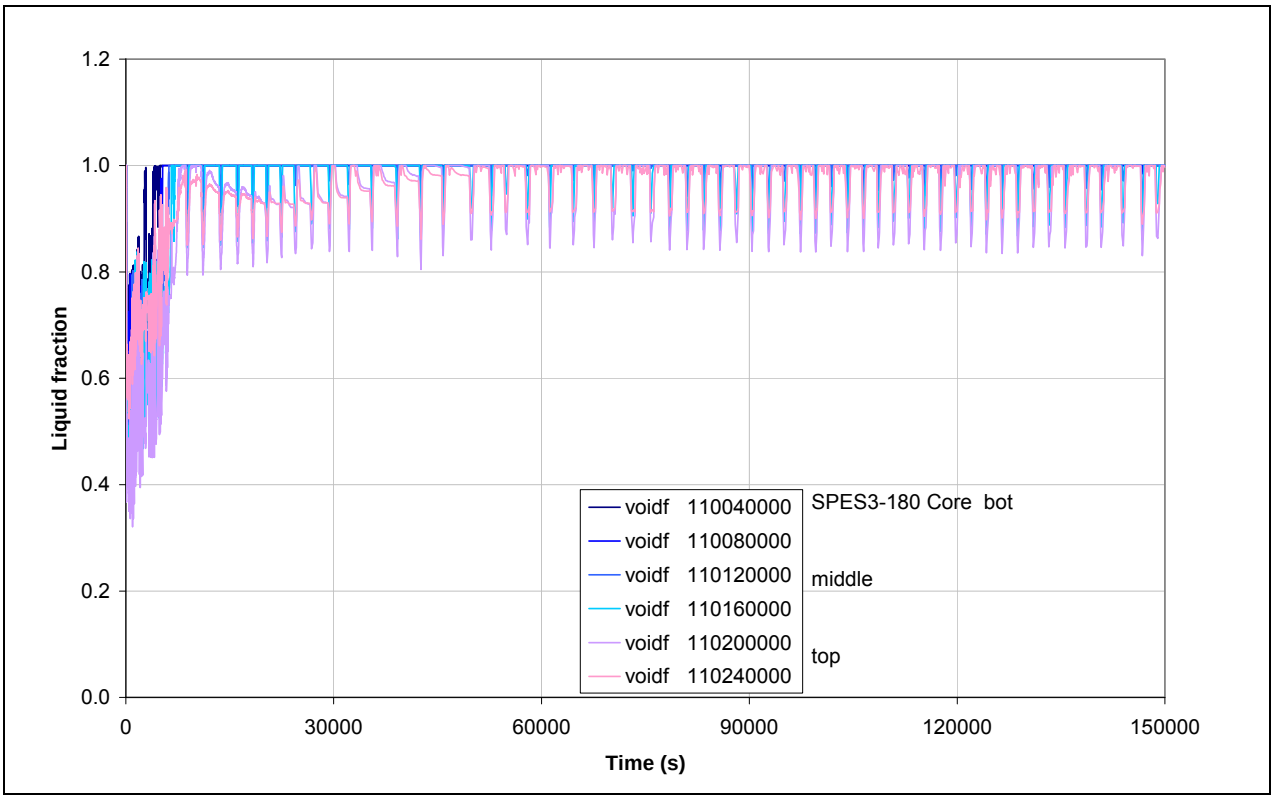

Fig.4.47 – SPES3-180 Core inlet and outlet temperatures (window)

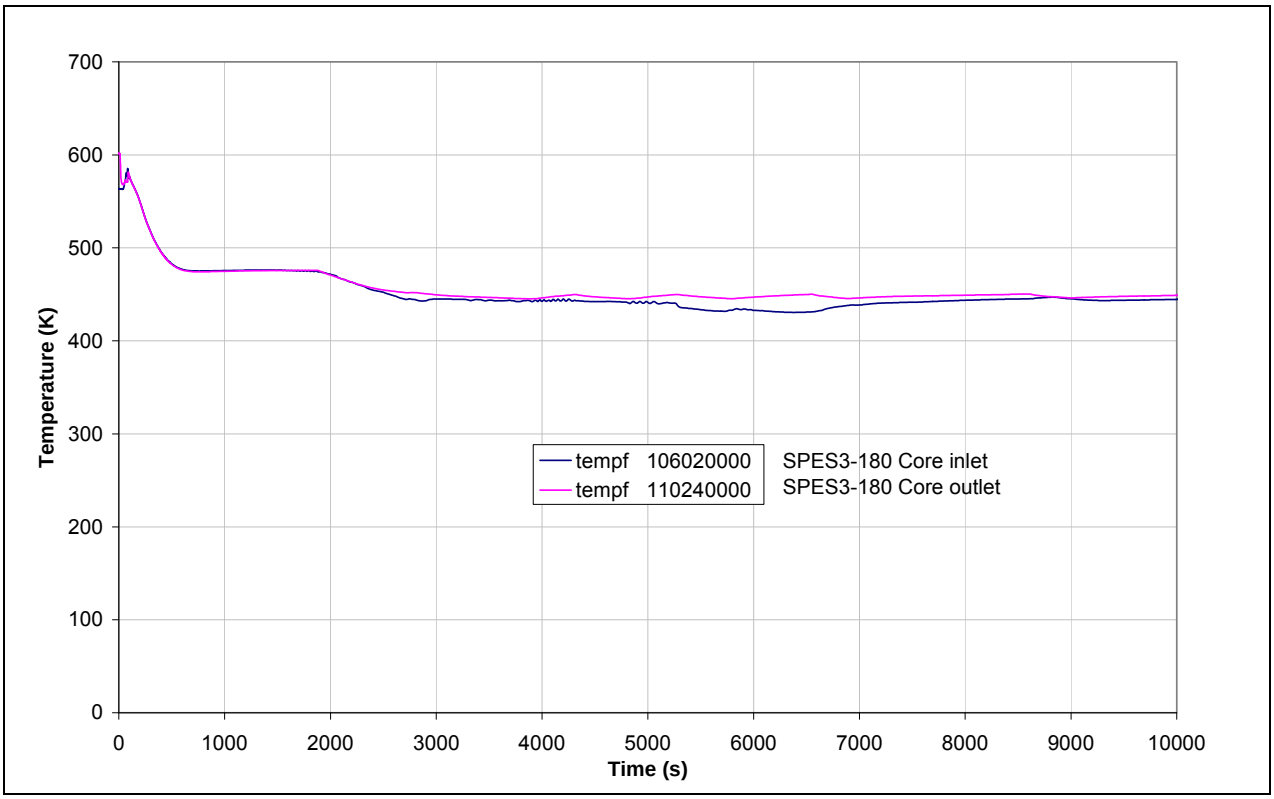

Fig.4.48 – SPES3-180 Core inlet and outlet temperatures

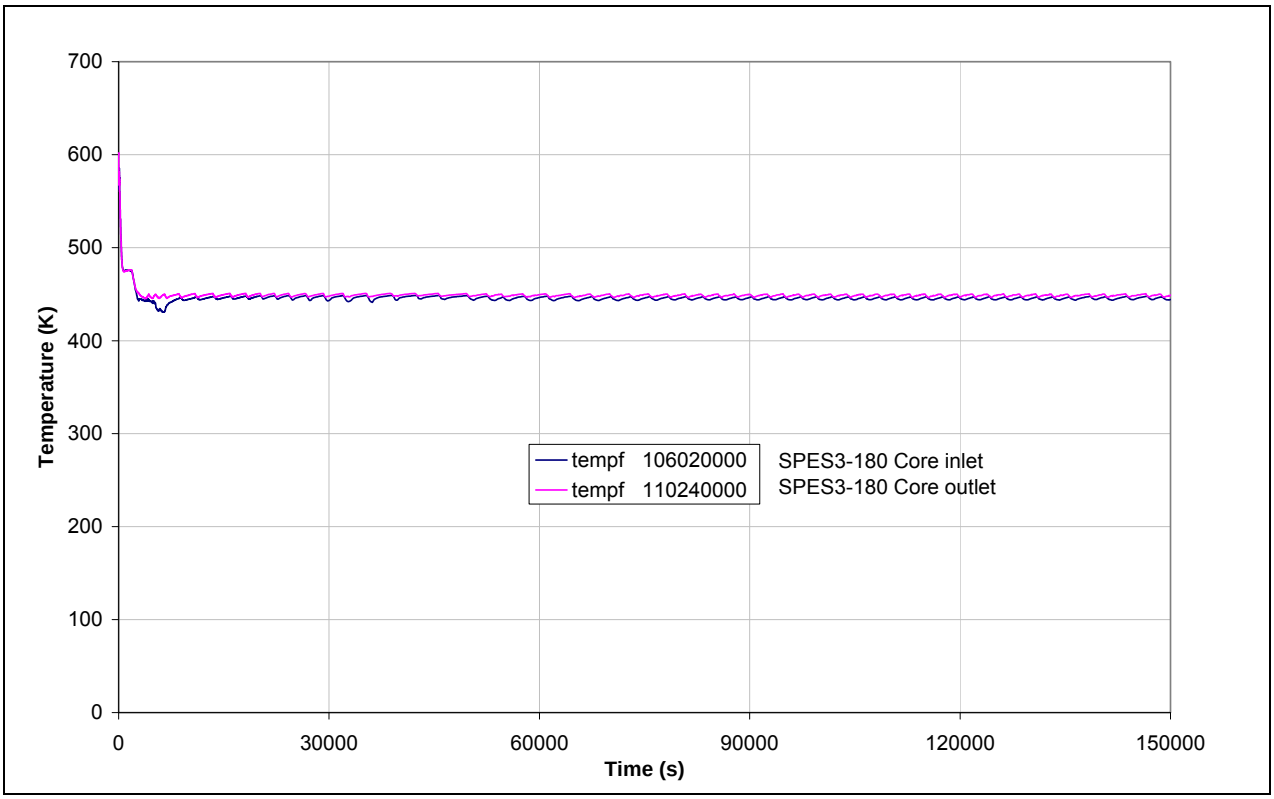

Fig.4.49 – SPES3-180 Core heater rod clad surface temperatures (normal rods)

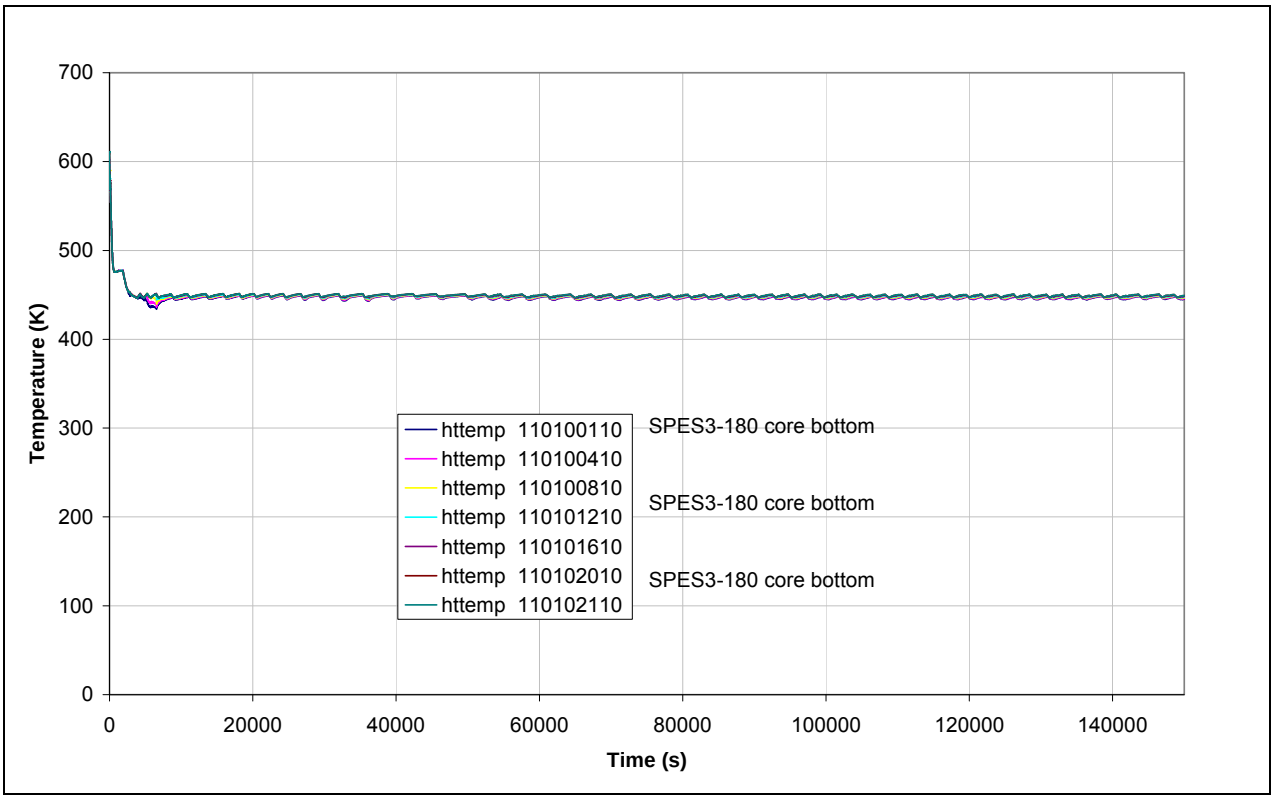

Fig.4.50 – SPES3-180 Core heater rod clad surface temperatures (hot rods)

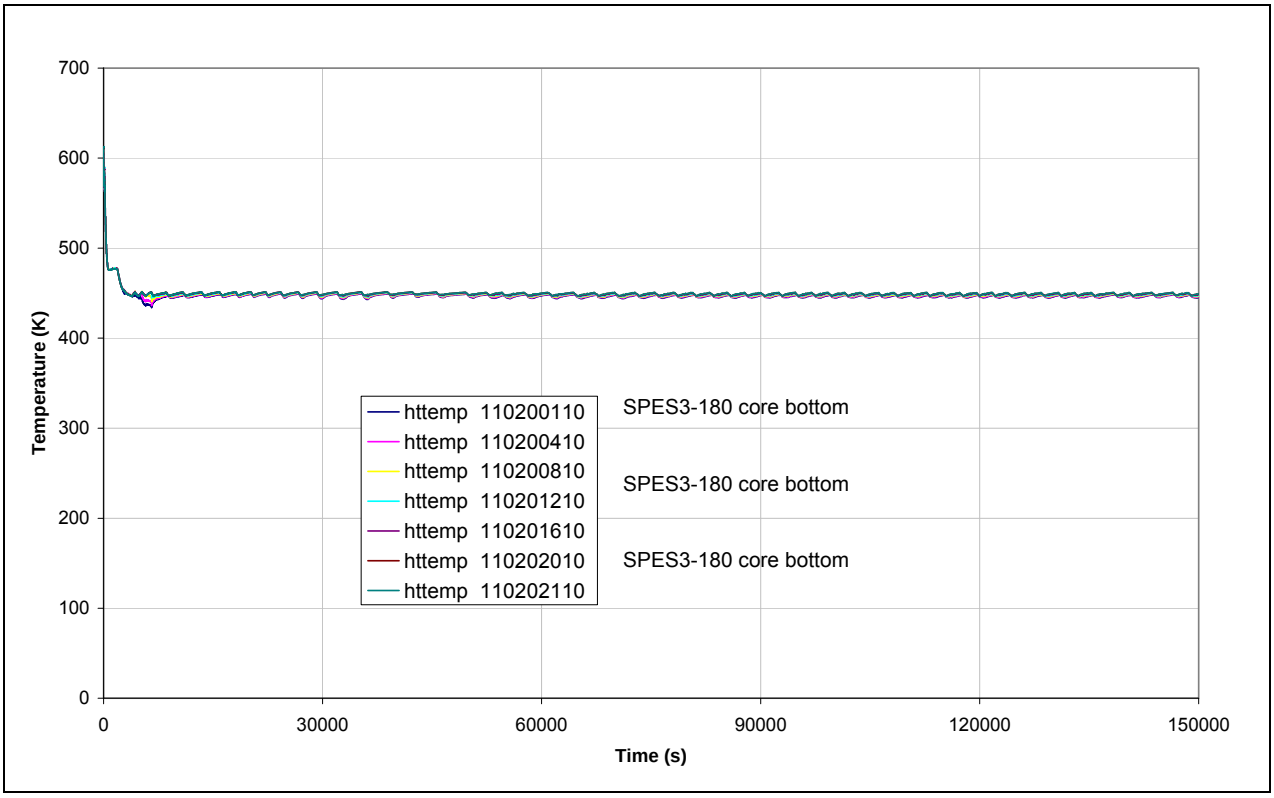

Fig.4.51 – SPES3-180 RPV mass

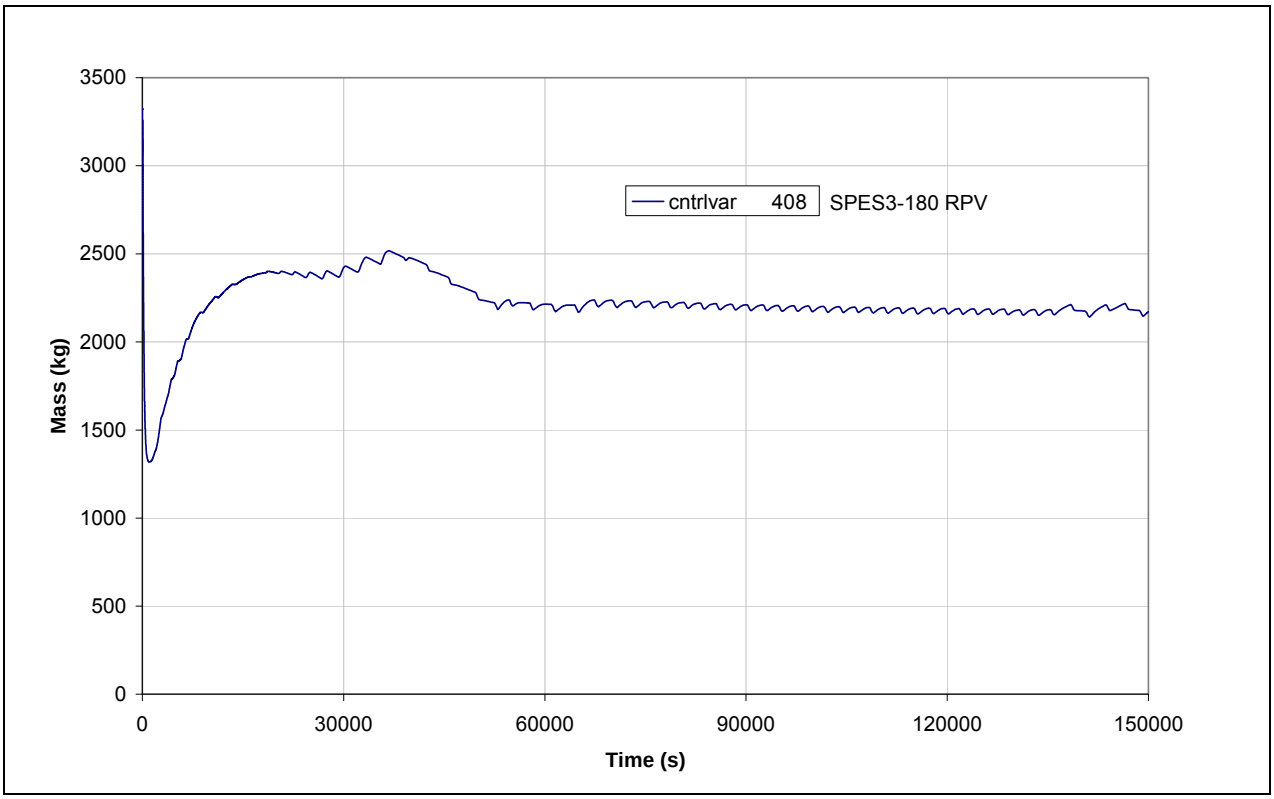

Fig.4.52 – SPES3-180 PCC mass flow

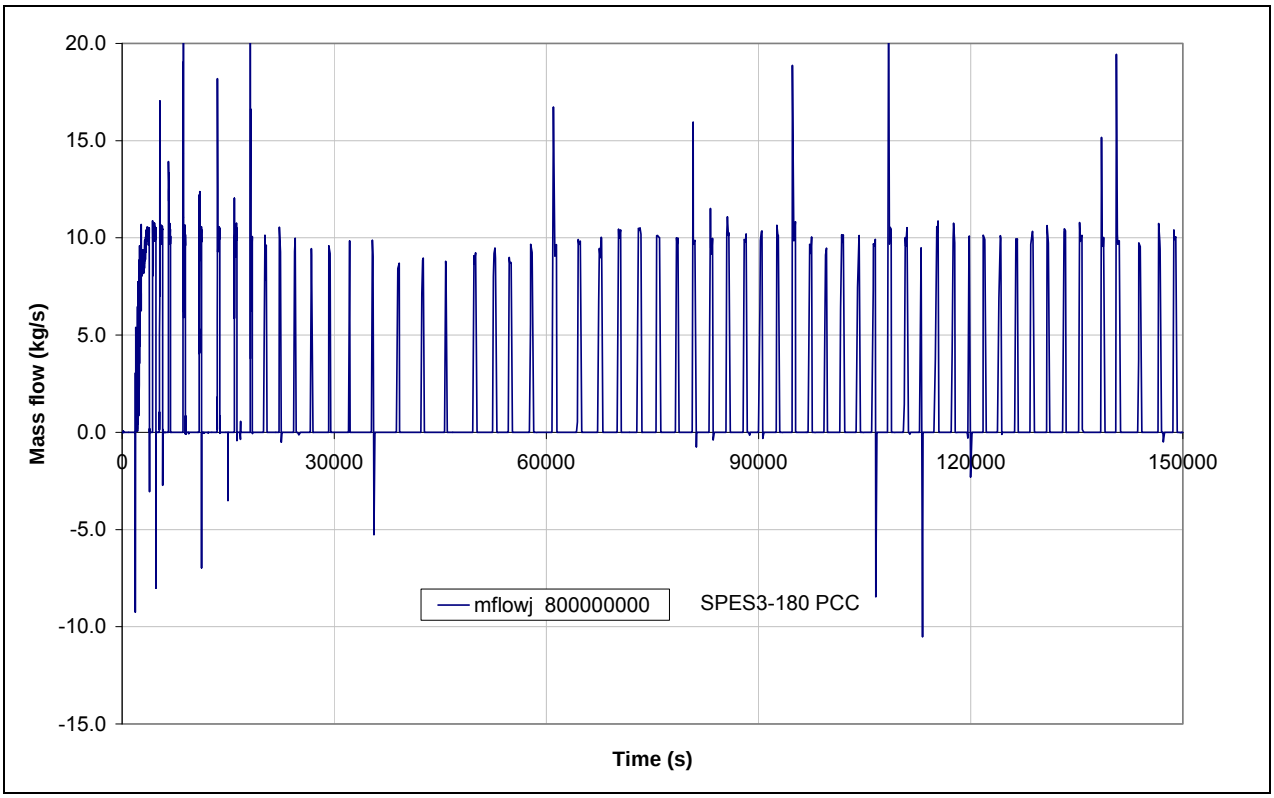

Fig.4.53 – SPES3-180 PCC tank level

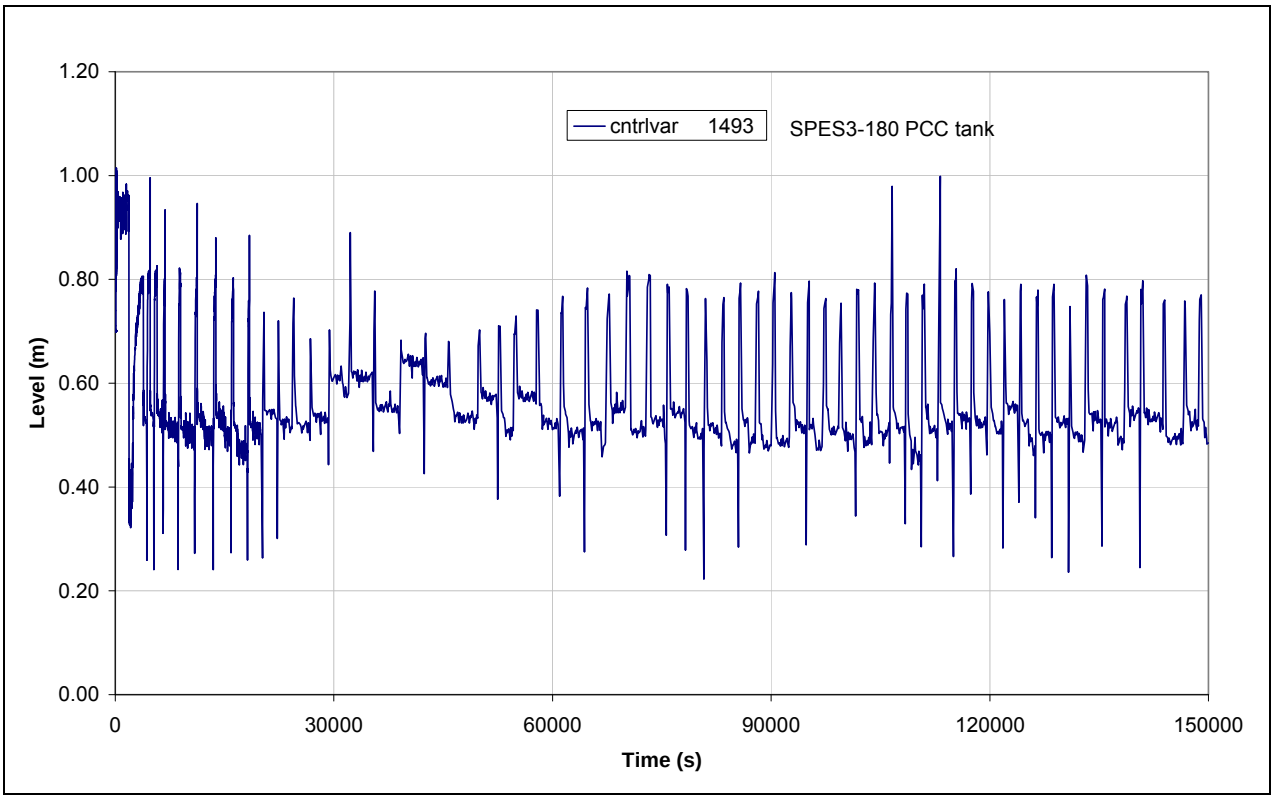

Fig.4.54 – SPES3-160 PCC inlet and outlet temperature

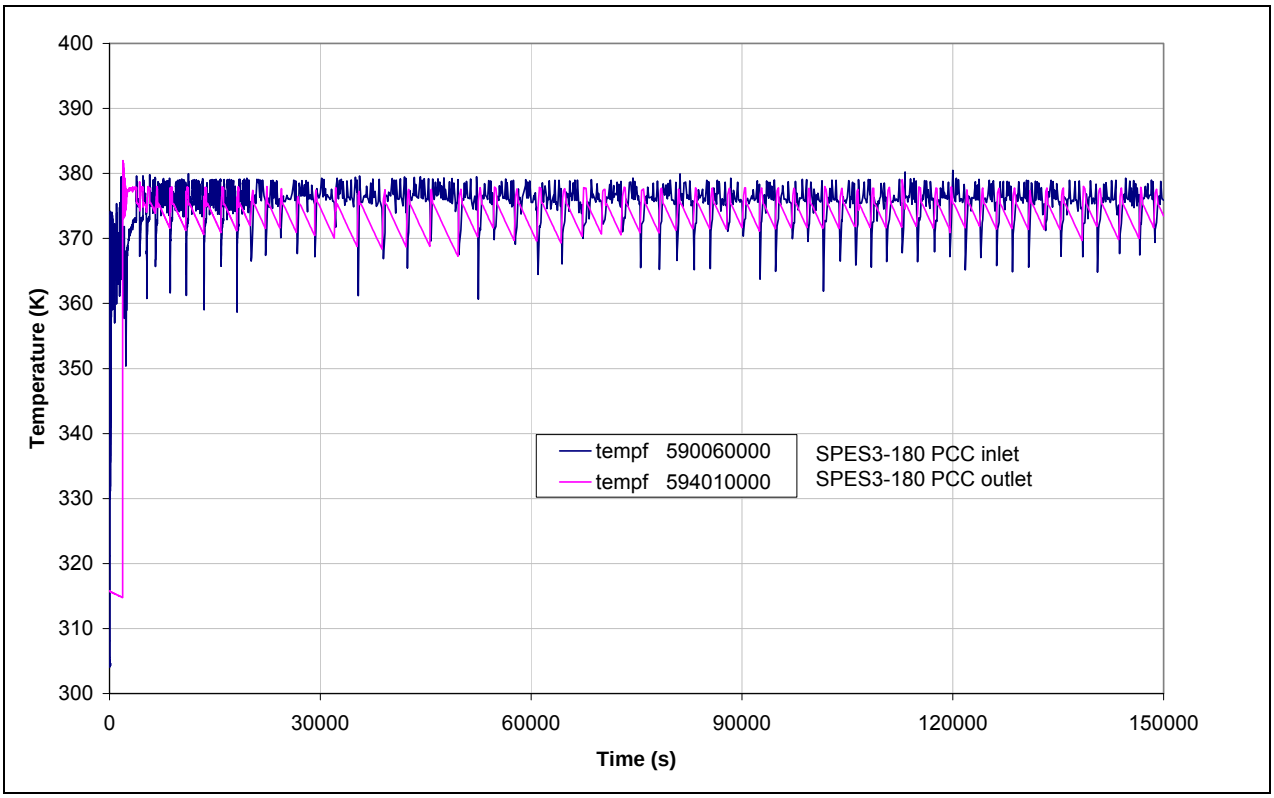

Fig.4.55 – SPES3-180 PCC liquid fraction (window)

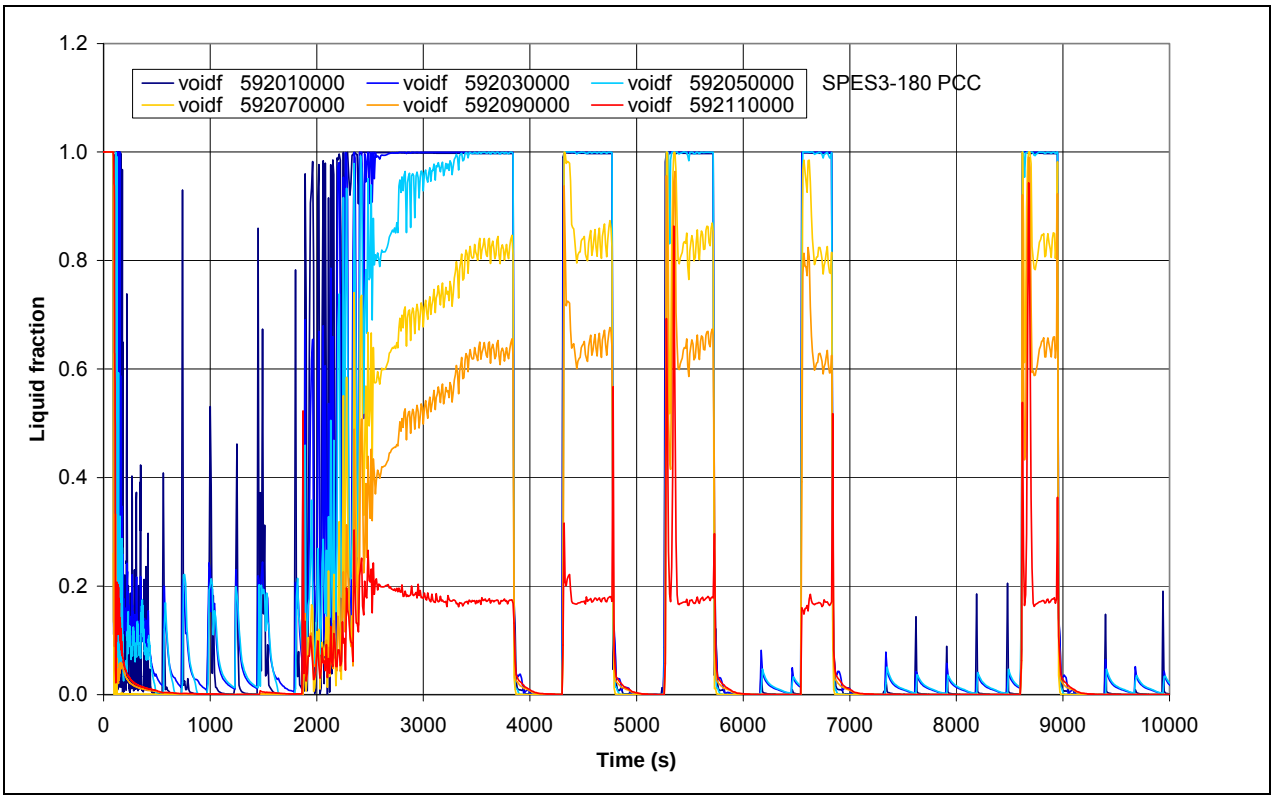

Fig.4.56 – SPES3-180 PCC liquid fraction

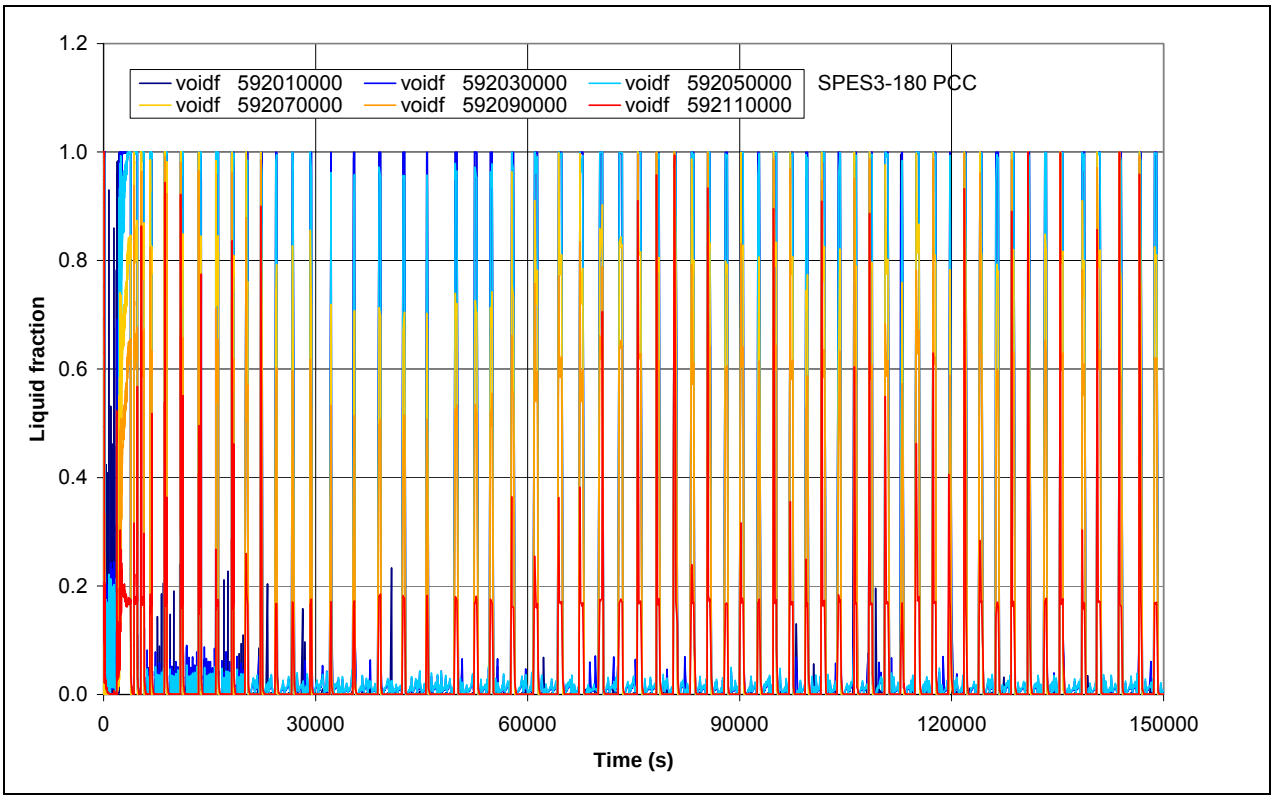

Fig.4.57 – SPES3-180 PCC power (window)

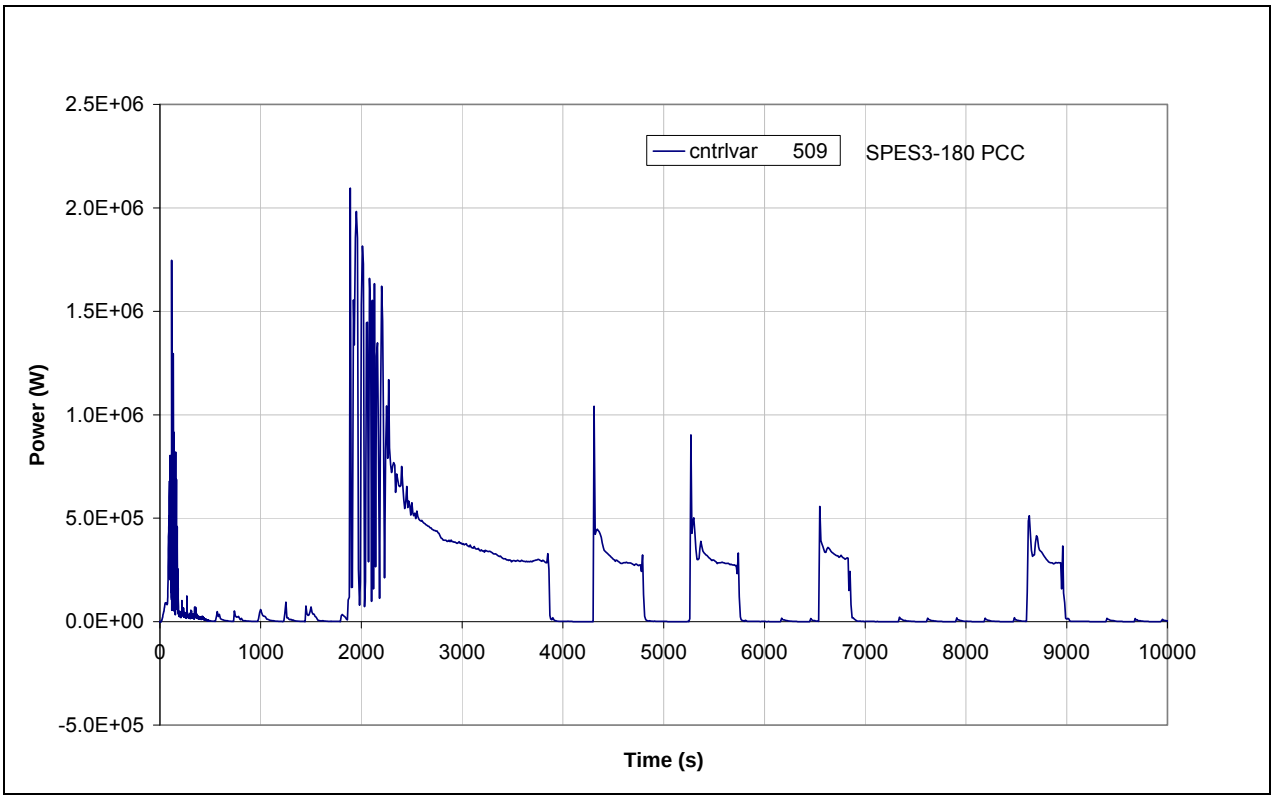

Fig.4.58 – SPES3-180 PCC power

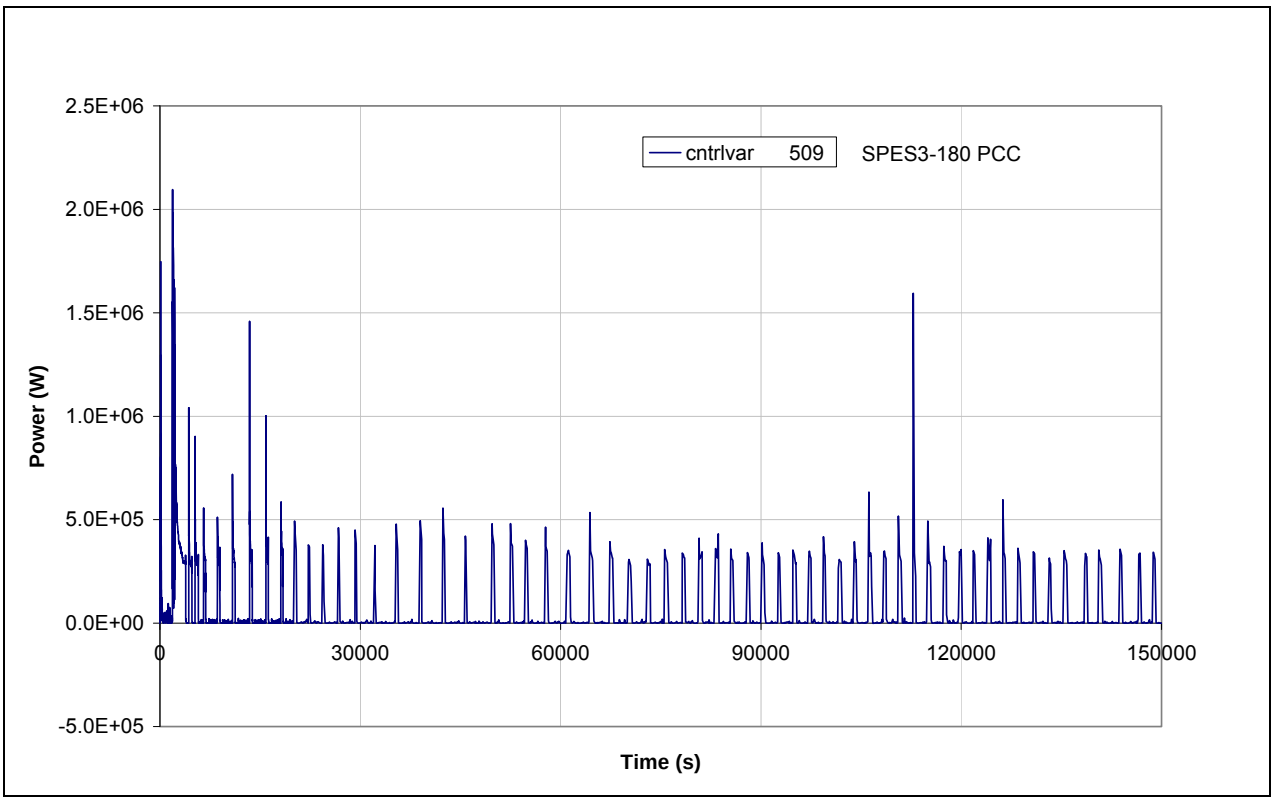

Fig.4.59 – SPES3-180 LGMS injection mass flow (window)

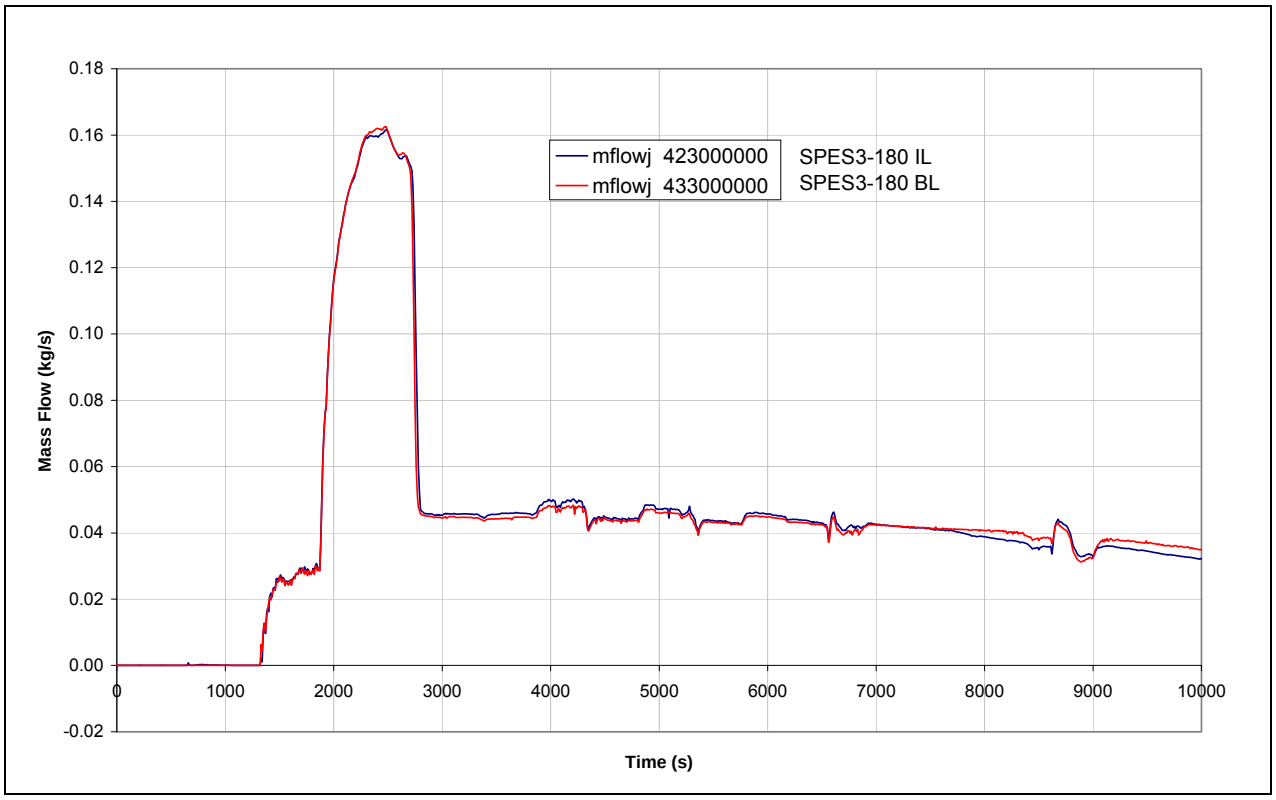

Fig.4.60 – SPES3-180 LGMS injection mass flow

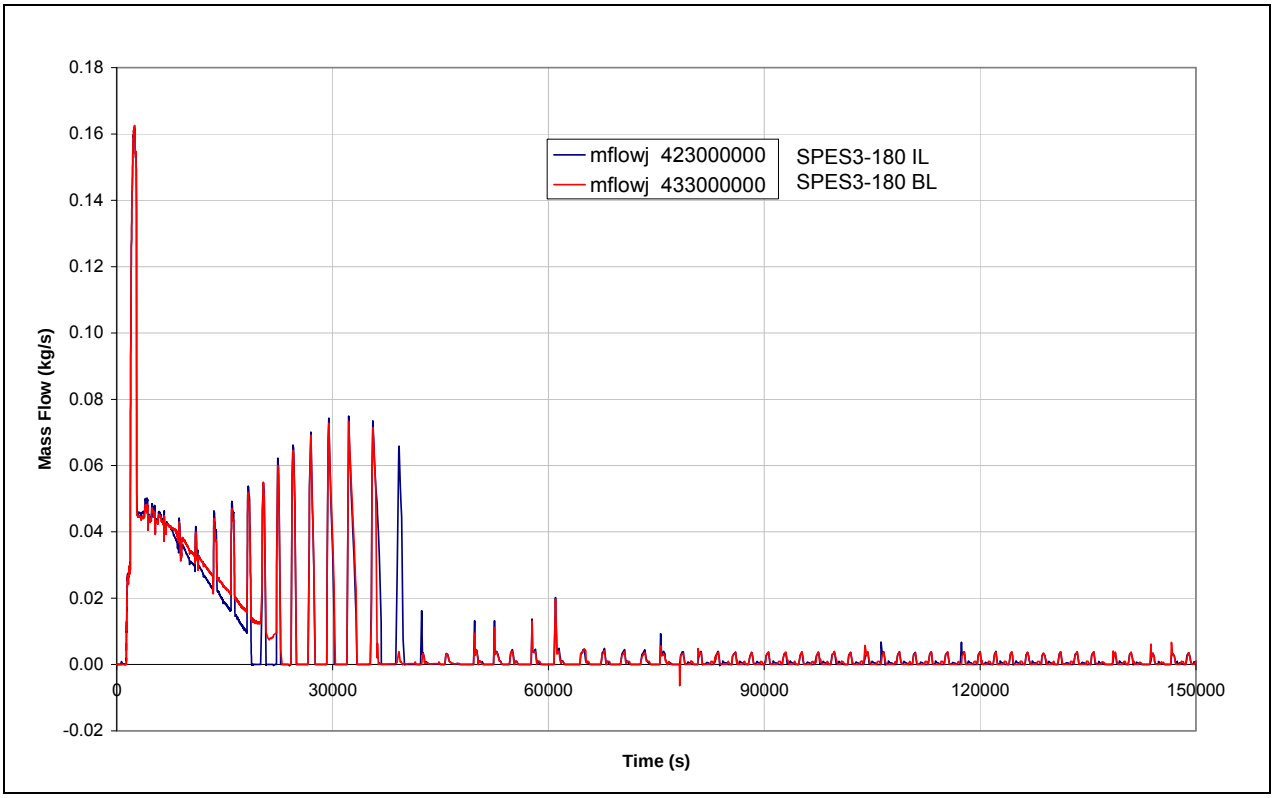

Fig.4.61 – SPES3-180 LGMS mass

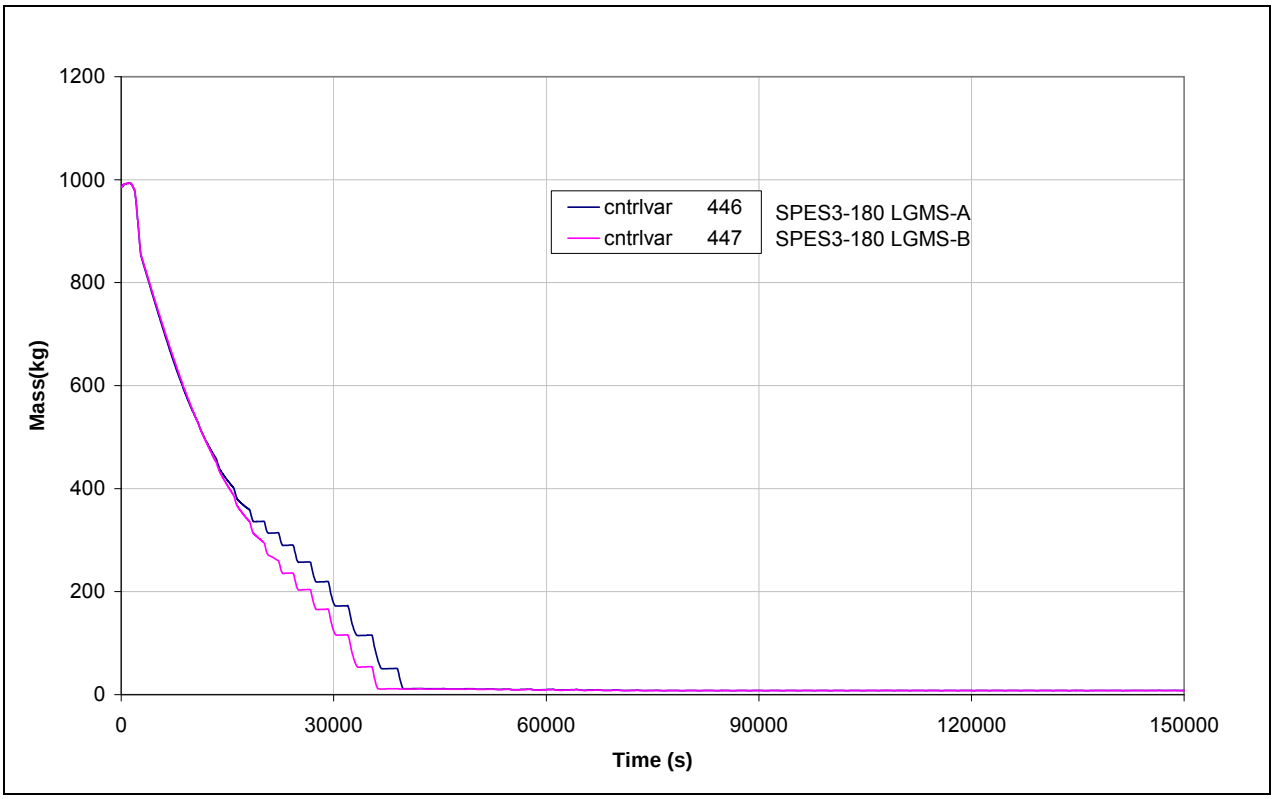

Fig.4.62 – SPES3-180 LGMS level

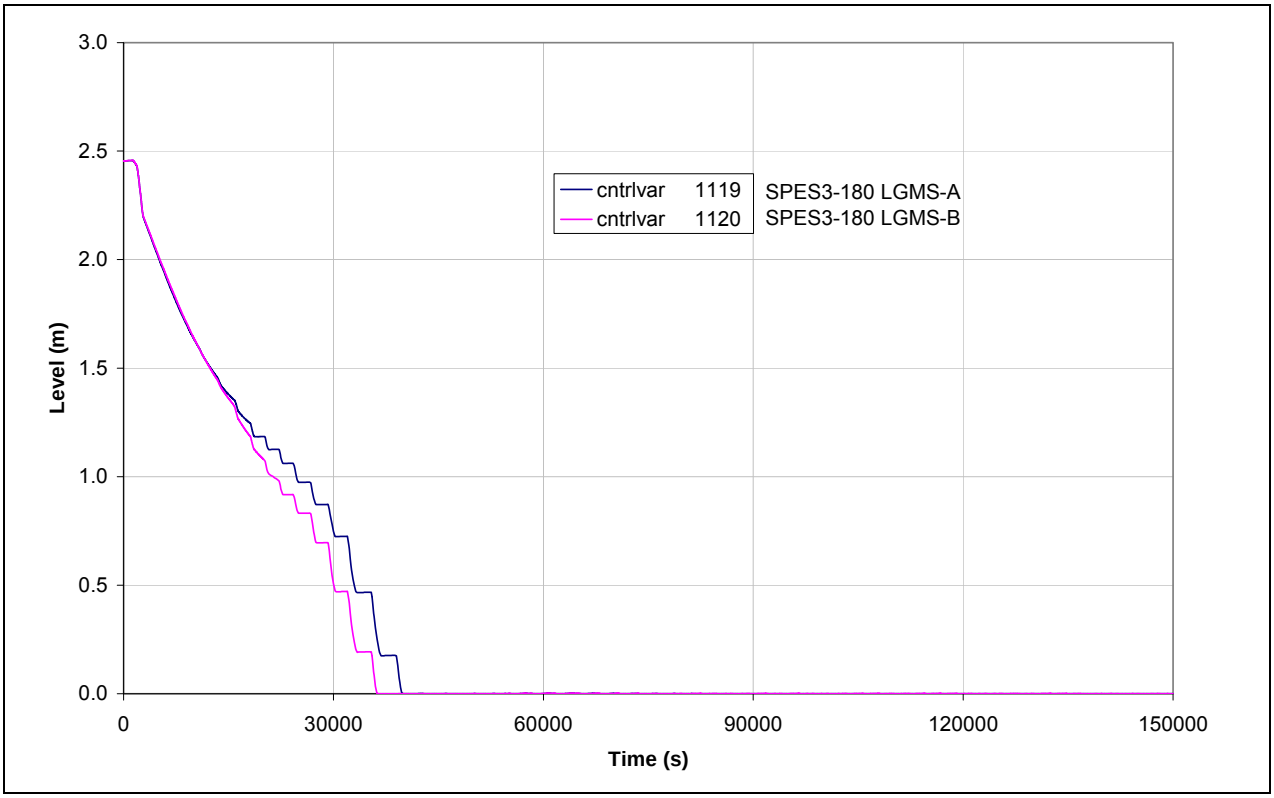

Fig.4.63 – SPES3-180 PSS and DW pressure (window)

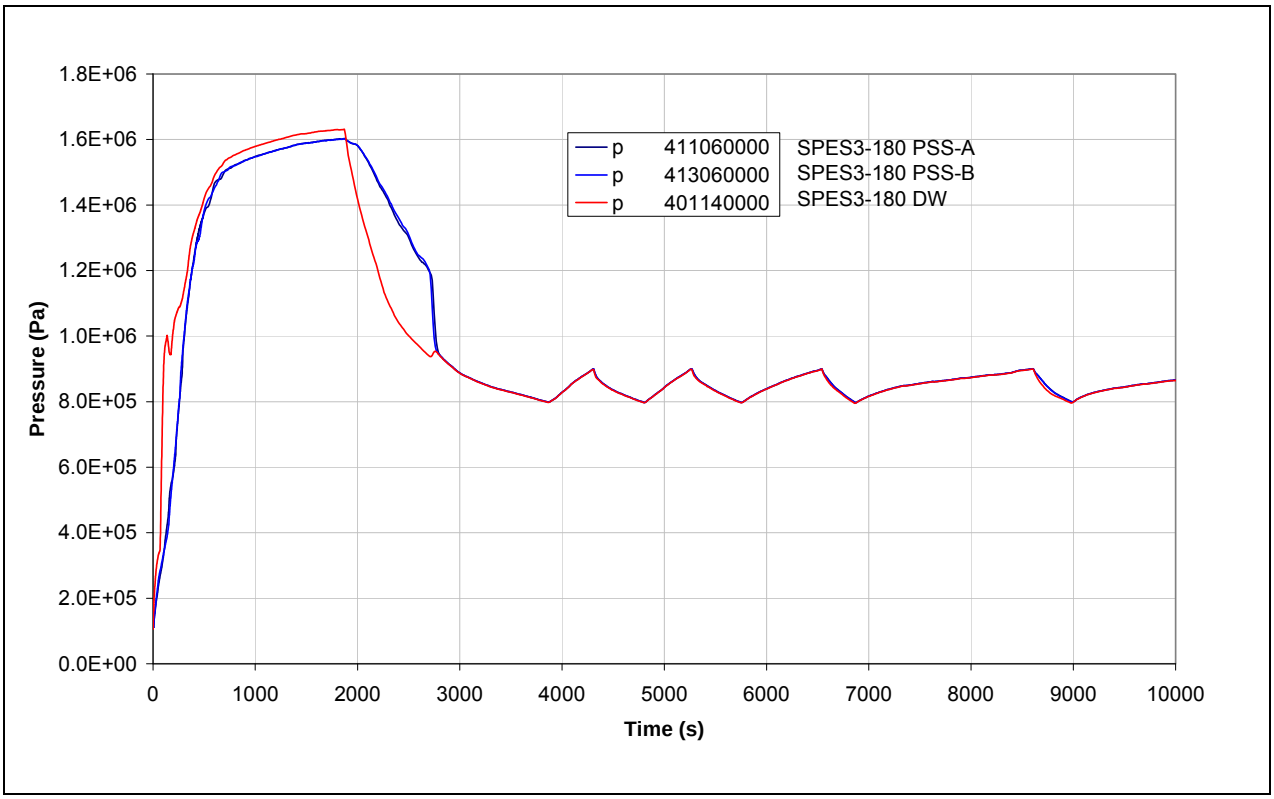

Fig.4.64 – SPES3-180 PSS and DW pressure

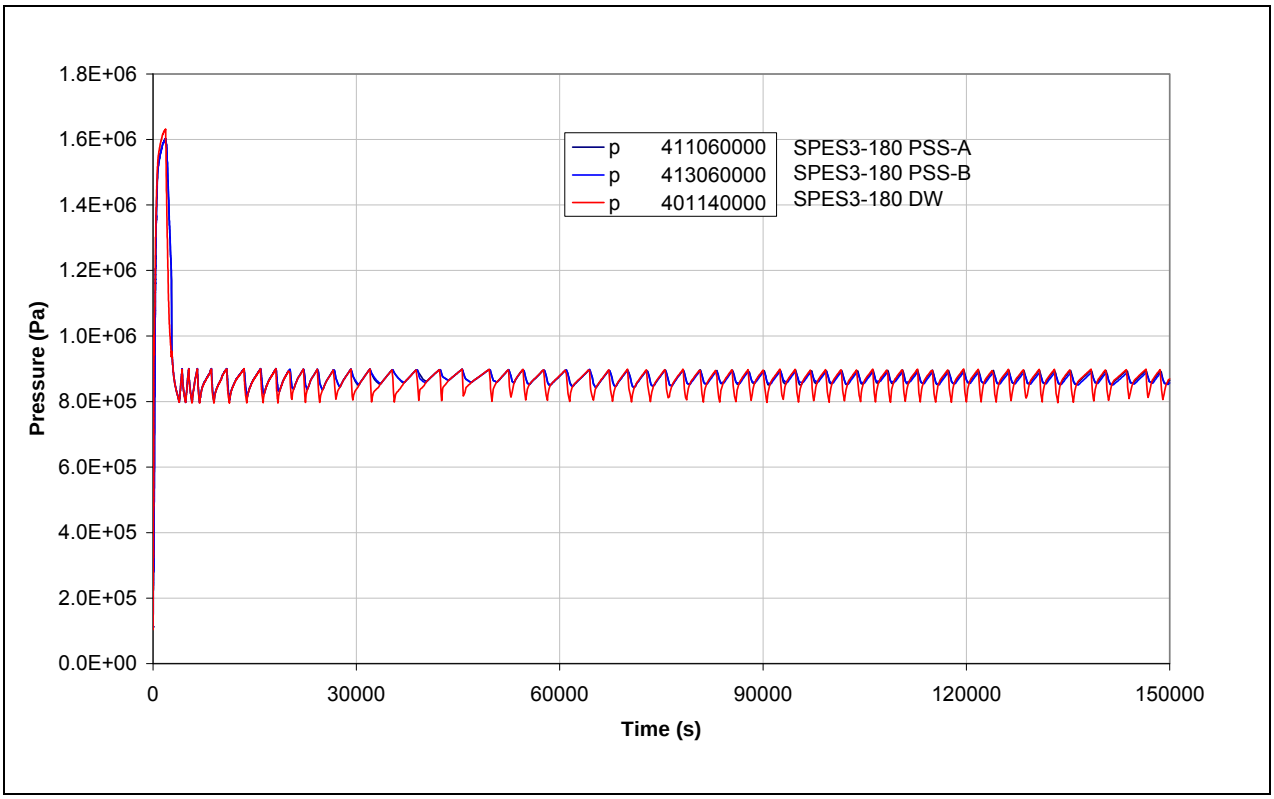

Fig.4.65 – SPES3-180 PSS vent pipe level (window)

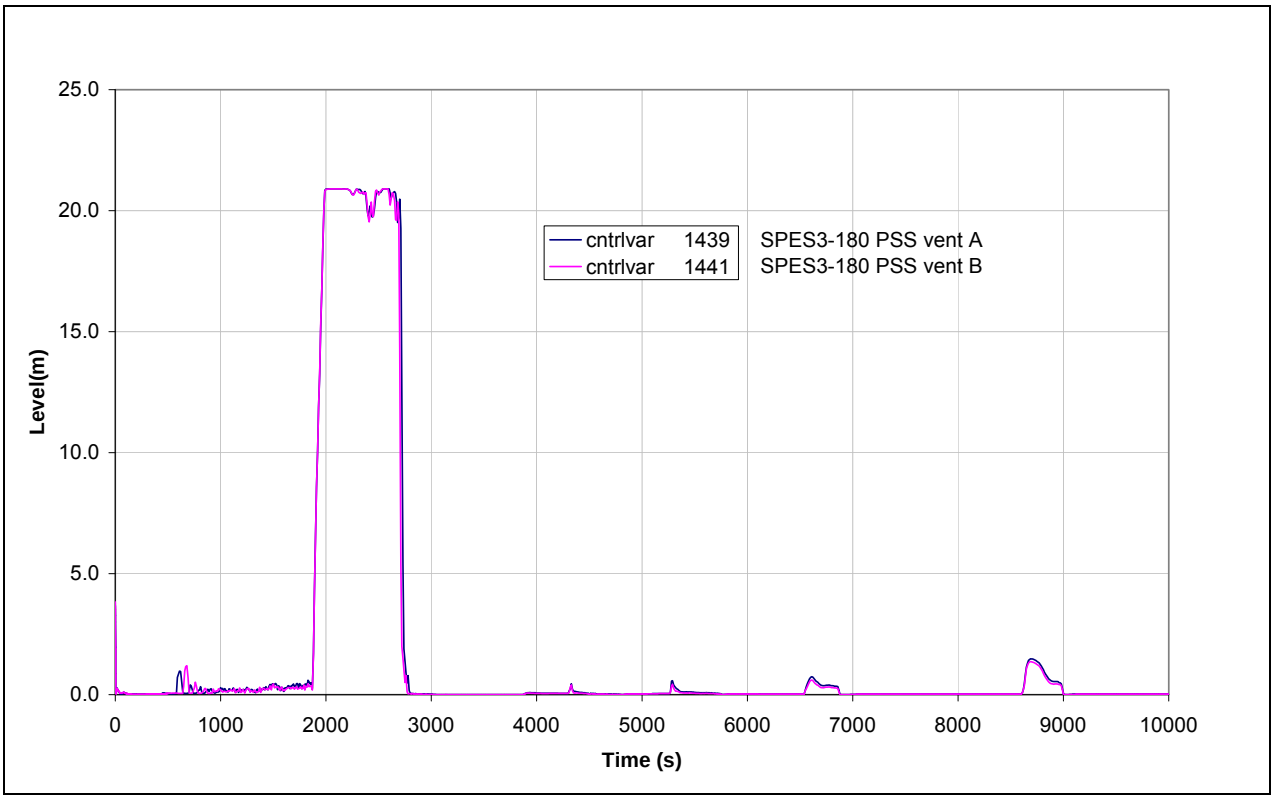

Fig.4.66 – SPES3-180 PSS vent pipe level

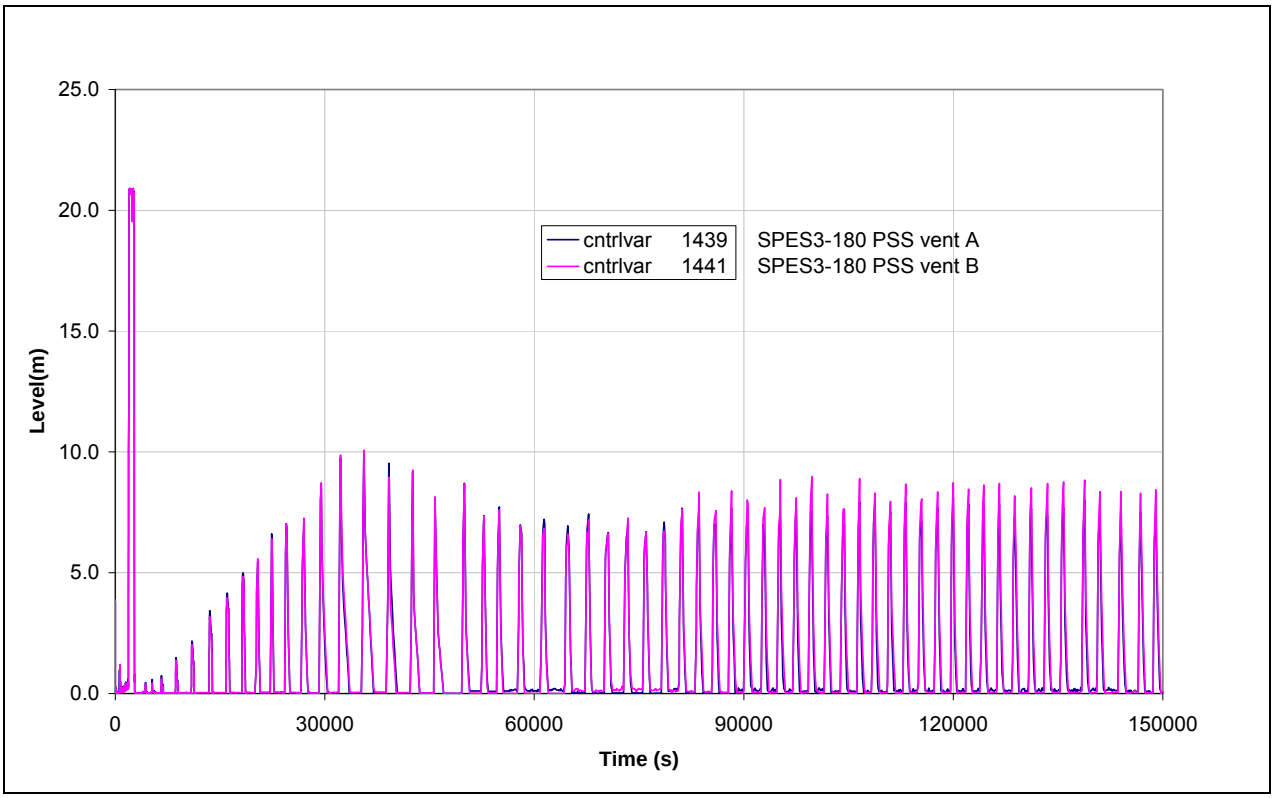

Fig.4.67 – SPES3-180 PSS level (window)

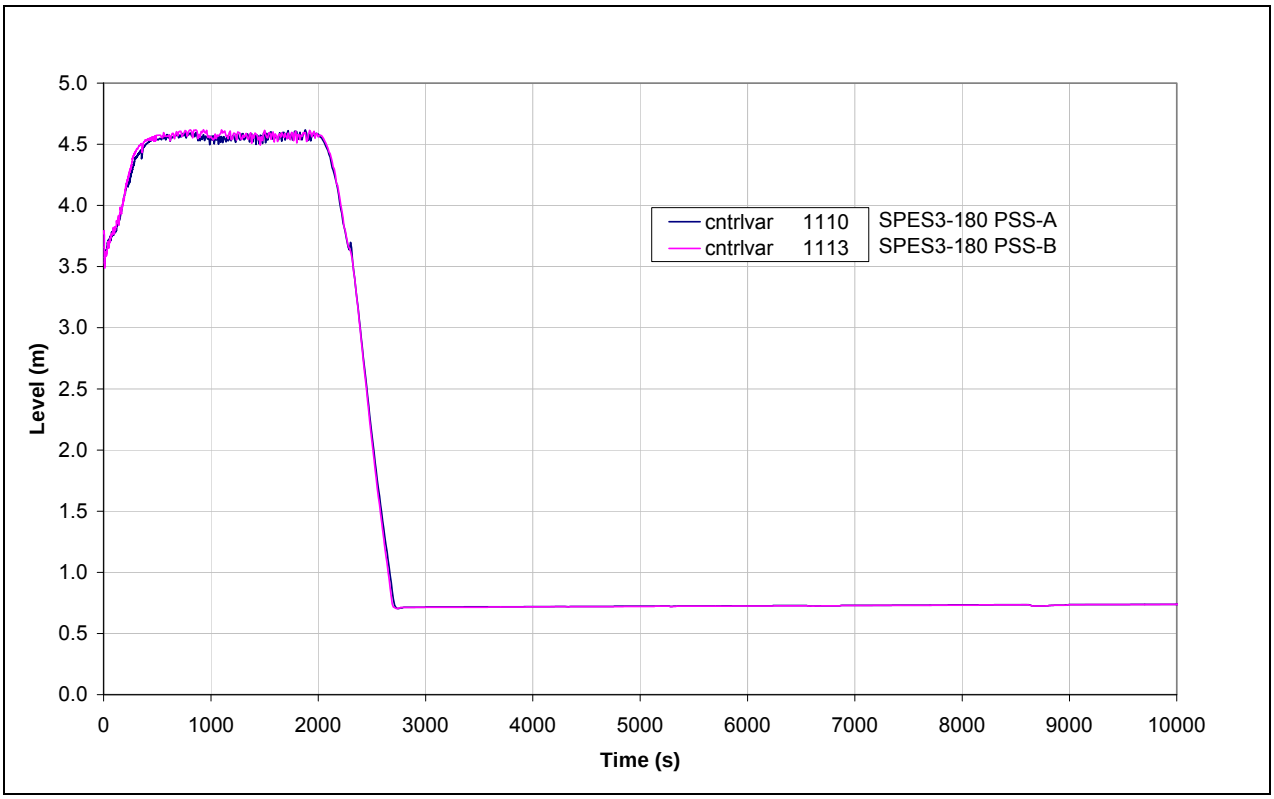

Fig.4.68 – SPES3-180 PSS level

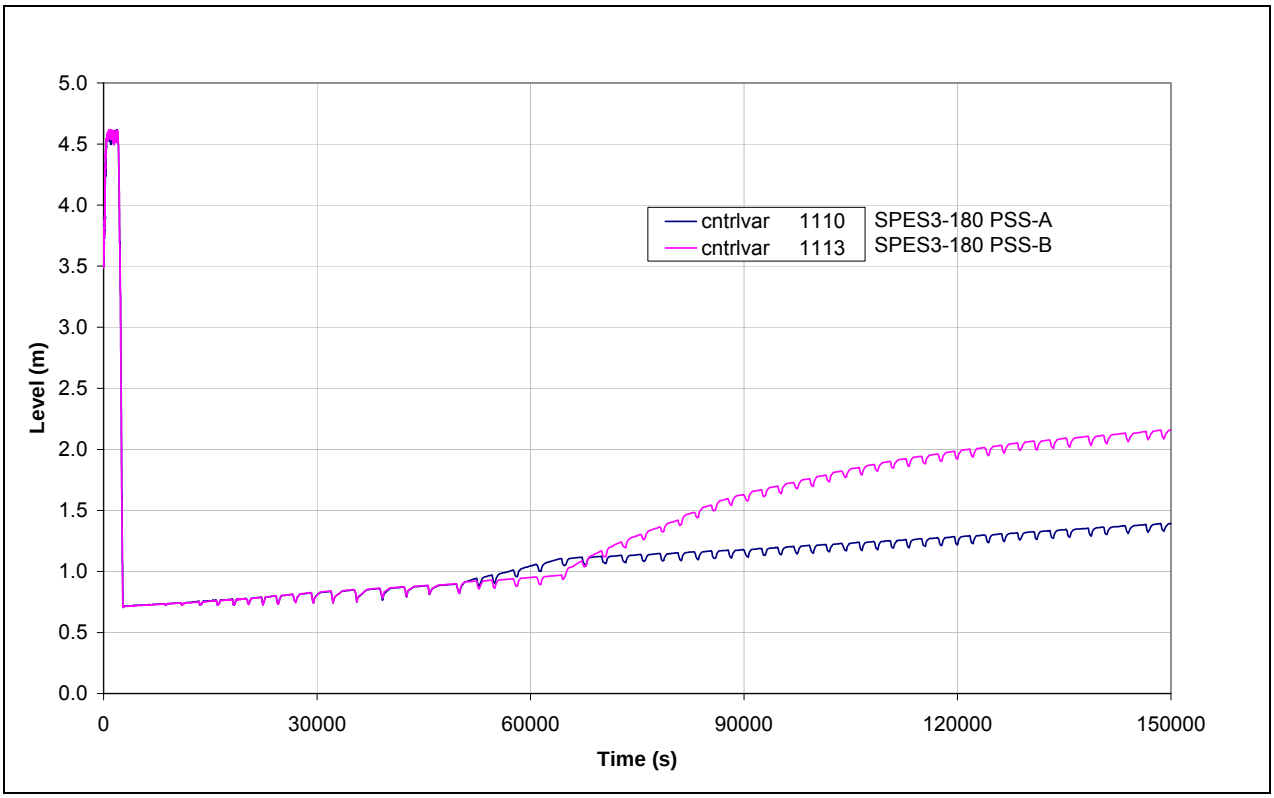

Fig.4.69 – SPES3-180 PSS mass

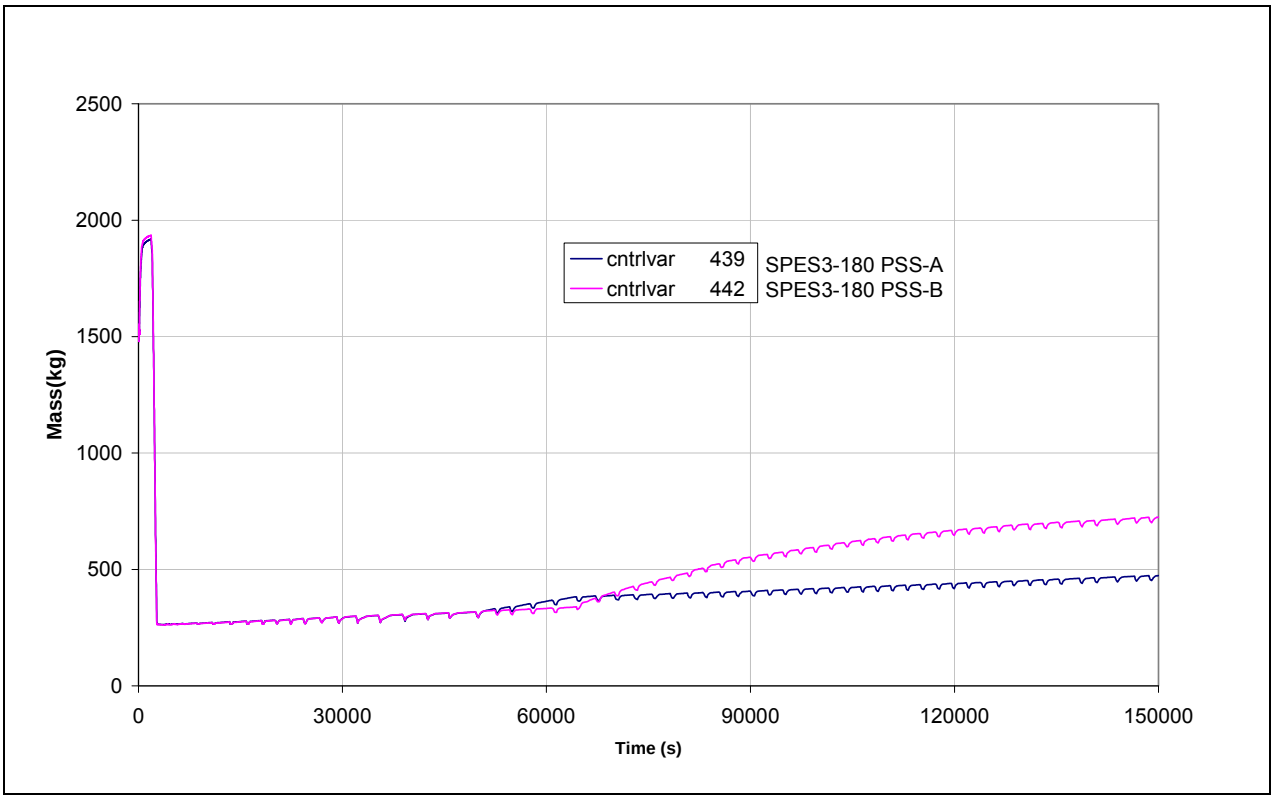

Fig.4.70 – SPES3-180 RC level (window)

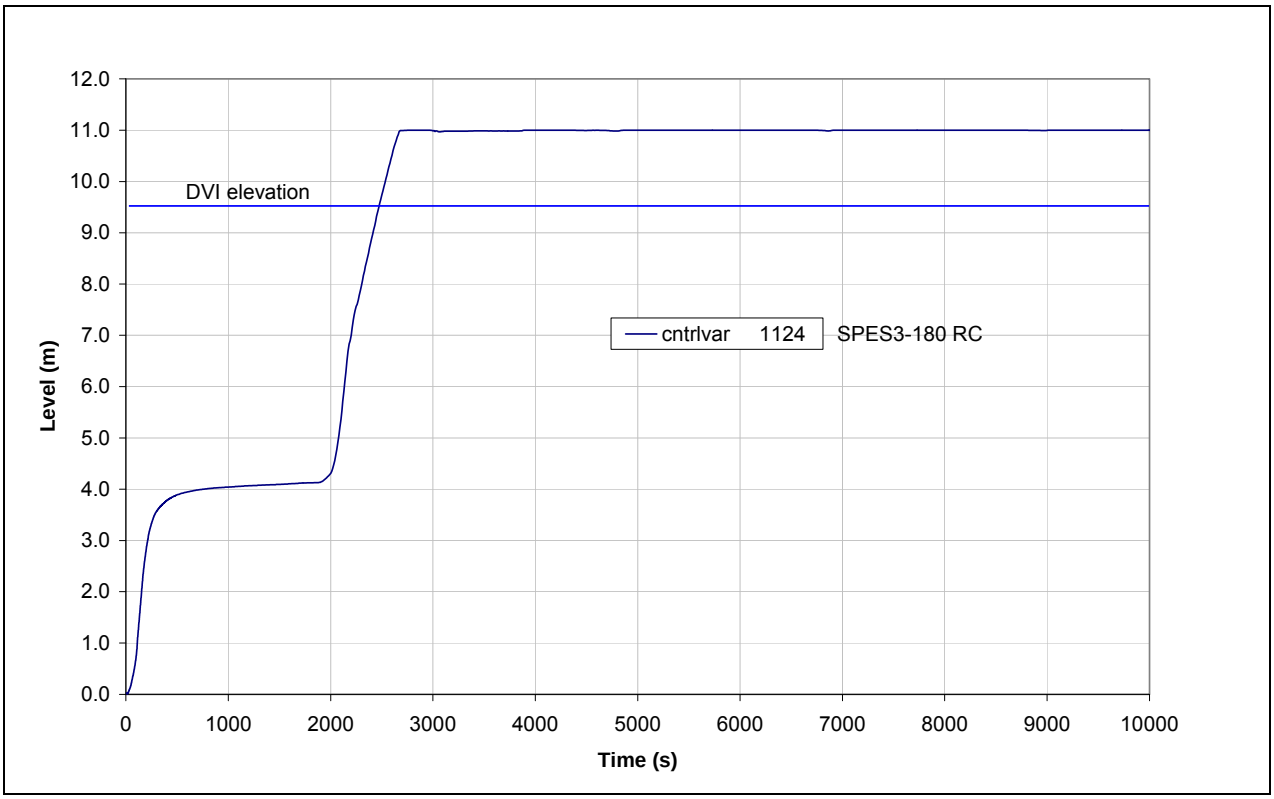

Fig.4.71 – SPES3-180 RC level

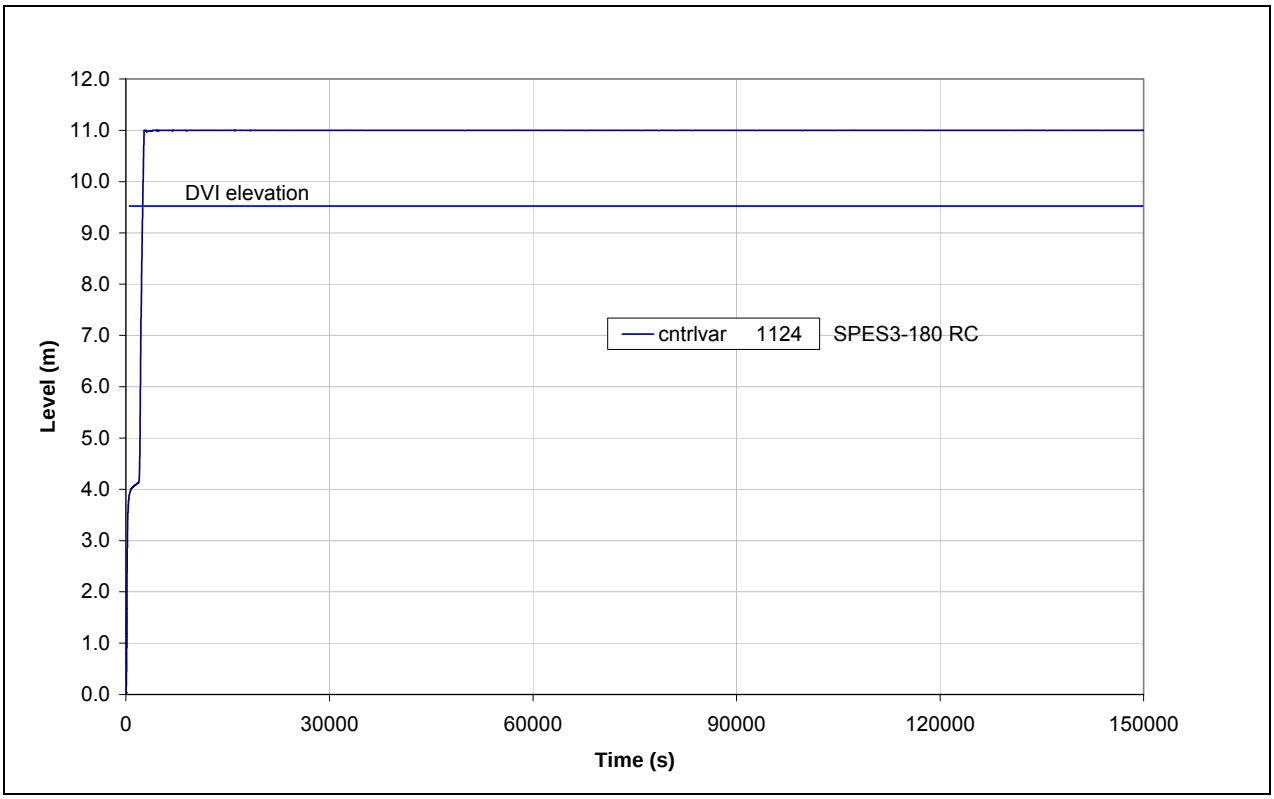

Fig.4.72 – SPES3-180 RC to DVI line mass flow

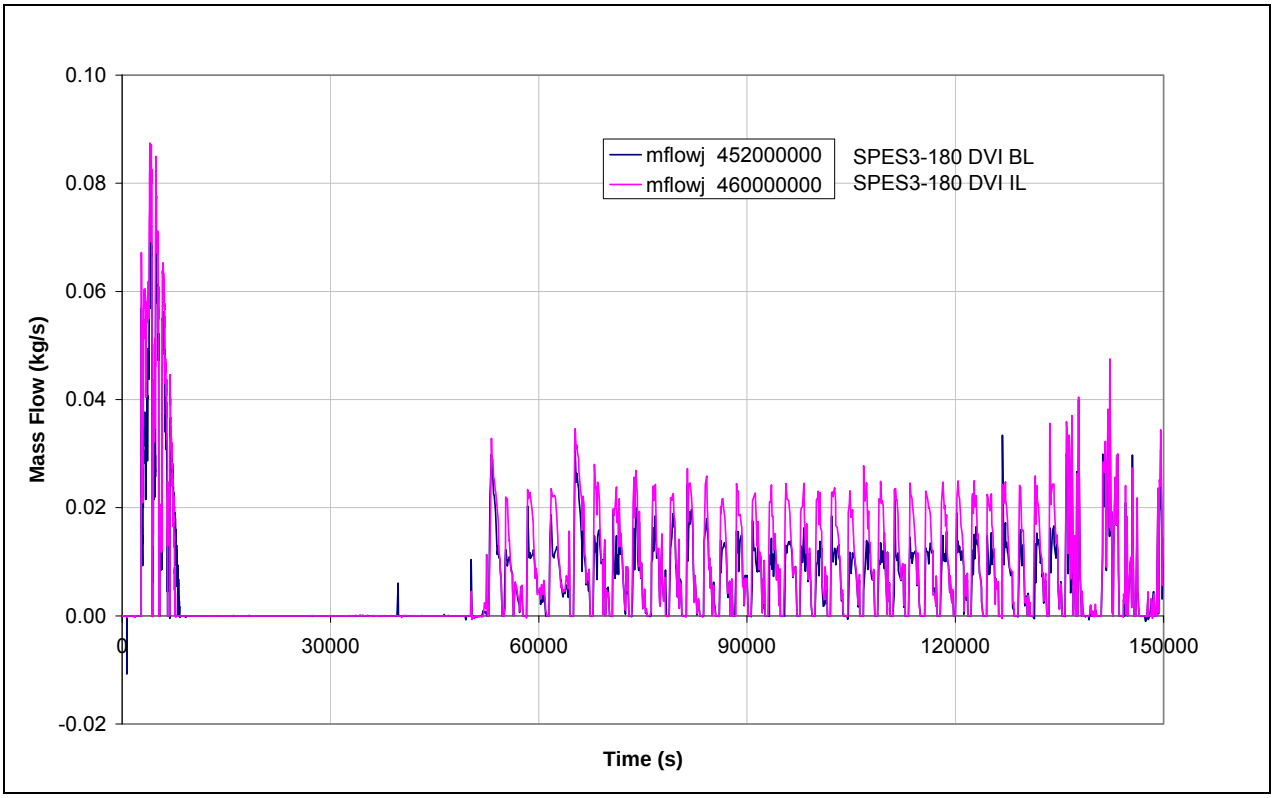

Fig.4.73 – SPES3-180 DVI line mass flow

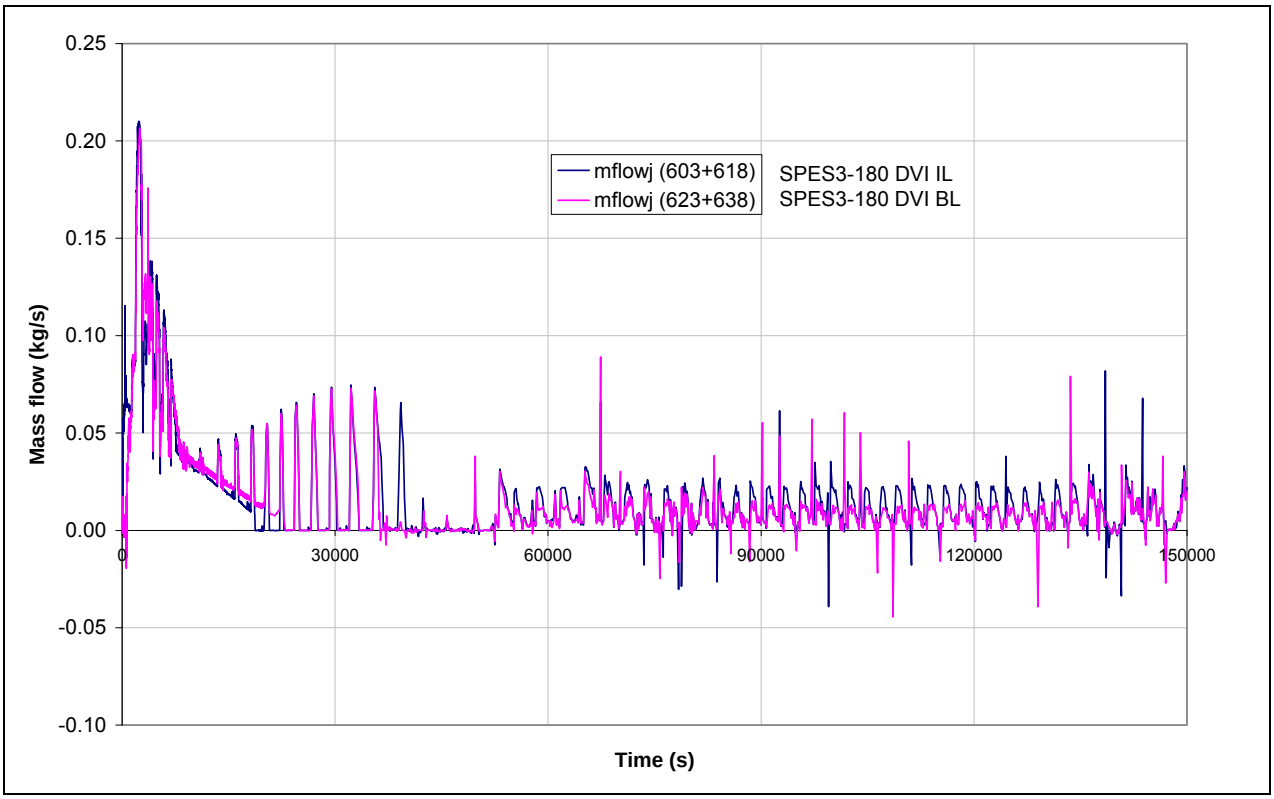

Fig.4.74 – SPES3-180 DW level

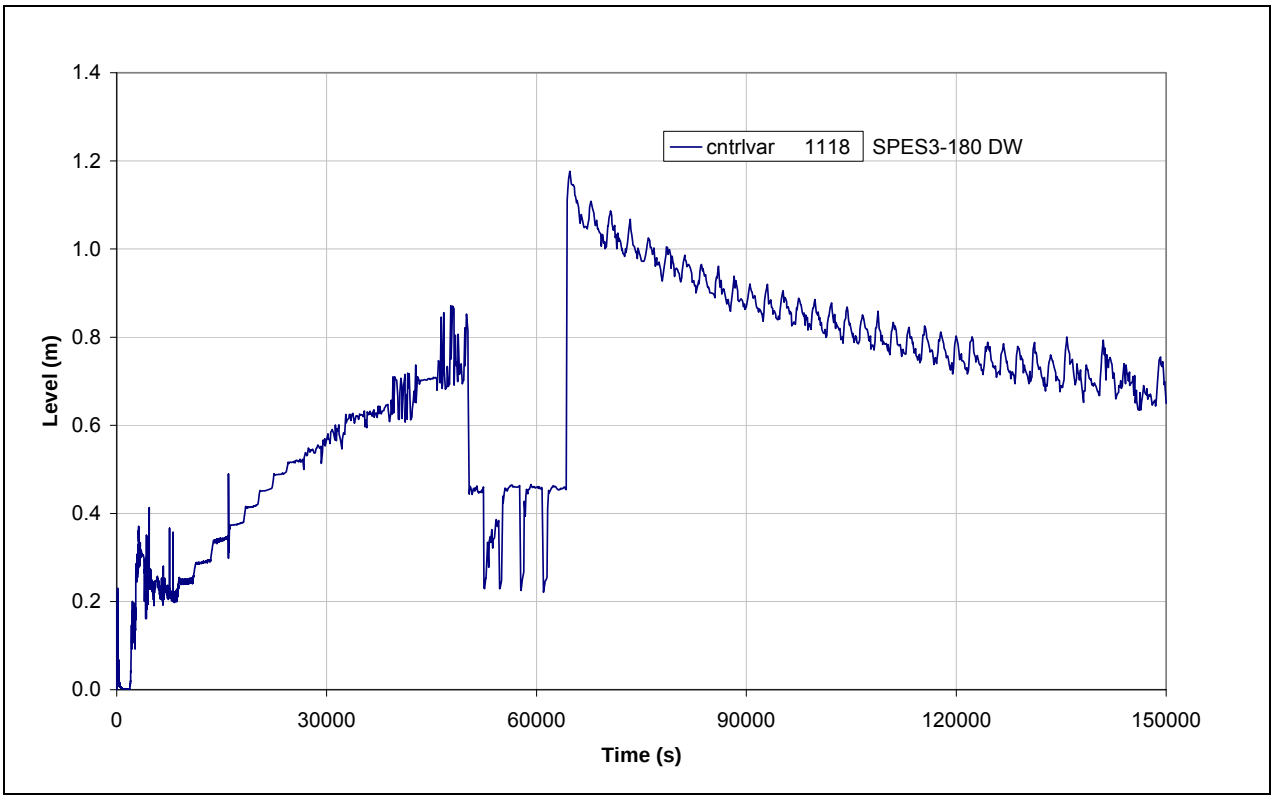

Fig.4.75 – SPES3-180 DW mass

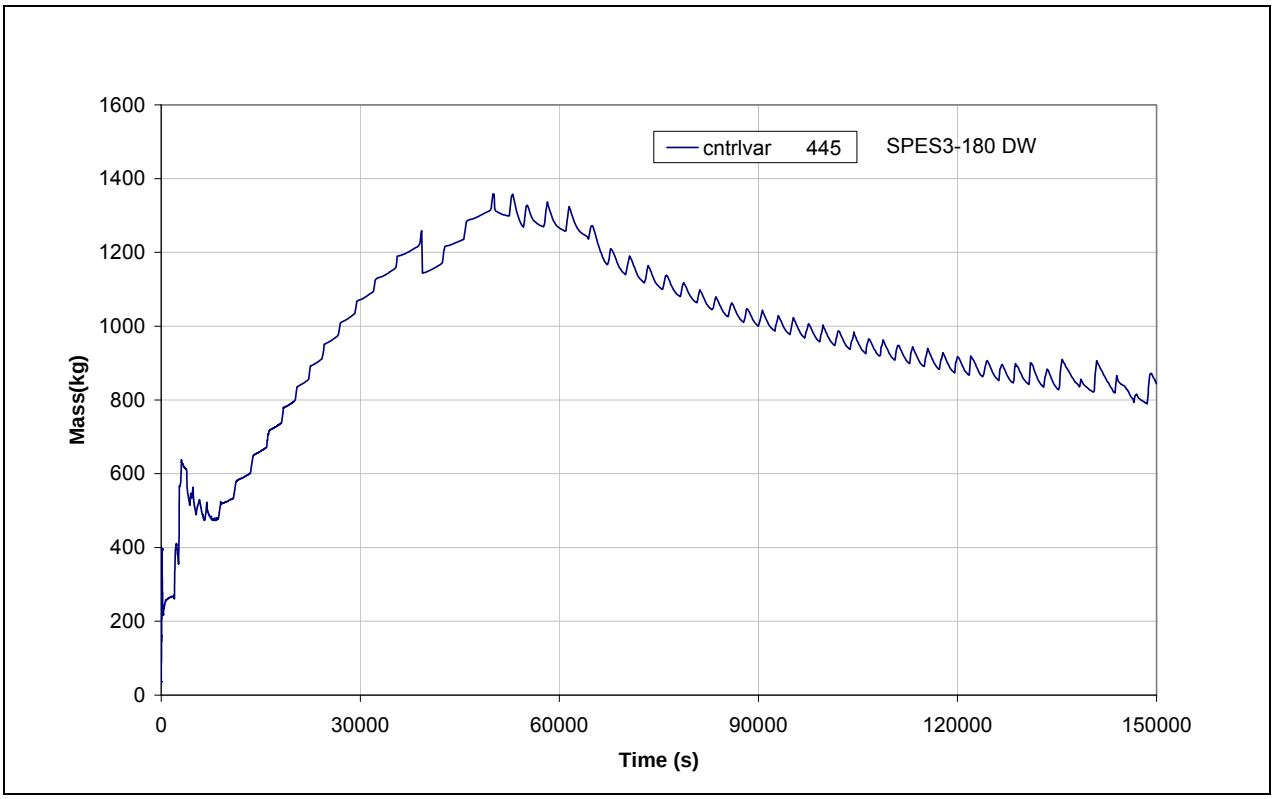

Fig.4.76 – SPES3-180 DW to RC mass flow (window)

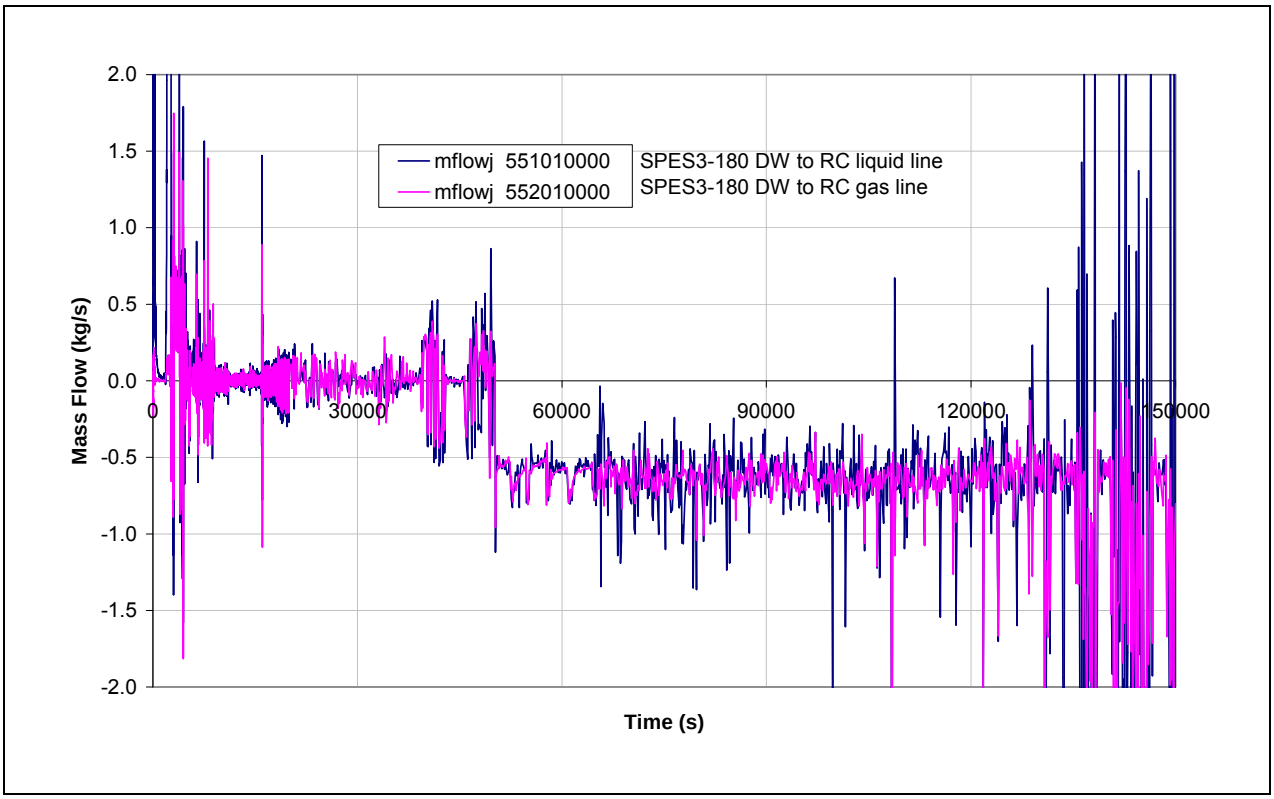

Fig.4.77 – SPES3-180 QT level

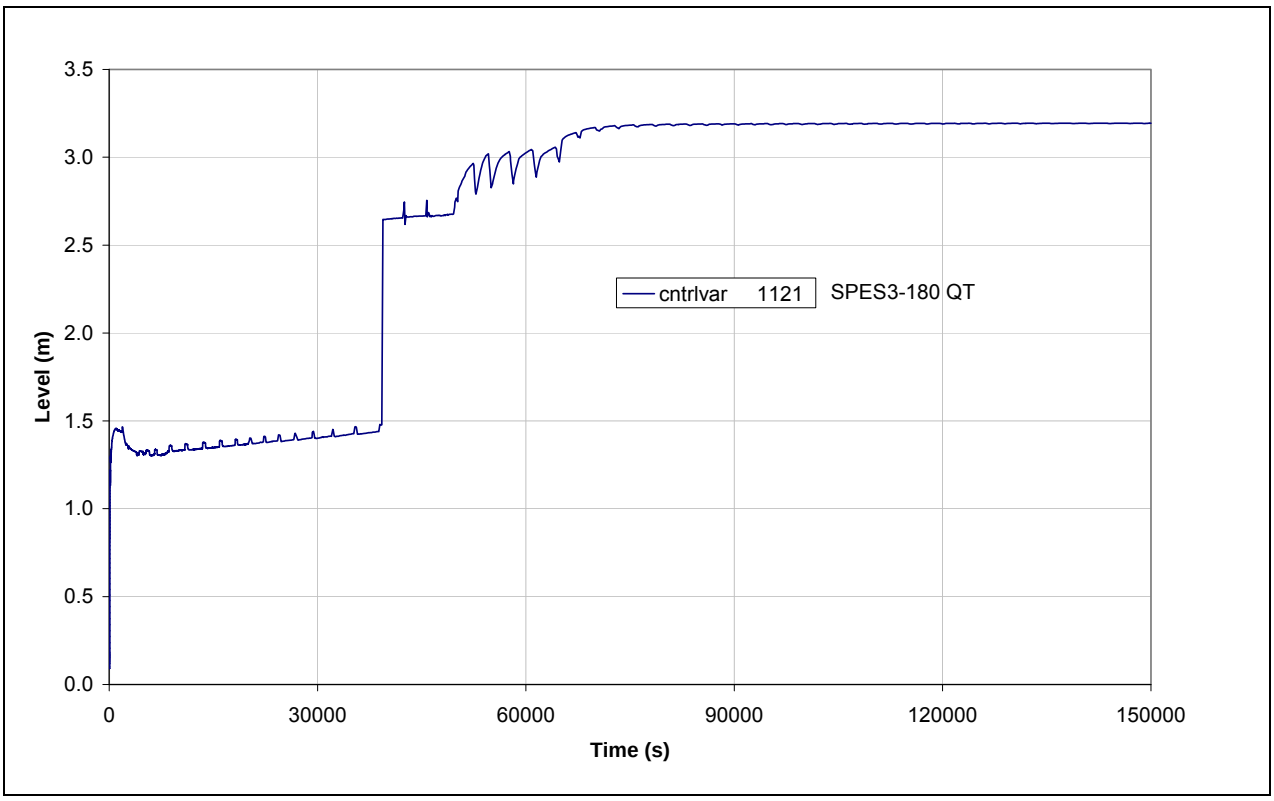

Fig.4.78 – SPES3-180 QT mass

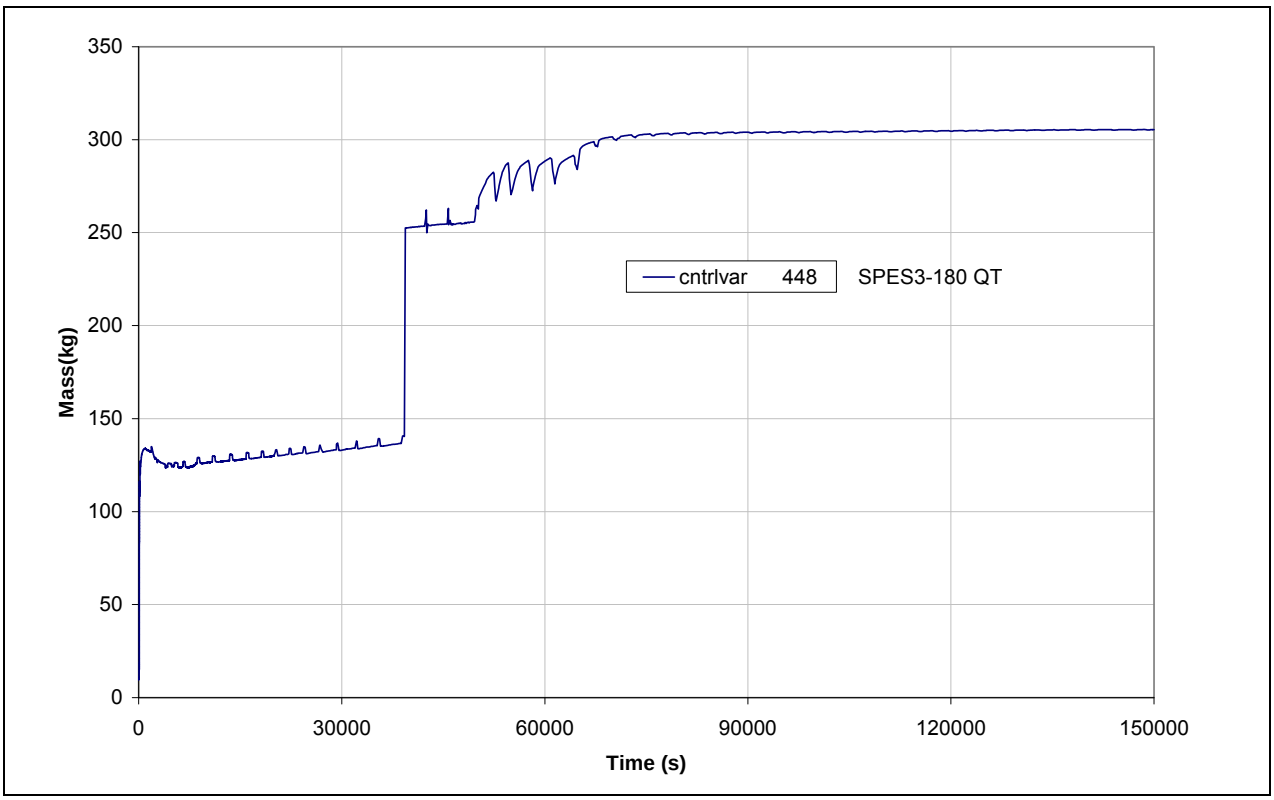

5. DBE DVI LINE 1-INCH EQUIVALENT SPLIT BREAK: SPES3-179

The design basis event of the DVI line split break is foreseen in the test matrix for SPES3 experimental program [1]. It is a 1-inch equivalent SBLOCA from the DVI-B, discharging directly into the reactor cavity.

SPES3-179 case is based on SPES3-175 nodalization, with 13 tubes SGs and the safety system actuation sequence typical of the design basis events [20].

SPES3-179 starts from steady conditions at 65% power, in order to investigate the actual SPES3 test conditions.

The RELAP5 nodalization used for SPES3-179 case is shown in Fig.3. 4, Fig.3. 5, Fig.3. 6.

The only changes in the model, with respect to SPES3-175 case, concern the break valves: the DVI-B line valve configuration is set to simulate a split break (i.e. a hole in the pipe), by opening the valve 666, Fig.3. 6, properly equipped with a 1-inch equivalent area orifice. The RC to DVI line orifice is set to 7 mm diameter for the mtrvlv 452 to correct a mistake in SPES3-175 (where it didn't affect the results).

The following paragraphs describe the DBE DVI line split break transient results.

5.1 SPES3-179

Steady conditions at 65% power, starting point for the transient, are summarized in Tab.4. 1.

The list of the main events occurring during the transient, with timing and quantities, is reported in Tab.5. 1.

5.1.1 SPES3-179 transient phases and description

The first 10 s of data (-10 s to 0 s) are steady state conditions.

All times of the events are given with respect to the break time, assumed as time 0 s.

The main phases of the transient are shortly summarized here, while a more detailed description is provided in the followings.

- The break opening causes RPV blowdown and depressurization, the containment pressurization, steam dumping into PSS with air build-up at PSS top and consequent pressurization;
- the S-signal (high DW pressure) triggers the reactor scram, the secondary loop isolation and EHRS-A and B actuation;
- the low PRZ water level signal triggers the pump coast-down and natural circulation in the core is guaranteed through the check valves connecting riser and downcomer, at one third of SG height; circulation lasts until the RI-DC check valves are covered;
- the LM-signal (high DW pressure and low PRZ pressure) triggers the ADS Stage-I to help RPV depressurization; triggers the EBT intervention, to inject cold borated water into the primary circuit; and actuates the EHRS-C;
- the low differential pressure signal between RPV and DW triggers the LGMS injection into the DVI line and opens the valves connecting RC and DVI line to increase the water reverse flow from the containment to the primary side;
- the PSS pressurization is never sufficiently high to overcome the PSS vent pipe gravity head and allow cold water flow from PSS to DW;
- the low LGMS mass signal opens the ADS stage-II, connecting the primary and containment systems at high elevation in the plant, with primary and containment pressure equalization and enhancement of flow from DW to RPV;

- in the long term, the plant is cooled by the EHRSs that reject the core decay heat to the RWSTs.

Break

The break line mass flow (SPLIT line), directly discharging into the RC, is shown in Fig.5. 1, Fig.5. 2 and Fig.5. 3. The peak of flow of 0.479 kg/s is observed at 2 s.

The EBT intervention, at 433.52 s, causes a steeper RPV depressurization with reduction of break flowrate, Fig.5. 4, Fig.5. 5, Fig.5. 6.

At 2940 s, LGMSs start to inject into the DVI lines. At 2970 s the containment pressure overcomes the RPV one, with interruption of the break flowrate between 2970 s and 8470 s, Fig.5. 7, Fig.5. 8, Fig.5. 9.

The break mass flow interrupts between 2970 s and 8470 s, when the containment pressure is higher than the RPV pressure, Fig.5. 8. Later, after RPV and containment pressure are equalized, it is driven by the liquid head in the RPV, above the DVI line. It stops definitively around 117000 s, when the Down Comer level and the RC level reach the DVI line elevation, Fig.5. 10, Fig.5. 11, Fig.5. 12.

Blowdown, RPV depressurization, containment pressurization

The blowdown phase depressurises the RPV with mass and energy transfer to the containment. The PRZ pressure is shown in Fig.5. 5, Fig.5. 6.

While PRZ depressurizes, the containment pressure increases as shown in Fig.5. 9, Fig.5. 13, Fig.5. 14 up to reach the pressure peak of 0.861 MPa at 2750 s.

Pressure increase at 433 s is due to ADS Stage-I intervention that discharges mass and energy into the DW, Fig.5. 15, Fig.5. 16.

ADS flowrate shows a two-peak trend, with the second peak due to water entrainment from the PRZ. The first mass flow peak occurs at 444 s, with 0.482 kg/s from the ST and 0.861 kg/s from the DT. The second peak occurs at 500 s with 0.629 kg/s from the ST and 1.25 kg/s from the DT. Smaller peaks follow still due to liquid fraction. When RPV and DW pressures equalize, ADS Stage-I mass flow stops and DW pressure decreases thanks to LGMS injection into the RPV, Fig.5. 15, Fig.5. 9, Fig.5. 7.

Steam dumping into PSS

Containment space (DW and RC) pressurization causes transfer of steam-gas mixture from DW to PSS, through the vent lines, starting at 60 s with a step increase at the ADS Stage-I intervention (433 s) and lasting until mass flow exits the ADS-Stage-I, Fig.5. 17, Fig.5. 16. Mass transferred from DW to PSS is shown in Fig.5. 18.

Non-condensable gas quality in the DW is shown in Fig.5. 19, Fig.5. 20. Rapidly, Steam sweeps away gas from the DW, toward the PSS. Non-condensable gas re-enters the DW only after the LGMS are empty (~20000 s) and the PSS gas space, connected to the LGMS top, has free way toward the DVI and the containment again, through the break line and the ADS Stage-II (~24500 s). In the long term of the transient, the DW non-condensable gas quality stabilizes around 0.55.

Steam is dumped underwater through the PSS sparger and air pressurizes the PSS and LGMS gas space, Fig.5. 21, Fig.5. 22, Fig.5. 23, Fig.5. 24. PSS and LGMS pressure follows the DW pressure trend, Fig.5. 25, Fig.5. 26, but PSS pressurization never reaches values high enough to overcome the PSS vent line gravity head and push water backward to the DW. PSS and LGMS pressure remains above the DW pressure until the break get uncovered and gas can flow from the LGMS to the RC, through the break line. The water level in the PSS vent pipes is shown in Fig.5. 27. It reaches the top around 6500 s, but only for a few seconds with no injection from PSS to DW.

The lack of water injection form PSS to DW limits the water availability to be injected back from containment to RPV and the RC level never reaches the top, Fig.5. 11.

The PSS water temperature increases, thanks to the mass transfer from the DW, Fig.5. 28. Both liquid and gas temperatures are reported in Fig.5. 28. Liquid and gas temperatures are similar both during the pressurization phase and in the long term, with PSS-A temperature higher than PSS-B of about 4 °K.

Temperatures always remain below saturation, Fig.5. 22, Fig.5. 28.

S-Signal: Reactor scram, secondary loop isolation, EHRS-A and B actuation

The high containment pressure set-point (1.7e5 Pa), reached at 122.96 s, triggers the S-signal.

The S-signal (Safeguard) starts the reactor SCRAM, isolates the three secondary loops and actuates the EHRS-A and B.

Power released to fluid in the core is shown in Fig.5. 29 and Fig.5. 30 together with power removed by the SGs. Steady state power is 6.5 MW. After the scram signal, the reduced power curve continues at 6.5 MW for 3.35 s, until it intersects the nominal decay power curve.

The peak of power, removed by the SGs, occurs following the EHRS-C intervention. After about 30000 s, a balance is reached between core and SG power.

The MFIV and MSIV of secondary loops are contemporarily closed in 5 s. Secondary loop mass flows are shown in Fig.5. 31, Fig.5. 32. They stop at secondary loop isolation and re-start at EHRS actuation. EHRS-A and B are actuated at secondary side isolation and natural circulation flow establishes. EHRS-C is actuated at LM-signal (LOCA mitigation), starting secondary loop natural circulation after 310 s from the loop isolation.

EHRS-A and B are actuated by opening in 2 s the related isolation valves (EHRS-C is actuated later on LM-signal). The peak mass flow of 0.263 kg/s is reached at 129 s. Between 1000 s and 8000 s, quite steady condition is reached with natural circulation flow of about 0.15 kg/s in the loops A and B, Fig.5. 33. After 8000 s, larger oscillations appear and mass flow decreases to low values around 0.02 kg/s in the long term, Fig.5. 34.

Power removed by EHRSs is shown in Fig.5. 35, Fig.5. 36. The EHRS-A and B peaks of removed power occurs at 285 s with 372 kW removed, each. The EHRS-C removed power peak occurs at 590 s with 716 kW value. Average power removed by EHRS-A and B in the long term is around 10.4 kW each.

The secondary side pressures are shown in Fig.5. 37, Fig.5. 38. After isolation, pressure increases due to heat transfer from the primary side that makes water contained in the SG tubes evaporate, up to reach 1.04 MPa at 183 s in SG-A, 1.07 MPa at 184 s in SG-B and 1.13 MPa at 185 s in SG-C. SG tube levels decrease until water stored in EHRS heat exchangers is poured into the loops and power begins to be removed, Fig.5. 39, Fig.5. 40.

Pump coast-down and primary circulation through RI-DC check valves

PRZ level is shown in Fig.5. 41. The early phase of level decrease, until ADS Stage-I intervention (433.5 s), is due to loss of mass from the break. Level increase, after the ADS Stage-I actuation, is due to suction at ADS nozzles with water entrainment that causes the ADS mass flow peak at 500 s, Fig.5. 15. When the RPV and containment pressures equalize (2990 s), the ADS discharge stops and PRZ level decreases down to zero, Fig.5. 9, Fig.5. 41.

Liquid fraction at the pump inlet is reported in Fig.5. 42. Due to the loss of mass from the break, the pump uncovers soon.

The pump coastdown is triggered by the Low PRZ level signal delayed of 15 s and it starts at 280.82 s. The pump velocity curve is shown in Fig.5. 43 and the pump is completely stopped at 384 s. Run at reduced

velocity in the steady state, due to 65% power, the pump velocity decay curve intersects the full power one, continuing at constant velocity for 2 s after the coast-down signal. After the pump coast-down signal, circulation occurs through the pump by-pass, until the pump suction is completely uncovered (490 s), Fig.5. 44, Fig.5. 42.

The core inlet flow is shown in Fig.5. 45, Fig.5. 46. Soon after the pump coast-down signal, the core mass flow falls to zero (304 s) to restart when mass flow starts through the pump by-pass, Fig.5. 44.

The pump head decrease, at the pump stop, let the RI-DC check valves open (300 s SG-A and B; 304 SG-C) and natural circulation occurs from the riser to the SG annuli, at lower level in the RPV. Mass flow is shown in Fig.5. 47, Fig.5. 48 for each SG annulus and it lasts until the RPV level decreases below the RI-DC check valves.

The loss of mass from the break and RPV depressurization rapidly cause flashing of the primary circuit and void begins at core outlet at 448 s, Fig.5. 49, Fig.5. 50, Fig.5. 51. Low liquid fraction in the core lasts until about 4000 s, when RPV mass is made-up by LGMS injection. In the long term of the transient (~87000 s), void occurs again in the core when the natural circulation through the RI-CD check valves decreases for low level in the RPV, Fig.5. 52, Fig.5. 46, Fig.5. 10.

LM-Signal: EHRS-C, ADS Stage-I and EBT actuation

The LM-Signal (LOCA mitigation) occurs at 433.52 s, when the low PRZ pressure set-point (11.72e6 Pa) is reached, Fig.5. 5.

The LM-signal actuates the EHRS-C and opens the ADS stage-I and EBT actuation valves.

The EHRS-C is actuated by opening in 2 s its isolation valves. The peak mass flow of 0.547 kg/s is reached at 437 s. After the peak, quite steady natural circulation of about 0.30 kg/s is present between 3400 s and 9000 s. After that, strong oscillations appears and mass flow decreases, Fig.5. 33, Fig.5. 34.

Power removed by EHRS-C is shown in Fig.5. 35, Fig.5. 36. The EHRS-C peak of removed power occurs at 590 s with a value of 716 kW. Average power removed by EHRS-C in the long term is around 18.1 kW.

The three trains of ADS Stage-I are actuated contemporarily on LM-signal and the actuation valves are fully opened in 10 s. ADS Stage-I mass flows are shown in Fig.5. 15, Fig.5. 16.

When ADS intervene, PRZ is empty, Fig.5. 41, and the ADS flow peak of 1.343 kg/s, at 444 s, is due to steam flowing toward the QT. At ADS intervention, water is sucked upwards and the PRZ level increases. The second ADS mass flow peak of 1.879 kg/s, at 500 s, is caused by increasing liquid void fraction at the PRZ top that decreases when the PRZ empties. Mass exited from the RPV through the ADS Stage-I is shown in Fig.5. 53.

The RPV mass is shown in Fig.5. 49, Fig.5. 50. It decreases until the LGMSs start to inject into the DVI lines, then, after the injection is over, RPV mass constantly decreases until the break is uncovered, Fig.5. 10. The value of residual mass in the RPV, in the long term of the transient, is around 1900 kg. Mixture enters the RPV from the RC, when the RPV pressure is lower than containment pressure, but mass flow values are very little, Fig.5. 54, Fig.5. 8.

The LM-signal triggers the EBT actuation, by fully opening the valves in 15 s. The EBT injection mass flow is shown in Fig.5. 4 and it is similar in the intact and broken loop. The EBT injection continues until both EBTs are empty, Fig.5. 55.

Soon after EBT actuation, liquid circulation from the RPV toward the EBT starts, at the EBT to RPV connection, then, after such connection is uncovered, steam replaces water contained in the EBT top lines and tanks, Fig.5. 56.

RPV saturation

The RPV mass decreases due to the loss of mass from the break, Fig.5. 49, Fig.5. 50. Fast RPV depressurization leads to reach the saturation conditions (core bottom liquid fraction < 1) at 590 s, Fig.5. 5, Fig.5. 51, Fig.5. 52. Two-phase mixture occurs in the core, but natural circulation through the RI-DC check valves allows to remove the decay heat. Core inlet and outlet temperature difference establishes again, after 3400 s, when core is under liquid single-phase, rewetted by LGMS. The inlet and outlet core temperatures are shown in Fig.5. 57, Fig.5. 58.

Core heater rod temperatures are shown in Fig.5. 59, Fig.5. 60, Fig.5. 61, Fig.5. 62 for the normal and hot rods, respectively. Notwithstanding the core liquid void fraction decrease, rod surface temperatures never overcomes maximum steady state temperature.

Low DP RPV-Containment signal, LGMS and RC to DVI line valve actuation

The containment pressure peak of 0.861 MPa occurs at 2750 s, Fig.5. 13.

The “Low DP RV-Containment” signal set point (50 kPa) is reached at 2810.79 s, Fig.5. 8.

The combination of LM-signal AND Low DP RV-Containment signal actuates the LGMSs and opens the valves on the lines connecting the RC to the DVI lines.

The LGMS isolation valves are fully open in 2 s as well as the RC to DVI line isolation valves.

LGMS injection is related both to gravity and to LGMS air space pressurization (through PSS to LGMS balance lines) by non-condensable gas entering the PSS from DW. The LGMS injection mass flow is shown in Fig.5. 7.

Containment and RPV pressure equalization, no water flow from PSS to DW, RC partial flooding, no reverse flow from containment to RPV

The RPV and containment pressures equalize at 2990 s, with the RPV pressure staying below the containment one until 8500 s. After this period, when pressures are equalized, the water level in the RPV drives the loss of mass through the break, until the DVI is uncovered, Fig.5. 3, Fig.5. 9, Fig.5. 10.

After the peak, the containment pressure decreases for steam condensation on the containment wall. After The RPV and containment pressure coupling, pressures decreases thanks to LGMS injection and to EHRS heat removal from the primary side. At 3190 s, the DW pressure decreases below the PSS pressure, Fig.5. 25, Fig.5. 26, but no reverse flow occurs from PSS to DW as the differential pressure is not sufficient to overcome the hydrostatic head of PSS vent pipes, Fig.5. 17.

The RC receives water from the break line, but level does not reach the top due to the lack of reverse flow from PSS to DW to RC, Fig.5. 11. This only allows mixture flow from containment to RPV when RPV pressure is lower than containment. The water mass flow entering the RPV, from the containment (RC to DVI line) is shown in Fig.5. 63, Fig.5. 64. Negative mass flow in the broken loop, shows water lost from the break.

The QT, initially empty, is partially filled-up by the ADS discharge, Fig.5. 65.

Low LGMS mass signal: ADS Stage-II actuation

The LGMS low mass signal occurs when, in both tanks, mass reaches 20% of initial mass (198 kg, 20% of 1 m^3 water at 48.9 °C), Fig.5. 66, Fig.5. 67.

The low LGMS mass signals actuates the ADS Stage-II valves, fully open in 10 s, to equalize primary and containment pressure and to allow steam circulation between RPV and DW in the upper part of the plant. This enhances steam condensation on the SG tubes in the long term, Fig.5. 68, Fig.5. 69.

SPES3 RWSTs begin to heat-up as soon as the EHRS are actuated, Fig.5. 70, and temperature reaches the saturation around 83000 s. RWST mass is shown in Fig.5. 71 and pressure in Fig.5. 72.

5.1.2 Case conclusions

The simulation of the DBE DVI line split break allowed to understand the phenomena occurring in the transient and to verify the plant conditions after this accident.

The results showed the size of the break (1-inch equivalent) is not large enough to cause a sufficient containment pressurization able to trigger the water back-flow from PSS to DW, observed in the 2-inch equivalent DVI DEG break. Notwithstanding the unavailability of PSS water to be injected from the RC into the RPV, the plant reaches a stable condition with the primary water level at the DVI elevation and decay heat rejected to the RWST by the EHRS.

Tab.5. 1– SPES3-179 list of the main events

	DVI-B line SPLIT break 1-inch equivalent	SPES3-179		
N.	**Phases and events**	**Time (s)**	**Quantity**	**Notes**
Break				
1	Break initiation	0		break valves stroke 2 s
2	Break flow peak	2	0.479 kg/s	
Blowdown, RPV depressurization, containment pressurization. Steam dumping into PSS				
3	Steam-air mixture begins to flow from DW to PSS	60		
S-Signal: Reactor scram, secondary loop isolation, EHRS-A and B actuation				
4	**High Containment pressure signal**	122.96	1.7e5 Pa	**S-signal. Set-point for safety analyses**
5	SCRAM begins	122.96		
6	MFIV-A,B,C closure start	122.96		MFIV-A,B,C stroke 5 s
7	MSIV-A-B-C closure start	122.96		MSIV-A,B,C stroke 5 s.
8	EHRS-A and B opening start (EHRS 1 and 3 in IRIS)	122.96		EHRS-A,B IV stroke 2 s.
9	EHRS-A and B peak mass flow	129	0.263 kg/s	
10	**High SG pressure signal**	139.9	9e6 Pa	
11	SG-A high pressure reached	139.9		
12	SG-B high pressure reached	141.28		
13	SG-C high pressure reached	141.67		
14	RWST-A/B begins to heat-up	168		
15	Secondary loop pressure peak	183 184 185	104e5 Pa 107e5 Pa 113e5 Pa	SG-A SG-B SG-C
Pump coast-down and primary circulation through RI-DC check valves				
15	**Low PRZ water level signal**	265.82	1.189 m	
17	RCP coast-down starts	280.82		Low PRZ level signal + 15 s delay
18	EHRS-A power peak	285	372 kW	
19	EHRS-B power peak	285	372 kW	
20	Natural circulation begins through shroud valves (RI-DC)	300, 304		SG-A and B, SG-C
LM-Signal: EHRS-C, ADS Stage-I and EBT actuation. RPV saturation				
21	**Low PRZ pressure signal**	433.52	11.72e6 Pa	**LM-Signal** (High P cont + Low P PRZ)
22	EHRS-C opening start (EHRS 2 and 4 in IRIS)	433.52		EHRS-C IV stroke 2 s.
23	ADS Stage I start opening (3 trains)	433.52		ADS valve stroke 10 s
24	EBT-A and B valve opening start	433.52		EBT valve stroke 15 s
25	EHRS-C peak mass flow	437	0.547 kg/s	
26	RWST-C begins to heat-up	476		
27	EHRS-C power peak	590	716 kW	
28	ADS Stage I first peak flow (3 trains)	444	1.343 kg/s	ST 0.482 kg/s; DT 0.861 kg/s
29	Flashing begins at core outlet	448	voidf 110 (core)	<1
30	ADS Stage I second peak flow (3 trains)	500	1.879 kg/s	ST 0.629 kg/s; DT 1.250 kg/s Due to liquid fraction.
31	Natural circulation interrupted at SGs top	490		Pump inlet uncovered (voidf 176-01 ~0)
32	EBT-RV connections uncovered	500, 510		EBT-B, EBT-A
33	Core in saturation conditions	590		
Low DP RPV-Containment signal, LGMS and RC to DVI valve actuation				
34	Containment pressure peak	2750	8.61e5 Pa	
35	**Low DP RPV-Containment**	2810.79	50e3 Pa	
36	LGMSA/B valve opening start	2810.79		LM + low DP RV-cont. LGMS valve stroke 2 s.
37	RC to DVI line valve opening	2810.79		RC to DVI valve stroke 2 s.
38	LGMS-B starts to inject into RC through DVI broken loop	2940		
39	LGMS-A starts to inject into RV through DVI intact loop	2940		
Containment and RV pressure equalization, no water flow from PSS to DW, no RC flooding from DW, no reverse flow from containment to RPV				
40	Containment and RPV pressure equalization	2990		
41	Mixture starts to flow from RC to DVI-A	3000		
42	DW pressure lower than PSS pressure	3190		
43	Steam and gas mixture flows again from RPV to QT	3660 to 3900		RPV P > DW P
44	EBT-A empty (intact loop)	4090		
45	EBT-B empty (broken loop)	4160		
Low LGMS mass signal: ADS Stage-II actuation				
46	Low LGMS mass	11049.19	20% mass (198 kg)	LGMS-A (intact loop)
46		12092.28	20% mass (198 kg)	LGMS-B (broken loop)
46	ADS stage-II start opening	12092.28		ADS Stage-II valve stroke 10 s.
49	RC level at DVI elevation	~120000		level just below the DVI
50	LGMS-A empty (intact loop)	16970		
51	LGMS-B empty (broken loop)	19100		
Long Term conditions				
52	Core power	150000	46.23 kW	Average between 100000-150000 s
53	SG total power	150000	42.79 kW	
54	RWST total power	150000	40.15 kW	
55	RWST-A/B temperature	150000	99 °C	almost saturated
56	RWST-C temperature	150000	99 °C	almost saturated

Fig.5. 1 - SPES3-179 DVI break mass flow (window)

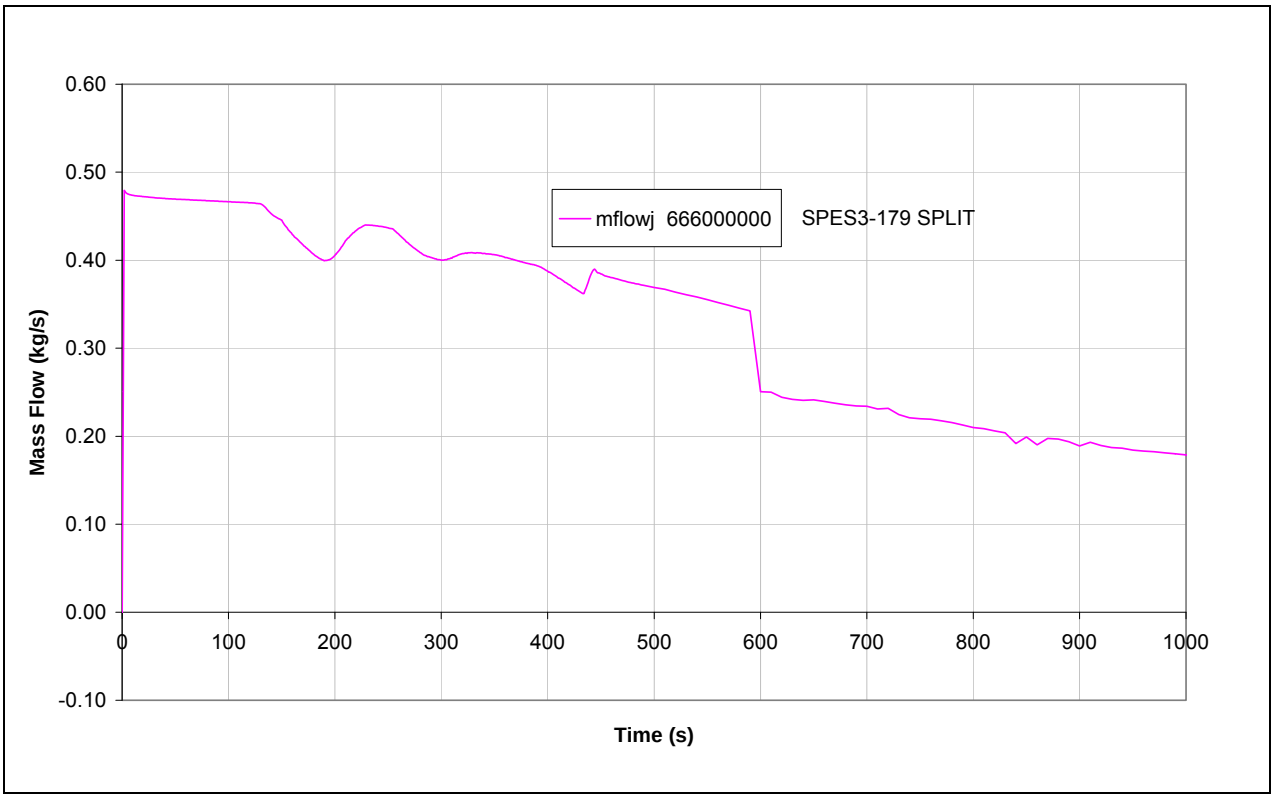

Fig.5. 2 - SPES3-179 DVI break mass flow (window)

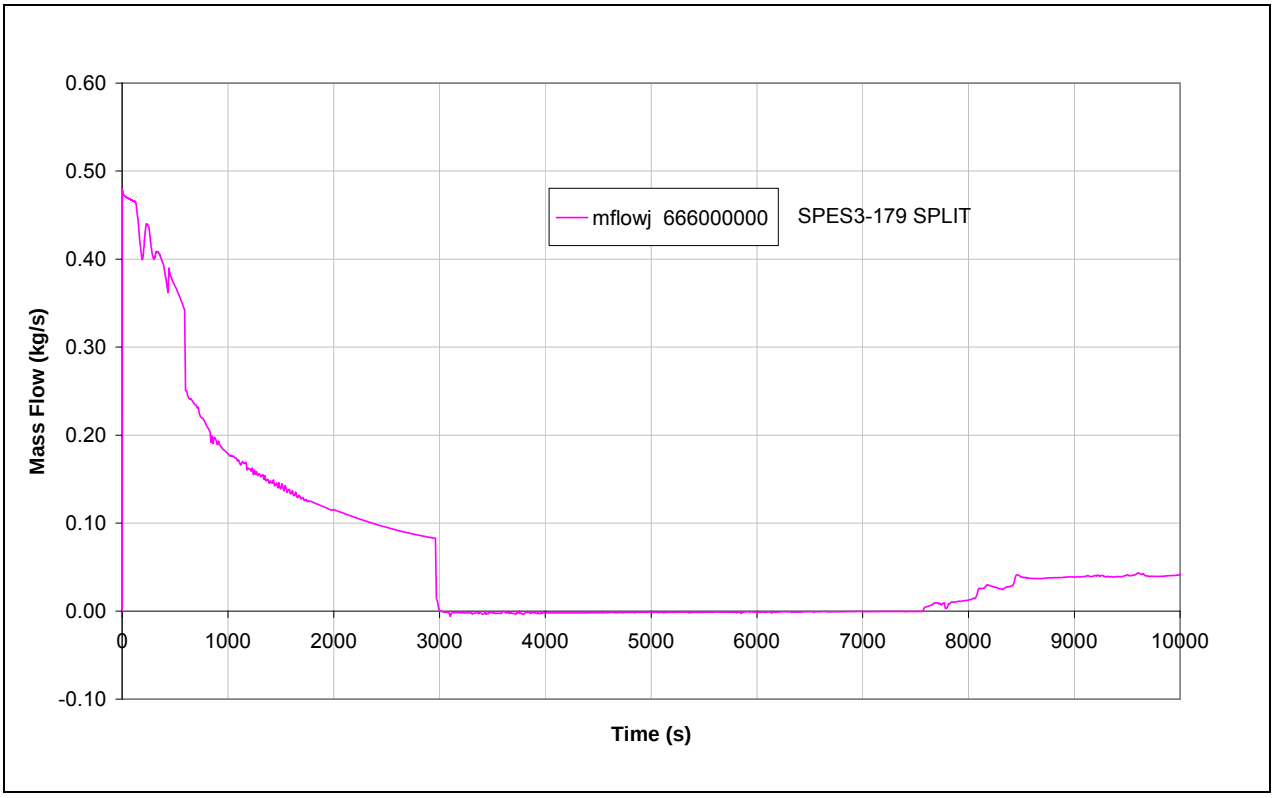

Fig.5. 3 - SPES3-179 DVI break mass flow

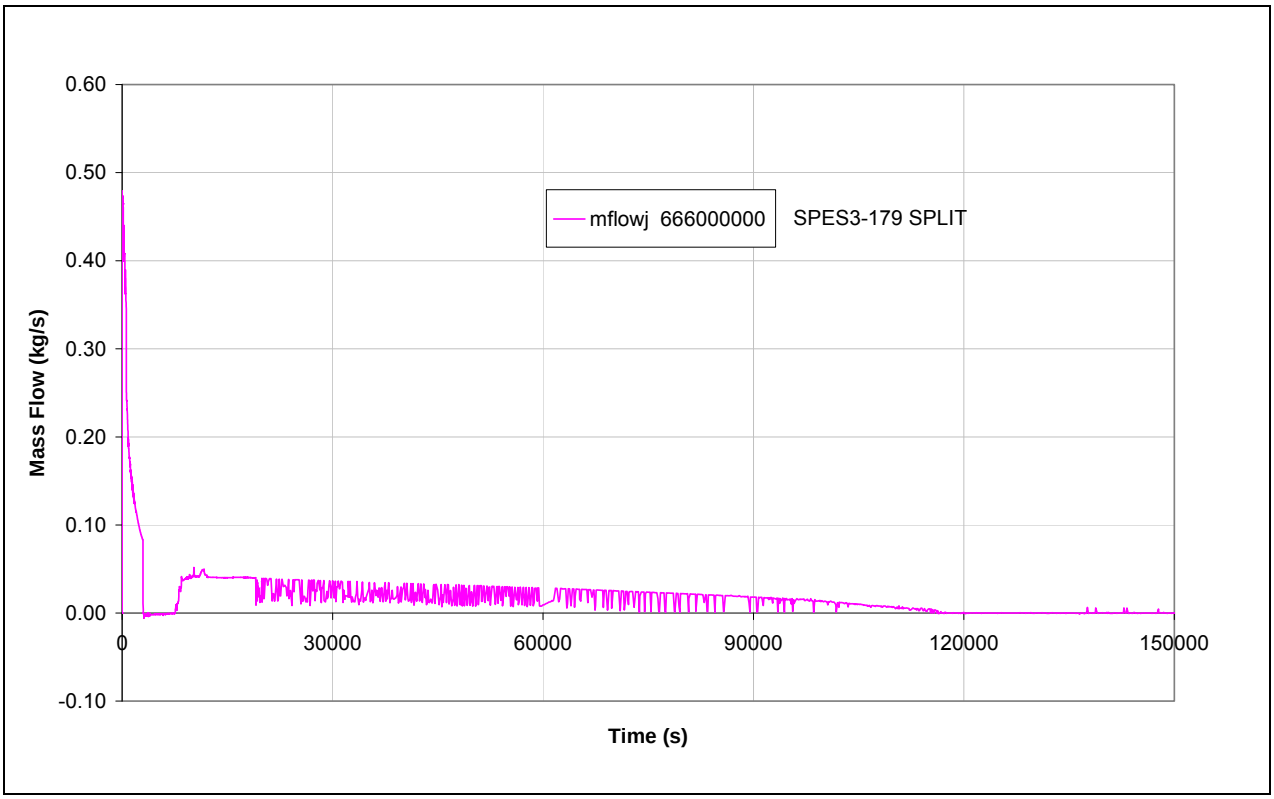

Fig.5. 4 - SPES3-179 EBT injection mass flow (window)

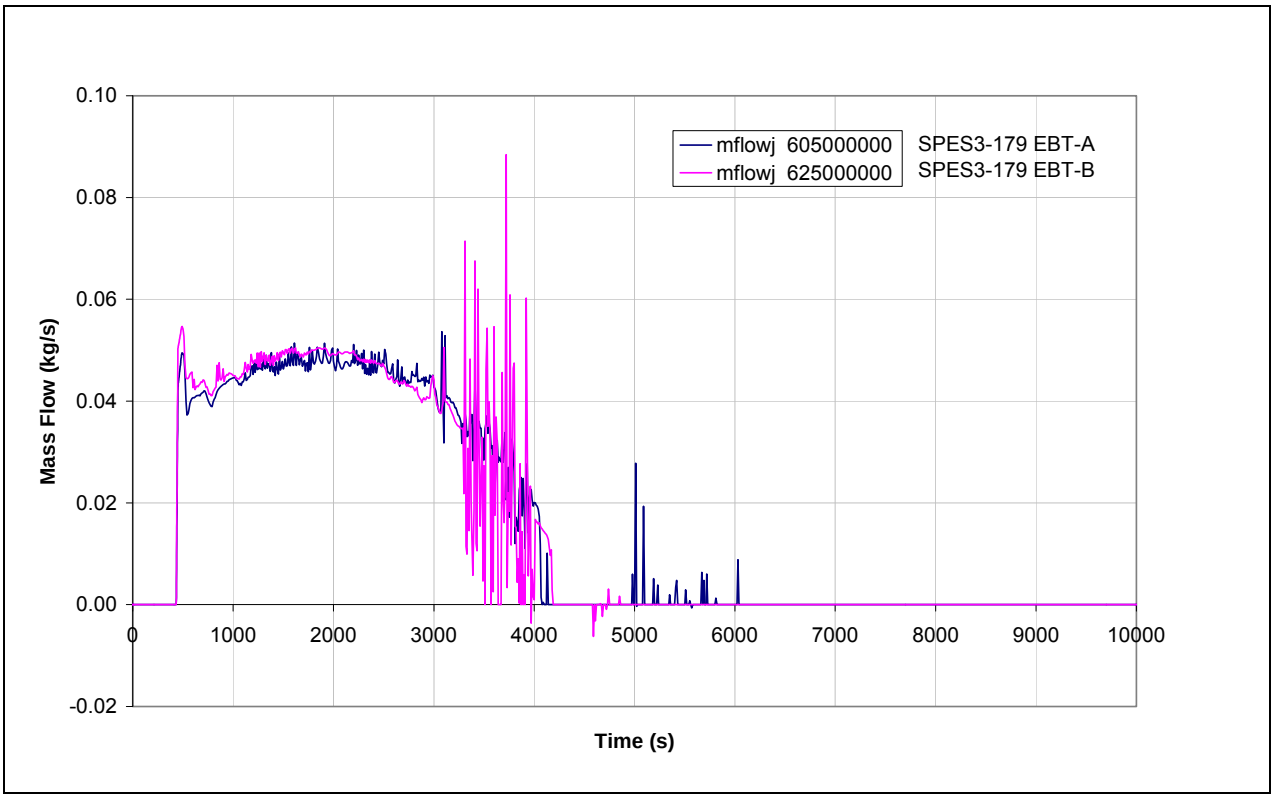

Fig.5. 5 - SPES3-179 PRZ pressure (window)

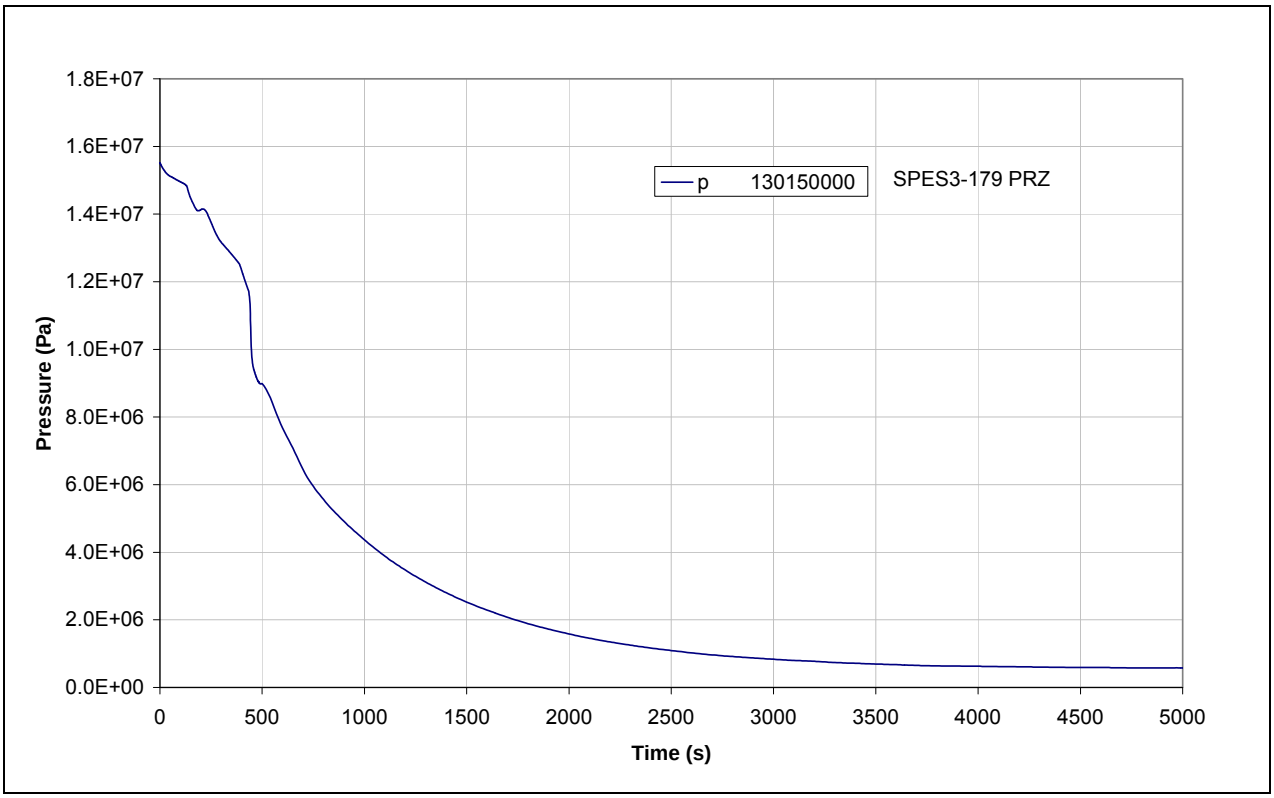

Fig.5. 6 - SPES3-179 PRZ pressure

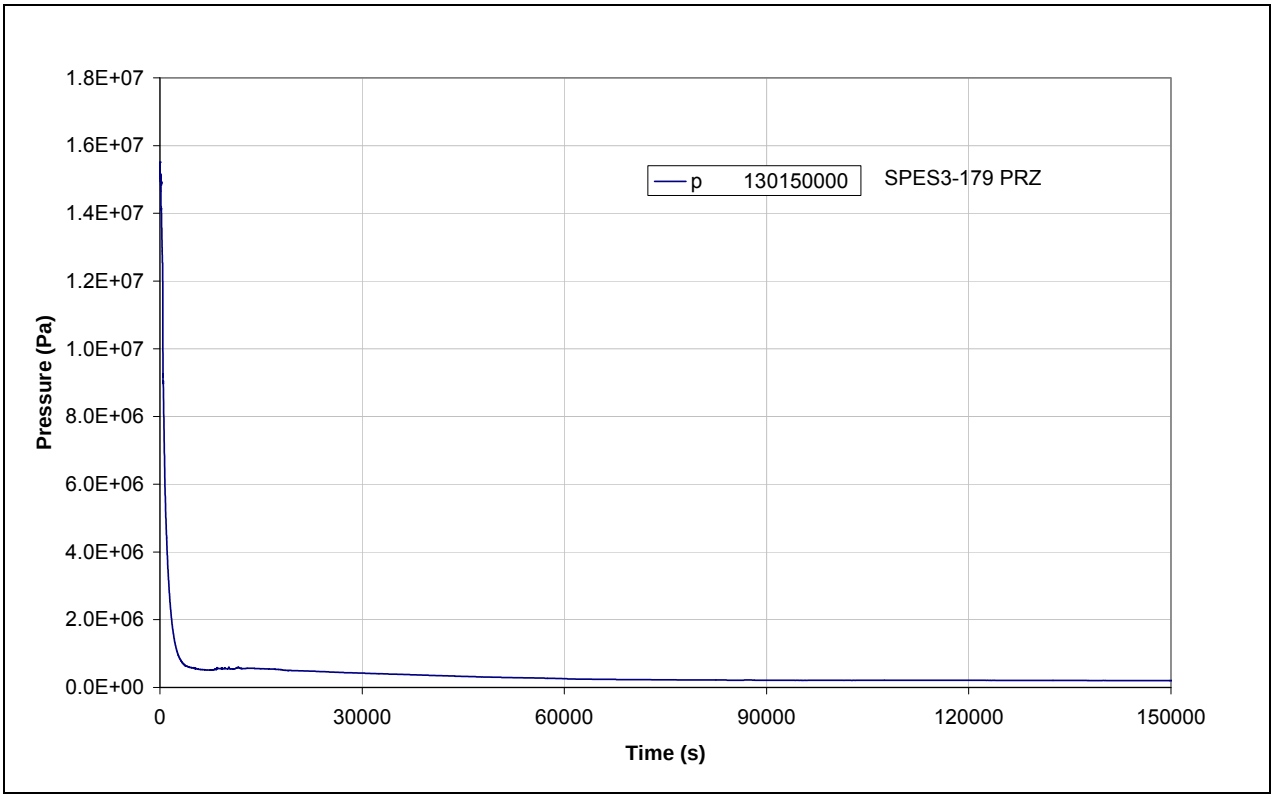

Fig.5. 7 - SPES3-179 LGMS mass flow (window)

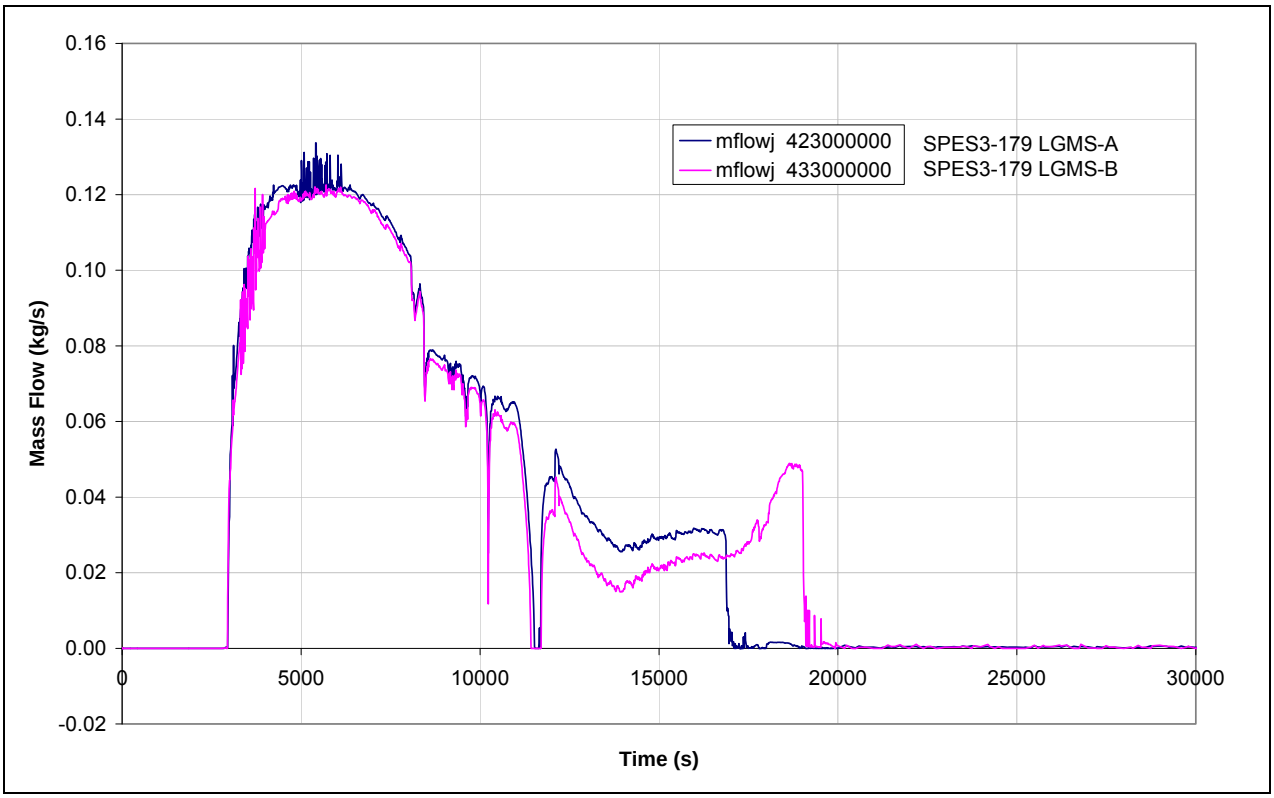

Fig.5. 8 - SPES3-179 PRZ and DW pressures (detail)

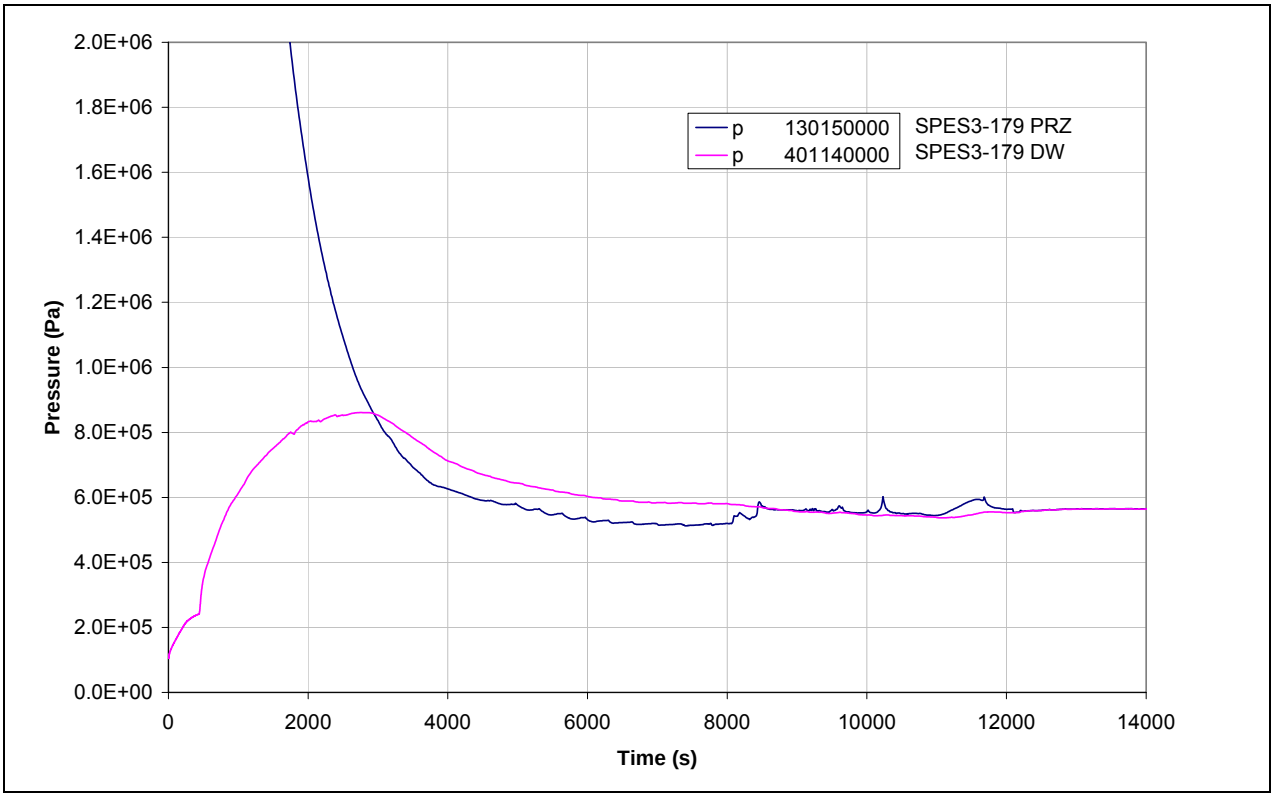

Fig.5. 9 - SPES3-179 PRZ and DW pressures (window)

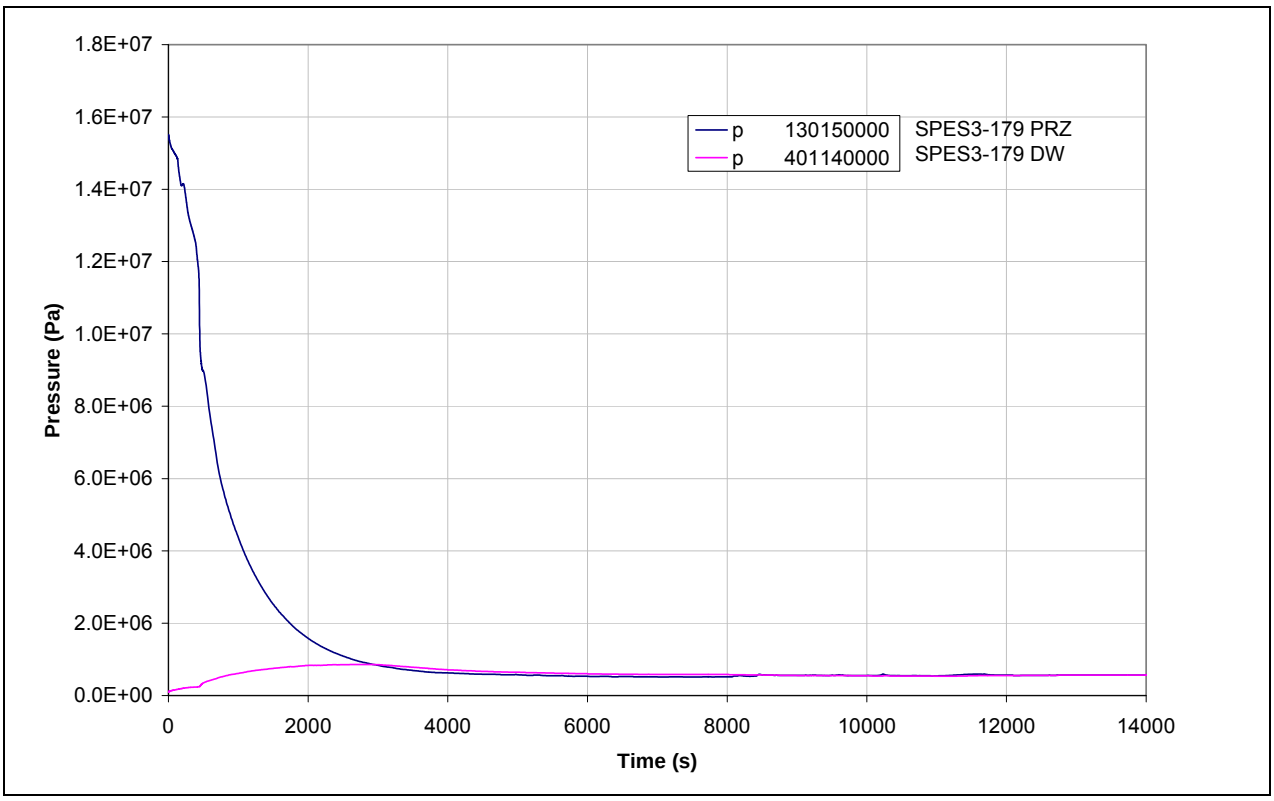

Fig.5. 10 - SPES3-179 RPV down domer level

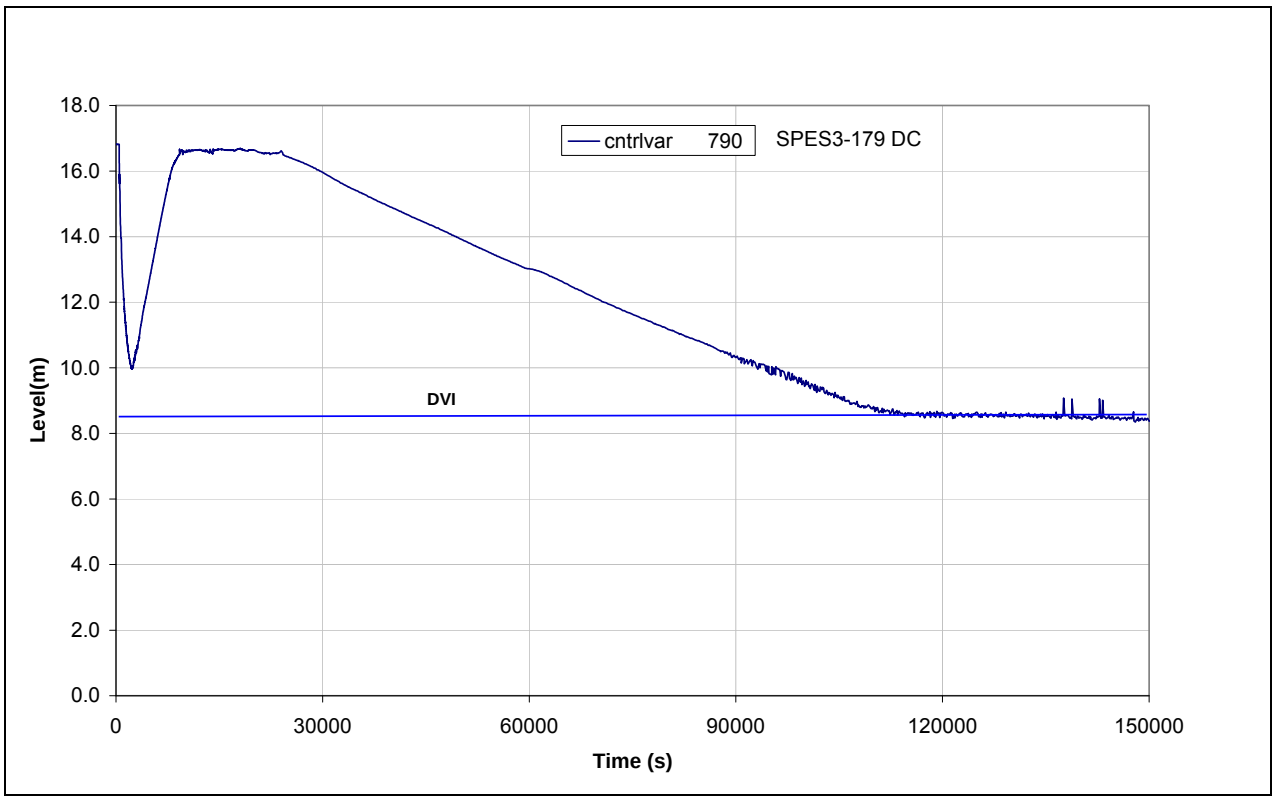

Note: DVI elevation referred to RPV bottom.

Fig.5. 11 - SPES3-179 RC level

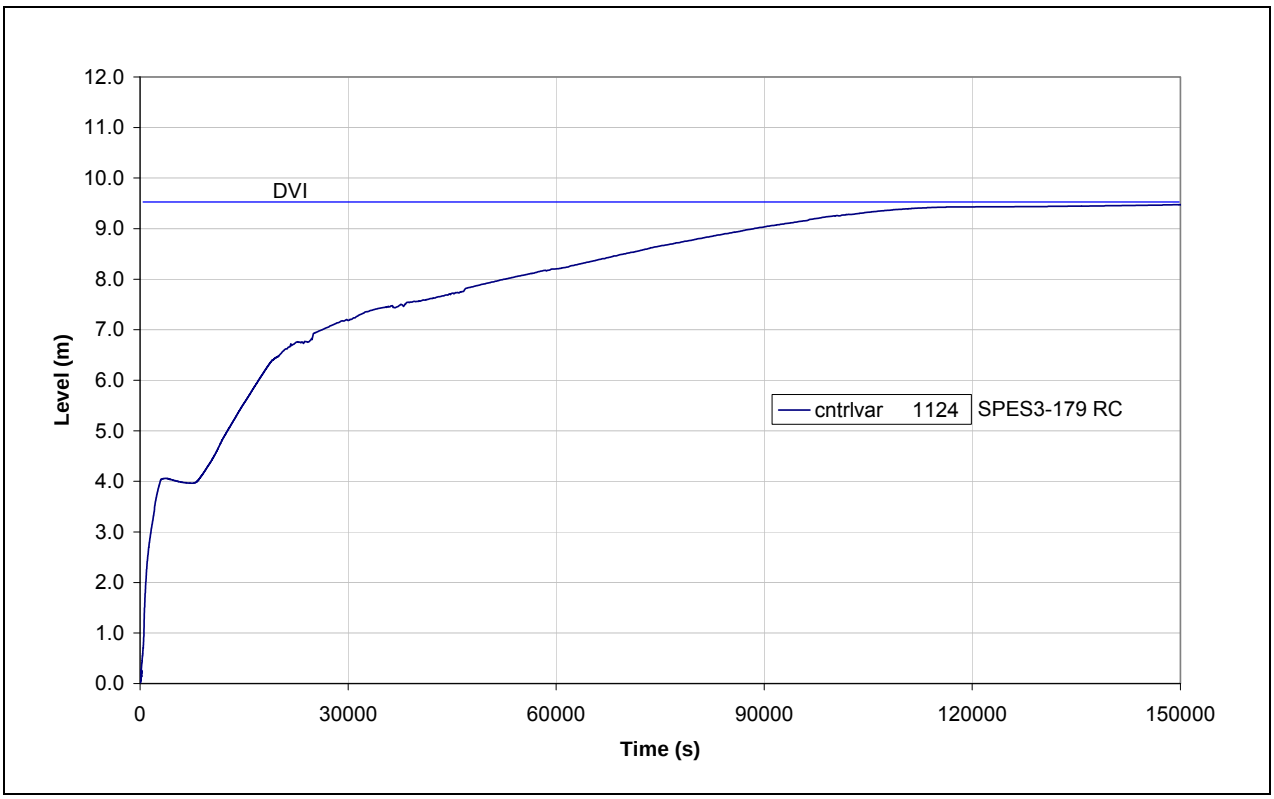

Note: DVI elevation referred to RC bottom.

Fig.5. 12 - SPES3-179 RC mass

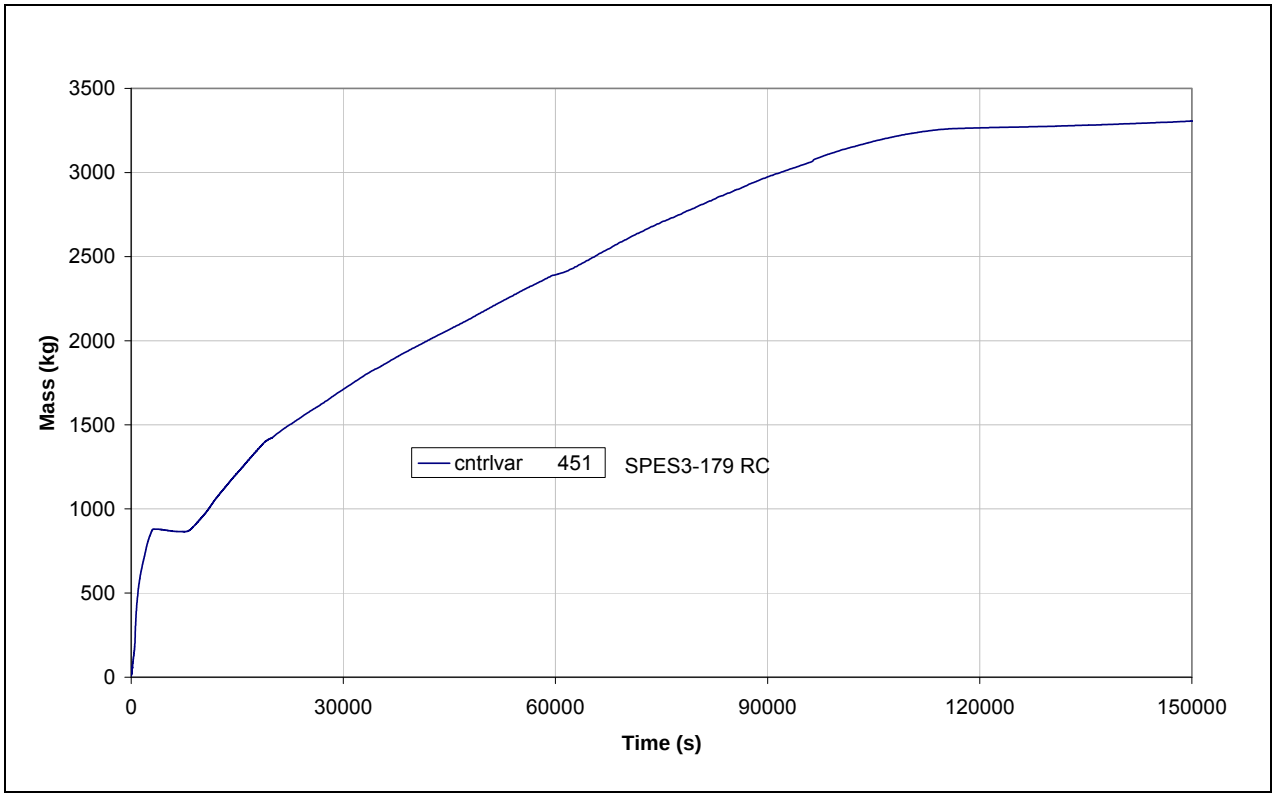

Fig.5. 13 - SPES3-179 DW pressure (window)

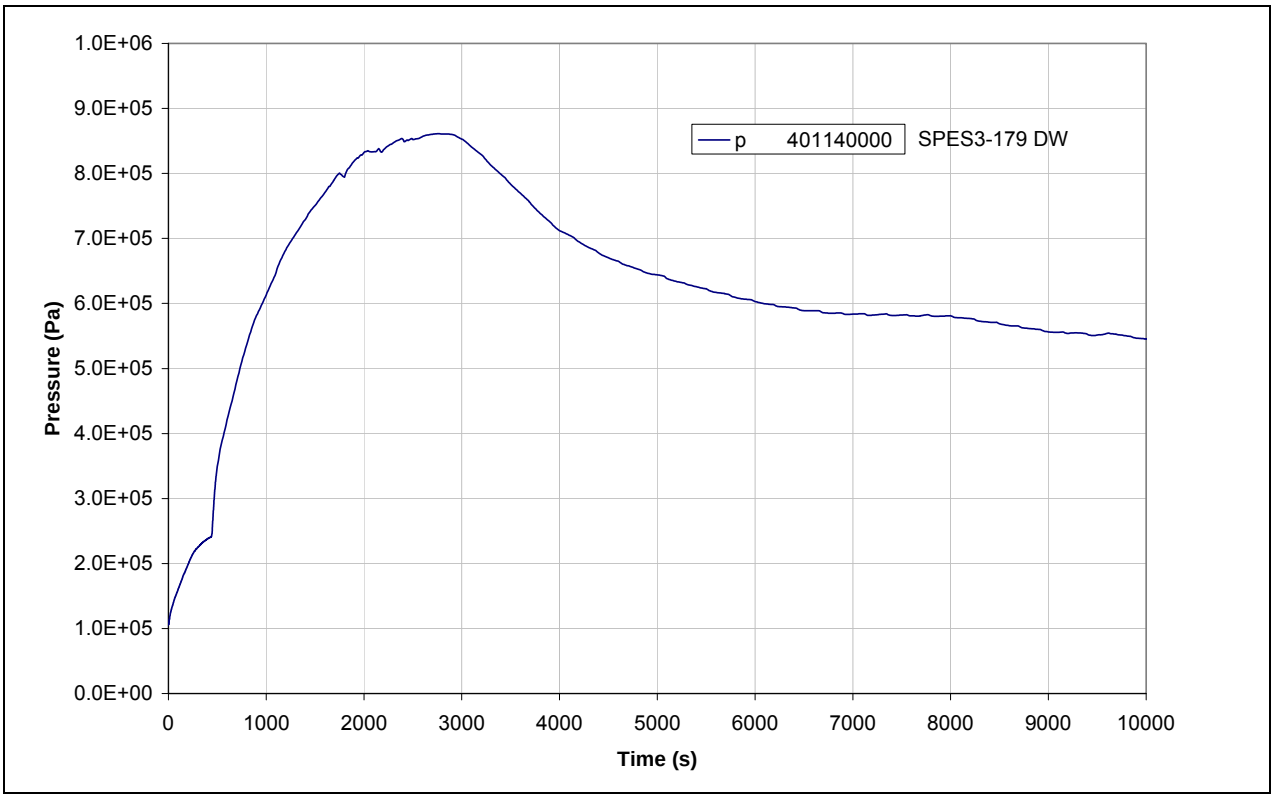

Fig.5. 14 - SPES3-179 DW pressure

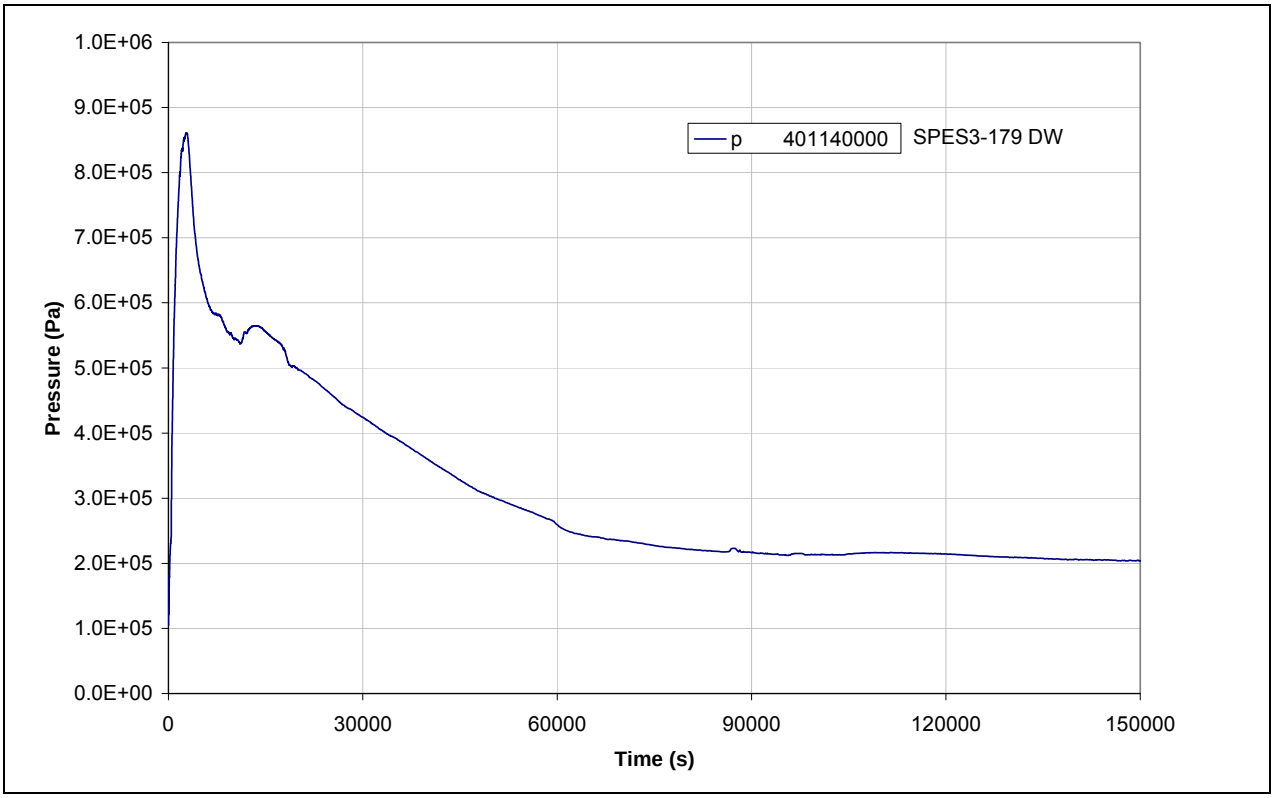

Fig.5. 15 - SPES3-179 ADS Stage-I mass flow (window)

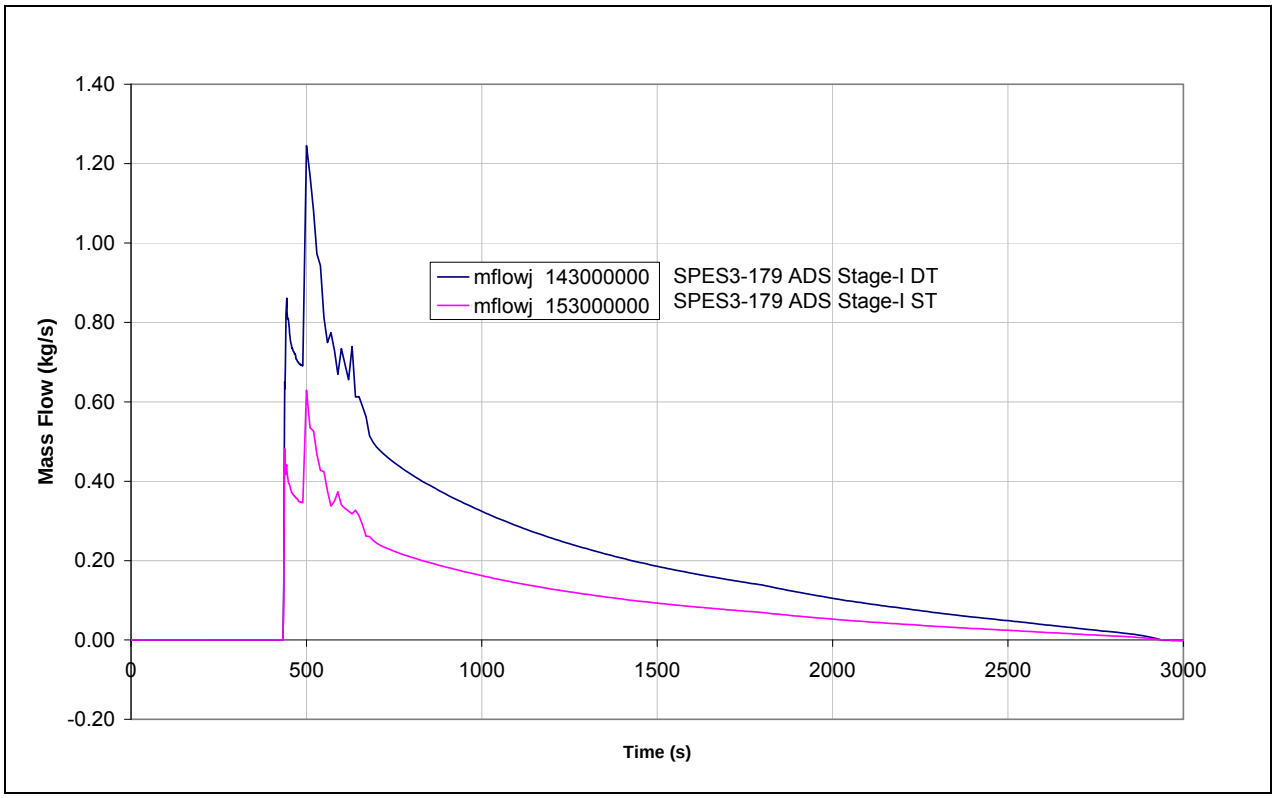

Fig.5. 16 - SPES3-179 ADS Stage-I mass flow (window)

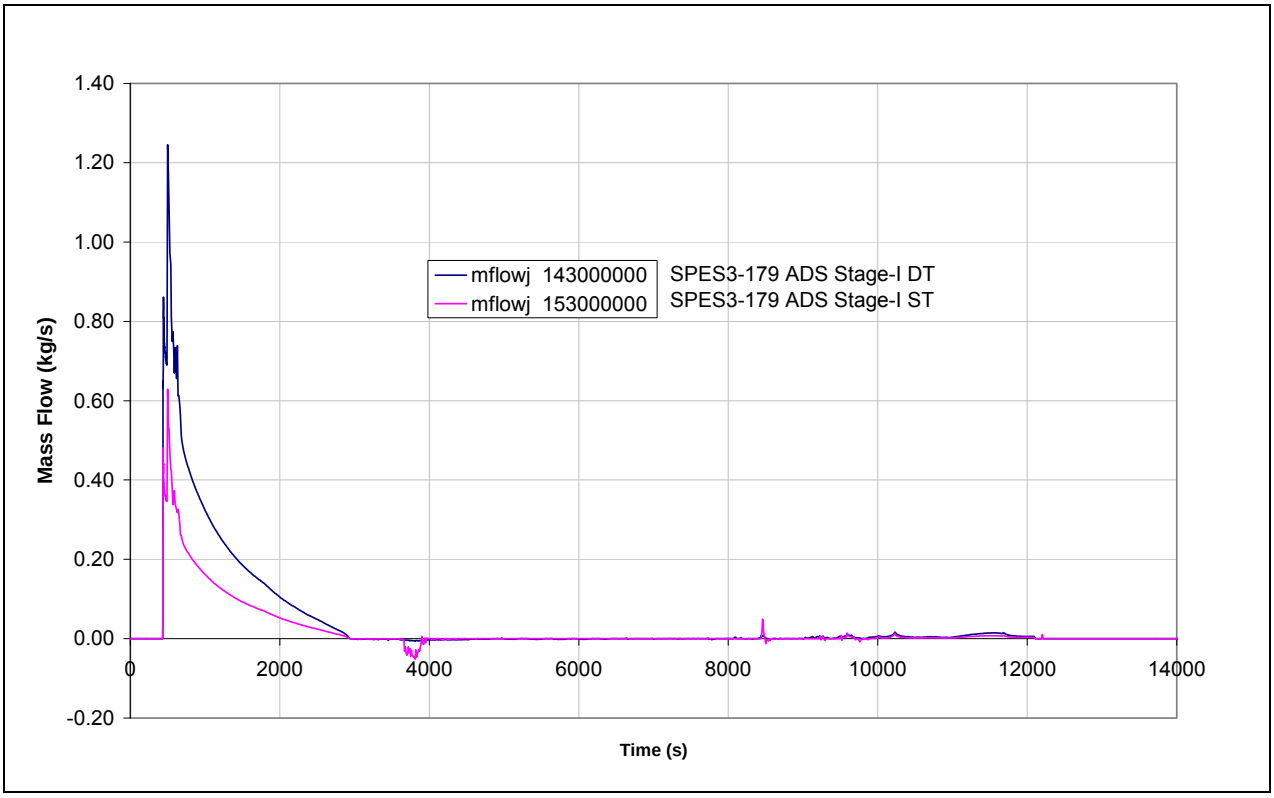

Fig.5. 17 - SPES3-179 DW to PSS mass flow (window)

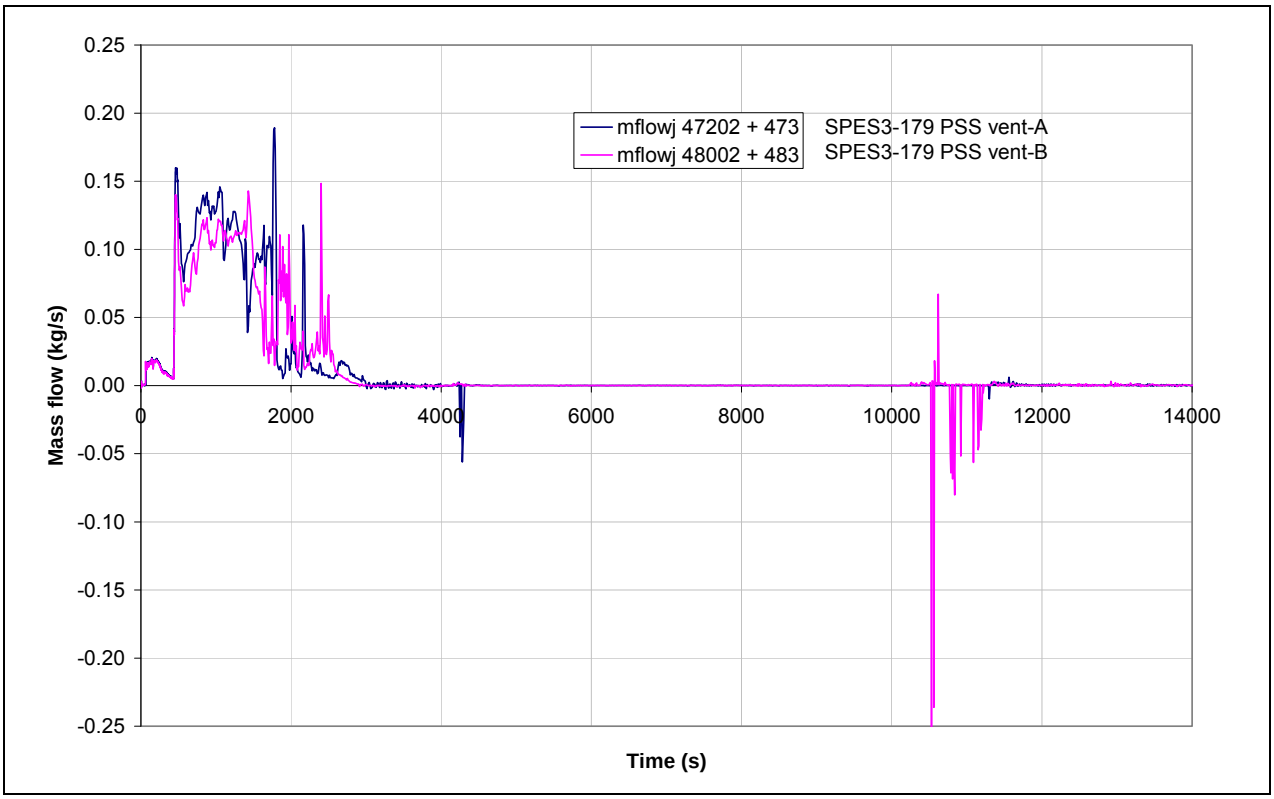

Fig.5. 18 - SPES3-179 DW to PSS integral flow (window)

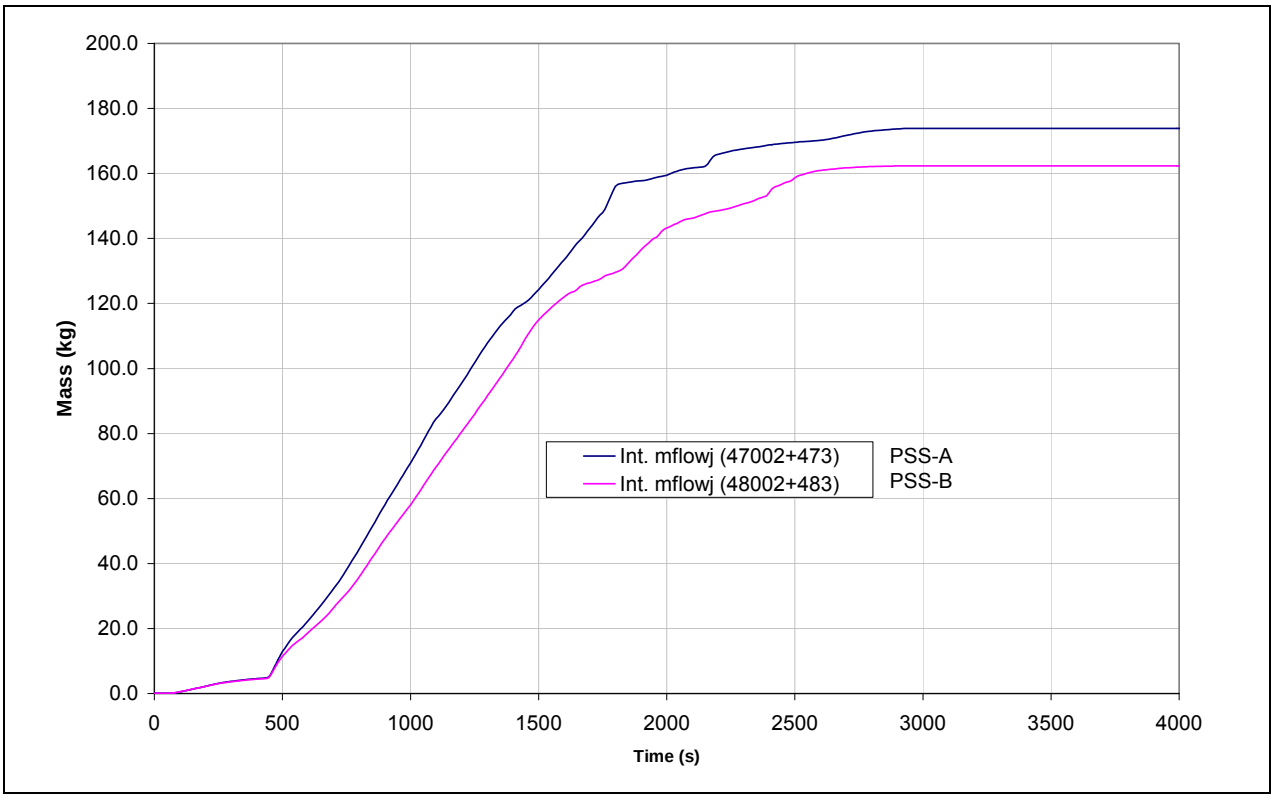

Fig.5. 19 - SPES3-179 DW non-condensable gas quality (window)

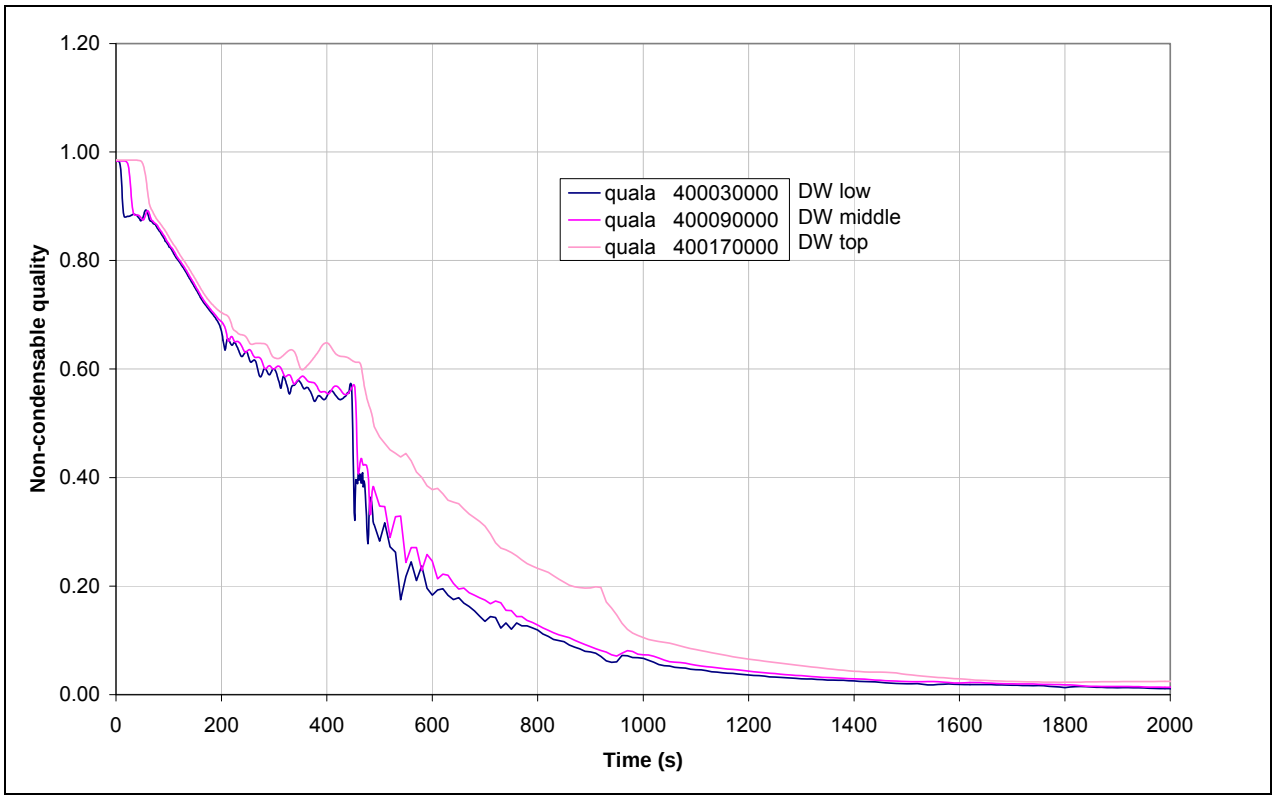

Fig.5. 20 - SPES3-179 DW non-condensable gas quality

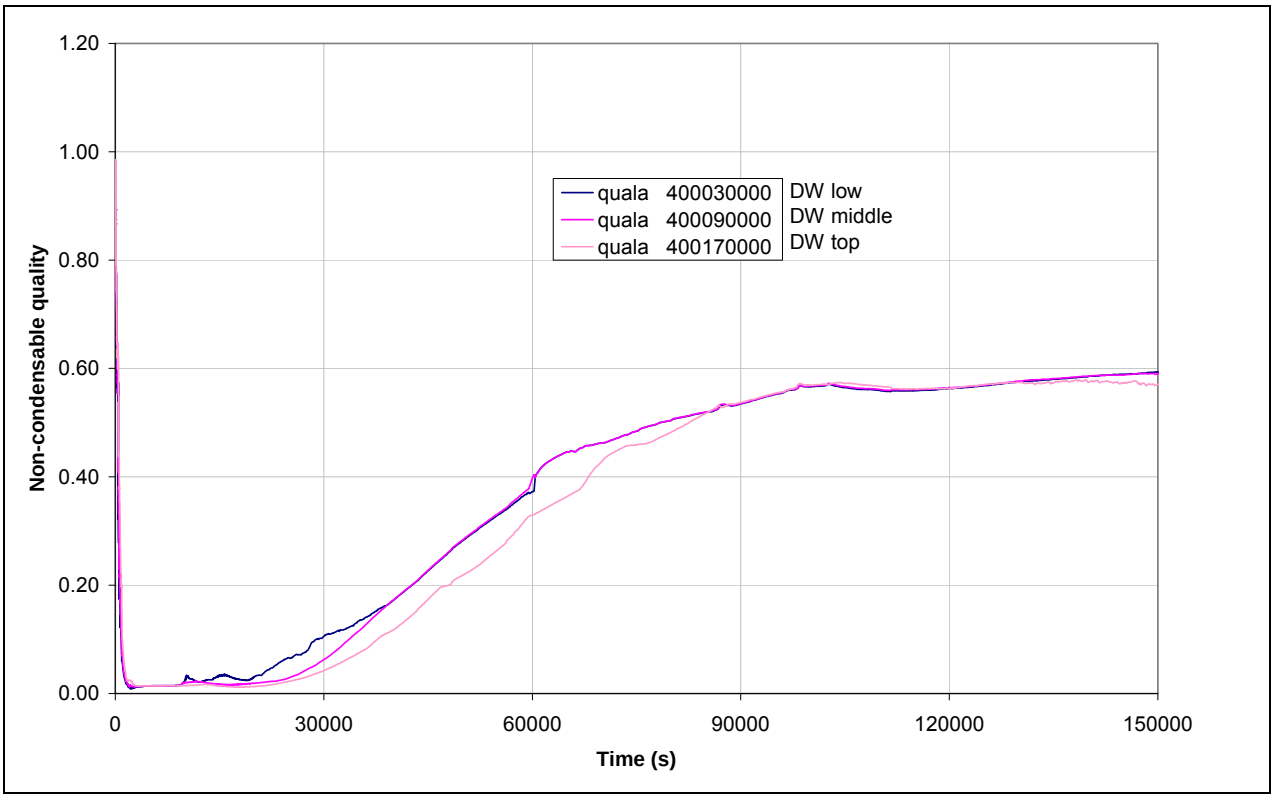

Fig.5. 21 - SPES3-179 PSS pressure (window)

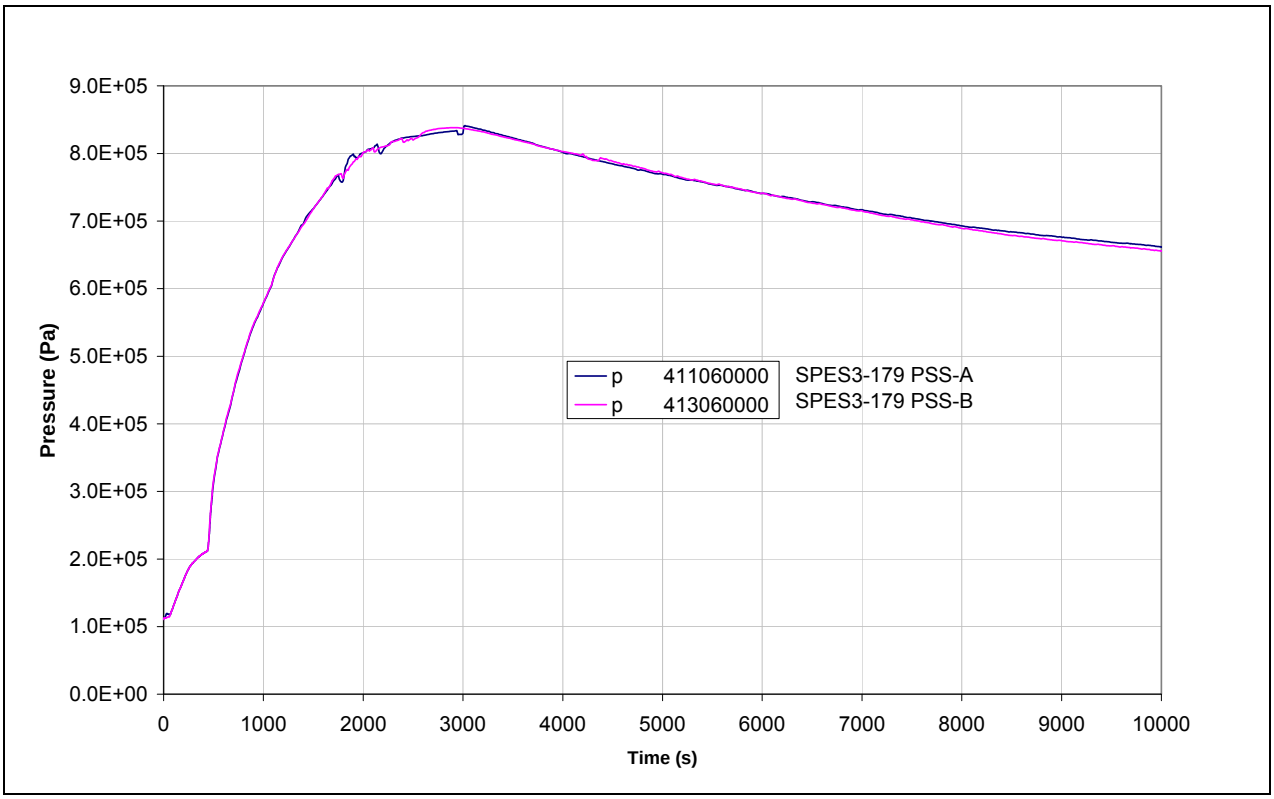

Fig.5. 22 - SPES3-179 PSS pressure

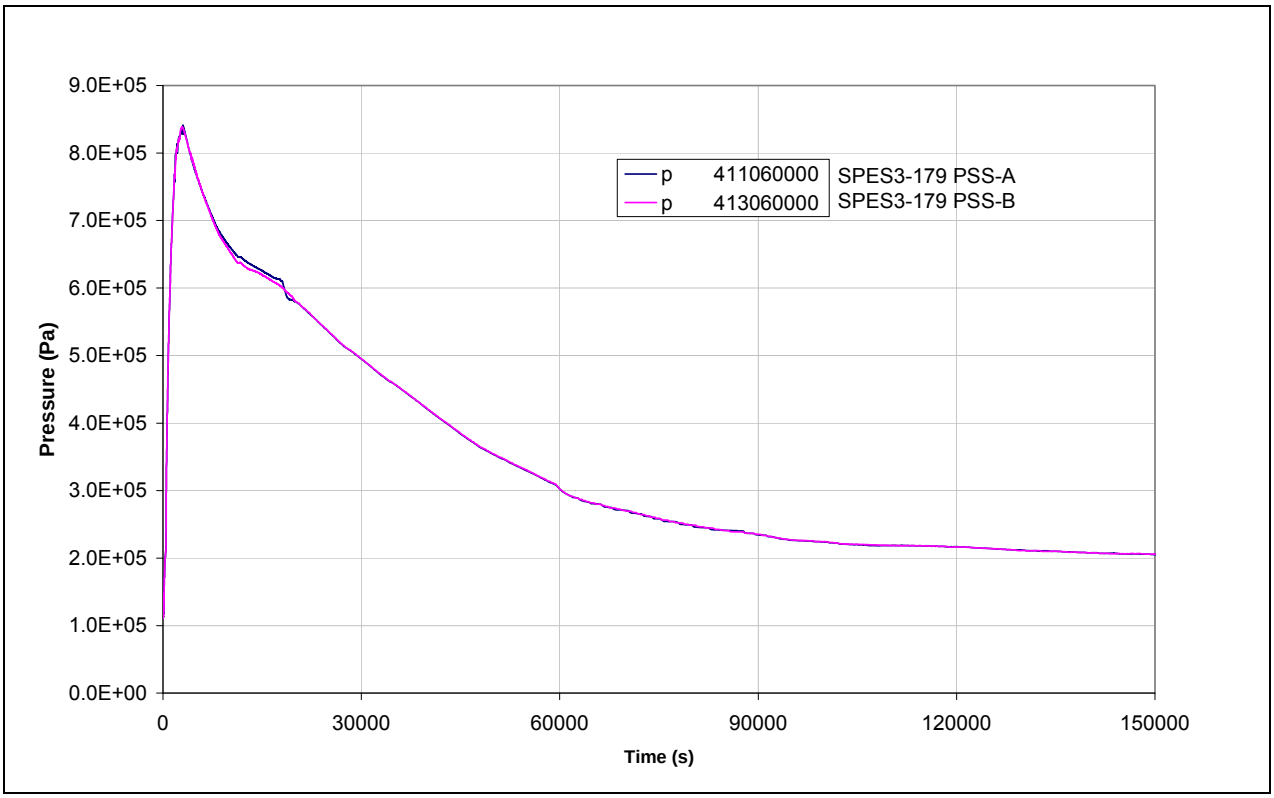

Fig.5. 23 - SPES3-179 LGMS pressure (window)

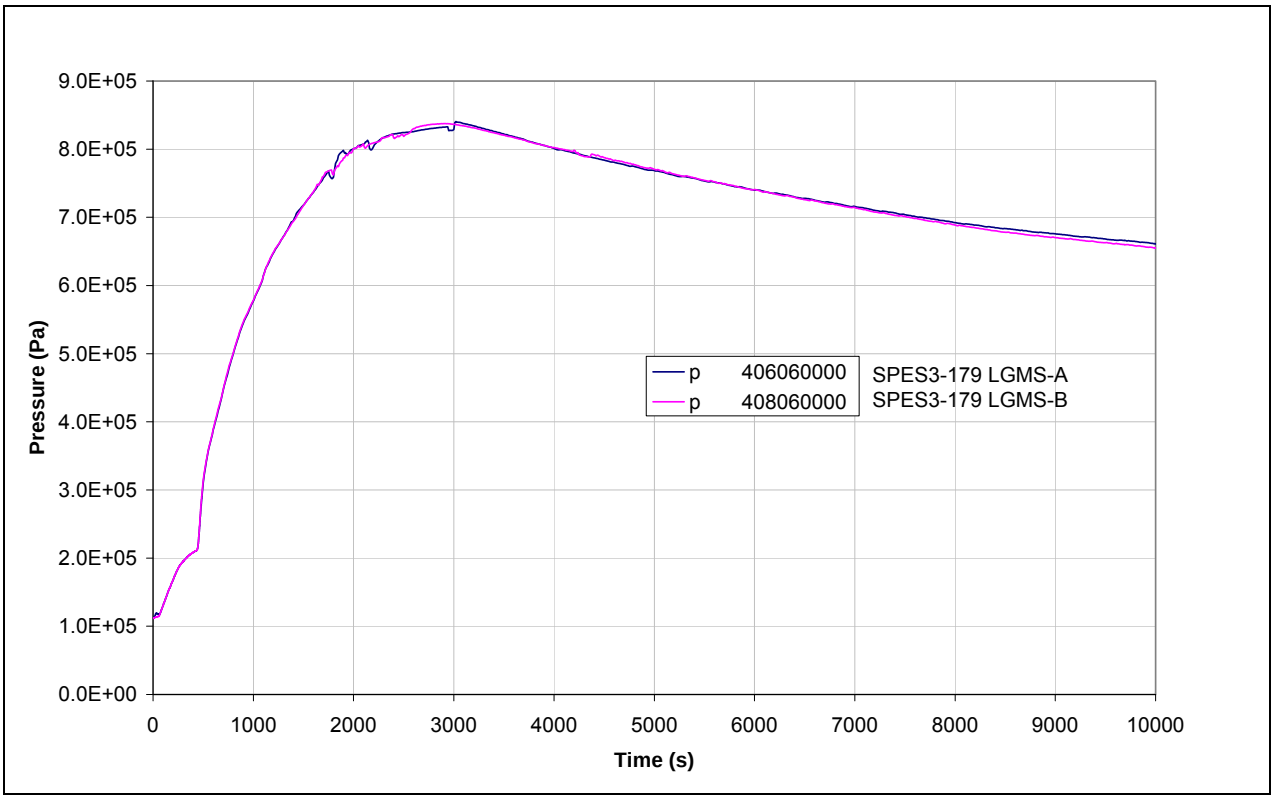

Fig.5. 24 - SPES3-179 LGMS pressure

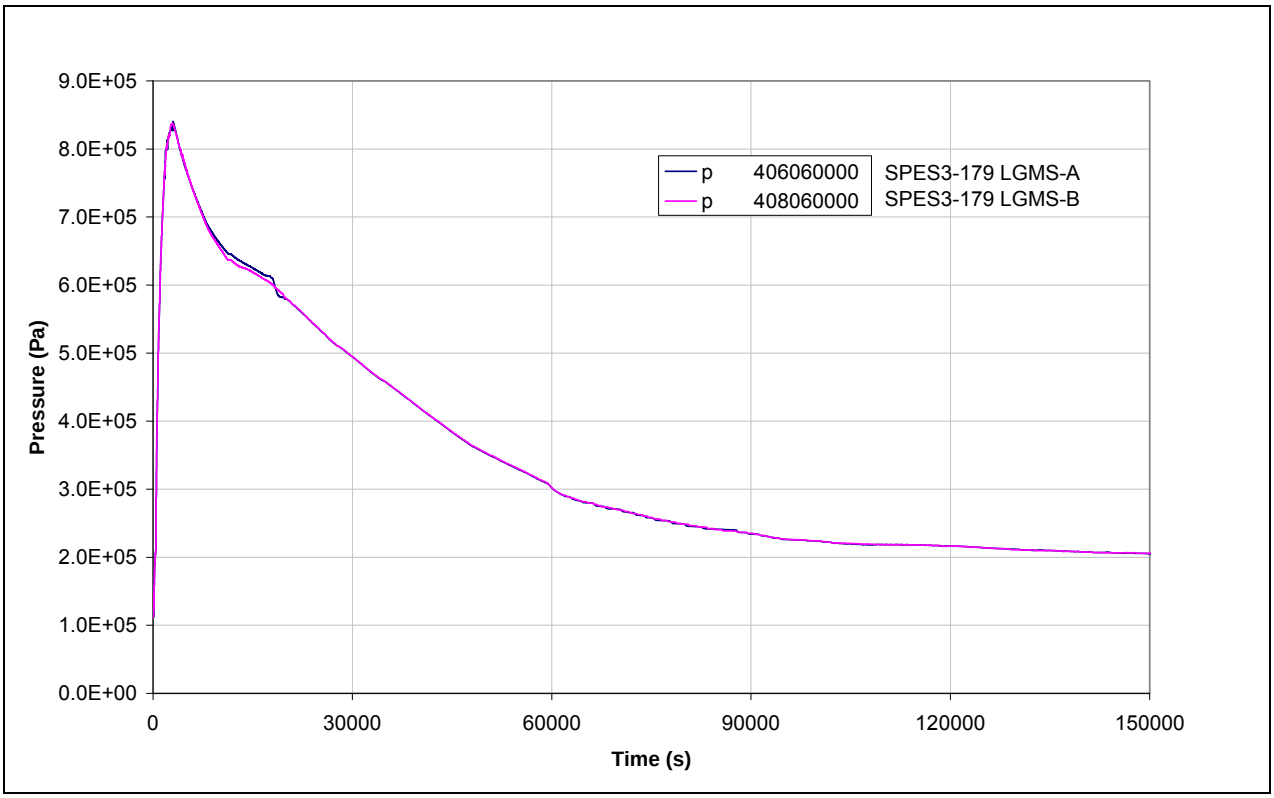

Fig.5. 25 - SPES3-179 DW and PSS pressure (window)

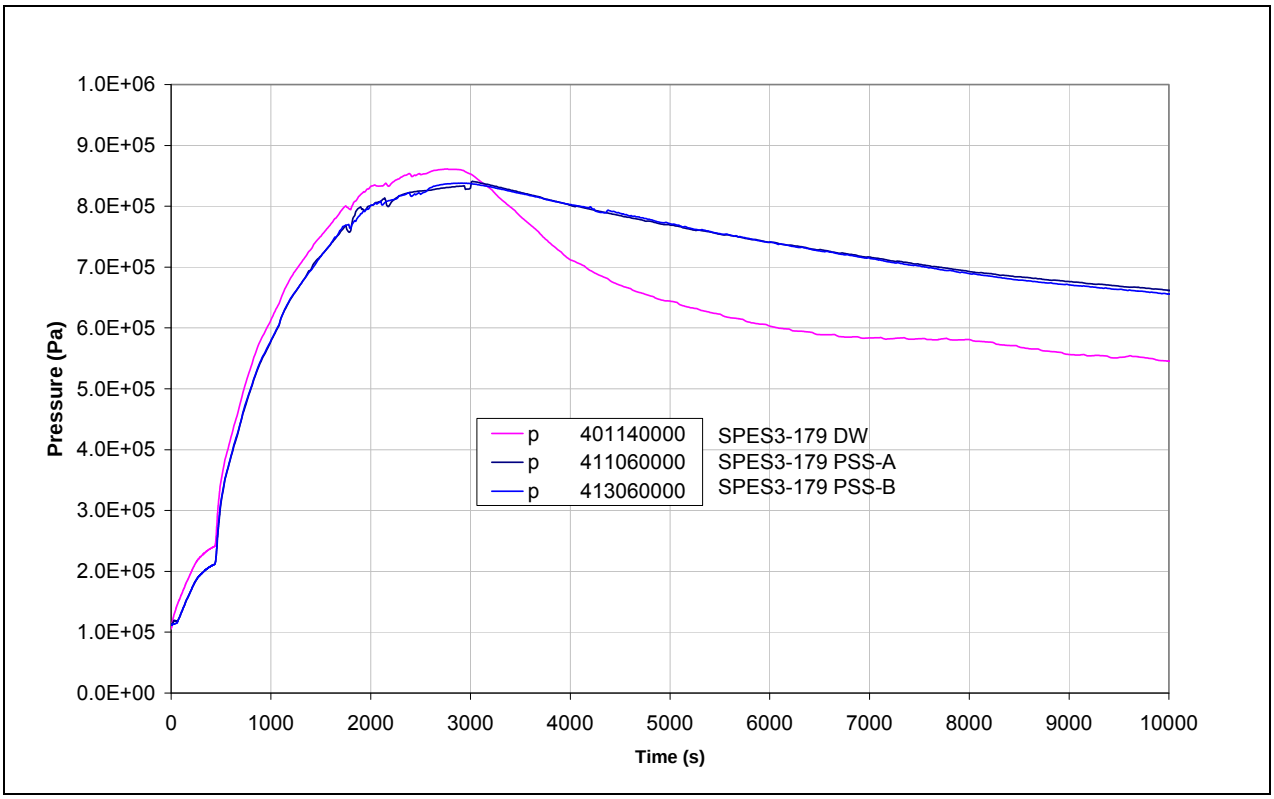

Fig.5. 26 - SPES3-179 DW and PSS pressure

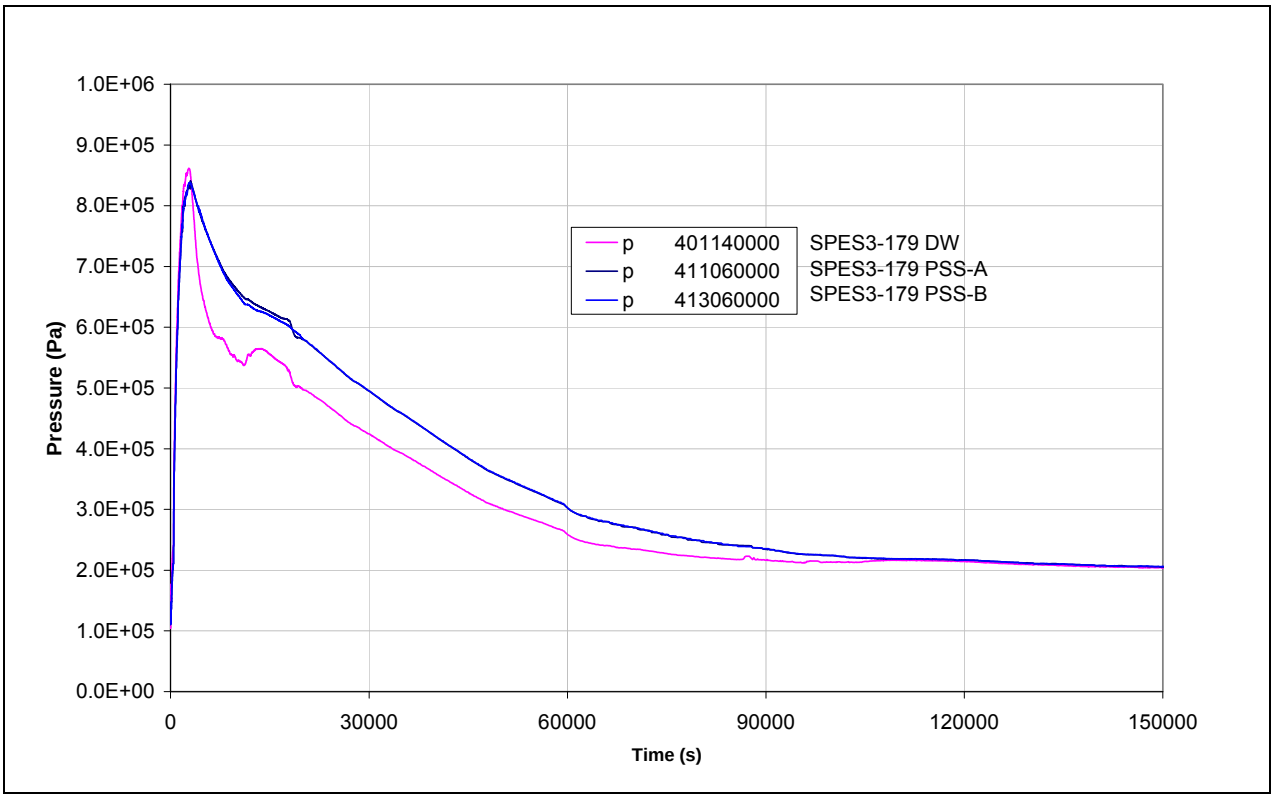

Fig.5. 27 - SPES3-179 PSS vent pipe level (window)

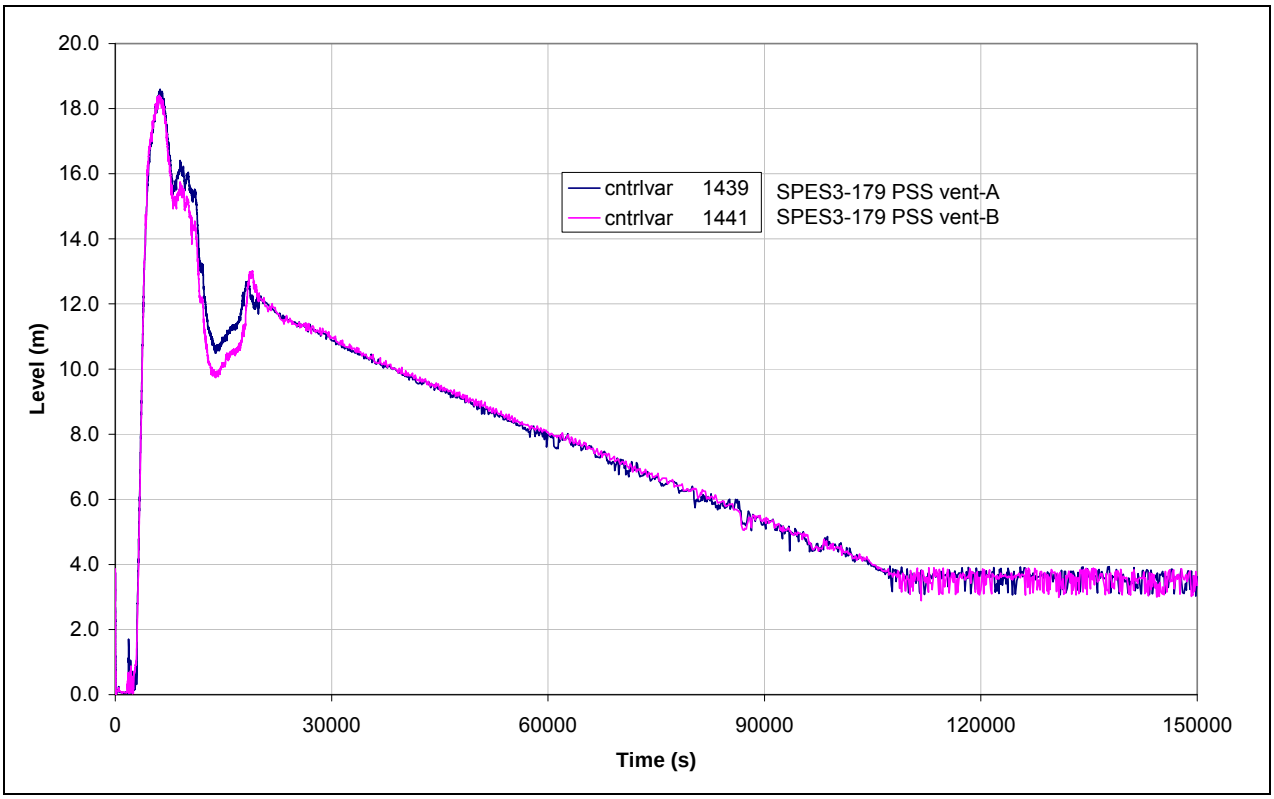

Fig.5. 28 - SPES3-179 PSS temperatures

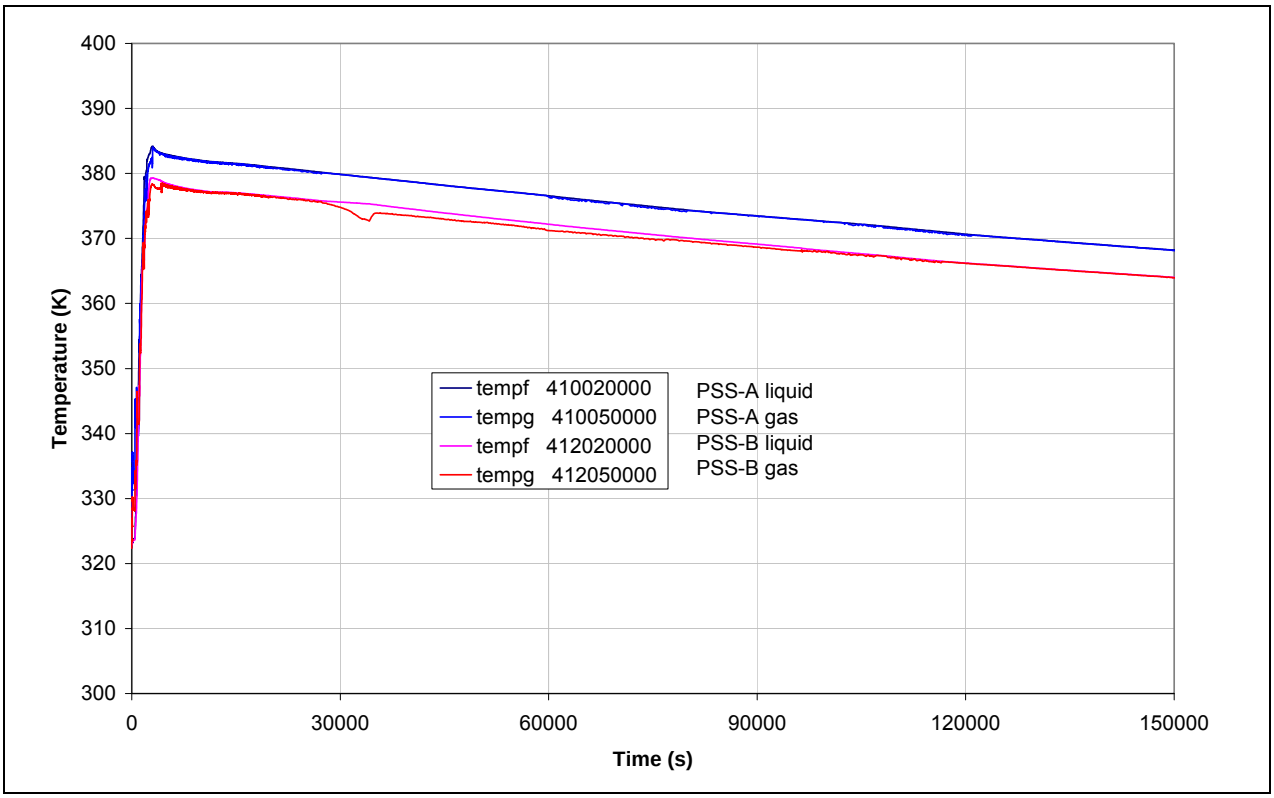

Fig.5. 29 - SPES3-179 Core and SG power(window)

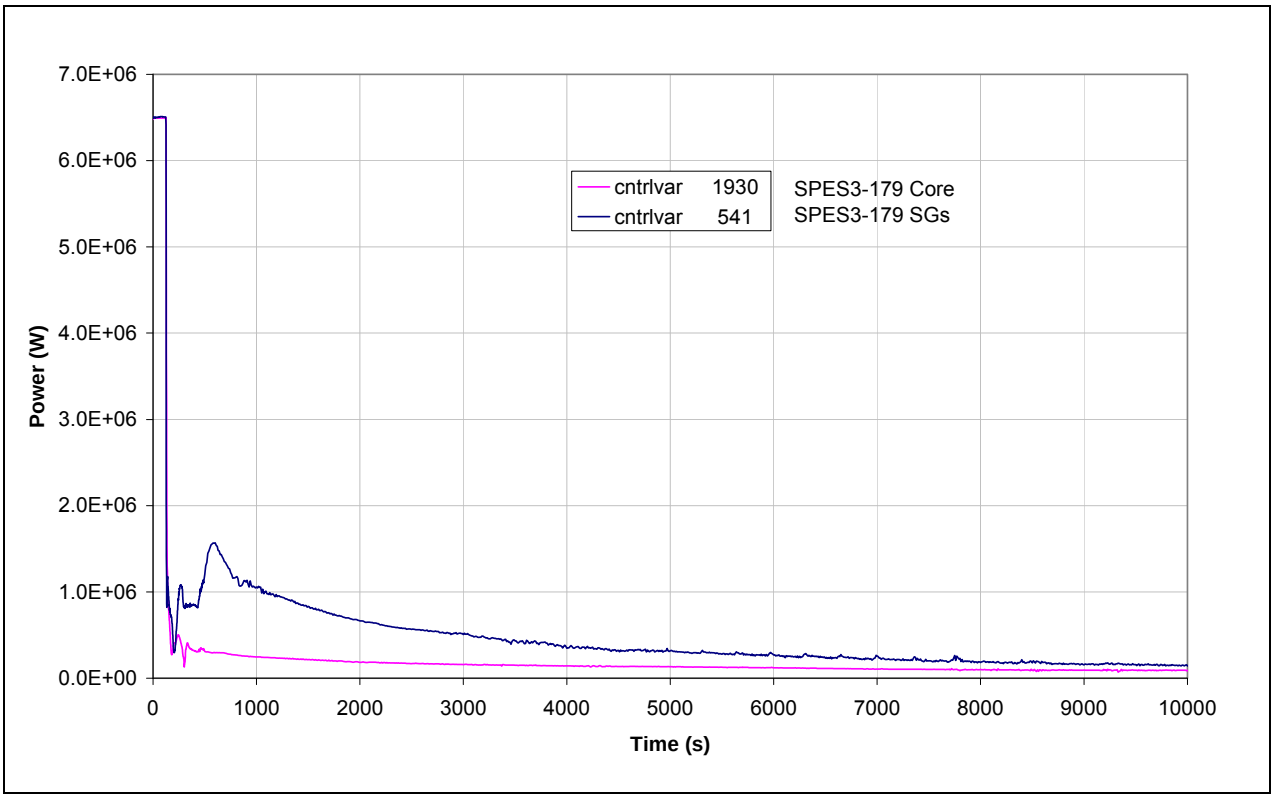

Fig.5. 30 - SPES3-179 Core and SG power

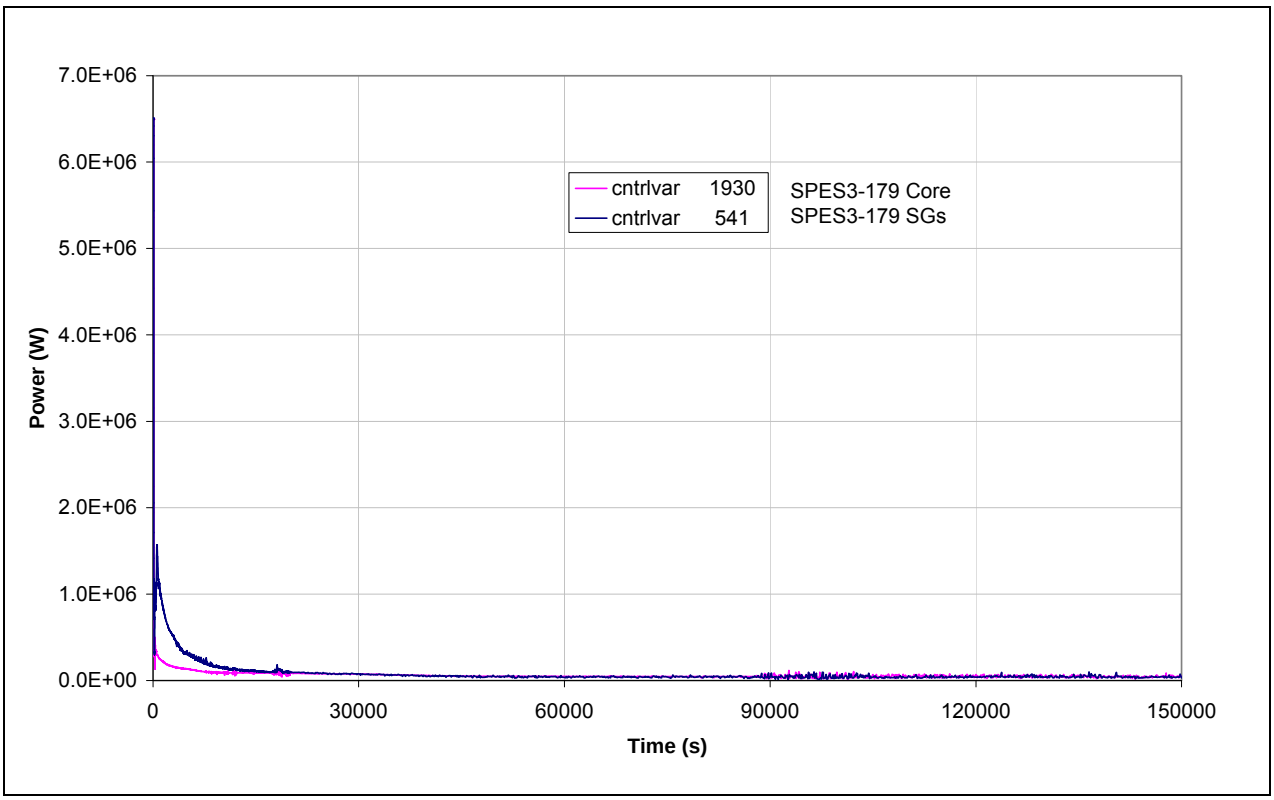

Fig.5. 31 - SPES3-179 SG secondary side mass flow (window)

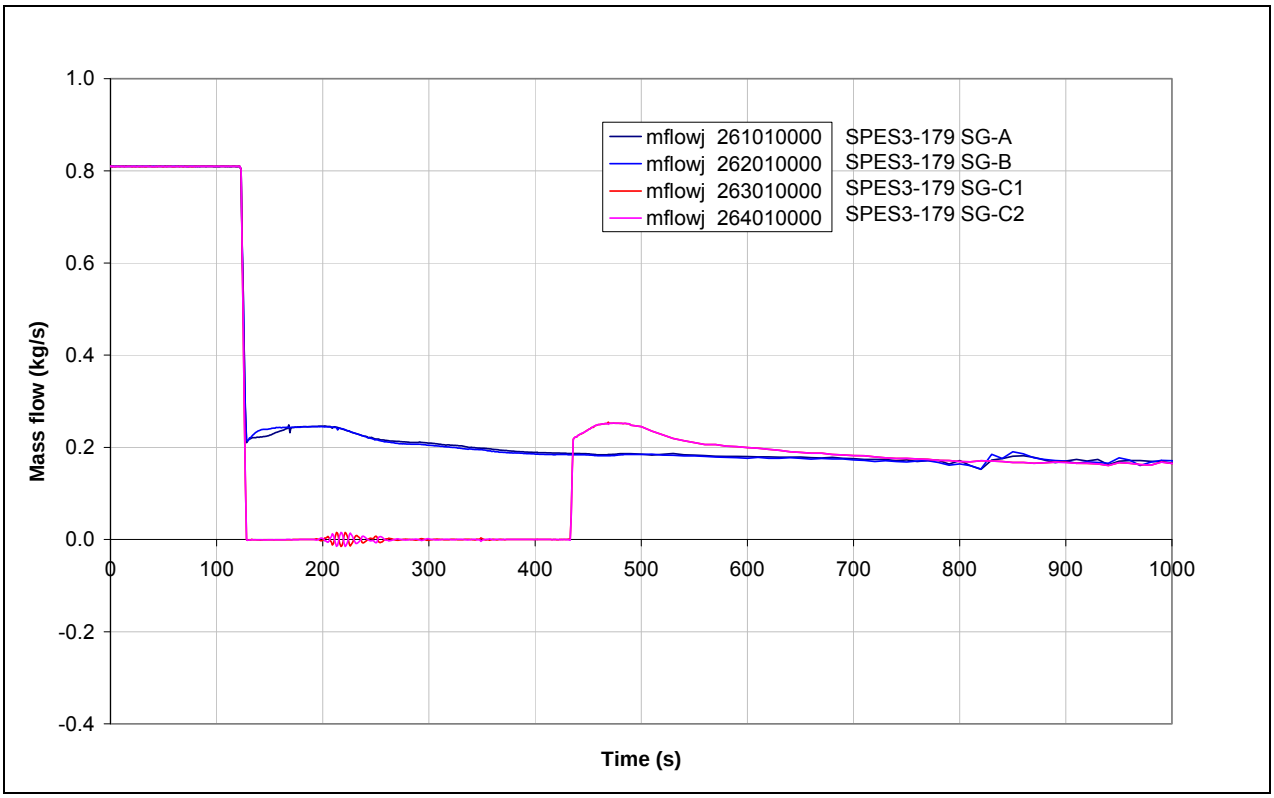

Fig.5. 32 - SPES3-179 SG secondary side mass flow

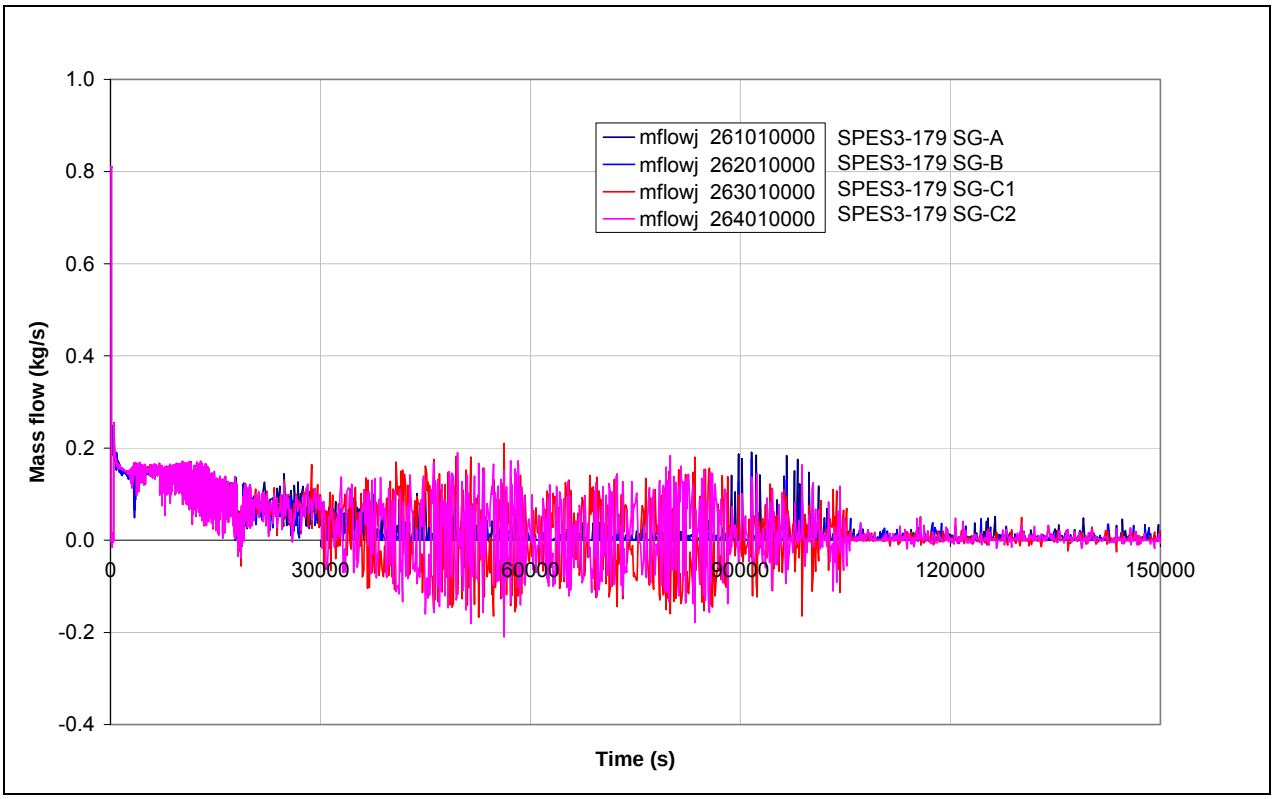

Fig.5. 33 - SPES3-179 EHRS cold leg mass flow (window)

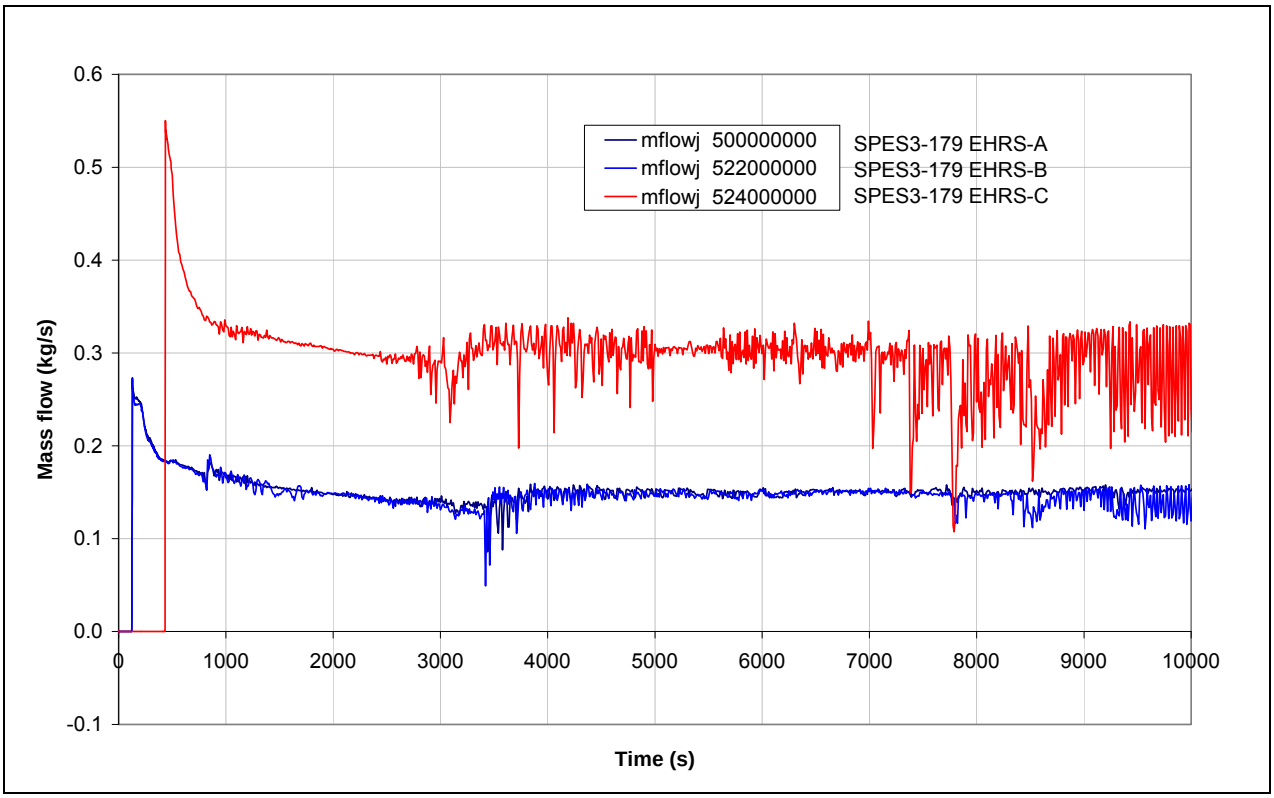

Fig.5. 34 - SPES3-179 EHRS cold leg mass flow

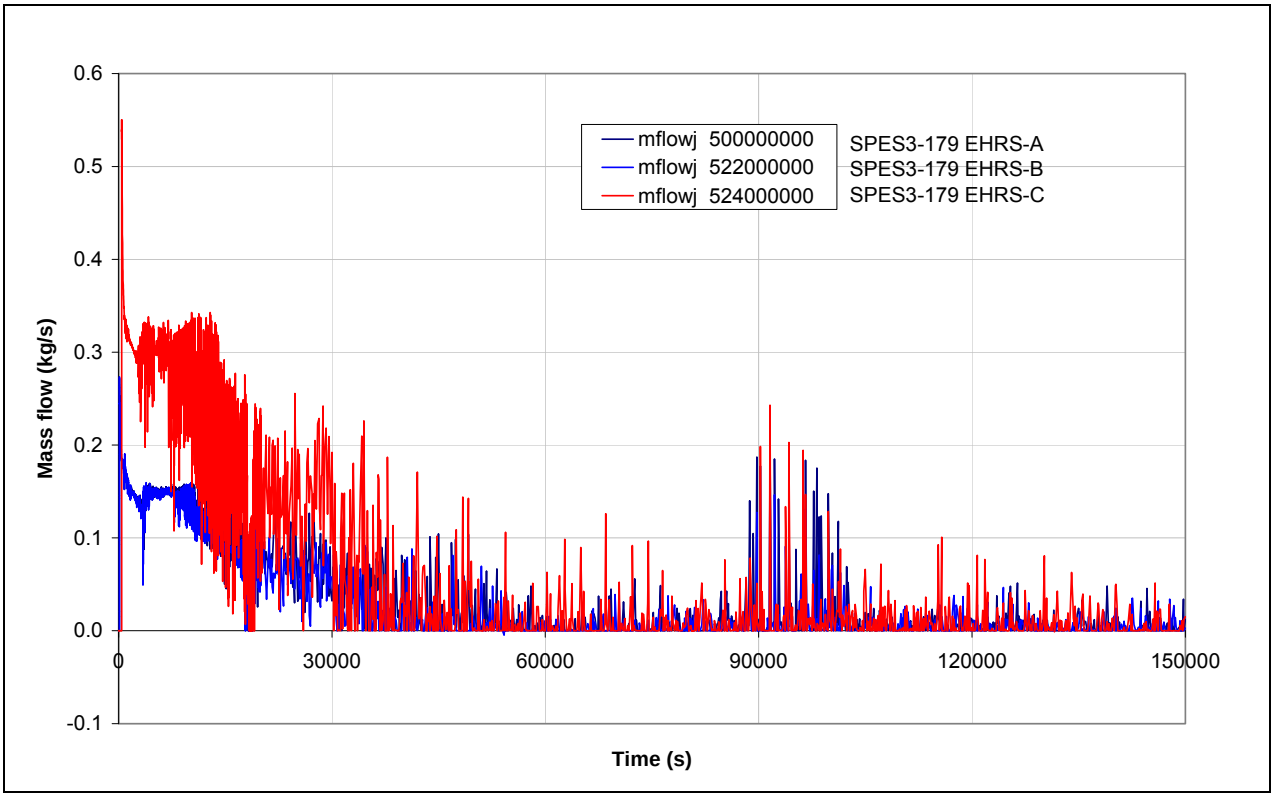

Fig.5. 35 - SPES3-179 EHRS power (window)

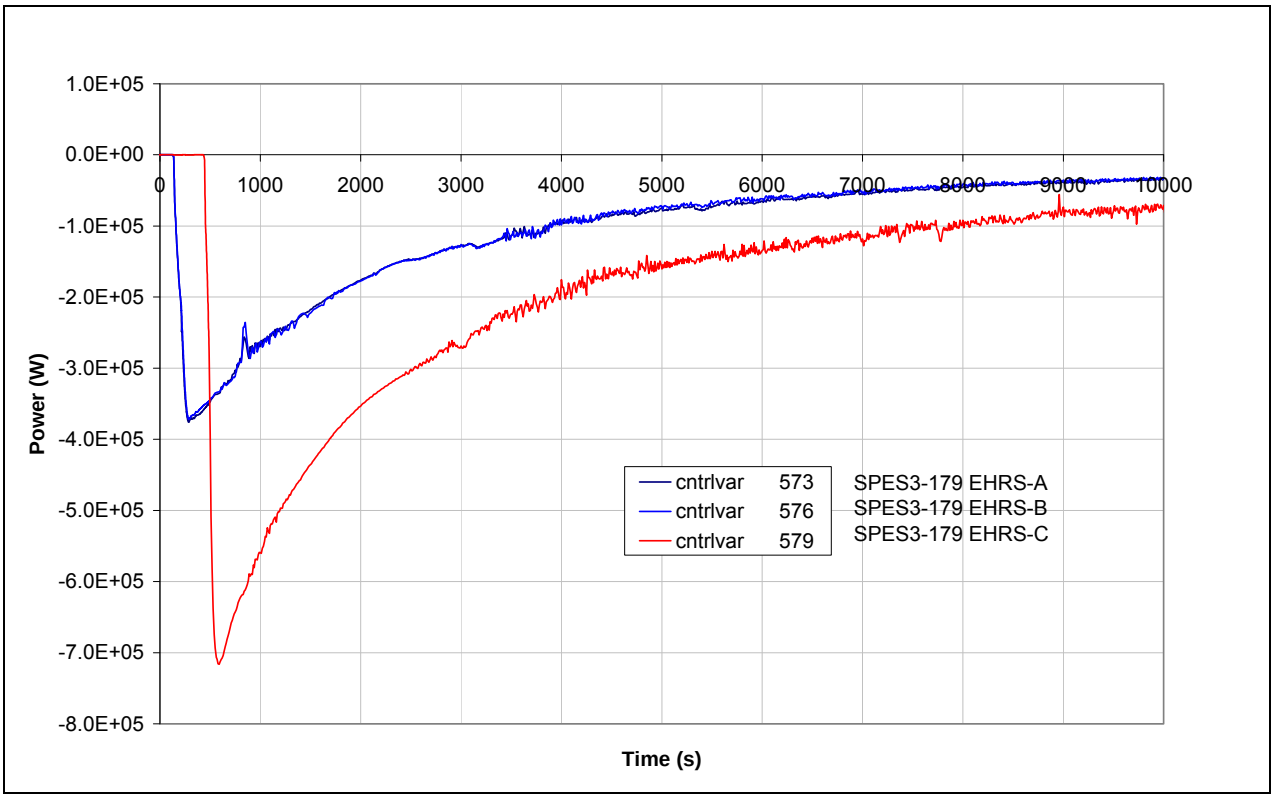

Fig.5. 36 - SPES3-179 EHRS power

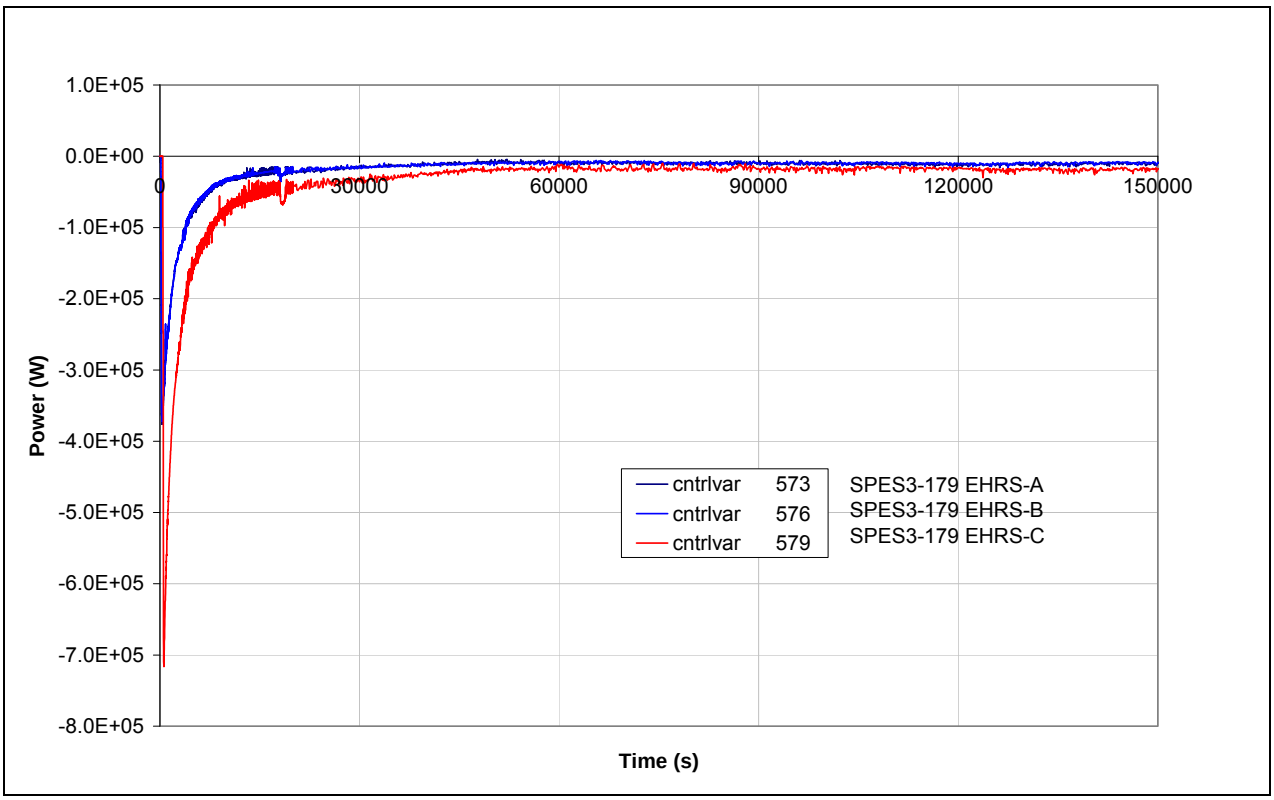

Fig.5. 37 - SPES3-179 SG secondary side outlet pressure (window)

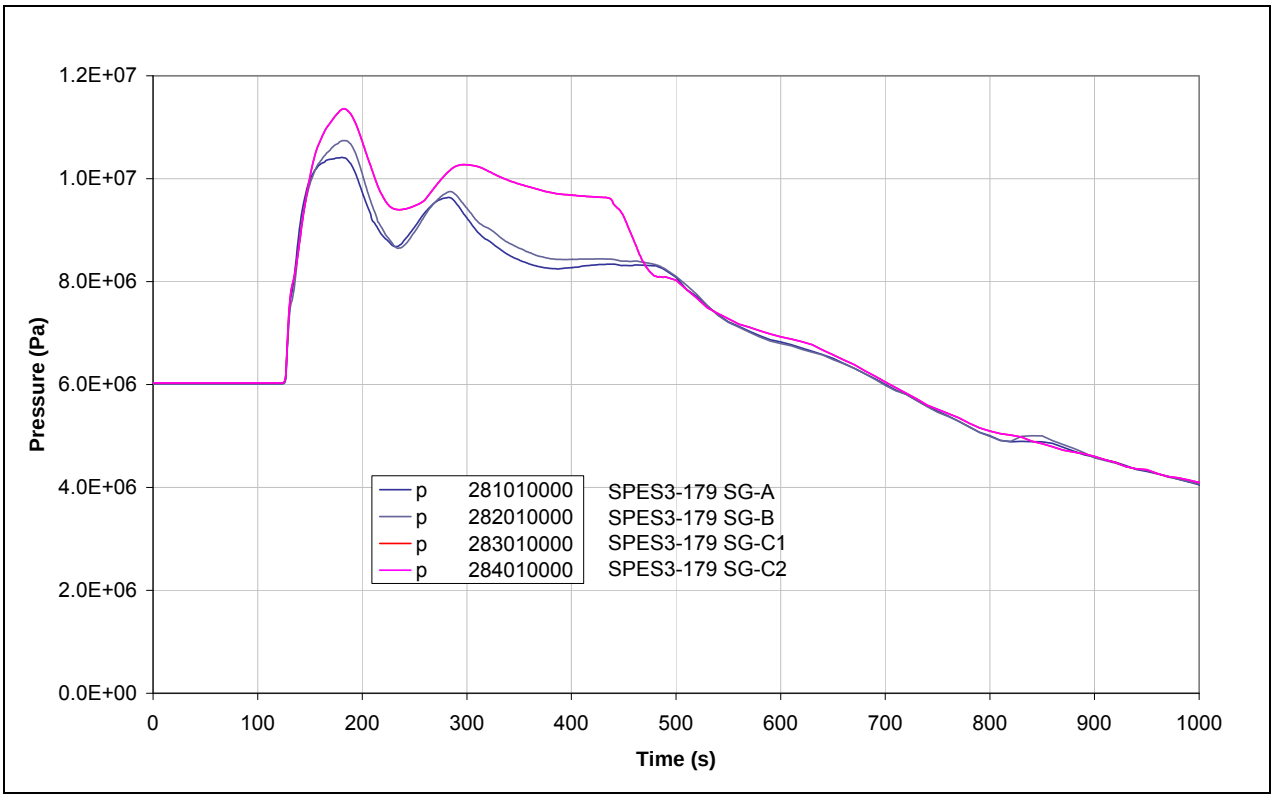

Fig.5. 38 - SPES3-179 SG secondary side outlet pressure

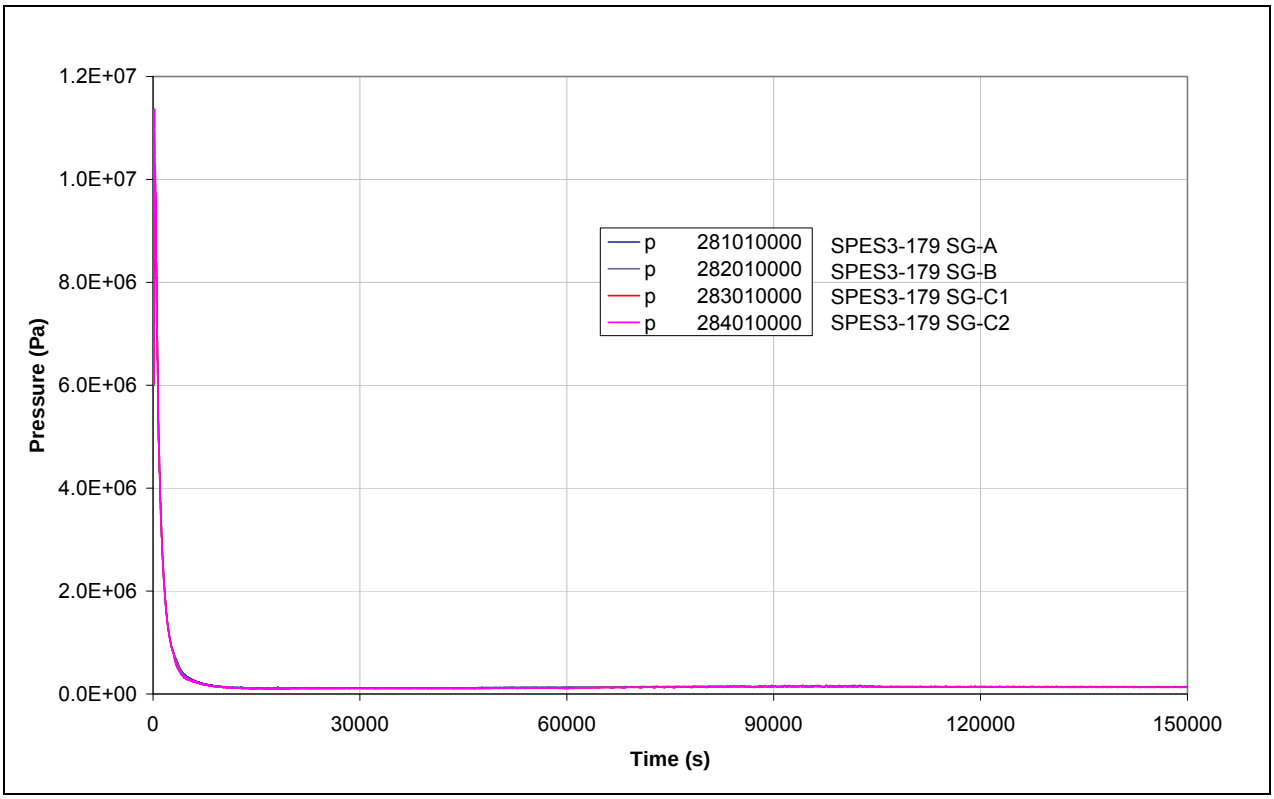

Fig.5. 39 - SPES3-179 SG secondary side collapsed level (window)

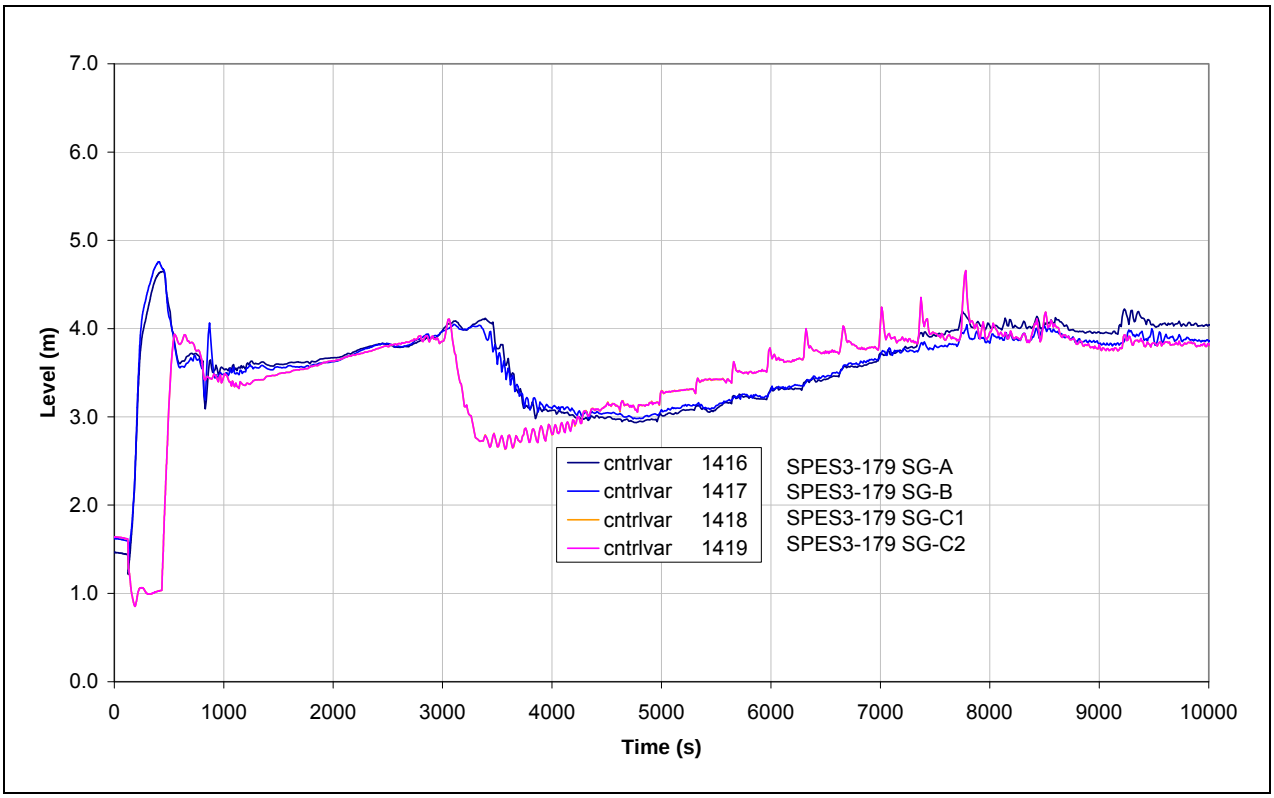

Fig.5. 40 - SPES3-179 SG secondary side collapsed level

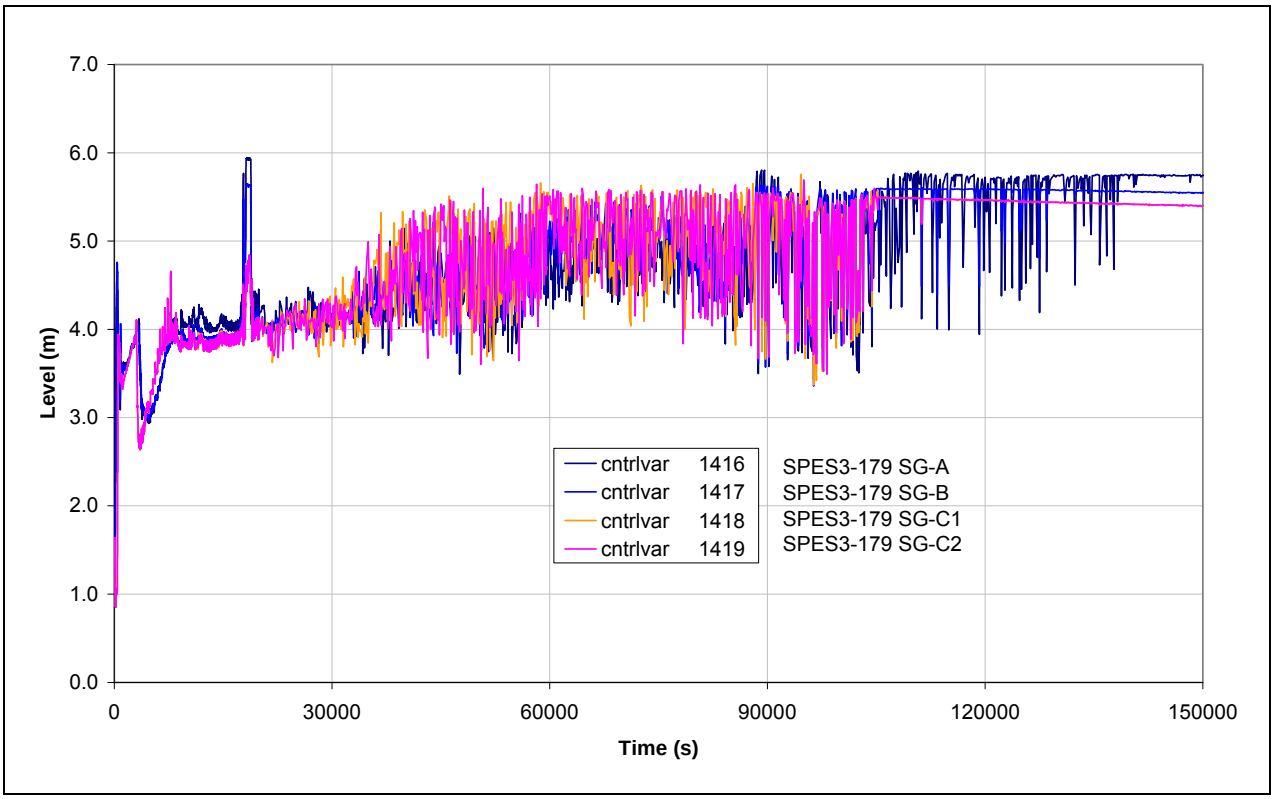

Fig.5. 41 - SPES3-179 PRZ level (window)

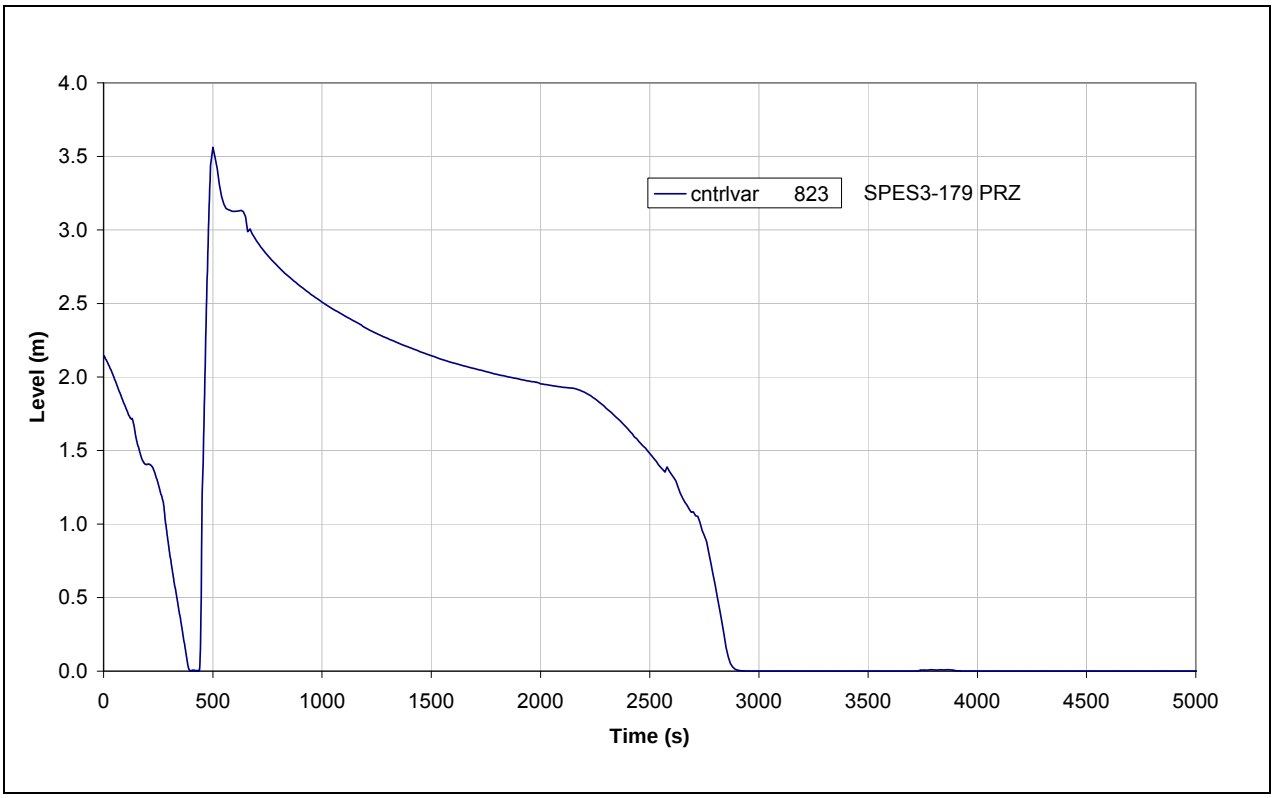

Fig.5. 42 - SPES3-179 Pump inlet liquid fraction (window)

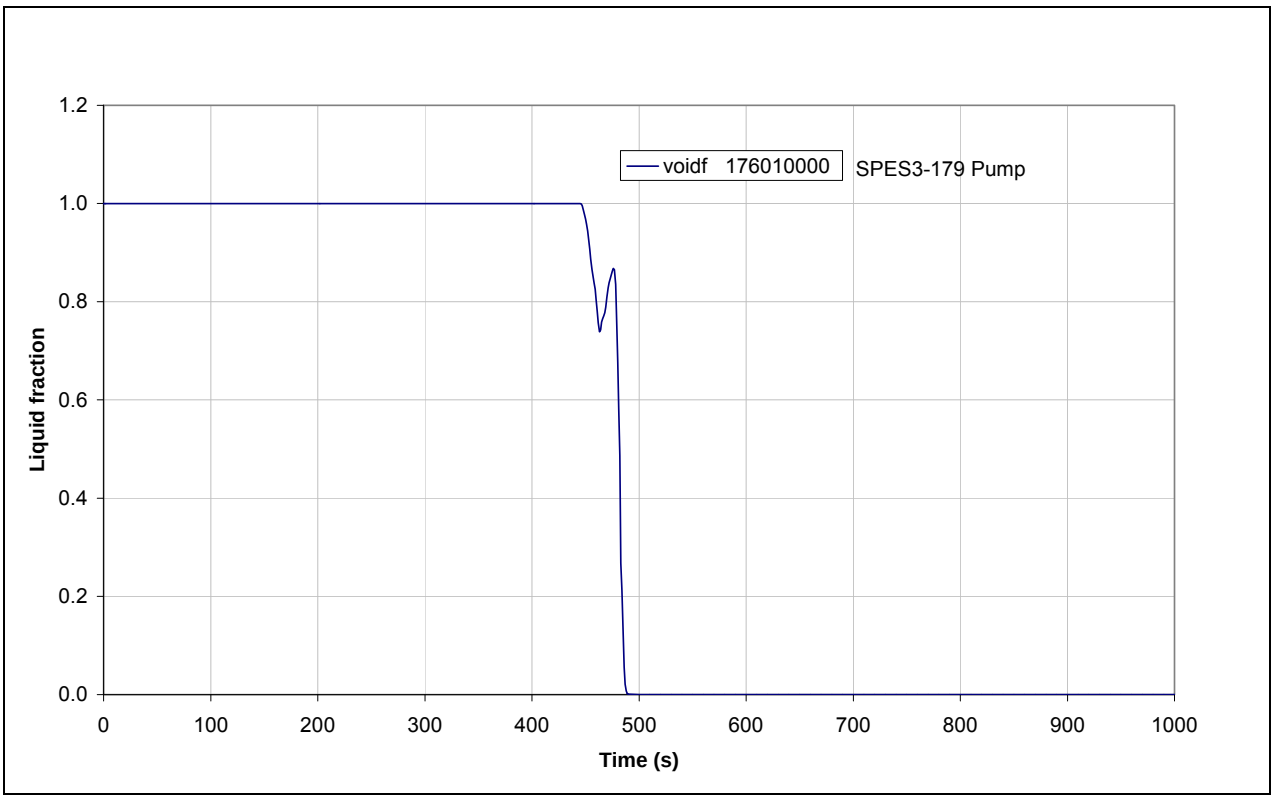

Fig.5. 43 - SPES3-179 Pump velocity (window)

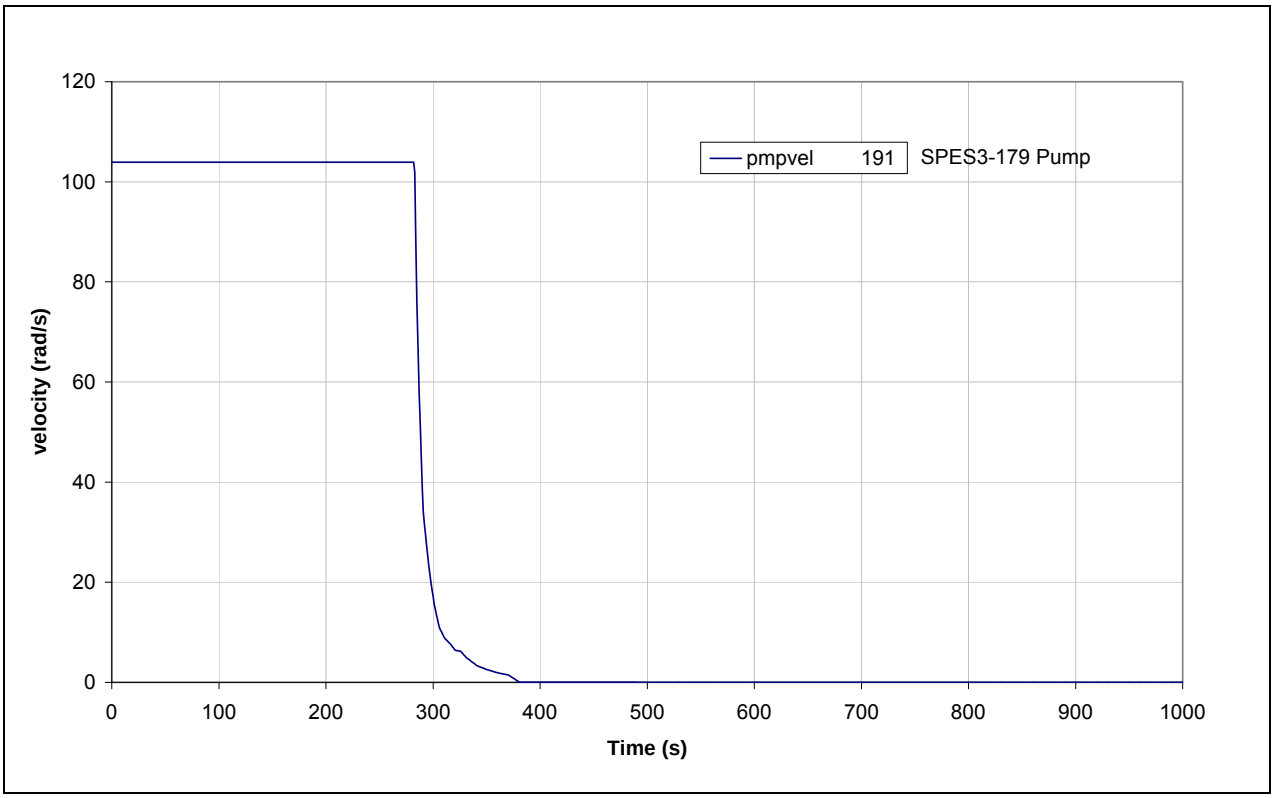

Fig.5. 44 - SPES3-179 Pump by-pass mass flow (window)

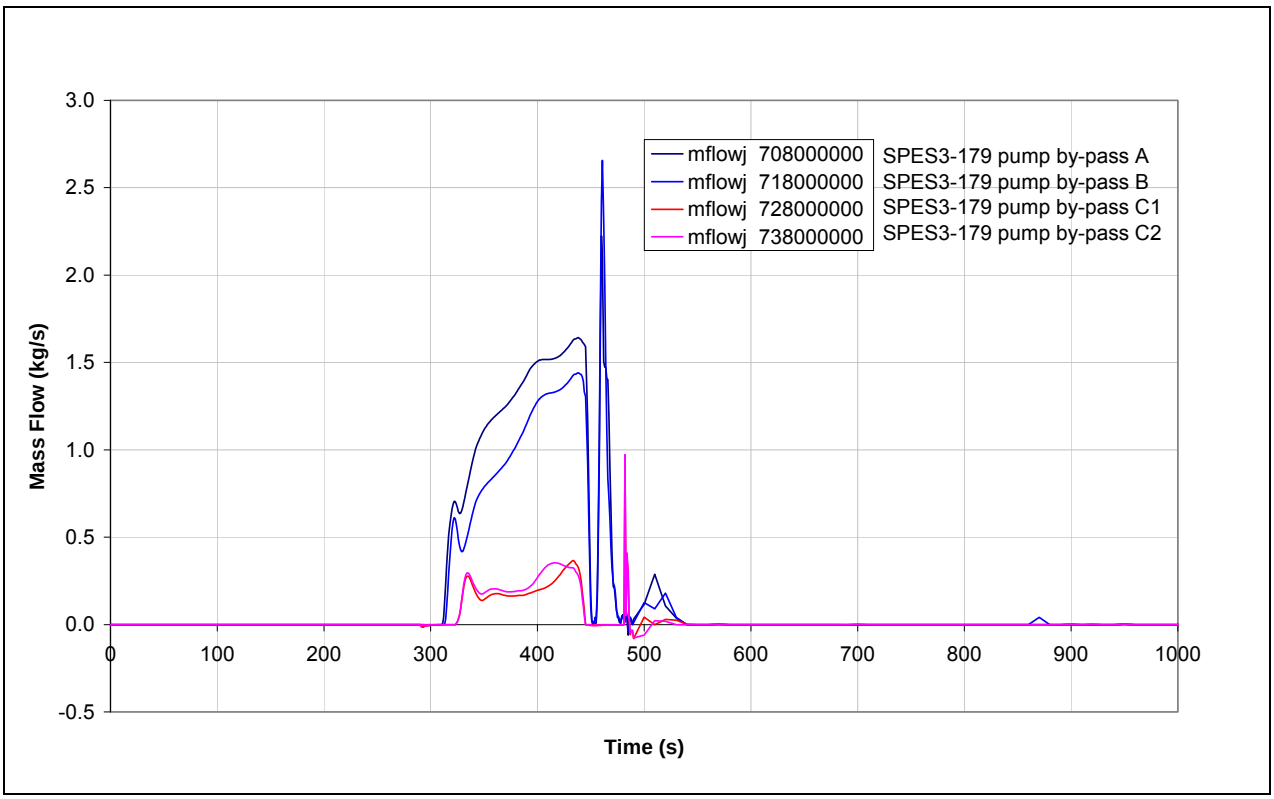

Fig.5. 45 - SPES3-179 Core inlet mass flow (window)

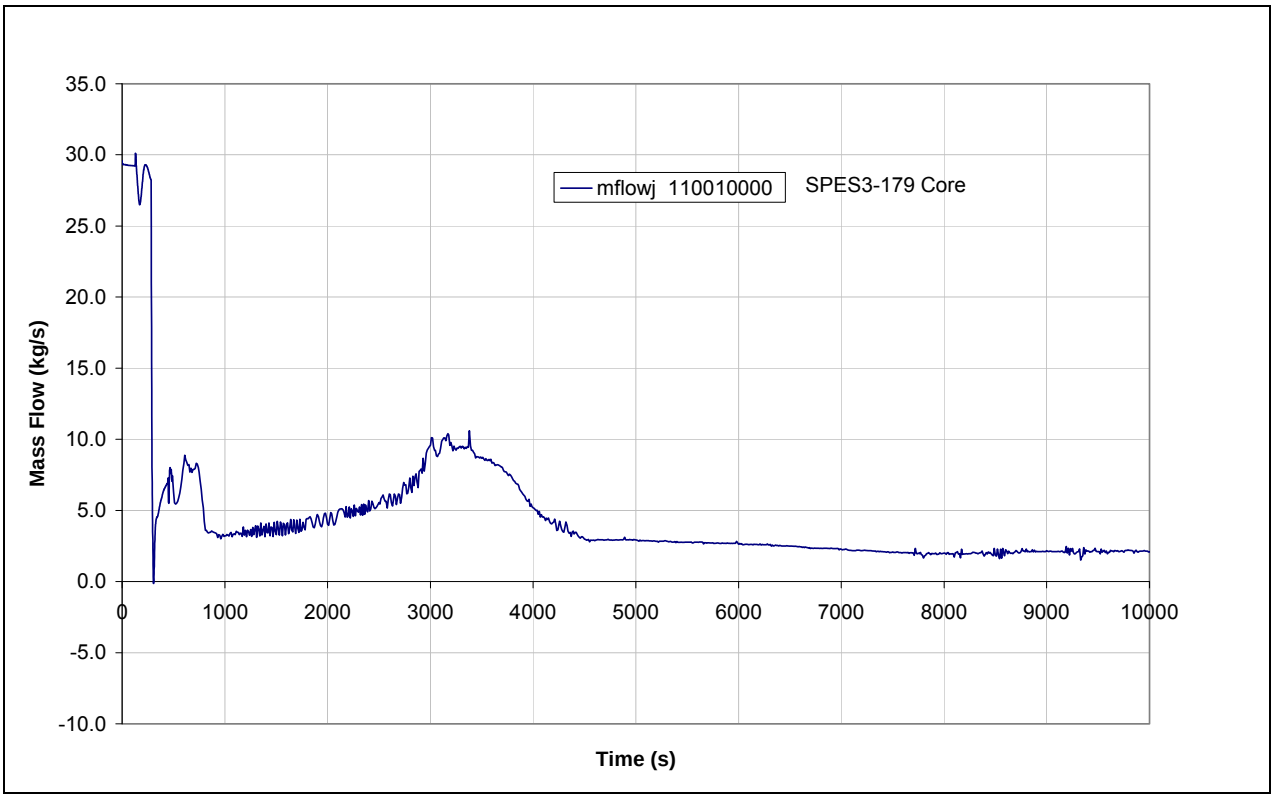

Fig.5. 46 - SPES3-179 Core inlet mass flow

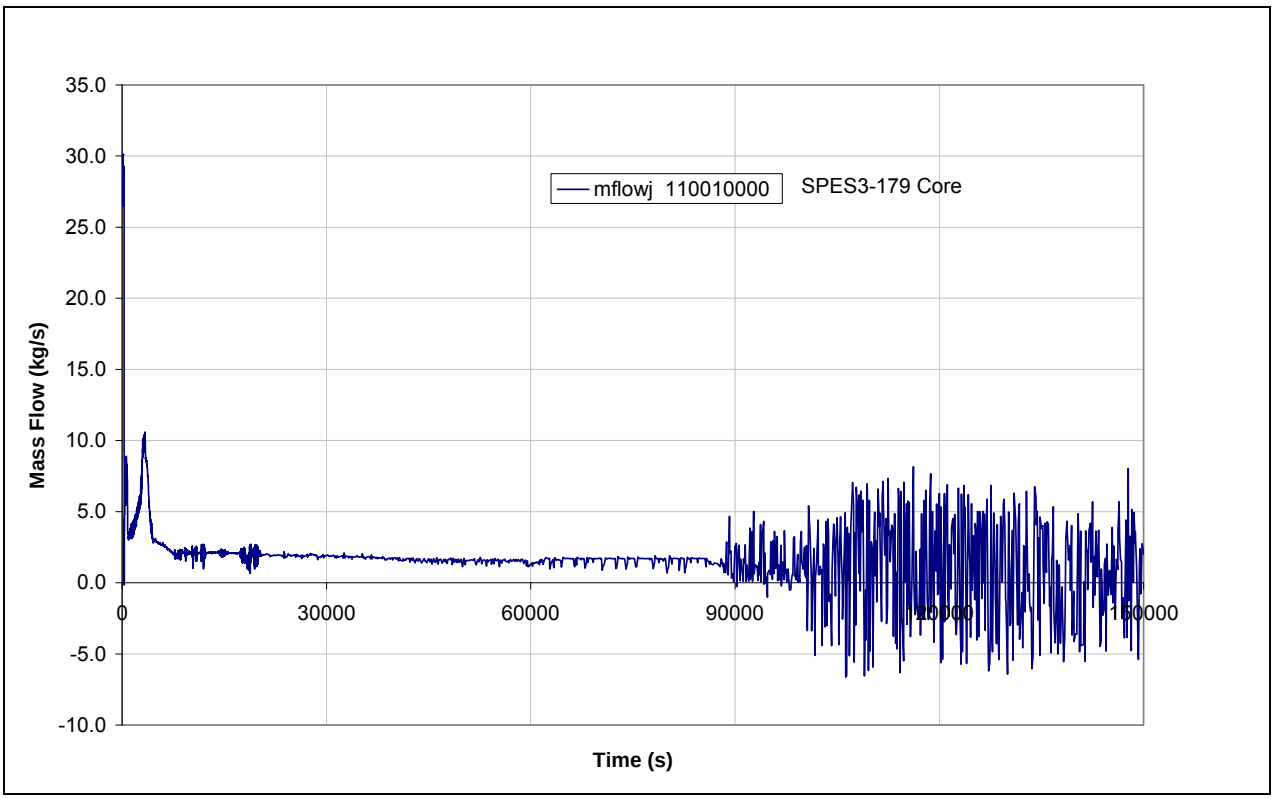

Fig.5. 47 - SPES3-179 RI-DC check valve mass flow (window)

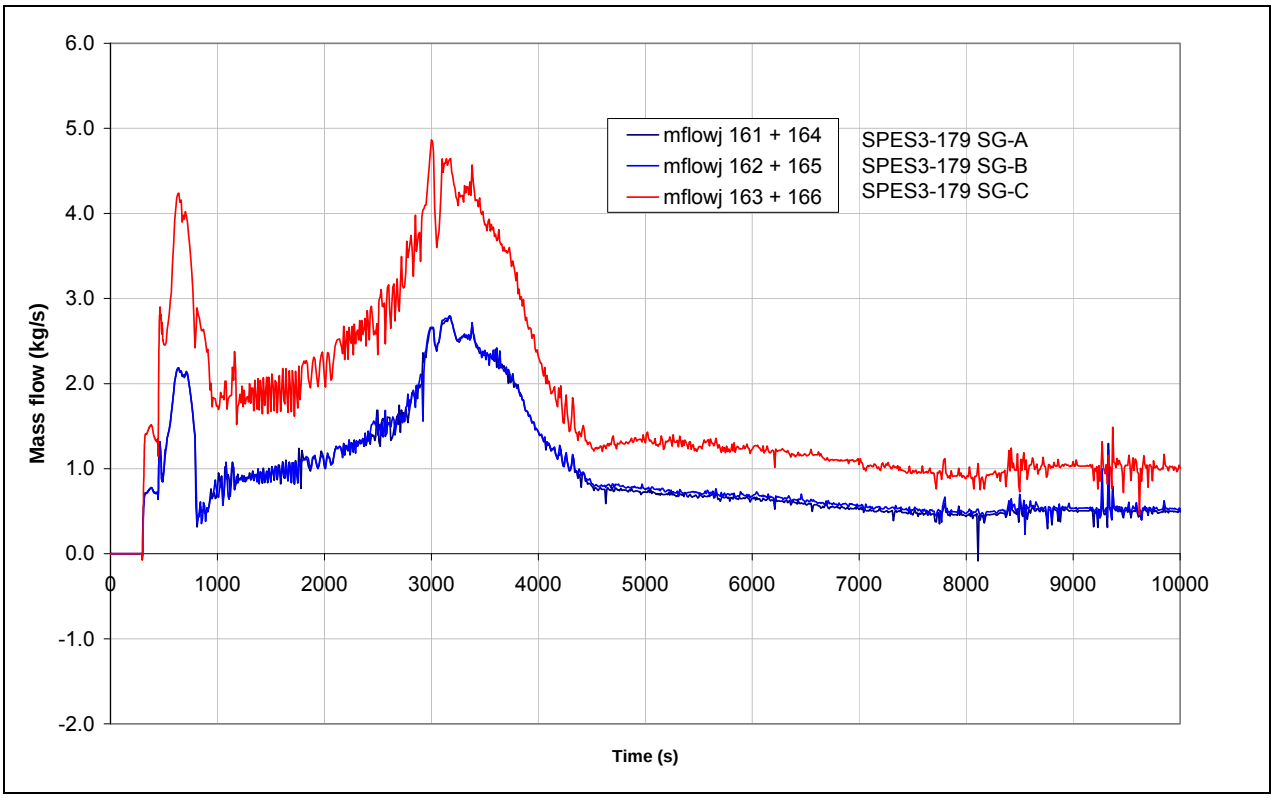

Fig.5. 48 - SPES3-179 RI-DC check valve mass flow

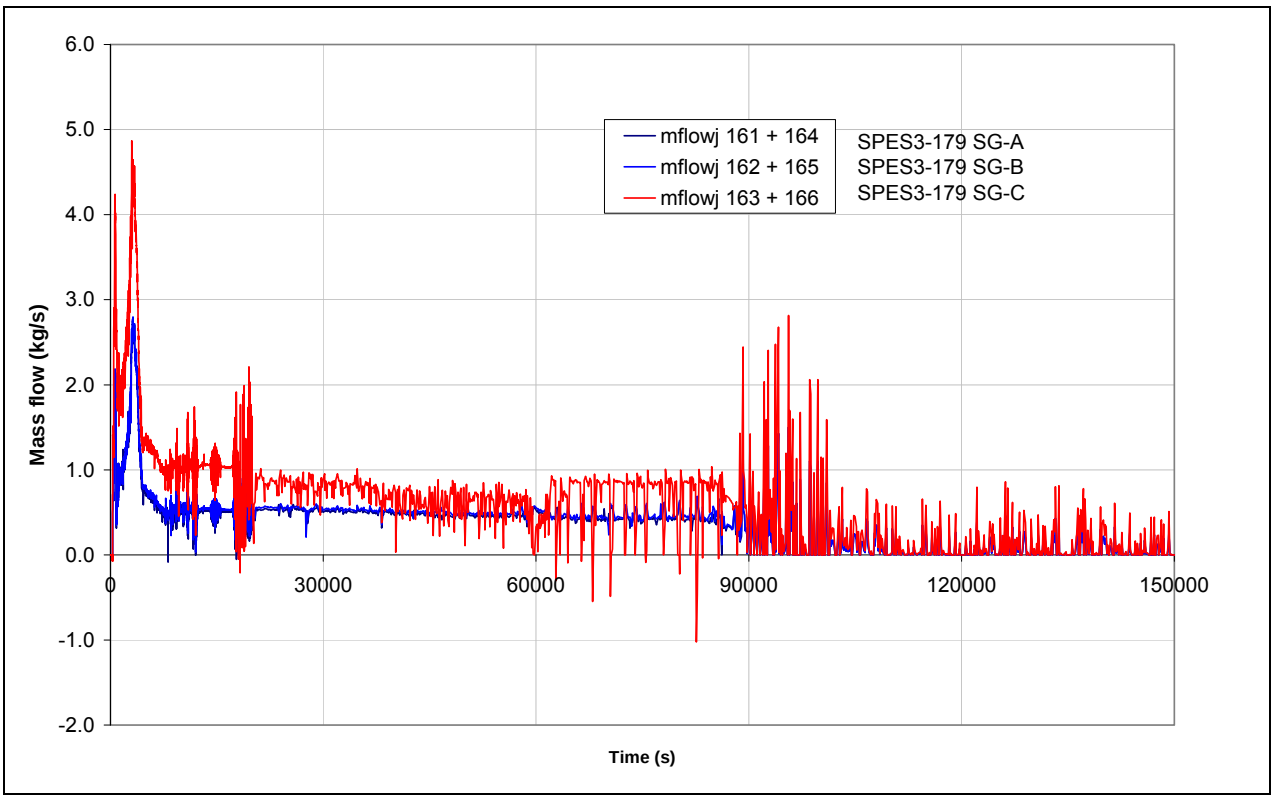

Fig.5. 49 - SPES3-179 RPV mass (window)

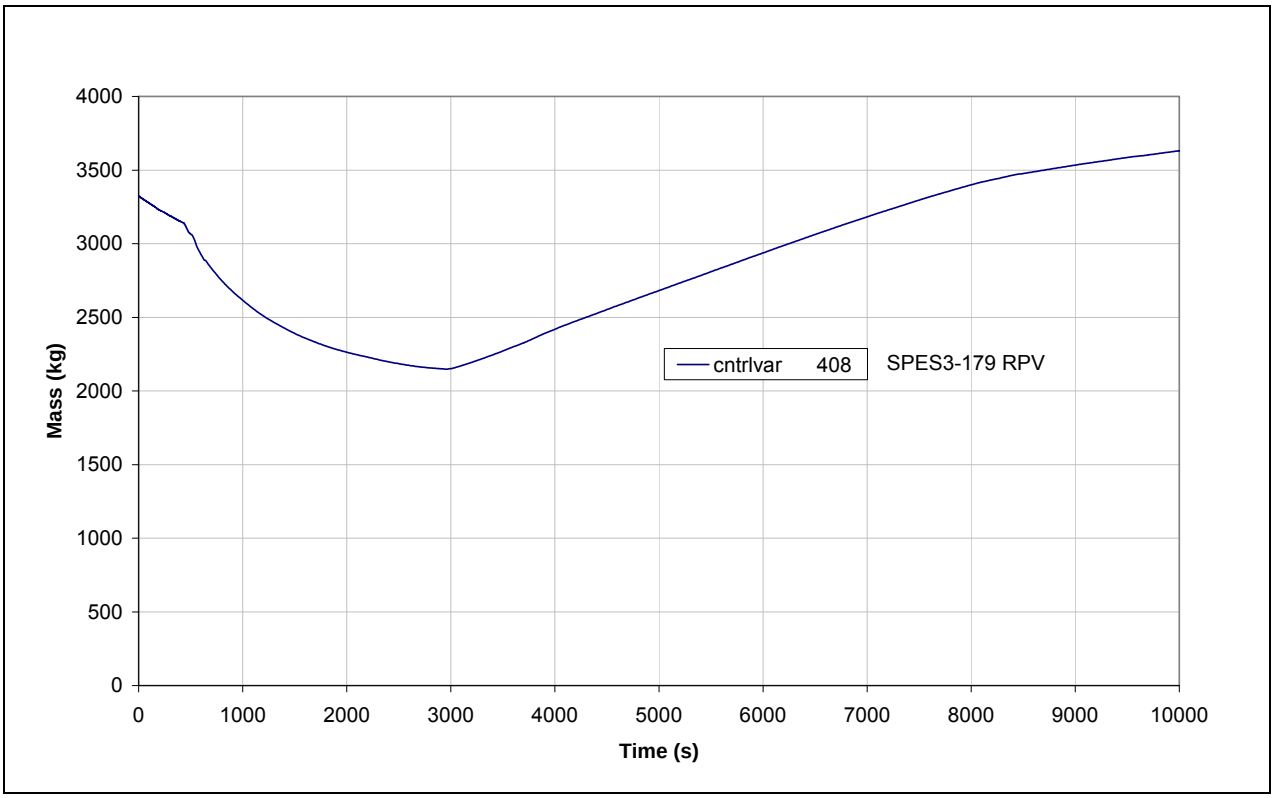

Fig.5. 50 - SPES3-179 RPV mass

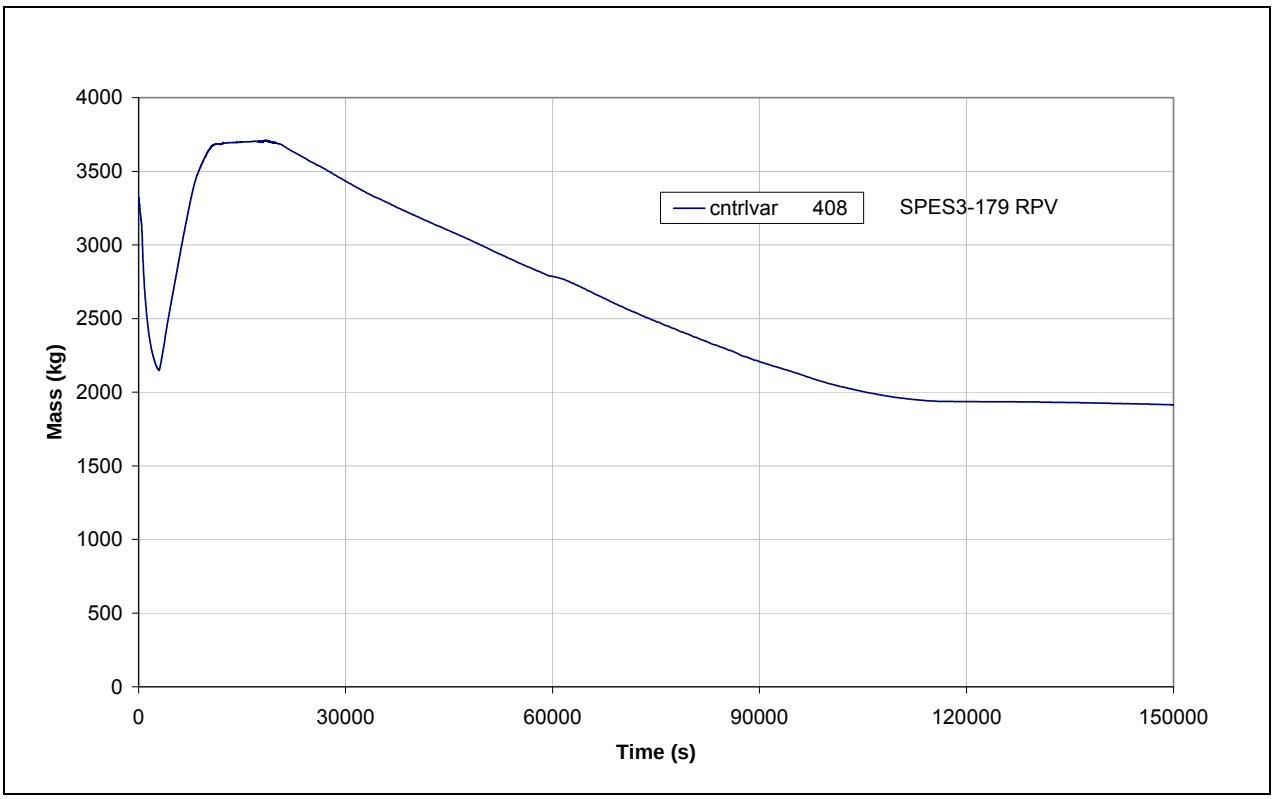

Fig.5. 51 - SPES3-179 Core liquid fraction (window)

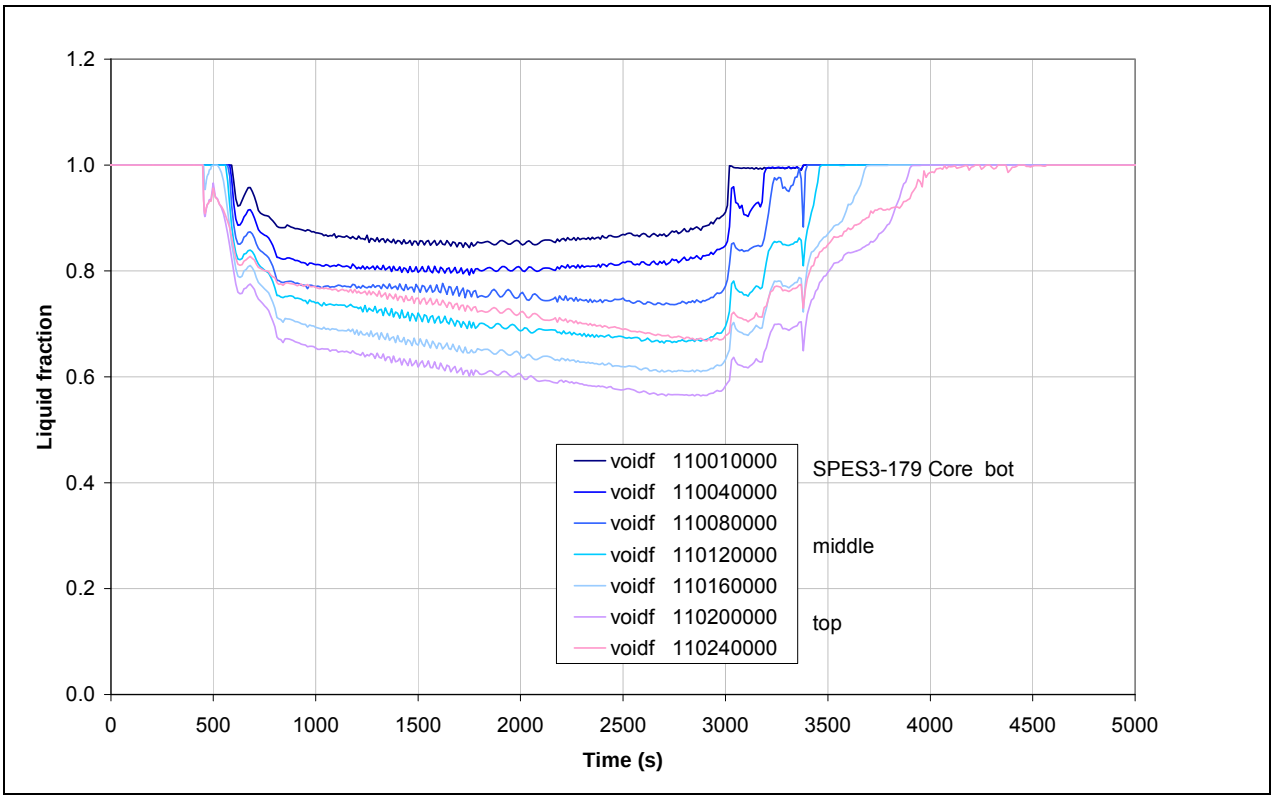

Fig.5. 52 - SPES3-179 Core liquid fraction

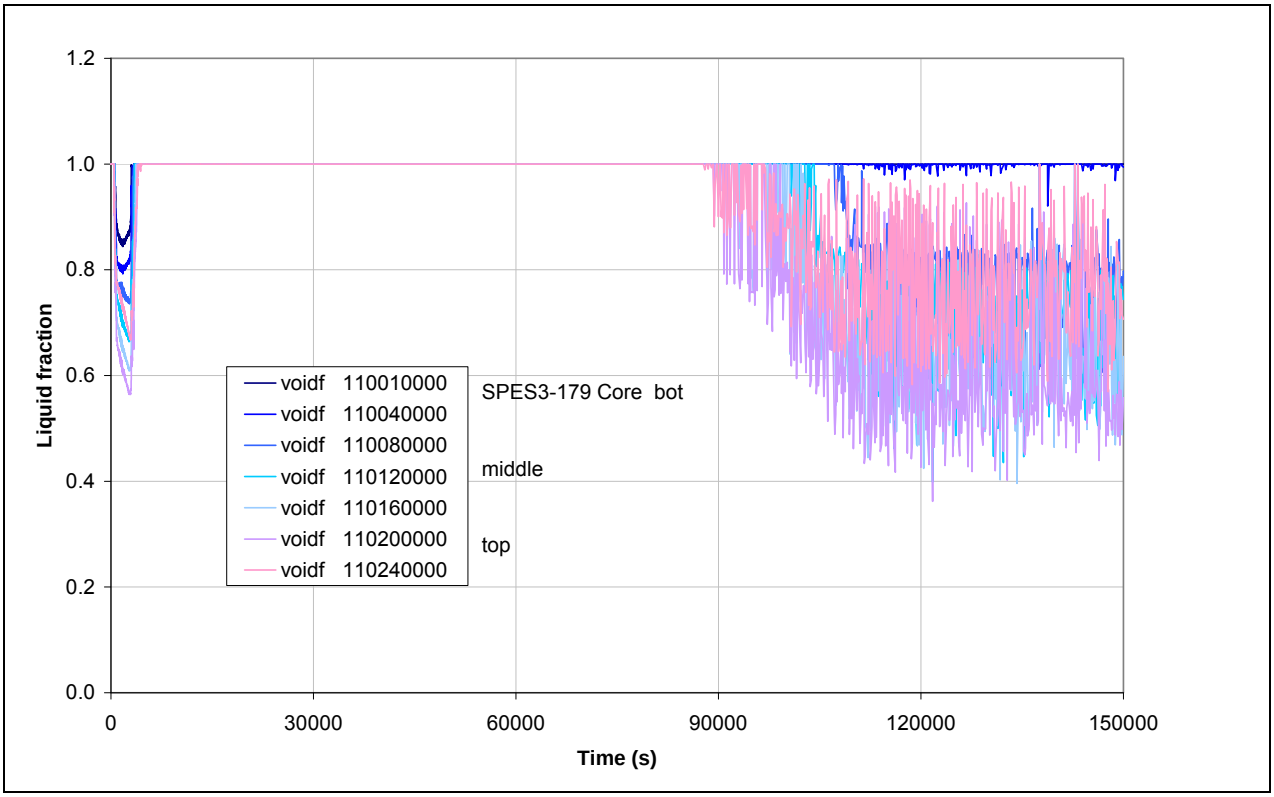

Fig.5. 53 - SPES3-179 ADS Stage-I integral flow

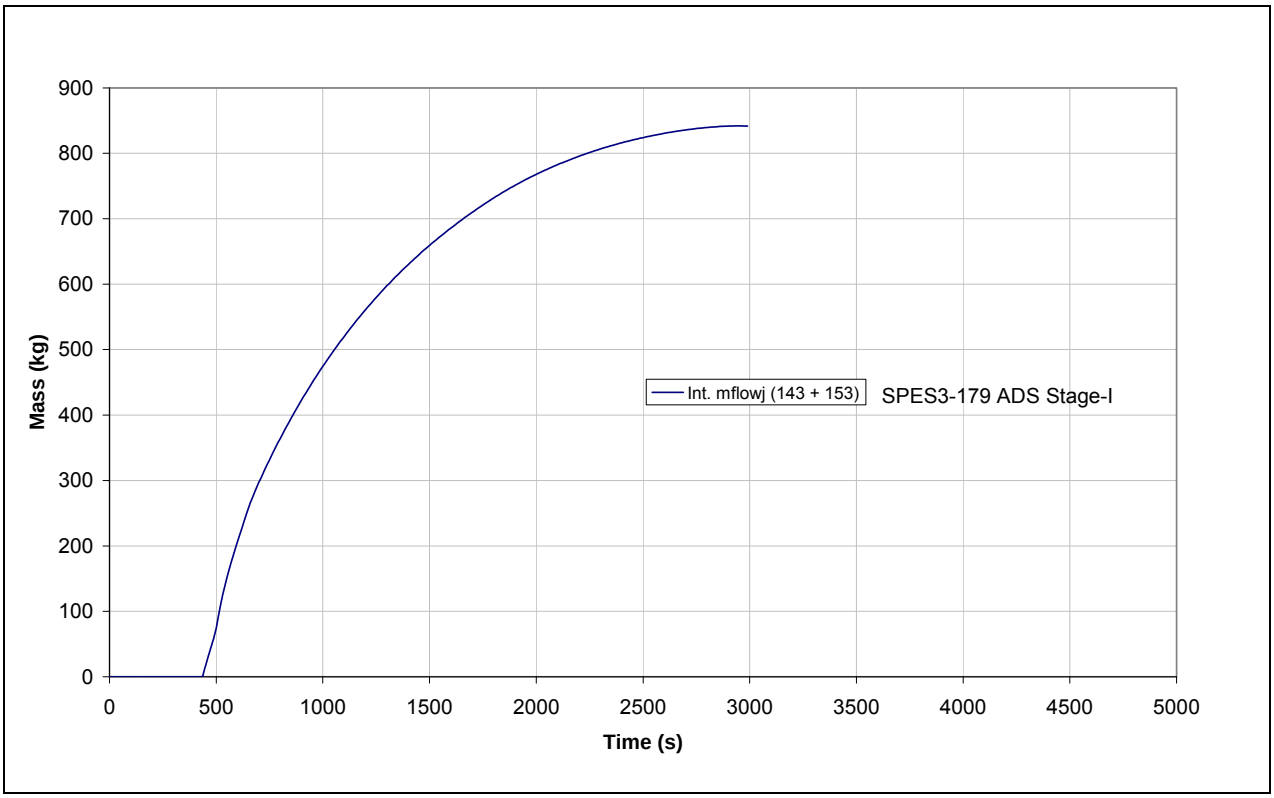

Fig.5. 54 - SPES3-179 RC to DVI mass flow (window)

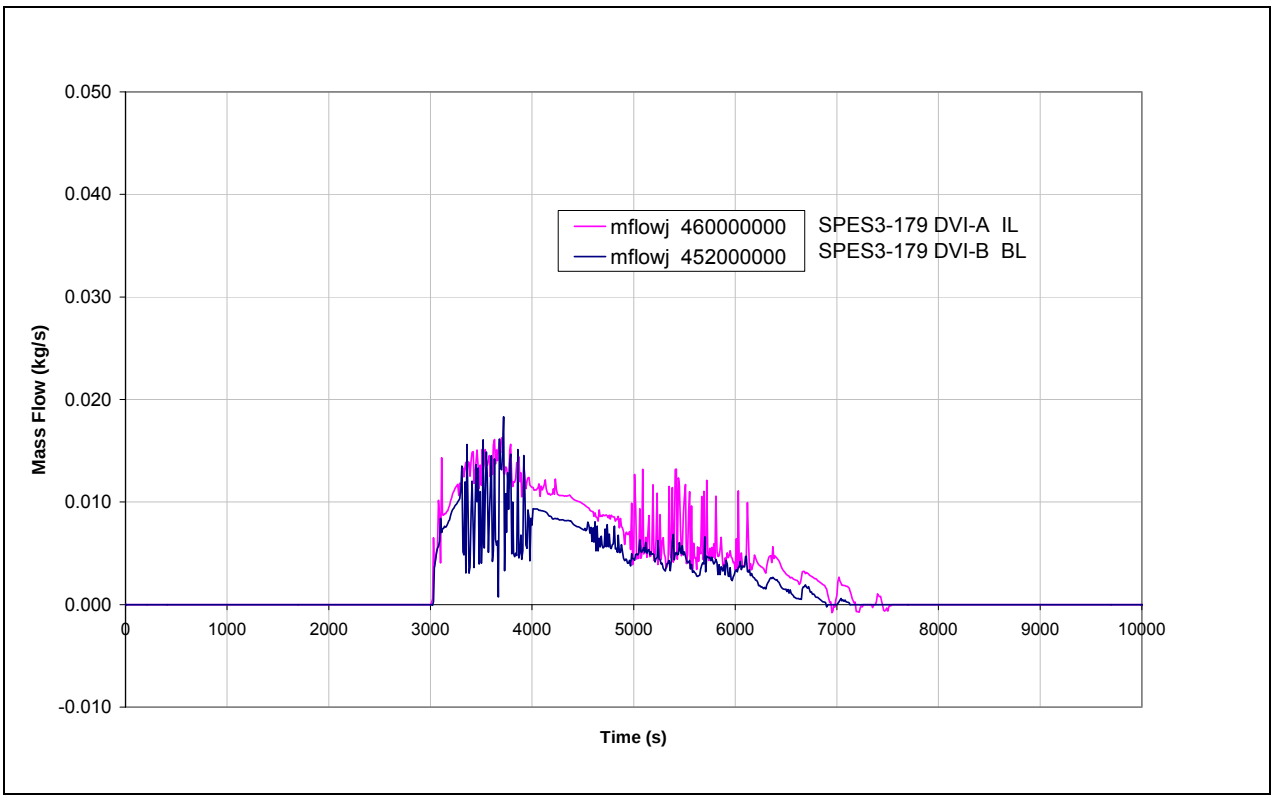

Fig.5. 55 - SPES3-179 EBT level (window)

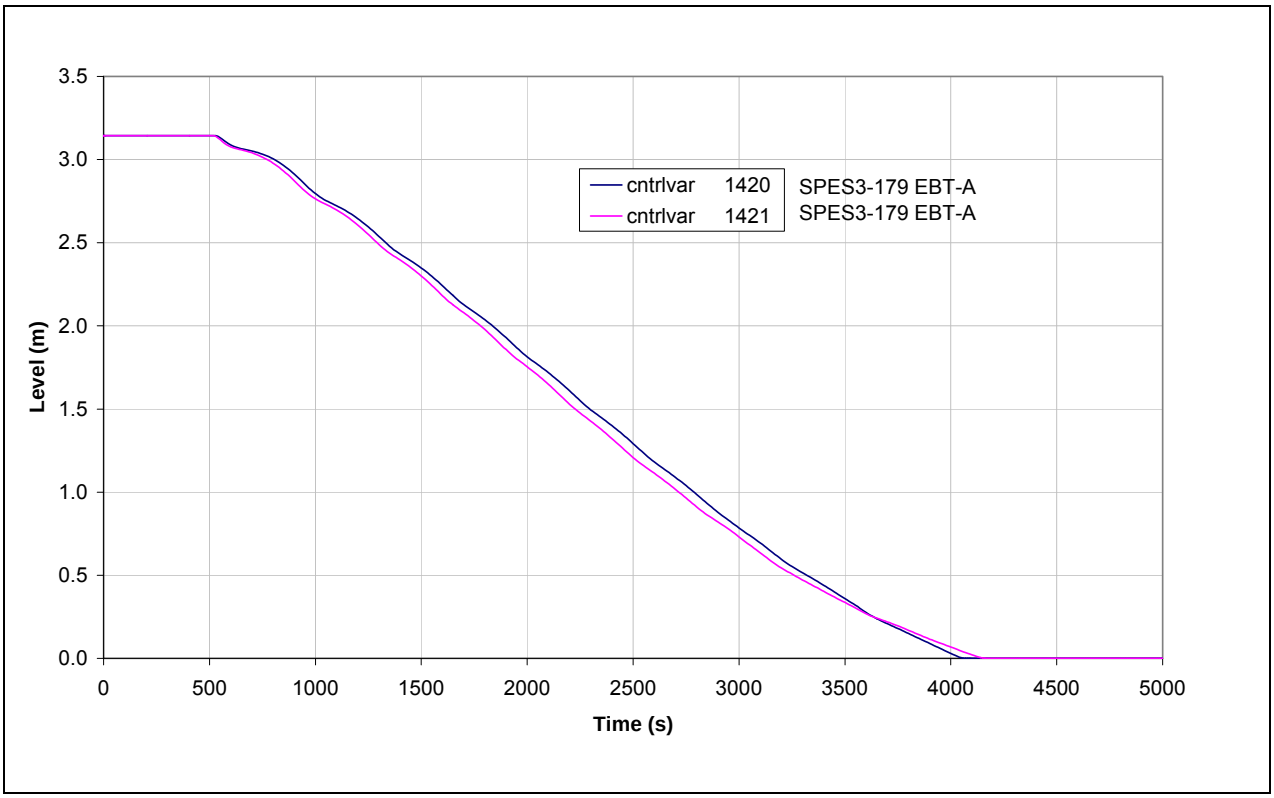

Fig.5. 56 - SPES3-179 EBT to RPV balance line mass flow (window)

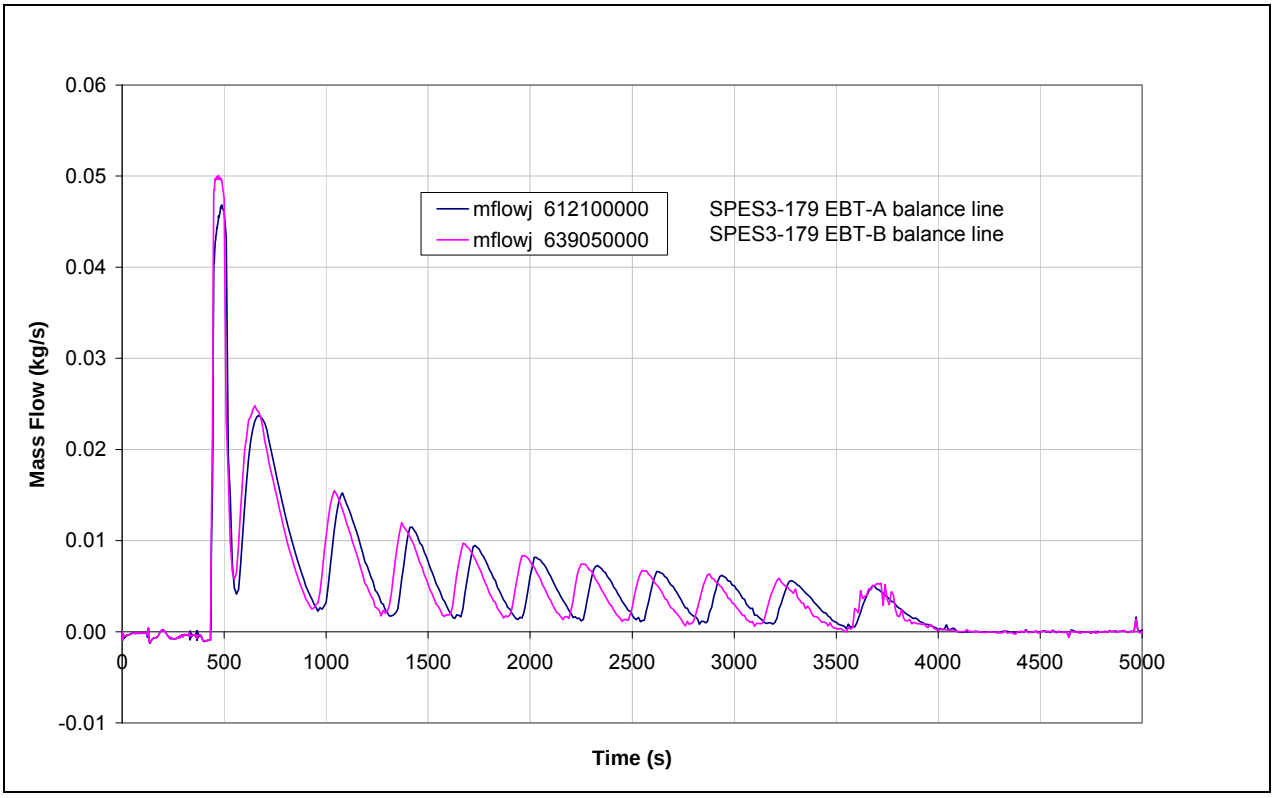

Fig.5. 57 - SPES3-179 Core inlet and outlet fluid temperature (window)

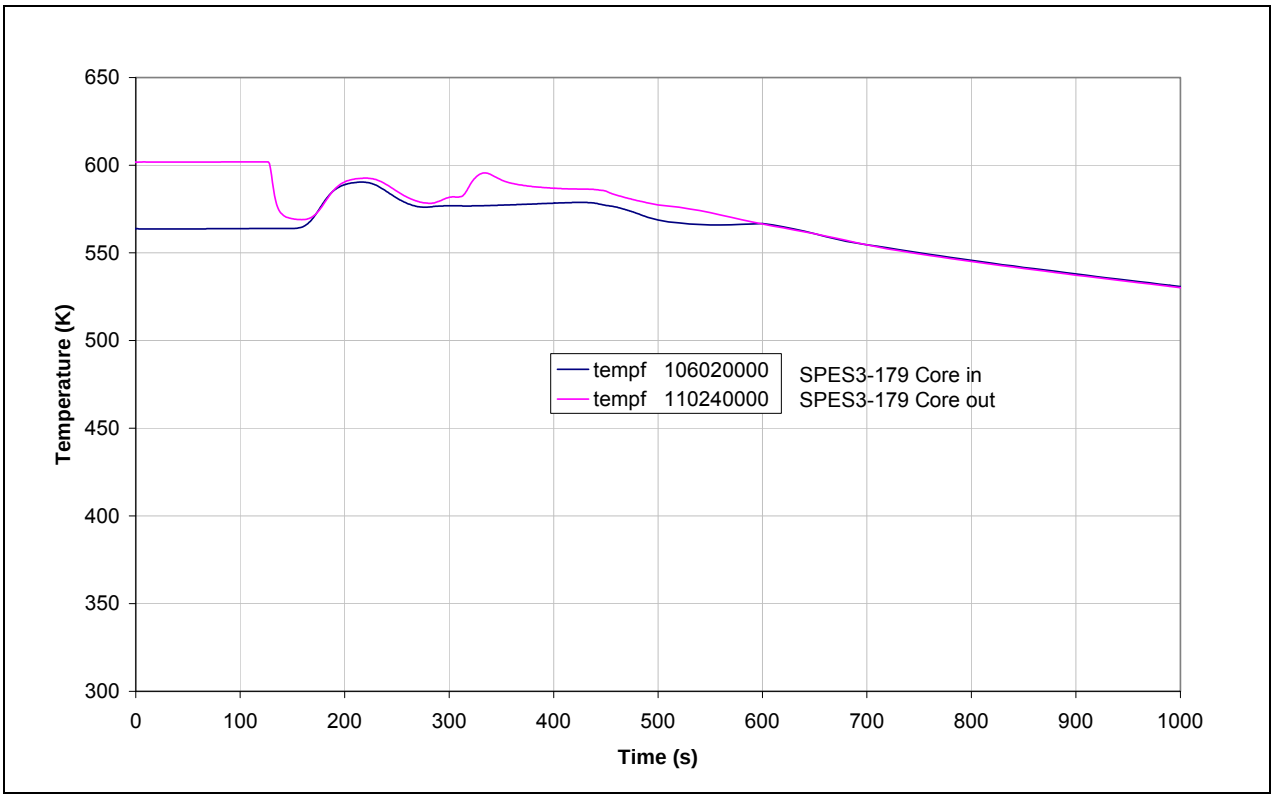

Fig.5. 58 - SPES3-179 Core inlet and outlet fluid temperature

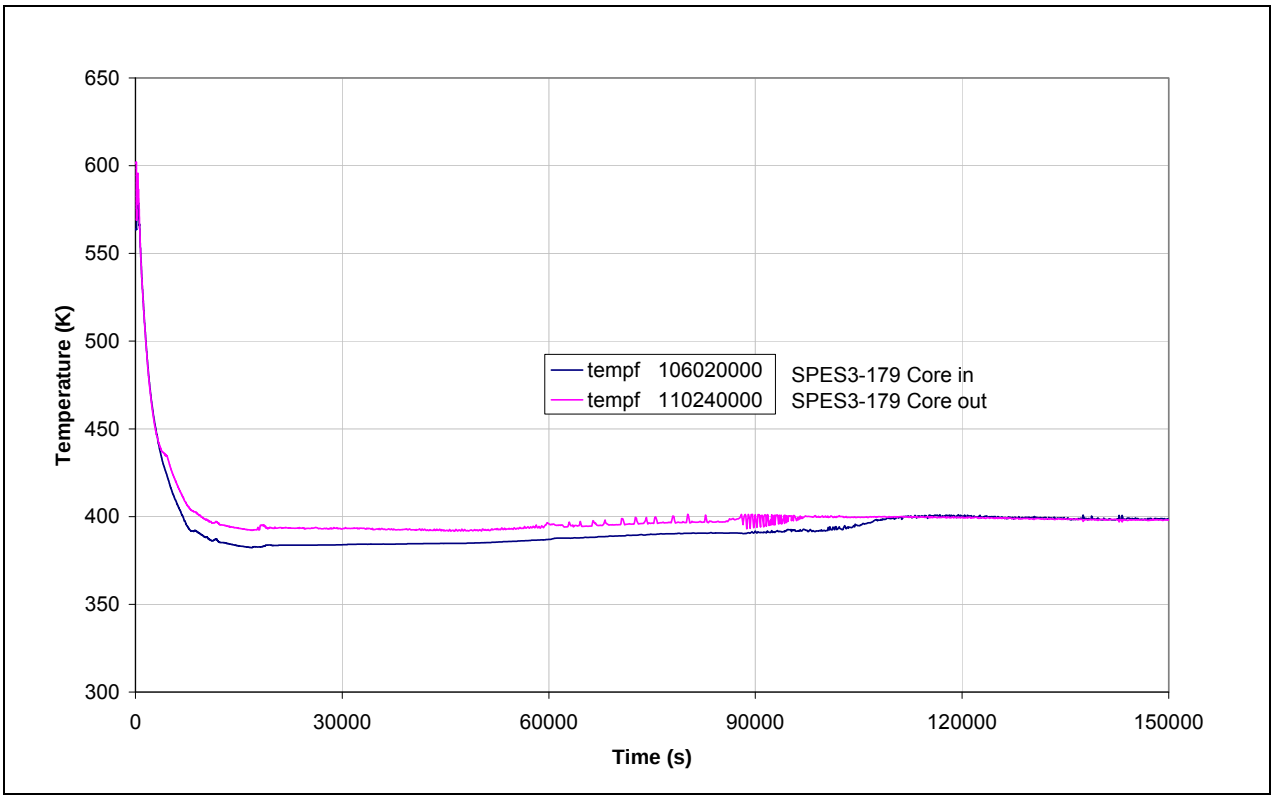

Fig.5. 59 - SPES3-179 Core heater rod surface temperature –normal rod (window)

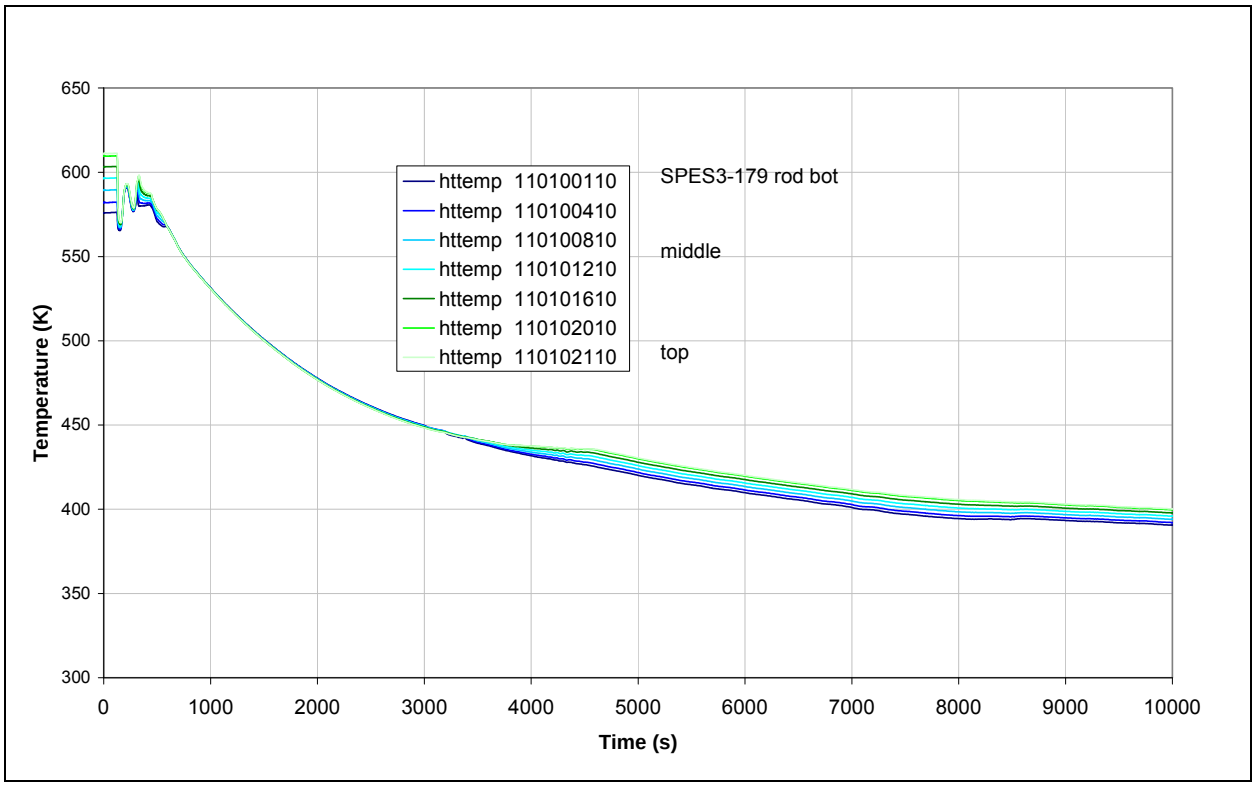

Fig.5. 60 - SPES3-179 Core heater rod surface temperature –normal rod

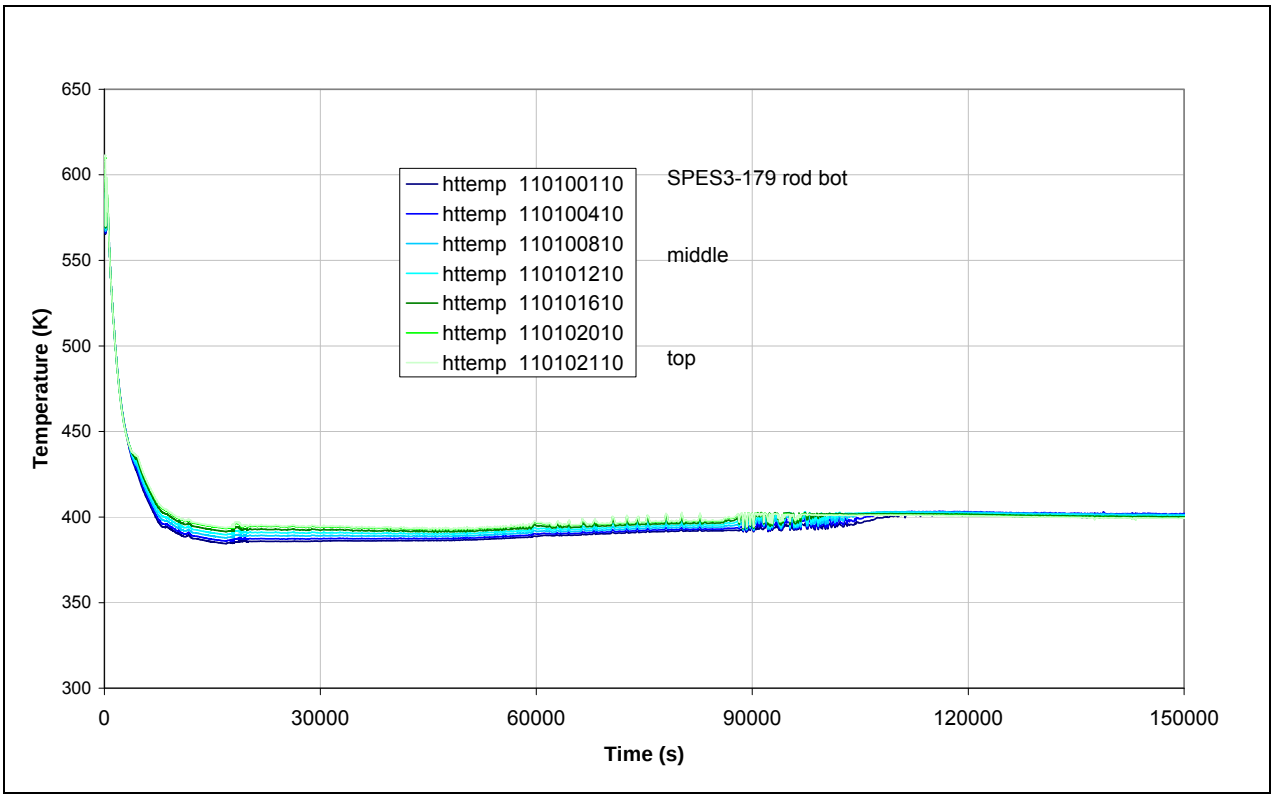

Fig.5. 61 - SPES3-179 Core heater rod surface temperature –hot rod (window)

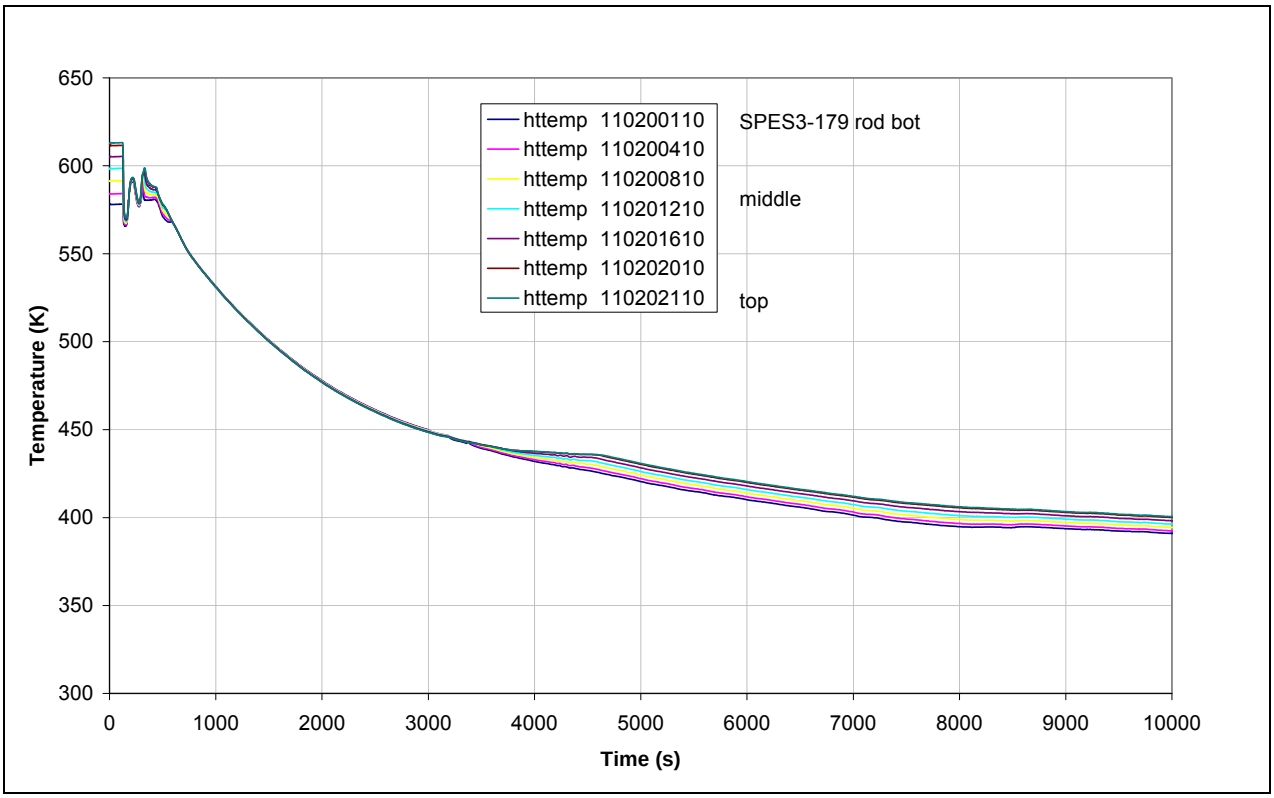

Fig.5. 62 - SPES3-179 Core heater rod surface temperature –hot rod

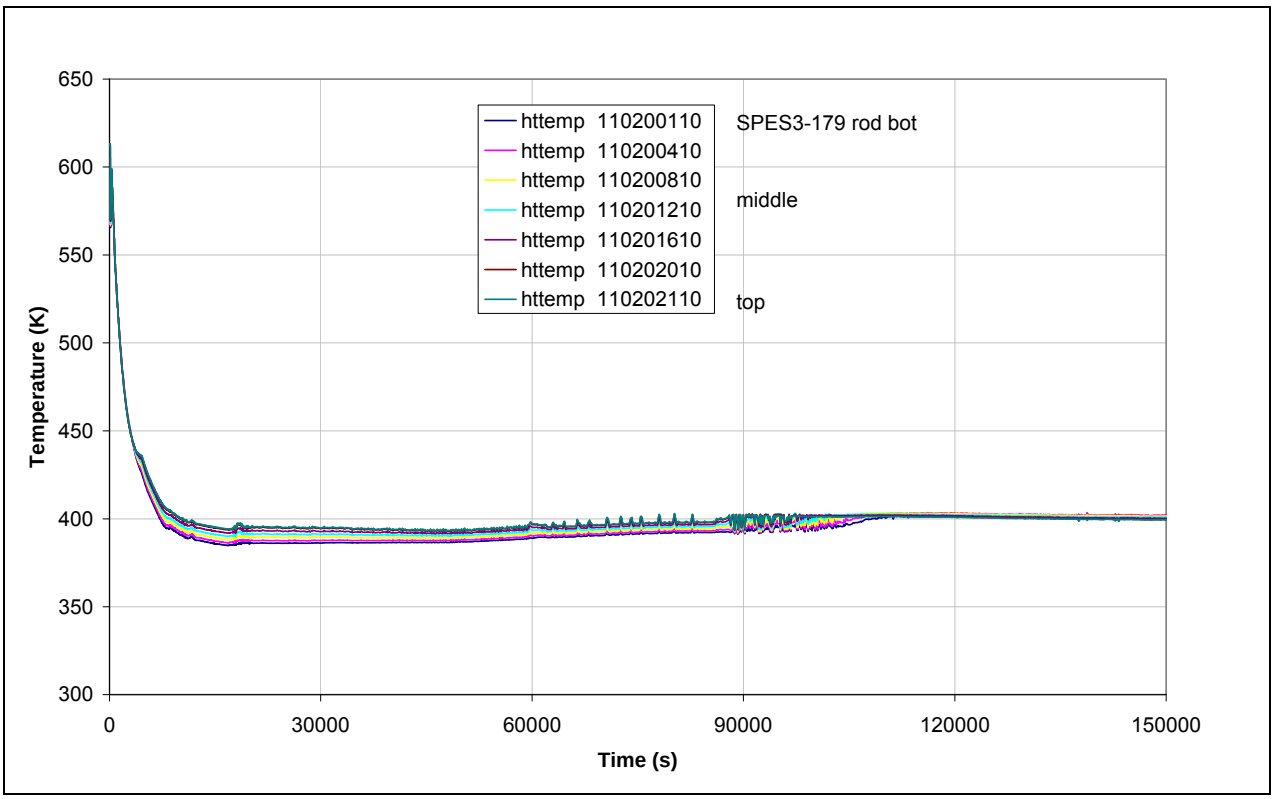

Fig.5. 63 - SPES3-179 DVI mass flow (window)

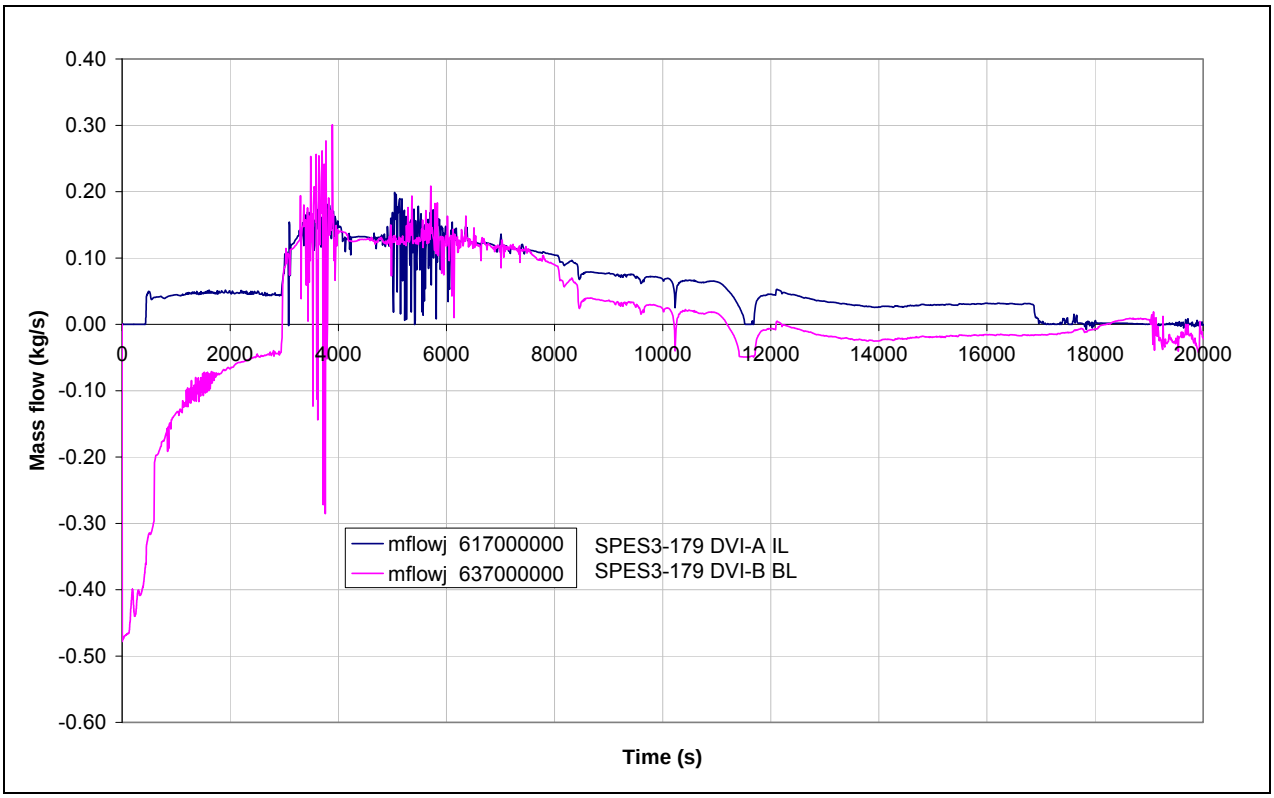

Fig.5. 64 - SPES3-179 DVI mass flow

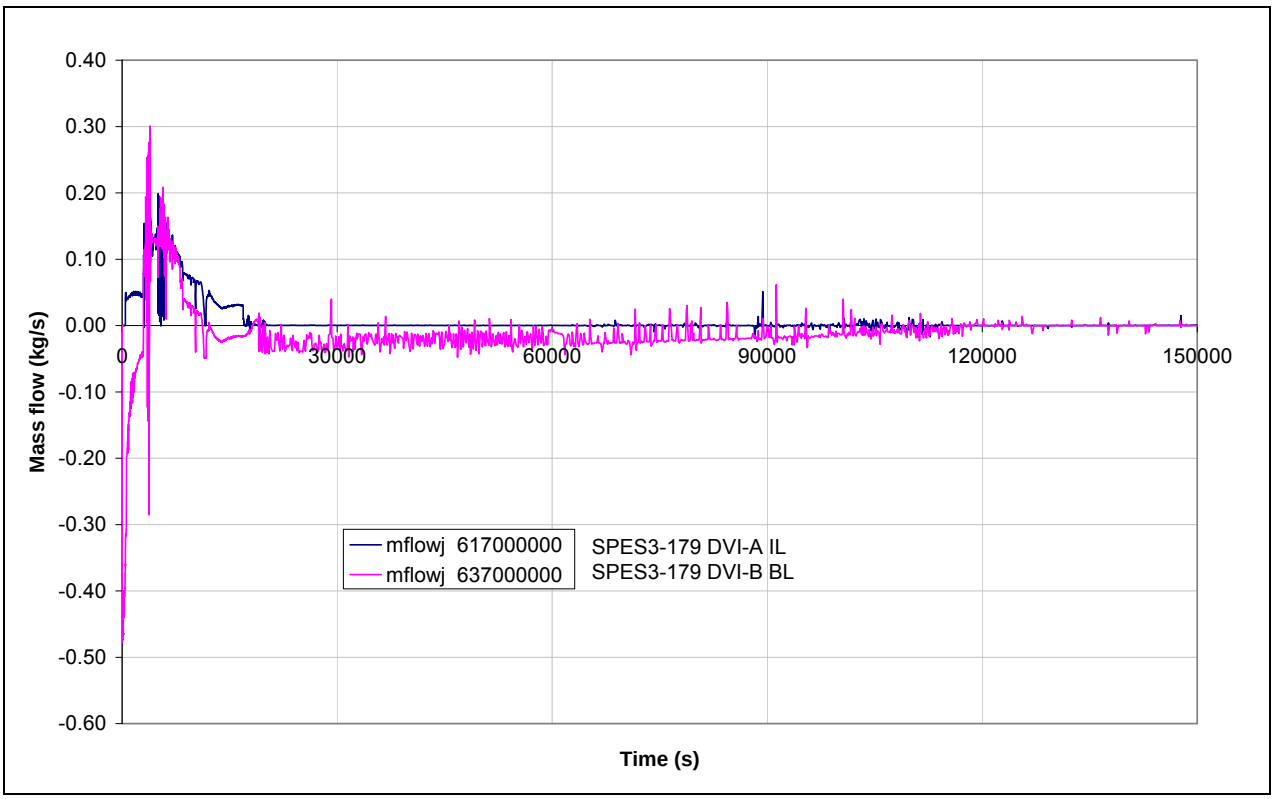

Fig.5. 65 - SPES3-179 QT level

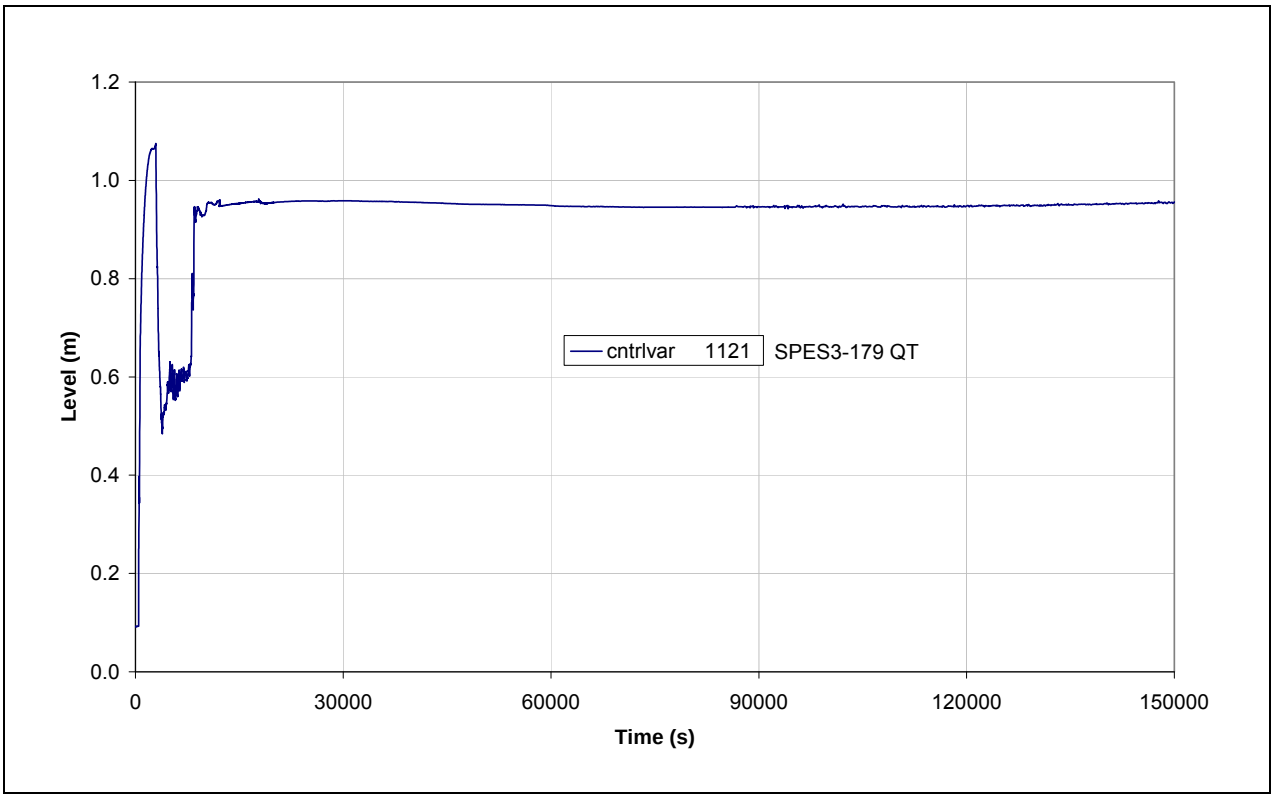

Fig.5. 66 - SPES3-179 LGMS level (window)

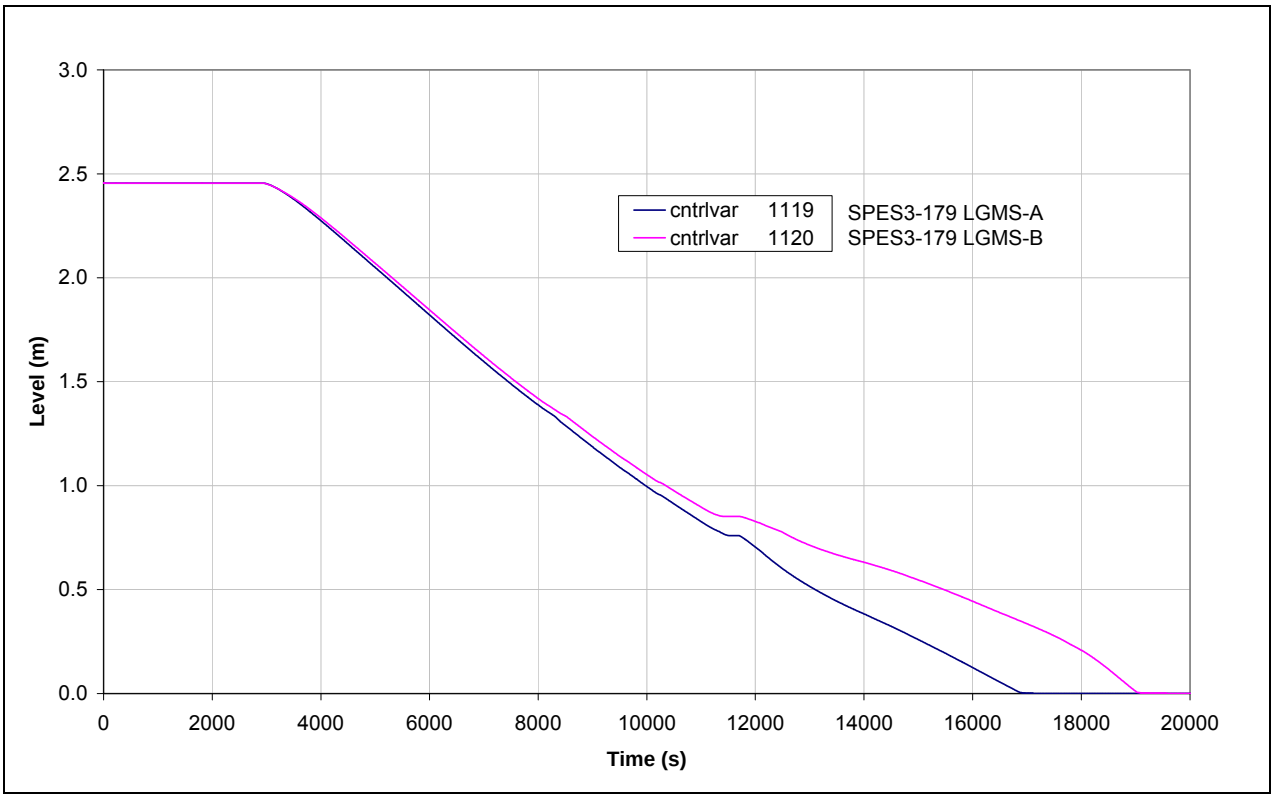

Fig.5. 67 - SPES3-179 LGMS mass (window)

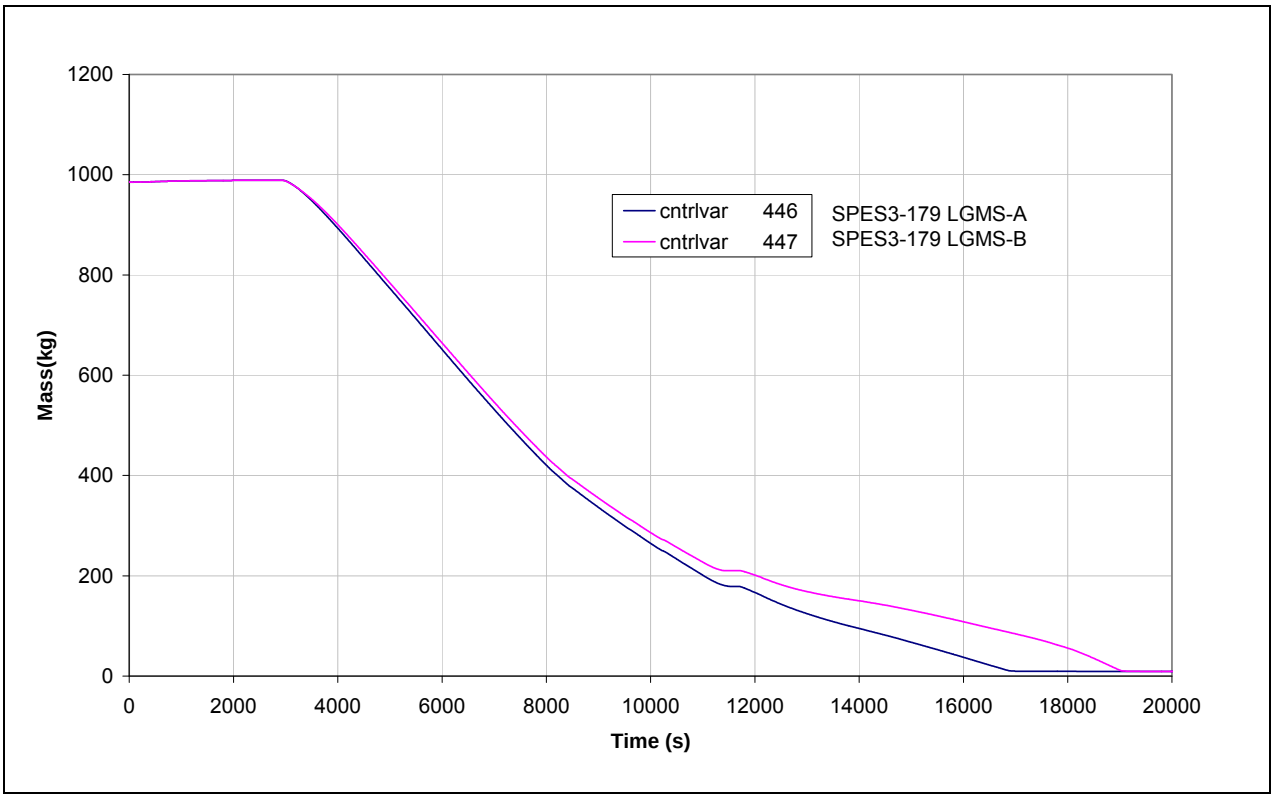

Fig.5. 68 - SPES3-179 ADS Stage-II mass flow (window)

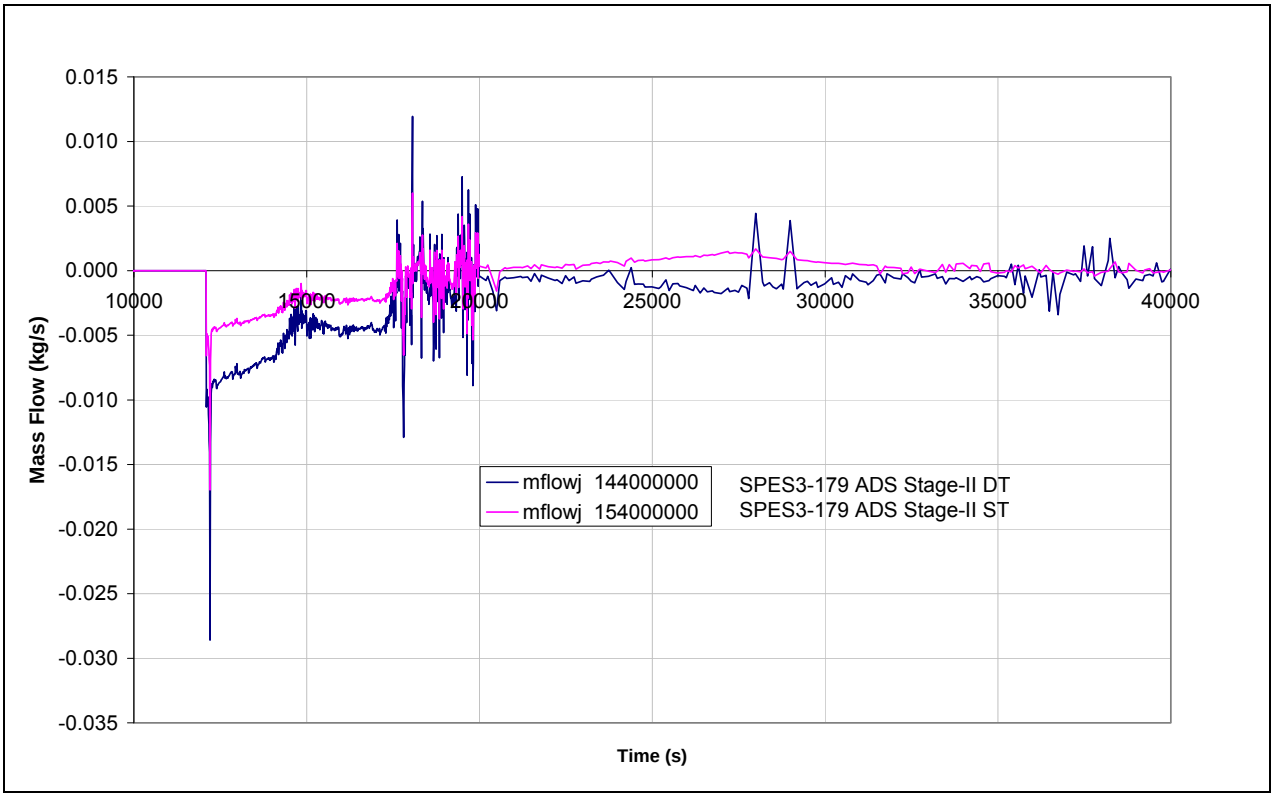

Fig.5. 69 - SPES3-179 ADS Stage-II mass flow

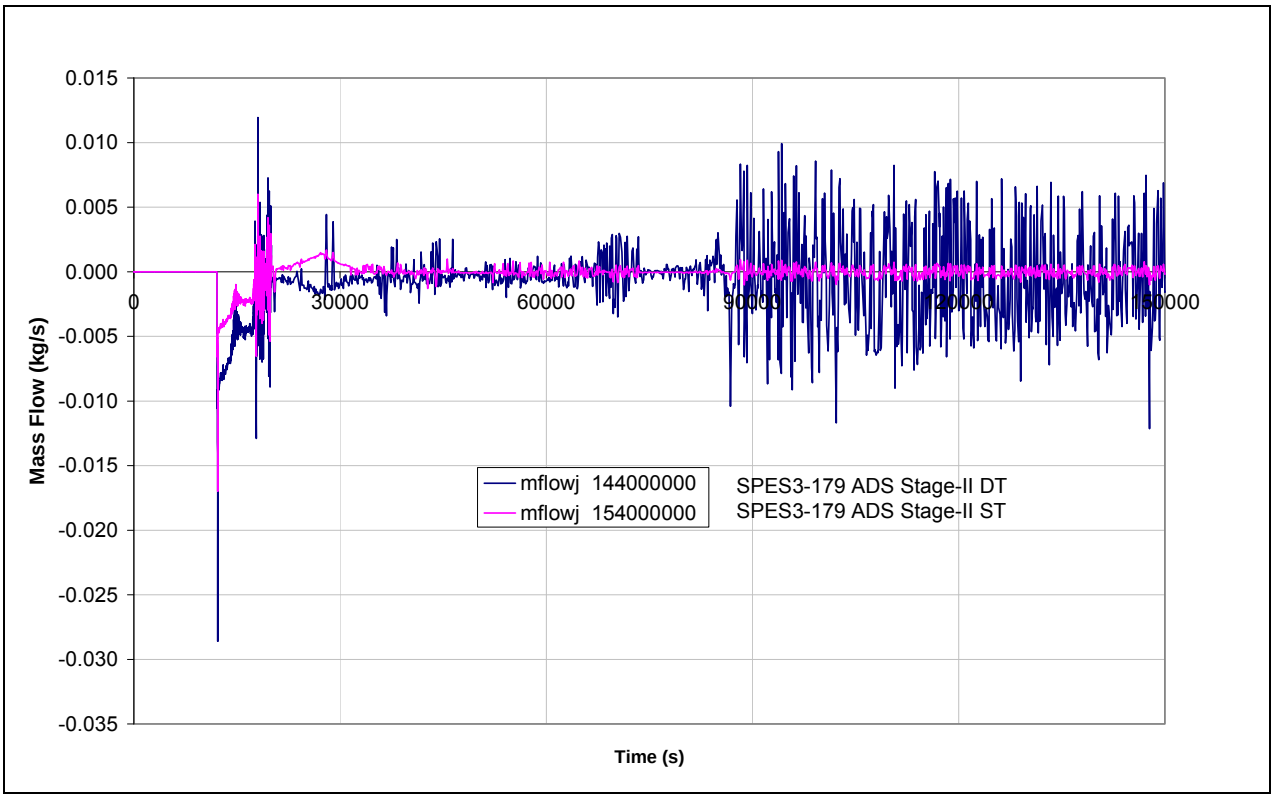

Fig.5. 70 - SPES3-179 RWST temperature

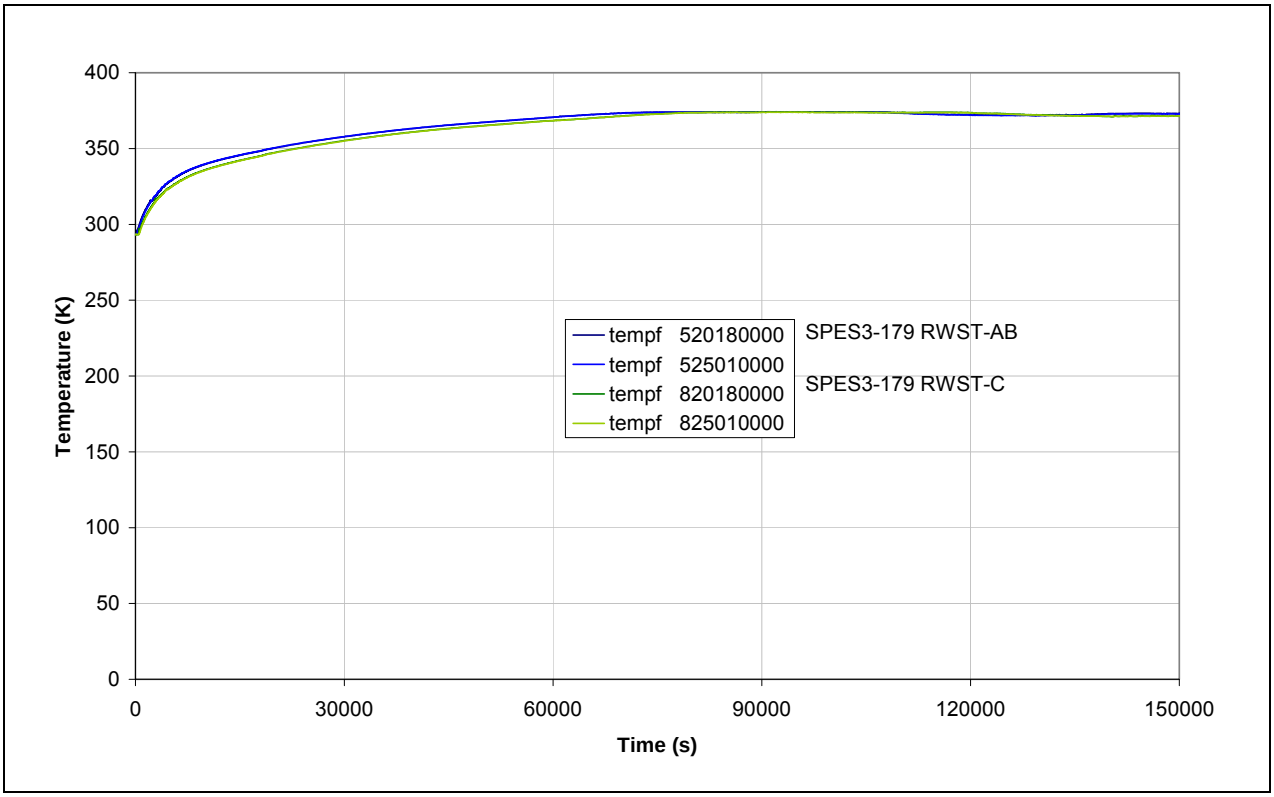

Fig.5. 71 - SPES3-179 RWST mass

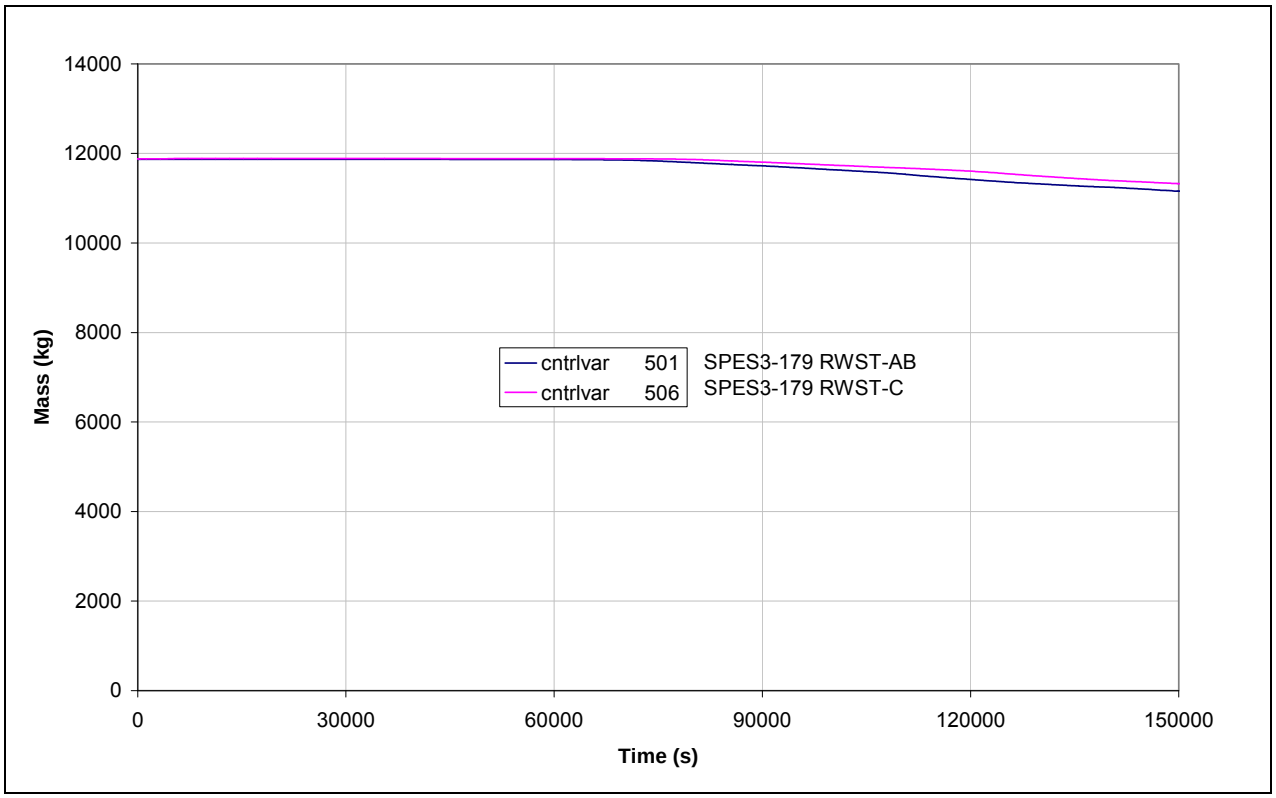

Fig.5. 72 - SPES3-179 RWST pressure

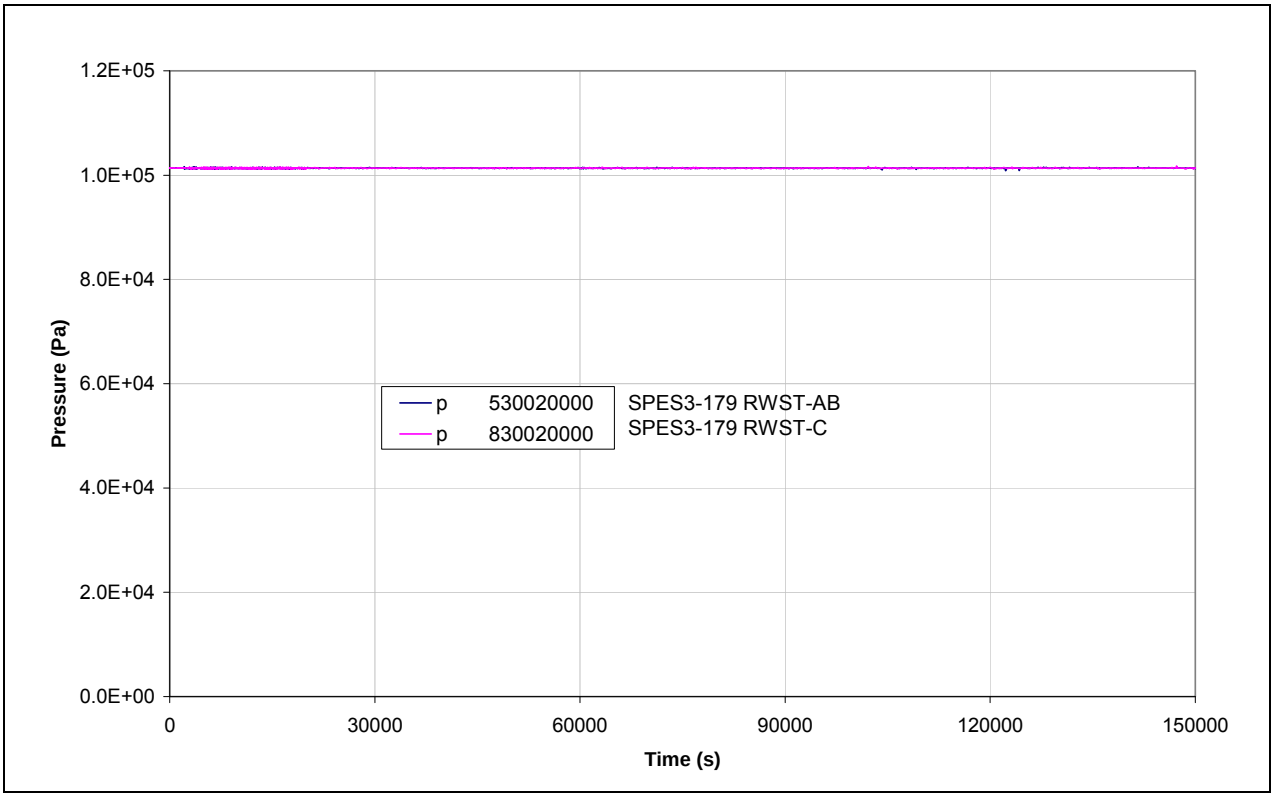

6. DBE STATION BLACK-OUT FUKUSHIMA TYPE: SPES3-177

The Fukushima accident occurred in Japan, on the 11th of March 2011, as a consequence of a 9.0 Magnitude earthquake followed by 14 m tsunami at the plant location. The basic sequence of events that triggered the accident is here summarized [21]:

- all the operating units were automatically shut-down when the earthquake occurred;
- the loss of off-site power occurred due to the earthquake;
- the emergency diesel generator properly operated until the tsunami flooded the area and made them inoperable;
- the accident resulted in a Station Black Out;
- all motor operated pumps (including ECCS pumps) became inoperable.

On the basis of the Fukushima accident, it was decided to perform a numerical simulation of the accidental sequence on the SPES3 facility in order to investigate the plant response and verify its adequacy to cope with a SBO.

The SBO was not included in the test matrix for SPES3 experimental program [1], and the definition of the sequence of events was performed on the basis of the Loss of Normal Feedwater/Loss of Offsite Power investigated in [22]. Moreover, according to [23], it was assumed the battery DC powered EHRS actuation valves, normally closed and fail-to-open type, are regularly automatically open by the devoted triggering signals and no later closure occurs (e.g. caused by tsunami).

SPES3-177 case is based on SPES3-175 nodalization, with 13 tubes SGs and the safety system actuation typical of the design basis events.

SPES3-177 starts from steady conditions at 65% power, in order to investigate the actual SPES3 test conditions.

The RELAP5 nodalization used for SPES3-177 case is shown in Fig.3. 4, Fig.3. 5, Fig.3. 6.

The changes in the model, with respect to SPES3-175 case, concern the break valves (set to leave the DVI-B intact) and the set-up of the trips to simulate the earthquake and the consequent reactor safety signal sequence. The triggering event of the transient is assumed to be the earthquake, set by TRIP 218 at time 0. The earthquake starts the reactor coolant pump and the main feed-water pump coast-down. The low feed-water signal trips (TRIP 225, 226 and 227) occur at 75% FW flow and trigger the reactor scram. The SG secondary side low collapsed level trips (TRIP 210, 211, 212) occur at 0.25 m level and isolate the secondary loops (MFIV and MSIV). The EHRS-A and B are actuated by the control system, on low SGss level OR high SG pressure. The EHRS-C is not actuated, being this transient a non-LOCA. The signal of low core inlet temperature actuates the EBT injection.

The following paragraphs describe the SBO transient results.

6.1 SPES3-177

Steady conditions at 65% power, starting point for the transient, are summarized in Tab.4. 1.

The list of the main events occurring during the transient, with timing and quantities, is reported in Tab.6. 1.

6.1.1 SPES3-177 transient phases and description

The first 10 s of data (-10 s to 0 s) are steady state conditions.

All times of the events are given with respect to the earthquake assumed as time 0 s.

The main phases of the transient are shortly summarized here, while a more detailed description is provided in the followings.

- The loss of off-site power is assumed to be contemporary to the earthquake and to trigger the RCP and MFW pump coast-down. Natural circulation establishes through the pump-bypass and RI-DC check valves;
- the low FW signal triggers the reactor scram;
- the start-up FW (foreseen in IRIS and not simulated in SPES3) is assumed to fail and this gives permission to isolate the SGs and trigger the EHRS-A and B;
- the low collapsed level signal in the SG, secondary side, triggers the SG isolation and actuates the EHRS-A and B; RPV level decreases for system cool-down and pump by-passes uncover. Natural circulation occurs through the RI-DC check valves. The RPV depressurizes;
- the low core inlet coolant temperature signal actuates the EBTs that inject water until RPV and EBT level equalize;
- in the long term, the plant is cooled by the EHRSs that reject the core decay heat to the RWSTs.

Earthquake and Loss of Off-site power: RCP and MFW pump trip

The earthquake occurs at time 0 and the loss of off-site electric power is contemporary. The pumps of the system are switched-off and the coast-down starts for the RCP and the FW pumps.

The RCP velocity is shown in Fig.6. 1 and it is completely stopped at 100 s. The pump head is shown in Fig.6. 2.

The pump head decrease let the RI-DC check valves open and allow natural circulation between riser and SG annuli at lower elevation in the RPV. Circulation starts at 11 s in SG-C and at 14 s in SG-A and B, Fig.6. 3, Fig.6. 4, Fig.6. 5.

When the pump head decreases, the pump by-pass check valves open and circulation starts also at high level in the RPV, at 18 s through the SG-C annulus and at 19 s through SG SG-A and B annuli, Fig.6. 6, Fig.6. 7. Around 400 s, natural circulation stops through the pump by-pass corresponding to SG-C, as no heat transfer occurs in SG-C since about 150 s, Fig.6. 8. Due to the RPV level decrease for system cooling, the pump uncovers at 2620 s and circulation stops through the pump by-pass, Fig.6. 9, Fig.6. 7.

The MFW pump is assumed to stop in 4.9 s and circulation in the secondary side re-starts only after the EHRS actuation, Fig.6. 10, Fig.6. 11.

Low FW signal: Reactor Scram; Start-up feed-water failure

The reactor scram occurs at 1.24 s, on Low FW signal, set at 75% of nominal feed-water mass flow. Being SPES3-177 a case starting form 65% power conditions, the signal set-point is 75% of steady value, reduced according to power. Core power is shown in Fig.6. 13, Fig.6. 14, Fig.6. 15 together with SG total power.

The Start-up feed-water, that should intervene at the reactor scram, is assumed to fail (it is not simulated in SPES3) and this gives permission for secondary loop isolation.

Low SG secondary side level signal: SG isolation and EHRS-A and B actuation

The loss of main feedwater causes the reduction of mass inventory in the SGs, secondary side. The SG low level signal occurs in SG-A at 31.13 s, when the collapsed level reaches 0.25 m, Fig.6. 16, Fig.6. 17, Fig.6. 18. The signal starts the secondary loop isolation and actuates the EHRS-A and B. The MFIV and MSIV are closed contemporarily in 5 s. The EHRS actuation valves are opened in 2 s.

Natural circulation restarts in SG-A and B, thanks to EHRS-A and B intervention, Fig.6. 10, Fig.6. 11, Fig.6. 12 allowing the decay power removal, Fig.6. 13, Fig.6. 14, Fig.6. 15.

The peak of water mass flow through the EHRS-A and B occurs at 37 s with 0.277 kg/s for loop-A and 0.273 for loop-B, Fig.6. 19, Fig.6. 20. Power transferred to the EHRS is shown in Fig.6. 21, Fig.6. 22. The peak of transferred power occurs at 212 s, 380 kW, for EHRS-A and at 220 s, 381 kW, for EHRS-B. Power is rejected to the RWST-AB that begins to heat-up at 51 s and reaches saturation at 9200 s, Fig.6. 23. The RWST-AB mass decreases for water evaporation, Fig.6. 24.

Heat removal by the EHRSs, through the SGs, enhances the natural circulation in the core that occurs through the RI-DC check valves, after the pump is uncovered, Fig.6. 3, Fig.6. 4, Fig.6. 5. The core inlet mass flow is reported in Fig.6. 25, Fig.6. 26, Fig.6. 27. After the pump stop, the core mass flow is around 4.3 kg/s, then it decreases of about 1 kg/s, around 2700 s, when circulation interrupts through the pump by-pass. In the long term, it is stable around 2 kg/s.

The SG isolation causes the secondary loop pressure increase up to the peak of 8.59 MPa in SG-A, at 129 s, of 8.63 MPa in SG-B, at 136 s, and of 7.87 MPa in SG-C, at 176 s, Fig.6. 28, Fig.6. 29.

Low Core inlet coolant temperature signal: EBT actuation

The primary side pressure decreases for the system cool-down and, in the long term, it is around 0.16 MPa, Fig.6. 30, Fig.6. 31. The inlet and outlet core temperatures are shown in Fig.6. 32, Fig.6. 33. Fig.6. 33 reports also the saturation temperature corresponding to core outlet pressure and it is possible to observe that, at 37390 s, the core outlet temperature is in saturation. Anyway, core is always under single-phase water, Fig.6. 34.

The primary system cool-down causes the water density increase with consequent water level decrease in the RPV. The PRZ level is shown in Fig.6. 35. The PRZ is empty at 1150 s. Water level in the down-comer is reported in Fig.6. 36 and in reaches a steady condition after about 60000 s.

The set-point of 533.15 K for the low core inlet coolant temperature is reached at 2583.04 s. The signal triggers the EBT actuation by opening the EBT valves in 15 s. Cold water is injected into the RPV, through the DVI lines, and hot water and steam replace the EBT water through the EBT top line, connected to the RPV, Fig.6. 37, Fig.6. 38, Fig.6. 39. The EBT injection stops around 4800 s, when the EBT and RPV levels are equalized. The EBT level is shown in Fig.6. 40.

The RPV mass inventory slightly increases thanks to the EBT injection and then it remains stable, Fig.6. 41.

No temperature excursion occurs on the heater rod cladding as circulation in the core is stable and liquid phase is always present, Fig.6. 42, Fig.6. 43, Fig.6. 44, Fig.6. 45, Fig.6. 26, Fig.6. 27, Fig.6. 34.

Long term conditions

In the long term, the EHRS-A and B remove the core decay power and slowly cool-down the system, Fig.6. 22, Fig.6. 33. The average power produced in the core, in the last 50000 s, is 29.78 kW. Power removed by the EHRS is 26.05 kW. The unbalance is due to the heat losses to the environment.

6.1.2 Case conclusions

The simulation of the SBO allowed to understand the phenomena occurring in the transient and to verify the plant is suitable to cope with this kind of accident. No particular or critical situation occurred and the system slowly cools-down.

Differently by the Fukushima NPPs, where the ECCS, driven by engines, were cut-out by the tsunami, the SPES3 emergency systems relay on natural circulation and do not require external or diesel power to

operate. In the IRIS system design, which logic is simulated in SPES3, power, provided by local AC batteries, is needed only to open the valves on triggering signals. Being fail-to-open type valves, an eventual delayed tsunami impairing them, could not lead to their re-closure, once open, nor could prevent their opening if still close.

Tab.6. 1 – SPES3-177 list of the main events

	SBO - Fukushima type	SPES3-177		
N.	**Phases and events**	**Time (s)**	**Quantity**	**Notes**
Earthquake and loss of off-site power: RCP and Main feedwater pump trip				
1	Earthquake	0		
2	Loss of off-site power	0		
3	RCP coast-down starts	0		pump completely stopped at 100 s
4	MFW pump coast-down starts	0		assumed to stop in 4.9 s
Low Feedwater signal: Reactor scram; Start-up feedwater fails				
5	**Low FW signal**	1.24	0.607 kg/s FW-A 0.607 kg/s FW-B 1.214 kg/s FW-C	**75% of nominal flow** (75% of mass flow at 65% power)
6	SCRAM begins	1.24		
7	Start-up FW actuation fails	1.24		
8	Natural circulation begins through shroud valves (RI-DC)	11, 14		SG-B and C; SG-A
9	Circulation begins through pump by-pass	18, 19		SG-C; SG-A and SG-B
Low SGss level signal: SG isolation, EHRS-A and B actuation				
10	**Low SGss level signal**	34.13	0.25 m	**Set point**
11	SGss low level	34.13, 55.35	SG-A, SG-C	Signal not reached in SG-B
12	MFIV-A,B,C closure start	34.13		MFIV-A,B,C stroke 5 s
13	MSIV-A-B-C closure start	34.13		MSIV-A,B,C stroke 5 s.
14	EHRS-A and B opening start (EHRS 1 and 3 in IRIS)	34.13		EHRS-A,B IV stroke 2 s.
15	EHRS-A peak mass flow	37	0.277 kg/s	
16	EHRS-B peak mass flow	37	0.273 kg/s	
17	RWST-A/B begins to heat-up	51		
18	Secondary loop-A pressure peak	129	8.59 MPa	
19	Secondary loop-B pressure peak	136	8.63 MPa	
20	Secondary loop-C pressure peak	176	7.87 MPa	
21	EHRS-A power peak	212	380 kW	
22	EHRS-B power peak	220	381 kW	
S-Signal				
23	**Low PRZ pressure**	1251.77	12.72 MPa	**Set point**
Low Core inlet coolant temperature signal: EBT actuation				
24	**Low core inlet coolant temperature**	2583.04	533.15 K	**Set-point**
25	EBT-A and B valve opening start	2583.04		EBT valve stroke 15 s
26	Natural circulation interrupted at SGs top	3190		Pump inlet uncovered (voidf 176-01 ~0)
27	EBT-RV connections uncovered	3270, 3290		EBT-A, EBT-B
28	EBT injection to RPV stop	4790		RPV and EBT level equalization
29	EBT-A empty	NO		
30	EBT-B empty	NO		
31	Core in saturation conditions	37390		T out Core ~ Tsat (Pout core). Liquid phase
Long Term conditions				
32	Core power	150000	29.78 kW	Average between 100000-150000 s
33	SG total power	150000	28.06 kW	Average between 100000-150000 s
34	RWST total power	150000	26.05 kW	Average between 100000-150000 s
35	RWST-A/B temperature	150000	102 °C	Saturated. Average between 100000-150000 s

Fig.6. 1 – SPES3-177 RCP velocity

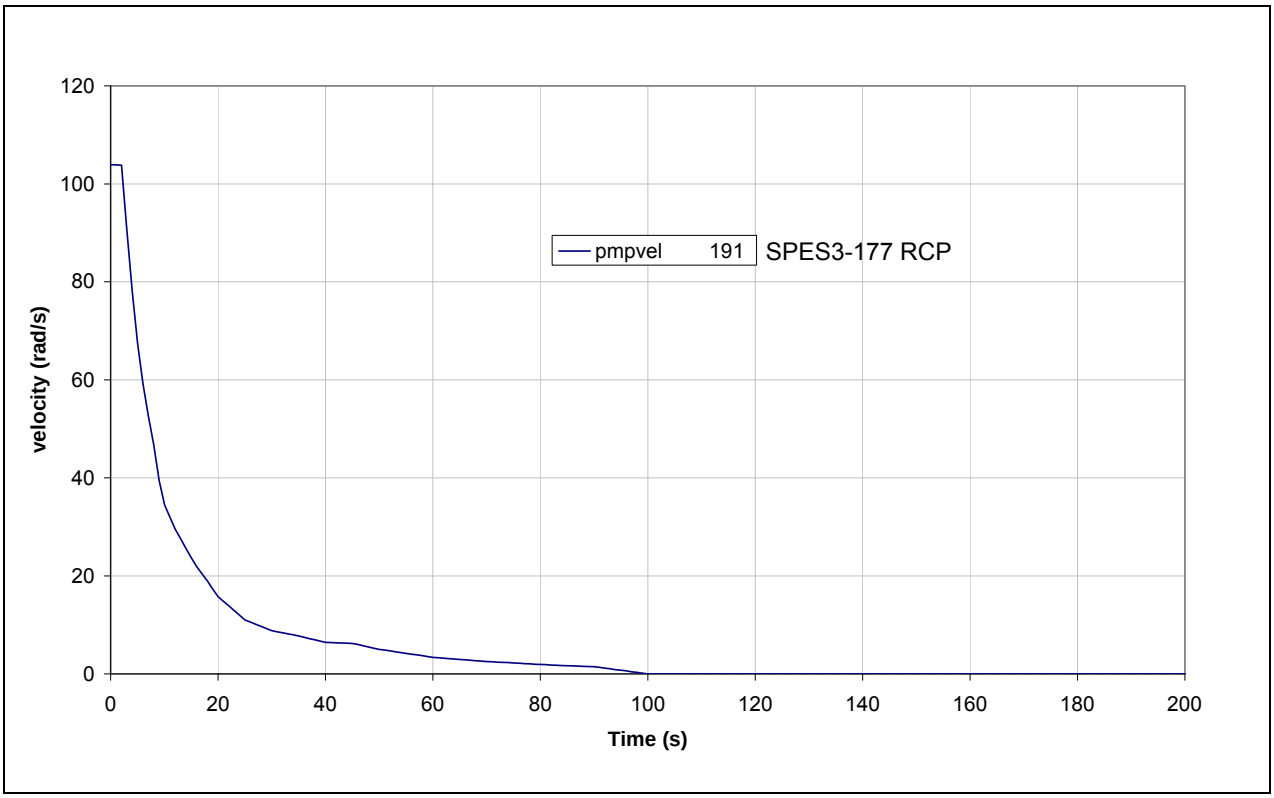

Fig.6. 2 – SPES3-177 RCP head

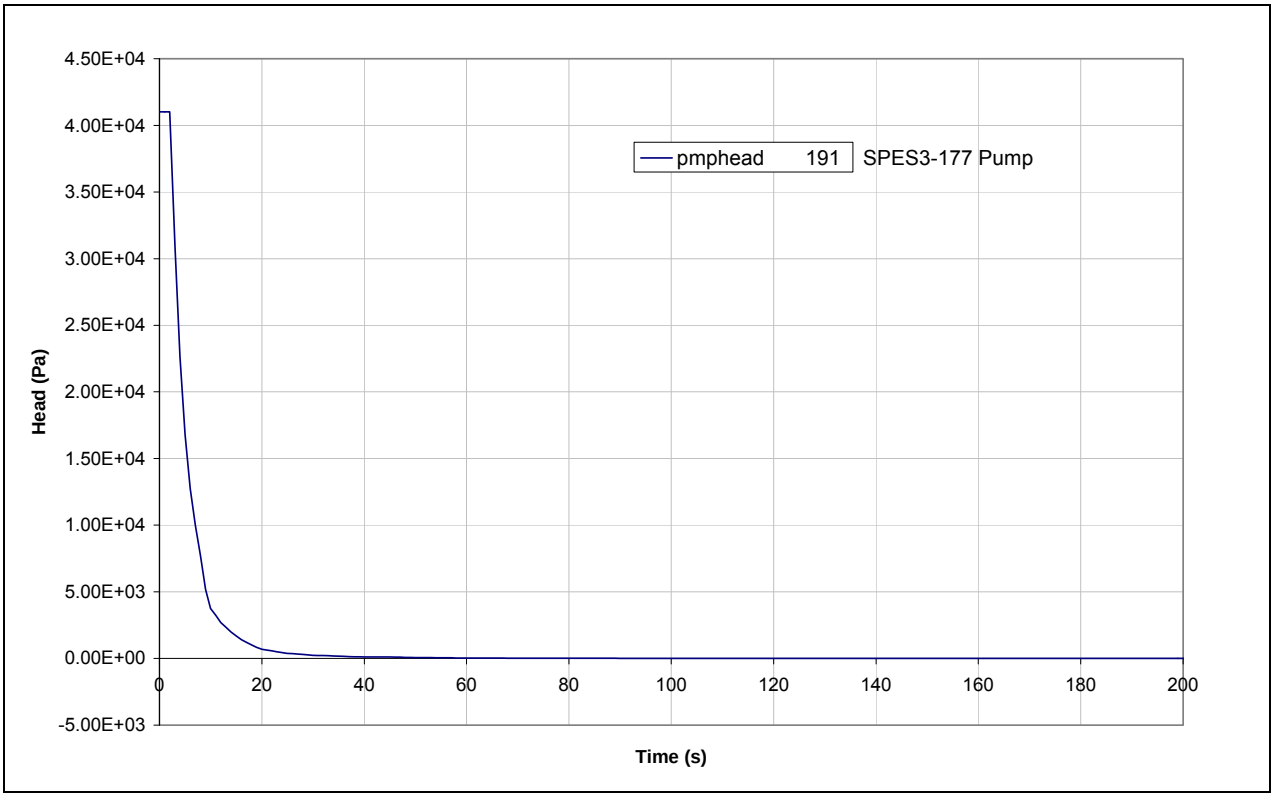

Fig.6. 3 – SPES3-177 RI-DC check valve mass flow (window)

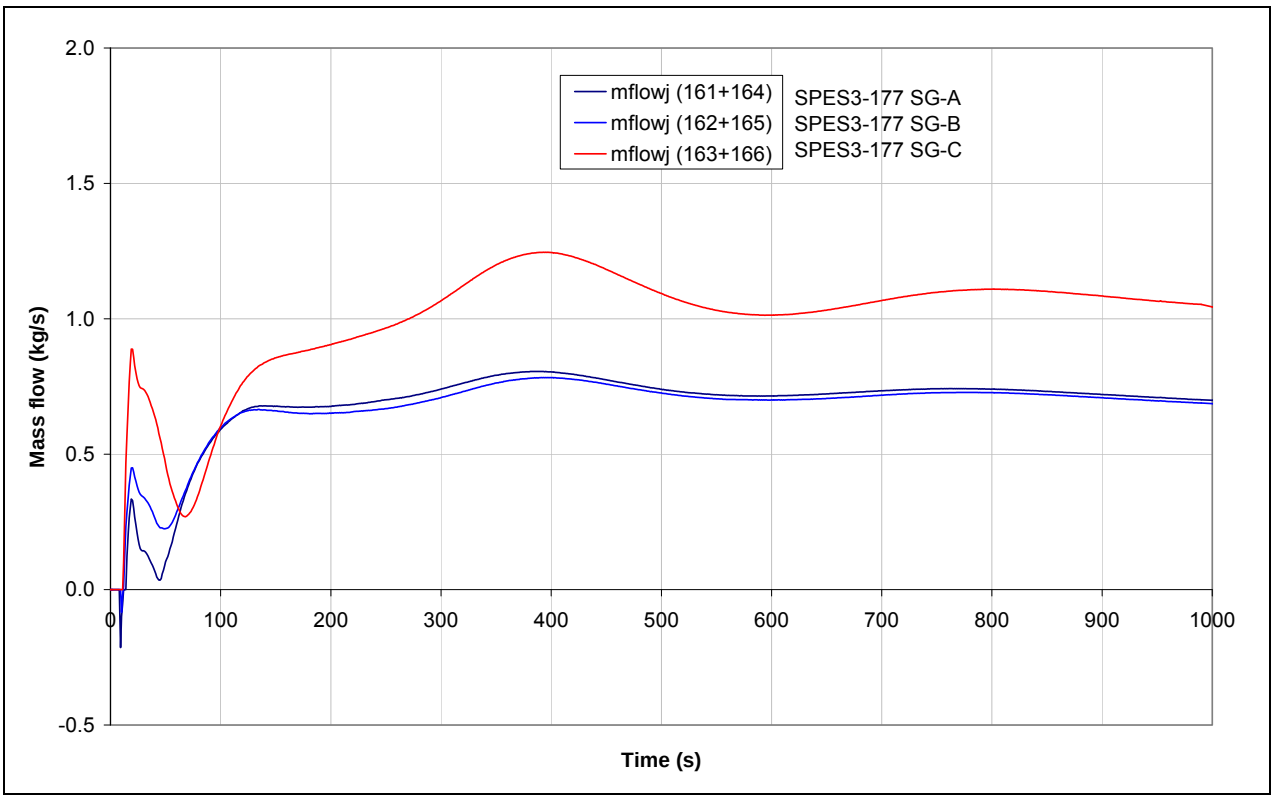

Fig.6. 4 – SPES3-177 RI-DC check valve mass flow (window)

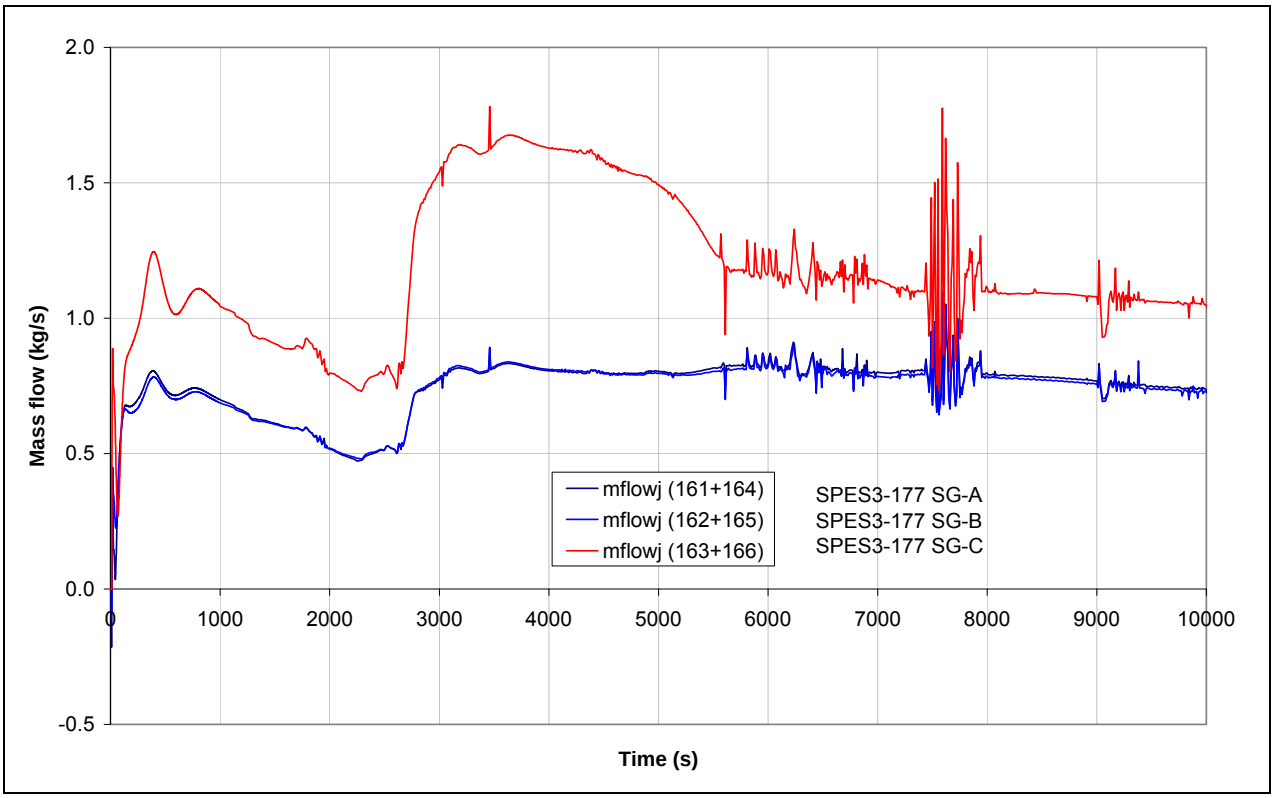

Fig.6. 5 – SPES3-177 RI-DC check valve mass flow

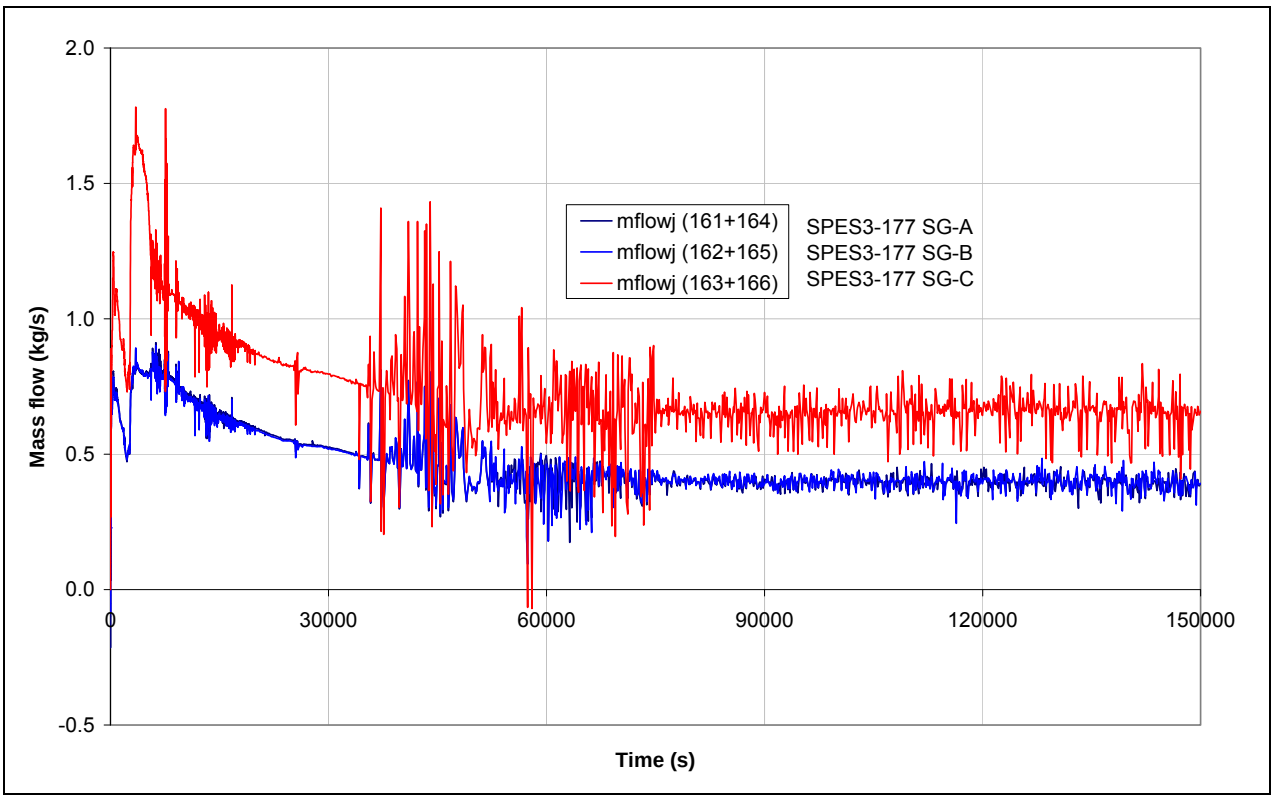

Fig.6. 6 – SPES3-177 Pump by-pass mass flow (window)

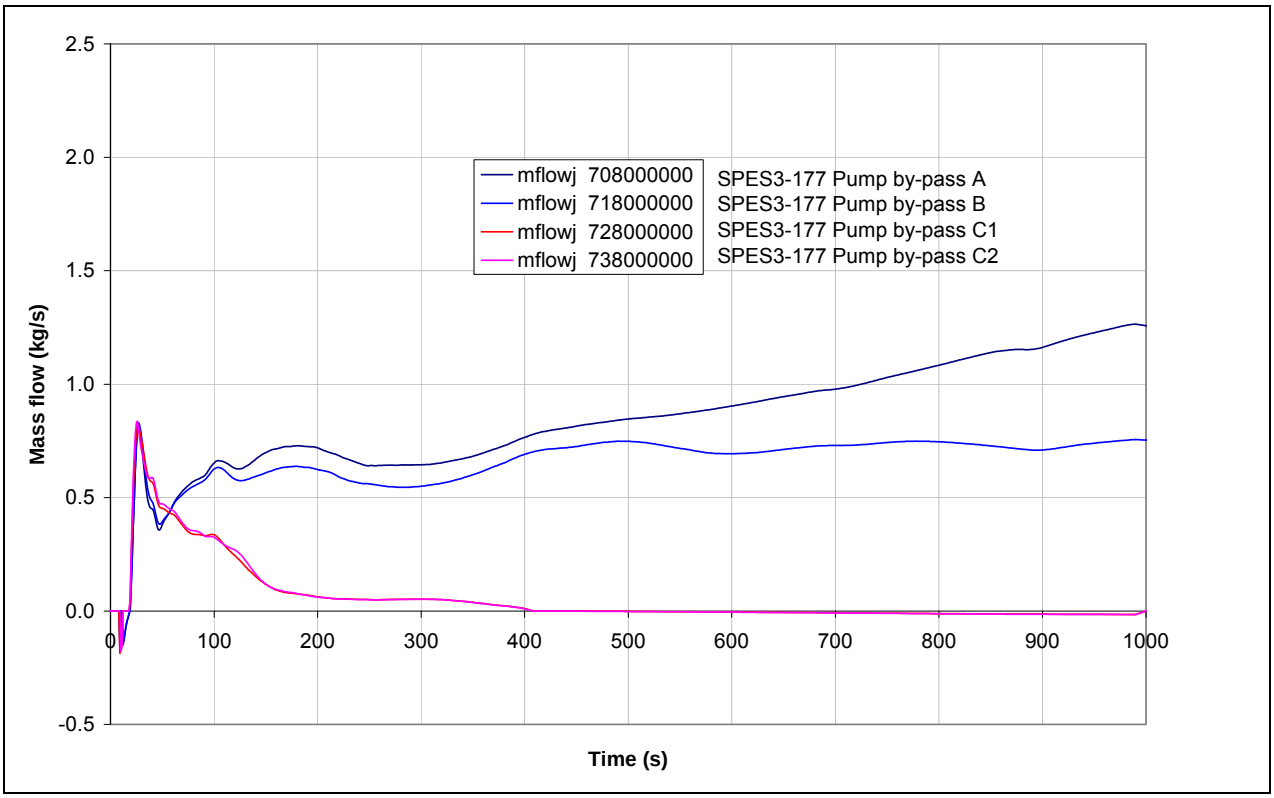

Fig.6. 7 – SPES3-177 Pump by-pass mass flow (window)

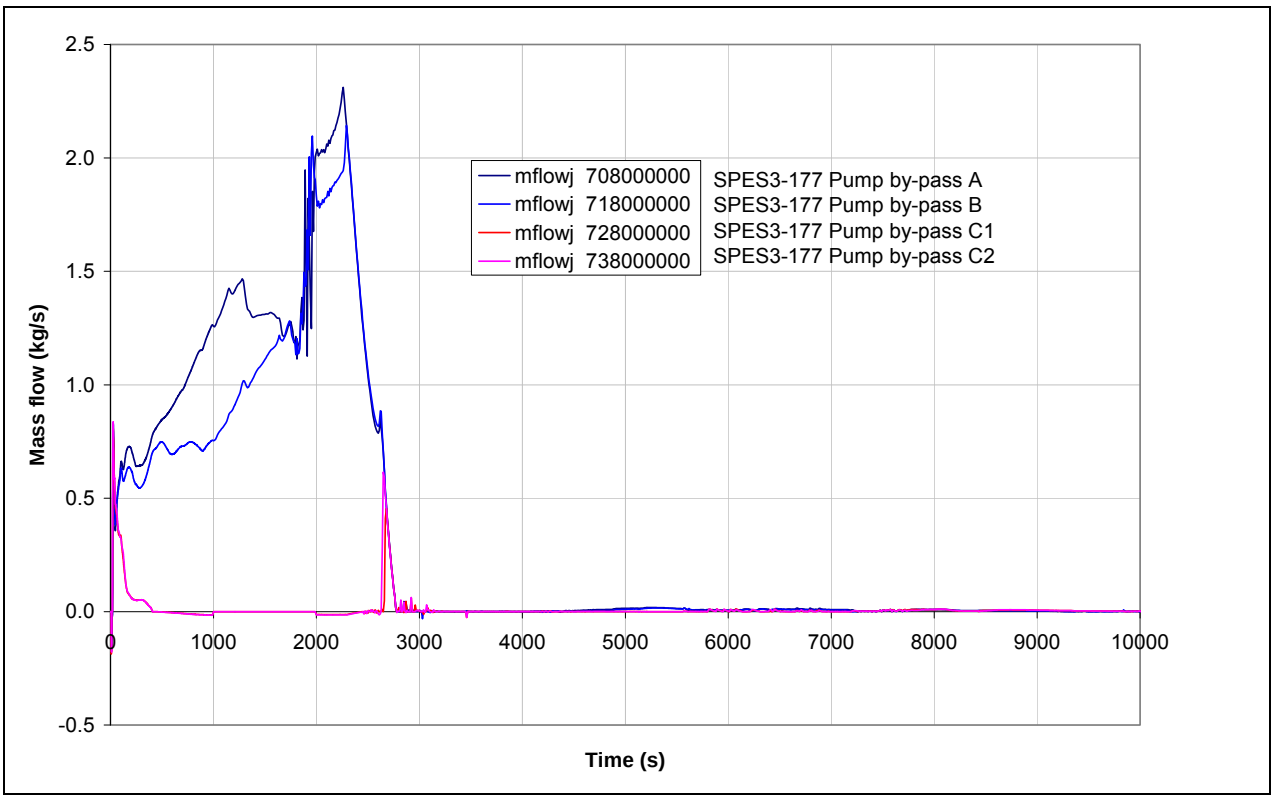

Fig.6. 8 – SPES3-177 SG power (window)

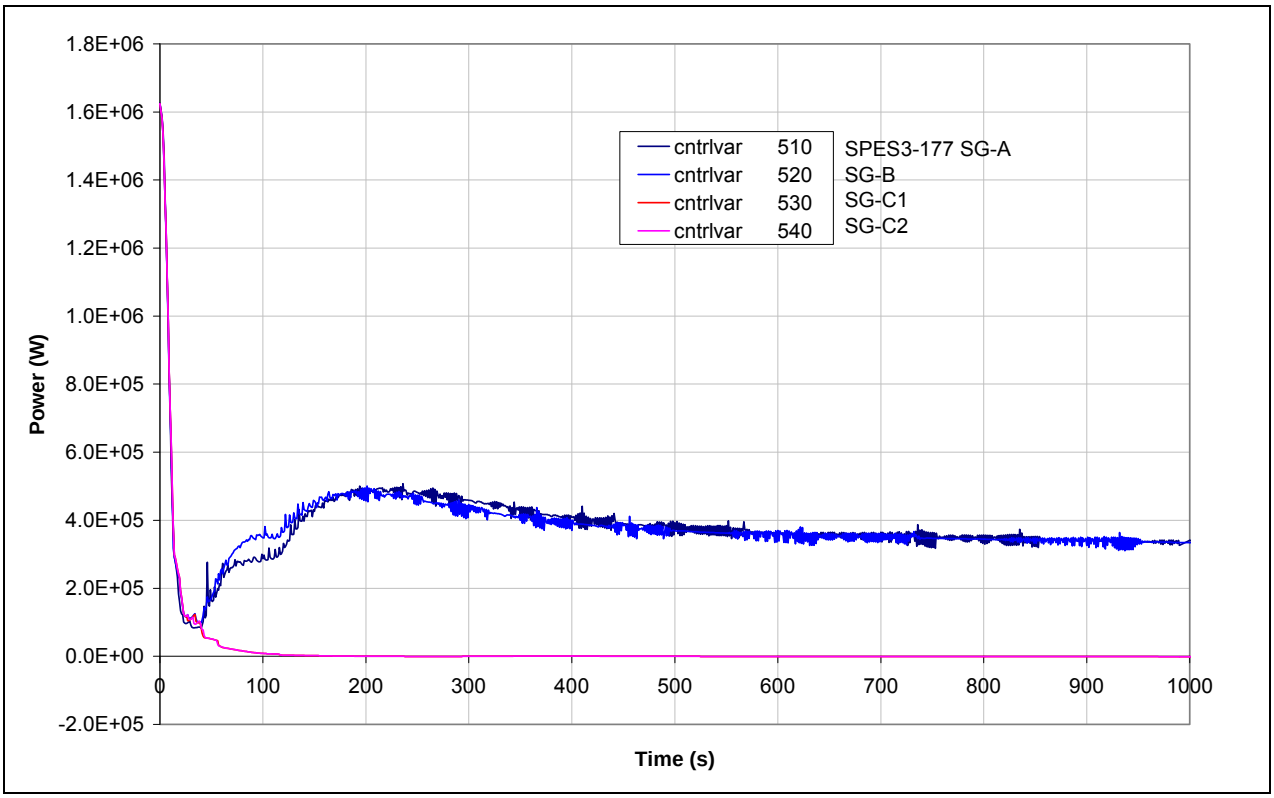

Fig.6. 9 – SPES3-177 Pump inlet liquid fraction (window)

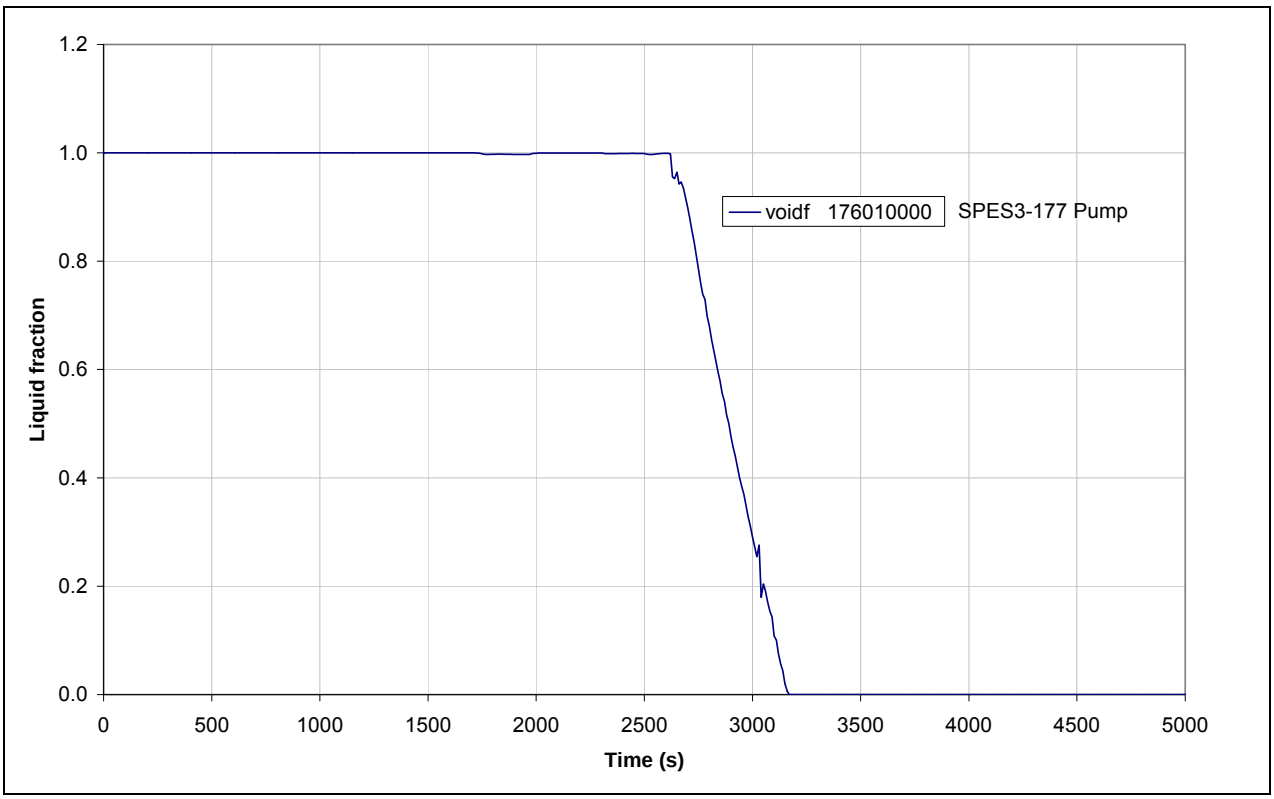

Fig.6. 10 – SPES3-177 SG secondary side mass flow (window)

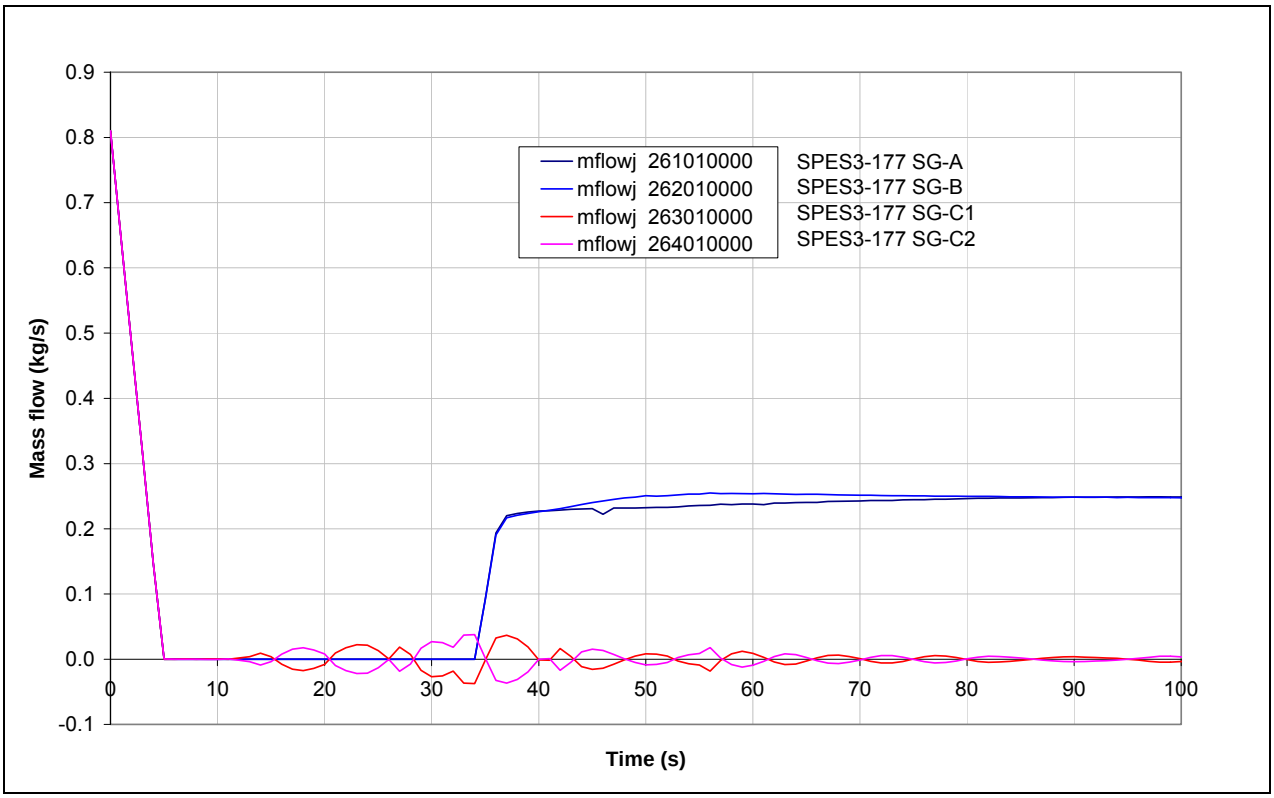

Fig.6. 11 – SPES3-177 SG secondary side mass flow (window)

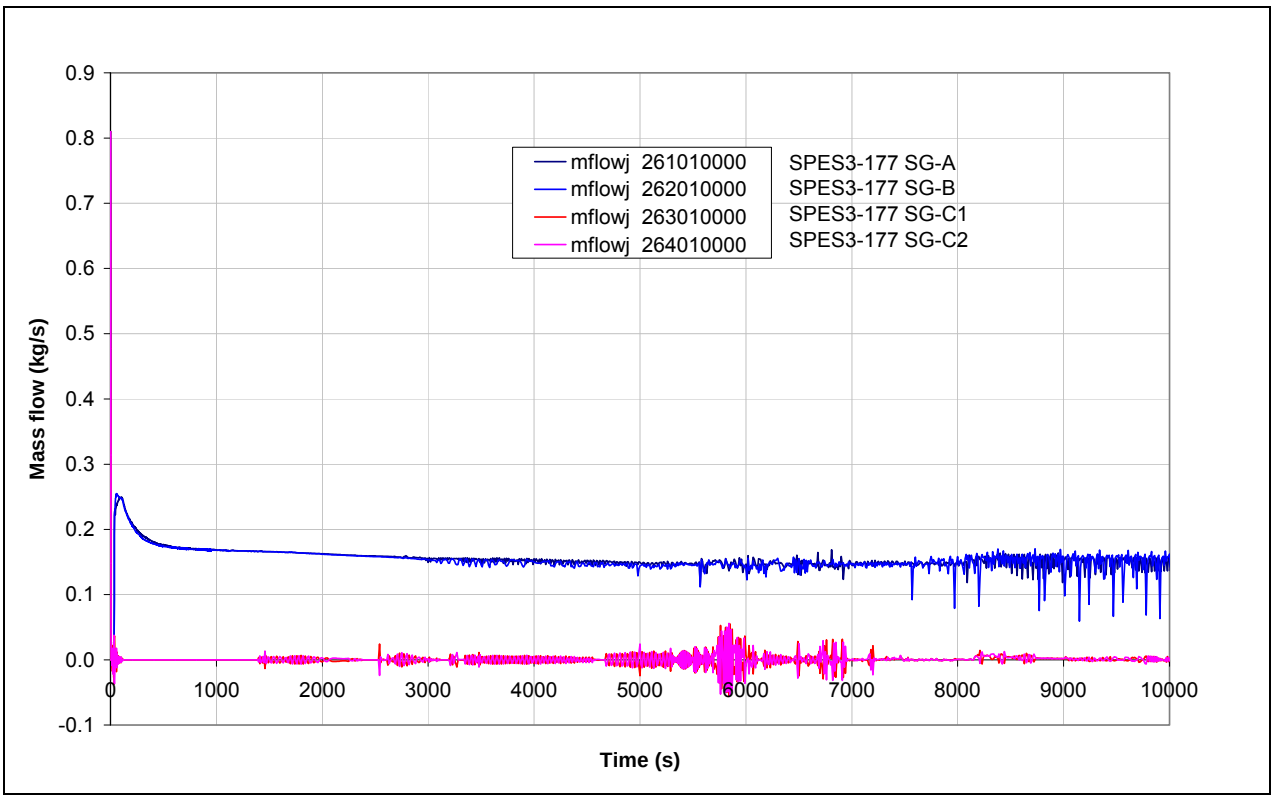

Fig.6. 12 – SPES3-177 SG secondary side mass flow

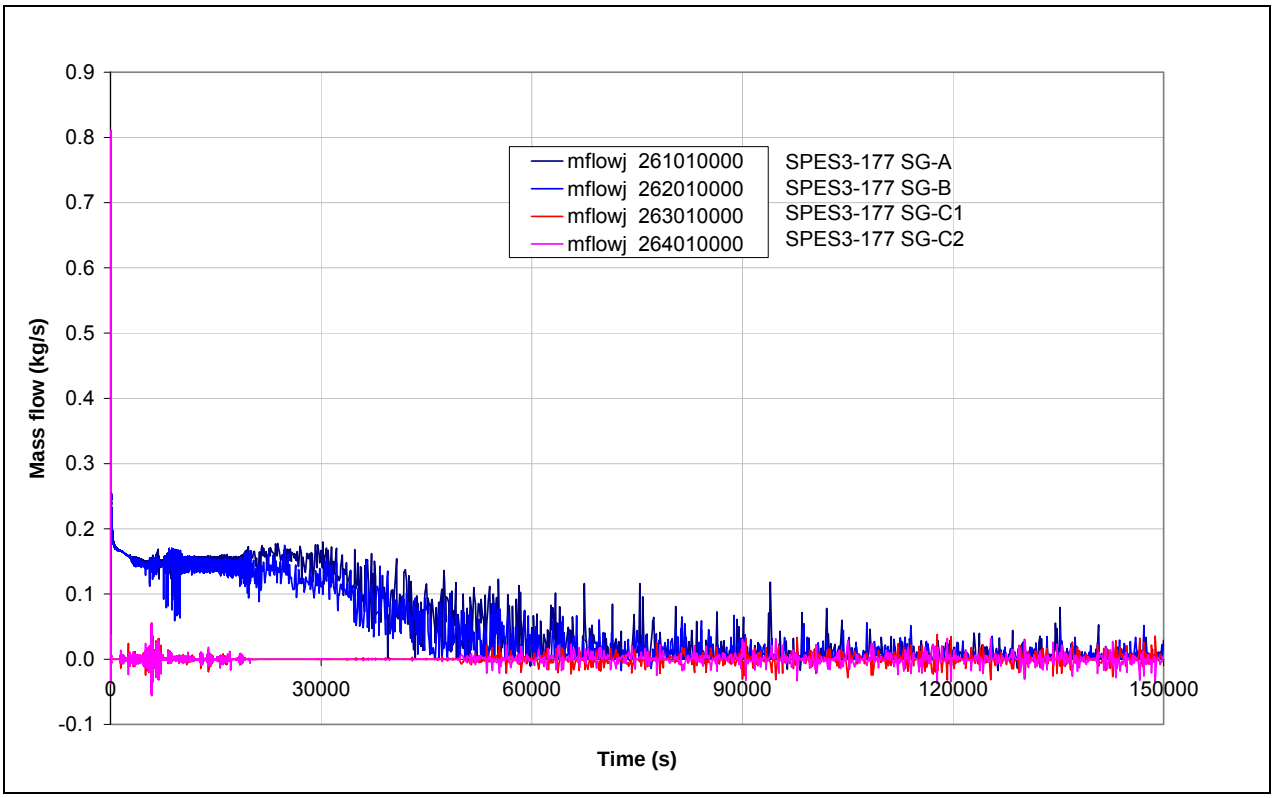

Fig.6. 13 – SPES3-177 Core and SG total power (window)

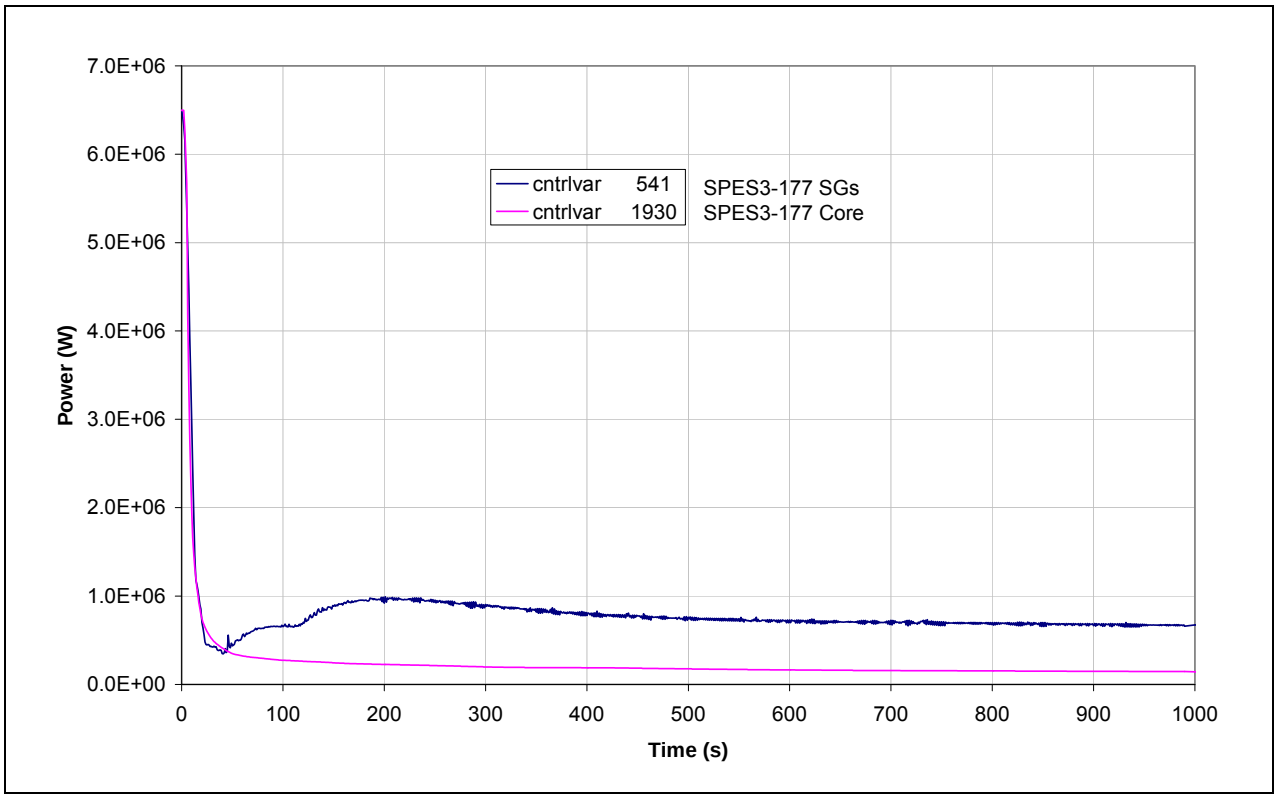

Fig.6. 14 – SPES3-177 Core and SG power (window)

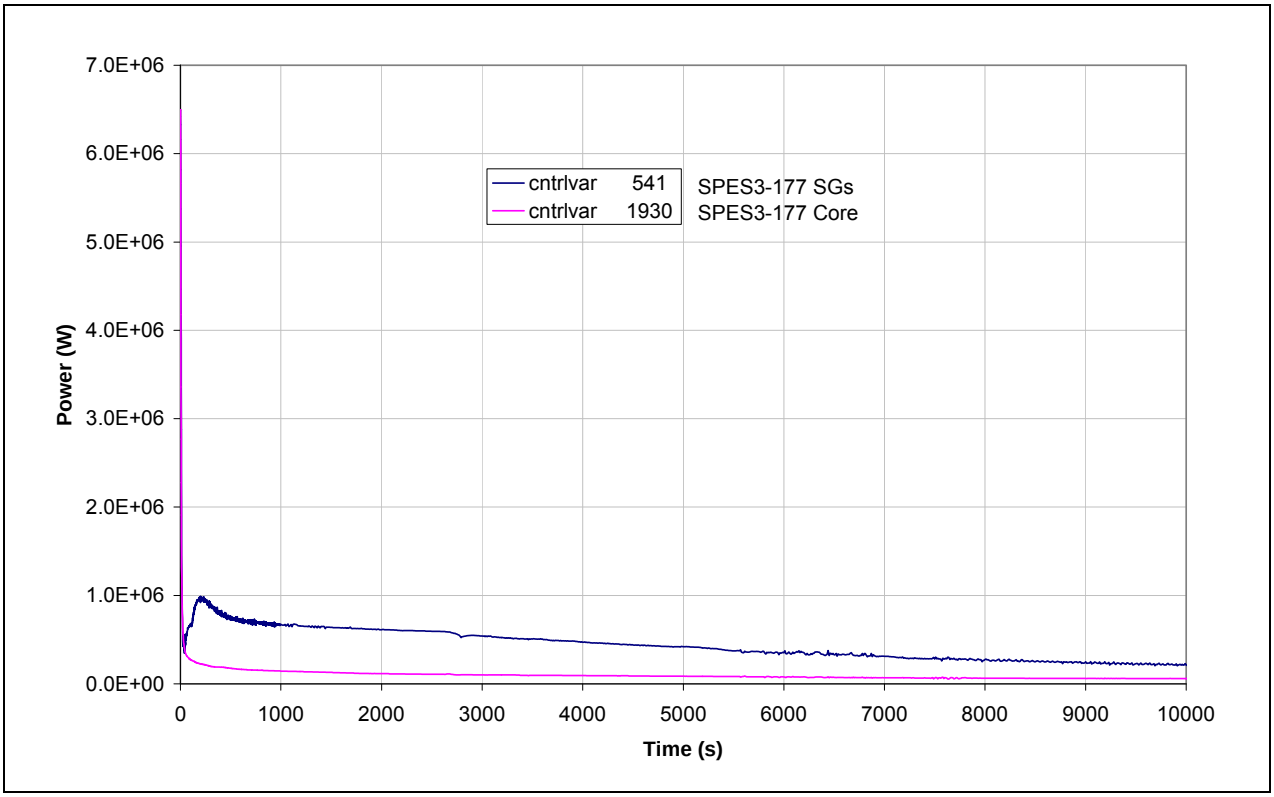

Fig.6. 15 – SPES3-177 Core and SG power

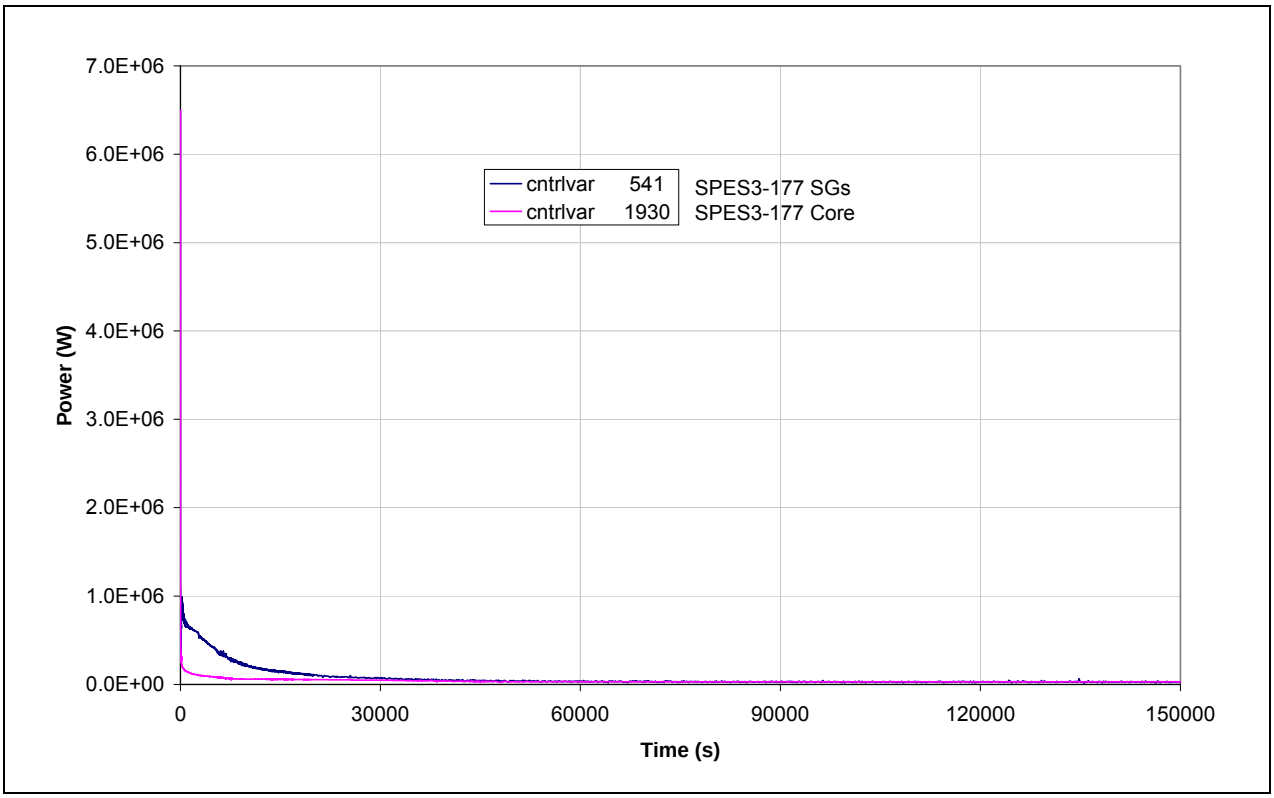

Fig.6. 16 – SPES3-177 SG secondary side collapsed level (window)

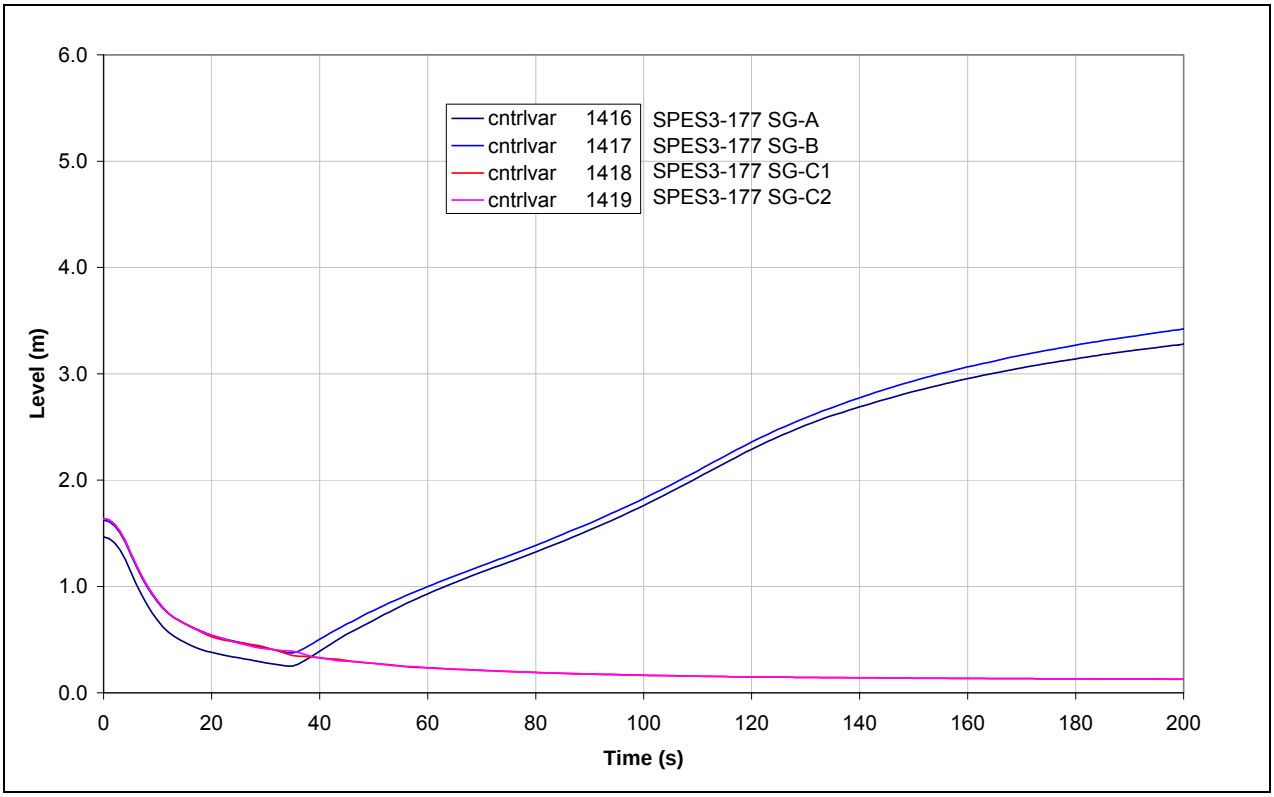

Fig.6. 17 – SPES3-177 SG secondary side collapsed level (window)

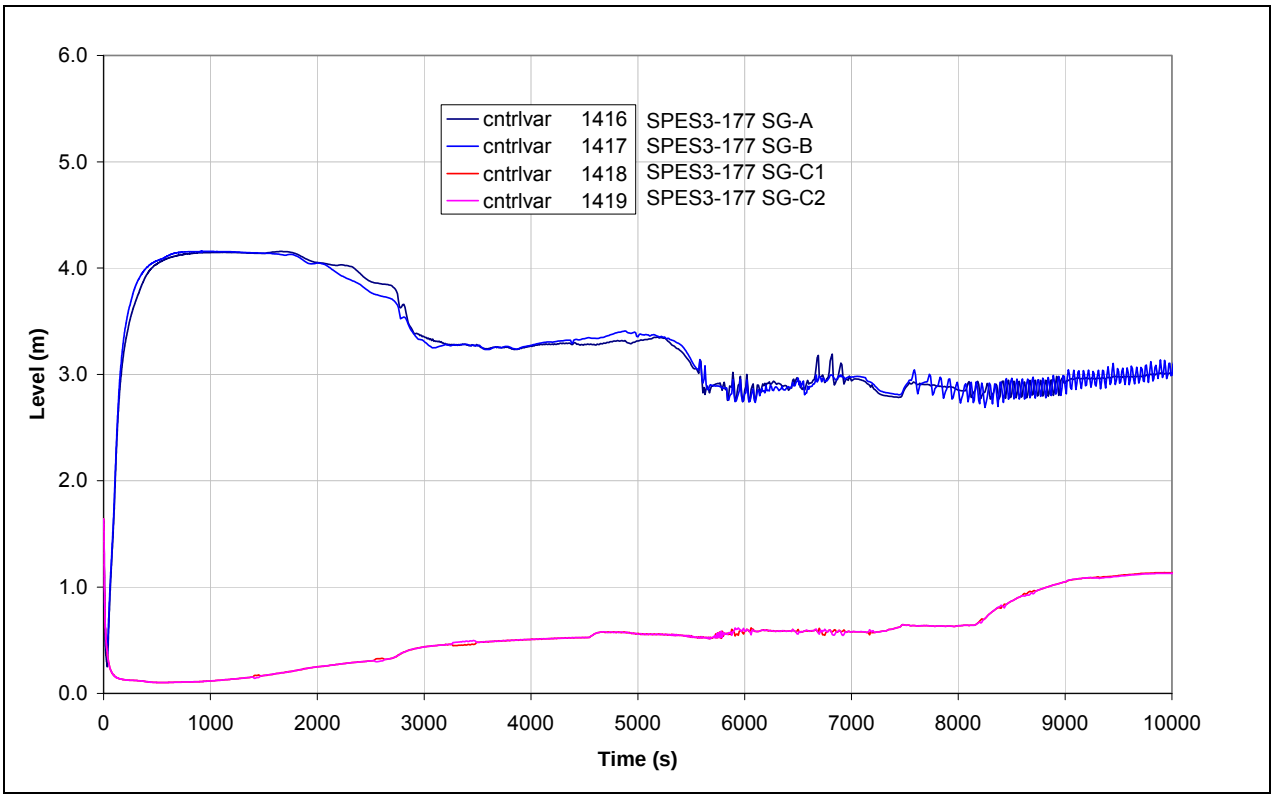

Fig.6. 18 – SPES3-177 SG secondary side collapsed level

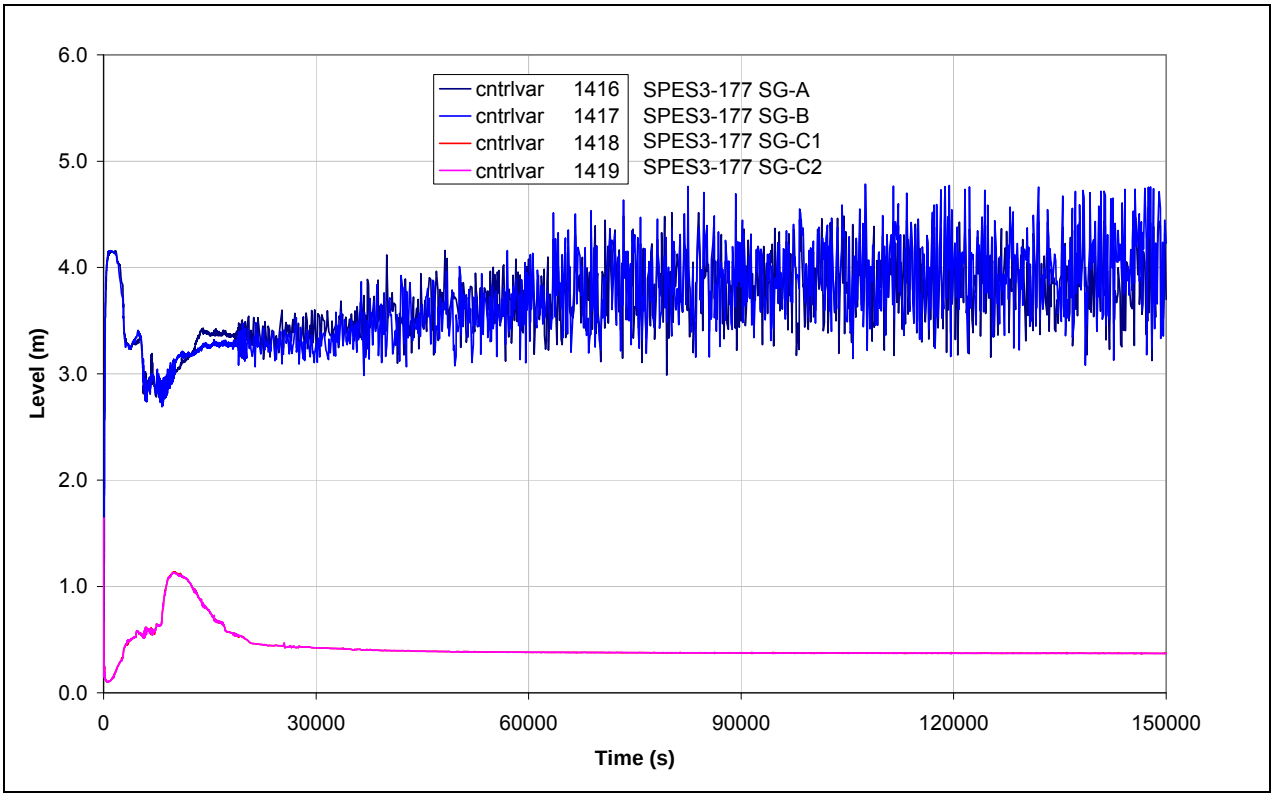

Fig.6. 19 – SPES3-177 EHRS cold leg mass flow (window)

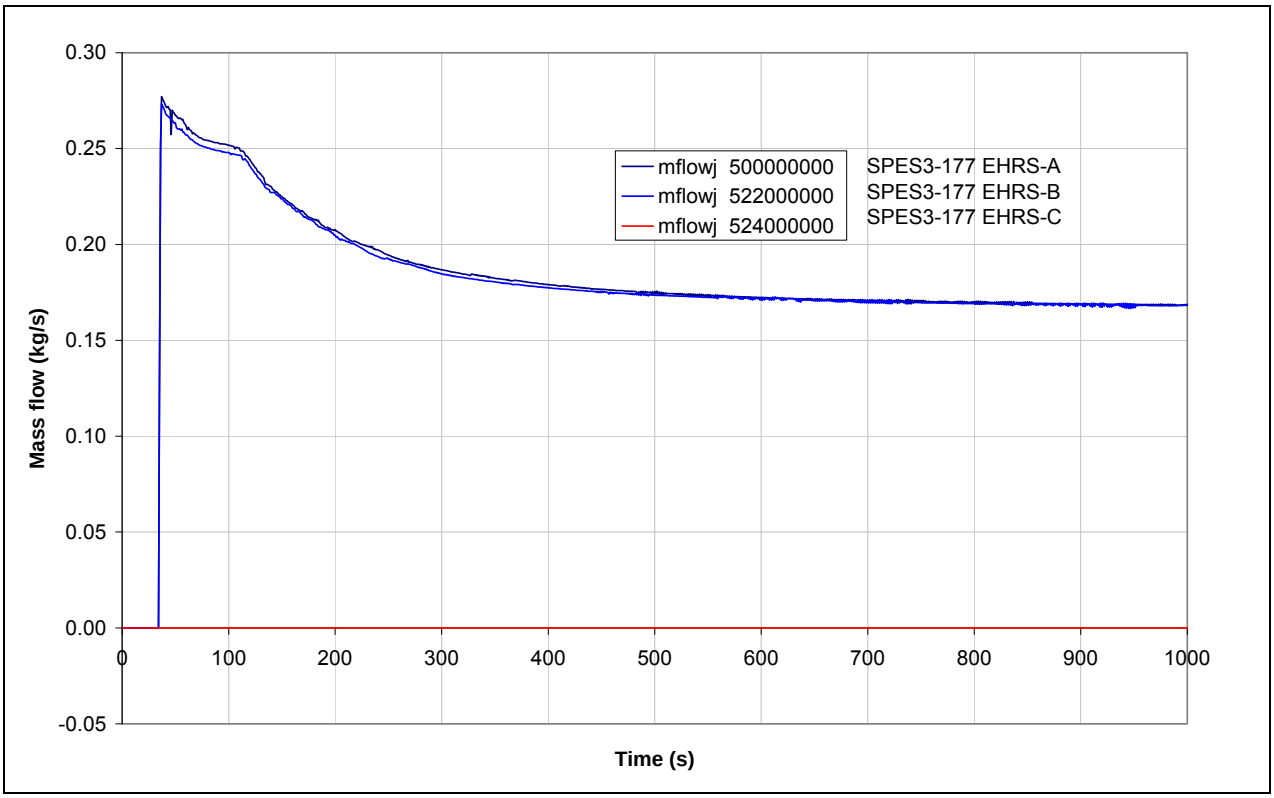

Fig.6. 20 – SPES3-177 EHRS cold leg mass flow

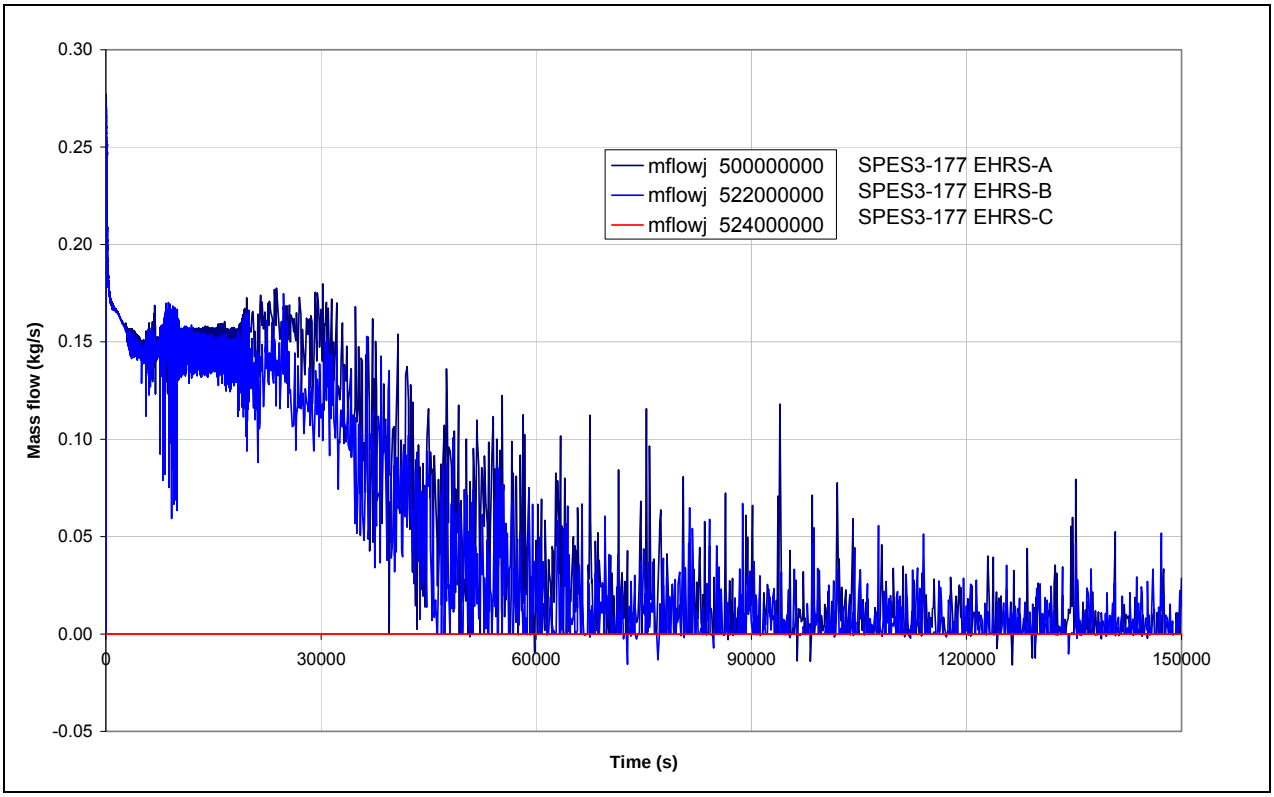

Fig.6. 21 – SPES3-177 EHRS power (window)

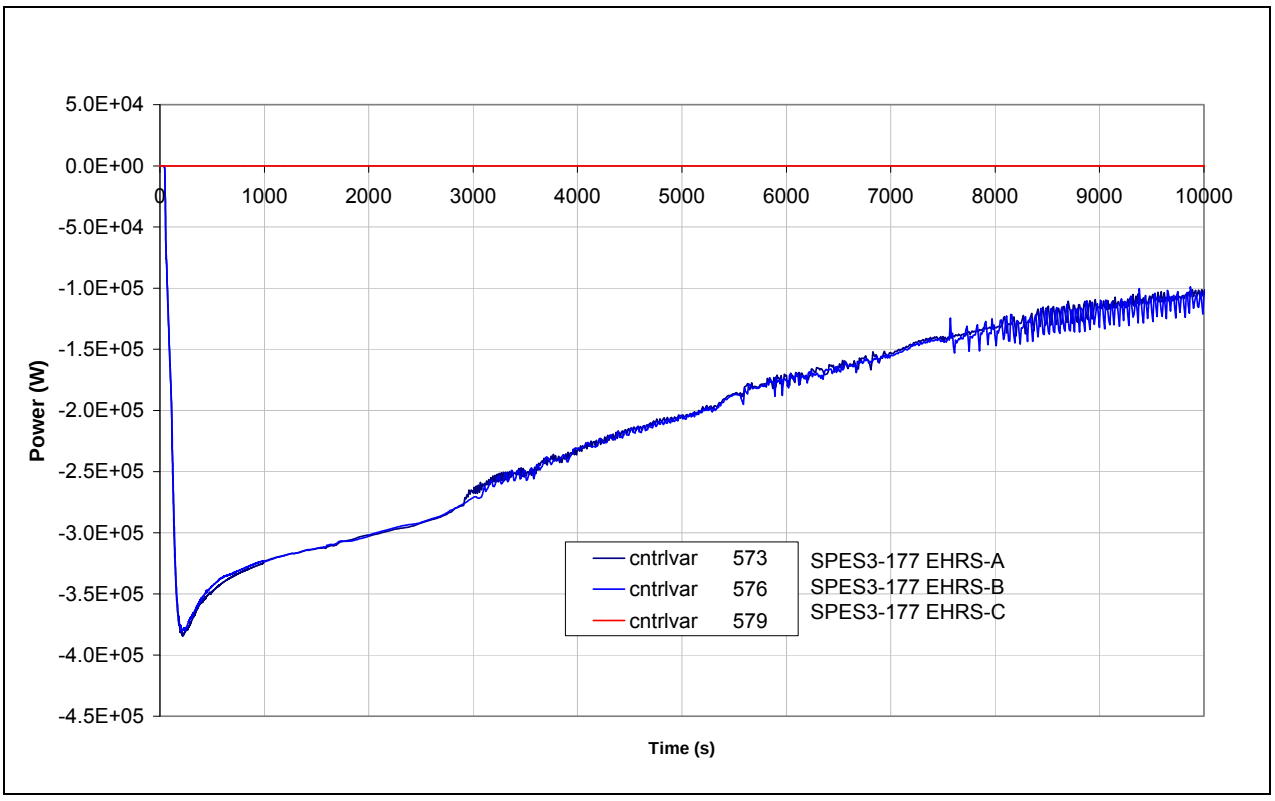

Fig.6. 22 – SPES3-177 EHRS power

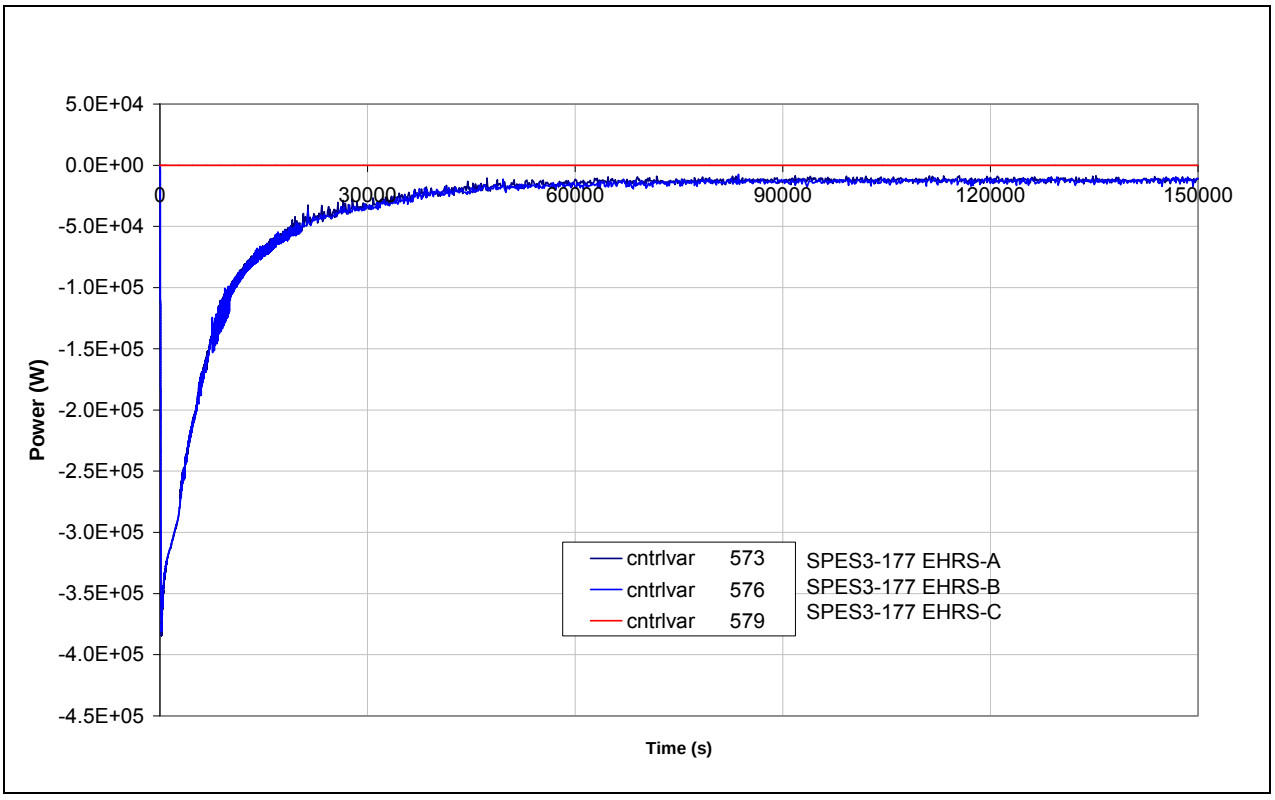

Fig.6. 23 – SPES3-177 RWST temperature

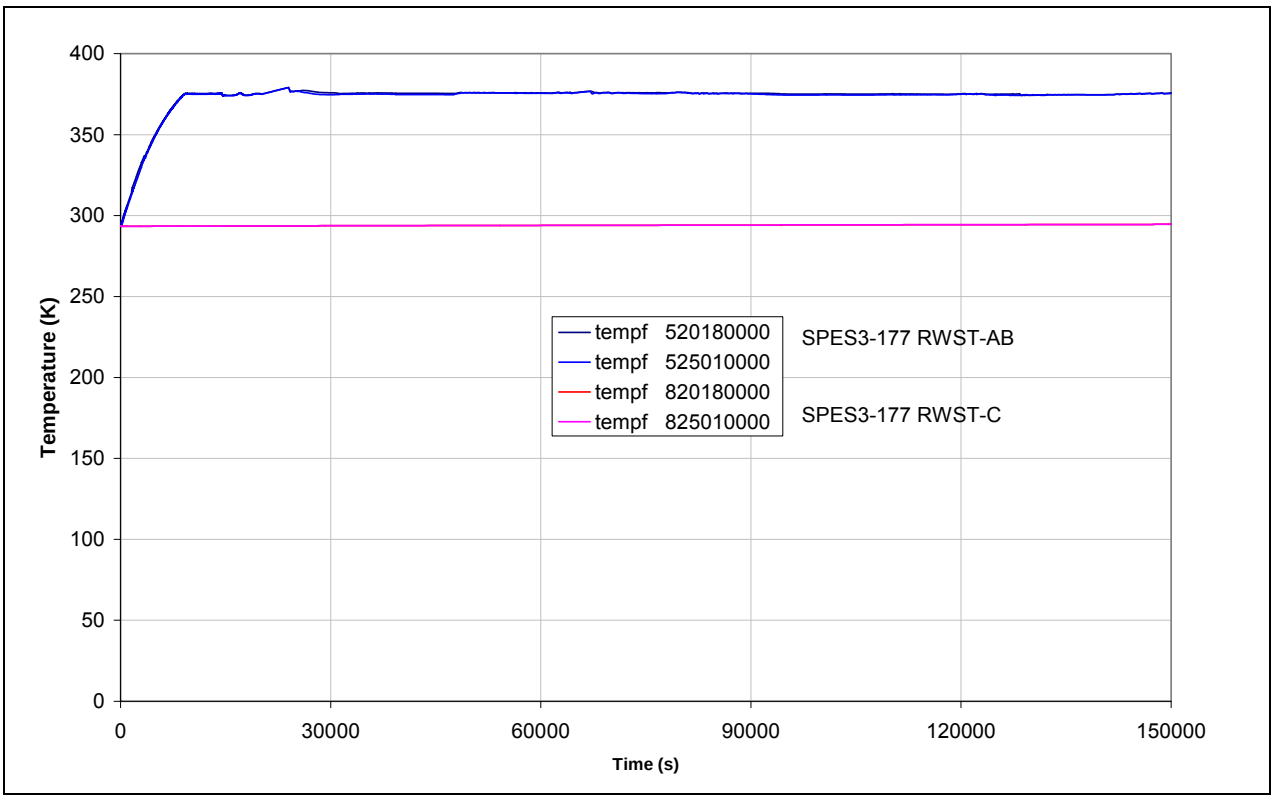

Fig.6. 24 – SPES3-177 RWST mass

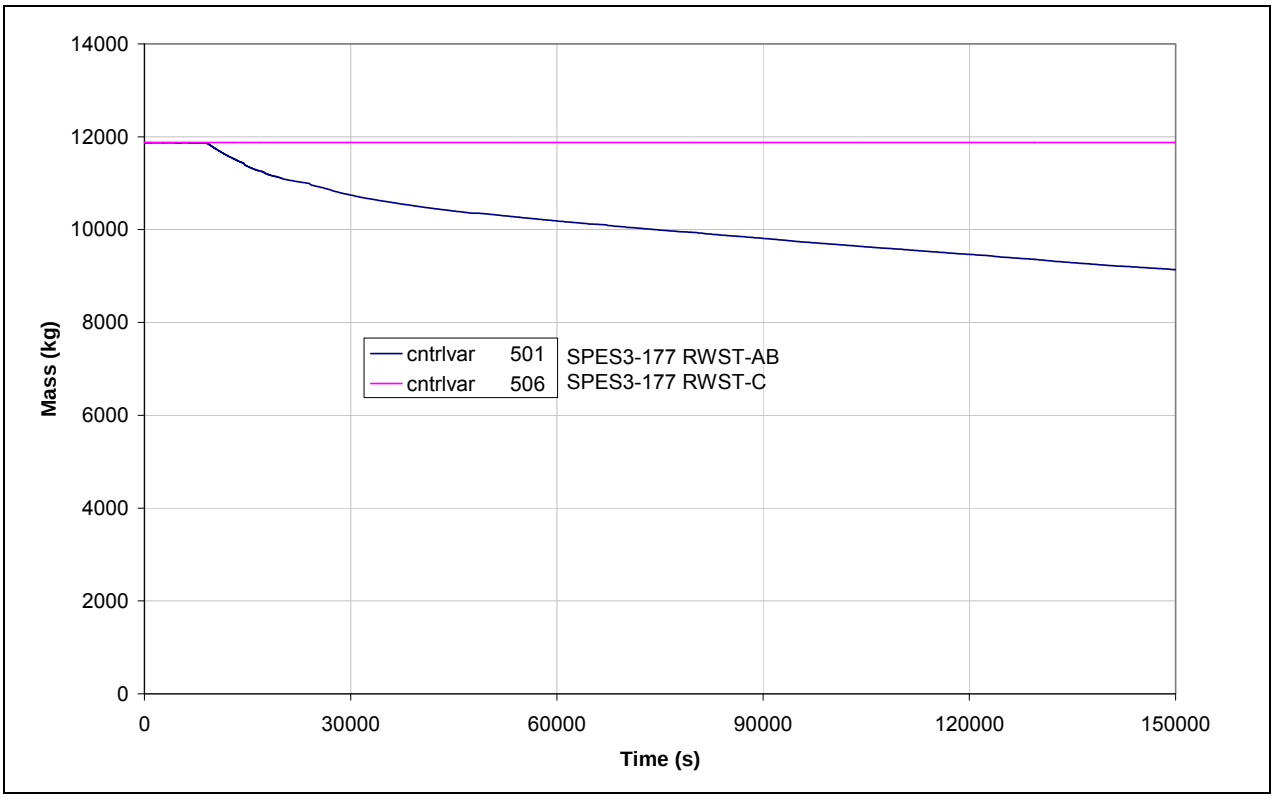

Fig.6. 25 – SPES3-177 Core mass flow (window)

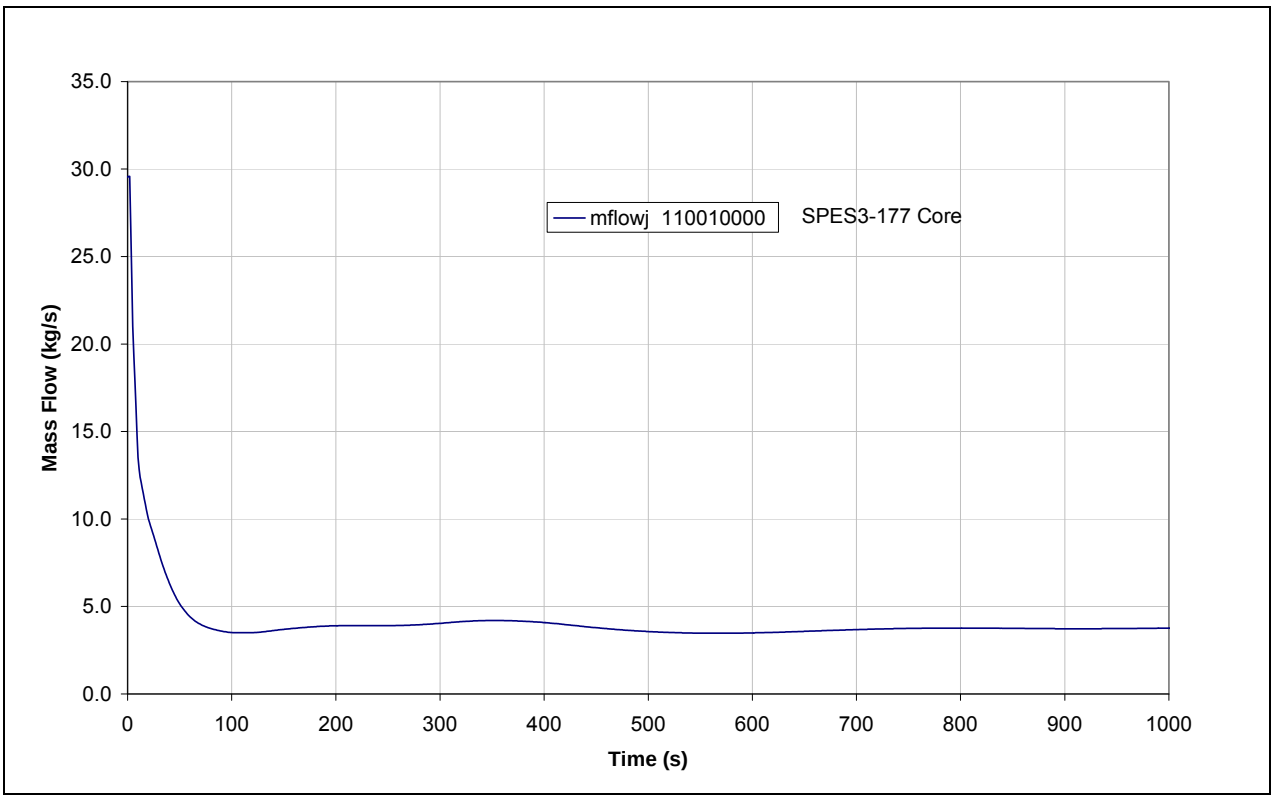

Fig.6. 26 – SPES3-177 Core mass flow (window)

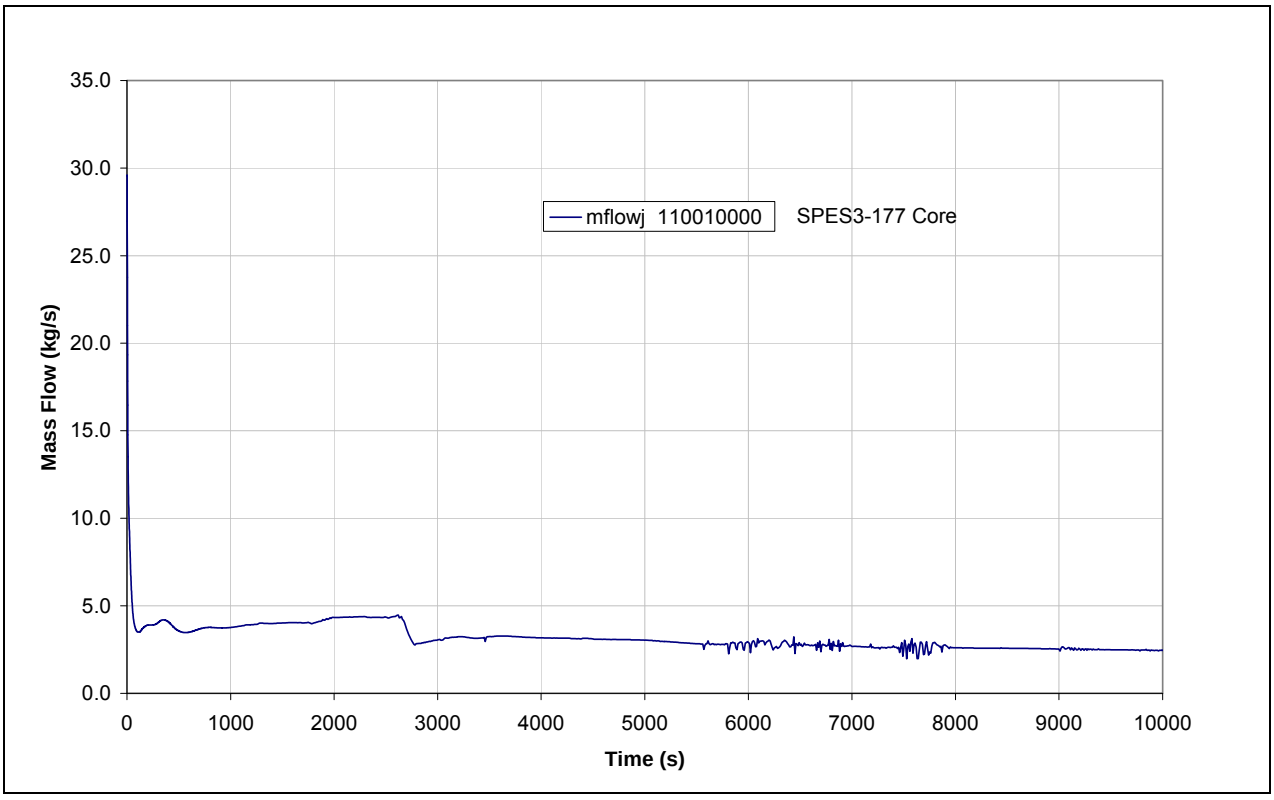

Fig.6. 27 – SPES3-177 Core mass flow

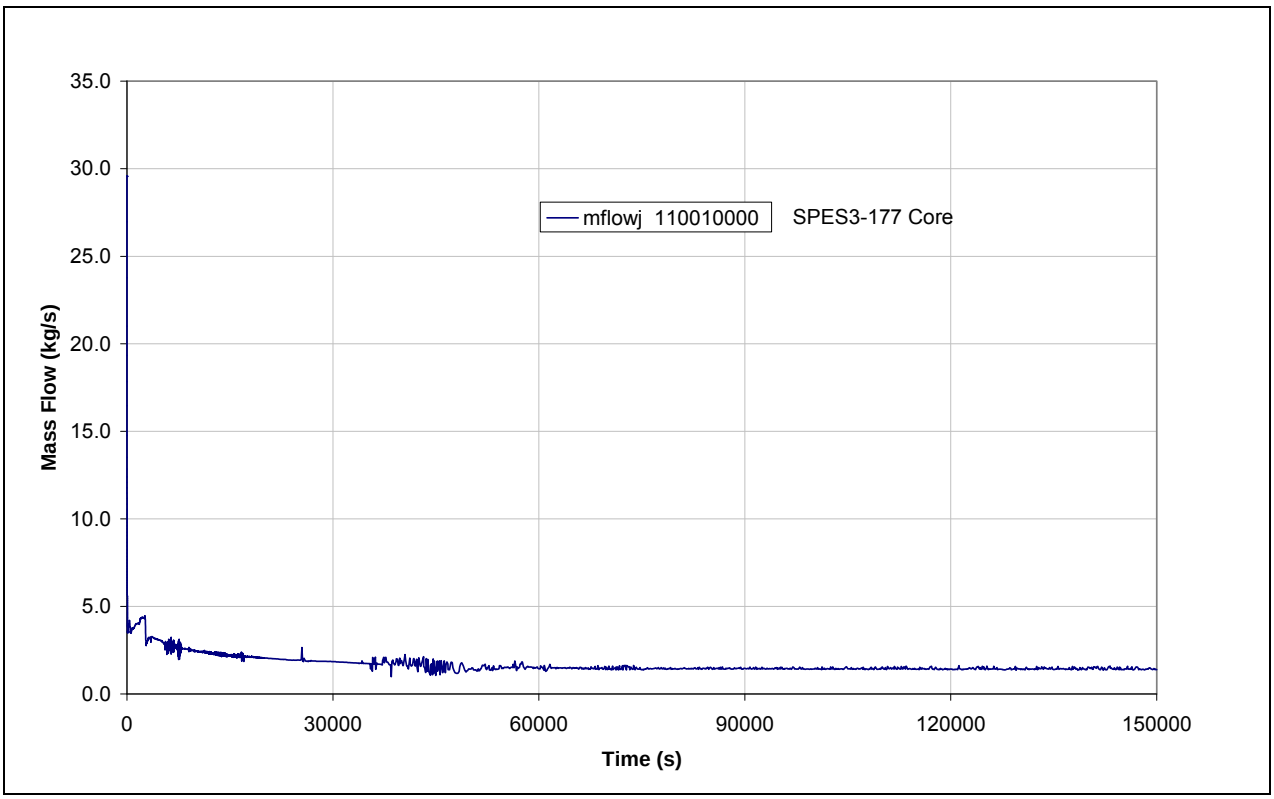

Fig.6. 28 – SPES3-177 SG secondary side outlet pressure (window)

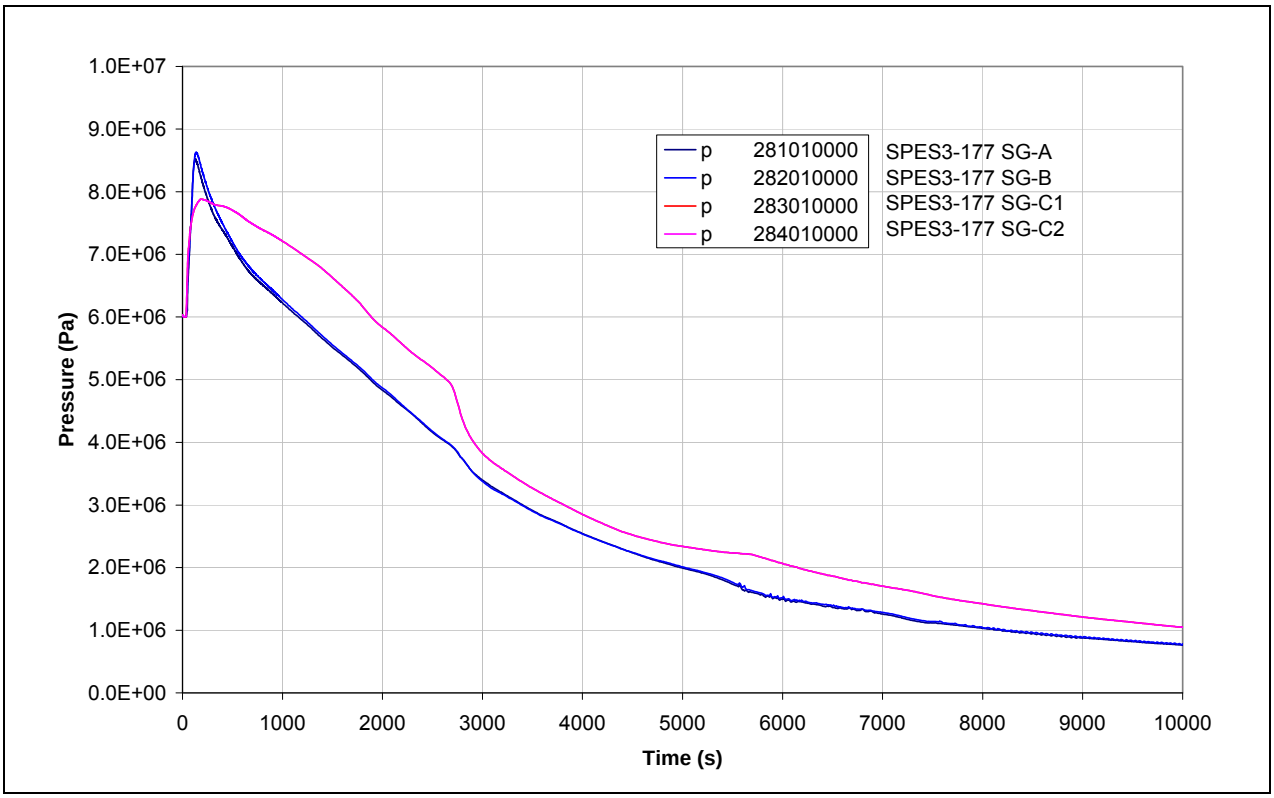

Fig.6. 29 – SPES3-177 SG secondary side outlet pressure

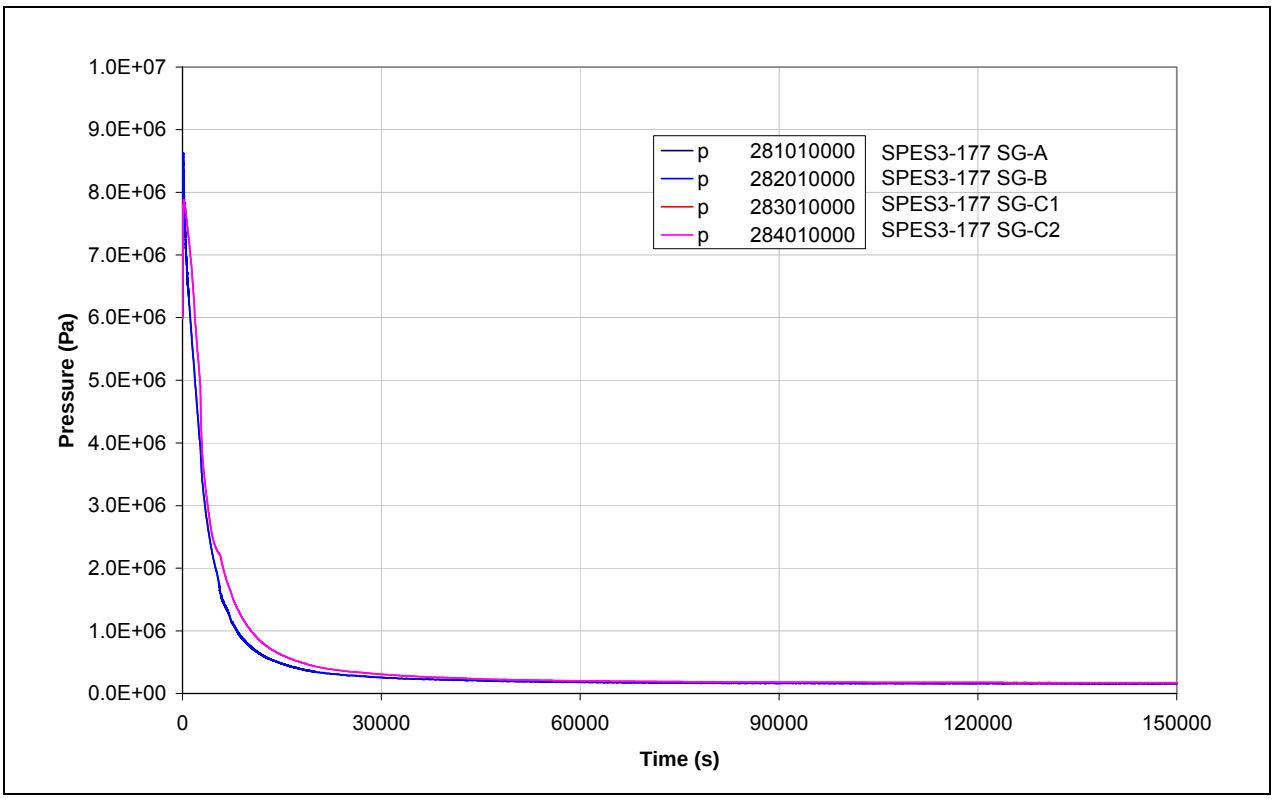

Fig.6. 30 – SPES3-177 PRZ pressure (window)

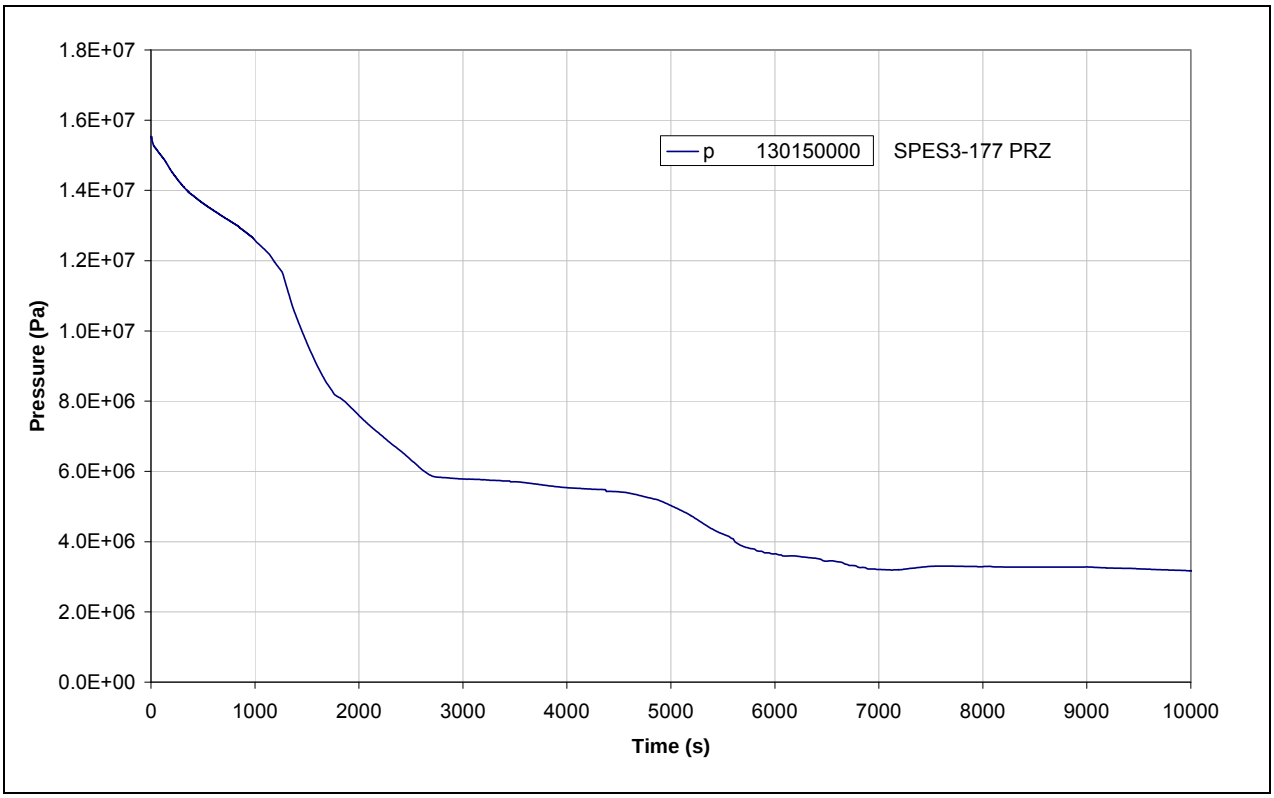

Fig.6. 31 – SPES3-177 PRZ pressure

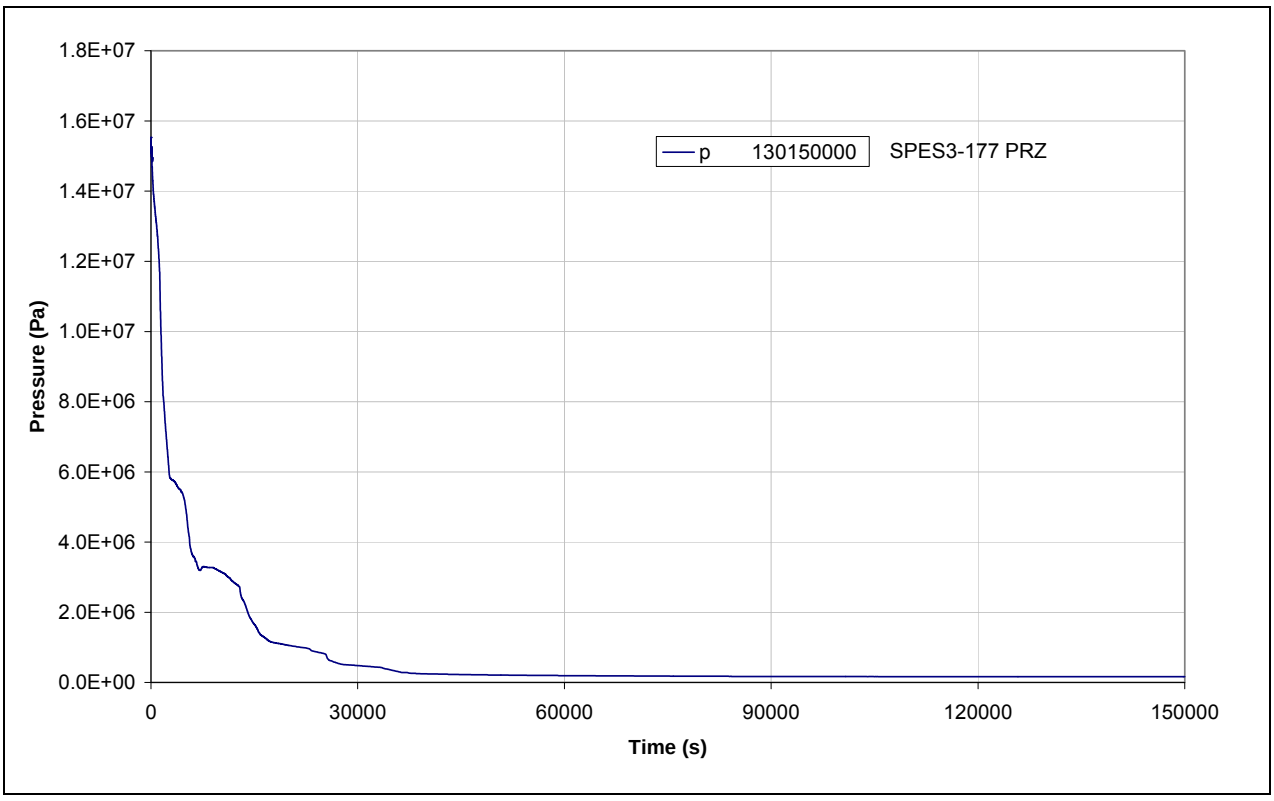

Fig.6. 32 – SPES3-177 Core inlet and outlet temperature (window)

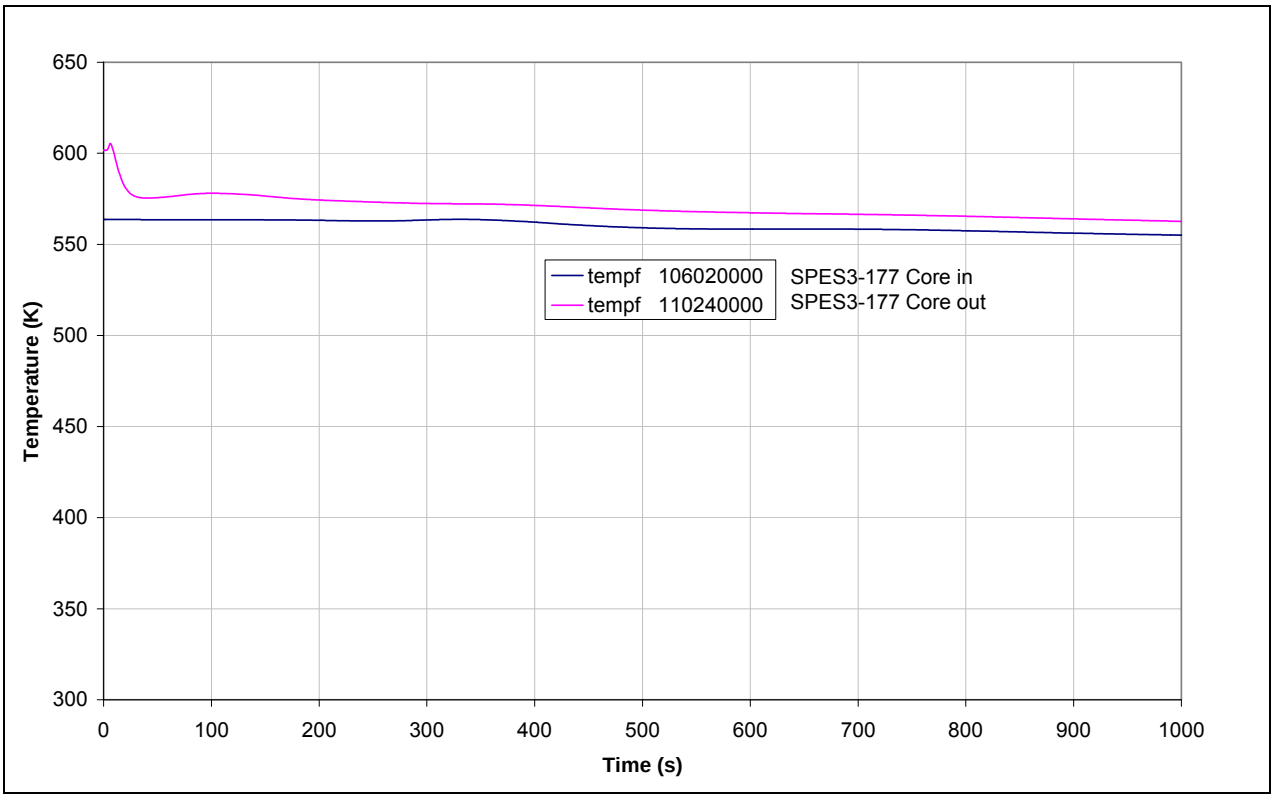

Fig.6. 33 – SPES3-177 Core inlet, outlet and saturation temperature

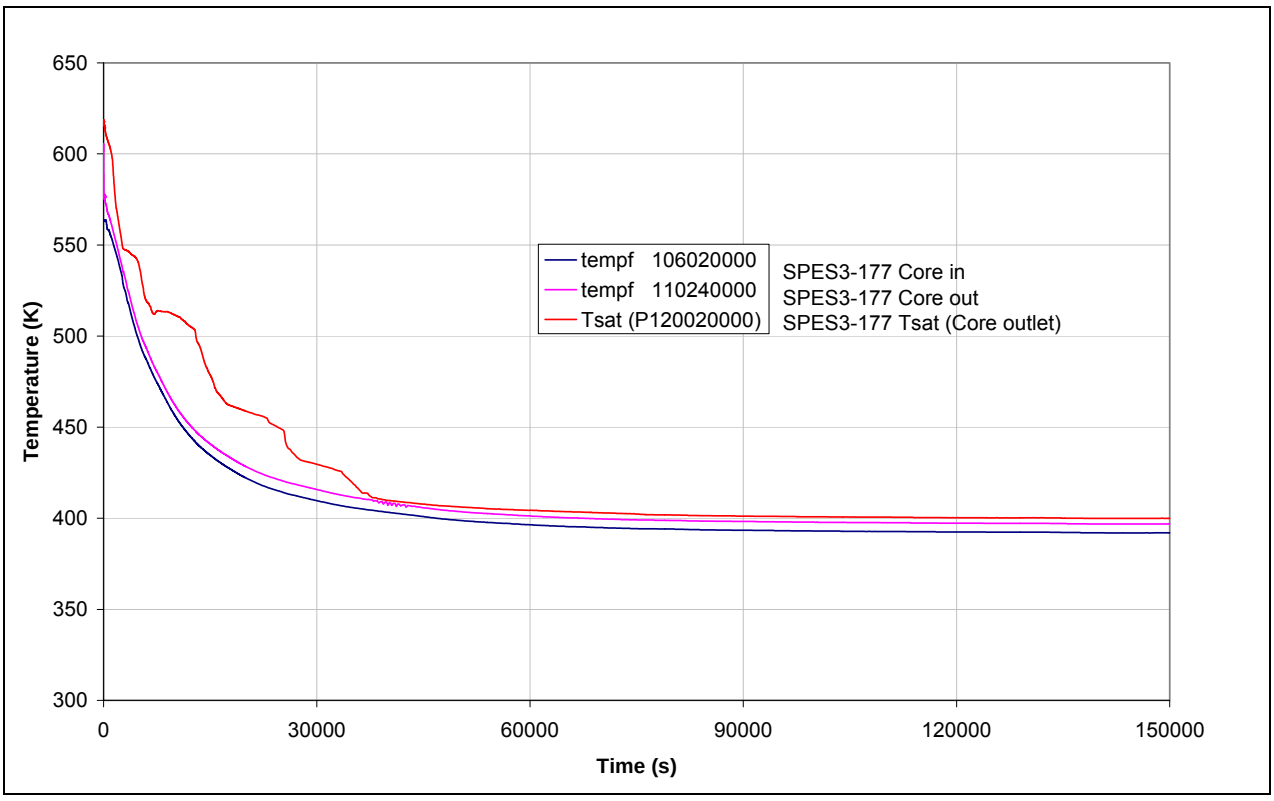

Fig.6. 34 – SPES3-177 Core liquid fraction

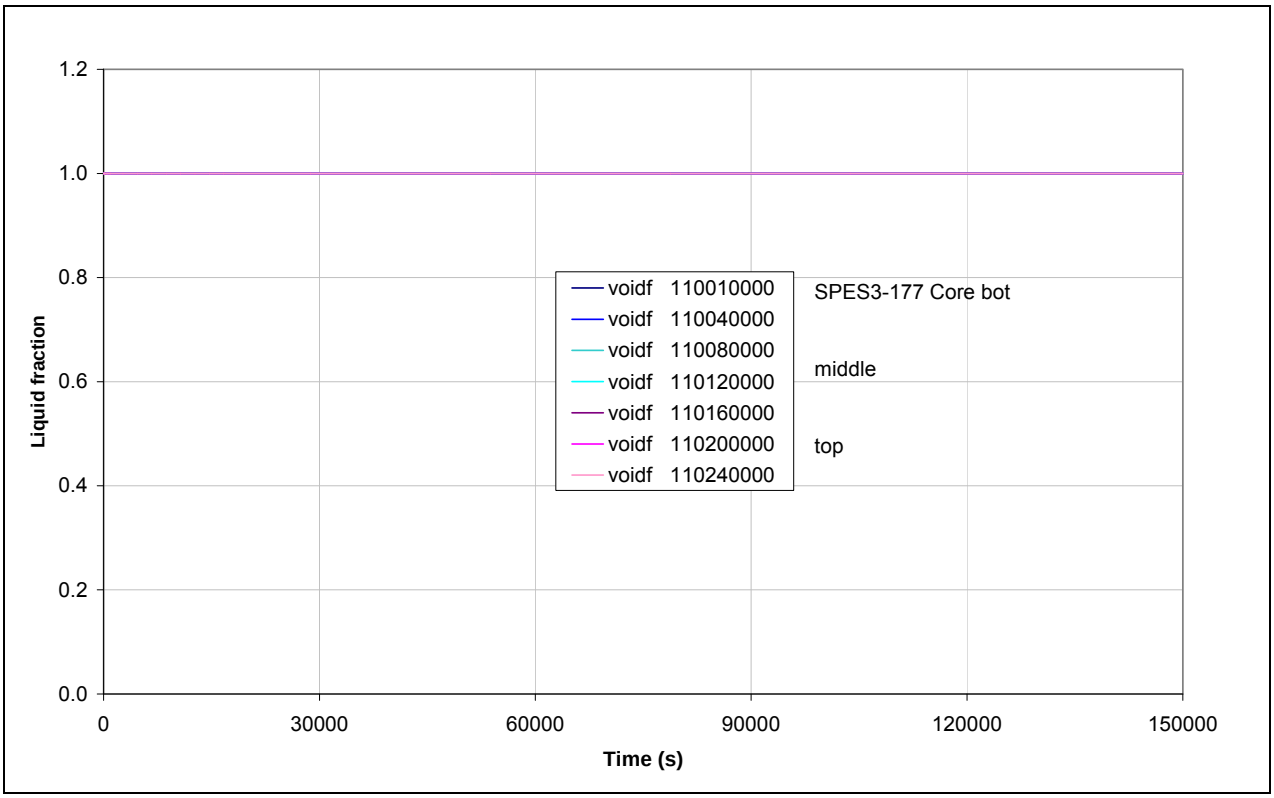

Fig.6. 35 – SPES3-177 PRZ level (window)

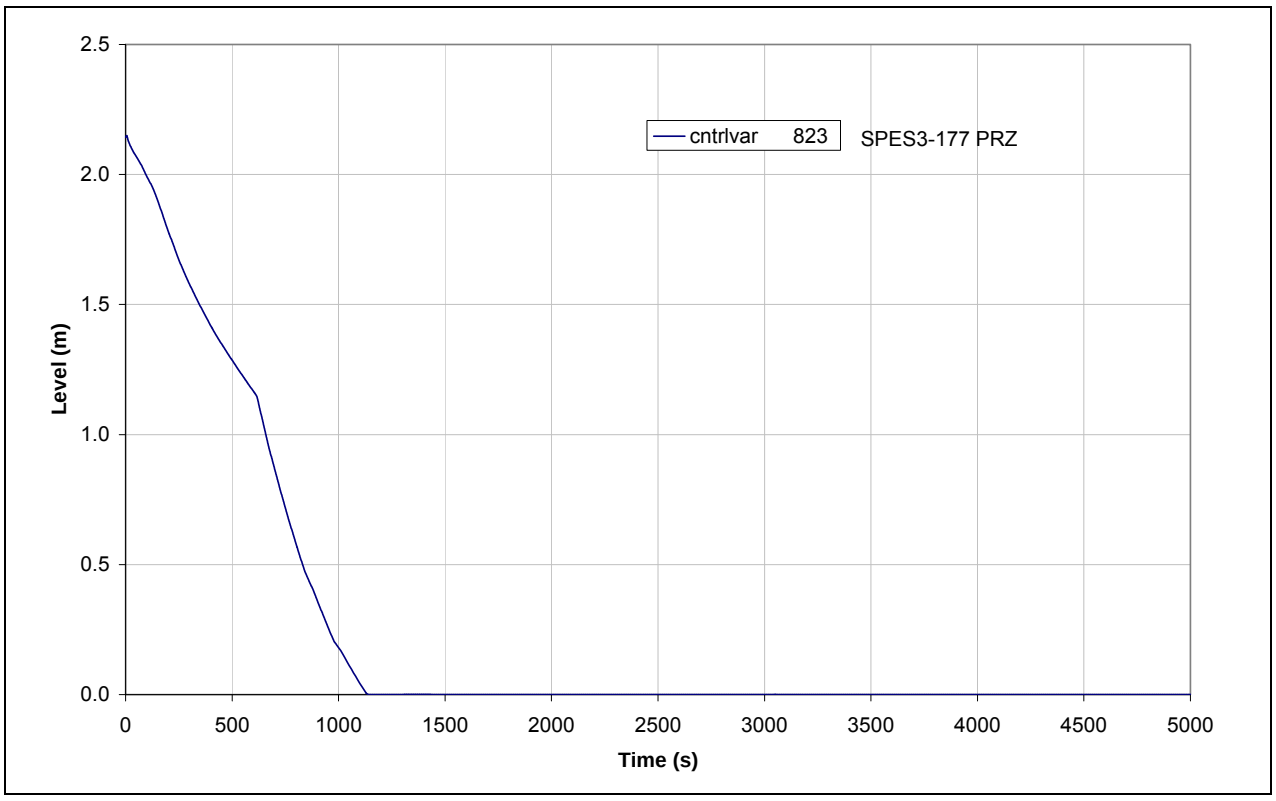

Fig.6. 36 – SPES3-177 RPV down comer level

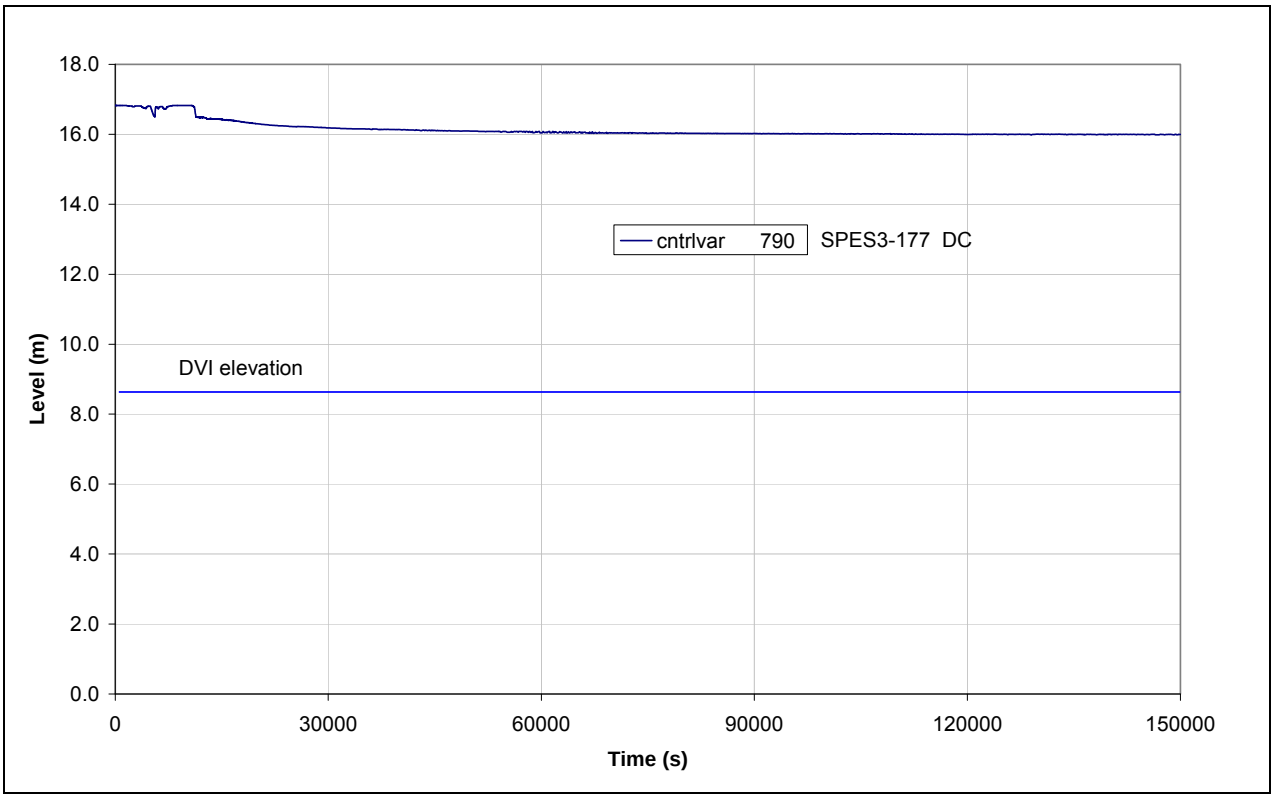

Note: DVI elevation referred to RPV bottom.

Fig.6. 37 – SPES3-177 EBT injection mass flow (window)

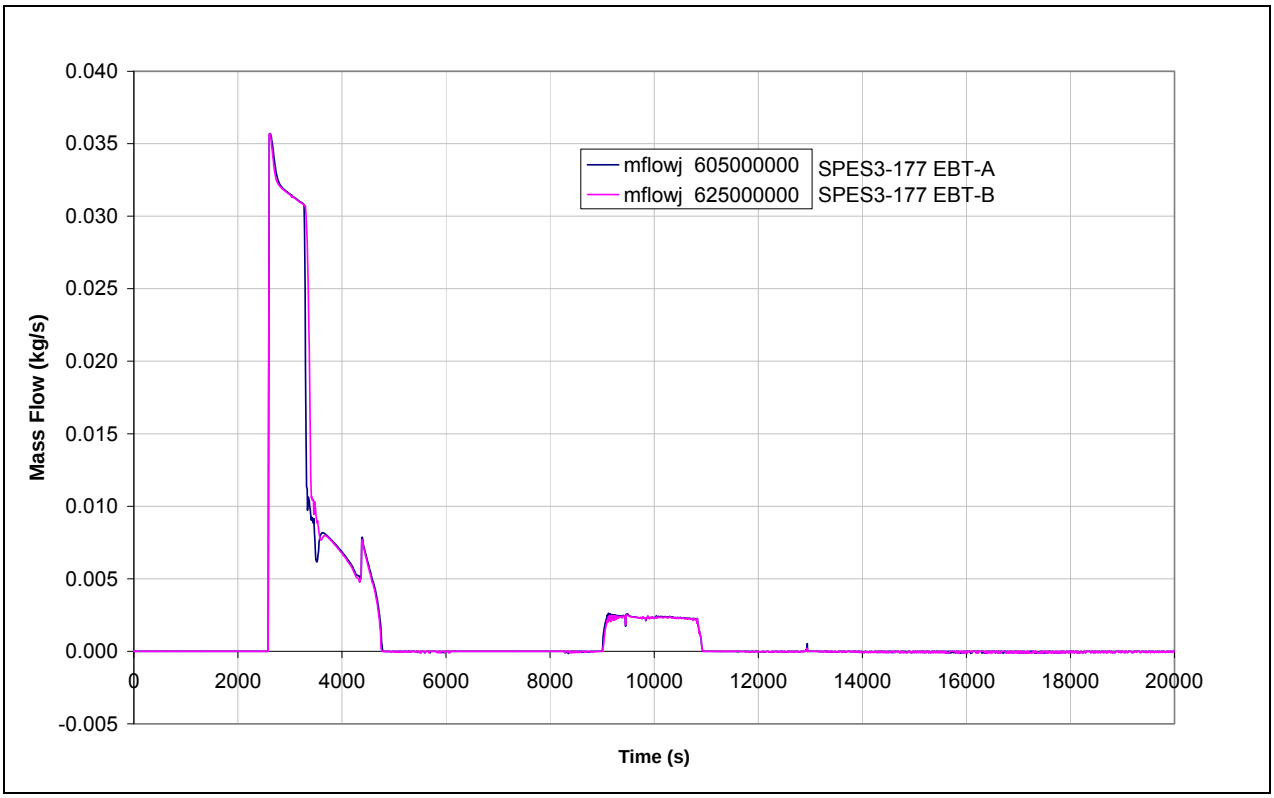

Fig.6. 38 – SPES3-177 EBT to RPV balance line mass flow (window)

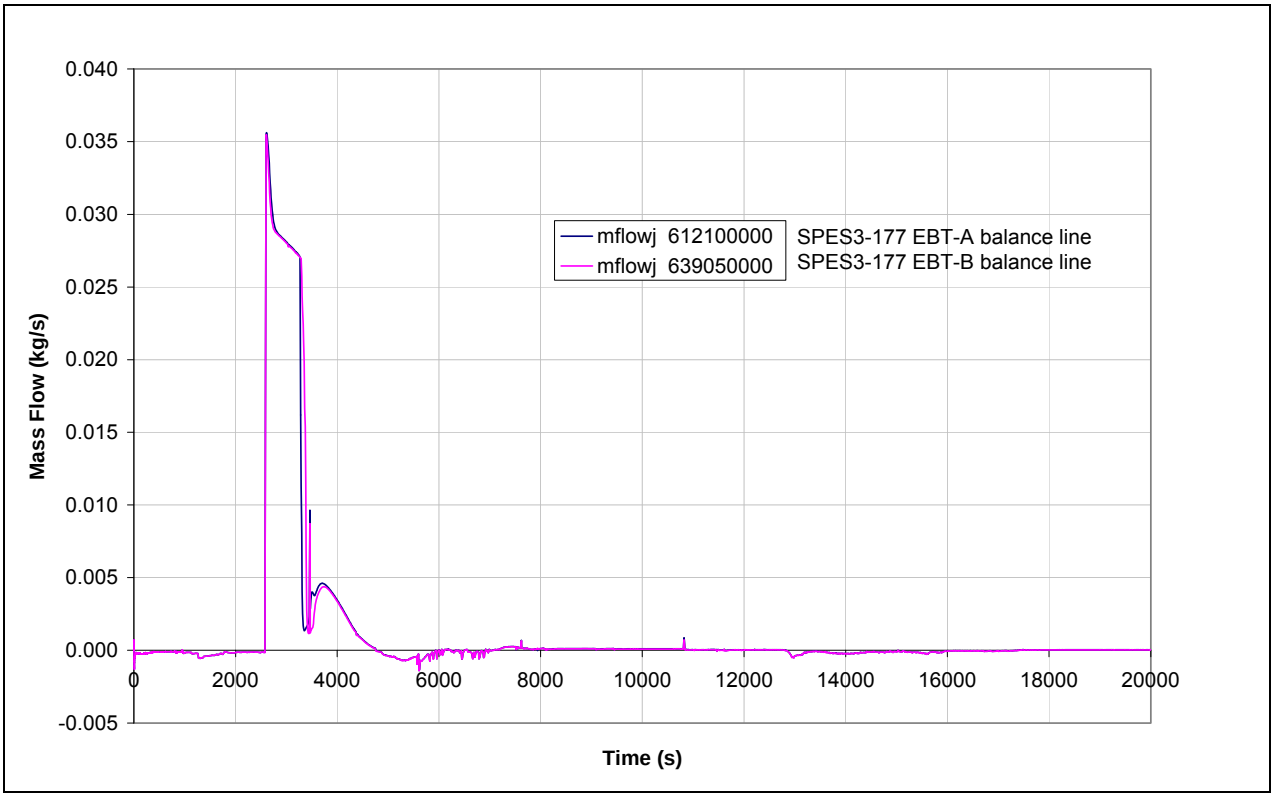

Fig.6. 39 – SPES3-177 DVI mass flow

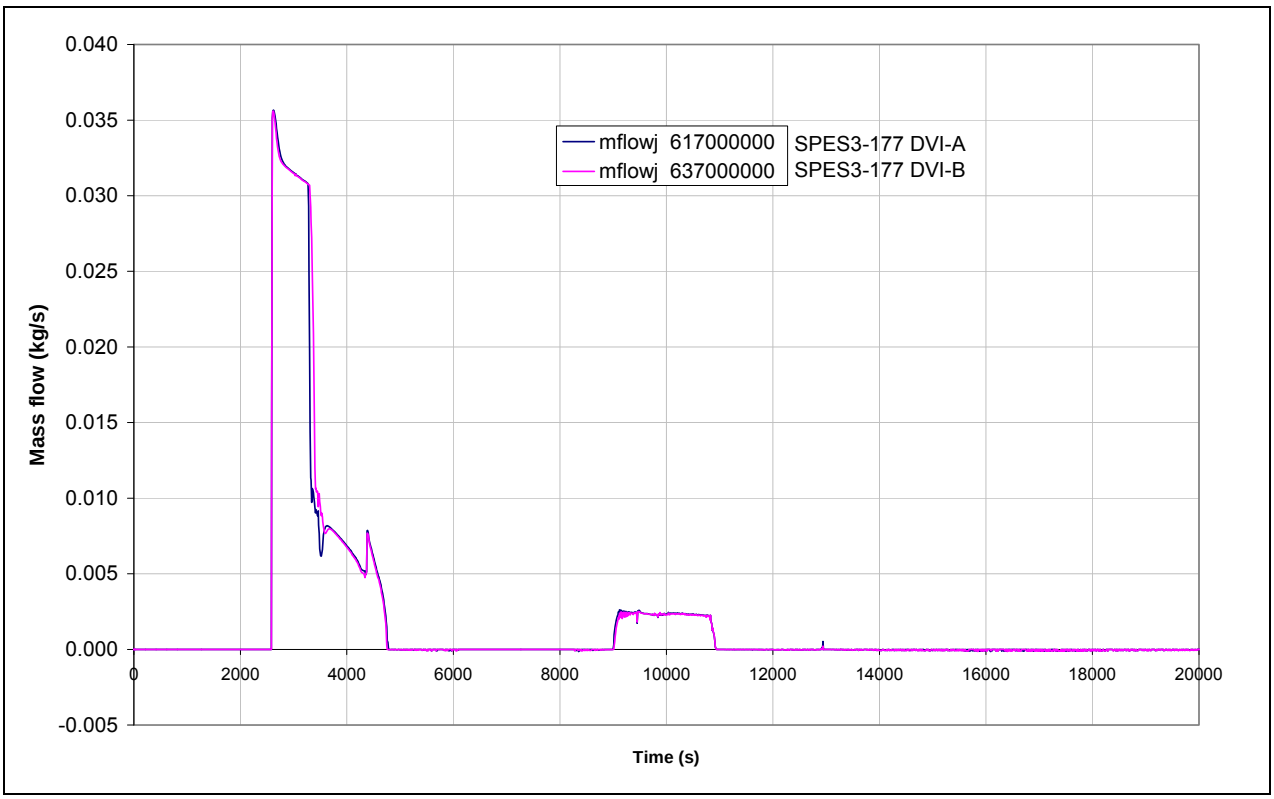

Fig.6. 40 – SPES3-177 EBT level

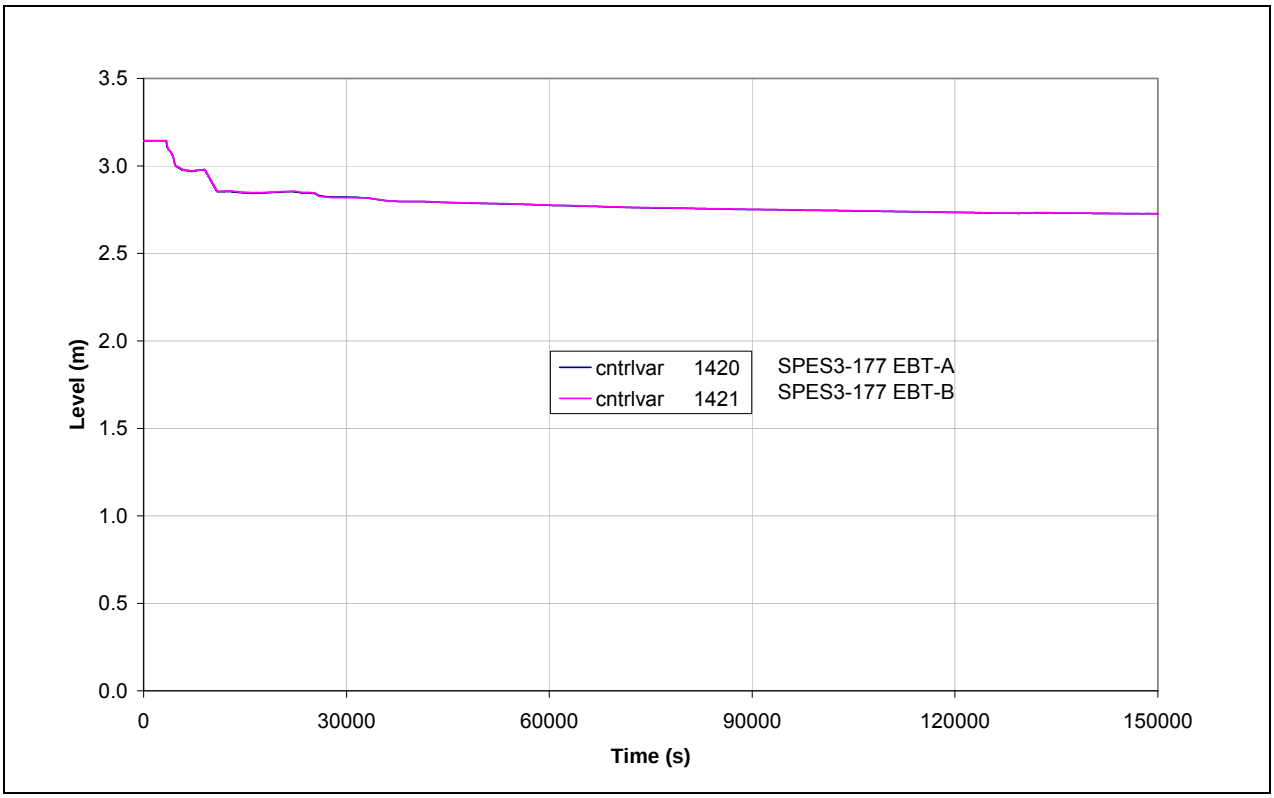

Fig.6. 41 – SPES3-177 RPV mass

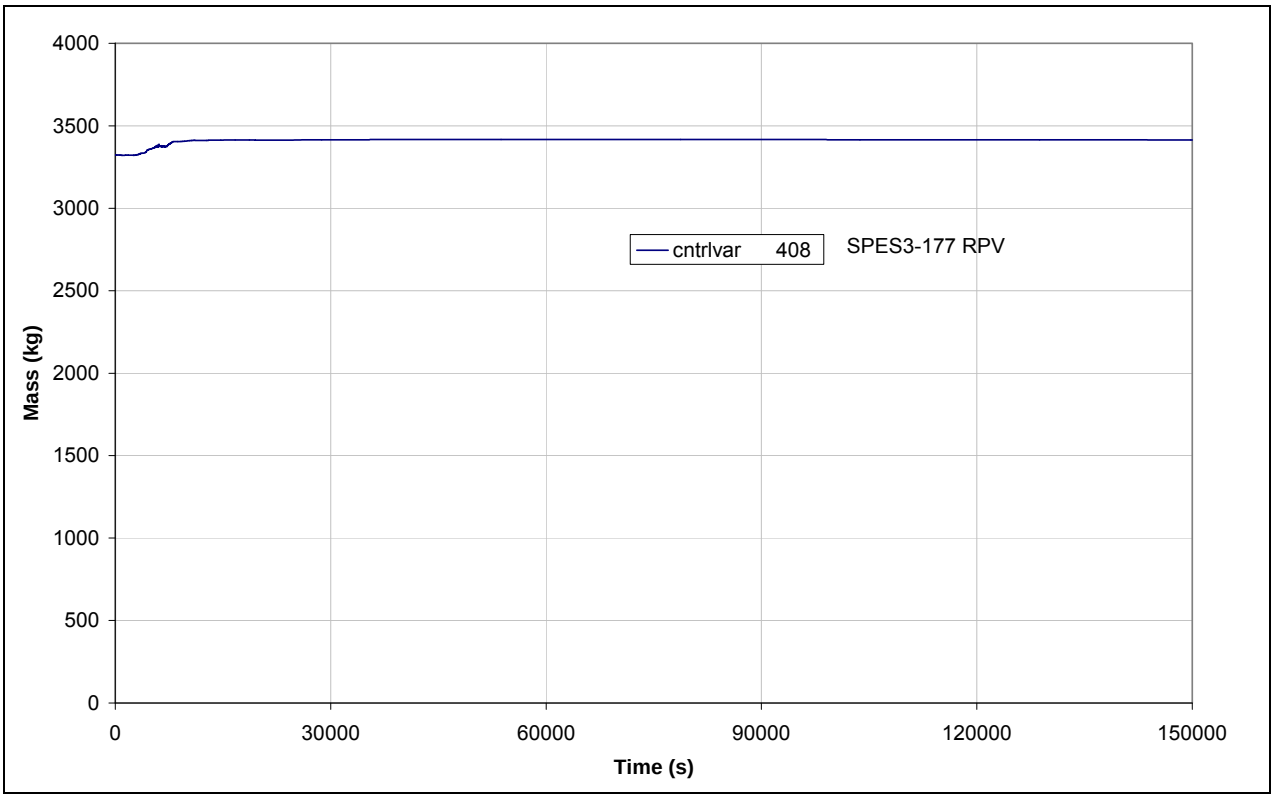

Fig.6. 42 – SPES3-177 Core heater rod surface temperature –normal rod (window)

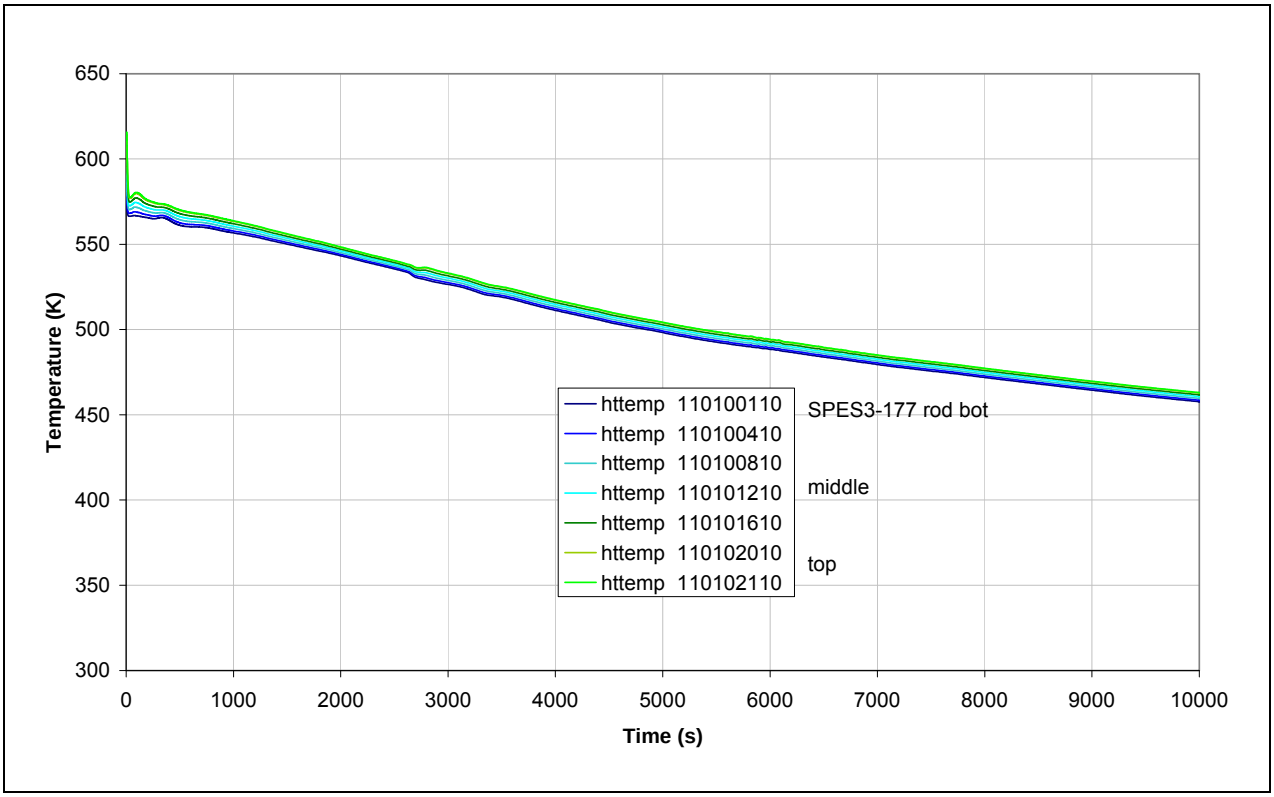

Fig.6. 43 – SPES3-177 Core heater rod surface temperature –normal rod

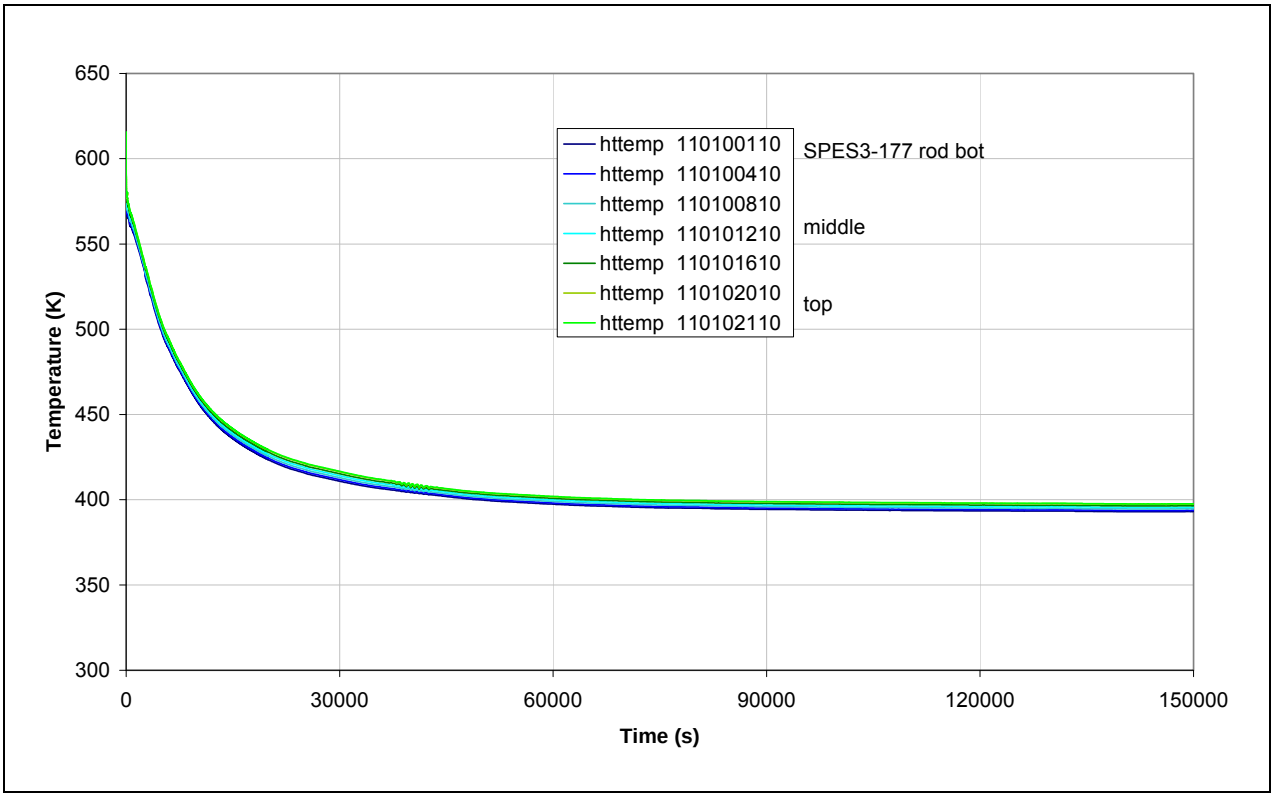

Fig.6. 44 – SPES3-177 Core heater rod surface temperature –hot rod (window)

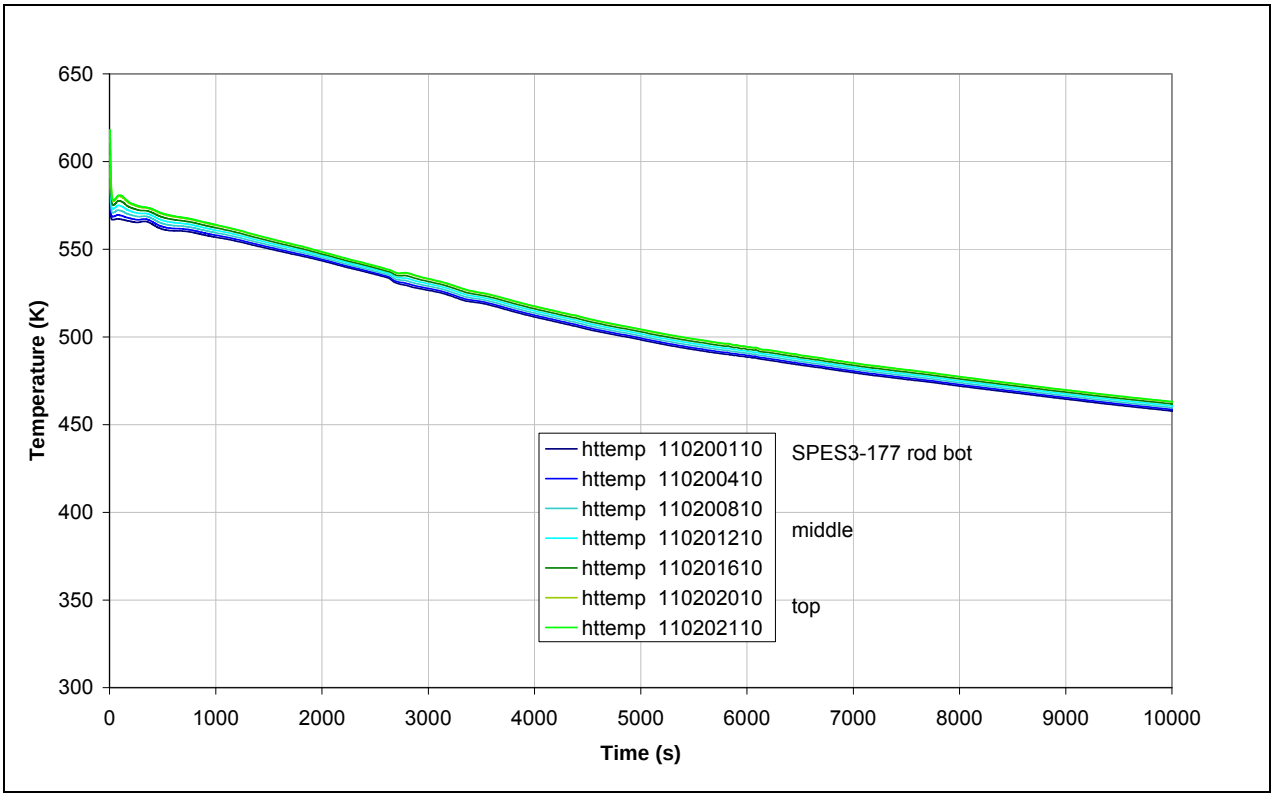

Fig.6. 45 – SPES3-177 Core heater rod surface temperature –hot rod

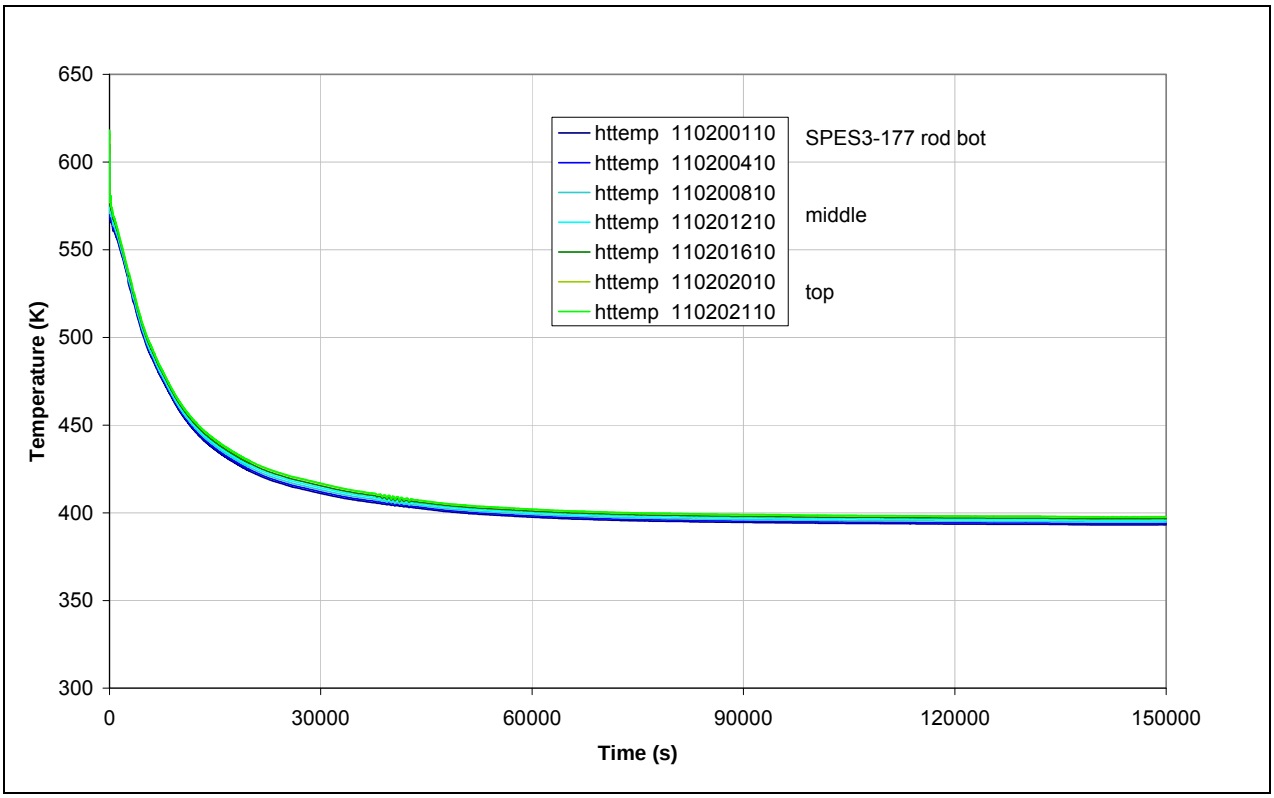

7. DBE DVI LINE DEG BREAK FROM 65% POWER – NEW EHRS: SPES3-181

The Chapter 3.2 explains the reasons why the EHRS tubes were changed with respect to the original design. The final tube configuration is: AISI 304 tubes, 60.3 mm outer diameter, 5.54 mm thickness. Different layers of Teflon insulation are foreseen for the EHRS-A/B and EHRS-C tubes to guarantee the exchanged power as in the original configuration that had thinner tubes. In particular, in the EHRS-A and B heat exchangers, the equivalent surface of a tube is covered with 0.096 mm Teflon and the headers are covered with 10 mm Teflon. In EHRS-C heat exchanger, no insulation is foreseen on the tubes while the headers are covered with 0.2 mm Teflon.

The SPES3-181 case is a DBE DVI line break transient run with the new EHRS tube geometry. It is exactly the same transient as SPES3-175 case, where the original EHRS tube geometry is simulated.

This chapter compares the SPES3-181 and SPES3-175 cases in order to verify that the EHRS re-design does not affect the heat rejection to RWST.

A deep analysis of the transient is reported in [20] for SPES3-175. The main quantities of the transients are compared here and, and differences explained on the basis of the changes to EHRS tubes.

7.1 SPES3-181 and SPES3-175 transient phases and description

The SPES3-181 and SPES3-175 cases are reduced power transients (65% power), starting from steady conditions as reported in Tab.4. 1.

The list of the main events occurring during the transients, with timing and quantities, is reported in Tab.7. 1.

7.1.1 SPES3-181 and SPES3-175 transient phases and description

The first 10 s of data (-10 s to 0 s) are steady state conditions.

All times of the events are given with respect to the break time, assumed as time 0 s.

Break

The break line mass flows, RPV side (SPLIT) and containment side (DEG), are compared in Fig.7. 1, Fig.7. 2, Fig.7. 3 for SPES3-181 and 175 cases. The trend is very similar for both RPV and containment side.

The mass flow, containment side (DEG), related to safety injection of EBT (~200 s) and later of LGMS (~2220 s), is very similar as well, Fig.7. 1, Fig.7. 2.

Reverse flow from containment to RPV is observed through the SPLIT line, after the RC level reaches the DVI line elevation, when the containment pressure is higher than the RPV pressure, Fig.7. 2, Fig.7. 3.

Blowdown, RPV depressurization, containment pressurization

The blowdown phase depressurises the RPV with mass and energy transfer to containment.

The PRZ pressure is shown in Fig.7. 4, Fig.7. 5, Fig.7. 6. Depressurization rate is very similar in SPES3-181 and 175 cases, with PRZ pressure slightly higher in SPES3-181 than 175 between 300 s and 1000 s.

While the PRZ depressurizes, the containment pressure increases as shown in Fig.7. 7, Fig.7. 8. Pressurization trend is very similar in the two cases. Reaching of the pressure peak is slightly anticipated in SPES3-181 (0.912 MPa at 2180 s, SPES3-181; 0.914 MPa at 2260 s, SPES3-175) and the depressurization phase is slightly anticipated as well. Between about 1500 s and 4000 s, both the PRZ and DW pressures in

SPES3-181 are lower than in SPES3-175. This depends on the slightly higher power, removed by the EHRS in this phase, Fig.7. 21.

Pressure increase around 200 s is due to ADS Stage-I intervention that discharges mass and energy into the DW. Depressurization, after the containment pressure peak, is due to the LGMS injection, followed by the PSS injection to DW, through the vent lines

Steam dumping into PSS

The containment space (DW and RC) pressurization causes transfer of steam-gas mixture from DW to PSS through the vent lines (~16 s) lasting until mass flow exits the ADS-Stage-I, Fig.7. 11.

Steam is dumped underwater through the PSS sparger and air pressurizes the PSS and LGMS gas space, Fig.7. 12, Fig.7. 13, Fig.7. 14. PSS and LGMS pressure follows the DW pressure trend. When PSS pressure is high enough to overcome the PSS vent line gravity head, water is pushed backward to the DW, enhancing the containment depressurization. PSS and LGMS pressure remains above the DW pressure until the PSS sparger is uncovered (~4500 s), i.e. the PSS vent pipes are empty. Afterwards, air flows from PSS to DW and DW, PSS and LGMS pressures equalize.

S-Signal: Reactor scram, secondary loop isolation, EHRS-A and B actuation

The high containment pressure set-point (1.7e5 Pa), reached at 31.54 s in SPES3-181 and 31.58 s in SPES3-175, triggers the S-signal.

The S-signal (Safeguard) starts the reactor SCRAM, isolates the three secondary loops and actuates the EHRS-A and B.

Power released to fluid in the core is shown in Fig.7. 15, Fig.7. 16. Steady state power is 6.5 MW. After the scram signal, the reduced power curve continues at 6.5 MW for 3.35 s, until it intersects the nominal decay power curve.
Power transferred to the steam generators is shown in Fig.7. 15, Fig.7. 16. The peak of removed power occurs following the EHRS-C intervention with similar values in SPES3-181 and SPES3-175 (1.63 MW at 327 s, SPES3-181; 1.66 MW at 320 s, SPES3-175). Power is slightly lower in SPES3-181 case due to lower power removed by EHRS-C between 250 s and 750 s, Fig.7. 21.
The MFIV and MSIV of secondary loops are contemporarily closed in 5 s. Secondary loop mass flows are shown in Fig.7. 17 and Fig.7. 18. They stop at secondary loop isolation and re-start at EHRS actuation. EHRS-A and B are actuated at secondary side isolation and natural circulation flow establishes. EHRS-C is actuated at LM-signal, starting secondary loop natural circulation after about 150 s from the loop isolation. After loop isolation, very similar mass flows are observed in the two cases.

EHRS-A and B are actuated by opening in 2 s the related isolation valves (EHRS-C is actuated later on LM-signal). The peak mass flow of 0.26 kg/s is reached at 37 s. Between 1000 s and 10000 s, quite steady condition is reached with natural circulation mass flow of about 0.16 kg/s in the loops A and B, Fig.7. 19. After 10000 s, larger oscillations appear and mass flow decreases to low values around 0.02 kg/s in the long term, Fig.7. 20.

Power removed by EHRSs is shown in Fig.7. 21 and Fig.7. 22. The EHRS-A and B peaks of removed power are very close in time and values for SPES3-181 and SPES3-175 (359 kW at 226 s, SPES3-181; 375 kW at 225 s, SPES3-175). The EHRS-C shows a difference between SPES3-181 and SPES3-175: less power is removed in the early phase of intervention (until ~750 s) and more power is removed in the second phase (until ~5000 s) in SPES3-181 than SPES3-175. After that, EHRS power is very similar in both cases.

Secondary side pressures are shown in Fig.7. 23 and Fig.7. 24. After isolation, pressure increases due to heat transfer from the primary side that makes water contained in the SG tubes evaporate. Very similar pressure peaks, in time and value, are reached in SPES3-181 and SPES3-175. The SG tube levels

decrease until water stored in EHRS heat exchangers is poured into the loops and power begins to be removed, Fig.7. 25, Fig.7. 26. Similar trends are observed for the two cases.

Pump coastdown and primary circulation through RI-DC check valves

The PRZ level is shown in Fig.7. 27. The early phase of level decrease, until ADS Stage-I intervention (~200 s), is due to loss of mass from the break. Level increase is due to the ADS Stage-I actuation. The PRZ level trend is very similar in SPES3-181 and SPES3-175.

The pump coastdown is triggered by the Low PRZ level signal delayed of 15 s. Run at reduced velocity in the steady state, the pump coast-down curve intersects the nominal one, continuing at constant velocity for 2 s after the coast-down signal. Afterwards, the curves are exactly the same.

Soon after the pump suction is uncovered, RPV natural circulation through the pump interrupts.

Core inlet flow is shown in Fig.7. 28 and Fig.7. 29. The trend is very similar for SPES3-181 and 175, until about 4500 s, the SPES3-181 case shows a little lower mass flow for about 6000 s. Afterwards, the curves are very similar.

The pump stop and pressure decrease in the DC let the RI-DC check valves open around 150 s and allow natural circulation from riser to SG annuli at lower level in the RPV. The RI-DC check valve mass flow is shown in Fig.7. 30 and Fig.7. 31 for each SG annulus. The trend and value of the RI-DC check valve mass flows are similar for SPES3-181 and SPES3-175 cases and they are strictly related to the core flow.

The fast RPV loss of mass and depressurization rapidly cause flashing of the primary circuit and void begins at core outlet at 238 s in SPES3-181 and 237 s in SPES3-175, Fig.7. 32, Fig.7. 33, Fig.7. 34. Low liquid fraction period in the core lasts until about 5000 s both in SPES3-181 and SPES3-175.

LM-Signal: EHRS-C, ADS Stage-I and EBT actuation

The LM-Signal (LOCA mitigation) occurs at 196.94 s in SPES3-181 and 196.42 s in SPES3-175, when the low PRZ pressure set-point (11.72e6 Pa) is reached, Fig.7. 4.

The LM-signal actuates the EHRS-C and opens the ADS stage-I and EBT actuation valves.

The EHRS-C is actuated by opening in 2 s the related isolation valves. The peak mass flow of 0.545 kg/s is reached at 201 s in SPES3-181 and of 0.547 kg/s at 200 s in SPES3-175. After the peak, quite steady natural circulation of about 0.32 kg/s is present between 3000 s and 9000 s. After that, strong oscillations appears and mass flow decreases. The long term values are very similar in the two cases, Fig.7. 19, Fig.7. 20.

Power removed by EHRS-C is shown in Fig.7. 21, Fig.7. 22. The EHRS-C peak of removed power occurs at 349 s (669 kW in SPES3-181) and at 334 s (719 kW in SPES3-175). The peak in case SPES3-181 is slightly lower than in SPES3-175, while transferred power is higher than in SPS3-175, between 750 s and 4000 s. The phenomenon can be explained considering that the increased tube thickness introduces a delay in the heat transfer, and later, the header contribution to the heat exchange, increases the transferred power. The average power removed by EHRS-C in the long term is around 20 kW.

The three trains of ADS Stage-I are actuated contemporarily on LM-signal and the actuation valves are fully opened in 10 s. ADS Stage-I mass flows are shown in Fig.7. 35.

When ADS intervene, PRZ is empty, Fig.7. 27, and the ADS flow peak is due to steam flowing toward the QT. At ADS intervention, water is sucked upwards and the PRZ level increases. The second ADS mass flow peak is caused by increasing liquid void fraction at the PRZ top that decreases when the PRZ empties. The curves are very similar in SPES3-181 and SPES3-185.

The RPV mass is shown in Fig.7. 32 and Fig.7. 33. The trend is similar in the two cases until about 5000 s. Between 5000 s and 10000 s, the SPES3-181 case shows lower mass increase related to the lower water back-flow from containment to RPV, through the RC to DVI line (intact loop), Fig.7. 36, Fig.7. 37. The mass injection from the containment to the RPV is higher in SPES3-175 as the containment pressure is higher than the RPV one, while they are very similar in SPES3-181, Fig.7. 9. The final value of mass in the RPV is around 2300 kg in both cases.

The LM-signal triggers EBT actuation, by fully opening the valves in 15 s. EBT injection mass flow is shown in Fig.7. 38 and it is very similar in SPES3-181 and SPES3-175. The EBT injection into the broken DVI line is initially about 14 times larger than injection into the intact DVI line, due to the presence of the break. The EBT injection continues until both EBTs are empty, Fig.7. 39.

RPV saturation

The RPV mass decreases due to the loss of mass from the break, Fig.7. 32, Fig.7. 33. The Fast RPV depressurization leads to reach the saturation conditions (core bottom liquid fraction < 1) at 238 s in SPES3-181 and 237 s in SPES3-175. Two-phase mixture occurs in the core, but natural circulation through the RI-DC check valves allows to remove the decay heat and temperature difference establishes again between the core inlet and outlet when core is under liquid single-phase, Fig.7. 34, Fig.7. 30, Fig.7. 40, Fig.7. 41. The inlet and outlet core temperatures are shown in Fig.7. 40, Fig.7. 41 and they are very similar in the two cases.

The core heater rod temperatures are shown in Fig.7. 42, Fig.7. 43, Fig.7. 44, Fig.7. 45 for the normal and hot rods, respectively. Notwithstanding the core liquid void fraction decrease, rod surface temperatures never overcomes the maximum steady state temperature.

Low DP RPV-Containment signal, LGMS and RC to DVI line valve actuation

The containment pressure peak of 0.912 MPa occurs at 2180 s in SPES3-181 and of 0.914 MPa at 2260 in SPES3-175, Fig.7. 7.

The “Low DP RV-Containment” signal set point (50 kPa) is reached at 2207.6 s in SPES3-181 and 2257.04 s in SPES3-175.

The combination of LM-signal AND Low DP RV-Containment signal actuates the LGMSs and opens the valves on the lines connecting the RC to the DVI lines.

The LGMS isolation valves are fully open in 2 s as well as the RC to DVI line isolation valves.

LGMS injection is related both to gravity and to LGMS air space pressurization (through PSS to LGMS balance lines) by non-condensable gas entering the PSS from DW. LGMS injection mass flow is shown in Fig.7. 46.

Containment and RPV pressure equalization, PSS water flow to DW, RC flooding, reverse flow from containment to RPV

RPV and containment pressure equalize at 2310 s in SPES3-181 and at 2390 s in SPES3-175.

After the peak, the containment pressure decreases for steam condensation on containment wall and for LGMS injection. After the RPV and containment pressures are coupled, they decreases thanks to EHRS heat removal from the primary side, Fig.7. 21, Fig.7. 22. At 2490 s in SPES3-181 and 2600 s in SPES3-175, the DW pressure decreases below the PSS pressure, Fig.7. 12. When the differential pressure between PSS and DW is sufficient to overcome the hydrostatic head of PSS vent pipes, a reverse flow starts from PSS to DW through the vent line extension, lasting for about 2000 s in both cases, Fig.7. 11.

The RC level, initially increased for the break and ADS mass flow collection, rapidly increases in correspondence of PSS injection up to the complete fill-up (11 m level from bottom) at 4200 s in SPES3-181 and 4490 s in SPES3-175, Fig.7. 47. In SPES3-175 case, RC level decreases below the top, in correspondence of strong water injection toward the RPV through the RC to DVI line, Fig.7. 36. The RC level is definitively restored around 13000 s.

Low LGMS mass signal: ADS Stage-II actuation

The LGMS low mass signal occurs when, in both tanks, mass reaches 20% initial mass (198 kg, 20% of 1 m^3 water at 48.9 °C), Fig.7. 48, Fig.7. 49. Empting in SPES3-181 is slightly delayed compared to SPES3-175. The reason is the greater injection from LGMS to DVI, in SPES3-175, between 4500 s and 10000 s, due to the higher differential pressure between containment and RPV, Fig.7. 46, Fig.7. 9.

The low LGMS mass signals actuates the ADS Stage-II valves, fully open in 10 s, to equalize primary and containment pressure and to allow steam circulation between RPV and DW in the upper part of the plant. The signal occurs at 24301 s in SPES3-181 and at 23321 s in SPES3-175. The ADS Stage-II mass flow s shown in Fig.7. 50.

The RWSTs begin to heat-up as soon as the EHRSs are actuated, Fig.7. 51, Fig.7. 52. Temperature increase is slower in SPES3-181 than SPES3-175, both in RWST-AB and RWST-C. In SPES3-181, saturation is reached with about 2000 s delay than in SPES3-175, Fig.7. 51.

7.1.2 Case conclusions

The comparison of the SPES3-181 and SPES3-175 case results, for the DBE DVI line DEG break, allowed to verify that the modification of the EHRS design does not affect the results in a meaningful way. Little differences were observed in the EHRS exchanged power, mainly regarding the EHRS-C. In fact, it results the most affected by the tube size modification with the need of reducing the Teflon layer thickness on the headers to compensate for the additional thermal resistance introduced by the tube metal thickness increase. EHRS-A and B behaves as in the case with the thinner tubes. Differences are considered negligible if compared to approximations introduce by the system modelling.

The new final design of SPES3 EHRS is adequate for the simulation of the IRIS EHRS.

Tab.7. 1 – SPES3-181 and SPES3-175 list of the main events

	DVI-B line DEG break 2 inch equivalent	SPES3-181		SPES3-175		
N.	**Phases and events**	**Time (s)**	**Quantity**	**Time (s)**	**Quantity**	**Notes**
Break						
1	Break initiation	0		0		break valves stroke 2 s
2	Break flow peak (Containment side)	1	0.688 kg/s	1	0.688 kg/s	Break flow = 0 kg/s at 11 s
3	Break flow peak (RV side)	2	1.33 kg/s	2	1.33 kg/s	
Blowdown, RV depressurization, containment pressurization. Steam dumping into PSS						
4	Steam-air mixture begins to flow from DW to PSS	16		16		
S-Signal: Reactor scram, secondary loop isolation, EHRS-A and B actuation						
5	**High Containment pressure signal**	31.54	1.7e5 Pa	31.58	1.7e5 Pa	**S-signal. Set-point for safety analyses**
6	SCRAM begins	31.54		31.58		
7	MFIV-A,B,C closure start	31.54		31.58		MFIV-A,B,C stroke 5 s
8	MSIV-A-B-C closure start	31.54		31.58		MSIV-A,B,C stroke 5 s.
9	EHRS-A and B opening start (EHRS 1 and 3 in IRIS)	31.54		31.58		EHRS-A,B IV stroke 2 s.
10	EHRS-A and B peak mass flow	37	0.262 kg/s	37	0.264 kg/s	
11	**High SG pressure signal**	48.54	9e6 Pa	48.58	9e6 Pa	
12	SG-A high pressure reached	48.54		48.58		
13	SG-B high pressure reached	49.93		49.96		
14	SG-C high pressure reached	50.35		50.38		
15	RWST-A/B begins to heat-up	64		59		
16	EHRS-A power peak	226	359 kW	220	380 kW	
17	EHRS-B power peak	226	359 kW	225	375 kW	
Pump coastdown and primary circulation through RI-DC check valves						
18	**Low PRZ water level signal**	121.75	1.189 m	121.72	1.189 m	
19	RCP coastdown starts	136.75		136.72		Low PRZ level signal + 15 s delay
20	Secondary loop pressure peak	89 89 91	104e5 Pa A 107e5 Pa B 114e5 Pa C	90 91 94	104e5 Pa 108e5 Pa 113e5 Pa	
21	Natural circulation begins through shroud valves	154, 161		154, 161		SG-A,B SG-C
22	Flashing begins at core outlet	238	voidf 110 (core)	237	voidf 110 (core)	<1
LM-Signal: EHRS-C, ADS Stage-I and EBT actuation. RV saturation						
23	**Low PRZ pressure signal**	196.94	11.72e6 Pa	196.42	11.72e6 Pa	**LM-Signal** (High P cont + Low P PRZ)
24	EHRS-C opening start (EHRS 2 and 4 in IRIS)	196.94		196.42		EHRS-C IV stroke 2 s.
25	EHRS-C peak mass flow	201	0.545 kg/s	200	0.547 kg/s	
26	RWST-C begins to heat-up	223		217		
27	EHRS-C power peak	349	669 kW	334	719 kW	
28	ADS Stage I start opening (3 trains)	196.94		196.42		ADS valve stroke 10 s
29	ADS Stage I first peak flow (3 trains)	207	1.301 kg/s	207	1.301 kg/s	ST 0.454 kg/s; DT 0.854 kg/s SPES3-181 ST 0.454 kg/s; DT 0.854 kg/s SPES3-175
30	ADS Stage I second peak flow (3 trains)	291	1.481 kg/s	291	1.481 kg/s	ST 0.471 kg/s; DT 1.010 kg/s SPES3-181 ST 0.471 kg/s; DT 1.010 kg/s SPES3-175 Due to liquid fraction.
31	EBT-A and B valve opening start	196.94		196.42		EBT valve stroke 15 s
32	Break flow peak (Containment side)	213	0.696 kg/s	214	0.695 kg/s	Due to EBT intervention
33	EBT-RV connections uncovered	244, 275		242, 274		EBT-B, EBT-A
32	Natural circulation interrupted at SGs top	249		247		Pump inlet uncovered (voidf 176-01 ~0)
36	Core in saturation conditions	242		339		
37	EBT-B empty (broken loop)	650		670		500 s (S3-181), 530 s (S3-175) almost empty; 650 s (S3-181), 670 s (S3-175) completely empty
Low DP RV-Containment signal, LGMS and RC to DVI valve actuation						
38	Containment pressure peak	2180	9.12e5 Pa	2260	9.14e5 Pa	
39	**Low DP RV-Containment**	2207.66	50e3 Pa	2257.04	50e3 Pa	
40	LGMSA/B valve opening start	2207.66		2257.04		LM + low DP RV-cont. LGMS valve stroke 2 s.
41	RC to DVI line valve opening	2207.66		2257.04		RC to DVI valve stroke 2 s.
42	LGMS-B starts to inject into RC through DVI broken loop	2240		2257.04		
43	LGMS-A starts to inject into RV through DVI intact loop	2280		2330		
Containment and RV pressure equalization, PSS water flow to DW, RC flooding, reverse flow from containment to RV						
44	Containment and RV pressure equalization	2310		2390		
45	Mixture starts to flow from RC to DVI-A	2330		2380		
46	DW pressure lower than PSS pressure	2490		2610		
47	EBT-A empty (intact loop)	3110		3100		
48	Water starts to flow from PSS to DW	3440, 3330		3570, 3520		PSS A, PSS-B
49	Steam and gas mixture flows again from RV to QT	3610 to 4320		3750 to 4510		RPV P > DW P
50	RC level at DVI elevation	3960		4130		
51	RC full of water	4200		4490		
52	QT fill-up starts from DW connection	10120		4470		
Low LGMS mass signal: ADS Stage-II actuation						
53	Low LGMS mass	19816.05	20% mass (198 kg)	17480.73	(185 kg)	LGMS-A (intact loop)
54		24301.98	20% mass (198 kg)	23321.78	(185 kg)	LGMS-B (broken loop)
55	ADS stage-II start opening	24301.98		23321.78		ADS Stage-II valve stroke 10 s.
56	Flow from RC to RV (intact loop) stable	33790		37790		
57	LGMS-A empty (intact loop)	45248		52790		~30 kg residual mass SPES3-181 ~30 kg residual mass SPES3-175
58	LGMS-B empty (broken loop)	45248		55990		~30 kg residual mass SPES3-181 ~00 kg residual mass SPES3-175
Long Term conditions						
59	Core power	150000	45.83 kW	150000	46.04 kW	Average between 100000-150000 s
60	SG tot power	150000	42.45 kW	150000	42.07 kW	
61	RWST tot power	150000	39.32 kW	150000	39.30 kW	
62	RWST-A/B temperature	150000	100.6 °C	150000	100 °C	saturated
63	RWST-C temperature	150000	100.6 °C	150000	100 °C	saturated

Fig.7. 1 - SPES3-181 and SPES3-175 DVI break mass flow (window)

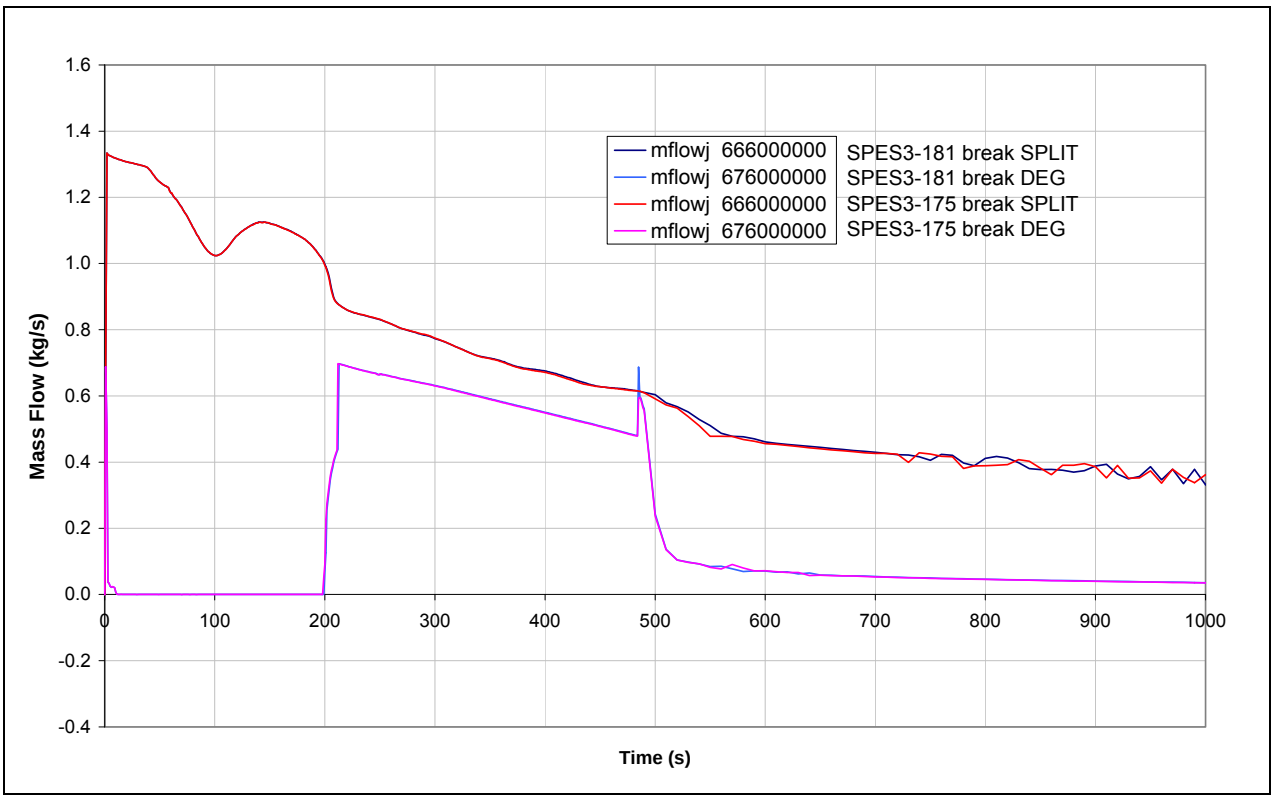

Fig.7. 2 - SPES3-181 and SPES3-175 DVI break mass flow (window)

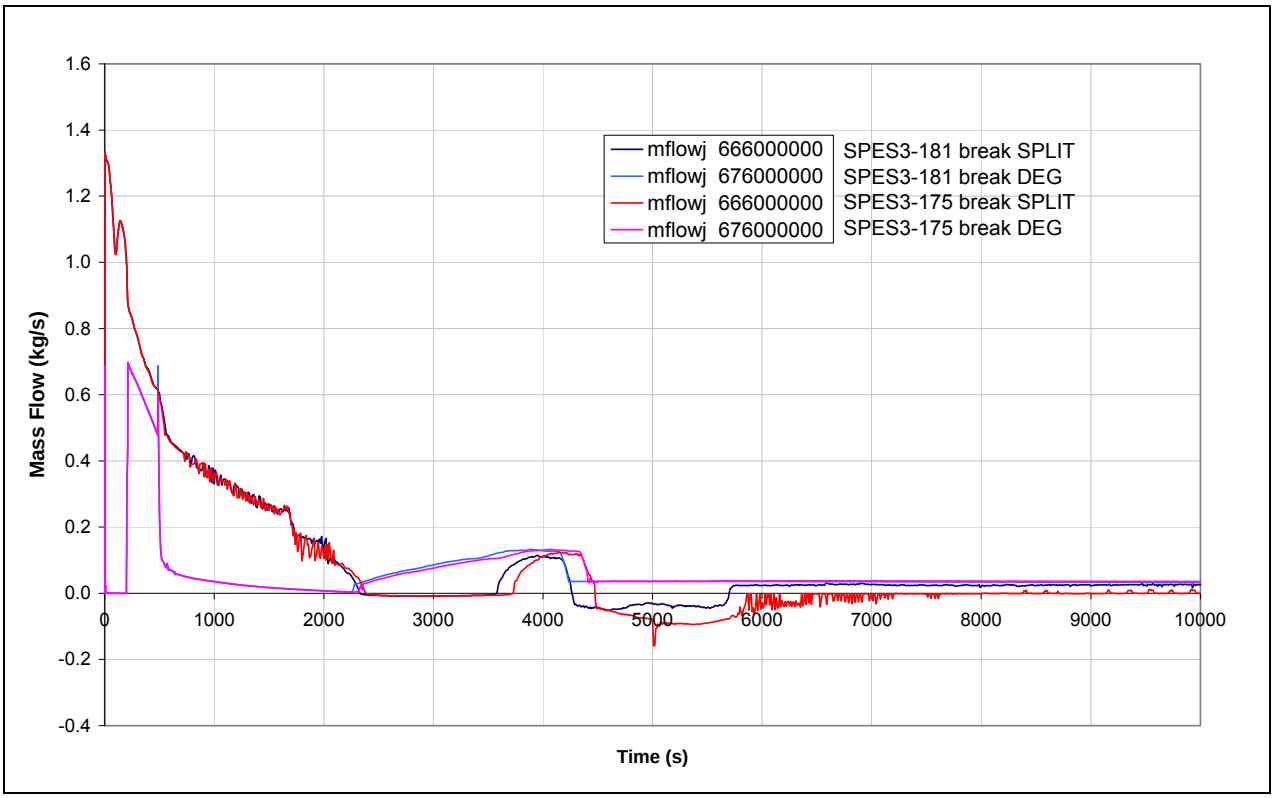

Fig.7. 3 - SPES3-181 and SPES3-175 DVI break mass flow

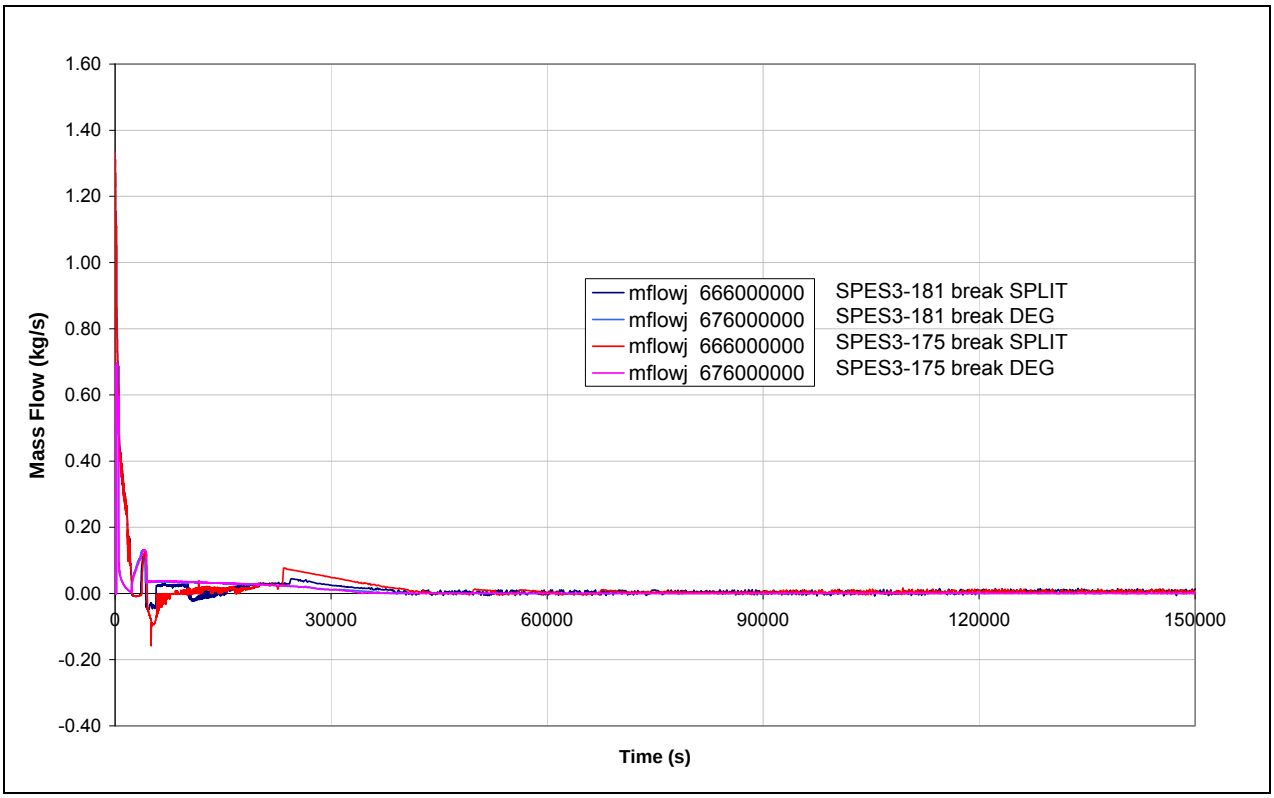

Fig.7. 4 - SPES3-172 and SPES3-175 PRZ pressure (window)

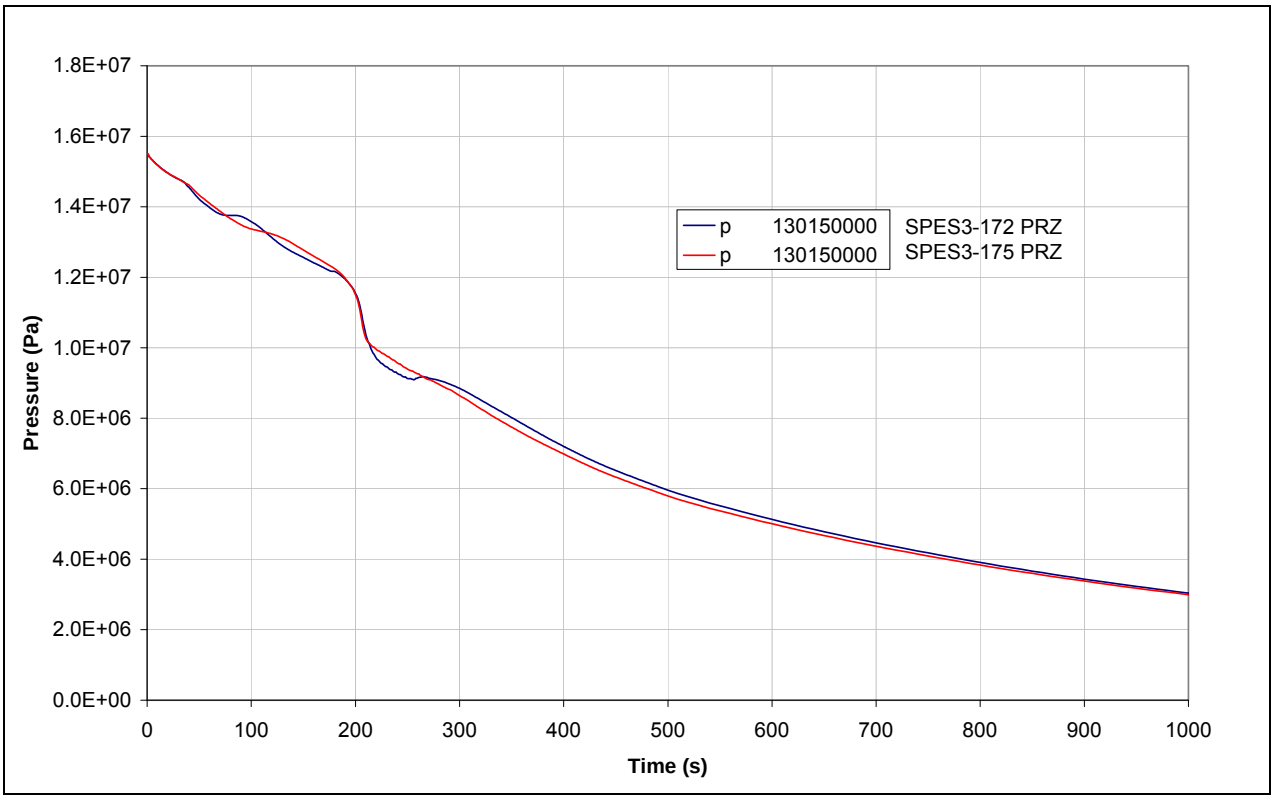

Fig.7. 5 - SPES3-181 and SPES3-175 PRZ pressure (window)

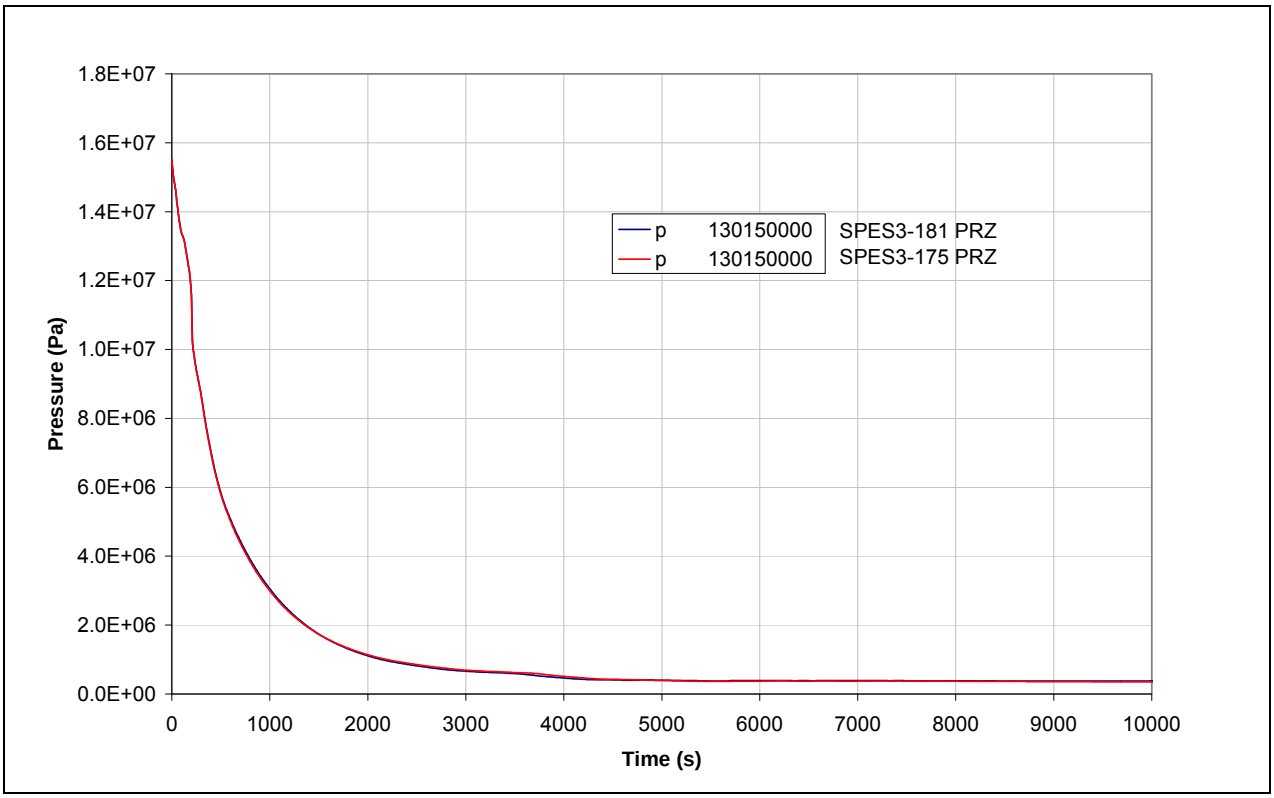

Fig.7. 6 - SPES3-181 and SPES3-175 PRZ pressure

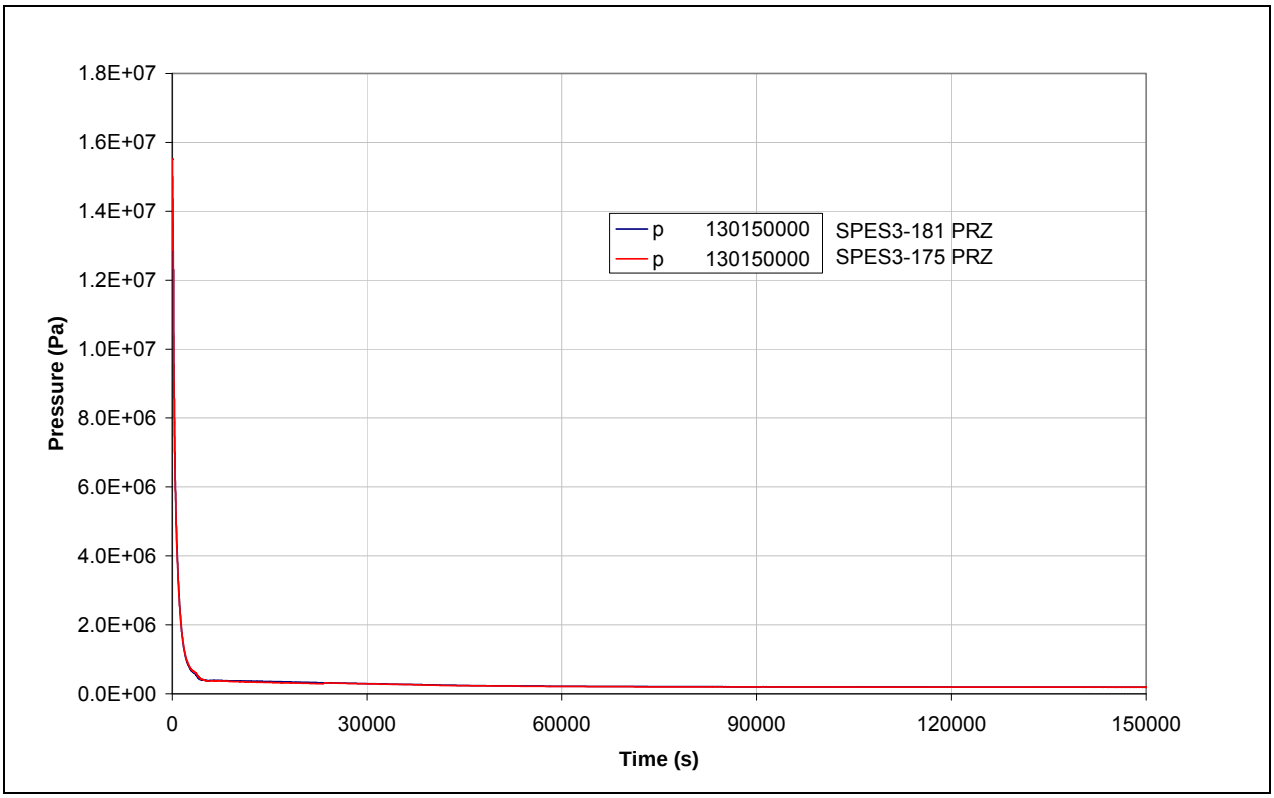

Fig.7. 7 - SPES3-181 and SPES3-175 DW pressure (window)

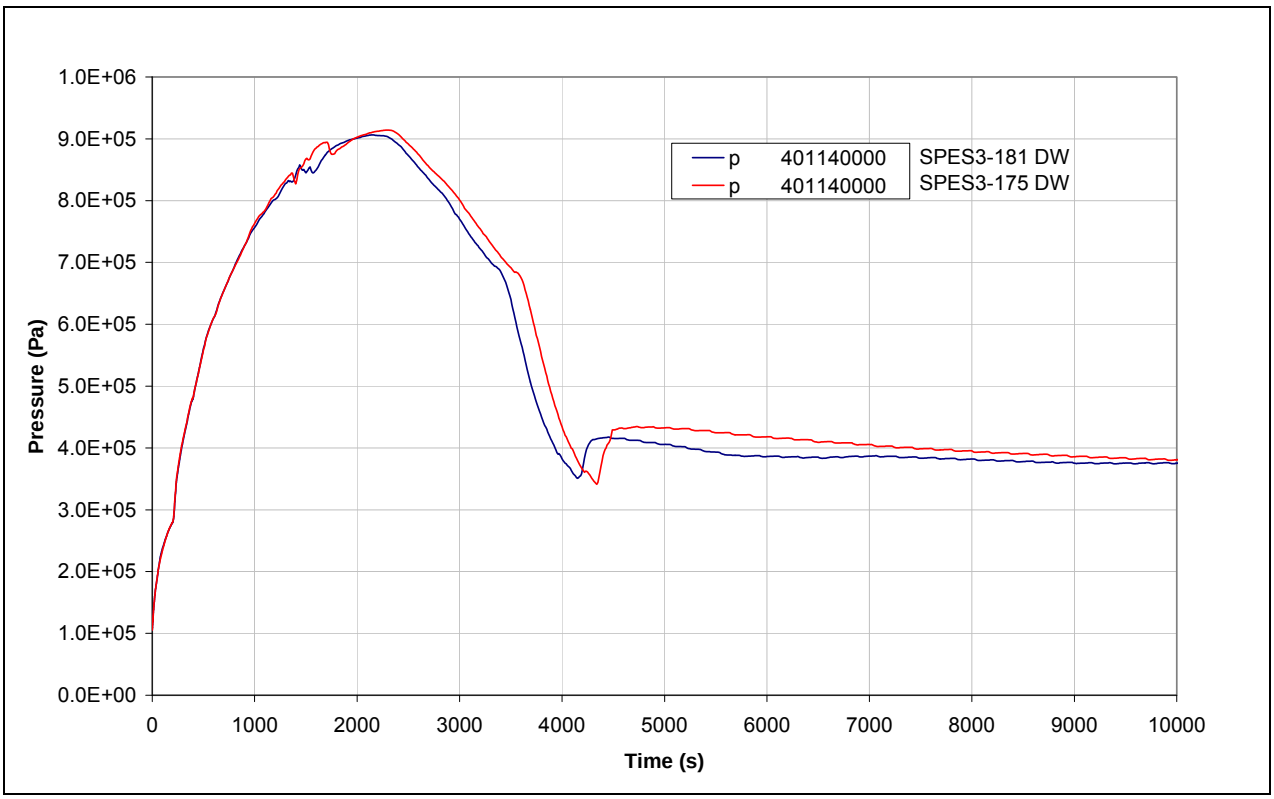

Fig.7. 8 - SPES3-181 and SPES3-175 DW pressure

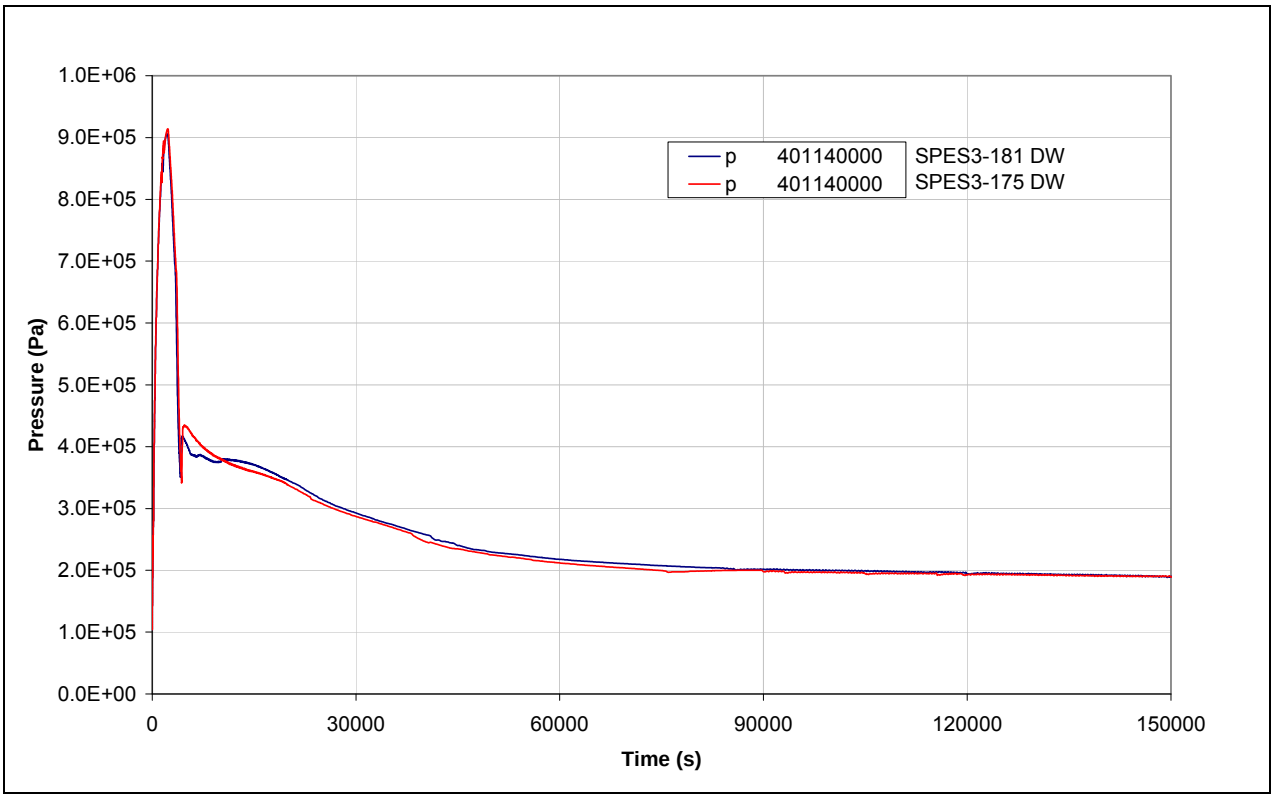

Fig.7. 9 - SPES3-181 and SPES3-175 PRZ and DW pressures (window)

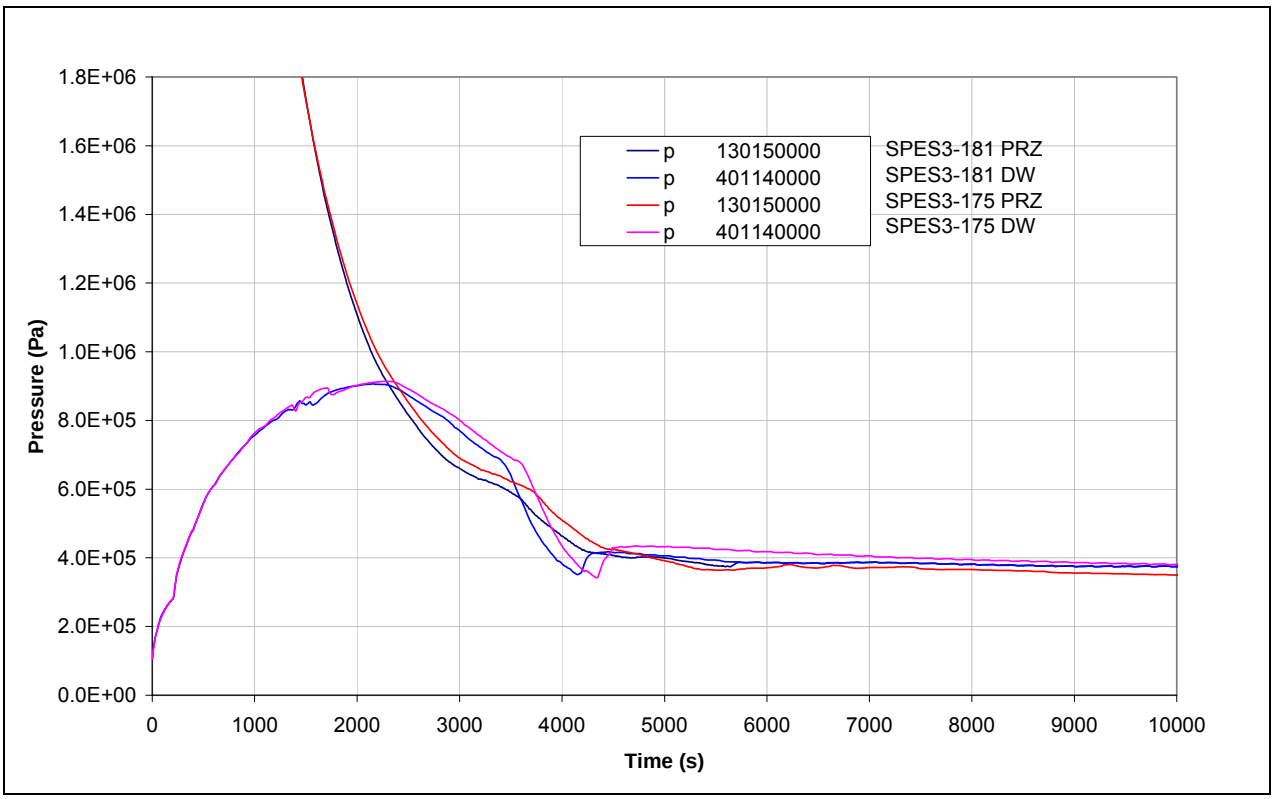

Fig.7. 10 - SPES3-181 and SPES3-175 PRZ and DW pressures

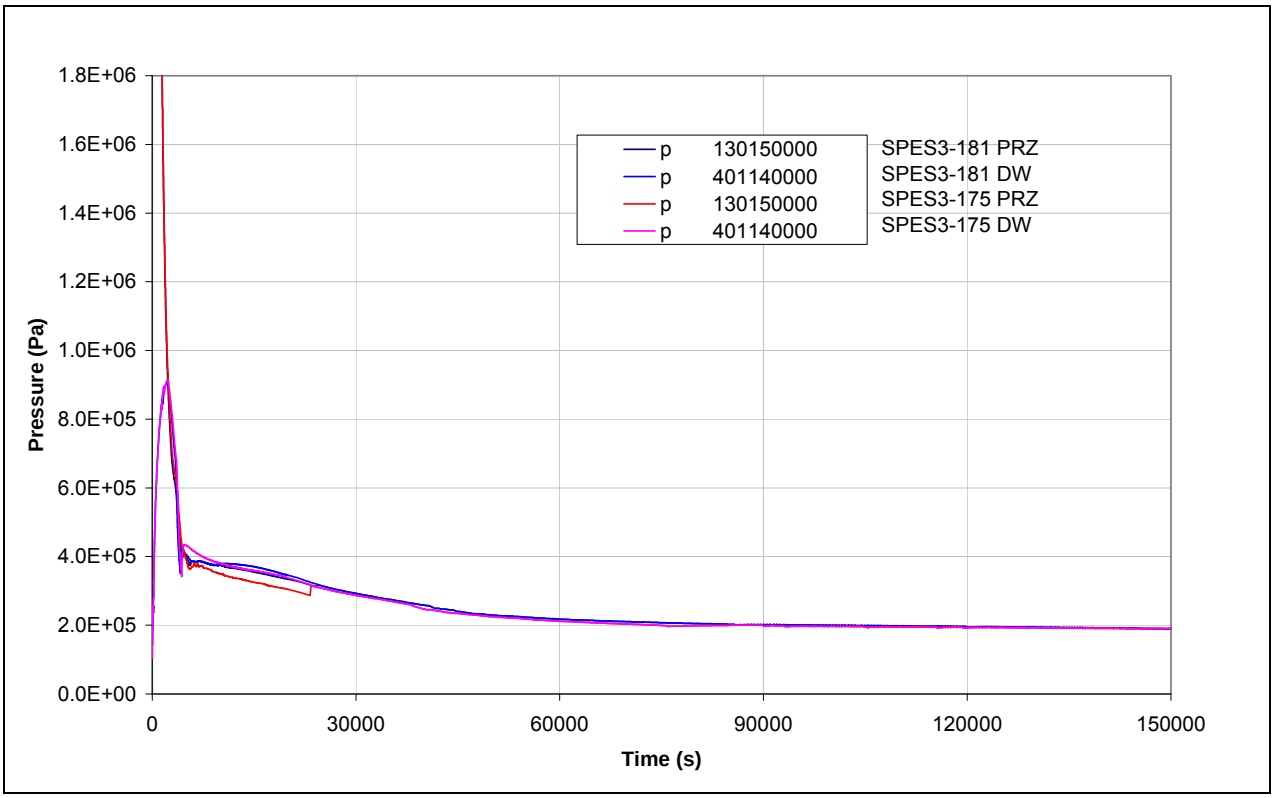

Fig.7. 11 - SPES3-181 and SPES3-175 DW to PSS mass flow (window)

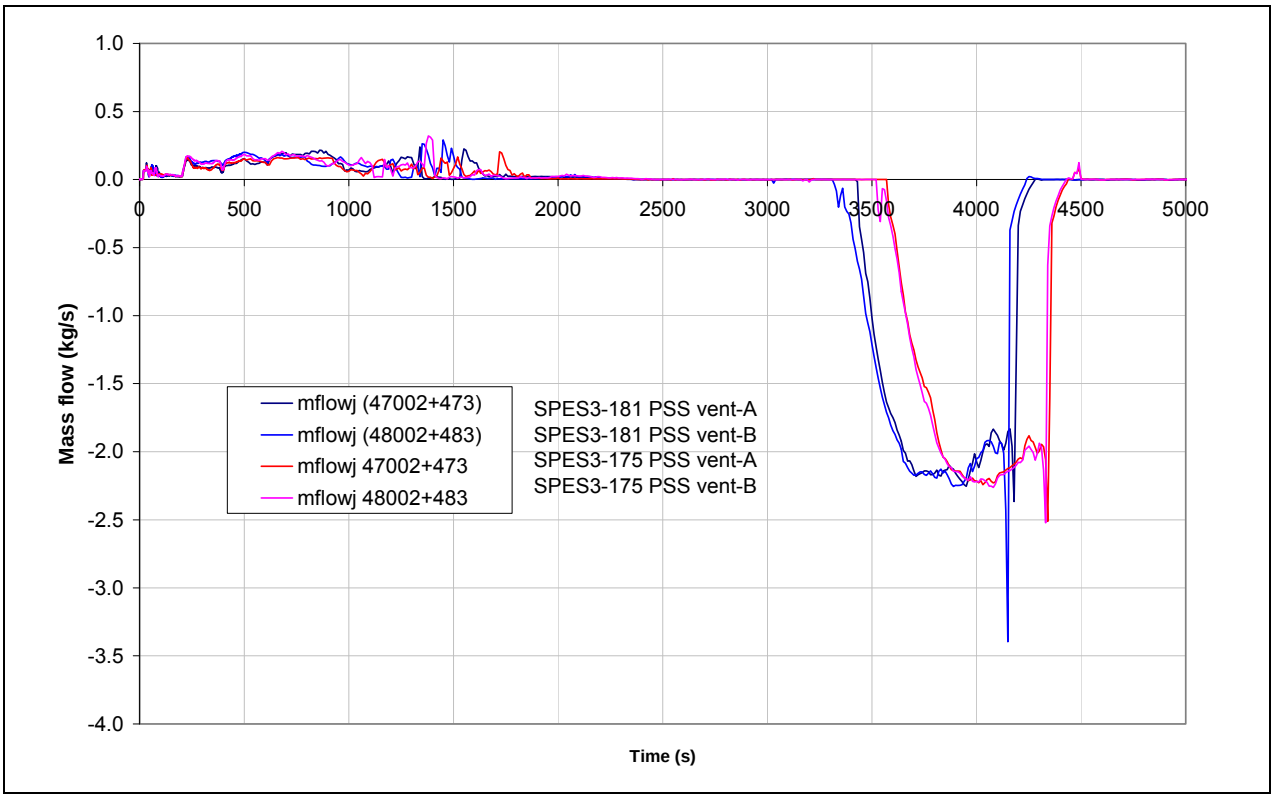

Fig.7. 12 - SPES3-181 and SPES3-175 DW and PSS pressure (window)

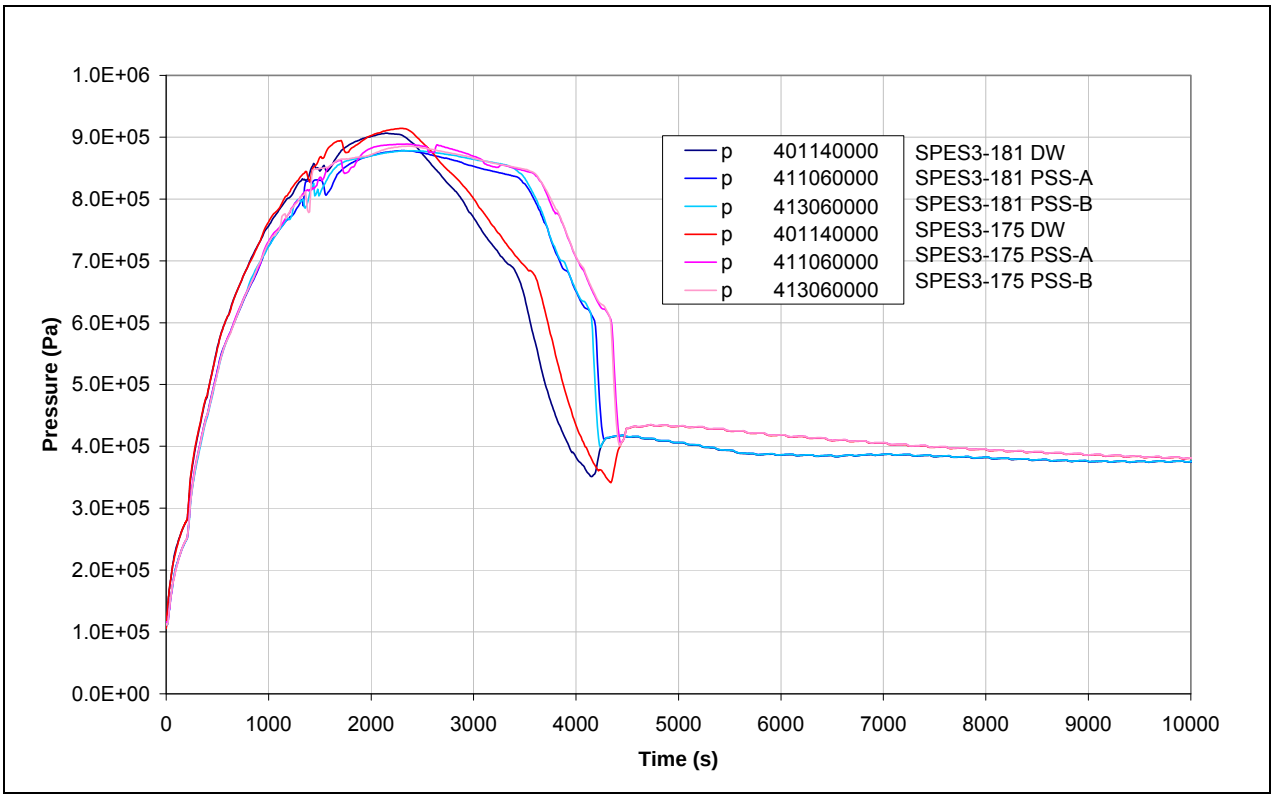

Fig.7. 13 - SPES3-181 and SPES3-175 DW and PSS pressure

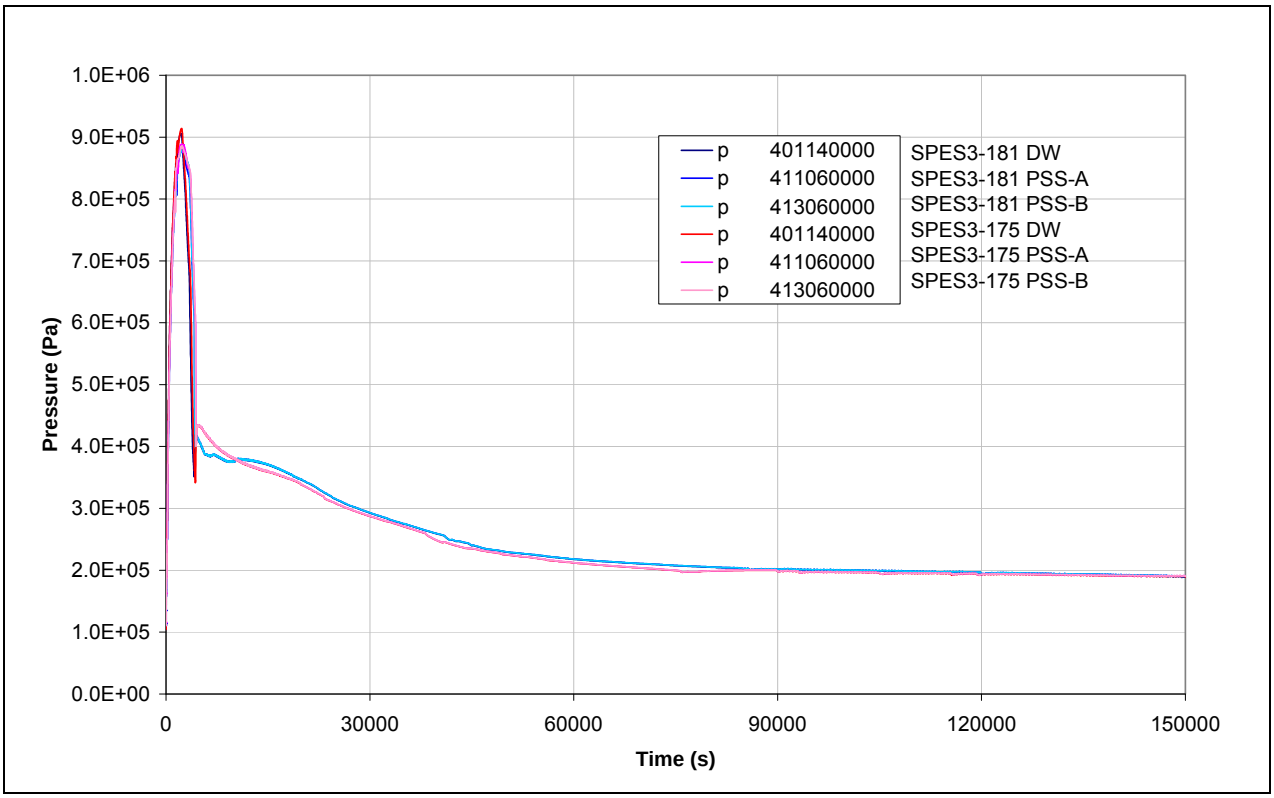

Fig.7. 14 - SPES3-181 and SPES3-175 LGMS pressure

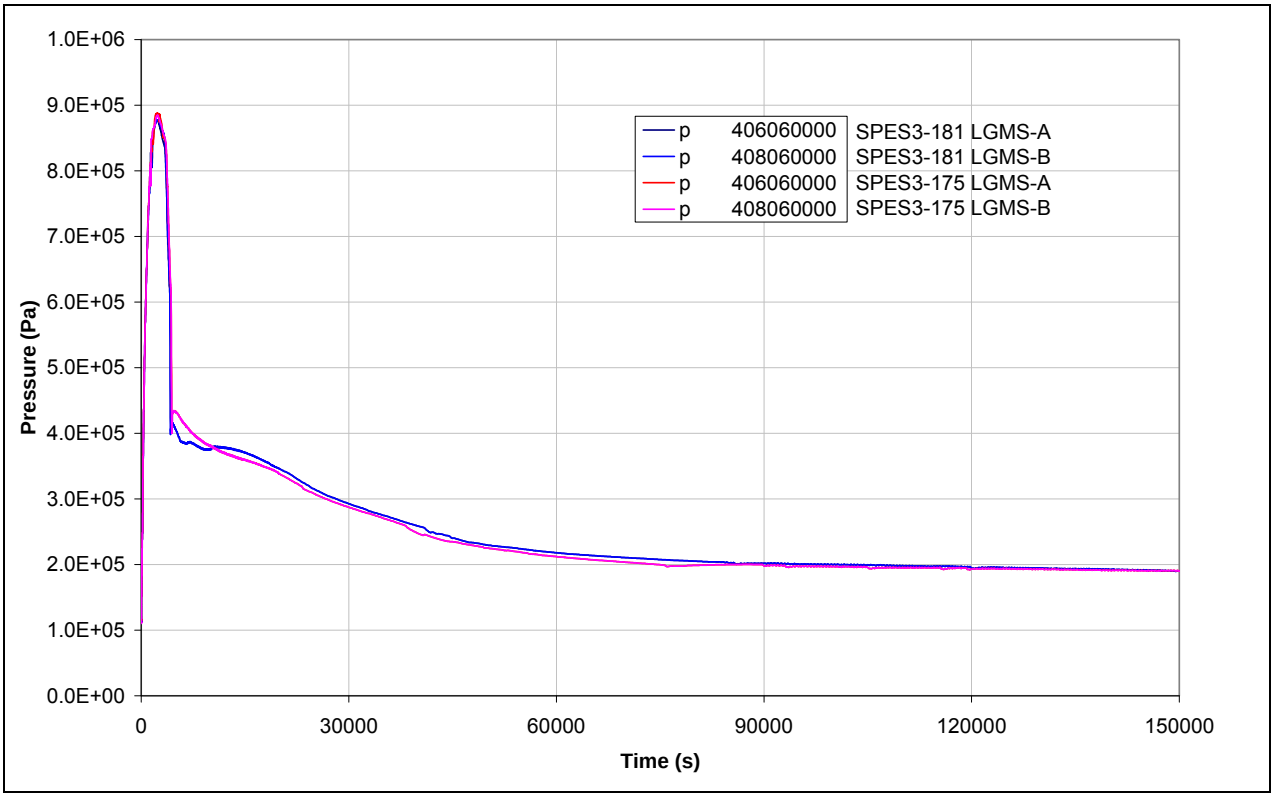

Fig.7. 15 - SPES3-181 and SPES3-175 Core and SG power (window)

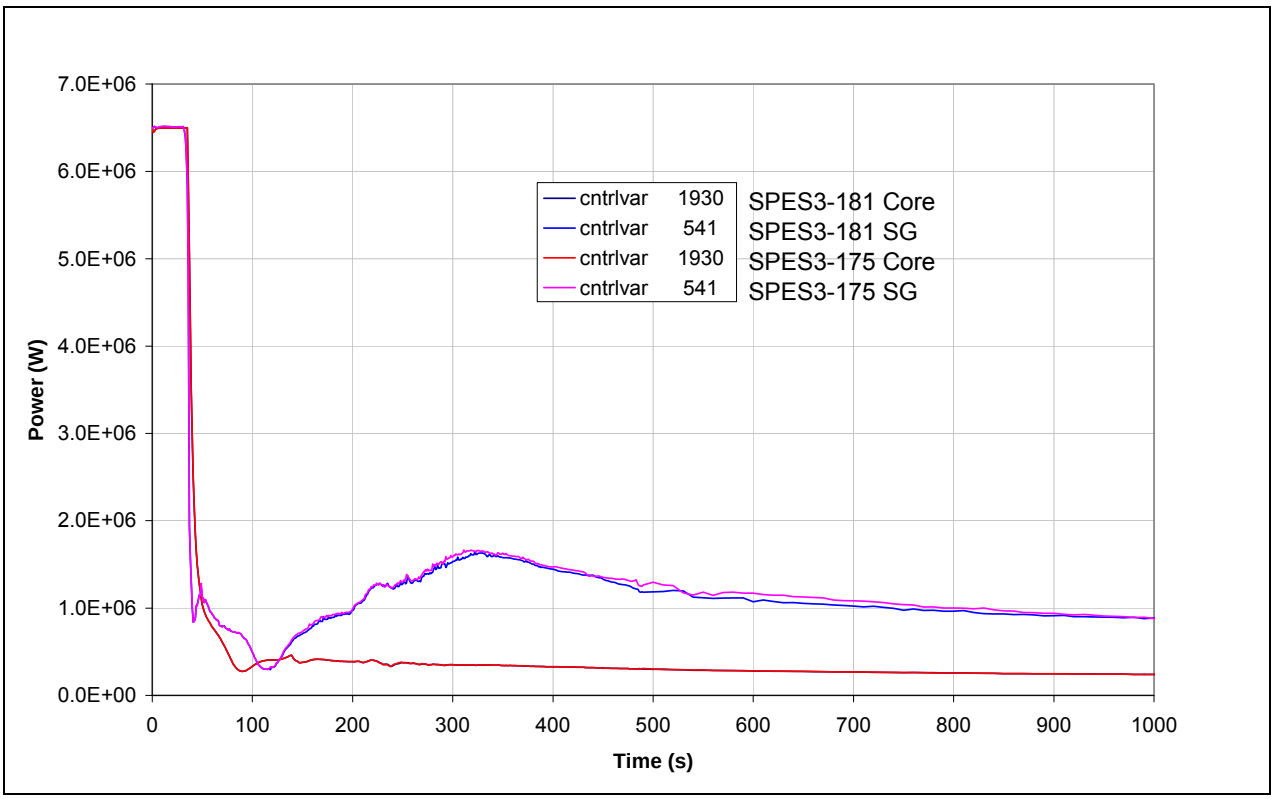

Fig.7. 16 - SPES3-172 and SPES3-175 Core and SG power

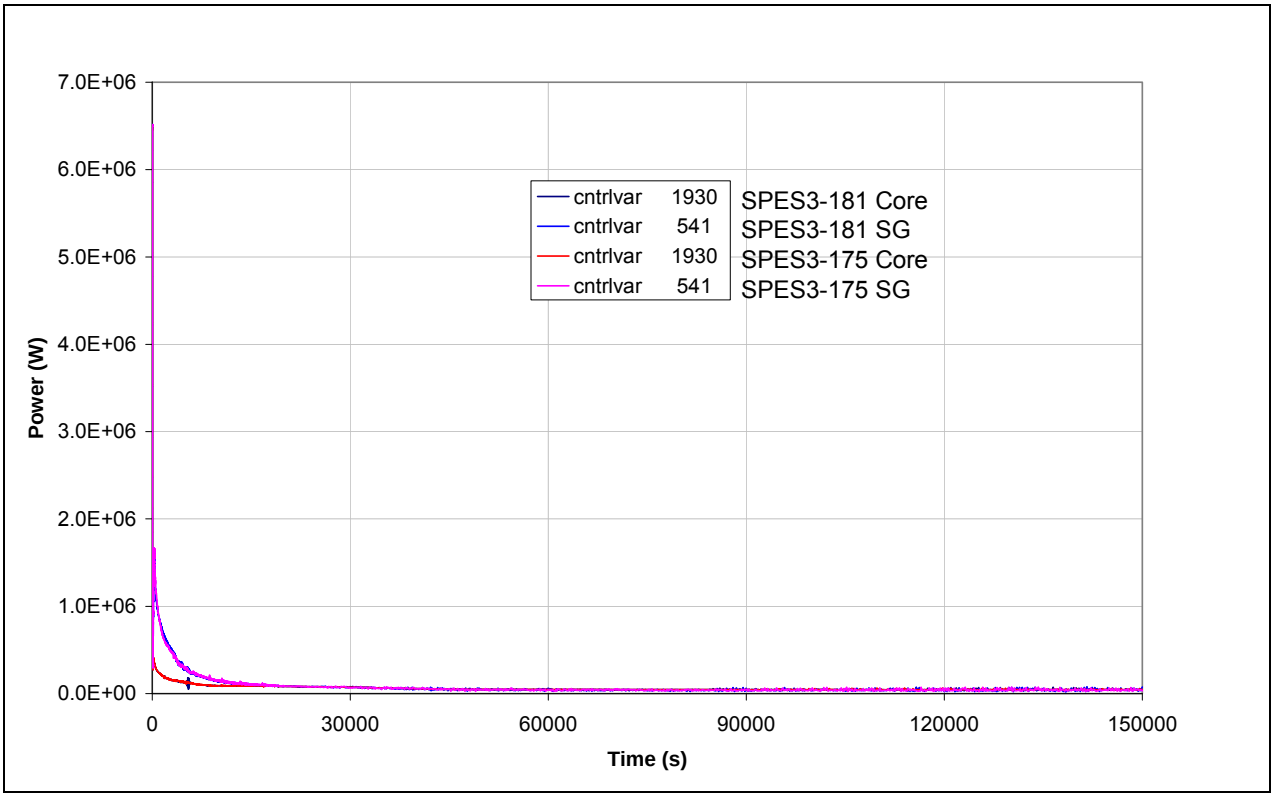

Fig.7. 17 - SPES3-181 and SPES3-175 SG ss mass flow (window)

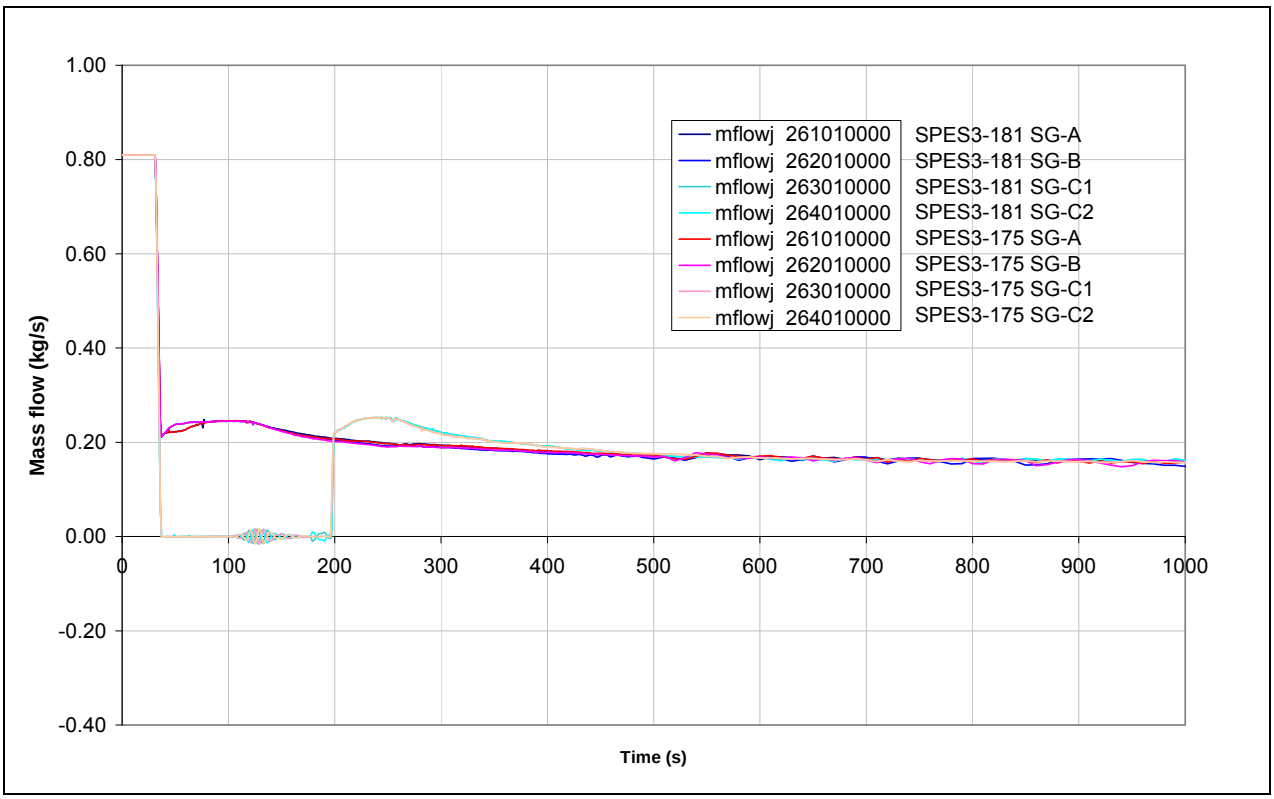

Fig.7. 18 - SPES3-181 and SPES3-175 SG ss mass flow

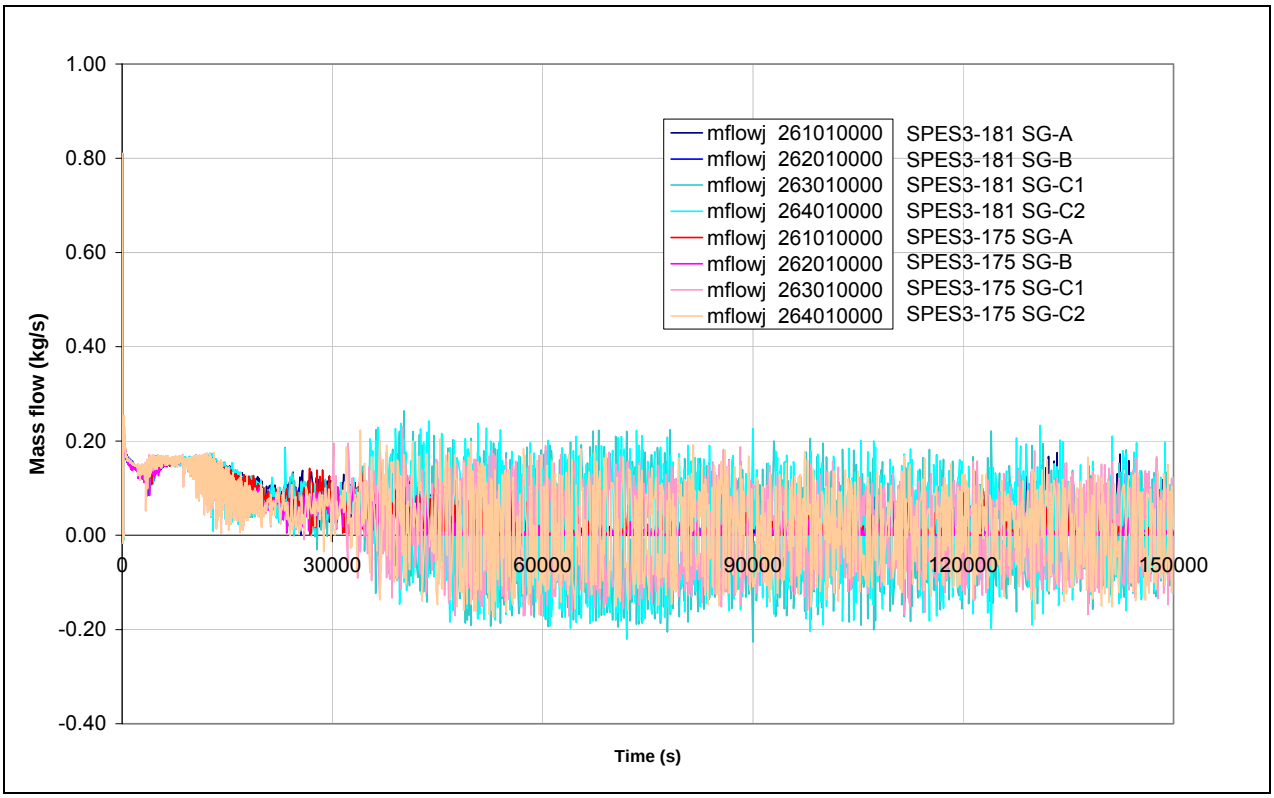

Fig.7. 19 - SPES3-181 and SPES3-175 EHRS cold leg mass flow (window)

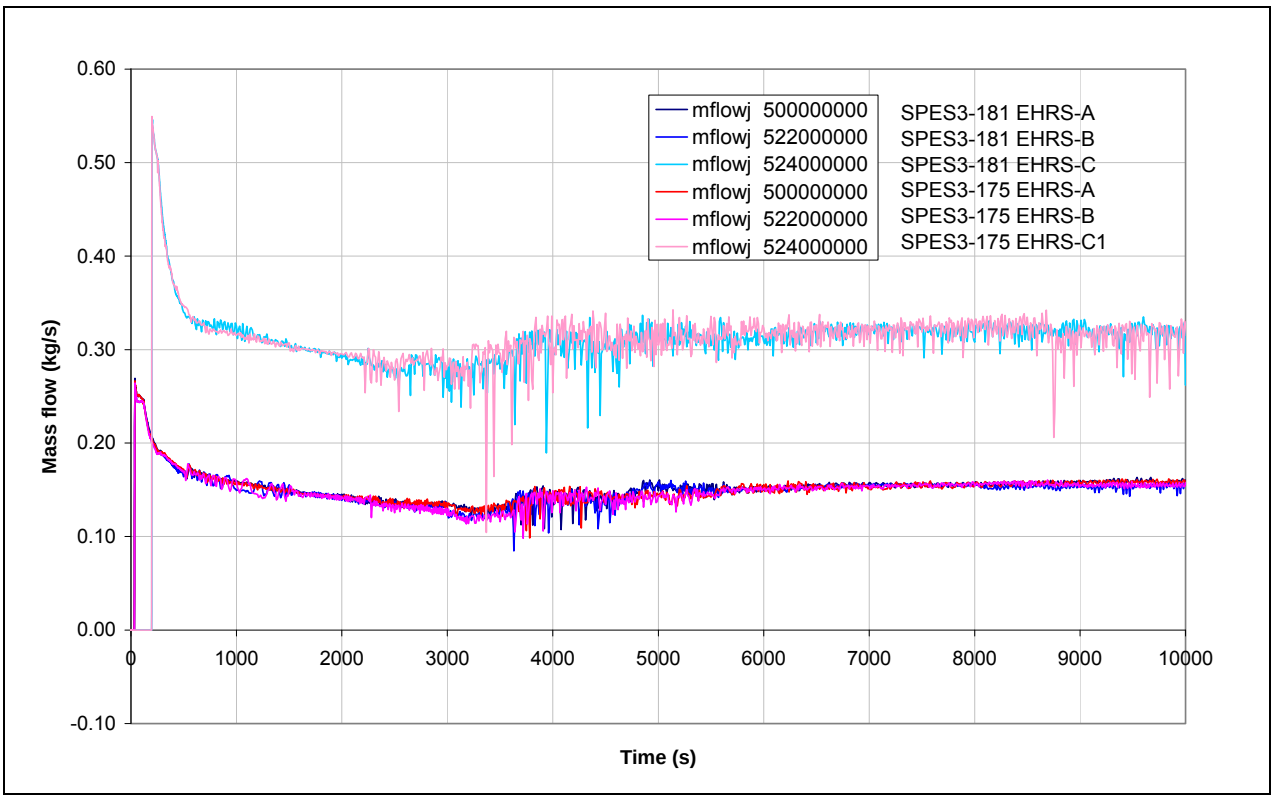

Fig.7. 20 - SPES3-181 and SPES3-175 EHRS cold leg mass flow

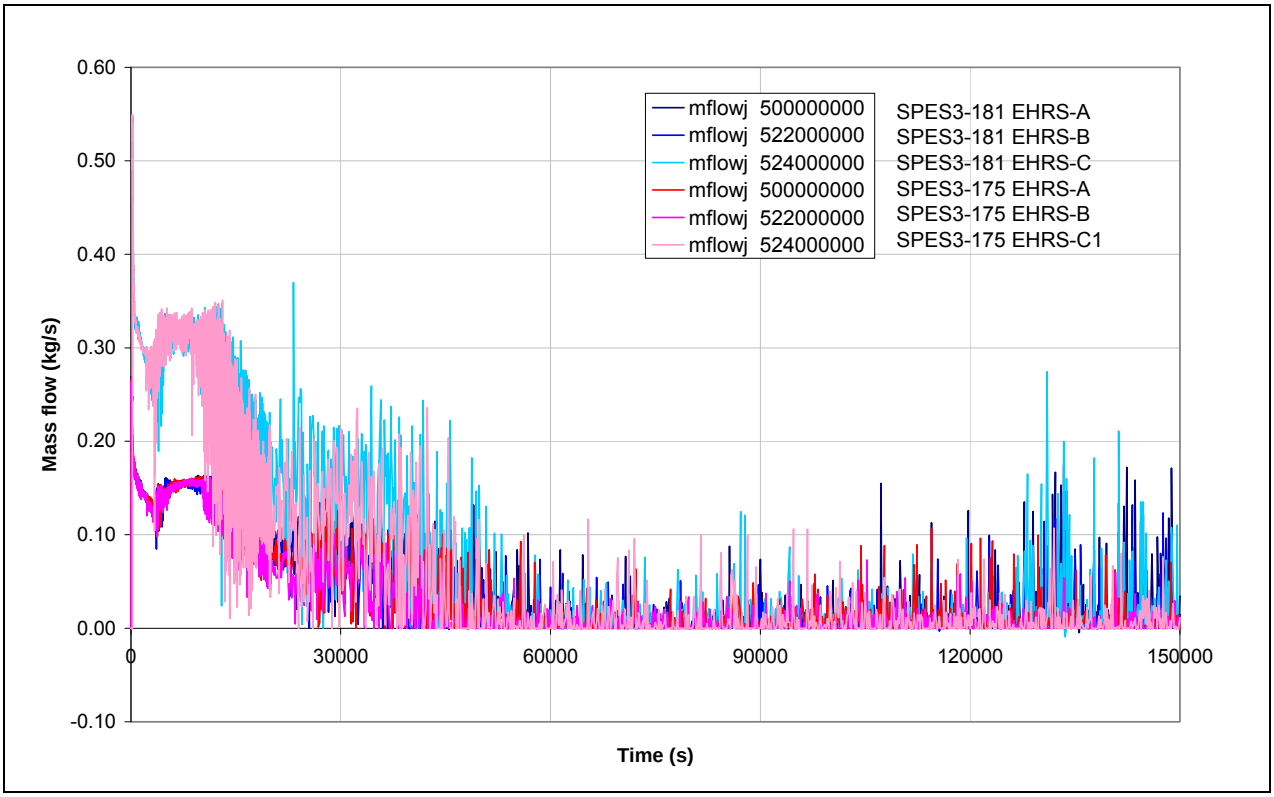

Fig.7. 21 - SPES3-181 and SPES3-175 EHRS power (window)

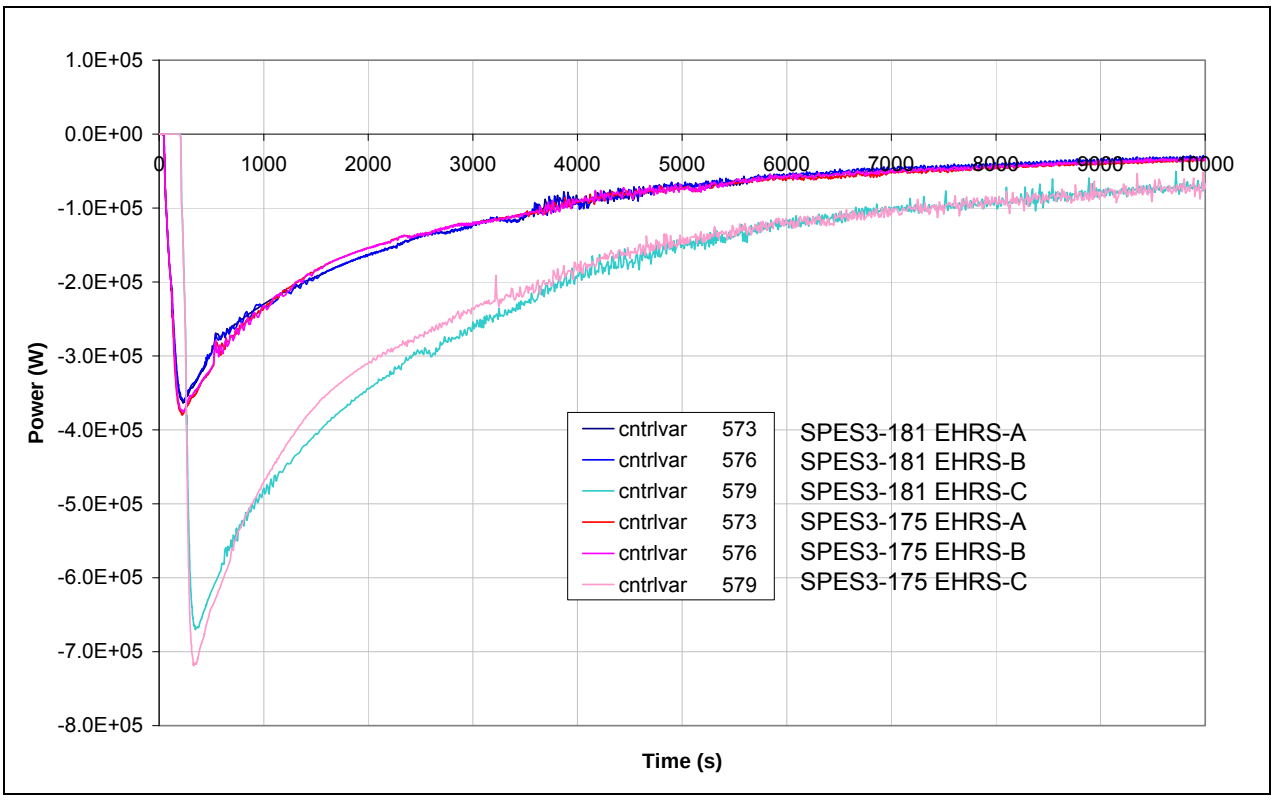

Fig.7. 22 - SPES3-181 and SPES3-175 EHRS power

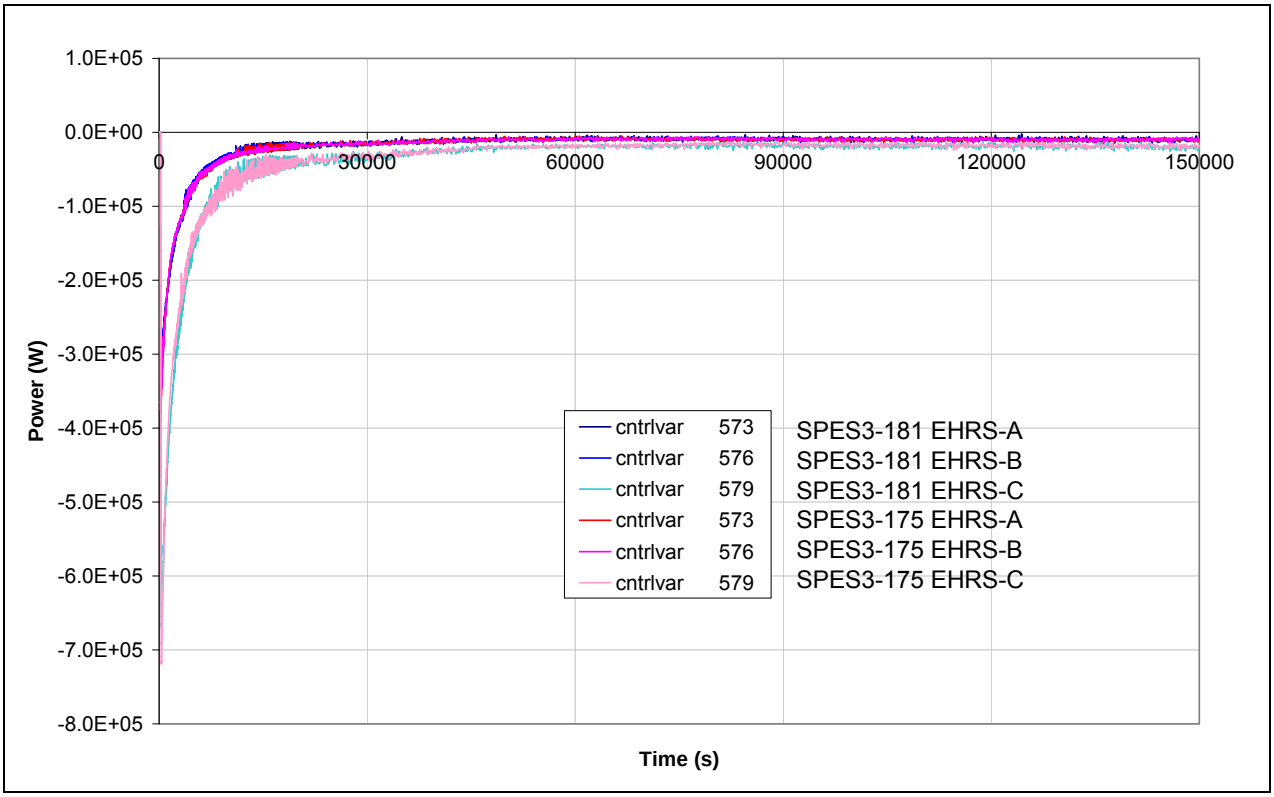

Fig.7. 23 - SPES3-181 and SPES3-175 SG ss outlet pressure (window)

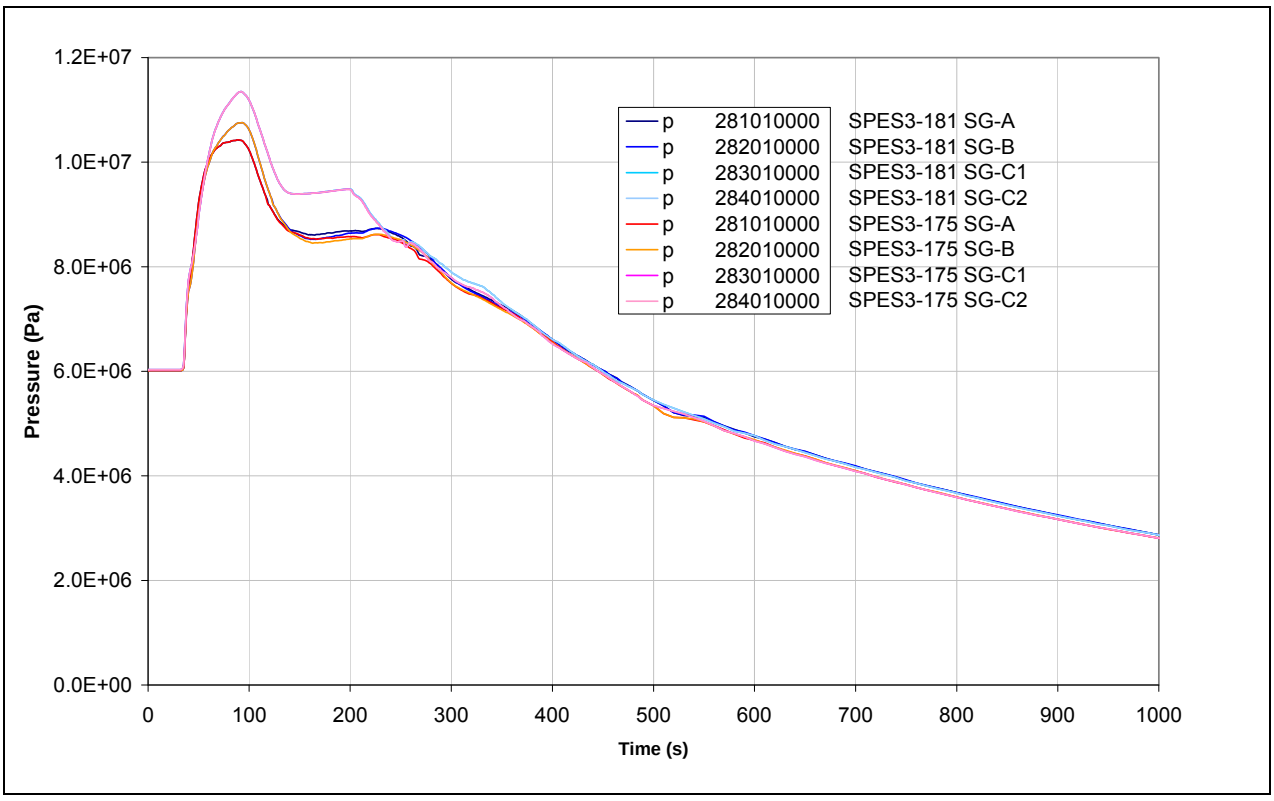

Fig.7. 24 - SPES3-181 and SPES3-175 SG ss outlet pressure

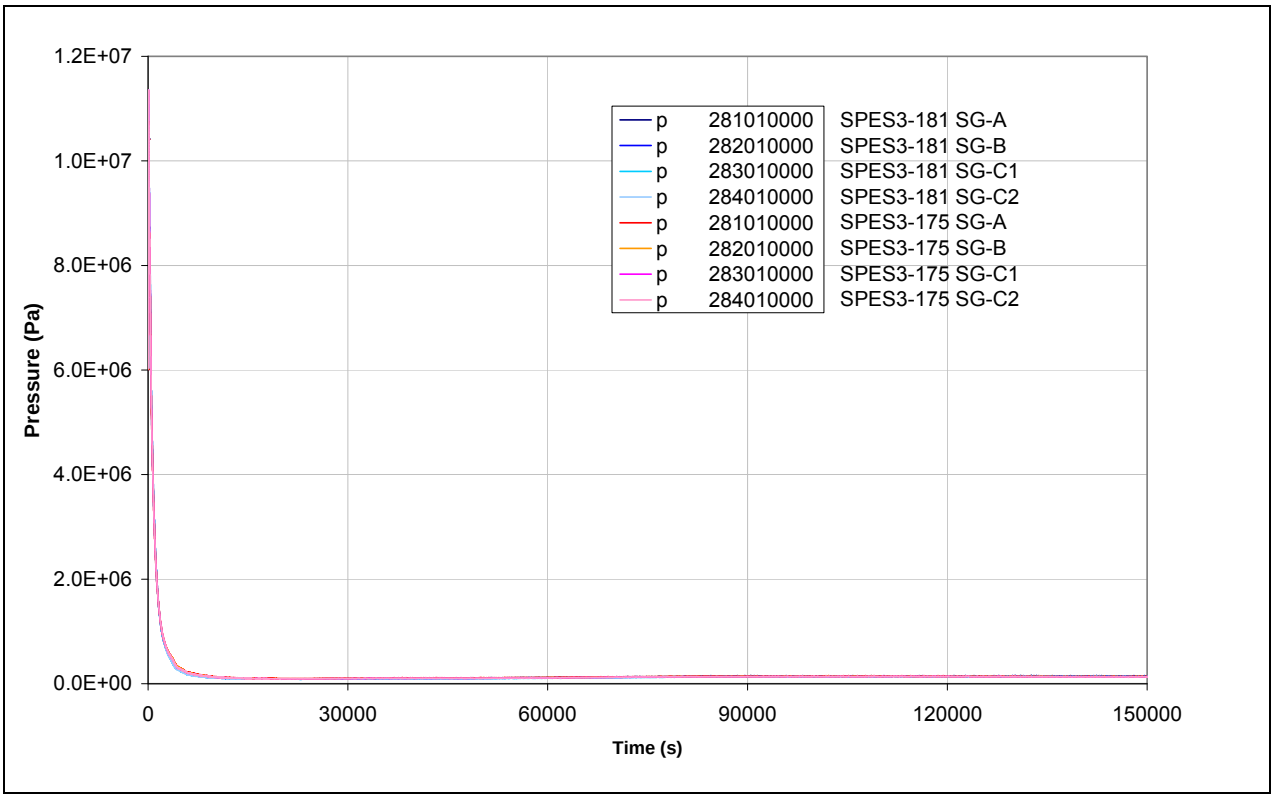

Fig.7. 25 - SPES3-181 and SPES3-175 SG-Ass collapsed level (window)

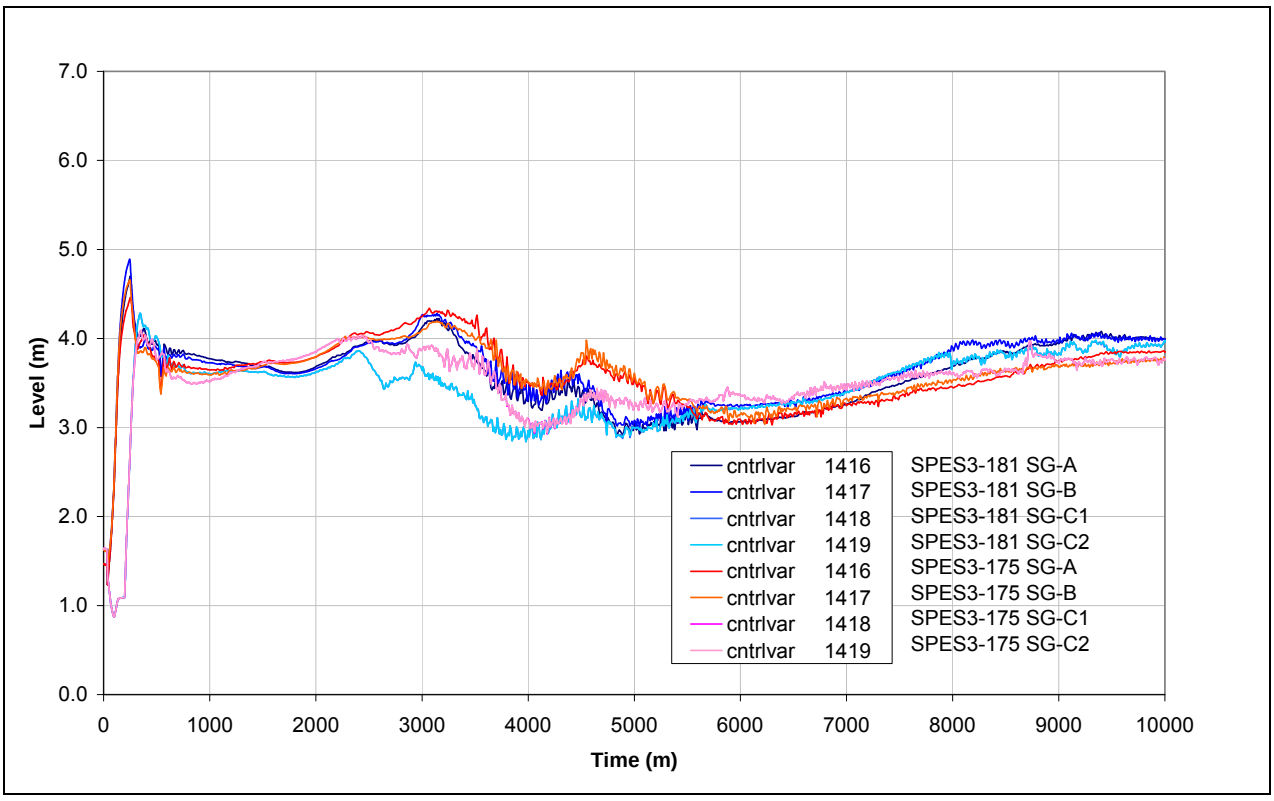

Fig.7. 26 - SPES3-181 and SPES3-175 SG-Ass collapsed level

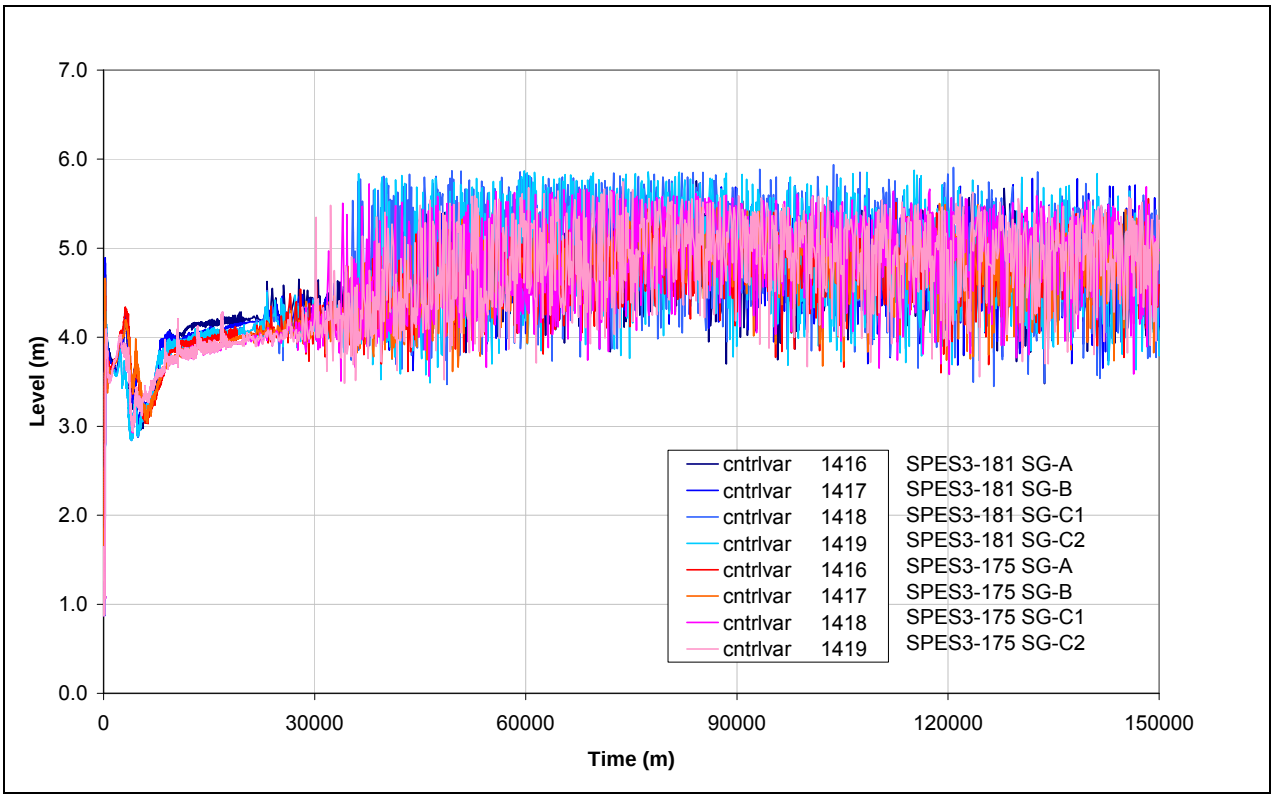

Fig.7. 27 - SPES3-181 and SPES3-175 PRZ level (window)

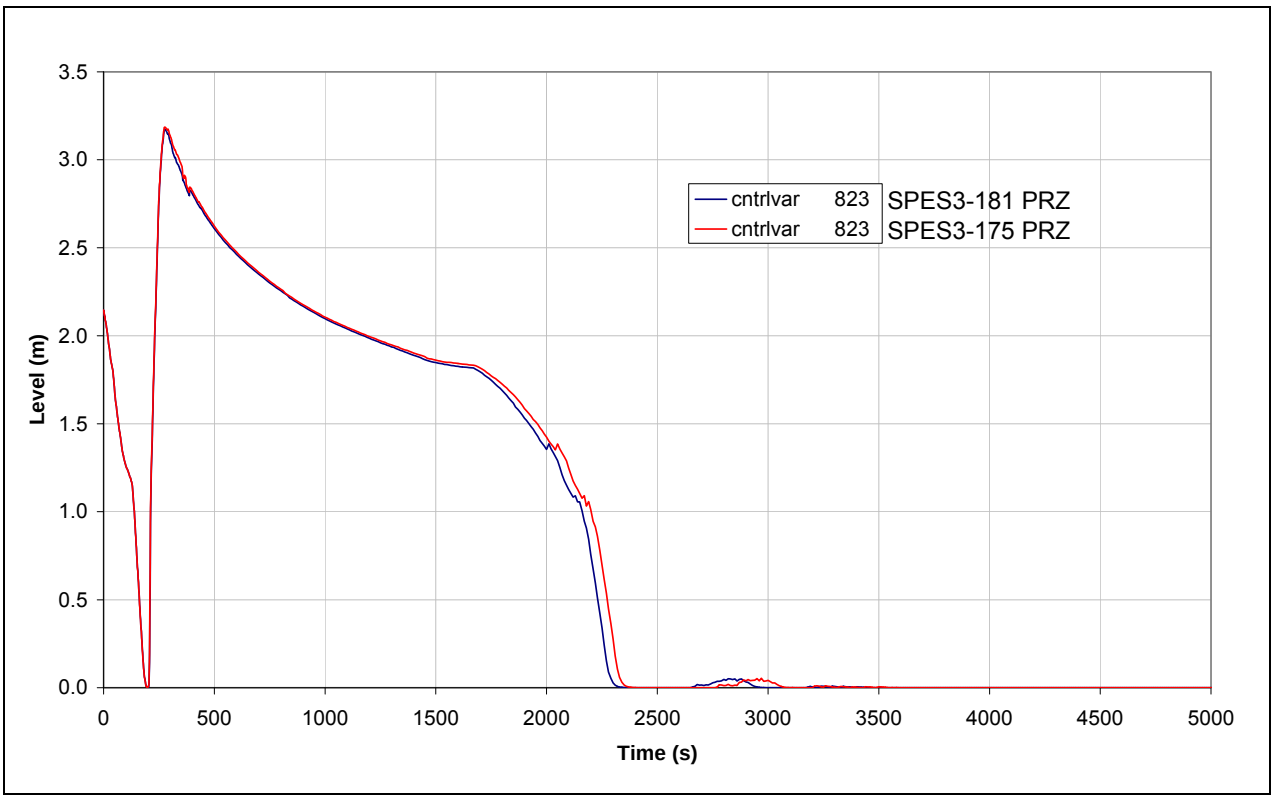

Fig.7. 28 - SPES3-181 and SPES3-175 Core inlet mass flow (window)

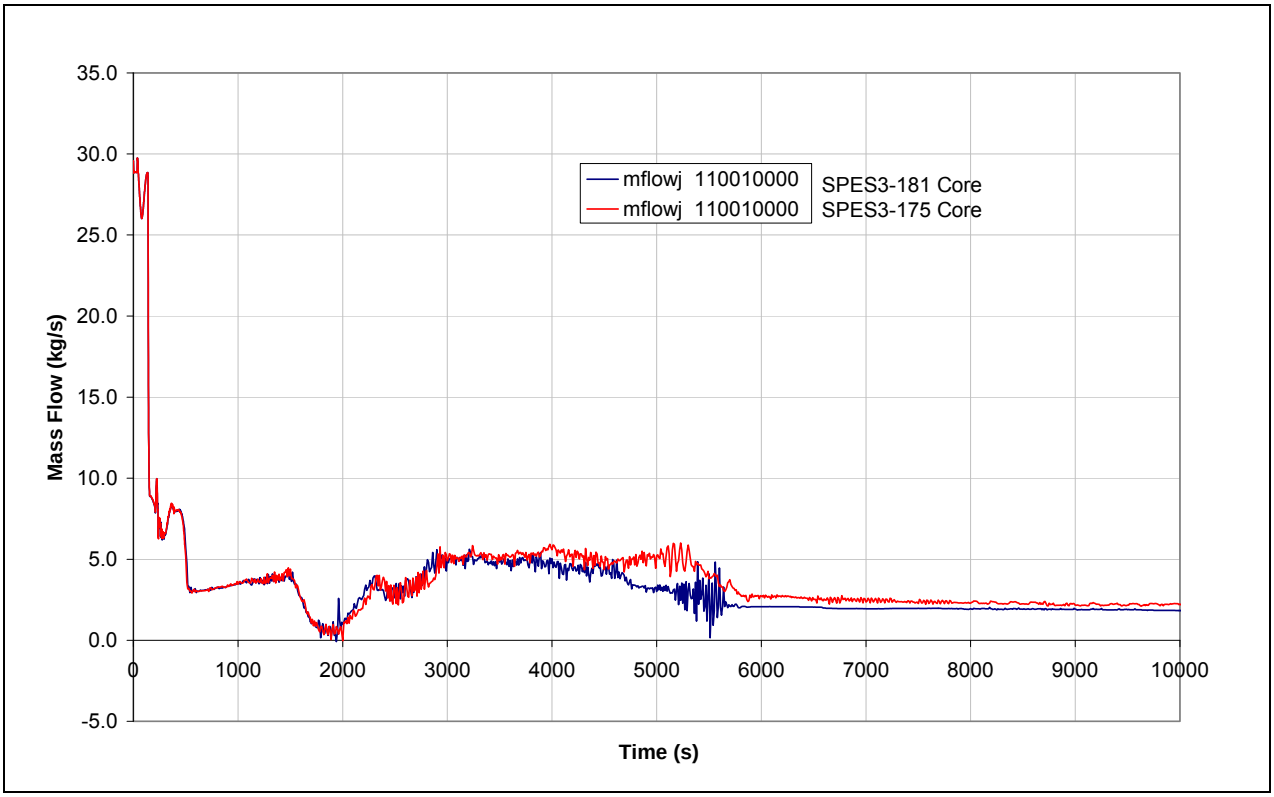

Fig.7. 29 - SPES3-181 and SPES3-175 Core inlet mass flow

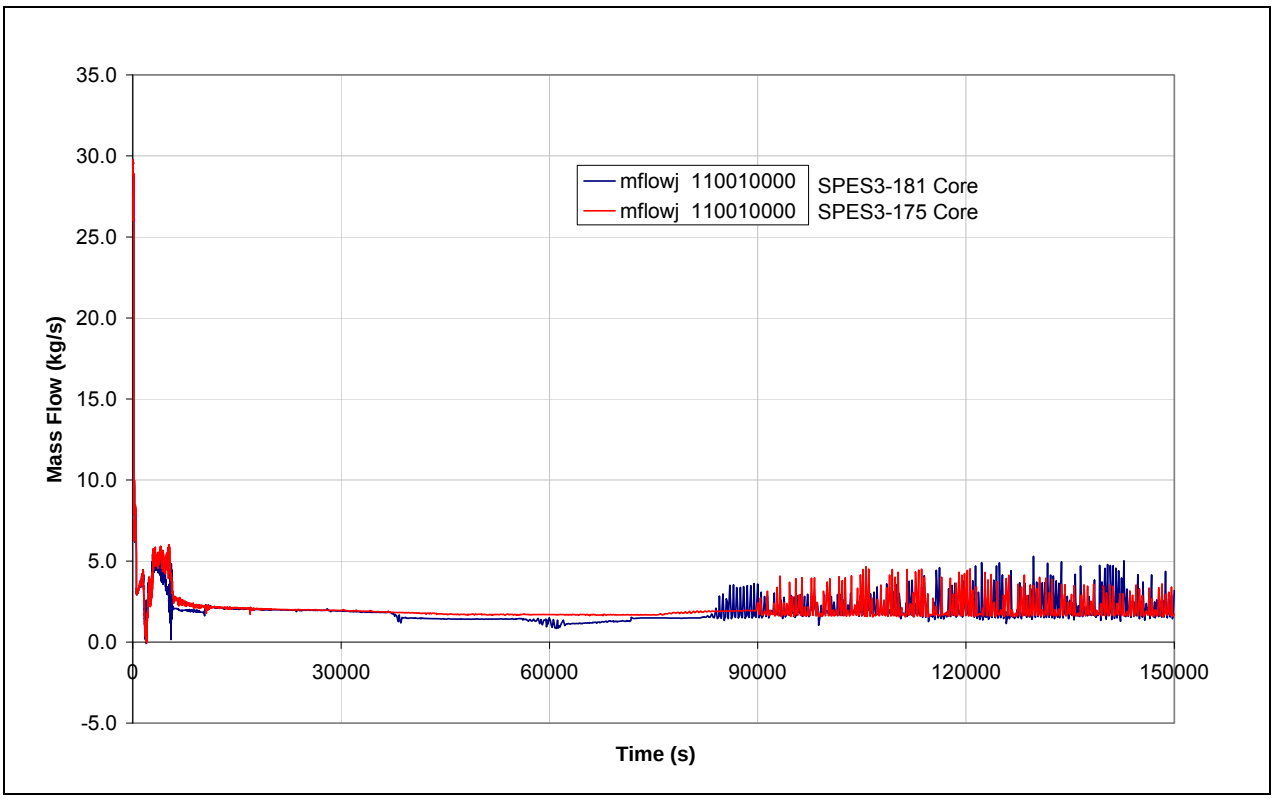

Fig.7. 30 - SPES3-181 and SPES3-175 RI-DC check valve mass flow (window)

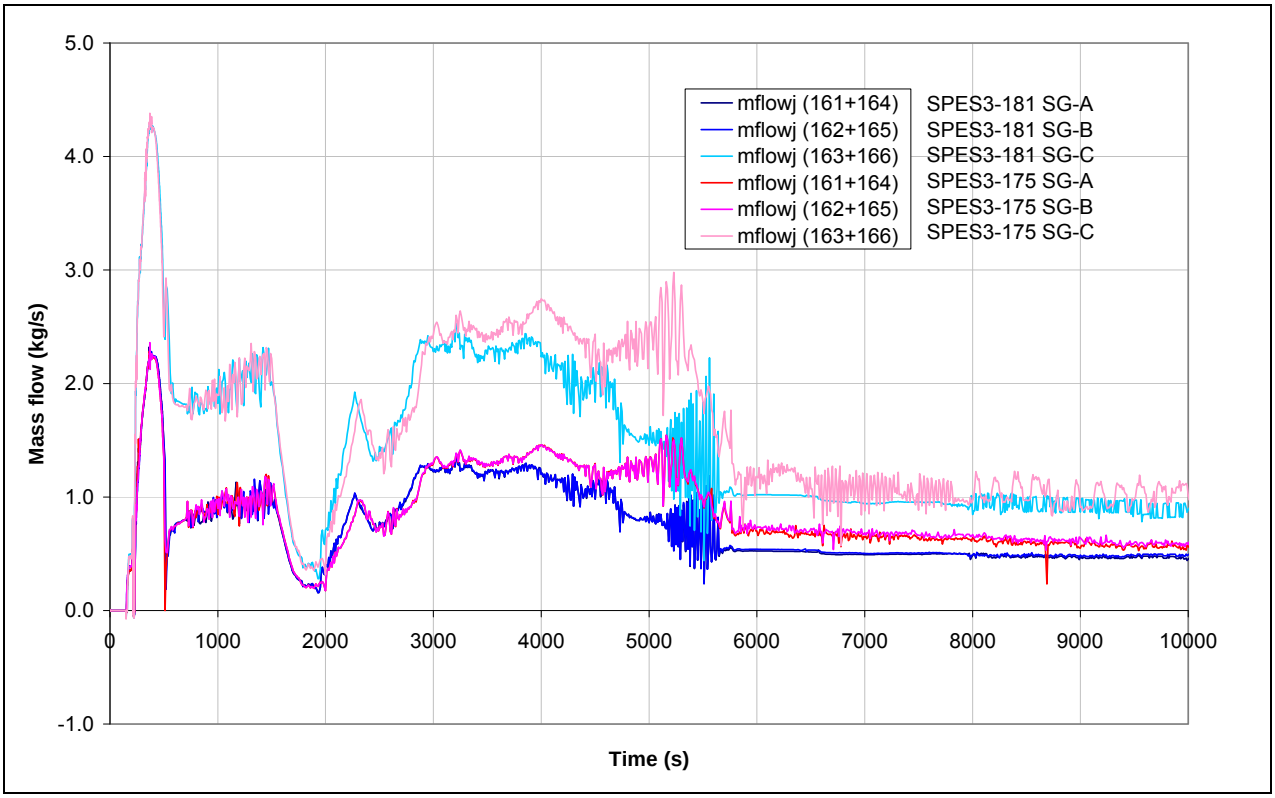

Fig.7. 31 - SPES3-181 and SPES3-175 RI-DC check valve mass flow

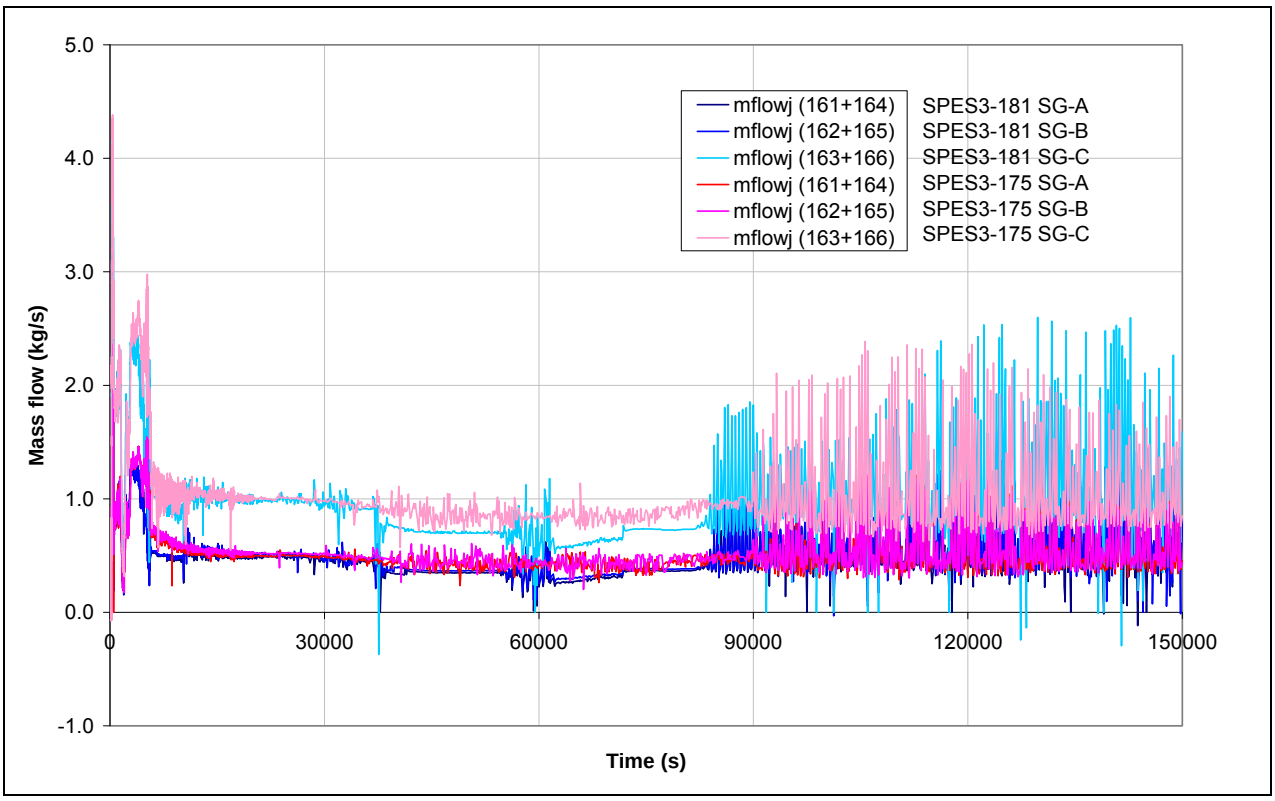

Fig.7. 32 - SPES3-181 and SPES3-175 RPV mass (window)

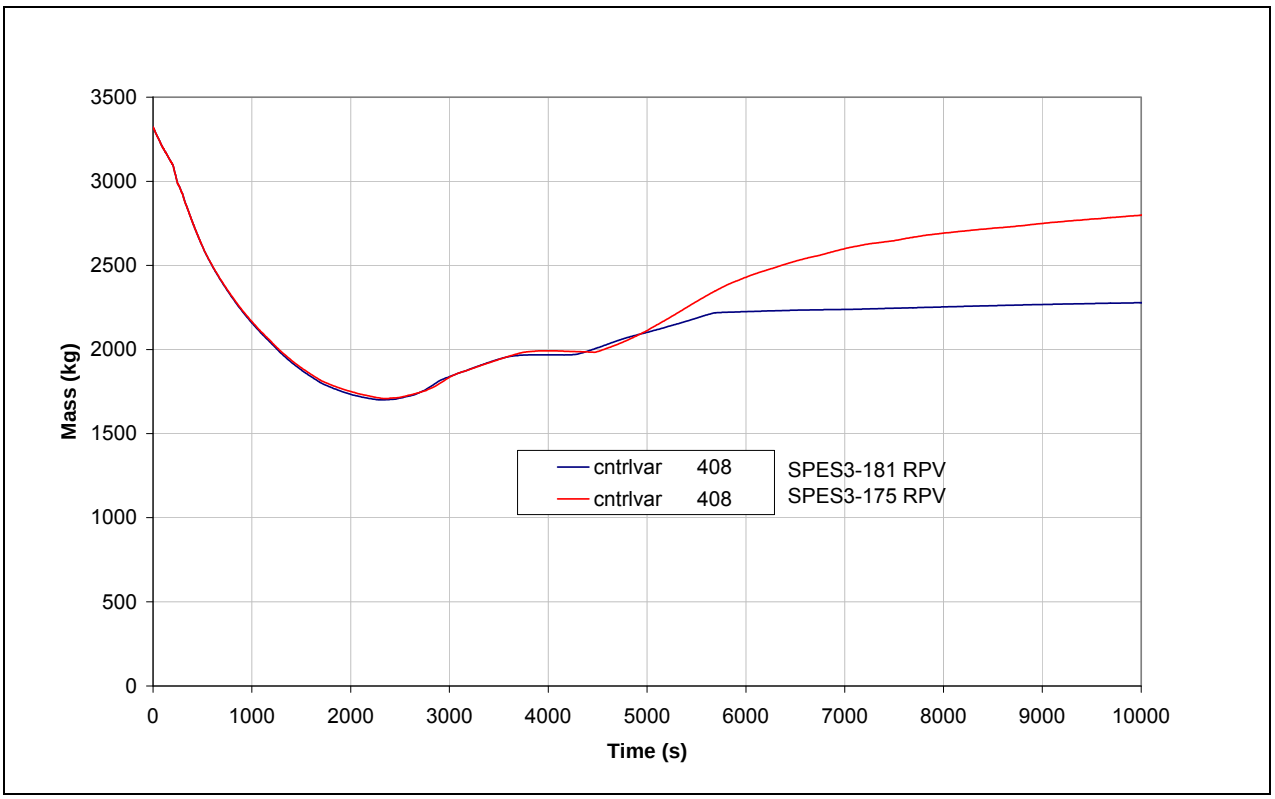

Fig.7. 33 - SPES3-181 and SPES3-175 RPV mass

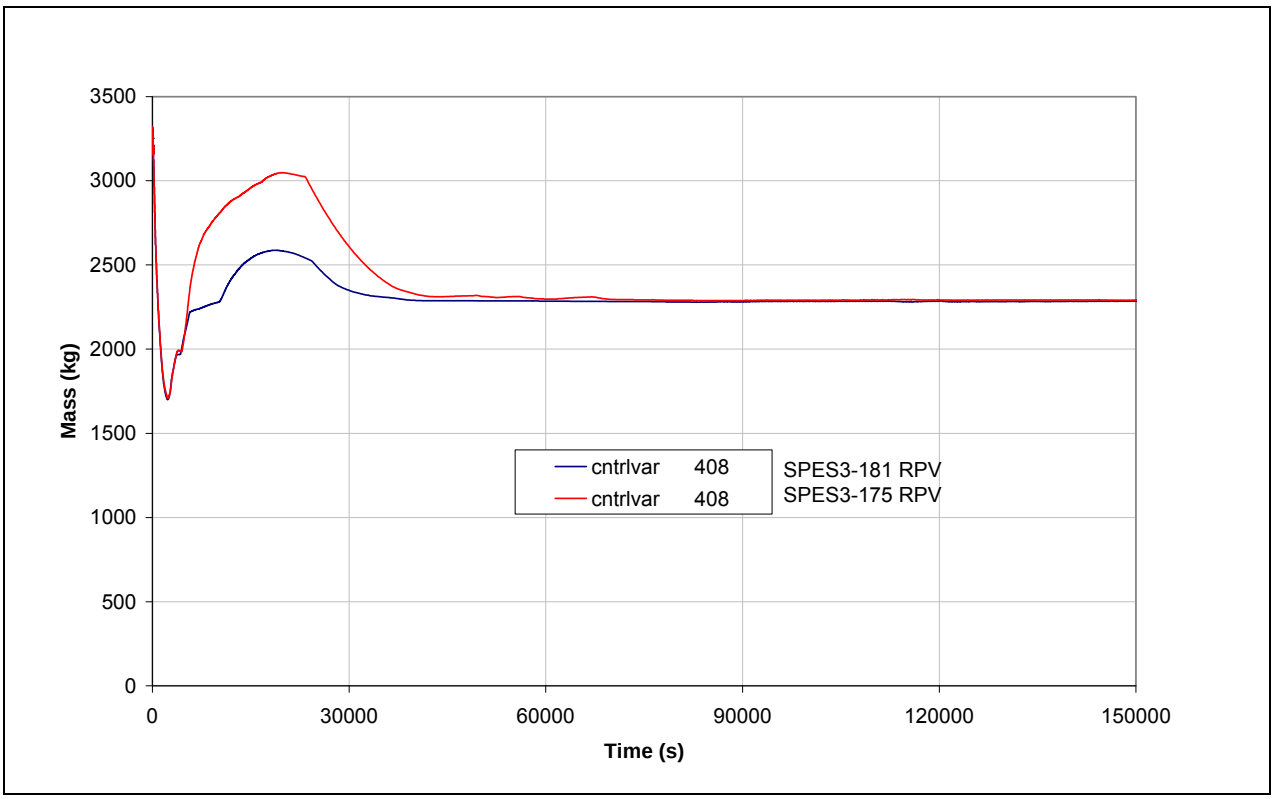

Fig.7. 34 - SPES3-181 and SPES3-175 Core liquid fraction (window)

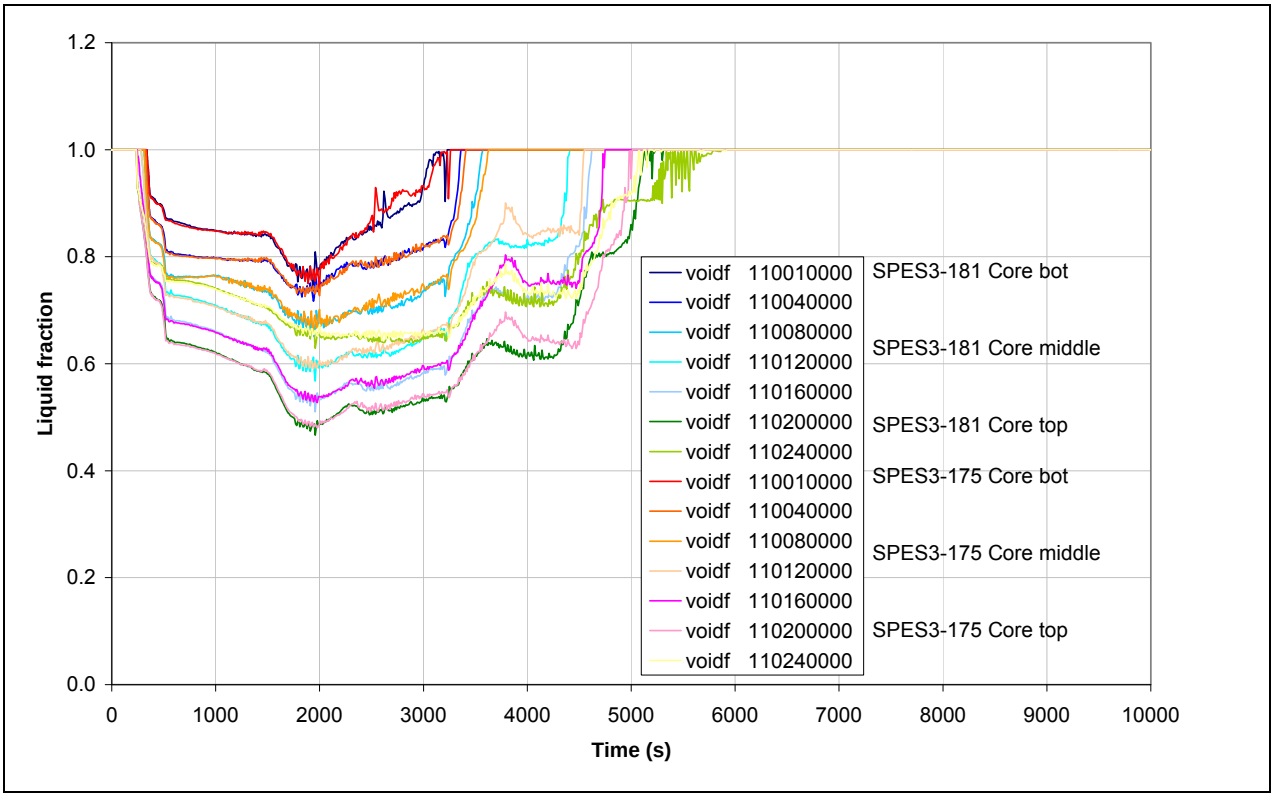

Fig.7. 35 - SPES3-181 and SPES3-175 ADS Stage-I mass flow (window)

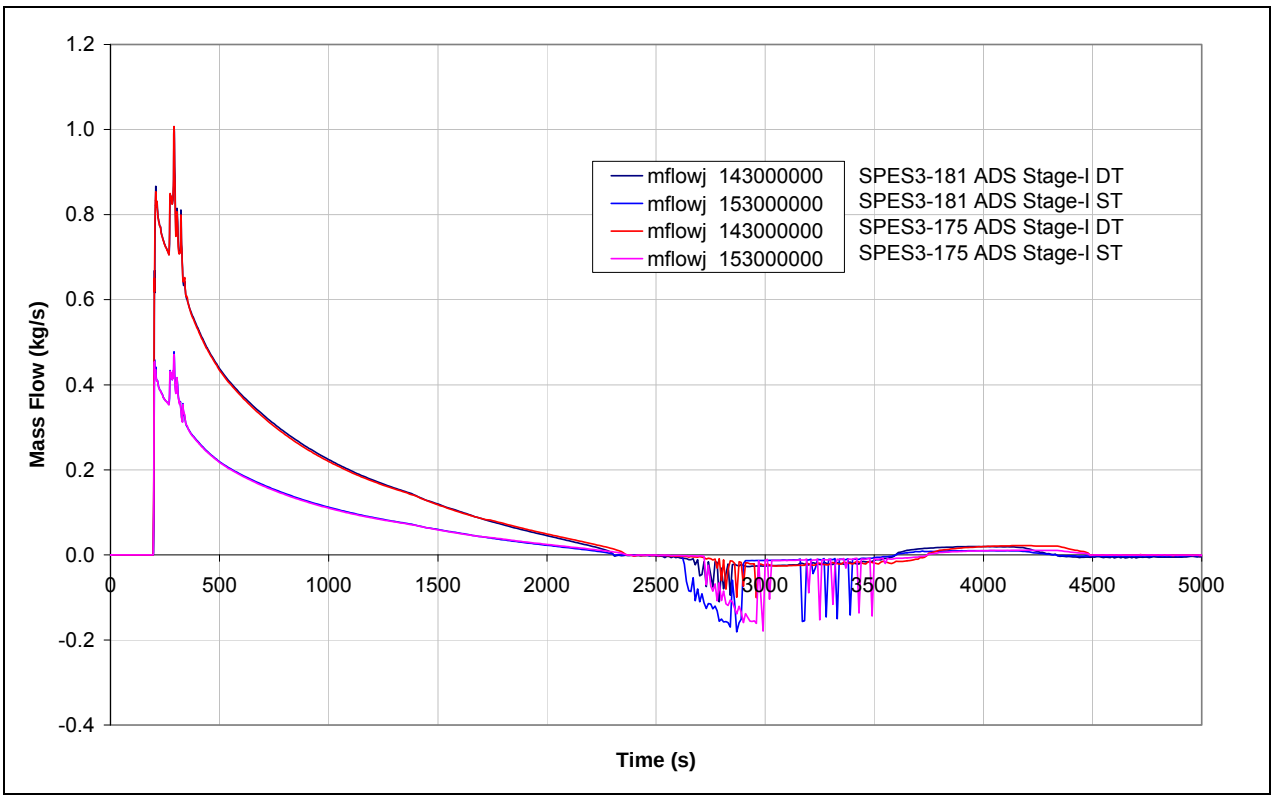

Fig.7. 36 - SPES3-181 and SPES3-175 RC to DVI mass flow IL (window)

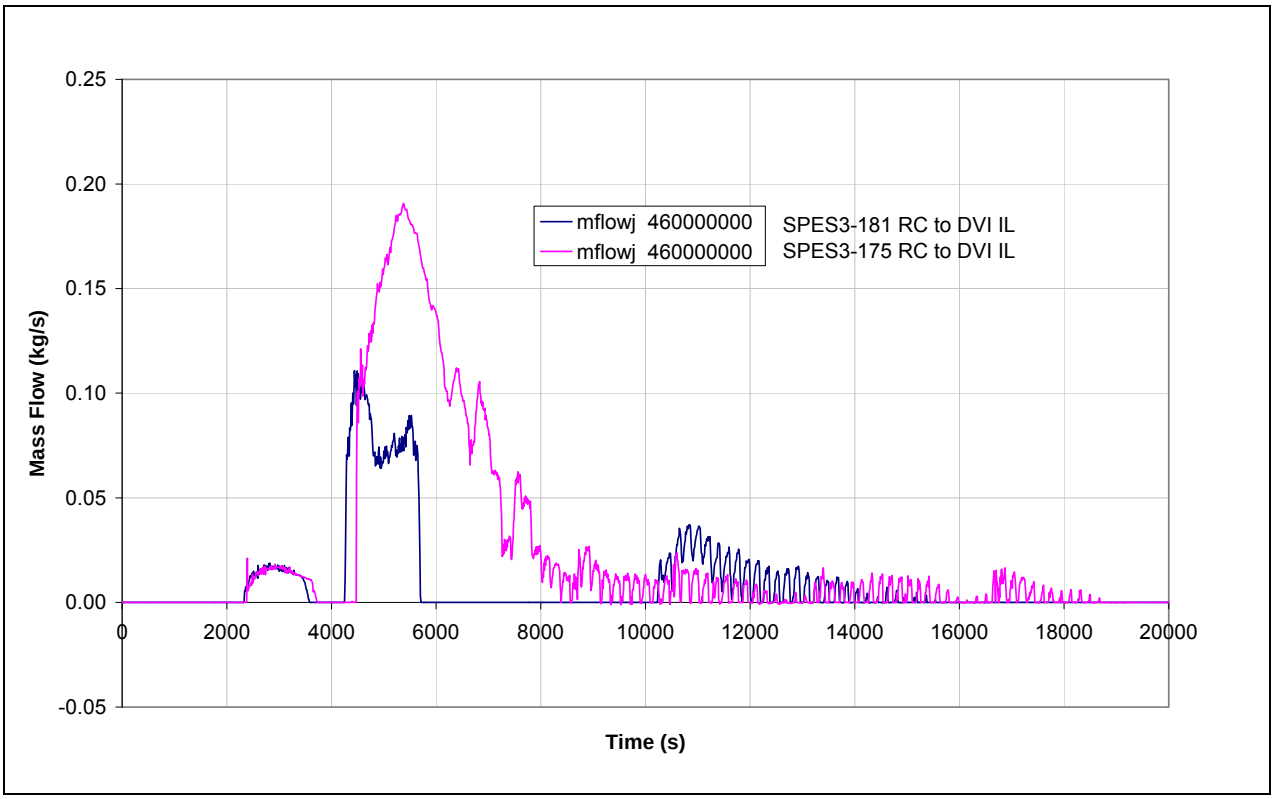

Fig.7. 37 - SPES3-181 and SPES3-175 RC to DVI mass flow IL

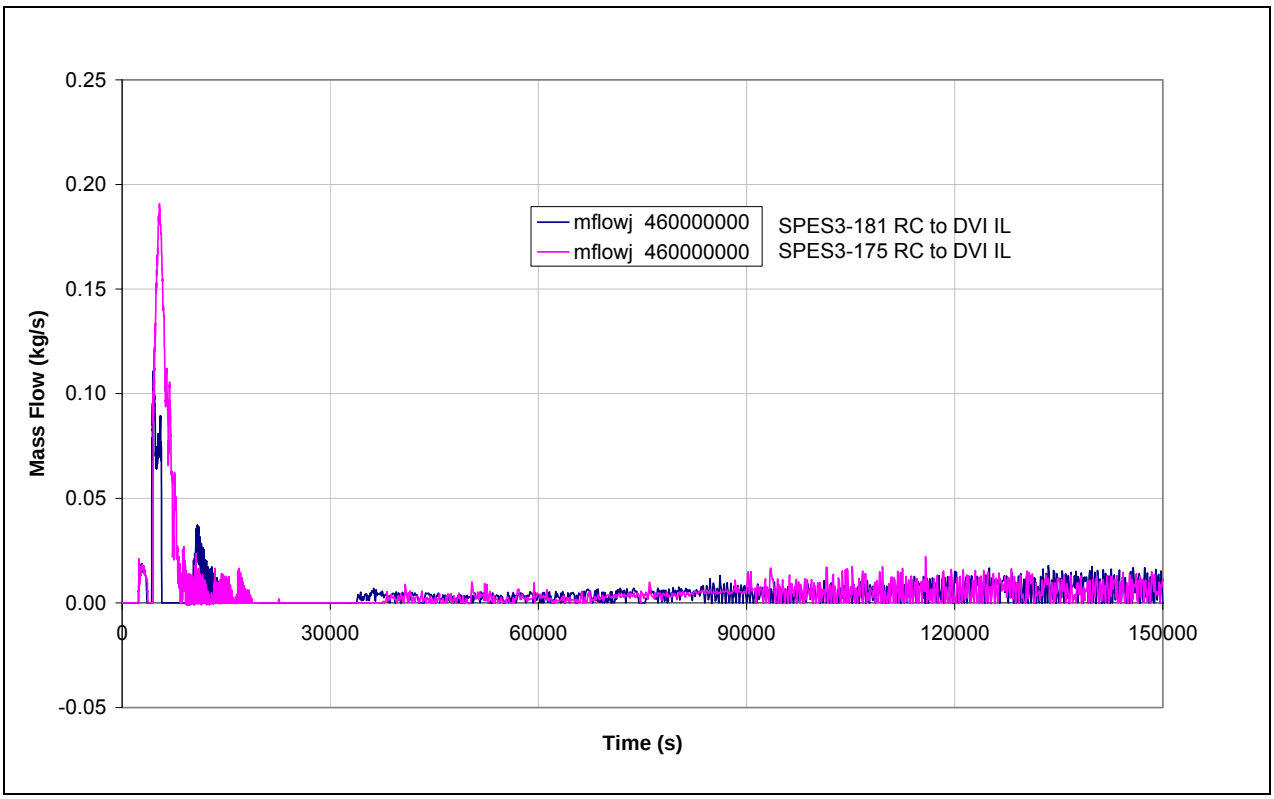

Fig.7. 38 - SPES3-181 and SPES3-175 EBT injection mass flow (window)

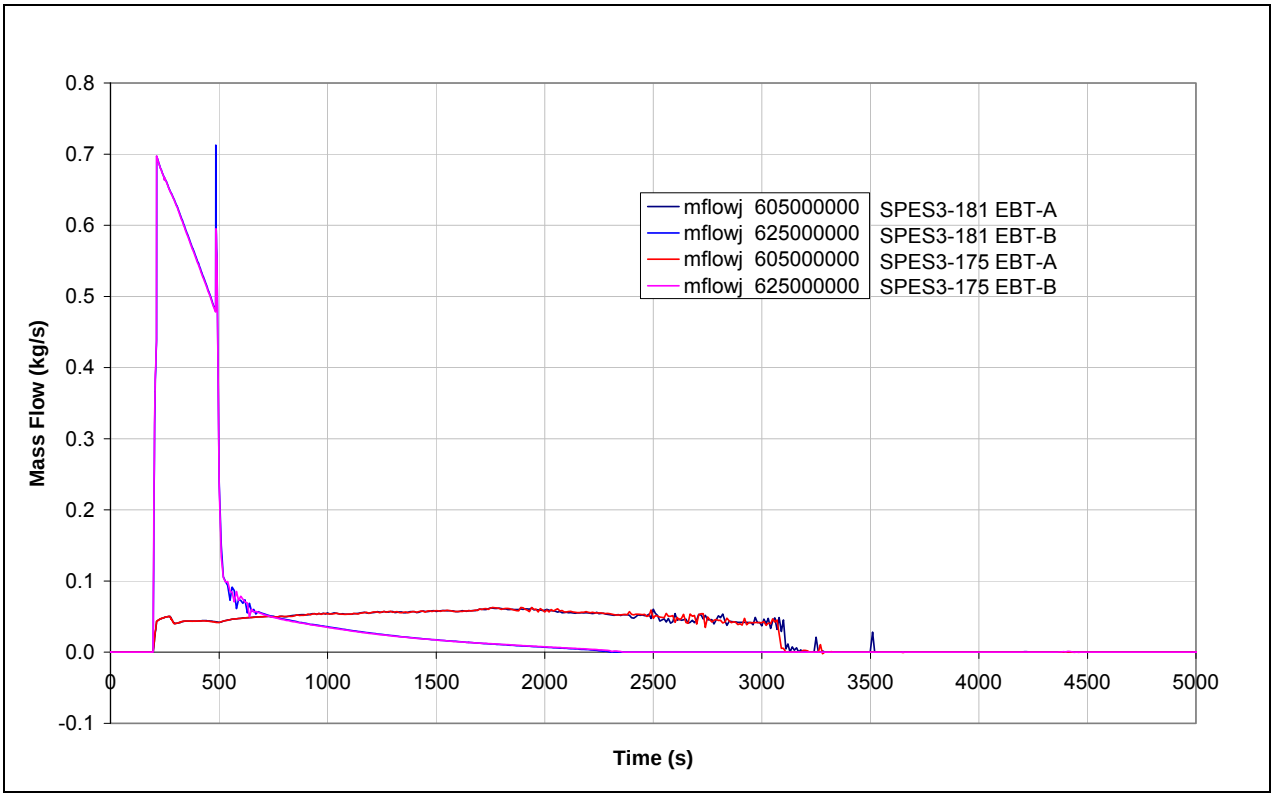

Fig.7. 39 - SPES3-181 and SPES3-175 EBT level (window)

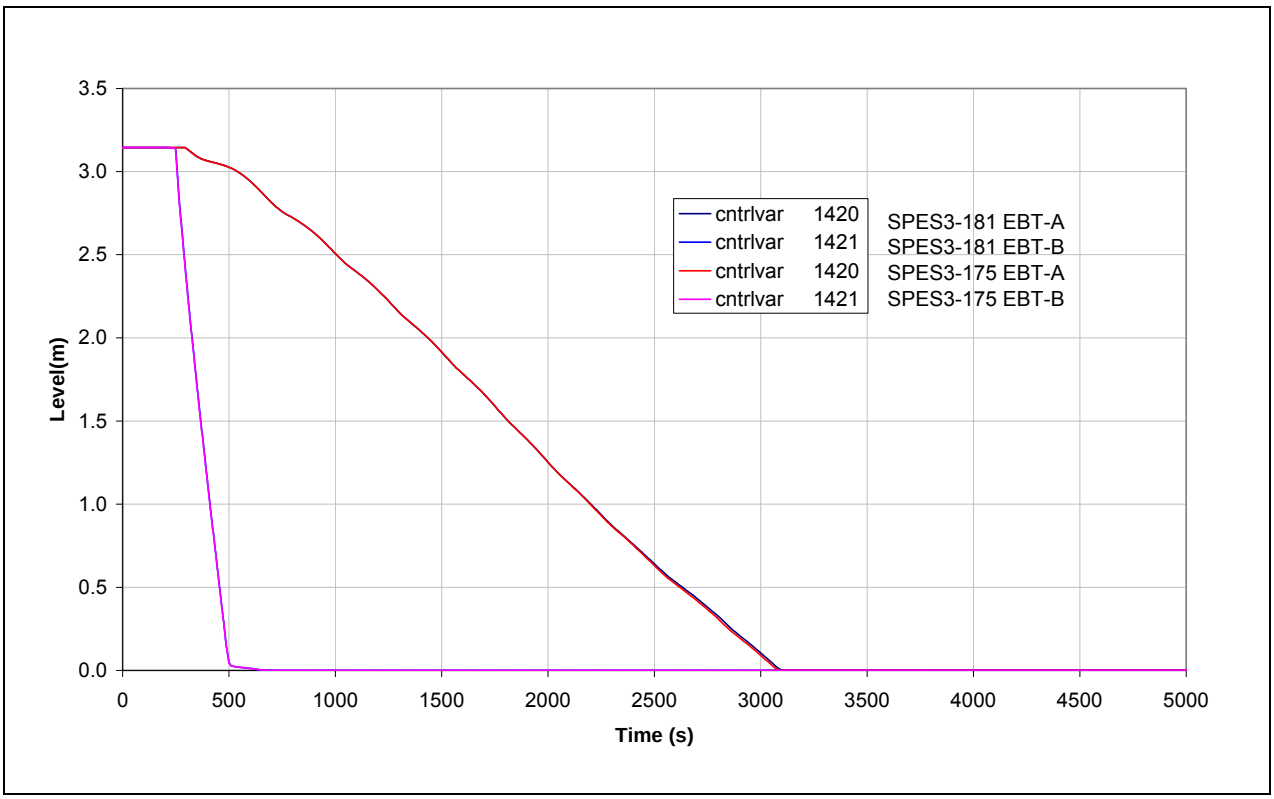

Fig.7. 40 - SPES3-181 and SPES3-175 Core inlet and outlet fluid temperature (window)

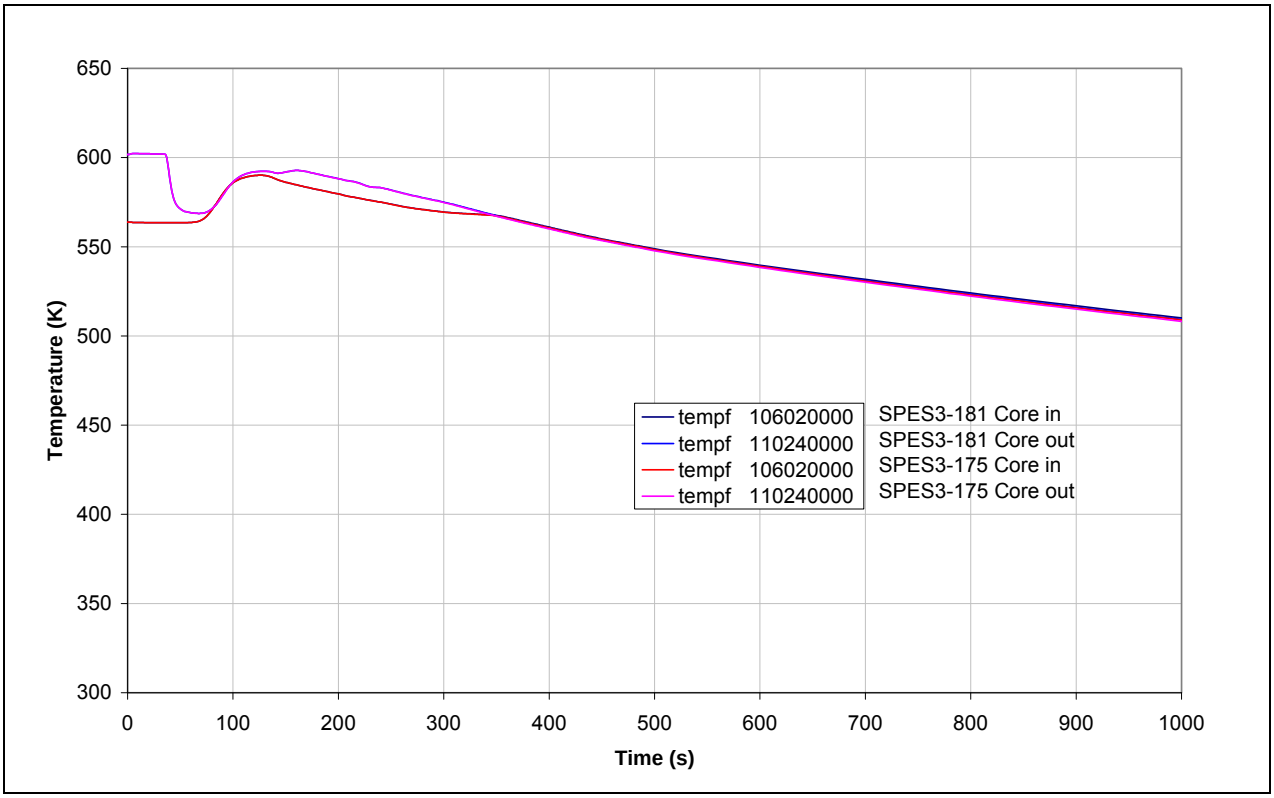

Fig.7. 41 - SPES3-181 and SPES3-175 Core inlet and outlet fluid temperature

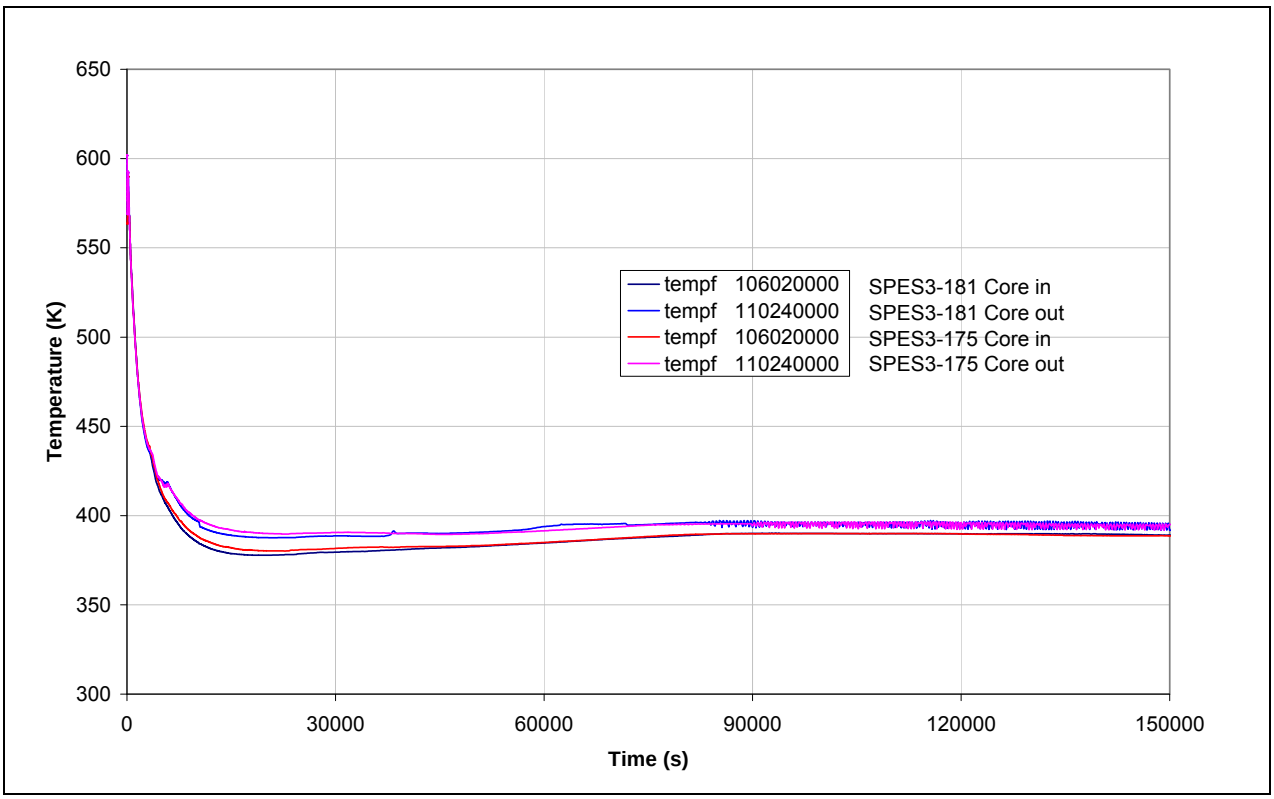

Fig.7. 42 - SPES3-181 and SPES3-175 Core heater rod surface temperature –normal rod (window)

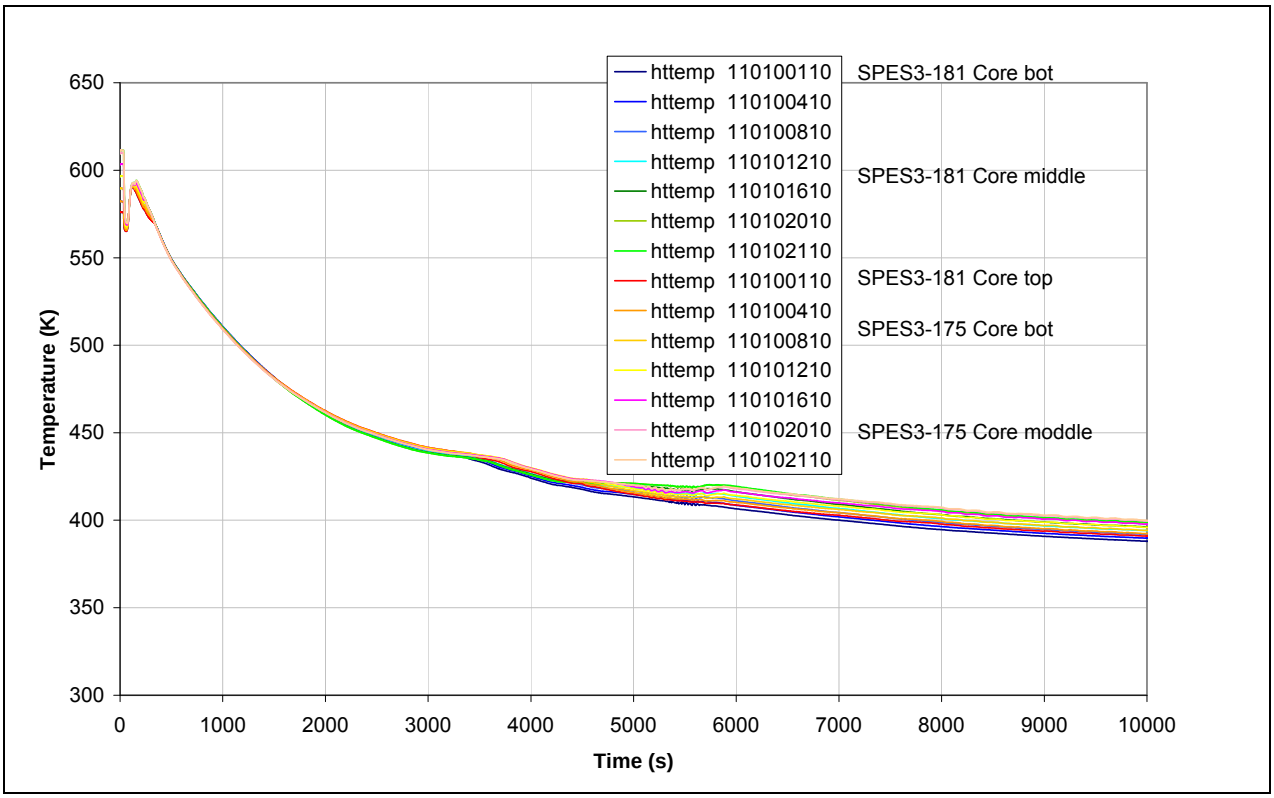

Fig.7. 43 - SPES3-181 and SPES3-175 Core heater rod surface temperature –normal rod

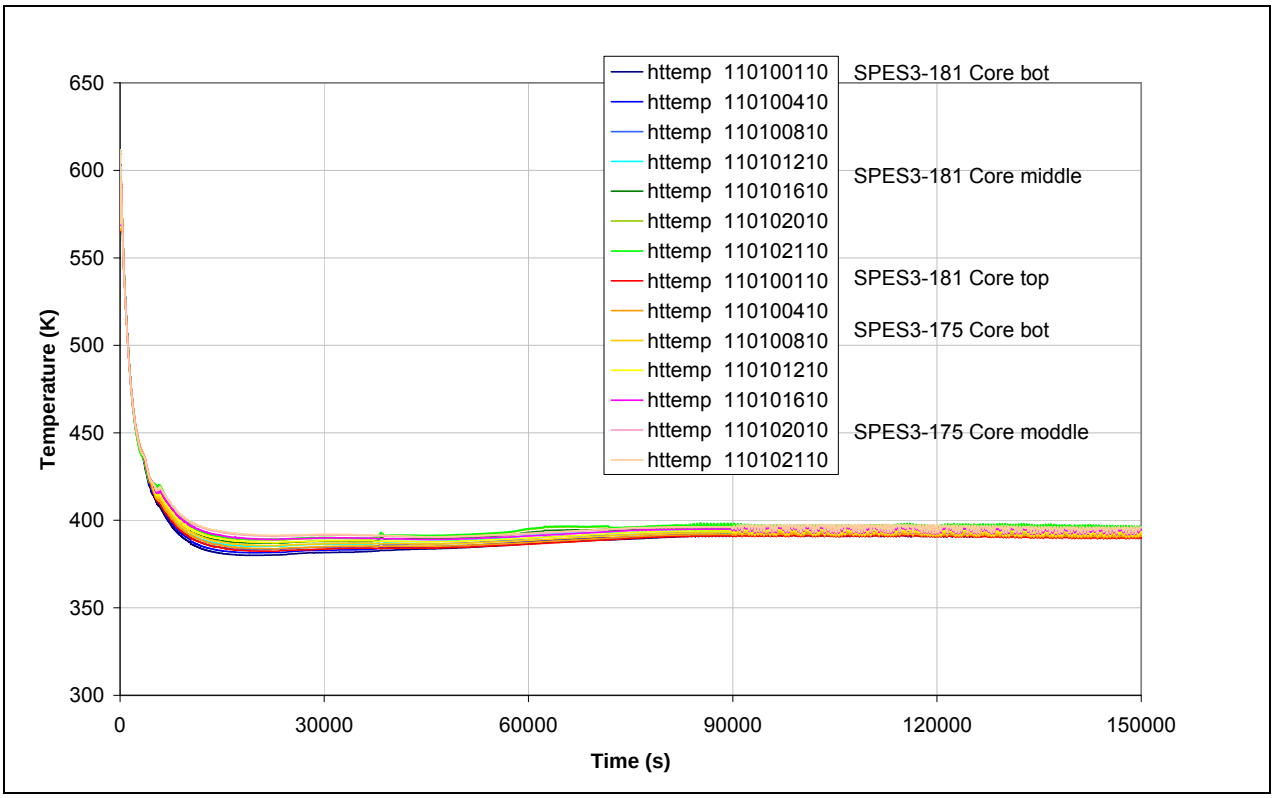

Fig.7. 44 - SPES3-181 and SPES3-175 Core heater rod surface temperature –hot rod (window)

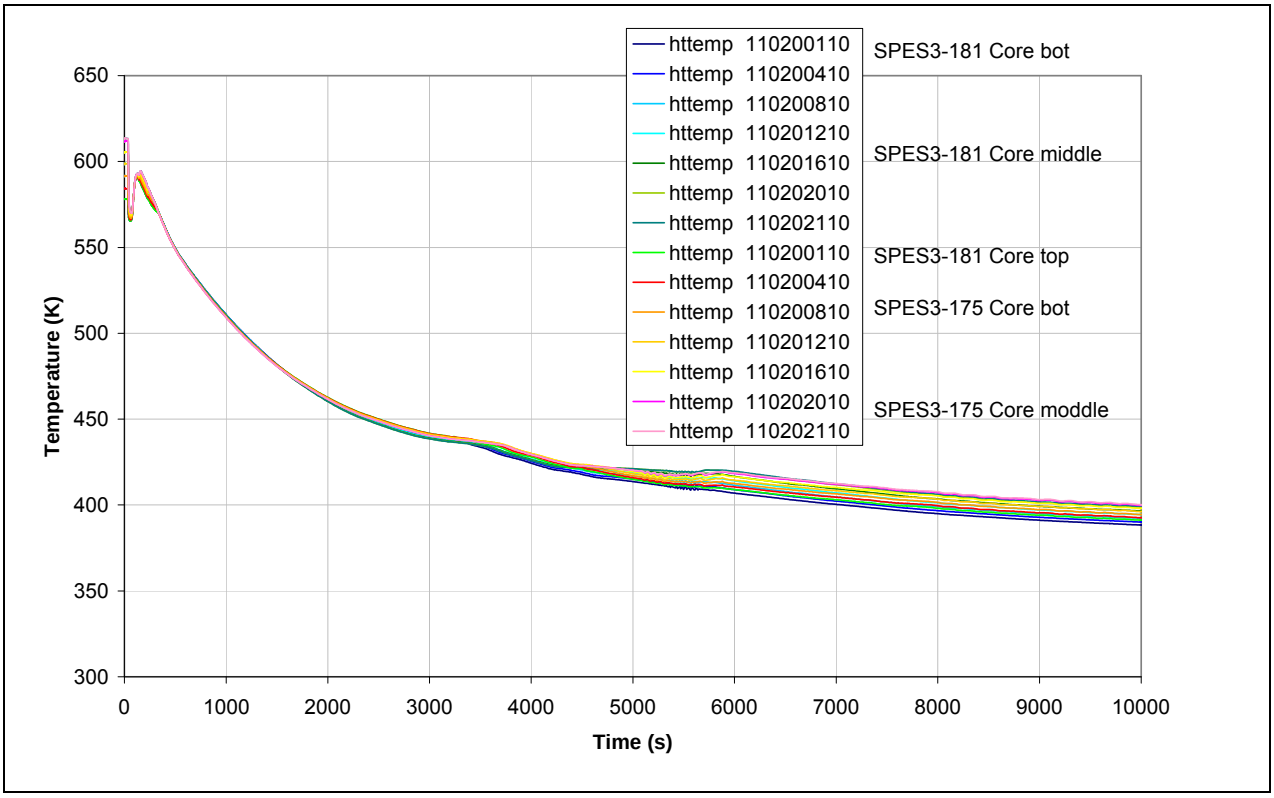

Fig.7. 45 - SPES3-181 and SPES3-175 Core heater rod surface temperature –hot rod

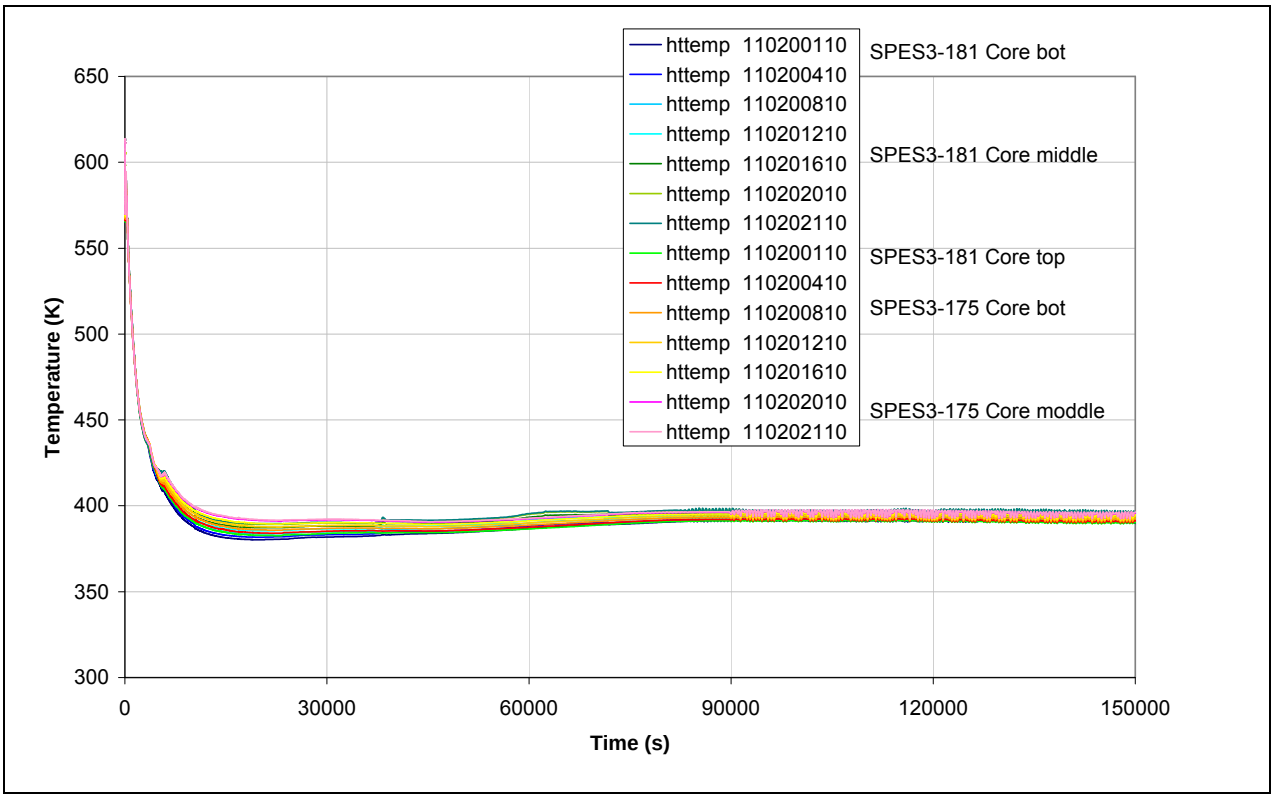

Fig.7. 46 - SPES3-181 and SPES3-175 LGMS injection mass flow (window)

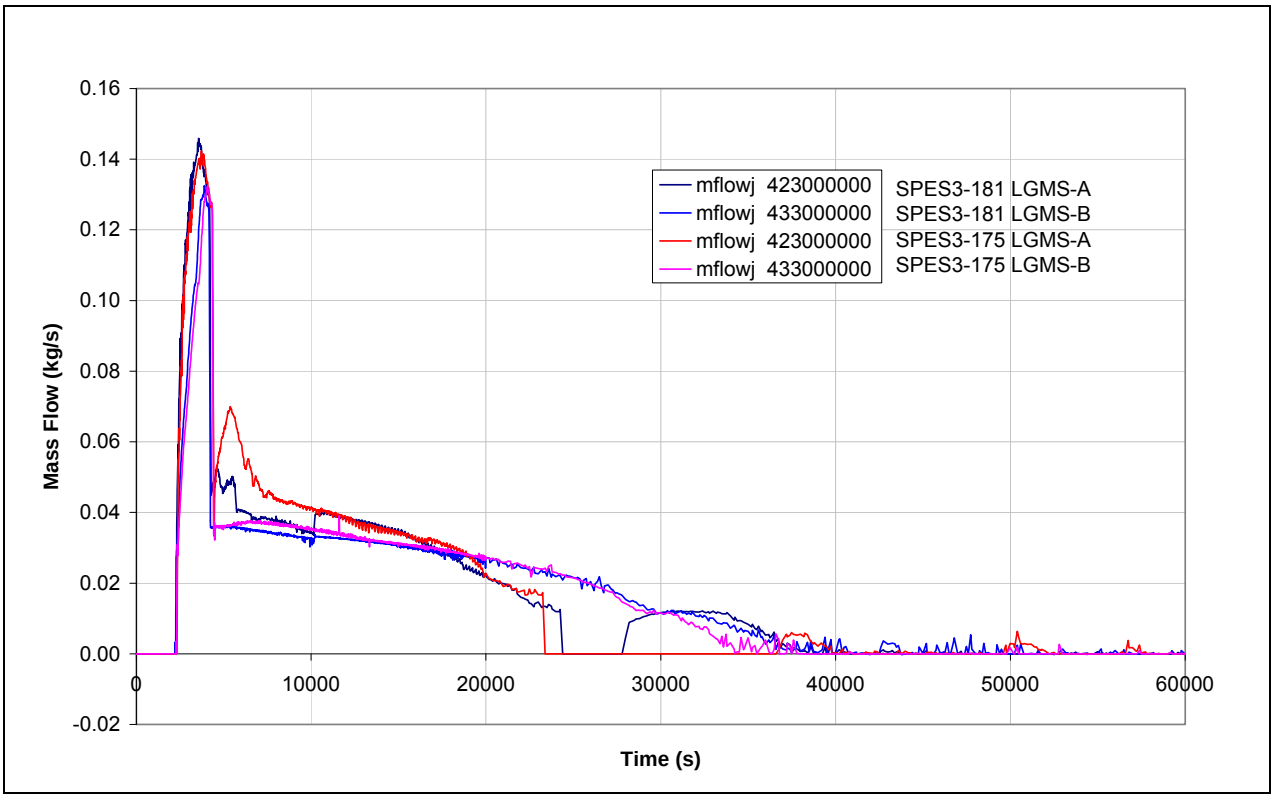

Fig.7. 47 - SPES3-181 and SPES3-175 RC level (window)

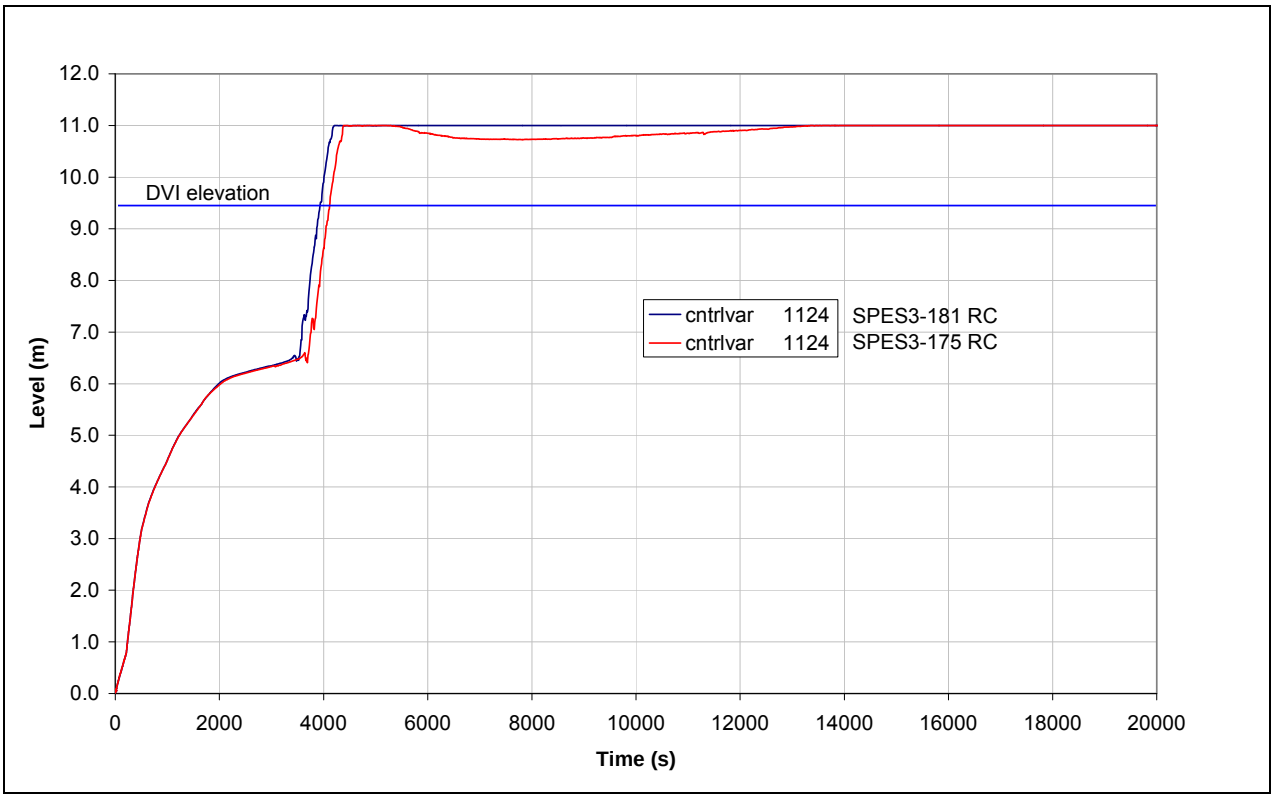

Fig.7. 48 - SPES3-181 and SPES3-175 LGMS level

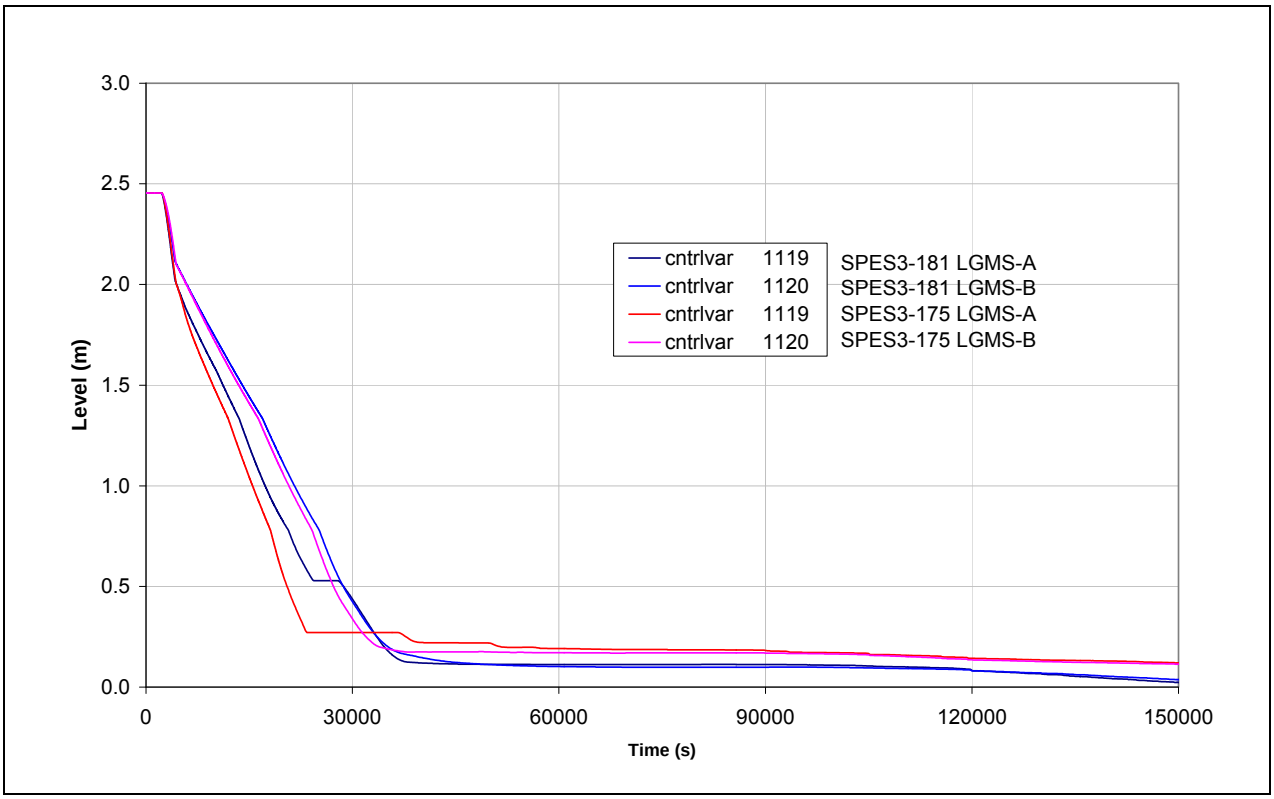

Fig.7. 49 - SPES3-181 and SPES3-175 LGMS mass

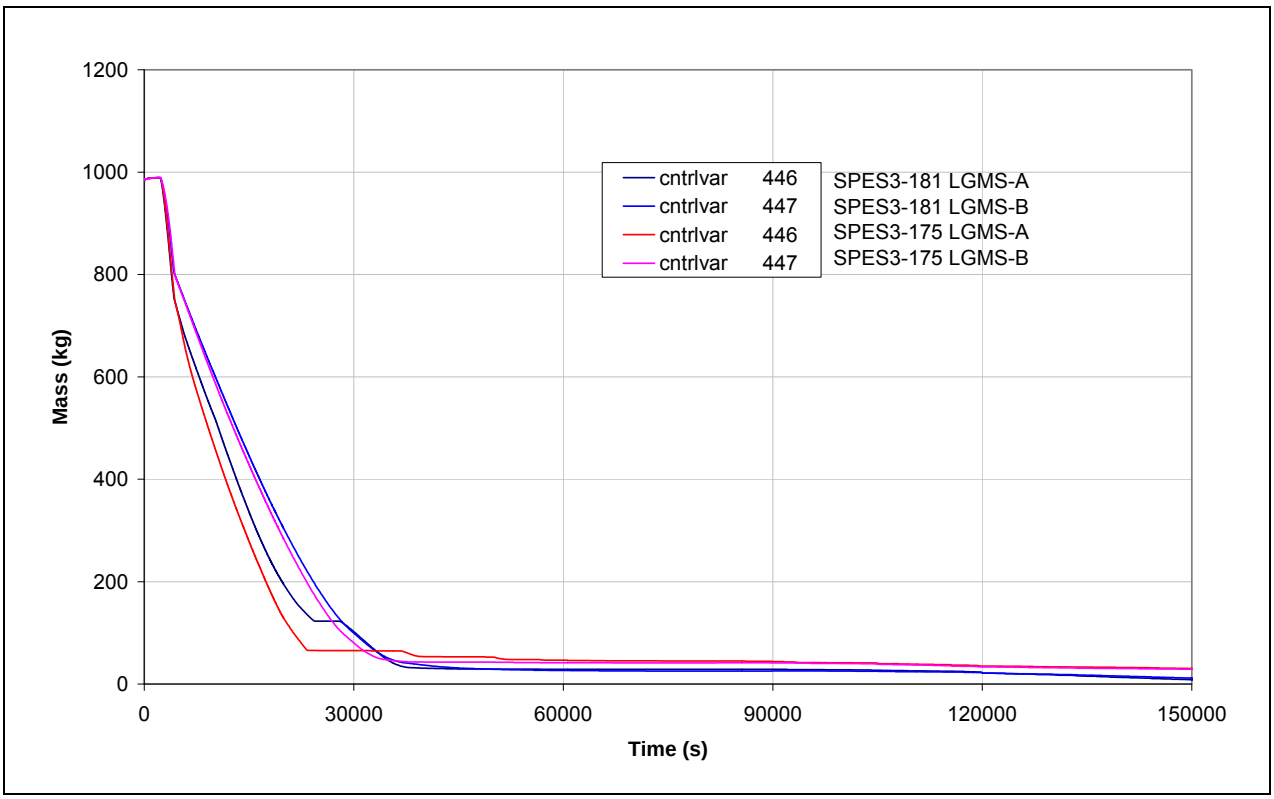

Fig.7. 50 - SPES3-181 and SPES3-175 ADS Stage-II mass flow

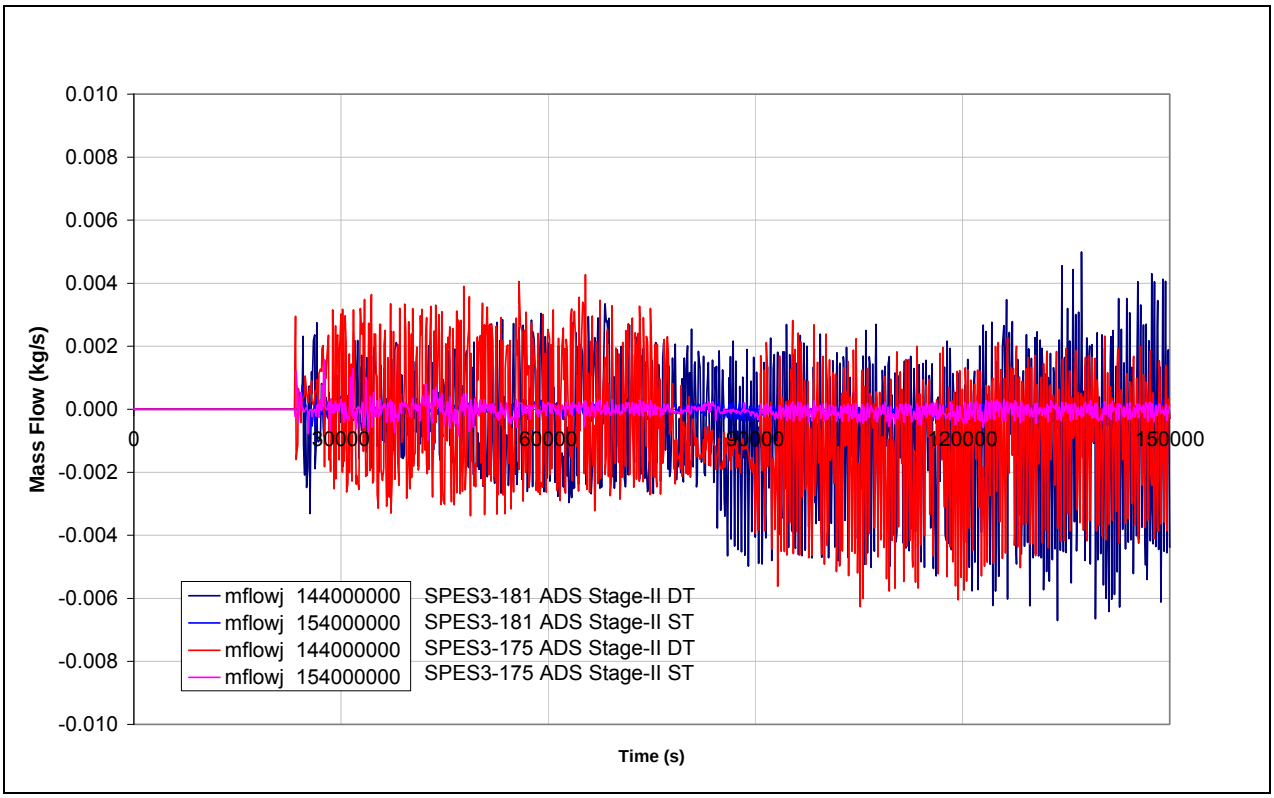

Fig.7. 51 - SPES3-181 and SPES3-175 RWST temperature (window)

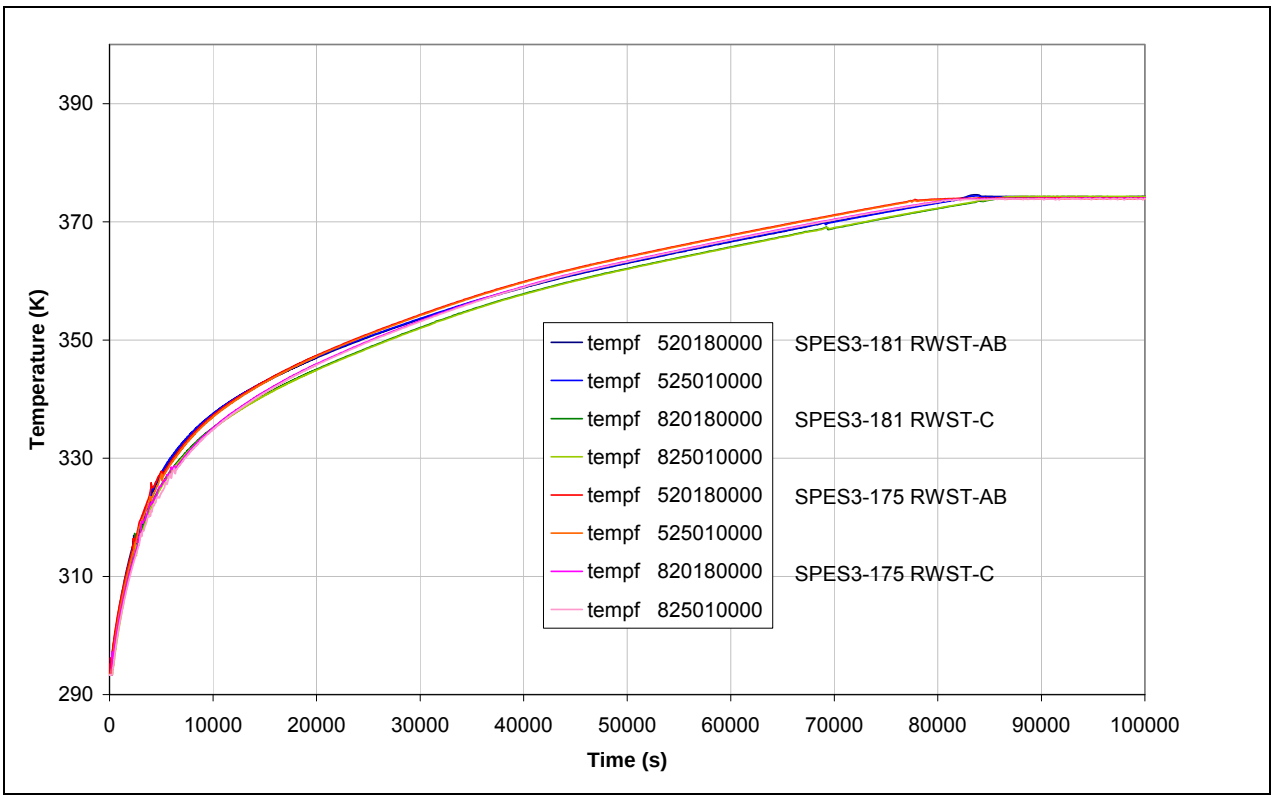

Fig.7. 52 - SPES3-181 and SPES3-175 RWST temperature

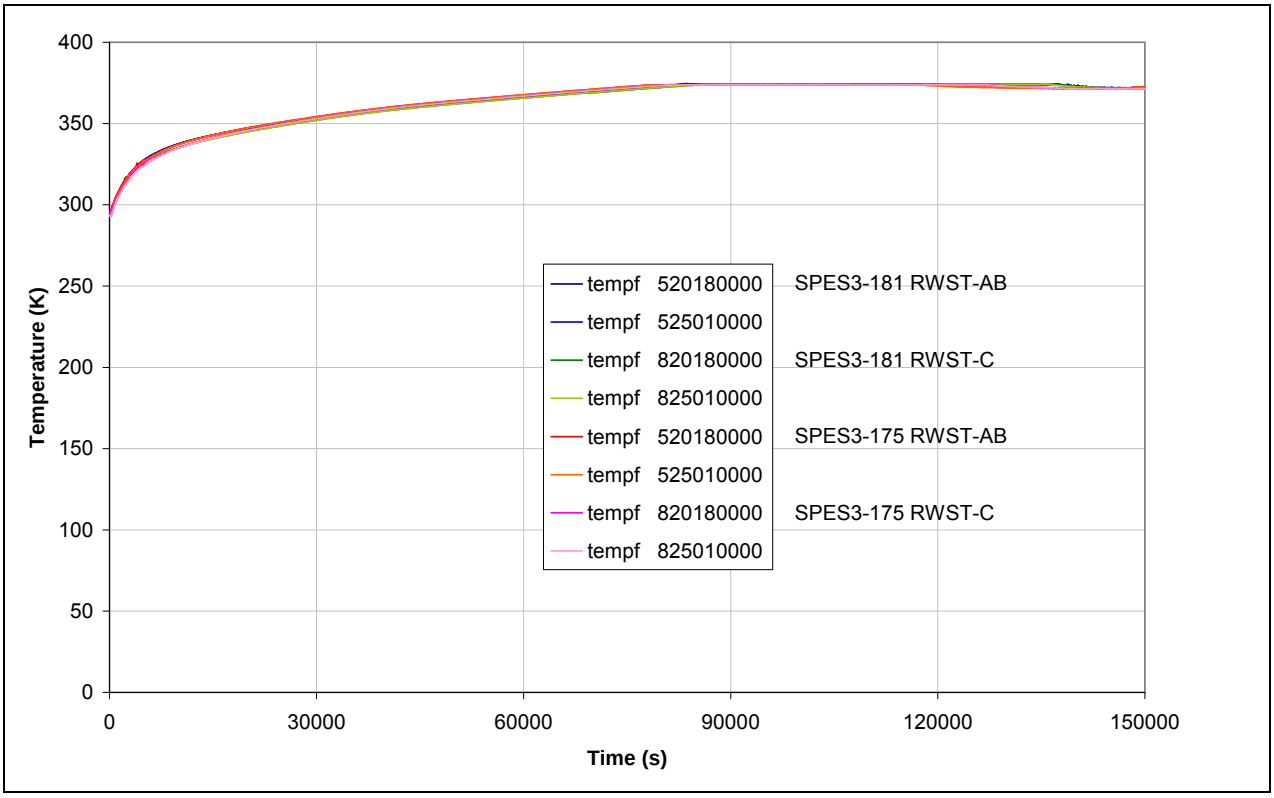

8. DBE STATION BLACK-OUT, FUKUSHIMA TYPE, FROM 65% POWER – NEW EHRS: SPES3-178

The Chapter 3.2 explains the reasons why the EHRS tubes were changed with respect to the original design. The final tube configuration is: AISI 304 tubes, 60.3 mm outer diameter, 5.54 mm thickness. Different layers of Teflon insulation are foreseen for the EHRS-A/B and EHRS-C tubes to guarantee the exchanged power as in the original configuration that had thinner tubes. In particular, in the EHRS-A and B heat exchangers, the equivalent surface of a tube is covered with 0.096 mm Teflon and the headers are covered with 10 mm Teflon. In EHRS-C heat exchanger, no insulation is foreseen on the tubes while the headers are covered with 0.2 mm Teflon.

The SPES3-178 case is a SBO transient, Fukushima type, run with the new EHRS tube geometry. It is exactly the same transient as SPES3-177 case, where the original EHRS tube geometry is simulated.

This chapter compares the SPES3-178 and SPES3-177 cases in order to verify that the EHRS re-design does not affect the heat rejection to RWST.

A deep analysis of the transient is reported in Chapter 6 for SPES3-177. Data related to SPES3-178 case are limited to about 70000 s, due to a numerical crash of the calculations. They are anyway sufficient for the comparison with SPES3-177 and the verification of the result similarity. The main quantities of the transients are compared and the differences are explained on the basis of the changes to the EHRS tubes.

8.1 SPES3-178 and SPES3-177

Steady conditions at 65% power, starting point for the transient, are summarized in Tab.4. 1.

The list of the main events occurring during the transient, with timing and quantities, is reported in Tab.8. 1.

8.1.1 SPES3-178 and SPES3-177 transient phases and description

The first 10 s of data (-10 s to 0 s) are steady state conditions.

All times of the events are given with respect to the earthquake assumed as time 0 s.

Earthquake and Loss of Off-site power: RCP and MFW pump trip

The earthquake occurs at time 0 and the loss of off-site electric power is contemporary. The pumps of the system are switched-off and the coast-down starts for the RCP and the FW pumps.

The RCP velocity is shown in Fig.8. 1 and it is completely stopped at 100 s. The pump head is shown in Fig.8. 2.

The pump head decreasing let the RI-DC check valves open and allows natural circulation between riser and SG annuli at lower elevation in the RPV. Circulation starts at 11 s in SG-C and at 14 s in SG-A and B, Fig.8. 3, Fig.8. 4, Fig.8. 5. Little differences between SPES3-177 and SPES3-178 cases are observed in the mass flow to stat from 200 s when the EHRS exchanged power is close to the maximum. The mass flow trend is delayed of about 100 s in SPES3-178, until around 6000 s. After that, no difference is observed.

When the pump head decreases, the pump by-pass check valves open and circulation starts also at high level in the RPV, at 18 s through the SG-C annulus and at 19 s through SG SG-A and B annuli, Fig.8. 6, Fig.8. 7. Around 400 s, natural circulation stops through the pump by-pass corresponding to SG-C, as no heat transfer occurs in SG-C since about 150 s, Fig.8. 8. Due to the RPV level decrease for system cooling, the pump uncovers at 2620 s in SPES3-177 and at 2710 s in SPES3-178 and circulation stops through the

pump by-pass, Fig.8. 9, Fig.8. 7. The pump uncovers later in SPES3-178, as in this phase of the transient, power removed by the EHRS is slightly lower than in SPES3-177 with a slower primary side cooling.

The MFW pump is assumed to stop in 4.9 s and circulation in the secondary side re-starts only after the EHRS actuation, Fig.8. 10, Fig.8. 11, Fig.8. 12.

Low FW signal: Reactor Scram; Start-up feed-water failure

The reactor scram occurs at 1.24 s, on Low FW signal, set at 75% of nominal feed-water mass flow. Being SPES3-177 and SPES3-178 cases starting form 65% power conditions, the signal set-point is 75% of steady value, reduced according to power. Core power is shown in Fig.8. 13, Fig.8. 14, Fig.8. 15 together with SG total power. After the secondary loop isolation, SG power is strictly related to the EHRS power and it appears a little lower in SPES3-178 than SPES3-177 between 120 s and 3000 s.

The Start-up feed-water, that should intervene at the reactor scram, is assumed to fail (it is not simulated in SPES3) and this gives permission for secondary loop isolation.

Low SG secondary side level signal: SG isolation and EHRS-A and B actuation

The loss of main feedwater causes the reduction of mass inventory in the SGs, secondary side. Both in SPES3-178 and SPES3-177 case, the SG low level signal occurs in SG-A at 34.13 s, when the collapsed level reaches 0.25 m, Fig.8. 16, Fig.8. 17, Fig.8. 18. The signal starts the secondary loop isolation and actuates the EHRS-A and B. The MFIV and MSIV are closed contemporarily in 5 s. The EHRS actuation valves are opened in 2 s.

Natural circulation restarts in SG-A and B, thanks to the EHRS-A and B intervention, Fig.8. 10, Fig.8. 11, Fig.8. 12 allowing the decay power removal, Fig.8. 13, Fig.8. 14, Fig.8. 15.

The peak of water mass flow through the EHRS-A and B occurs at 37 s with 0.277 kg/s for loop-A and 0.273 for loop-B, both in SPES3-178 and SPES3-177, Fig.8. 19, Fig.8. 20. Power transferred to the EHRS is shown in Fig.8. 21, Fig.8. 22. The peak of transferred power occurs at 212 s, 380 kW, for EHRS-A and at 220 s, 381 kW, for EHRS-B in SPES3-177 and at 222 s, 368 kW, for EHRS-A and at 243 s, 365 kW, for EHRS-B in SPES3-178. It appears a little delay and lower peak in SPES3-178, mainly caused by the increased tube thickness that delays the heat transfer in the early phases of the transient. After 3000 s, no difference in the exchanged power is observed between the cases. Power is rejected to the RWST-AB that begins to heat-up at 51 s in SPES3-177, and reaches saturation at 9200 s, and at 53 s in SPES3-178, and reaches saturation at 9600 s, Fig.8. 23. The RWST-AB mass decreases for water evaporation, Fig.8. 24.

Heat removal by the EHRSs, through the SGs, enhances the natural circulation in the core that occurs through the RI-DC check valves, after the pump is uncovered, Fig.8. 3, Fig.8. 4, Fig.8. 5. The core inlet mass flow is reported in Fig.8. 25, Fig.8. 26, Fig.8. 27. After the pump stop, the core mass flow is around 4.3 kg/s, then it decreases of about 1 kg/s, around 2700 s, when circulation interrupts through the pump by-pass. In the long term, it is stable around 2 kg/s. A great similarity is observed between SPES3-178 and SPES3-177.

The SG isolation causes the secondary loop pressure increase up to the peak of 8.59 MPa in SG-A, at 129 s, of 8.63 MPa in SG-B, at 136 s, and of 7.87 MPa in SG-C, at 176 s, in SPES3-177 and of 8.59 MPa in SG-A, at 137 s, of 8.70 MPa in SG-B, at 147 s, and of 7.88 MPa in SG-C, at 186 s, in SPES3-178, Fig.8. 28, Fig.8. 29.

Low Core inlet coolant temperature signal: EBT actuation

The primary side pressure decreases for the system cool-down and around 70000 s, end of calculation, it is around 0.19 MPa for both cases, Fig.8. 30, Fig.8. 31. The inlet and outlet core temperatures are shown in Fig.8. 32, Fig.8. 33. The Fig.8. 33 reports also the saturation temperature corresponding to core outlet

pressure and it is possible to observe that, at 37390 s in SPES3-177 and 37990 s in SPES3-178, the core outlet temperature is in saturation. Anyway, core is always under single-phase water, Fig.8. 34.

The primary system cool-down causes the water density increase with consequent water level decrease in the RPV. The PRZ level is shown in Fig.8. 35. The PRZ is empty at 1150 s in SPES3-177 and 1240 s in SPES3-178. Water level in the down-comer is reported in Fig.8. 36 and in reaches a steady condition after about 60000 s.

The set-point of 533.15 K for the low core inlet coolant temperature is reached at 2583.04 s in SPES3-177 and at 2668.88 s in SPES3-178. The signal triggers the EBT actuation by opening the EBT valves in 15 s. Cold water is injected into the RPV, through the DVI lines, and hot water and steam replace the EBT water through the EBT top line, connected to the RPV, Fig.8. 37, Fig.8. 38, Fig.8. 39. The EBT injection stops around 4800 s, when the EBT and RPV levels are equalized. The EBT level is shown in Fig.8. 40. A part the slight delay of SPES-178 case compared to SPES3-177, the two cases are very similar.

The RPV mass inventory slightly increases thanks to the EBT injection and then it remains stable, Fig.8. 41.

No temperature excursion occurs on the heater rod cladding as circulation in the core is stable and liquid phase is always present, Fig.8. 42, Fig.8. 43, Fig.8. 44, Fig.8. 45, Fig.8. 26, Fig.8. 27, Fig.8. 34.

Long term conditions

In the long term, the EHRS-A and B remove the core decay power and slowly cool-down the system, Fig.8. 22, Fig.8. 33. The average power produced in the core, between 60000 and 70000 s, is 30.36 kW in SPES3-177 and 30.47 kW in SPES3-178. Power removed by the EHRS is 30.73 kW in SPES3-177 and 30.75 kW in SPES3-178. Very similar values are observed in the two cases.

8.1.2 Case conclusions

The comparison of the SPES3-178 and SPES3-177 case results, for the SBO, allowed to verify that the modification of the EHRS design does not affect the results in an meaningful way. Little differences were observed in the EHRS-A and B exchanged power, while EHRS-C never intervened in the transient. Such differences are considered negligible if compared to approximations introduce by the system modelling.

As concluded for the DBE DVI line DEG break, described in Chapter 7., also in this case the conclusion is that the new final design of SPES3 EHRS is adequate for the simulation of the IRIS EHRS.

Tab.8. 1 – SPES3-178 and SPES3-177 list of the main events

	BDBE DVI-B line DEG break (2-inch equivalent)	**SPES3-178**		**SPES3-177**		
N.	**Phases and events**	**Time (s)**	**Quantity**	**Time (s)**	**Quantity**	**Notes**
Earthquake and loss of off-site power: RCP and Main feedwater pump trip						
1	Earthquake	0		0		
2	Loss of off-site power	0		0		
3	RCP coast-down starts	0		0		pump completely stopped at 100 s
4	MFW pump coast-down starts	0		0		assumed to stop in 4.9 s
Low Feedwater signal: Reactor scram; Start-up feedwater fails						
5	**Low FW signal**	1.24	0.607 kg/s FW-A 0.607 kg/s FW-B 1.214 kg/s FW-C	1.24	0.607 kg/s FW-A 0.607 kg/s FW-B 1.214 kg/s FW-C	**75% of nominal flow** (75% of mass flow at 65% power)
6	SCRAM begins	1.24		1.24		
7	Start-up FW actuation fails	1.24		1.24		
8	Natural circulation begins through shroud valves (RI-DC)	11, 14		11, 14		SG-B and C; SG-A
9	Circulation begins through pump by-pass	18, 19		18, 19		SG-C; SG-A and SG-B
Low SGss level signal: SG isolation, EHRS-A and B actuation						
10	**Low SGss level signal**	34.13	0.25 m	34.13	0.25 m	**Set point**
11	SGss low level	34.13, 55.35		34.13, 55.35	SG-A, SG-C	Signal not reached in SG-B
12	MFIV-A,B,C closure start	34.13		34.13		MFIV-A,B,C stroke 5 s
13	MSIV-A-B-C closure start	34.13		34.13		MSIV-A,B,C stroke 5 s.
14	EHRS-A and B opening start (EHRS 1 and 3 in IRIS)	34.13		34.13		EHRS-A,B IV stroke 2 s.
15	EHRS-A peak mass flow	37	0.277 kg/s	37	0.277 kg/s	
16	EHRS-B peak mass flow	37	0.273 kg/s	37	0.273 kg/s	
17	RWST-A/B begins to heat-up	53		51		
18	Secondary loop-A pressure peak	137	8.59 MPa	129	8.59 MPa	
19	Secondary loop-B pressure peak	147	8.70 MPa	136	8.63 MPa	
20	Secondary loop-C pressure peak	186	7.88 MPa	176	7.87 MPa	
21	EHRS-A power peak	222	368 kW	212	380 kW	
22	EHRS-B power peak	243	365 kW	220	381 kW	
S-Signal						
23	**Low PRZ pressure**	1302.58	12.72 MPa	1251.77	12.72 MPa	**Set point**
Low Core inlet coolant temperature signal: EBT actuation						
24	**Low core inlet coolant temperature**	2668.88	533.15 K	2583.04	533.15 K	**Set-point**
25	EBT-A and B valve opening start	2668.88		2583.04		EBT valve stroke 15 s
26	Natural circulation interrupted at SGs top	3290		3190		Pump inlet uncovered (voidf 176-01 ~0)
27	EBT-RV connections uncovered	3389, 3410		3270, 3290		EBT-A, EBT-B
28	EBT injection to RPV stop	4980		4790		RPV and EBT level equalization
29	EBT-A empty	NO		NO		
30	EBT-B empty	NO		NO		
31	Core in saturation conditions	37990		37390		T out Core ~ Tsat (Pout core). Liquid phase
Long Term conditions						
32	Core power	70000	30.47 [2]	70000	30.36 kW	Average between 60000-70000 s
33	SG total power	70000	32.56	70000	32.60 kW	Average between 60000-70000 s
34	RWST total power	70000	30.75	70000	30.73 kW	Average between 60000-70000 s
35	RWST-A/B temperature	70000	103	70000	103 °C	Saturated. Average between 60000-70000 s

[2] SPES3-178 data available until 67583 s. Average values calculated between 60000 s and 67583 s.

Fig.8. 1 – SPES3-178 and SPES3-177 RCP velocity (window)

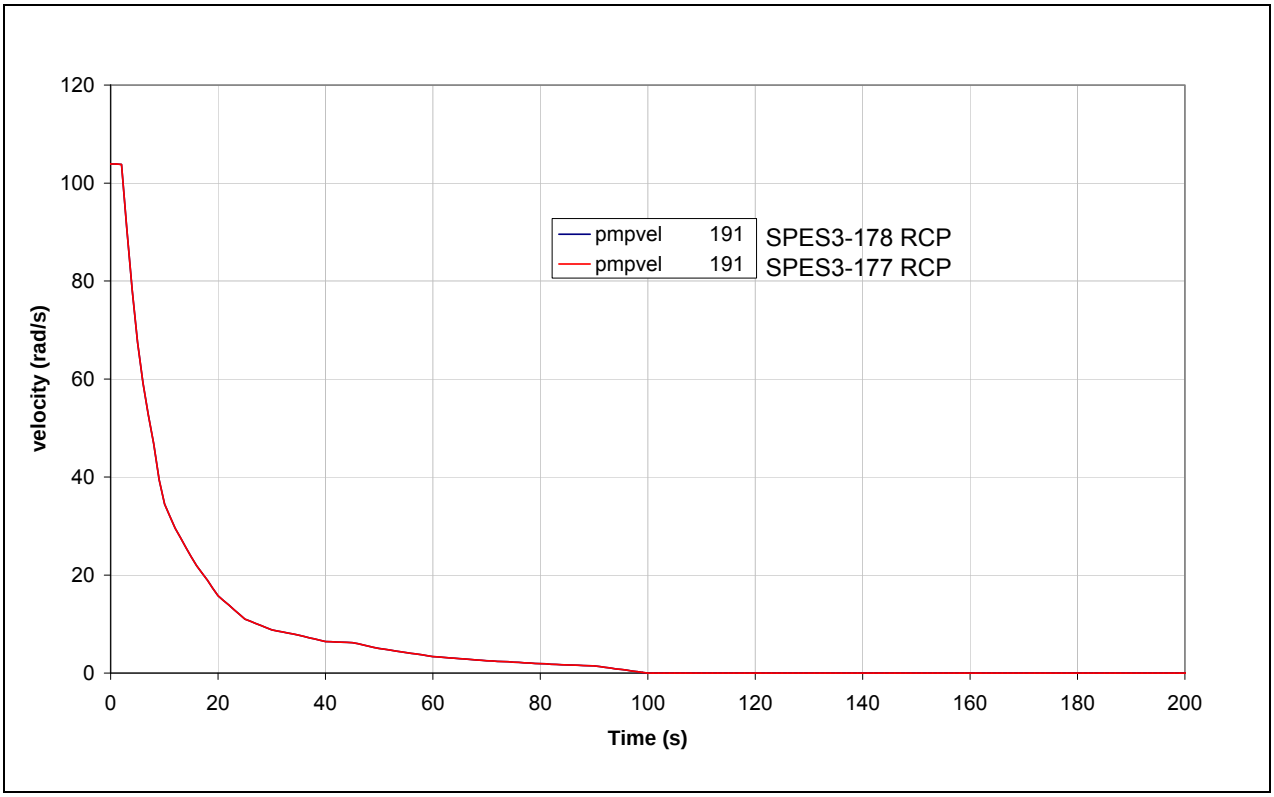

Fig.8. 2 – SPES3-178 and SPES3-177 RCP head (window)

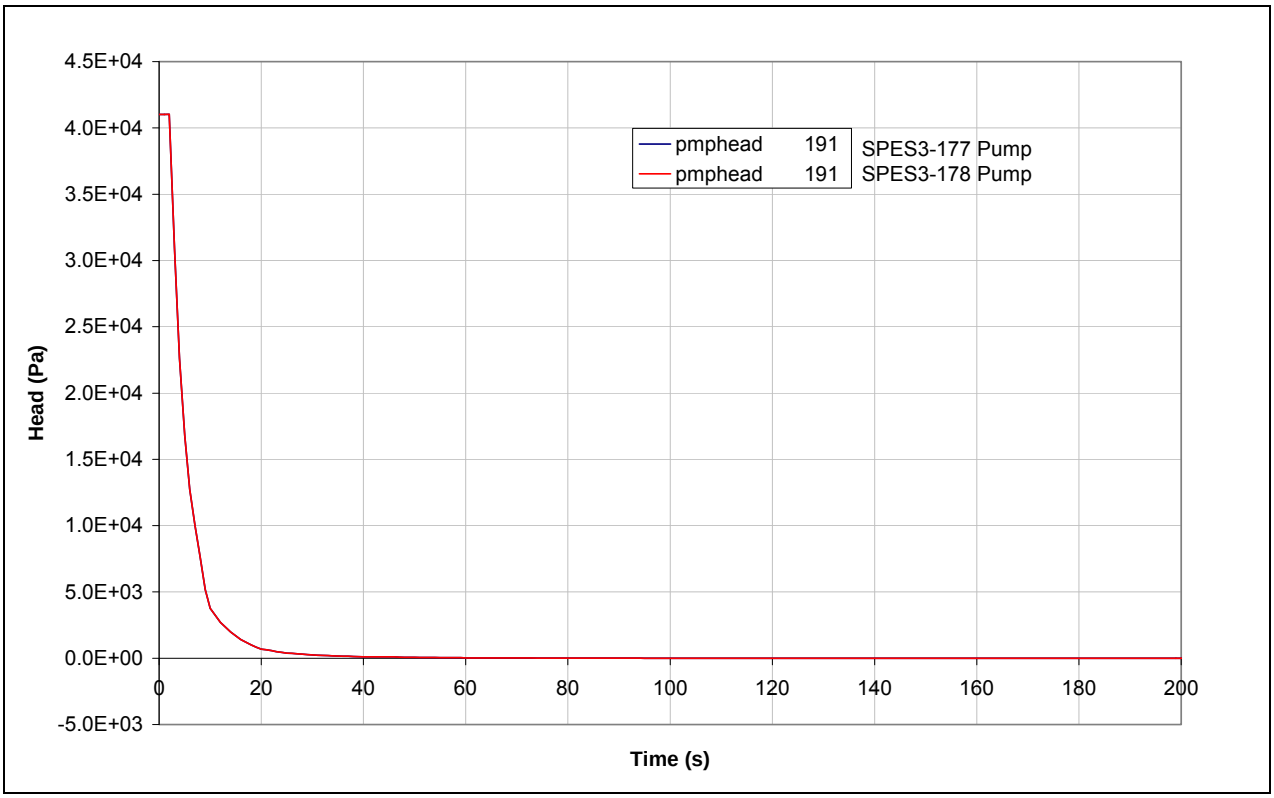

Fig.8. 3 – SPES3-178 and SPES3-177 RI-DC check valve mass flow (window)

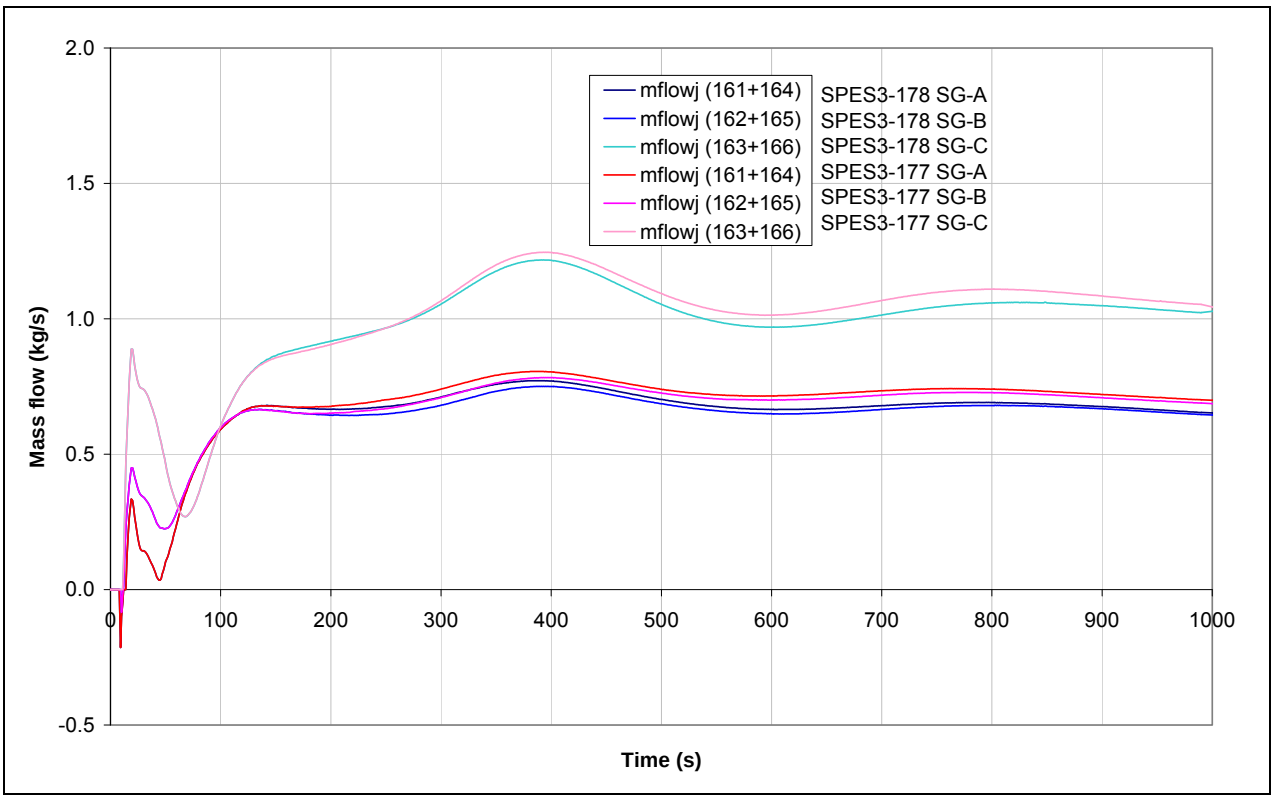

Fig.8. 4 – SPES3-178 and SPES3-177 RI-DC check valve mass flow (window)

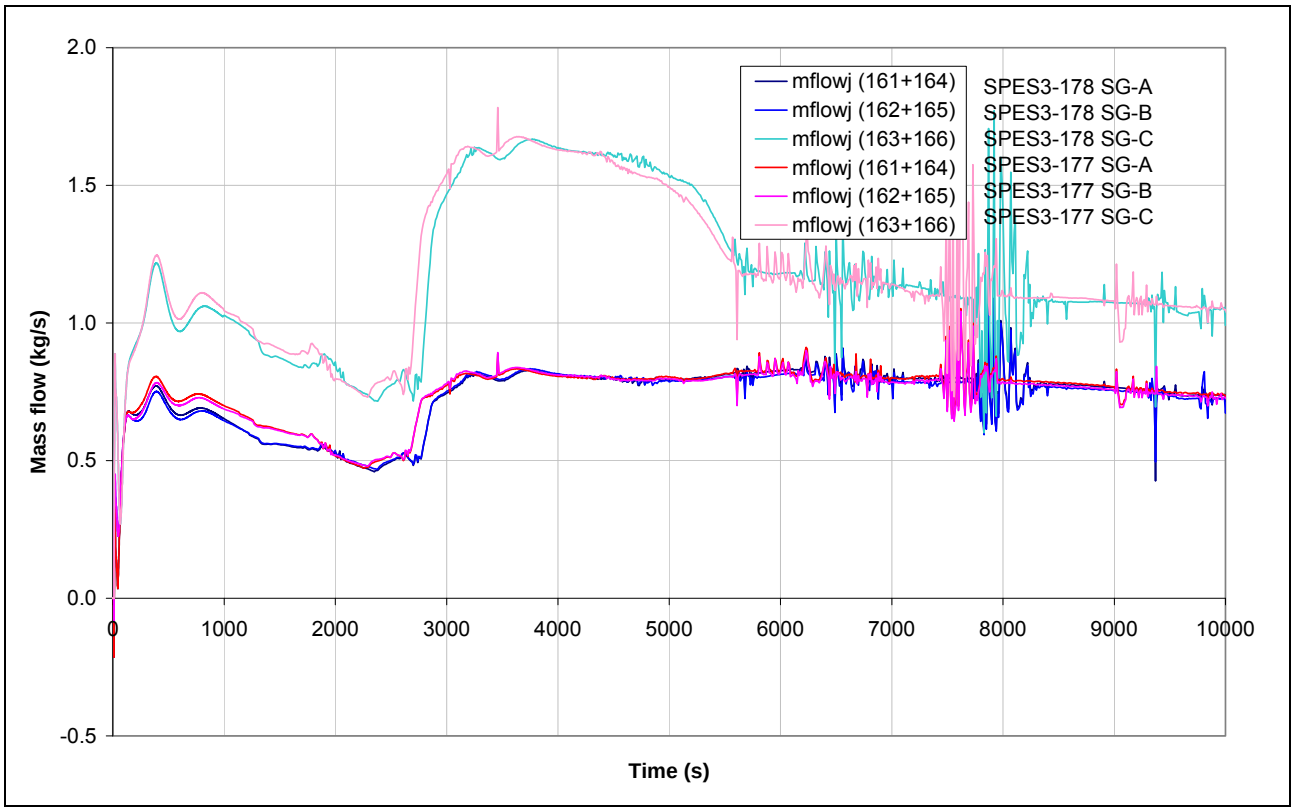

Fig.8. 5 – SPES3-178 and SPES3-177 RI-DC check valve mass flow

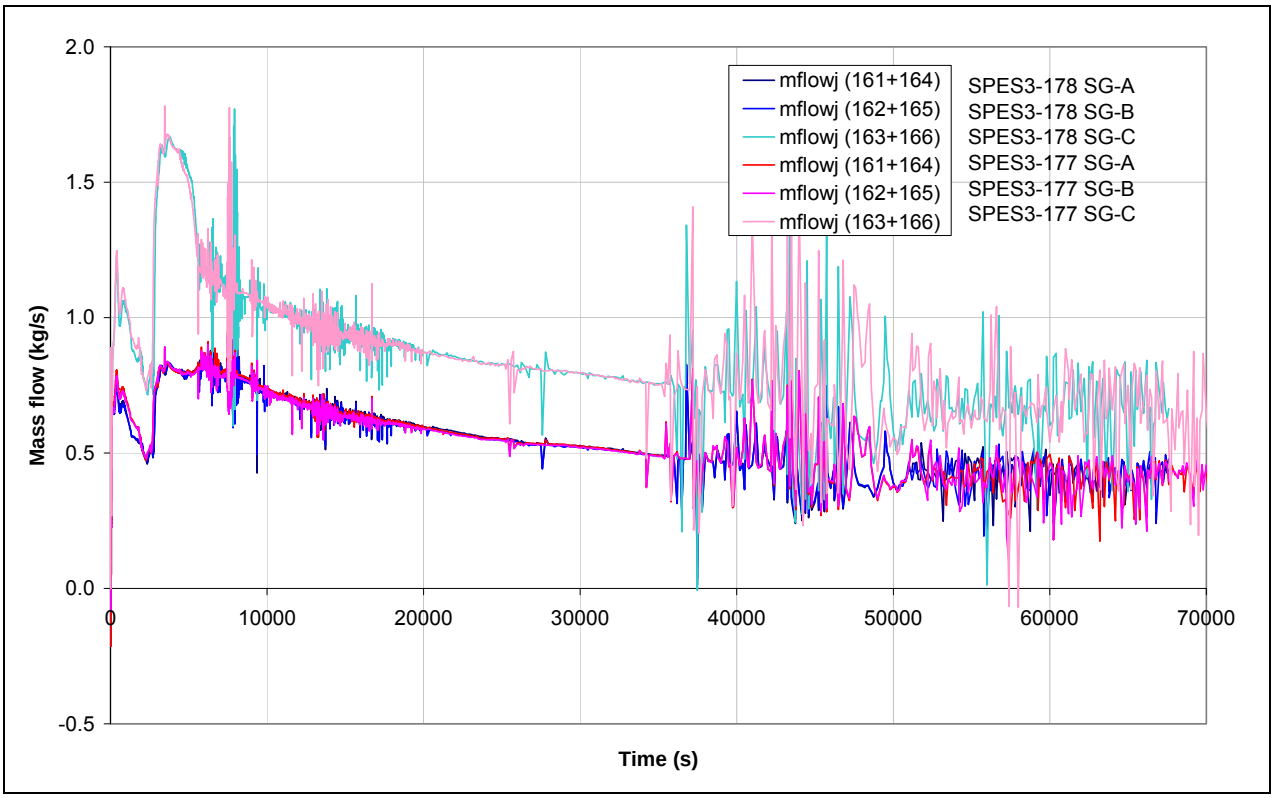

Fig.8. 6 – SPES3-178 and SPES3-177 Pump by-pass mass flow (window)

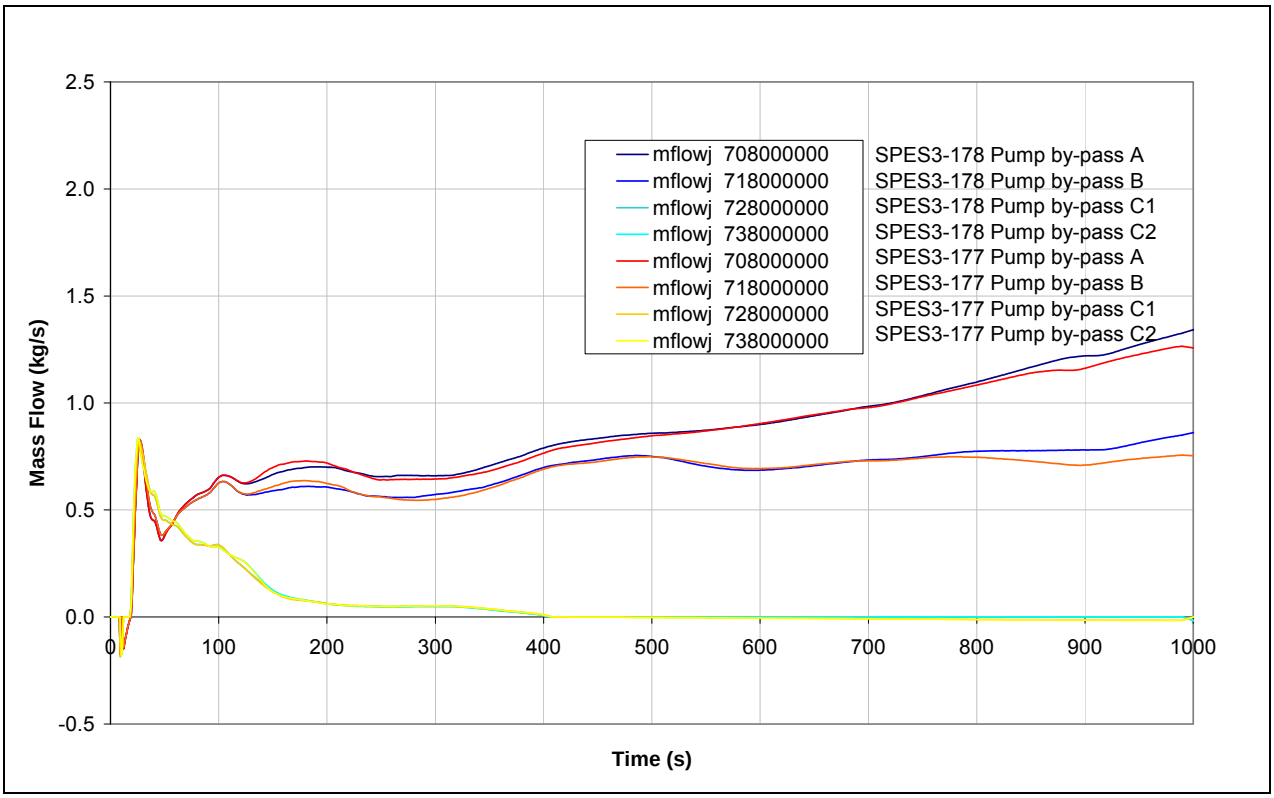

Fig.8. 7 – SPES3-178 and SPES3-177 Pump by-pass mass flow (window)

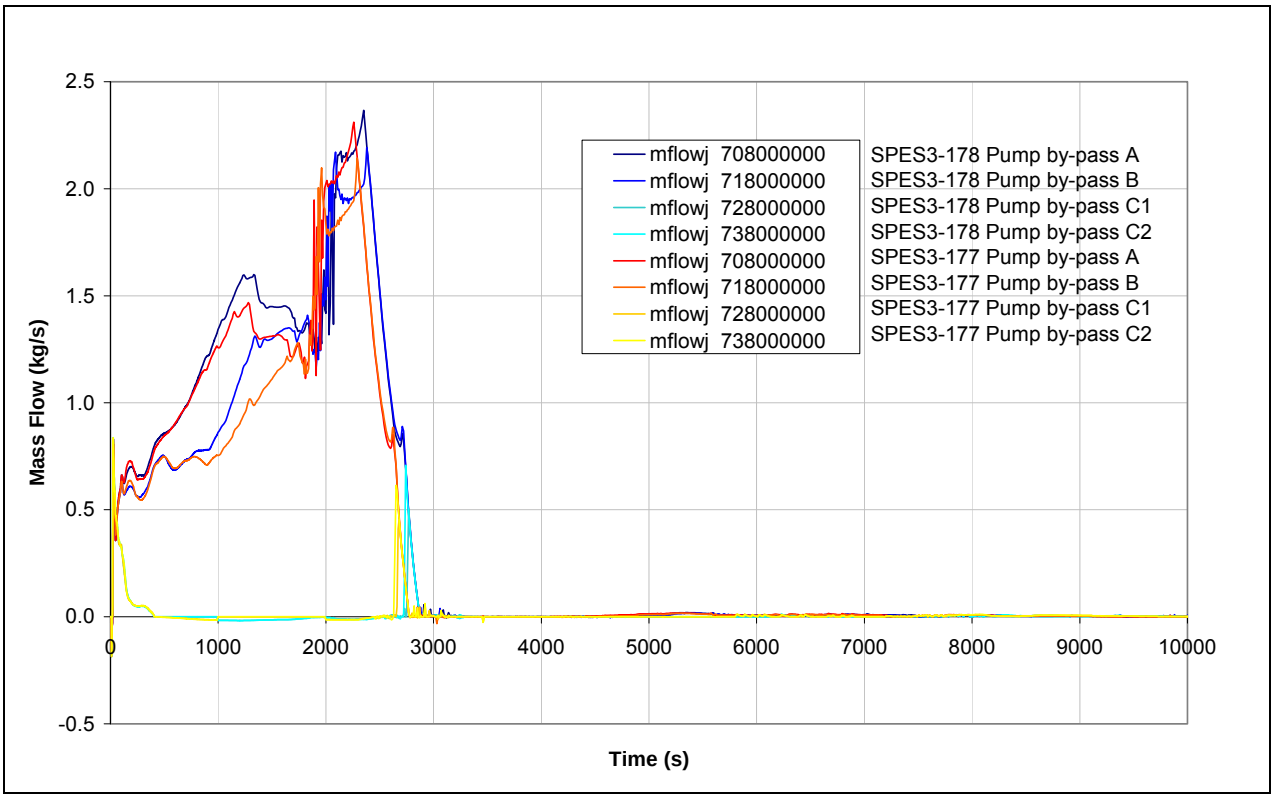

Fig.8. 8 – SPES3-178 and SPES3-177 SG power (window)

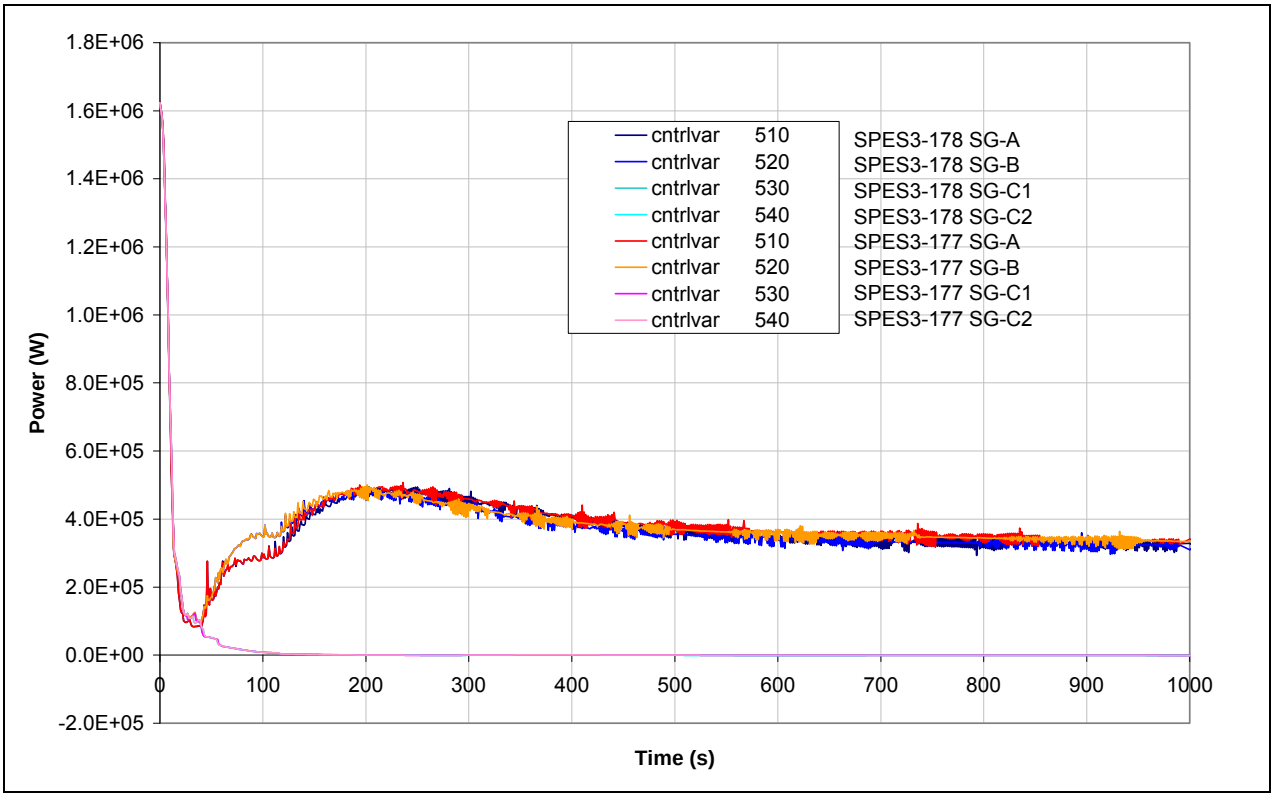

Fig.8. 9 – SPES3-178 and SPES3-177 Pump inlet liquid fraction (window)

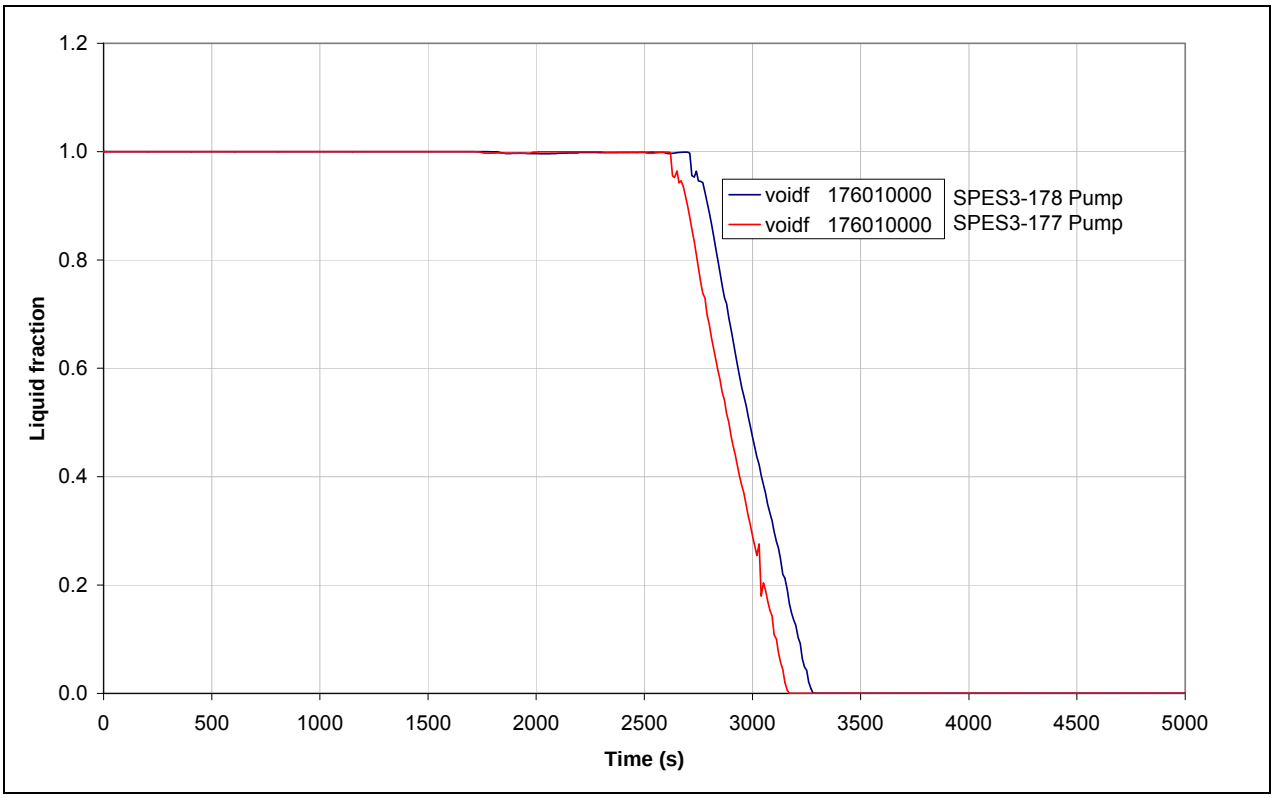

Fig.8. 10 – SPES3-178 and SPES3-177 SG secondary side mass flow (window)

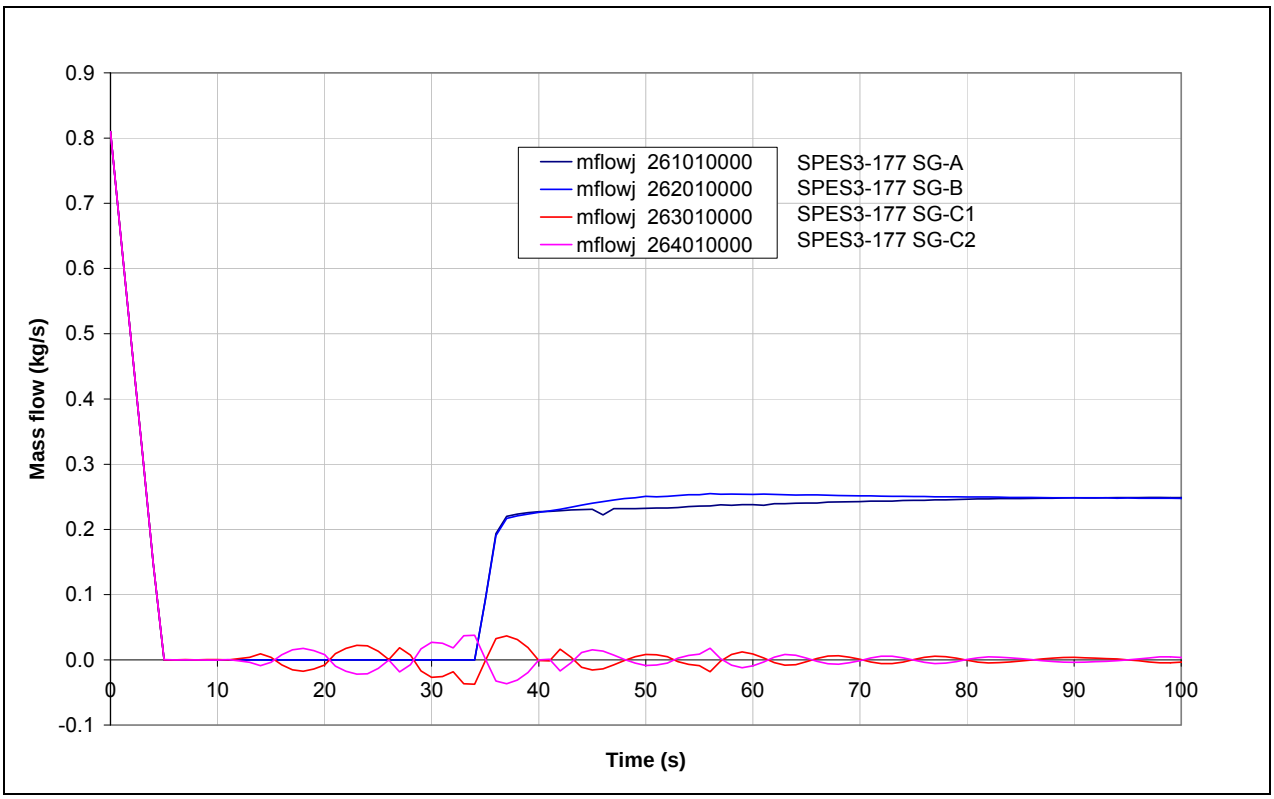

Fig.8. 11 – SPES3-178 and SPES3-177 SG secondary side mass flow (window)

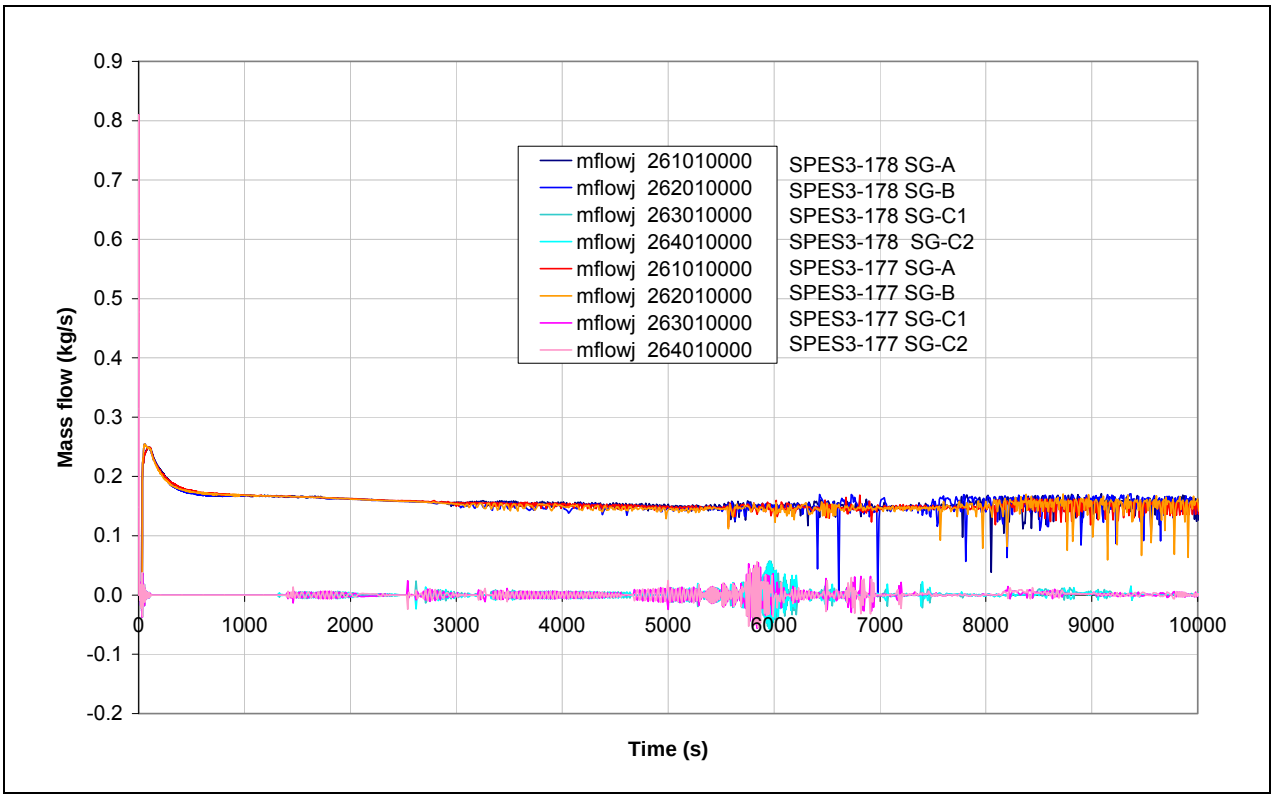

Fig.8. 12 – SPES3-178 and SPES3-177 SG secondary side mass flow

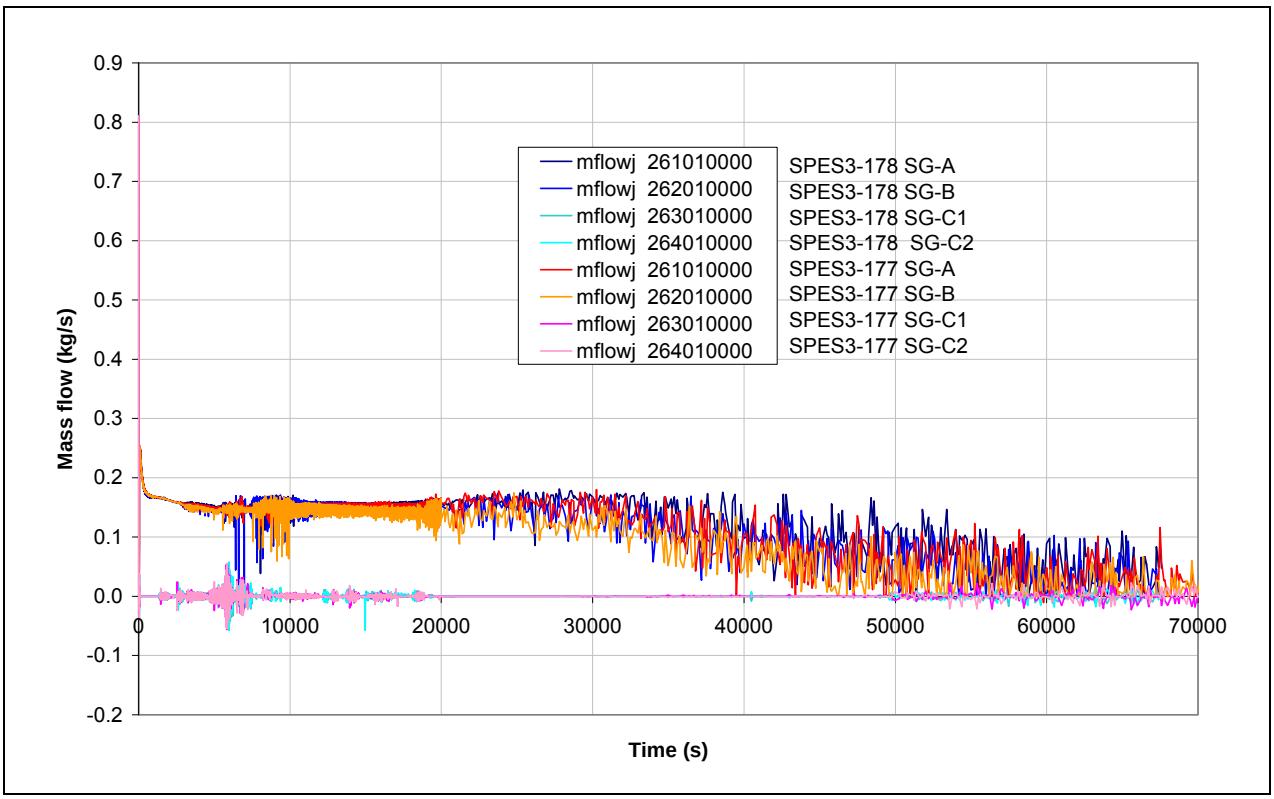

Fig.8. 13 – SPES3-178 and SPES3-177 Core and SG total power (window)

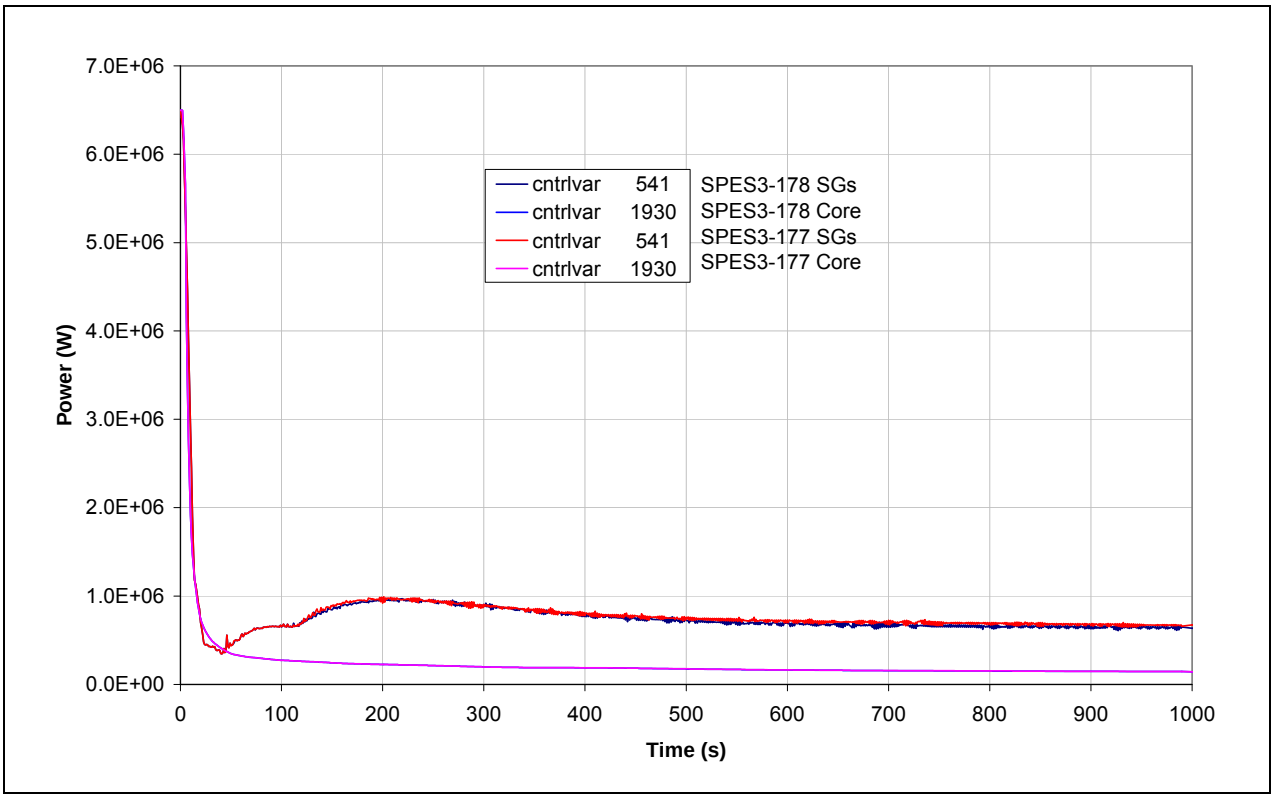

Fig.8. 14 – SPES3-178 and SPES3-177 Core and SG power (window)

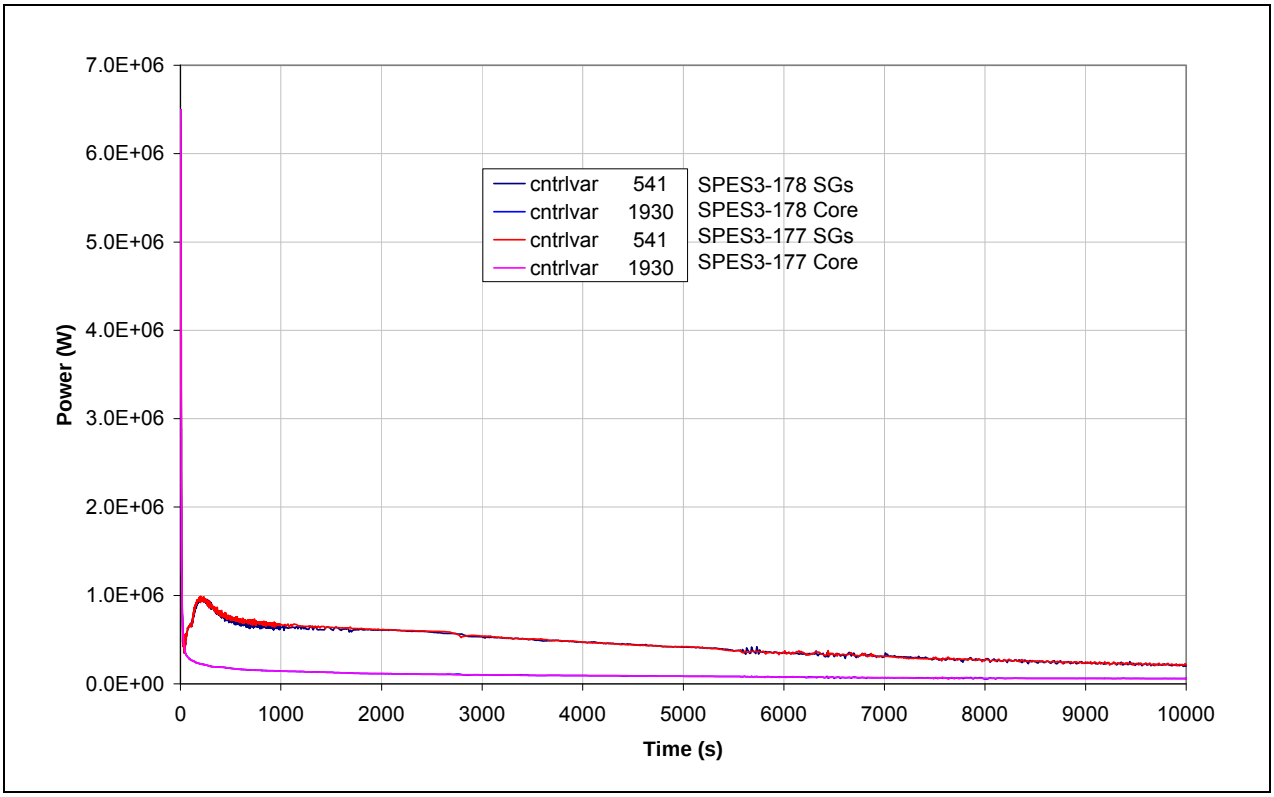

Fig.8. 15 – SPES3-178 and SPES3-177 Core and SG power

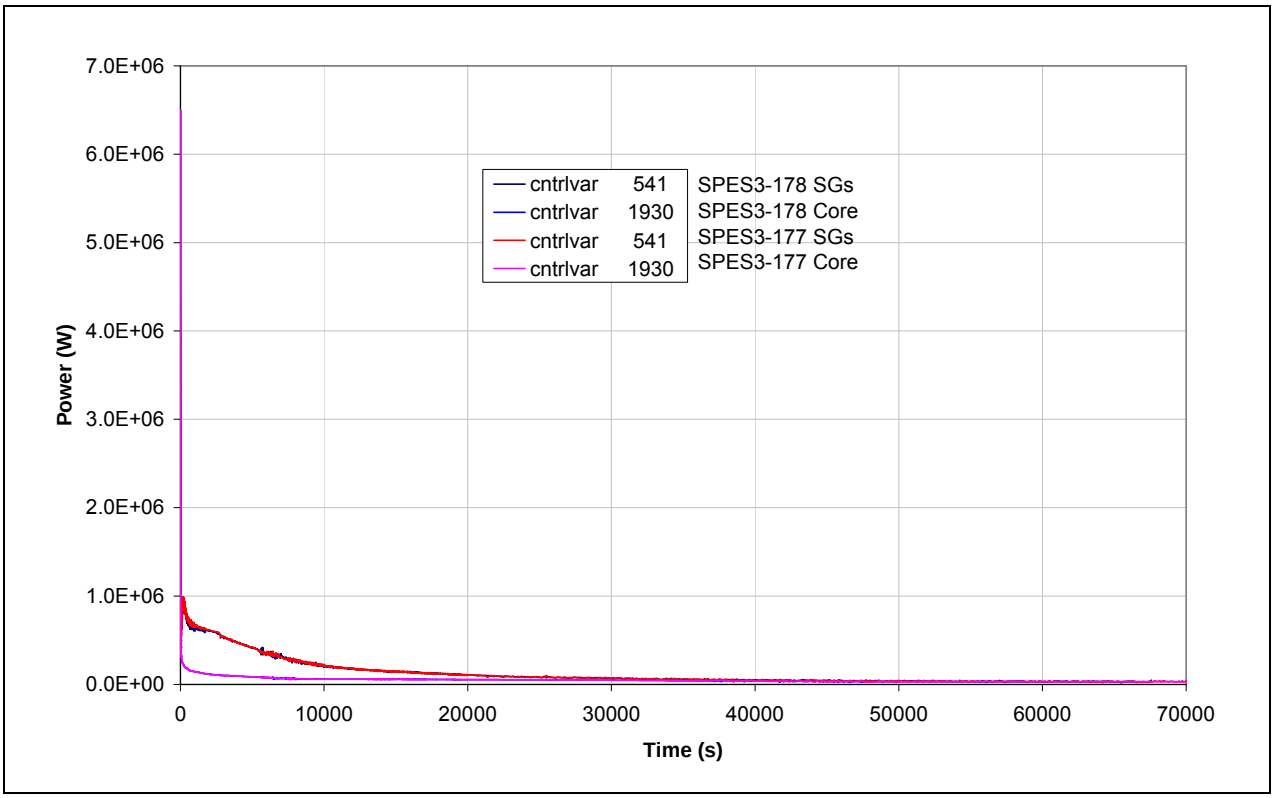

Fig.8. 16 – SPES3-178 and SPES3-177 SG secondary side collapsed level (window)

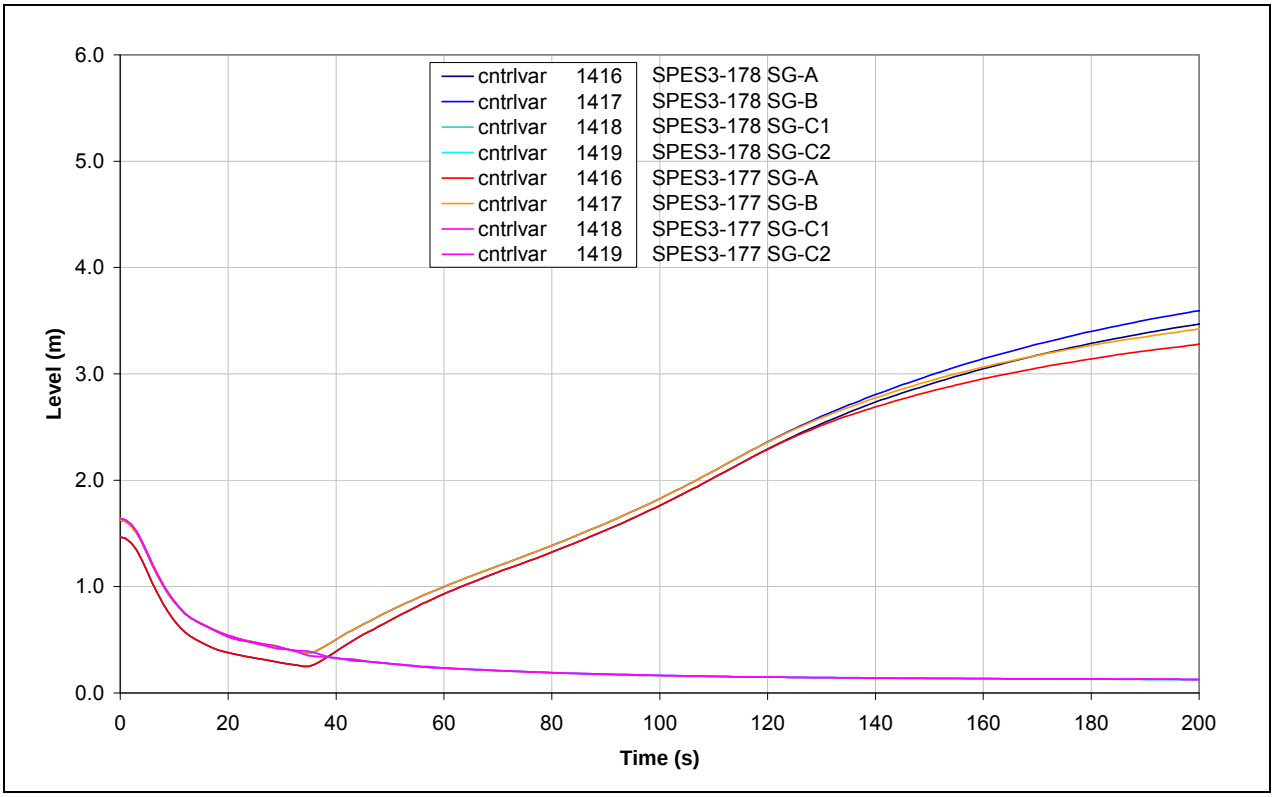

Fig.8. 17 – SPES3-178 and SPES3-177 SG secondary side collapsed level (window)

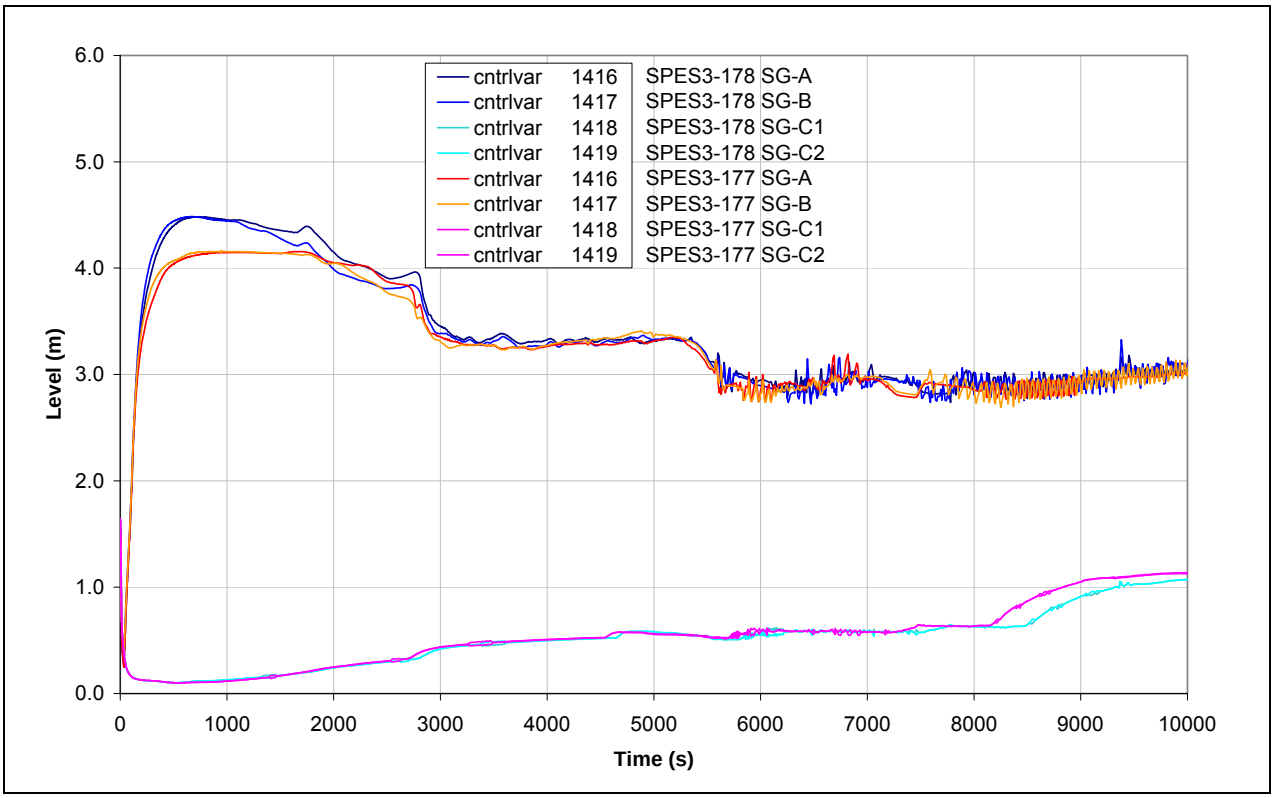

Fig.8. 18 – SPES3-178 and SPES3-177 SG secondary side collapsed level

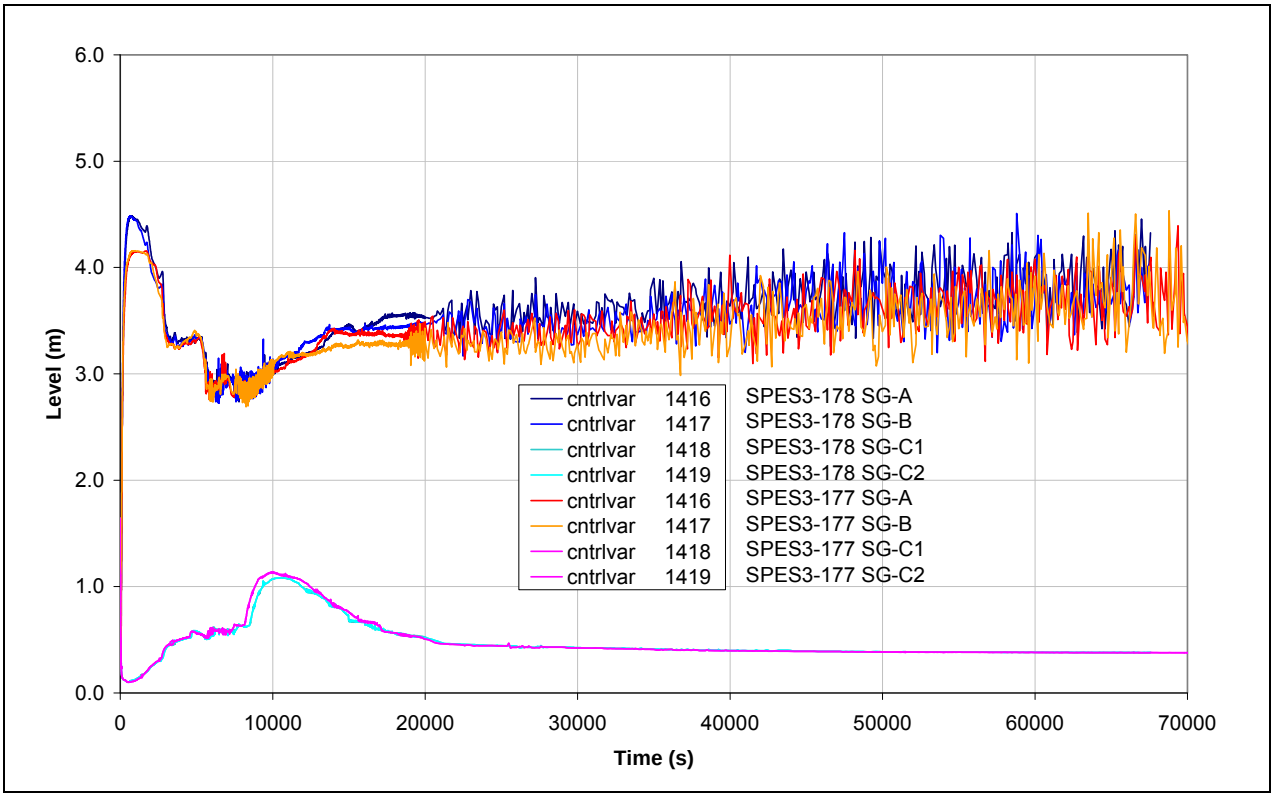

Fig.8. 19 – SPES3-178 and SPES3-177 EHRS cold leg mass flow (window)

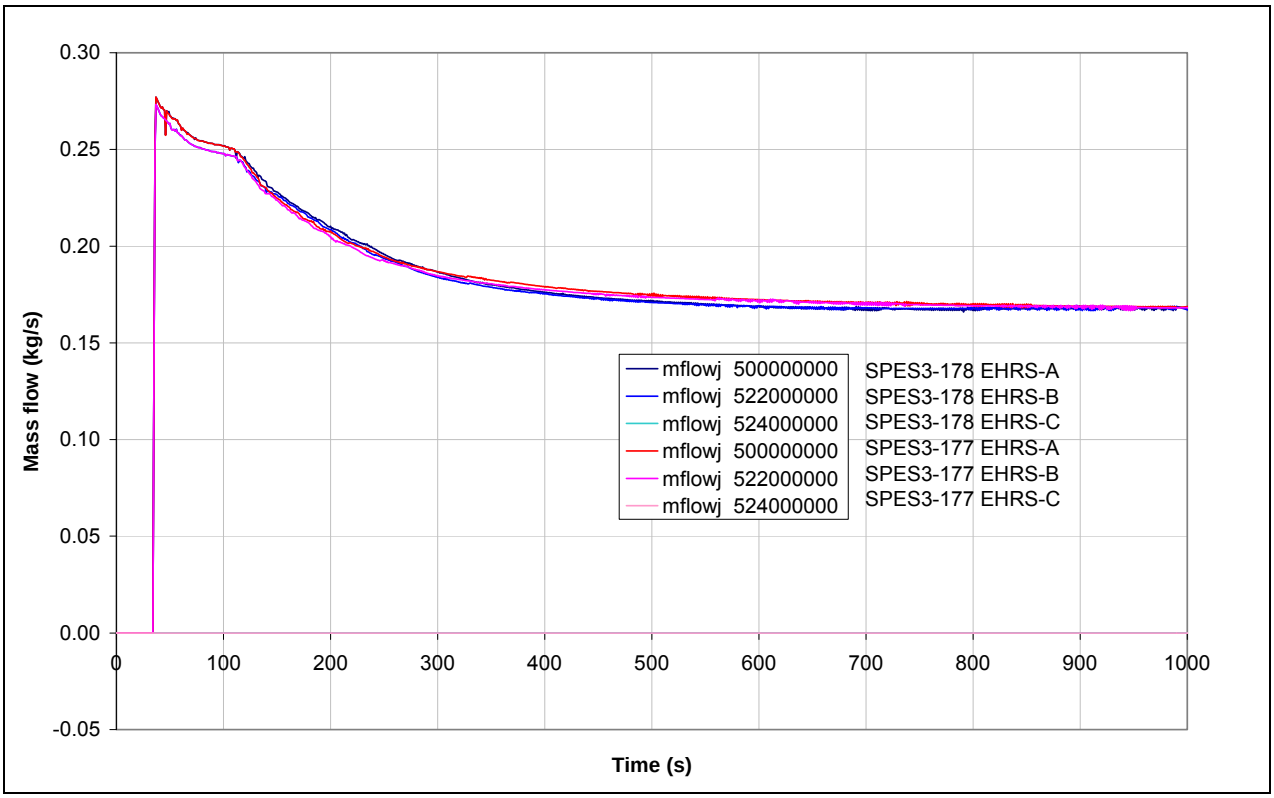

Fig.8. 20 – SPES3-178 and SPES3-177 EHRS cold leg mass flow

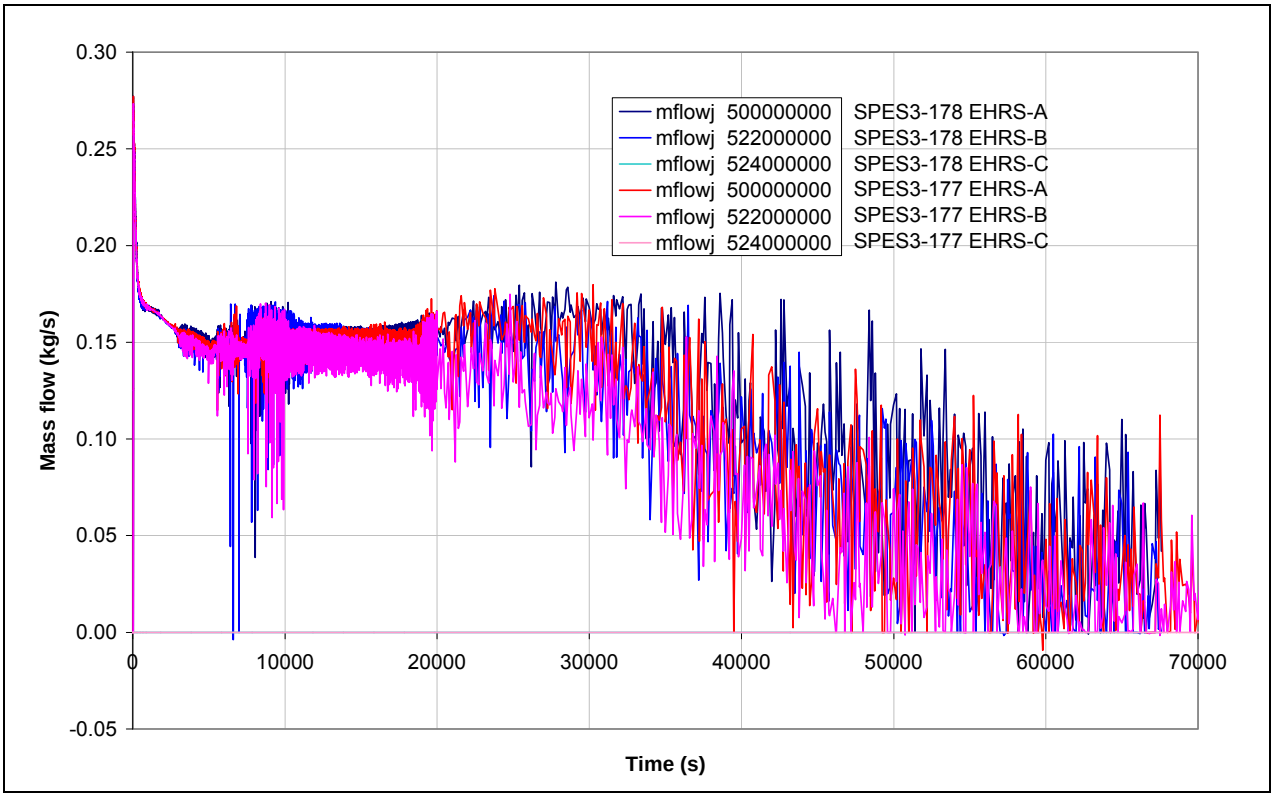

Fig.8. 21 – SPES3-178 and SPES3-177 EHRS power (window)

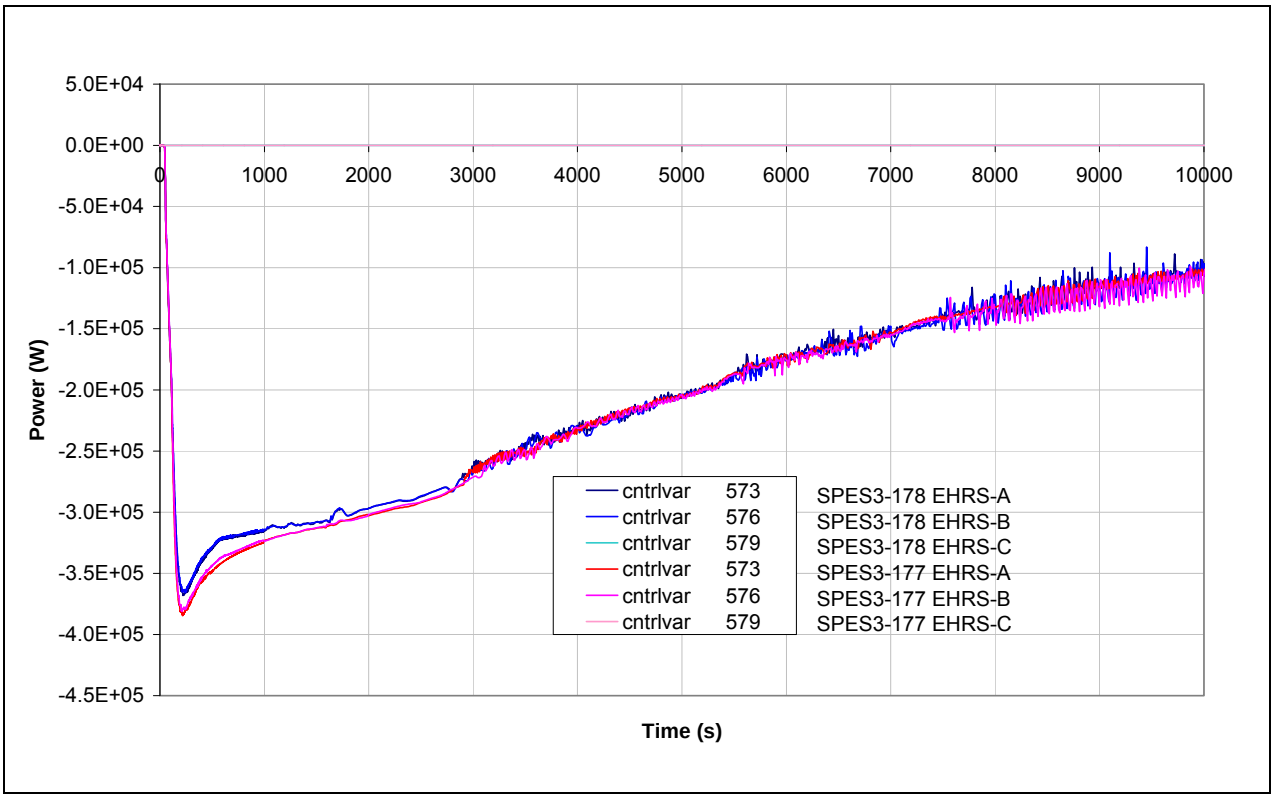

Fig.8. 22 – SPES3-178 and SPES3-177 EHRS power

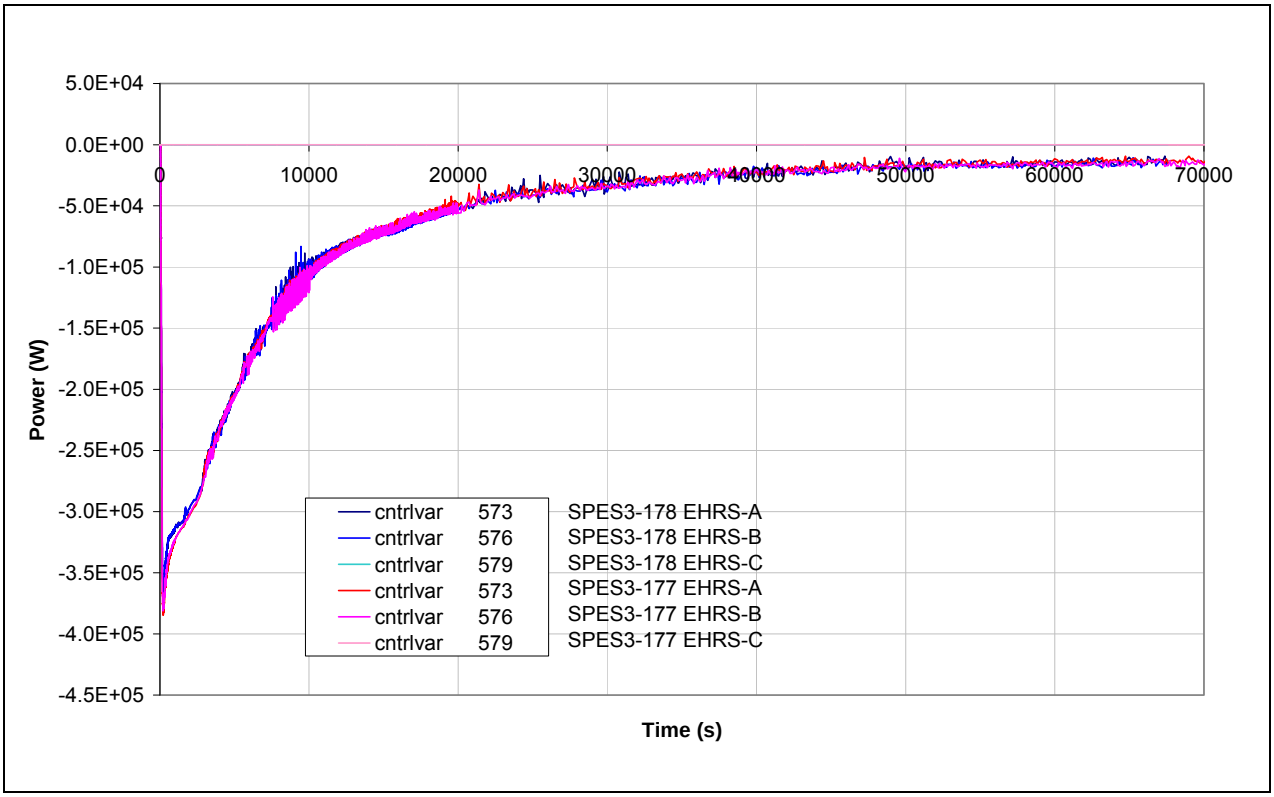

Fig.8. 23 – SPES3-178 and SPES3-177 RWST temperature

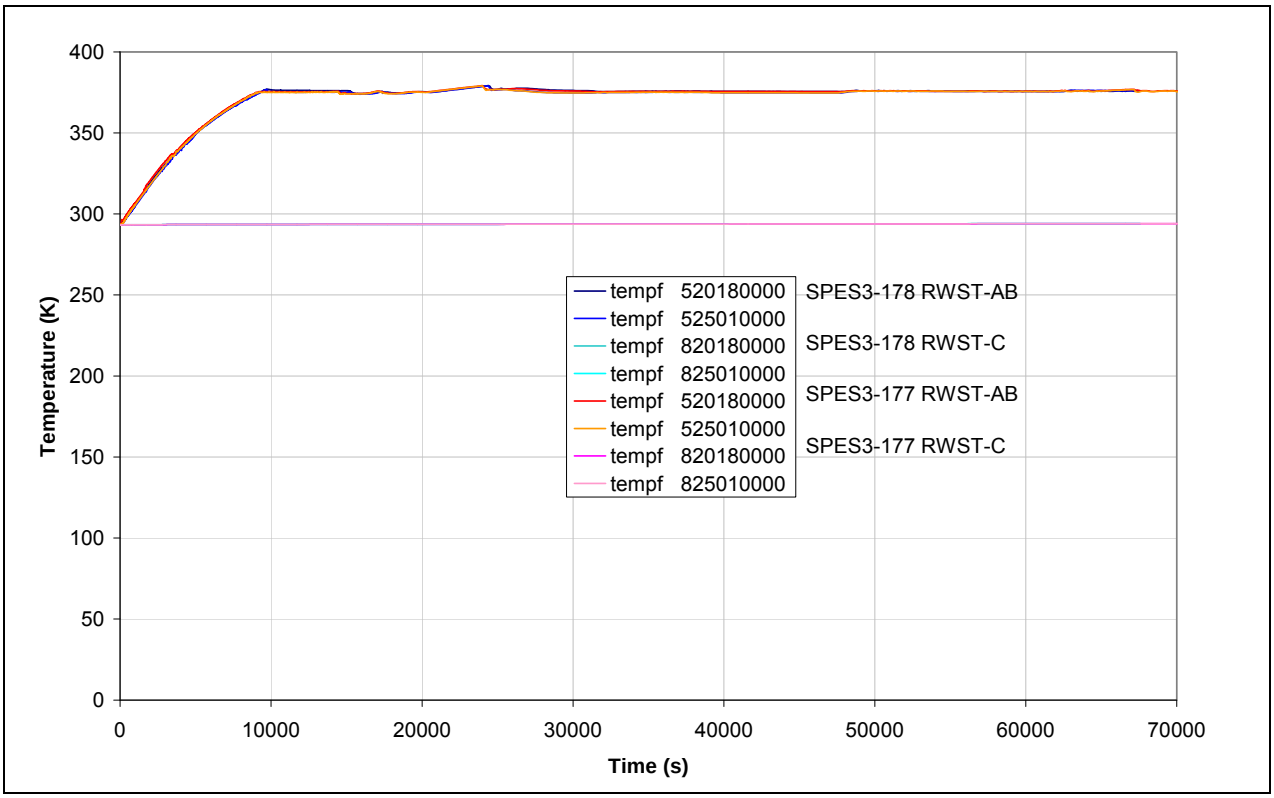

Fig.8. 24 – SPES3-178 and SPES3-177 RWST mass

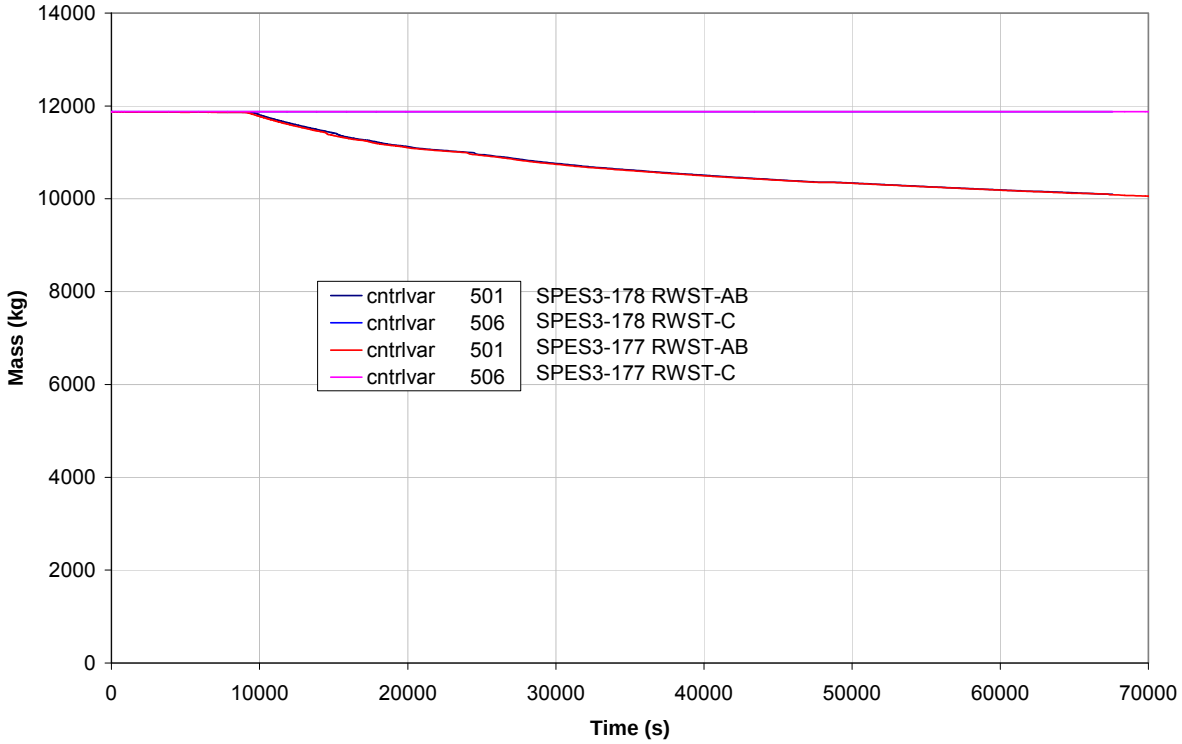

Fig.8. 25 – SPES3-178 and SPES3-177 Core mass flow (window)

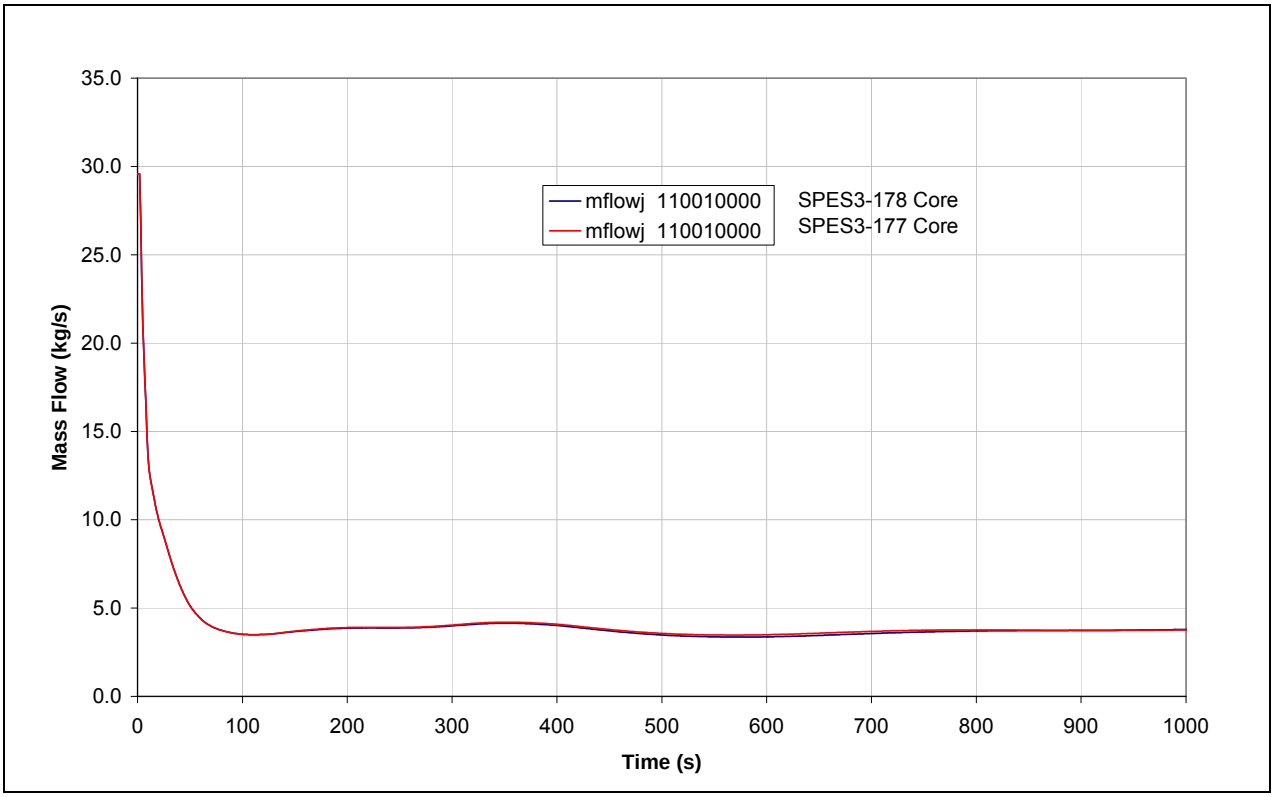

Fig.8. 26 – SPES3-178 and SPES3-177 Core mass flow (window)

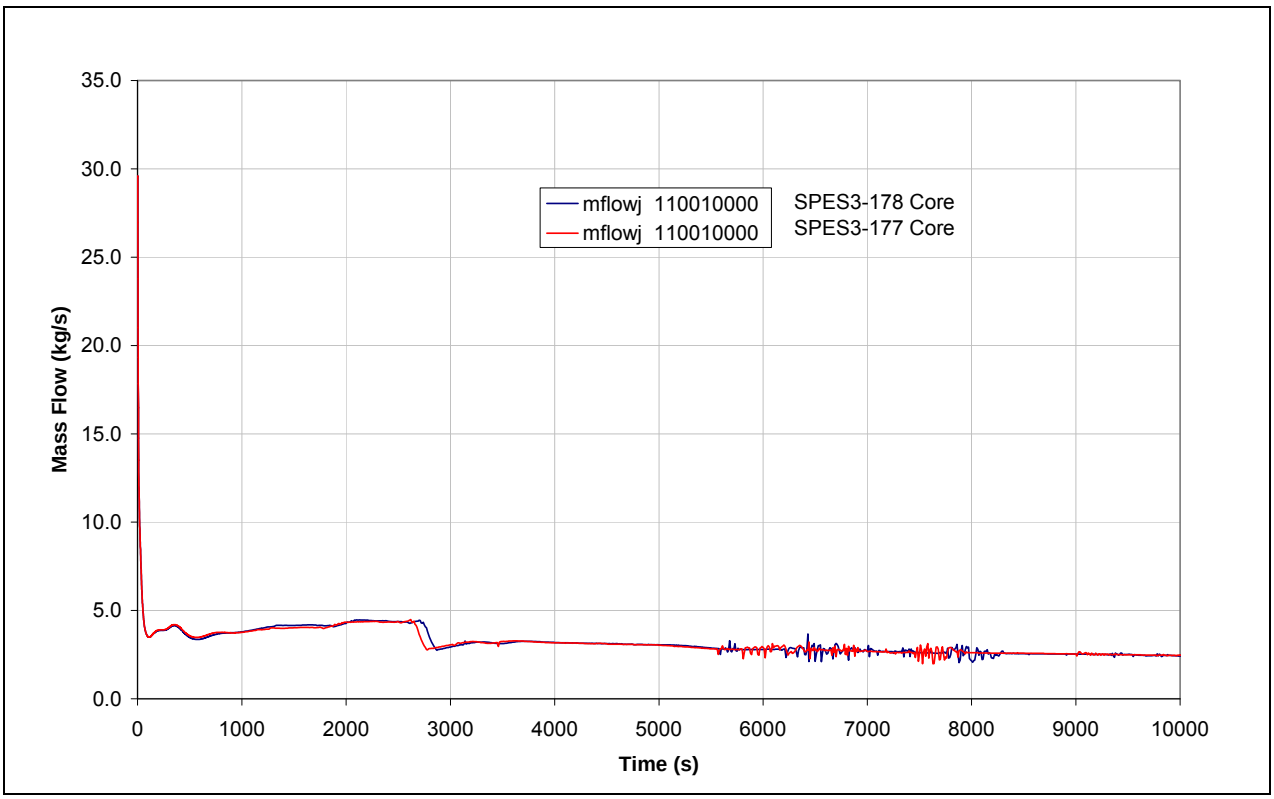

Fig.8. 27 – SPES3-178 and SPES3-177 Core mass flow

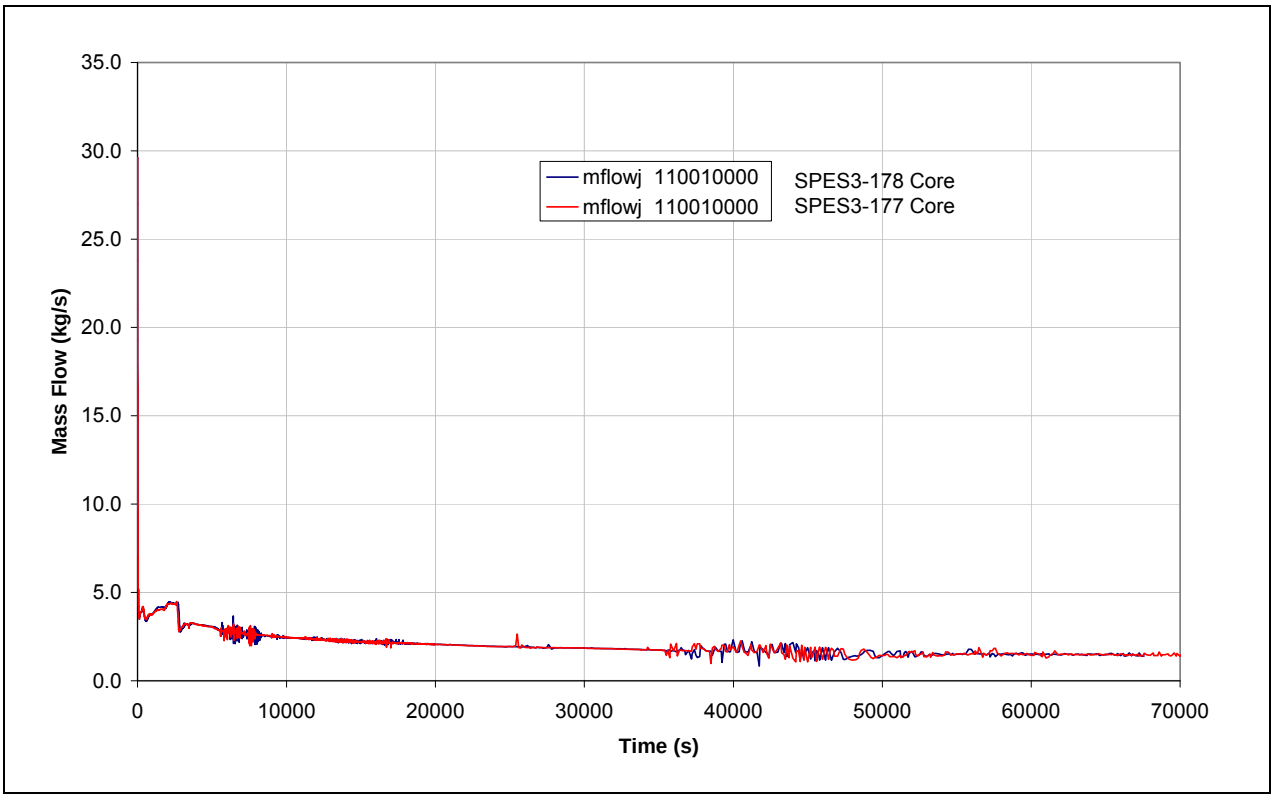

Fig.8. 28 – SPES3-178 and SPES3-177 SG secondary side outlet pressure (window)

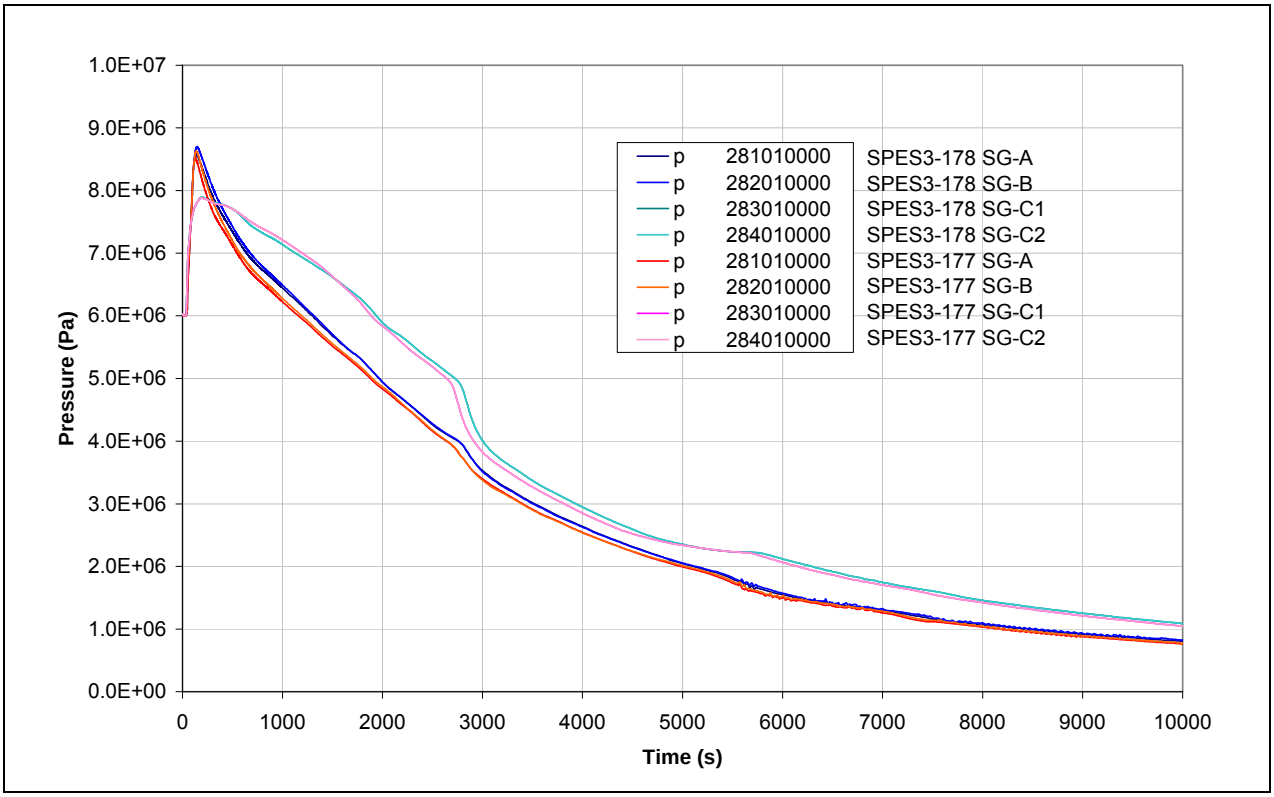

Fig.8. 29 – SPES3-178 and SPES3-177 SG secondary side outlet pressure

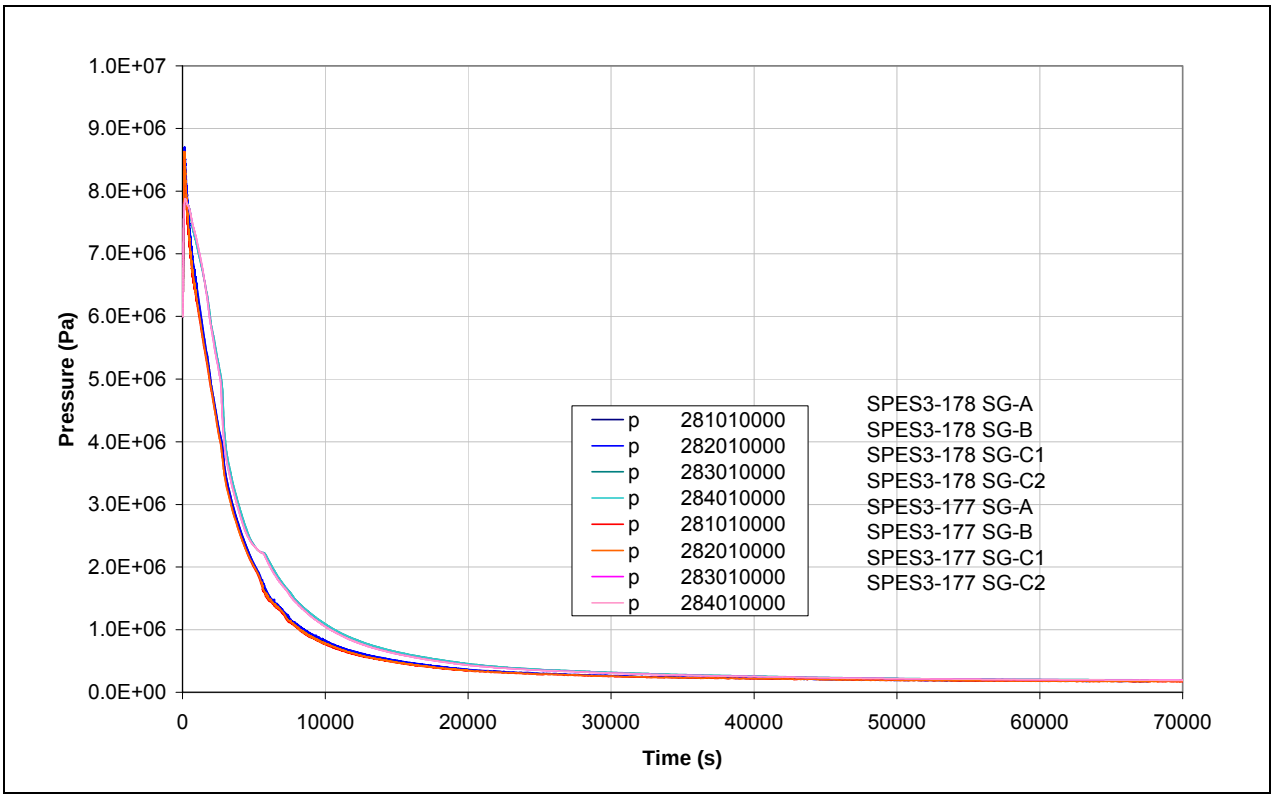

Fig.8. 30 – SPES3-178 and SPES3-177 PRZ pressure (window)

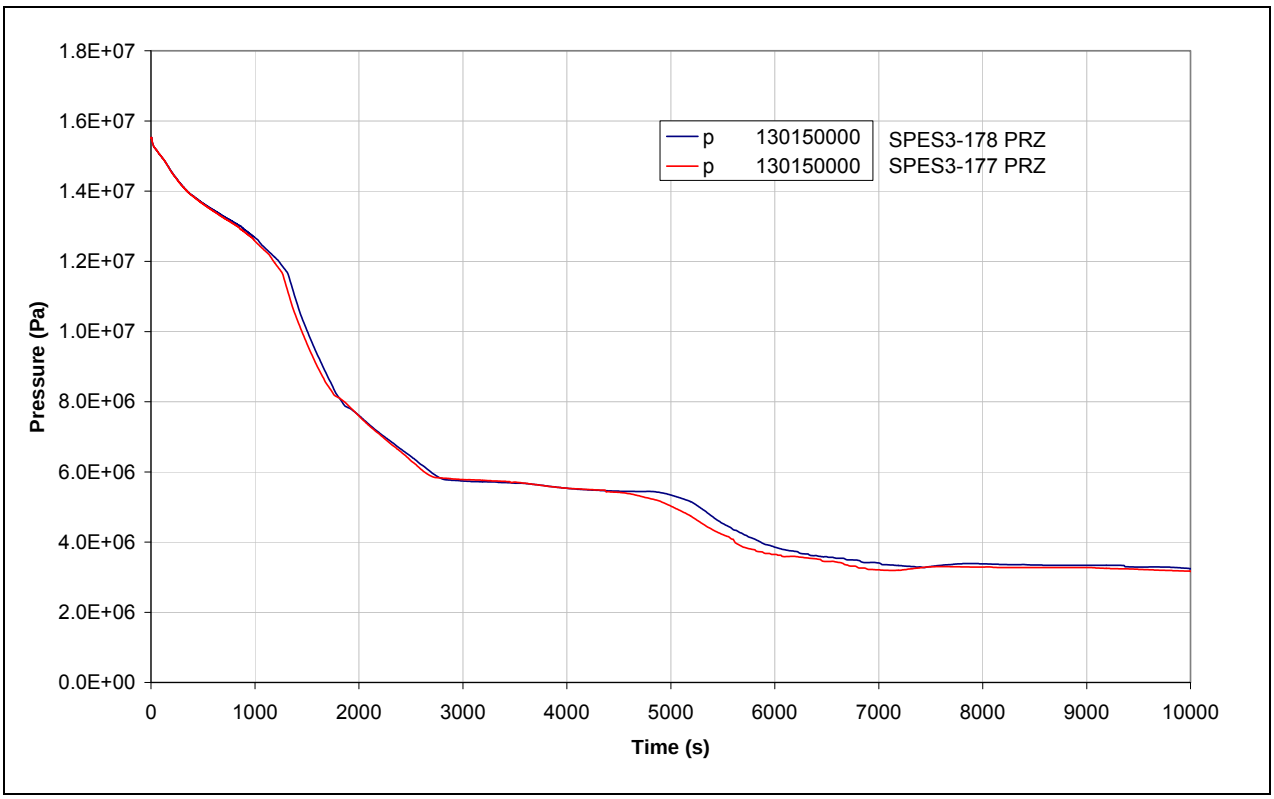

Fig.8. 31 – SPES3-178 and SPES3-177 PRZ pressure

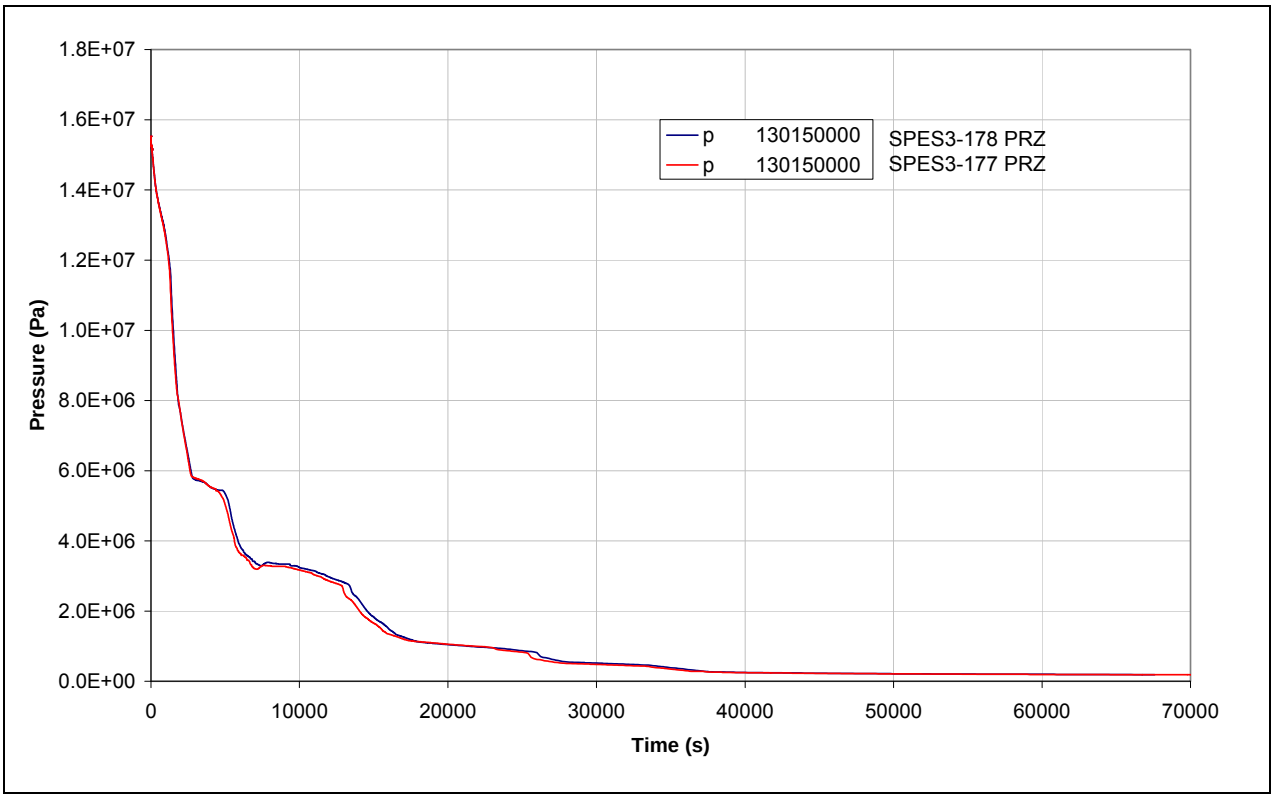

Fig.8. 32 – SPES3-178 and SPES3-177 Core inlet and outlet temperature (window)

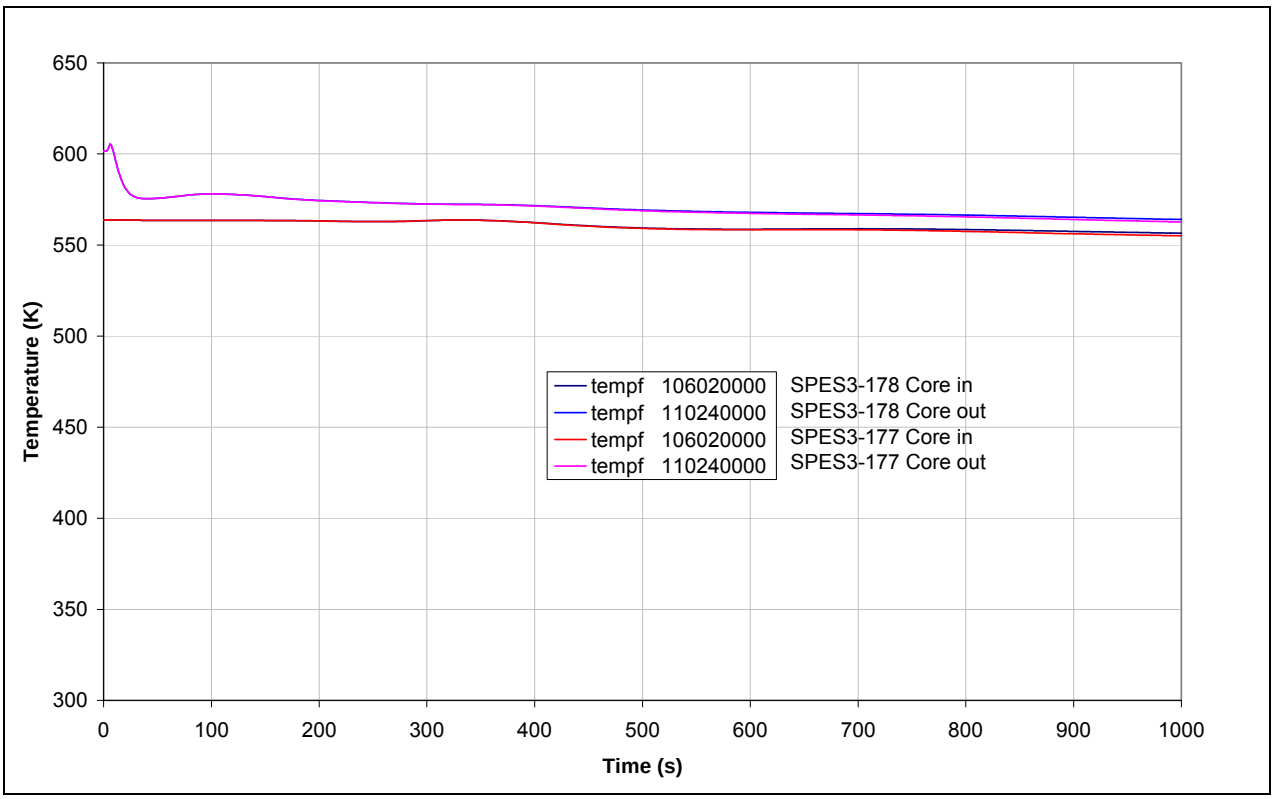

Fig.8. 33 – SPES3-178 and SPES3-177 Core inlet, outlet and saturation temperature

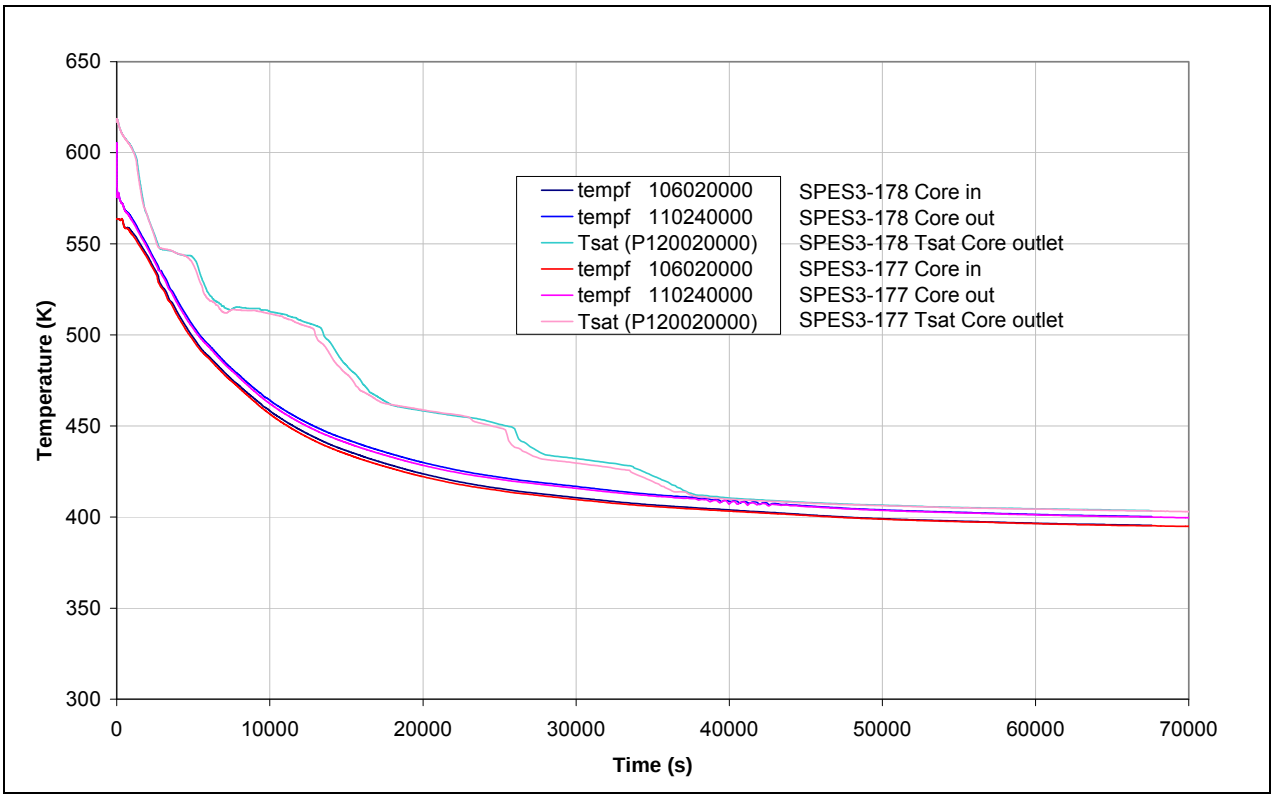

Fig.8. 34 – SPES3-178 and SPES3-177 Core liquid fraction

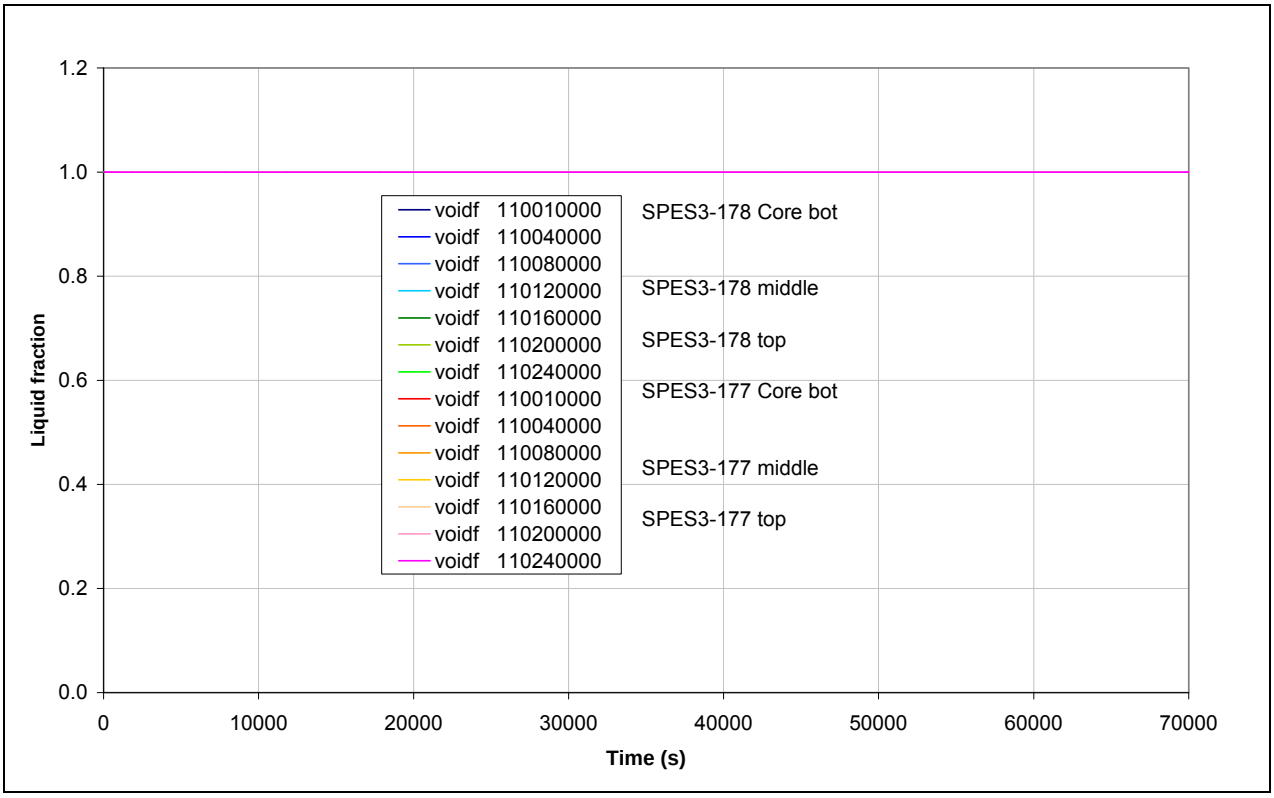

Fig.8. 35 – SPES3-178 and SPES3-177 PRZ level (window)

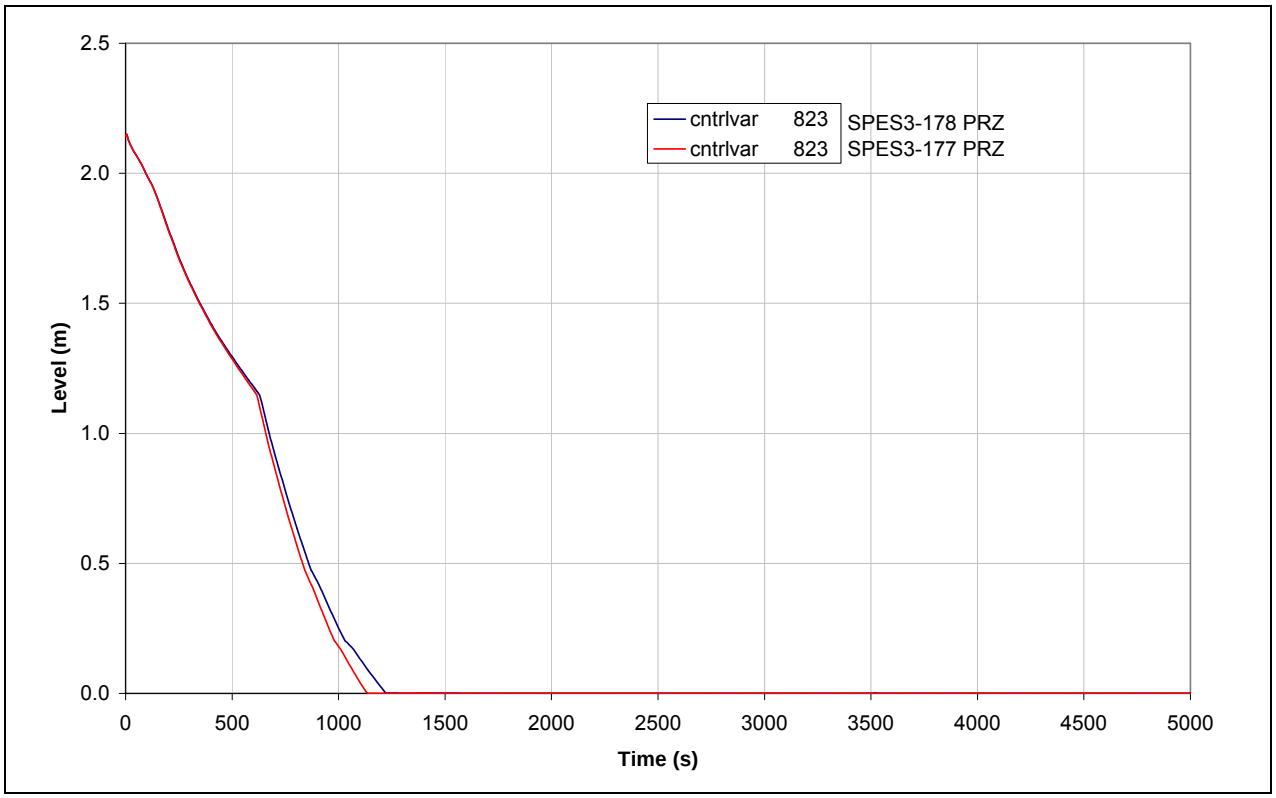

Fig.8. 36 – SPES3-178 and SPES3-177 RPV down comer level

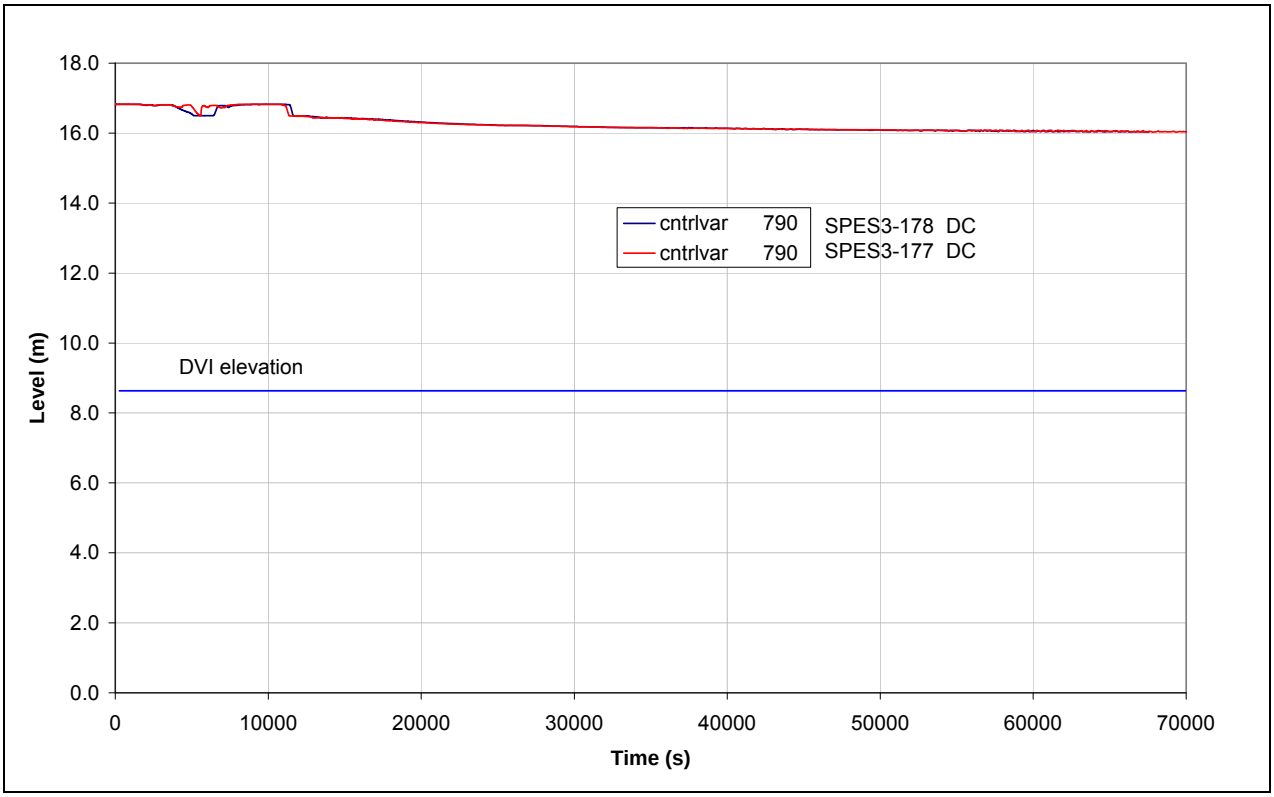

Note: DVI elevation referred to RPV bottom.

Fig.8. 37 – SPES3-178 and SPES3-177 EBT injection mass flow (window)

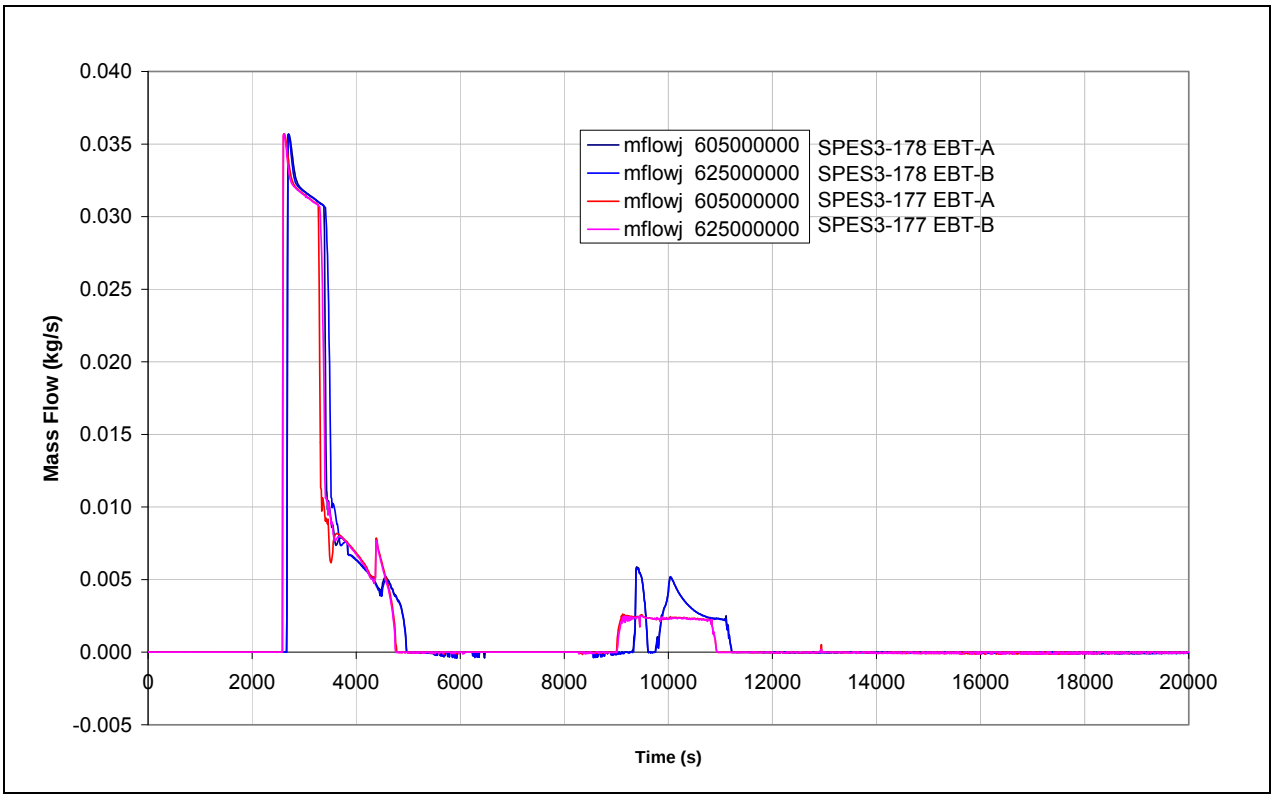

Fig.8. 38 – SPES3-178 and SPES3-177 EBT to RPV balance line mass flow (window)

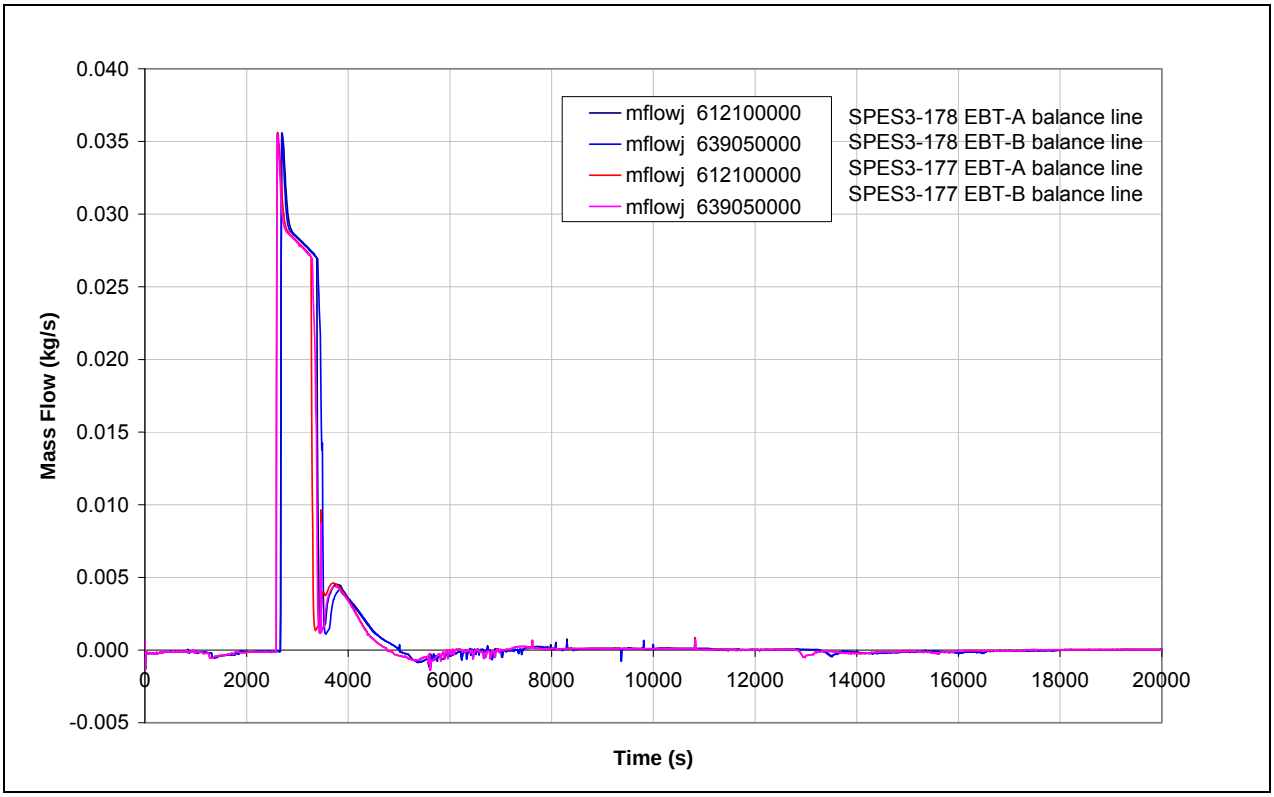

Fig.8. 39 – SPES3-178 and SPES3-177 DVI mass flow

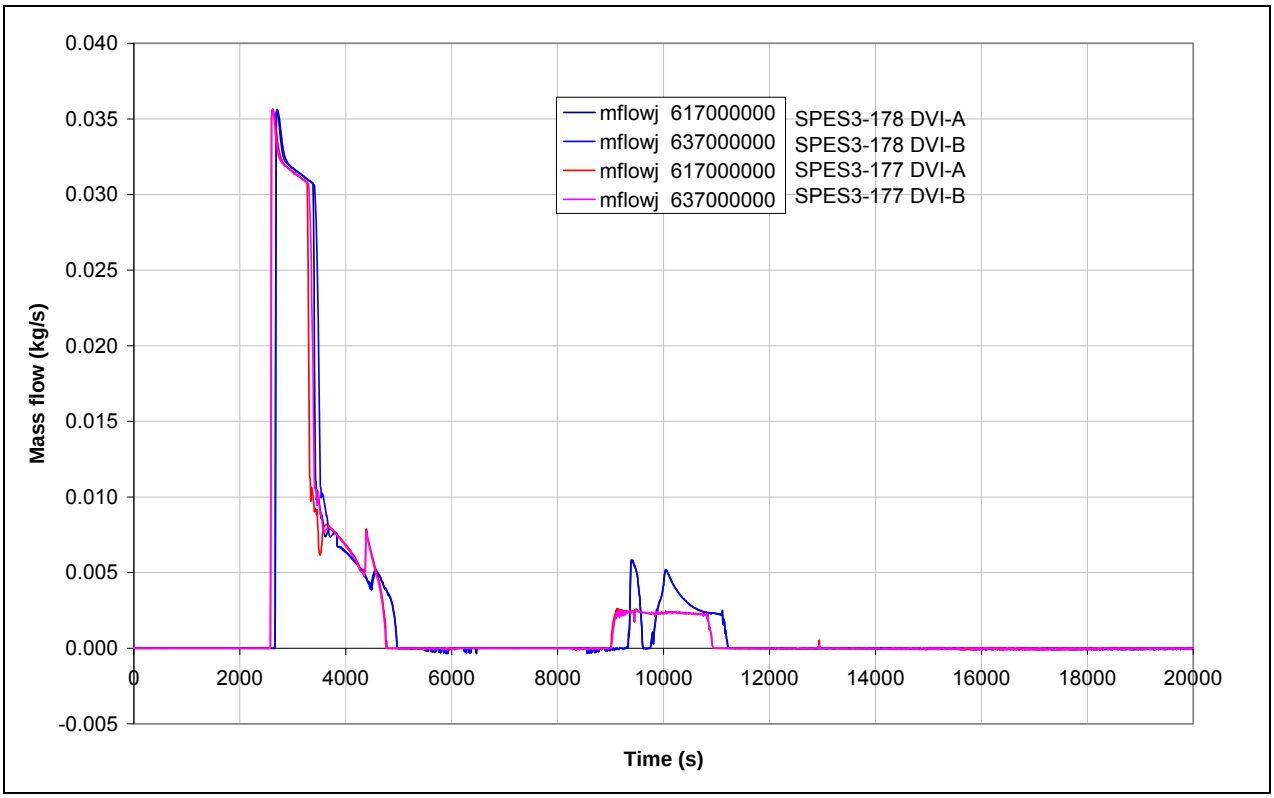

Fig.8. 40 – SPES3-178 and SPES3-177 EBT level

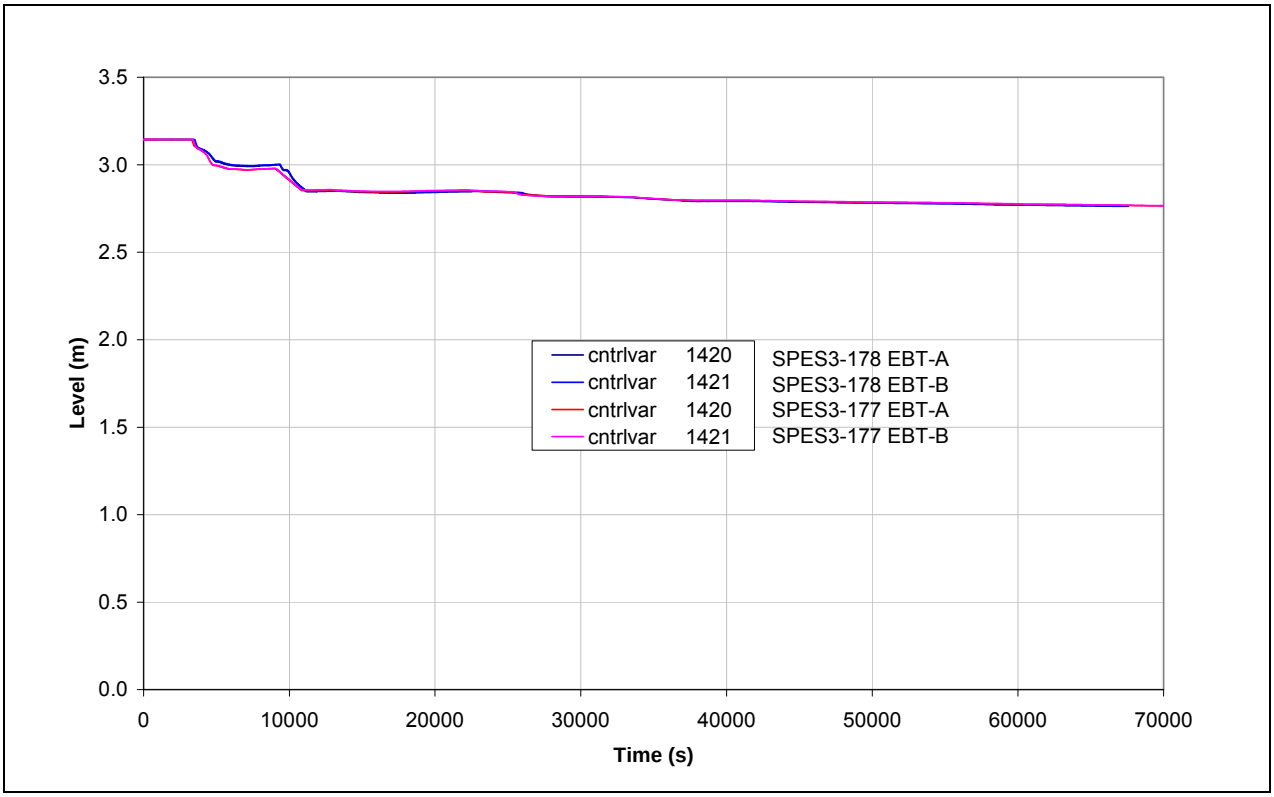

Fig.8. 41 – SPES3-178 and SPES3-177 RPV mass

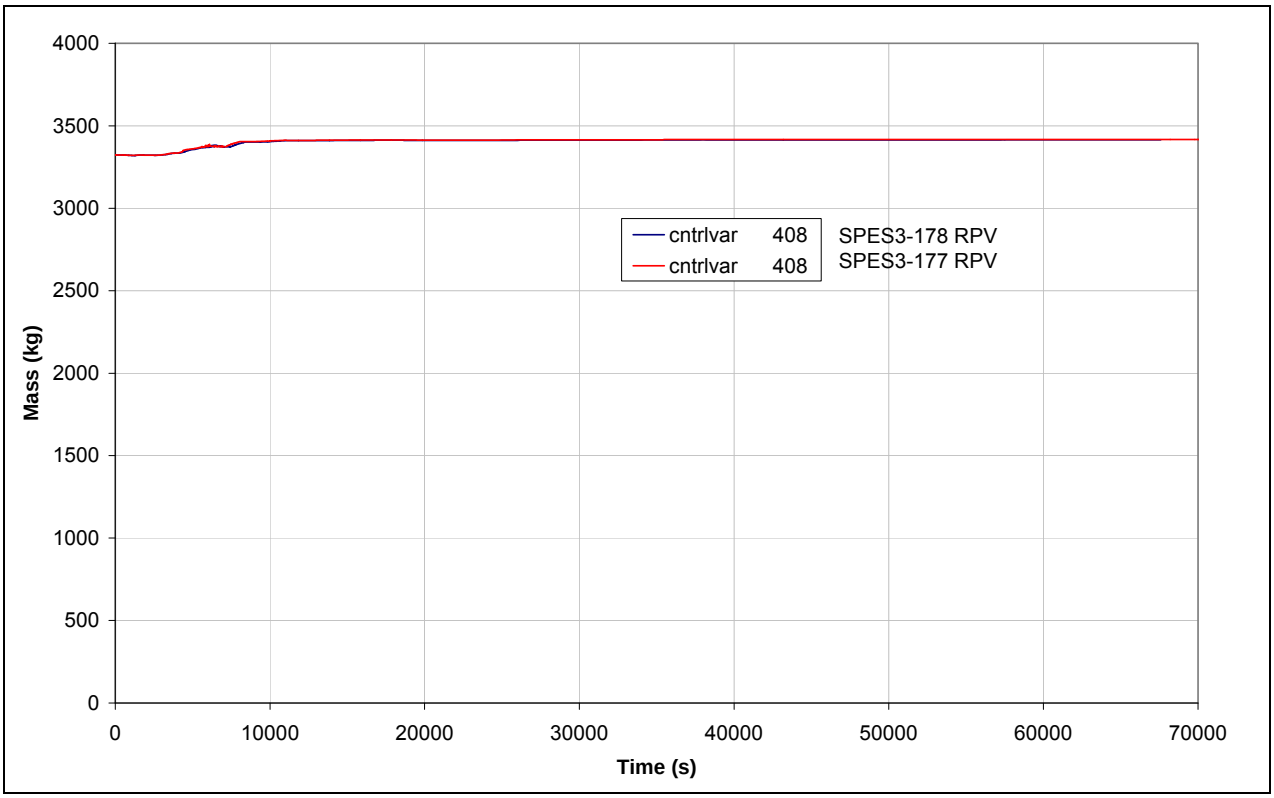

Fig.8. 42 – SPES3-178 and SPES3-177 Core heater rod surface temperature –normal rod (window)

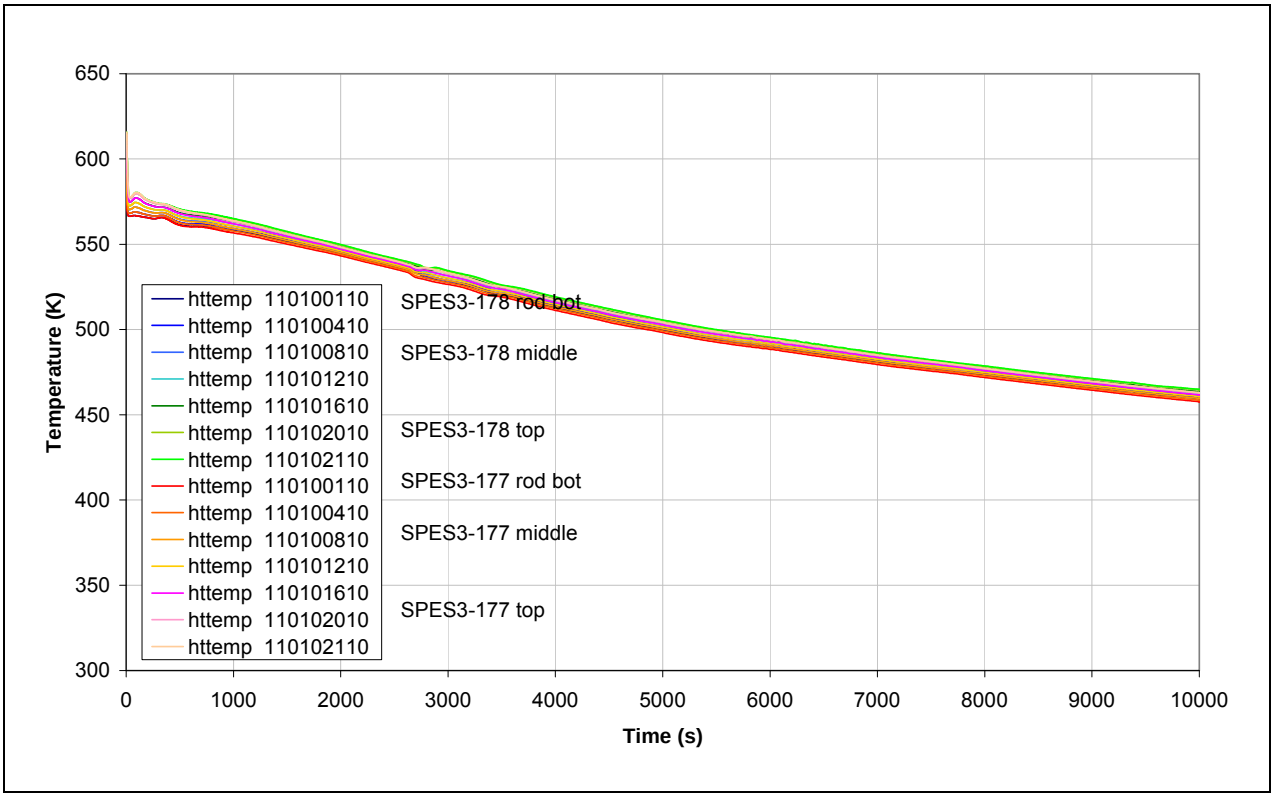

Fig.8. 43 – SPES3-178 and SPES3-177 Core heater rod surface temperature –normal rod

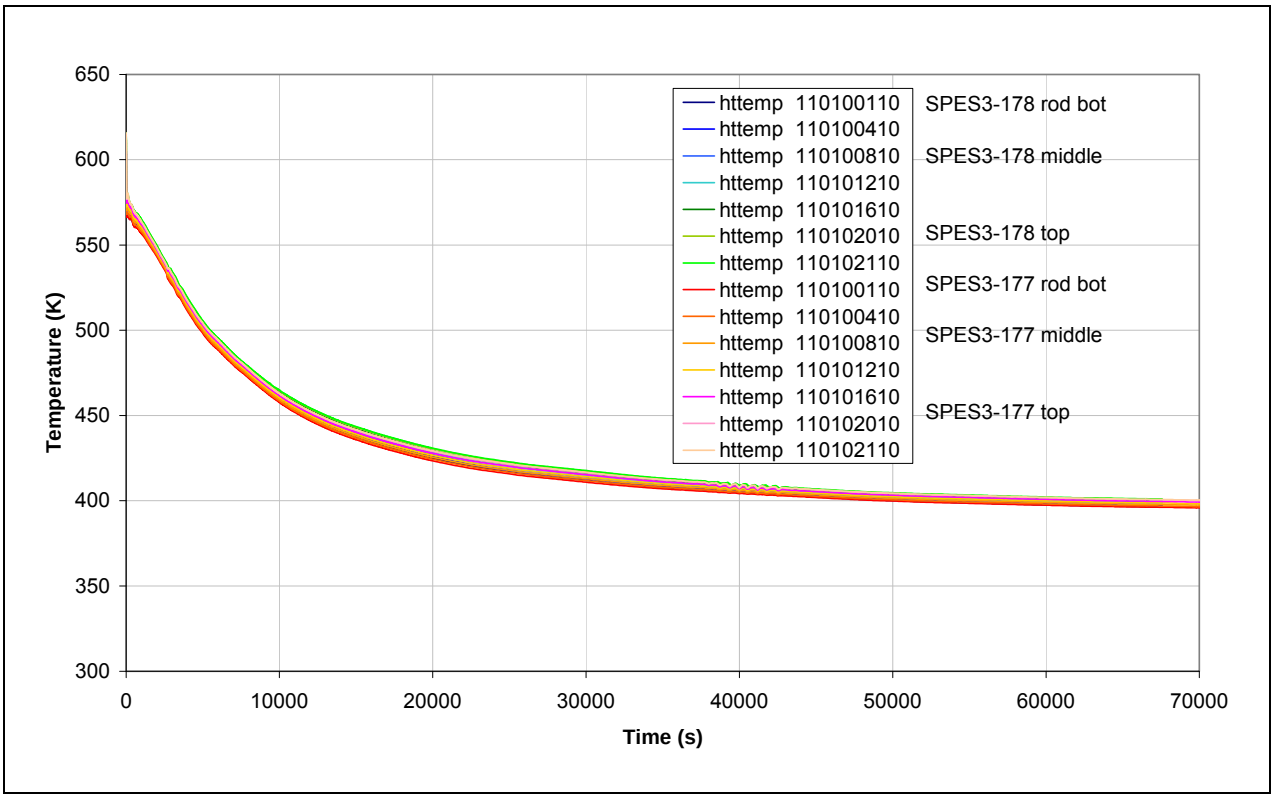

Fig.8. 44 – SPES3-178 and SPES3-177 Core heater rod surface temperature –hot rod (window)

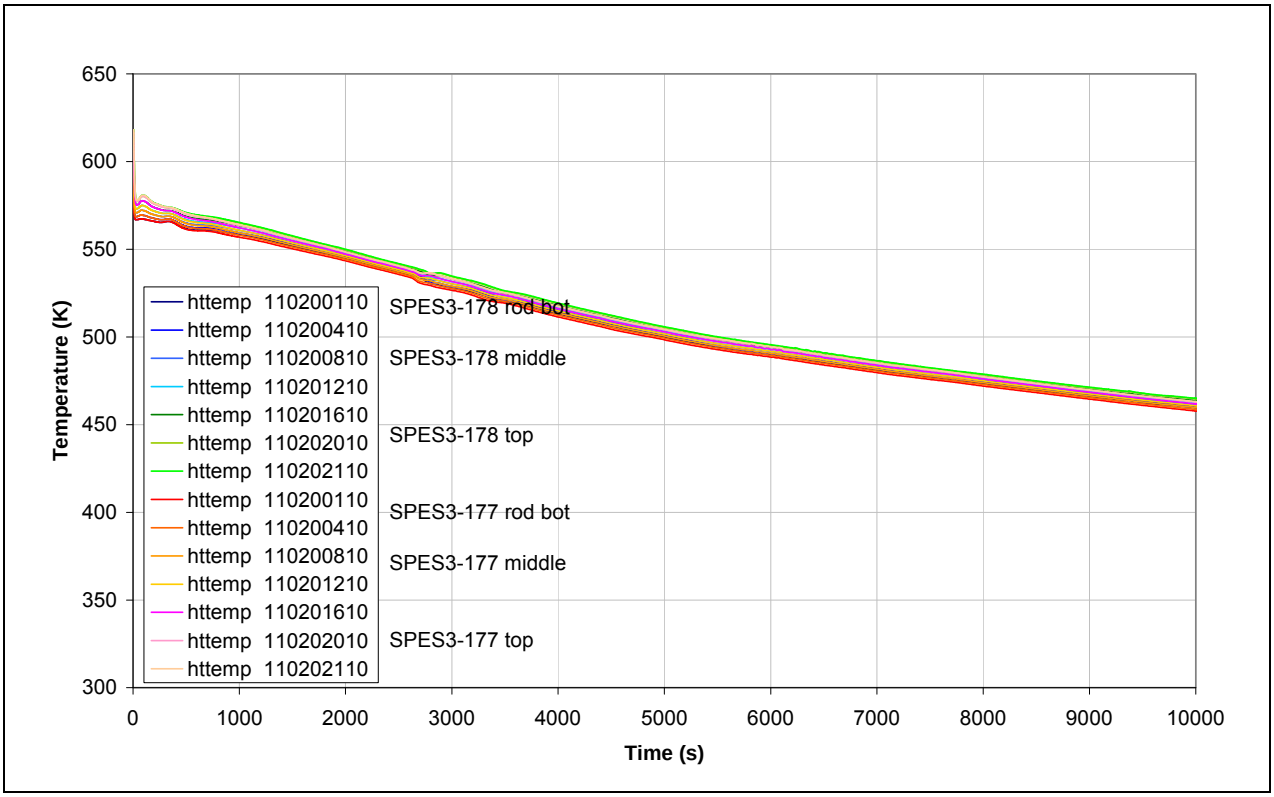

Fig.8. 45 – SPES3-178 and SPES3-177 Core heater rod surface temperature –hot rod

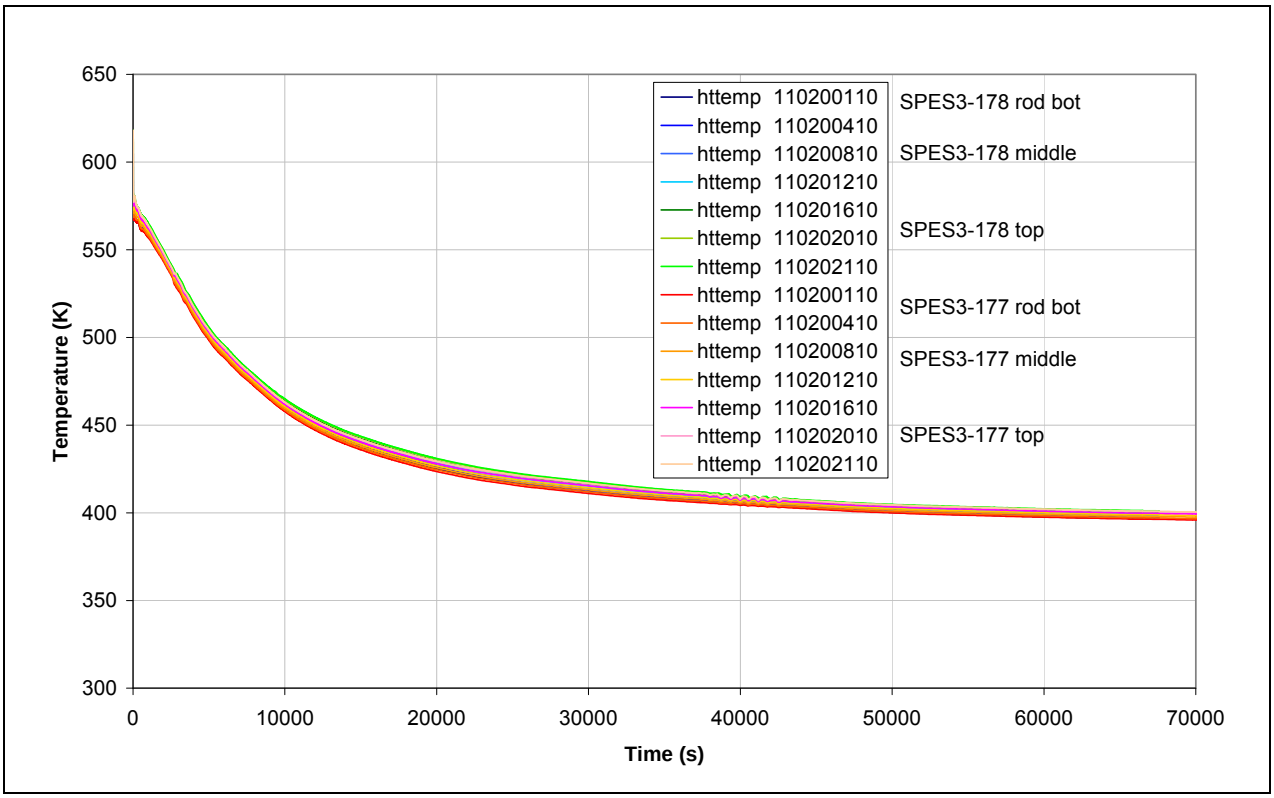

9. CONCLUSIONS

This document reports the results of the RELAP5 simulation of two tests foreseen in the test matrix [1], in particular the DVI line 1-inch equivalent spit break, in design basis conditions, and the EBT top line 4-inch equivalent DEG break, in beyond design conditions. Moreover it reports the results of a SBO simulation based on the Fukushima accident sequence. All the transients are simulated starting from 65% power steady state, typical of the test conditions at SIET.

In all cases, the analysis of the incidental sequence of events showed the capability of SPES3 simulator to cope with the accident. The sequence of intervention of the emergency safety systems assures the plant cooling even in the most challenging conditions. In particular, the Fukushima type SBO simulation showed that, for the emergency system characteristics in IRIS, simulated in SPES3, that, once actuated, relay on natural circulation, the decay hear removal function is always assured by the EHRS.

The final mechanical design of the EHRS heat exchangers and the decision of using AISI 304 instead of Inconel imposed to modify the tube thickness according to the PED directive. In order to guarantee the required heat transfer, the insulating Teflon layer, foreseen on HX tubes, was modified. In order to verify the appropriateness of the new solution, two cases were run with the RELAP5 code, including the new EHRS heat exchanger design, and the results compared with those obtained by the same transient simulations with the original EHRS configuration. The DVI line 2-inch equivalent DEG break and the SBO transients were compared and the results showed very little differences. This assures the new EHRS geometry is suitable to provide the required heat transfer.

In the future, other transients included in the test matrix will be simulated.

10. REFERENCES

[1] G. D. Storrick: IRIS integral system test specification. Westinghouse Electric Company STD-AR-08-01 Rev.2, June 2010.

[2]. M.D. Carelli, L.E. Conway, L. Oriani, B. Petrović, C.V. Lombardi, M.E. Ricotti, A.C.O. Barroso, J.M. Collado, L. Cinotti, N.E. Todreas, D. Grgić, M.M. Moraes, R.D. Boroughs, H. Ninokata, D.T. Ingersoll, F. Oriolo: The Design and Safety Features of the IRIS Reactor. Nuclear Engineering and Design 2004, 230, pp. 151-167.

[3]. M. D. Carelli, B. Petrovic, L.E. Conway, L. Oriani, C.L. Kling, K. Miller, C.V. Lombardi, M.E. Ricotti, A.C.O. Barroso, J.M. Collado, L. Cinotti, S. Storai, F. Berra, N.E. Todreas, H. Ninokata, N. Cavlina, D. Grgic, F. Oriolo, M.M. Moraes, C. Frederico, F. Henning, W. Griffith, J. Love, D.T. Ingersoll, R. Wood, G. Alonso, N. Kodochigov, V. Polunichev, J. Augutis, R. Alzbutas, R.D. Boroughs, A. Naviglio, B. Panella: IRIS design overview and status update. ICONE13-50442 Beijing, China. May 16-20, 2005.

[4] R. Ferri, C. Congiu: Conceptual design of the SPES3-IRIS facility. SIET 01 334 RT 07 Rev.1. Piacenza (I), September 5th, 2008

[5] R. Ferri: Impianto SPES3 – Progetto esecutivo: Elenco elaborati. SIET 01 488 ST 09 Rev.0. Piacenza (I), 25 Marzo 2009.

[6] A. Achilli: Impianto SPES3 – Progetto esecutivo: Dimensionamento e caratteristiche delle tubazioni. SIET 01 487 ST 09 Rev.0. Piacenza (I), 25 Marzo 2009.

[7] C. Congiu, G. Tortora: Impianto SPES3 – Design review del piping. SIET 01 662 RT 10 Rev. 0. Piacenza (I), 24 Settembre 2010.

[8] S. Botti: Impianto SPES3 – Progetto esecutivo: Specifica tecnica dei serbatoi. SIET 01 338 ST 07 Rev.0. Piacenza (I), 19 Marzo 2009.

[9] C. Congiu: Impianto SPES3: Specifica tecnica per la fornitura di serbatoi e scambiatori di calore. SIET 01 338 ST 07 Rev.1. Piacenza (I), 24 Maggio 2011.

[10] A. Achilli: Dossier di progettazione del canale centrale dell'impianto SPES3: Elenco documenti. SIET 01 556 ED 09 Rev.1. Piacenza (I), 29 Marzo 2010.

[11] R. Ferri: Dossier di progettazione del canale centrale dell'impianto SPES3: Specifiche e relazioni. SIET 01 593 ED 10 Rev.0. Piacenza (I), 29 Marzo 2010.

[12] R. Ferri: Dossier di progettazione del canale centrale dell'impianto SPES3: Disegni. SIET 01 594 ED 10 Rev.0. Piacenza (I), 29 Marzo 2010.

[13] R. Ferri: Dossier di progettazione del canale centrale dell'impianto SPES3: Note e rapporti di calcolo. SIET 01 595 ED 10 Rev.0. Piacenza (I), 29 Marzo 2010.

[14] RELAP5 MOD3.3 code manual. NUREG/CR-5535/Rev P3. Idaho National Engineering Laboratory (USA), March 2003.

[15] R. Ferri, C. Congiu: SPES3-IRIS facility nodalization for RELAP5 Mod.3.3 code and steady state qualification. SIET 01 423 RT 08 Rev.0. Piacenza (I), January 30th, 2009.

[16] R. Ferri, C. Congiu: SPES3-IRIS facility RELAP5 base case transient analyses for design support. SIET 01 489 RT 09 Rev.0. Piacenza (I), April 7th, 2009.

[17] R. Ferri, C. Congiu: SPES3-IRIS facility RELAP5 sensitivity analyses of the Lower Break transient for design support. SIET 01 499 RT 09 Rev.0. Piacenza (I), June 11th, 2009.

[18] R. Ferri: SPES3-IRIS facility RELAP5 sensitivity analyses on the containment system for design review. SIET 01 526 RT 09 Rev.0. Piacenza (I), August 31st, 2010.

[19] R. Ferri, P. Meloni: Approach for a correct simulation of the SPES3-IRIS Emergency Heat Removal System with the RELAP5/MOD3 code. SIET 01 745 RT 11 Rev.0. Piacenza (I), May 31st, 2011.

[20] R. Ferri: SPES3 facility: RELAP5 simulations of the DBE and BDBE DVI line DEG break from 65% and 100% power for design support. SIET 01 743 RT 11 Rev.0. Piacenza (I), August 2nd, 2011.

[21] The 2011 off the Pacific coast of Tohoku Pacific Earthquake and the seismic damage to the NPPs. Nuclear and Industrial Safety Agency (NISA); Japan Nuclear Energy Safety Organization (JNES). Japan, April 4th 2011.

[22] L.E. Conway, A. Frisani, L. Oriani: Phenomena Identification and Ranking Table (PIRT) for IRIS Non-LOCA transients and accidents. Westinghouse Electric Company STD-ES-05-02 Rev.0, June 2005.

[23] Westinghouse Electric Company: IRIS plant description document. WCAP-16062-P. March 21, 2003.

11. ATTACHMENTS

The RELAP5 input deck files and results are provided for all cases described in this document.
The list of files and details are reported in Tab.11. 1.

Tab.11. 1 – Files attached to this document

Case	File	Notes
SPES3-169	spes3-169.i	Steady state input-deck (10000 s) 65% power
SPES3-180	restart-180.i	Restart of spes3-169 since 10000 s
	restart-180_1.i	Restart of restart-180 since 40000 s
	spes3-180a.xls spes3-180a_1.xls spes3-180c.xls spes3-180c.xls spes3-180d.xls spes3-180e.xls spes3-180f.xls spes3-180g.xls spes3-180i.xls spes3-180l.xls	Results
SPES3-179	restart-179.i	Restart of spes3-169 since 10000 s
	spes3-179a.xls spes3-179a_1.xls spes3-179c.xls spes3-179c.xls spes3-179d.xls spes3-179e.xls spes3-179f.xls spes3-179g.xls spes3-179i.xls spes3-179l.xls	Results
SPES3-177	restart-177.i	Restart of spes3-169 since 10000 s
	restart-177_1.i	Restart of restart-177 since 125000 s
	spes3-177a.xls spes3-177a_1.xls spes3-177c.xls spes3-177c.xls spes3-177d.xls spes3-177e.xls spes3-177f.xls spes3-177g.xls spes3-177i.xls spes3-177l.xls	Results

Case	File	Notes
SPES3-181	restart-181.i	Restart of spes3-169 since 10000 s
	spes3-181a.xls spes3-181a_1.xls spes3-181c.xls spes3-181c.xls spes3-181d.xls spes3-181e.xls spes3-181f.xls spes3-181g.xls spes3-181i.xls spes3-181l.xls	Results
SPES3-178	restart-178.i	Restart of spes3-169 since 10000 s
	spes3-178a.xls spes3-178a_1.xls spes3-178c.xls spes3-178c.xls spes3-178d.xls spes3-178e.xls spes3-178f.xls spes3-178g.xls spes3-178i.xls spes3-178l.xls	Results